THE UNIVERSITY OF MANITOBA

LIBRARY

AUTHOR ....WISE, Michael Anthony....

TITLE ....GEOCHEMISTRY AND CRYSTAL CHEMISTRY OF Nb, Ta AND Sn MINERALS FROM THE YELLOWKNIFE PEGMATITE FIELD, N.W.T.....

THESIS ....Ph.D., 1987....

I, the undersigned, agree to refrain from producing, or reproducing, the above-named work, or any part thereof, in any material form, without the written consent of the author:

Geochemistry and Crystal Chemistry of Nb, Ta and Sn Minerals from the Yellowknife Pegmatite Field, N. W. T.

Michael Anthony Wise
Smithfield, Virginia

B.A., University of Virginia, 1979

A thesis presented to the
Faculty of Graduate Studies of the University of Manitoba
in partial fulfillment of the requirements for the degree of
Doctor of Philosophy
in
Geological Sciences

June, 1987 

ISBN 0-315-37403-9

THE UNIVERSITY OF MANITOBA

FACULTY OF GRADUATE STUDIES

The undersigned certify that they have read, and recommend to the Faculty of Graduate Studies for acceptance, a Ph.D. thesis entitled:

GEOCHEMISTRY AND CRYSTAL CHEMISTRY OF Nb, Ta and Sn MINERALS FROM THE YELLOWKNIFE PEGMATITE FIELD, N.W.T.

submitted by MICHAEL ANTHONY WISE

in partial fulfilment of the requirements for the Ph.D. degree.

Advisor

Advisor

Dr. E.E. Foord
External Examiner
Senior Researcher
U.S. Geological Survey
Denver Federal Center
Denver, Colorado

Date of oral examination: May 1, 1987

The student has satisfactorily completed and passed the Ph.D. oral examination.

P K Isaac
Chairman of Ph.D. Oral*

(*The signature of the Chairman does not necessarily signify that the Chairman has read the complete thesis.)

GEOCHEMISTRY AND CRYSTAL CHEMISTRY OF Nb, Ta and Sn MINERALS FROM THE YELLOWKNIFE PEGMATITE FIELD, N.W.T.

BY

MICHAEL ANTHONY WISE

A thesis submitted to the Faculty of Graduate Studies of the University of Manitoba in partial fulfillment of the requirements of the degree of

DOCTOR OF PHILOSOPHY

ABSTRACT

The 12,000 km^2 Yellowknife pegmatite field, Northwest Territories, is populated by numerous granitic pegmatites varying from barren to complex rare-element types, many of which host accessory Nb-, Ta- and Sn-oxide minerals. Columbite-tantalite, ferrotapiolite, ixiolite, cassiterite and microlite have been identified by X-ray diffraction and electron microprobe analysis; they occur in pegmatites which also carry subordinate to minor accumulations of beryl, amblygonite-montebrasite and/or spodumene. The bulk of the Nb-Ta-Sn mineralization occurs in the intermediate zone of complex pegmatites; however, oxide minerals have also been found in the core and in saccharoidal albite bodies.

Columbite-tantalite is the most common oxide mineral in the field, with typically ferrocolumbite compositions which grade mainly into ferrotantalite, and only rarely into manganocolumbite and manganotantalite. Members of the series show variable degrees of order, but most show intermediate structural states.

Ferrotapiolite and cassiterite are the next most abundant oxide minerals present. Ferrotapiolite is found primarily in pegmatites containing little or no spodumene, in areas of relatively advanced Ta fractionation, and compositions are less variable than in columbite-tantalite. Structurally, ferrotapiolite shows variable degrees of order. Cassiterite occurs almost exclusively in spodumene-bearing pegmatites and is often enriched in Ta, Nb and Fe.

Occurrences of ixiolite and microlite are rare. Ixiolite shows fairly uniform chemistry and typically shows extreme structural disorder. Microlite occurs predominantly as a replacement of primary columbite-tantalite or ferrotapiolite. Microlite compositions display strong variations in their content of Ca, Na, U and Pb. Partitioning of elements in coexisting mineral pairs generally conforms to the preference of the tetragonal phase for Fe and Ta, with Mn and Nb preferring the orthorhombic phases.

A crystallographic study of ixiolite shows the true symmetry of ixiolite to be monoclinic with ß very close to 90°. The apparent orthorhombic nature of most of its single-crystal diffraction patterns is interpreted to be the result of twinning. Additional evidence supporting an ixiolite-wodginite relationship is indicated by the close similarites in composition. This strongly supports an ixiolite-wodginite order-disorder relationship.

The chemistry of the Yellowknife tapiolites shows less extreme Fe-Mn and Nb-Ta substitution and greater concentration of Fe^{3+} as compared to columbite-tantalite. Structural analysis of a partially disordered tapiolite showed it to be 74% ordered with a trirutile structure.

The overall chemical signature of the Yellowknife pegmatite field is one of Fe and Nb enrichment with local accumulations of Ta, Ti and Sn. The fractionation of Ta within pegmatite bodies, pegmatite swarms, pegmatite series and the entire field is relatively extensive, whereas Mn fractionation is fairly limited. The geochemical nature of the pegmatite melts/fluids is characterized by the general evolution of Nb- and Ta-oxide minerals, which typically proceeds from ferrocolumbite to ferrotantalite, ferrotapiolite, ixiolite and cassiterite. This Fe- and Nb-rich pegmatitic

environment, as characterized by Nb- and Ta-oxide mineral chemistry, is probably due to the low activity of F in the pegmatite melts before and during Nb and Ta precipitation. Local areas displaying anomalous Mn enrichment can, in most cases, be explained by higher F activity relative to the remainder of the pegmatite field. The local enrichment of Ti and Sn in Nb- and Ta-bearing minerals is the result of normal fractionation of Ti- and Sn-enriched granite magmas, which are rarely affected by assimilated host rock material.

Similar ranges of Mn/(Mn + Fe) and Ta/(Ta + Nb) are observed in columbite-tantalite from primary units and metasomatic saccharoidal albite bodies. Columbite-tantalite compositions suggest that saccharoidal albite originated from a medium that largely did not differ in its minor and trace element content from that crystallizing from primary zones. This also may suggest that the timing of solidification of the two kinds of units was not particularly different.

Regional variations in structural state, and the Mn and Ta contents of columbite-tantalite in pegmatite aureoles surrounding granite plutons are in part irregular. Non-systematic increases (or decreases) in structural states, and Mn and Ta contents away from granitoid plutons predominates. However, in some areas regular increasing or decreasing trends do occur.

The low Ta content and conspicuous presence of Ti and Sn within Nb and Ta minerals, in addition to unfavorable market conditions, location and areal distribution of Ta-bearing pegmatites make economic development of the area for tantalum unfeasible at this time.

ACKNOWLEDGEMENTS

The author is greatly indebted to Dr. P. Černý of the Department of Geological Sciences, University of Manitoba, for his supervision of the thesis research and to Drs. F.C. Hawthorne, A. Secco (Univ. of Manitoba) and E.E. Foord (USGS) for their critical reviews of the manuscript.

The writer wishes to thank the Tantalum Mining Corporation of Canada Limited and the Geology Division, Department of Indian Affairs and Northern Development, Yellowknife, for their financial and field support.

Special thanks go to R.E. Meintzer for providing valuable field support, chemical data on pegmatites of the area and for his helpful discussions. Special accolades are also extended to Dr. T.S. Ercit for his numerous helpful discussions and assistance in various aspects of this research. The writer also thanks R. Chapman for analyzing several samples in the early stages of the research and R. Pryhitko for his photographic services.

The author gratefully acknowledges the field assistance of R. Chaoka, R. Alers, R. Gaba, K. Ferreira, K. Meintzer, F. Ostrop, L. Chackowsky and B. Schmidke. Last, but not least, special thanks are extended to C. Grenfell for her help and constant support throughout the final stages of the thesis writing.

CONTENTS

LIST OF FIGURES

LIST OF TABLES

CHAPTER 1

Introduction

Prior to the early 1940's, commercial consumption of tantalum was small; its primary use being filament material for incandescent light bulbs. During World War II, tantalum consumption increased dramatically due mainly to the rapid technological advances in the field of electronics. The development of tantalum capacitors absorbed the bulk of domestic tantalum consumption. By 1958, the commercial use of tantalum had expanded into other areas. Tantalum carbide in machine cutting tools became the second largest use of tantalum in the United States. Its resistance to corrosion and chemical attack made tantalum particularly suitable for the manufacture of acid-resistant laboratory equipment. Its high melting point made it appropriate for use in refractory alloys used in rockets, jet engines and gas turbine parts. Finally, the medical field benefited from its use in surgical instruments and prosthetics.

Unfortunately, the economic exploitation of tantalum metal has been quite erratic as evidenced by the fluctuating price trend. Over a period of twenty years (1955-1975), the market price of tantalum concentrate suffered through a series of "peaks and valleys" , yet the average straight line trend value showed a small increase in price from $6 to $14/lb. However, in 1980 the price of tantalum rose rapidly and peaked at $125/lb. The sudden escalation of tantalum prices was influenced by anticipated greater tantalum demand and concerns of dwindling world supply. Three years later, the world market price for tantalum fell sharply to $30/lb.

This decline in price was due primarily to the development of new less expensive alloys and ceramics.

The period during which the demand for tantalum was greatest led to an increase in the number of exploration programs aimed at locating new tantalum deposits. In the United States and Canada, these programs targeted rare-element pegmatites which were known to be an important source of tantalum. This resulted in an increased interest in granitic pegmatites and subsequently, extensive research on their mineralogy and geochemistry. This in turn prompted extensive studies on the geochemistry of niobium, tantalum, beryllium and lithium.

General Geochemistry of Niobium and Tantalum

The first major comprehensive study on the geochemistry of Nb and Ta was completed by Rankama (1944,1948). In these works, most of the basic geochemical characteristics were outlined. Works by Kuzmenko (1959,1964) and Eskova (1964) supplied additional information to the study. Excellent summaries of the geochemical behavior of Nb and Ta are offered by Vlasov (1966a,1966b), Parker and Fleischer (1968) and Gorzhevskaya et al. (1974).

Niobium was first discovered in 1801 and tantalum in 1802. Both are Group Va transition metal elements with similar physical, chemical and crystallochemical properties, and consequently are always found together in nature (Table 1). The very similar ionic radii and identical valence states in terrestrial environments result in nearly unlimited isomorphous substitution in a large number of crystal structures, despite the considerable difference in their atomic masses. The close relationship between Nb and Ta is a direct consequence of the lanthanide contraction. The strong

lithophile nature of niobium and tantalum is evident by their enrichment in the earth's crust and by their strong affinity for forming oxygen-based minerals. Average crustal abundances (clarke values) for Nb and Ta have been estimated at 23 and 2 ppm respectively (Flörke et al., 1974). About 85% of the known Nb- and Ta-bearing minerals are oxides with the remaining species consisting of a few silicates, two phosphates and a borate.

Table 1: Physical and chemical properties of niobium and tantalum.

	Niobium	Tantalum
Atomic number	41	73
Atomic weight (a.m.u.)	92.9064	180.9479
Melting point (°C)	2468 ± 10	2996
Boiling point (°C)	4742	5425 ± 100
Specific gravity (20°C,g/cm^3)	8.57	16.654
Oxidation state	$^{+}$5 (3,2,4?)	$^{+}$5 (3,2?,4?)
Ionic radius (Å)*	0.64	0.64
Electron configuration	[Kr]4d^{4}5s^1	[Xe]4f^{14}5d^{3}6s^2
Electronegativity	1.6	1.5

*Shannon (1976). All other data obtained from Weast et al. (1986).

Niobium and tantalum are known to occur in increased concentrations in various igneous rock types and some sedimentary rocks, such as clays, laterites and bauxites. By far the greatest accumulation occurs in both felsic and mafic igneous rocks. Their contents generally increase slightly

from ultrabasic to acidic rocks during magmatic differentiation in both calc-alkalic and peralkaline suites. The highest concentration occurs in the final stages of magmatic crystallization, during the formation of pegmatites and high-temperature hydrothermal assemblages. Niobium is the dominant element in alkalic rock series of anorogenic origin (syenites, alkali granites, carbonatites), whereas tantalum is dominant in the late stages of calc-alkalic and peraluminous granitoid sequences of orogenic affiliation. The partial separation of Nb from Ta in these two different petrochemical and petrogenetic environments is considered due to the affinity of Nb to carbonate complexes, as opposed to the fluorophile character of Ta (Aleksandrov et al., 1969; Aleksandrov and Trusikova, 1973).

In calc-alkaline and peraluminous sequences, the absolute contents of Nb and Ta begin to show significant increases in silicic leucogranites and pegmatitic granites. The contents of Nb and Ta in these rocks increase to approximately 150 and 40 ppm respectively (Beus et al., 1968), and the trend is extended to about 500 ppm Nb and 4500 ppm Ta in associated rare-element granitic pegmatites (Černý et al., 1985a). This increase in rare-metal content has been attributed to the relative stabilities of Nb and Ta complexes at high temperatures, and to their affinity to a hydrous phase in liquid fractionation and volatile-related transport (Hildreth, 1981; Černý et al., 1985a).

In granites parental to Nb- and Ta-bearing pegmatites, Nb and Ta are mostly dispersed in micas, garnet, tourmaline, ilmenite and zircon, and rarely form minerals of the columbite-tantalite group. Nb- and Ta-bearing minerals are generally restricted to pegmatitic phases and usually occur with minerals of Sn, Ti, Zr, Hf, Be and Li as rare accessories in both sim-

ple and complex pegmatites. Most Nb and Ta minerals occur in albite + muscovite-rich intermediate zones or metasomatic bodies and in lepidolite-rich units. The border and wall zones are usually poor in Nb- and Ta-bearing minerals.

The general fractionation trend of Nb and Ta in an individual pegmatite shows a tendency for the Ta/(Ta + Nb) ratio to increase with progressive crystallization of primary zones and metasomatic units. This is shown in a general way by the increasing enrichment of Ta in Nb and Ta minerals from the wall zone inwards to the core and into the replacement units (Cameron et al.,1949; Page et al., 1953), a phenomenon which is explained by the difference in thermal stability of Nb and Ta complexes in pegmatitic systems. Specifically, it is suggested that Nb and Ta exist mainly as fluoride complexes in granitic melts or fluids, and that these complexes have significantly different temperatures of stability. According to Wang et al. (1982), Ta-fluoride complexes are generally stable to lower temperatures than Nb-fluoride complexes. Thus the availability of Nb for early crystallizing phases would be due to the breakdown of its complexes at higher temperatures. Reversals of this trend (increased Nb contents with fractionation) have been reported in the literature but not thoroughly documented (Fersman, 1940; Kornetova, 1961; Ferreira, 1984).

The regional distribution of Nb and Ta is also dependent on the overall degree of fractionation attained by different pegmatites and on the extent of metasomatic processes (Kuzmenko,1959). In cogenetic pegmatite groups, variations in the Nb/Ta ratio is regulated by the same factors as outlined above for the internal evolution of individual pegmatite bodies. Poorly fractionated, unreplaced pegmatites close to parental granites usually carry Nb-rich mineral phases, whereas Ta-rich species are more common

in the most exterior pegmatites displaying a high degree of fractionation and metasomatic replacement.

The mineralogy of Nb and Ta depends not only on the Nb/Ta signature of the parent melt or derived fluids , but also upon the overall chemical signature of the melt or fluid. The relationships among the activities of Fe, Mn, Mg, Na, Ca, Y, REE's, and those of OH and F are particularly important. This multitude of geochemical variables leads to considerable diversity in the mineralogy of Nb and Ta.

An extensive data-base of Nb and Ta assemblages in individual pegmatites and pegmatite groups of the rare-element class has been compiled by Černý and Ercit (1985) and their data allowed them to characterize the paragenesis of Nb- and Ta- bearing minerals in various types of rare-element pegmatites (Table 2). Their list of rare-element pegmatite types and the Nb and Ta minerals characteristic to each type is presented here:

1. Gadolinite type (rare-element type of Table 2): aeschynite, niobo-aeschynite, samarskite, fergusonite, formanite, (yttrocolumbite), yttrotantalite, polymignite, euxenite, polycrase, ferrocolumbite, (ixiolite), niobian rutile, ilmenite, (pyrochlore), betafite, microlite, fersmite, (rynersonite).
2. Beryl-columbite type (beryl type of Table 2): ferrocolumbite, manganocolumbite, (ferrotantalite), ixiolite, ferrotapiolite, niobian rutile, cassiterite, microlites (also with U, Bi, Sn), (stibiobetafite).
3. Complex (complex type,spodumene subtype): fersmite, (rynersonite), manganocolumbite, manganotantalite, (ferrotantalite), ferrotapiolite, ixiolite, (wodginite), tantalian rutile, cassiterite, (staringite), thoreaulite, microlites (also with U, Sb, Sn).

4. Complex (complex type, petalite subtype): manganocolumbite, manganotantalite, ferrotapiolite, (ixiolite), wodginite, (tantalian rutile), cassiterite, microlites (also with U, Bi, Sb, Cs, Pb, Ba), cesstibtantite, natrobistantite, stibiotantalite, (bismutotantalite), simpsonite, alumotantite, natrotantite, calciotantite, lithiotantite, tantite, sosedkoite, rankamaite, holtite, behierite.
5. Complex (complex type, lepidolite subtype): manganocolumbite, (manganotantalite), microlites (also with Bi, U), stibiotantalite.
6. Albite-spodumene type: columbite-tantalite, cassiterite, (microlite).

Purpose of the study

The compositional and structural variability of complex Nb- and Ta-oxide minerals occurring in rare-element pegmatites is relatively well-documented, but still poorly understood. Recent works by Foord (1982) and Černý and Ercit (1985) have greatly contributed to the better understanding of the chemical and structural features of this mineral family. Despite their efforts, much remains to be done.

Although progress is continually being made in crystallochemical studies of Nb and Ta minerals, the intricacies of their structural and chemical relationships still require additional work (Komkov, 1970; Graham and Thornber, 1974a; Ercit, 1986; Wise and Černý, 1986; M.A. Wise, unpubl. ms.). Studies dealing with the evolution of Nb and Ta minerals in individual pegmatites have broadened our understanding of Fe/Mn and Nb/Ta fractionation paths (Foord, 1976; Ferreira, 1984; Černý et al., 1985b; Ercit, 1986; Lumpkin et al., 1986). Regional studies involving pegmatites of dif-

ferent types at the group or field scale are particularly sparse (Černý et al., 1981; Anderson, 1984; Černý et al., 1986b).

The purpose of this study is to examine the Nb-, Ta- and Sn-oxide minerals of the Yellowknife pegmatite field and to document their structural, chemical and paragenetic variations. Specifically, the objectives of this study are fivefold:

1. to investigate the compositional variation of complex Nb-, Ta- and Sn-oxide minerals of different geochemical and paragenetic pegmatite types, and to establish these variations within and among different pegmatite series of the field,
2. to establish the general structural and compositional relationships of two mineral species typical of the field, tapiolite and ixiolite,
3. to investigate relationships between chemical composition and structural state of the columbite-related minerals,
4. to characterize the partitioning behavior of Fe, Mn, Nb, Ta, Sn and Ti among coexisting mineral phases,
5. to correlate Fe/Mn and Nb/Ta fractionation trends with rare-alkali fractionation of the parent pegmatites.

The results of this study are expected:

1. to establish the behavior of Nb and Ta in the particular pegmatite types represented in the Yellowknife field,
2. to lead to the development of guidelines for the exploration of Ta-bearing pegmatites in the Yellowknife field
3. to provide a better understanding of the general geochemistry and crystal chemistry of selected Nb- and Ta-oxide minerals in the pegmatitic environment.

Table 2: Paragenesis of Nb- and Ta-bearing minerals in selected rare-element pegmatites. After Černý and Ercit (1985).

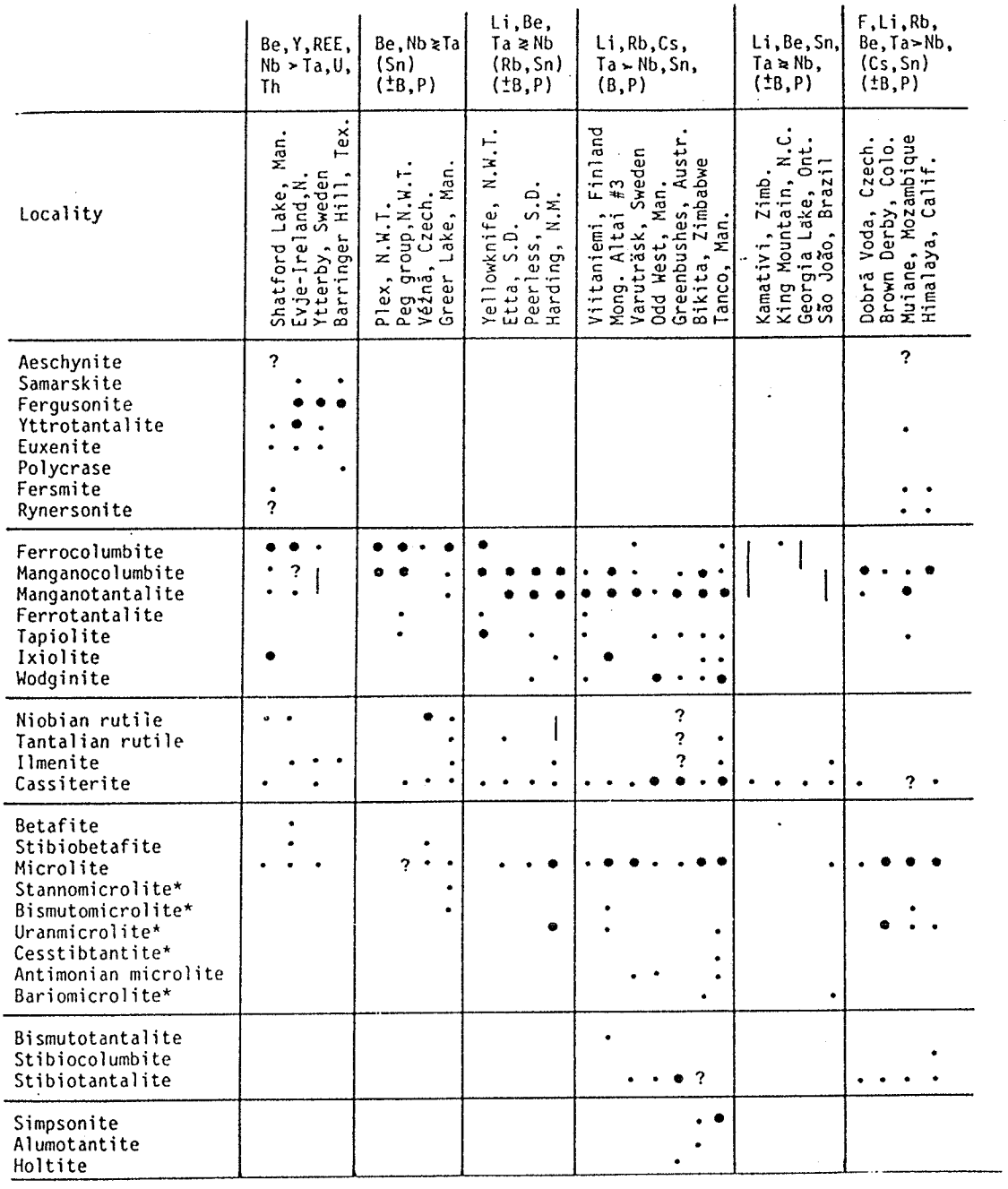

Large dot represents a particularly abundant mineral.
Vertical line marks an uncertainty about composition in a mineral group.
Question mark signifies uncertain identification or paragenetic affiliation.
*Includes microlite with elevated contents of the typical A-cations.

Sponsorship for the study

The project was conceived and supervised by Dr. Petr Černý with field sampling commencing in June 1980. Financial support was provided by the Geology Office, Division of Indian Affairs and Northern Development, Yellowknife contracts 1980-1981, 1983-1984, 1984-1985; Tantalum Mining Corporation of Canada, Ltd. grants 1981-1982, 1982-1983; Department of Energy, Mines and Resources, Ottawa, Research Agreements 1983-1984, 1984-1985, 1985-1986; and NSERC Operating Grants to Dr. P. Černý 1981-1987.

CHAPTER 2

Location and general geology

Location and access

The Yellowknife pegmatite field, at one time a major mineral producing area of northern Canada, is populated by large granitoid plutons and numerous pegmatite bodies, some of which contain rare-elements of economic importance. The study area is located north of the eastern arm of the Great Slave Lake and east of the city of Yellowknife in the District of Mackenzie, Northwest Territories (Figure 1). The area covers approximately 12,000 km^2 between the latitudes 62° and 63° N and longitudes 112° and 114° 30' W. The topography of the area is generally of low relief with rocky hills and ridges and contains numerous lakes, swamps and low areas covered by muskeg and infested by black flies and mosquitoes. Pegmatite outcrops are well-exposed throughout most of the area, and are easily identified on aerial photographs. Limited eastern segments of the pegmatite field are accessible by roads; however, most of the pegmatites can be reached only by float-equipped aircraft onto nearby lakes or by helicopter service from Yellowknife. The short summer season (typically June to late August) greatly limited the amount of field work completed each year. Ice-covered lakes (until late May) made early access to the pegmatite field virtually impossible. The beginning of the fall school session necessitated the completion of field work by early September.

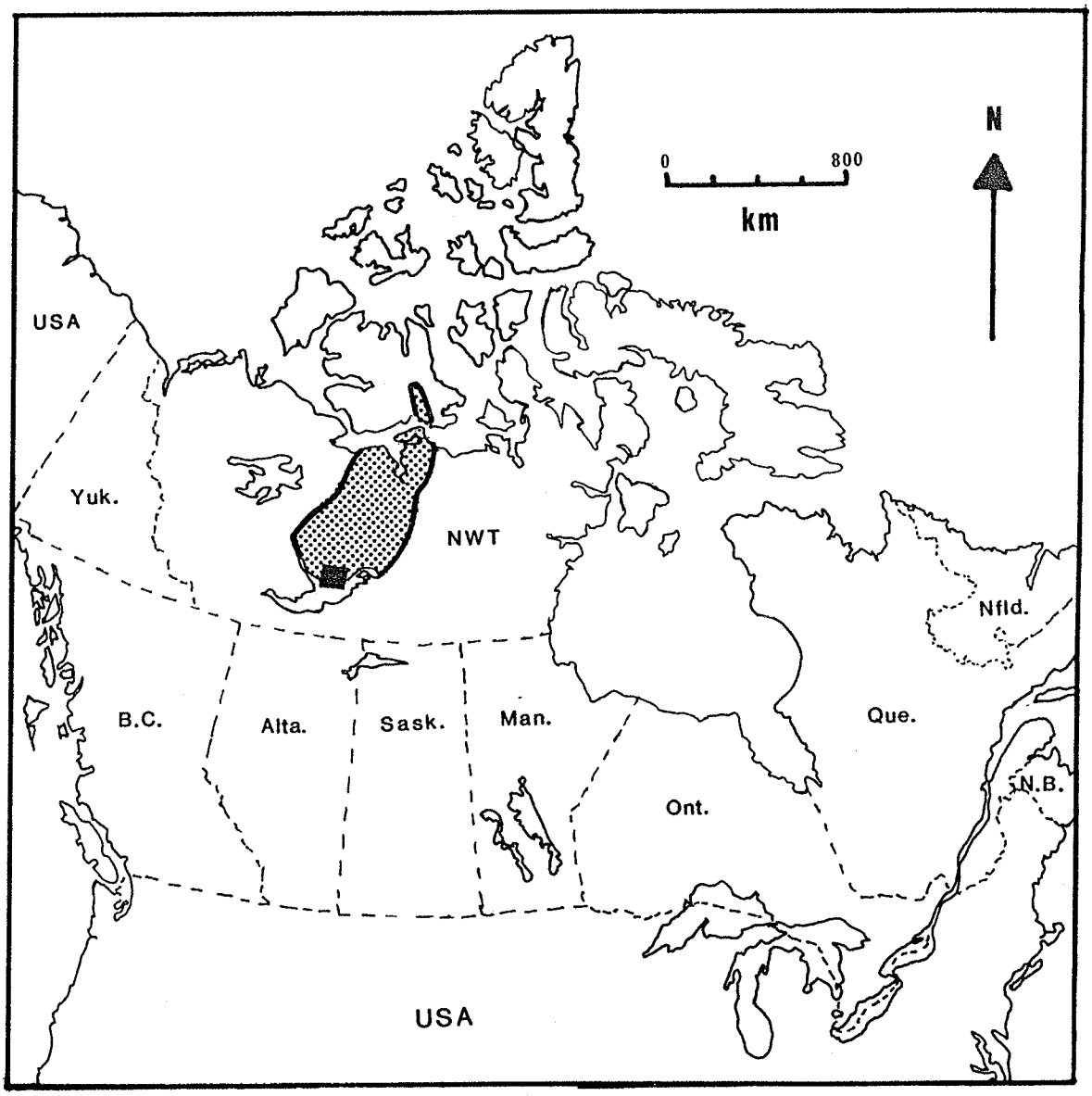

Figure 1: Location map of the Yellowknife pegmatite field in the District of Mackenzie, Northwest Territories. Dotted pattern denotes the area defined by the Archean Slave Structural Province. The position of the Yellowknife pegmatite field is shown by the black rectangle.

Regional geology

The Yellowknife pegmatite field lies within the extreme southwestern portion of the Archean Slave Structural Province of the Canadian Shield (Figure 2). The province, which is underlain by Late Archean rocks (3.0 - 2.5 Ga), has remained relatively stable since the close of the Archean era, except for minor faulting, folding and local intrusions during the early Proterozoic. The geology of the province has been documented by McGlynn and Henderson (1972), McGlynn (1977) and recently summarized by Padgham (1985).

The pegmatite field is underlain largely by granitoids and metasedimentary rocks and to a lesser extent by metavolcanic and gabbroid/dioritoid rocks (Figure 3). A thick sequence of metavolcanics and metasedimentary rocks comprises the supracrustal rocks of the Yellowknife Supergroup. The metavolcanic rocks are dominantly andesite, dacite and basalt flows which outcrop in an arcuate belt in the northwestern portion of the field and along the edge of folded metasediments in the west. The metasedimentary rocks consist largely of a thick sequence of interbedded graywacke-mudstone turbidites. The entire sequence of Yellowknife Supergroup rocks has been complexly folded, and regionally metamorphosed (greenschist to middle amphibolite facies). This low pressure metamorphism generated quartz-biotite schists and hornfels of amphibolite facies which contain conspicuous nodules of cordierite and, less commonly, andalusite.

Late Archean syntectonic and late-tectonic rocks of tonalitic, granodioritic and granitic compositions intruded the supracrustal and basement rocks at various times, and in part contributed to the complex folding of the metasediments. In addition, these late intrusions generated contact-

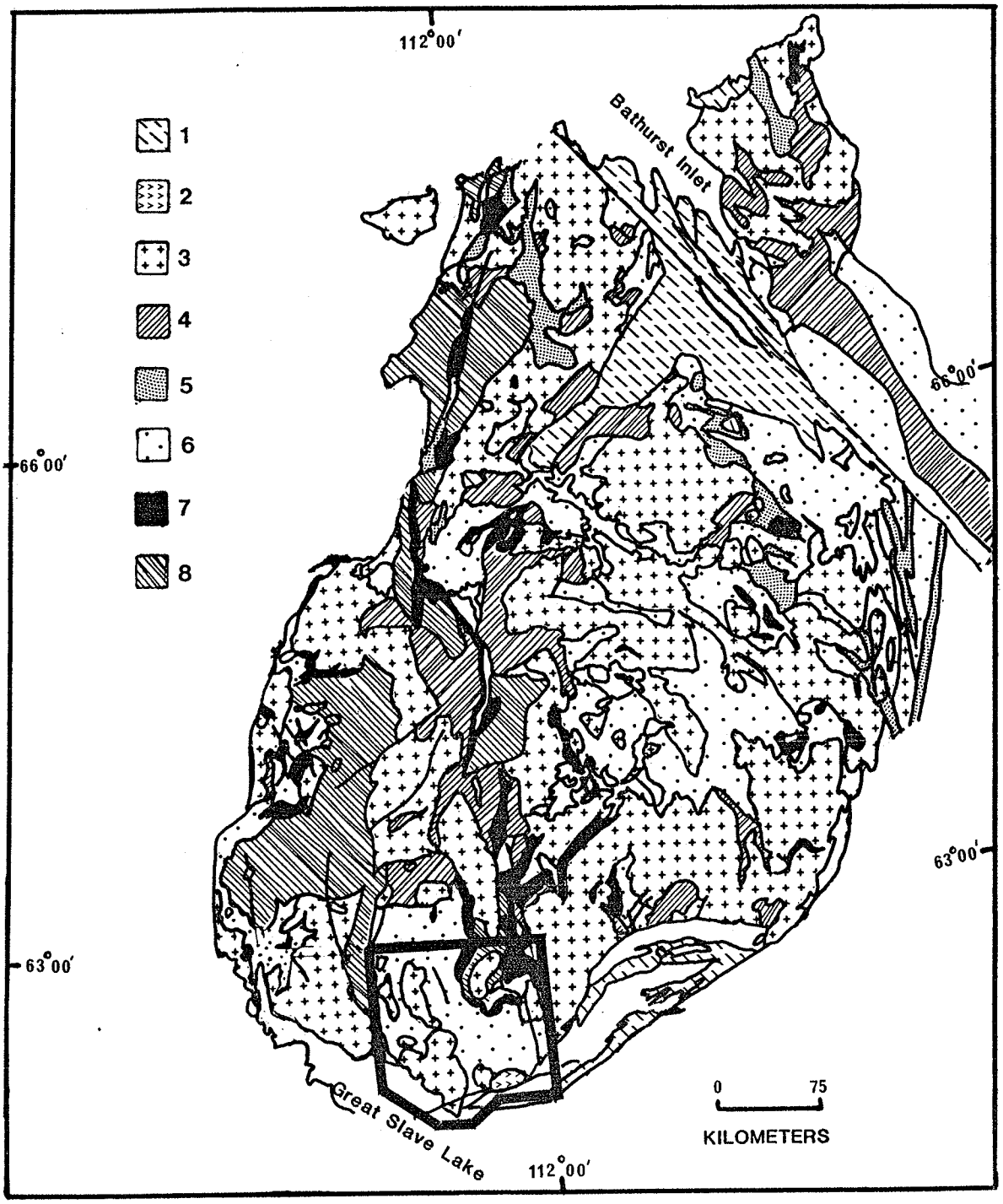

Figure 2: General geology map of the Slave Structural Province. The Yellowknife pegmatite field is outlined. Major rock units are numbered as follows: 1) Proterozoic cover rocks; 2) Proterozoic metamorphic and intrusive rocks; 3) Granitoid intrusions; 4) Migmatite; 5) Dominantly felsic volcanic belts; 6) Metasedimentary rocks, mainly turbidites; 7) Dominantly basaltic volcanic belts; 8) Metamorphic and intrusive rocks including pre-Yellowknife Supergroup granitoid rocks. Map modified after Padgham (1985).

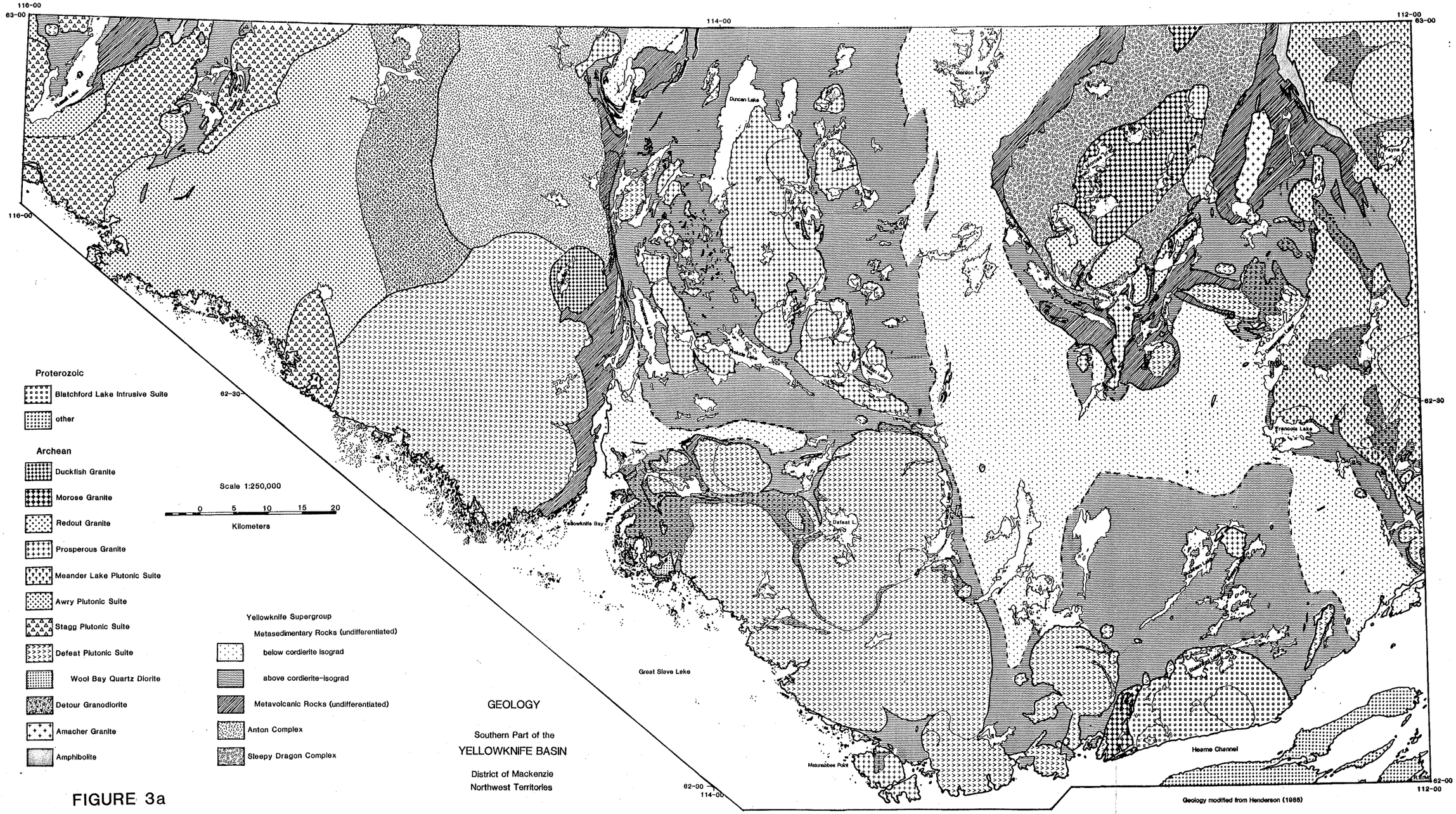
116-00
63-00
114-00
112-00
63-00
116-00
62-30
62-30
62-00
114-00
62-00
112-00
Hottah Lake
Duncan Lake
Gordon Lake
Wynne
Yellowknife Bay
Defeat L.
Great Slave Lake
Mezonabbee Point
Heame Channel
Francois Lake
Geology modified from Henderson (1985)
Proterozoic
Blatchford Lake Intrusive Suite
other
Archean
Duckfish Granite
Morose Granite
Redout Granite
Prosperous Granite
Meander Lake Plutonic Suite
Awry Plutonic Suite
Stagg Plutonic Suite
Defeat Plutonic Suite
Wool Bay Quartz Diorite
Detour Granodiorite
Amacher Granite
Amphibolite
Scale 1:250,000
0 5 10 15 20
Kilometers
Yellowknife Supergroup
Metasedimentary Rocks (undifferentiated)
below cordierite isograd
above cordierite-isograd
Metavolcanic Rocks (undifferentiated)
Anton Complex
Sleepy Dragon Complex
GEOLOGY
Southern Part of the
YELLOWKNIFE BASIN
District of Mackenzie
Northwest Territories

FIGURE 3a

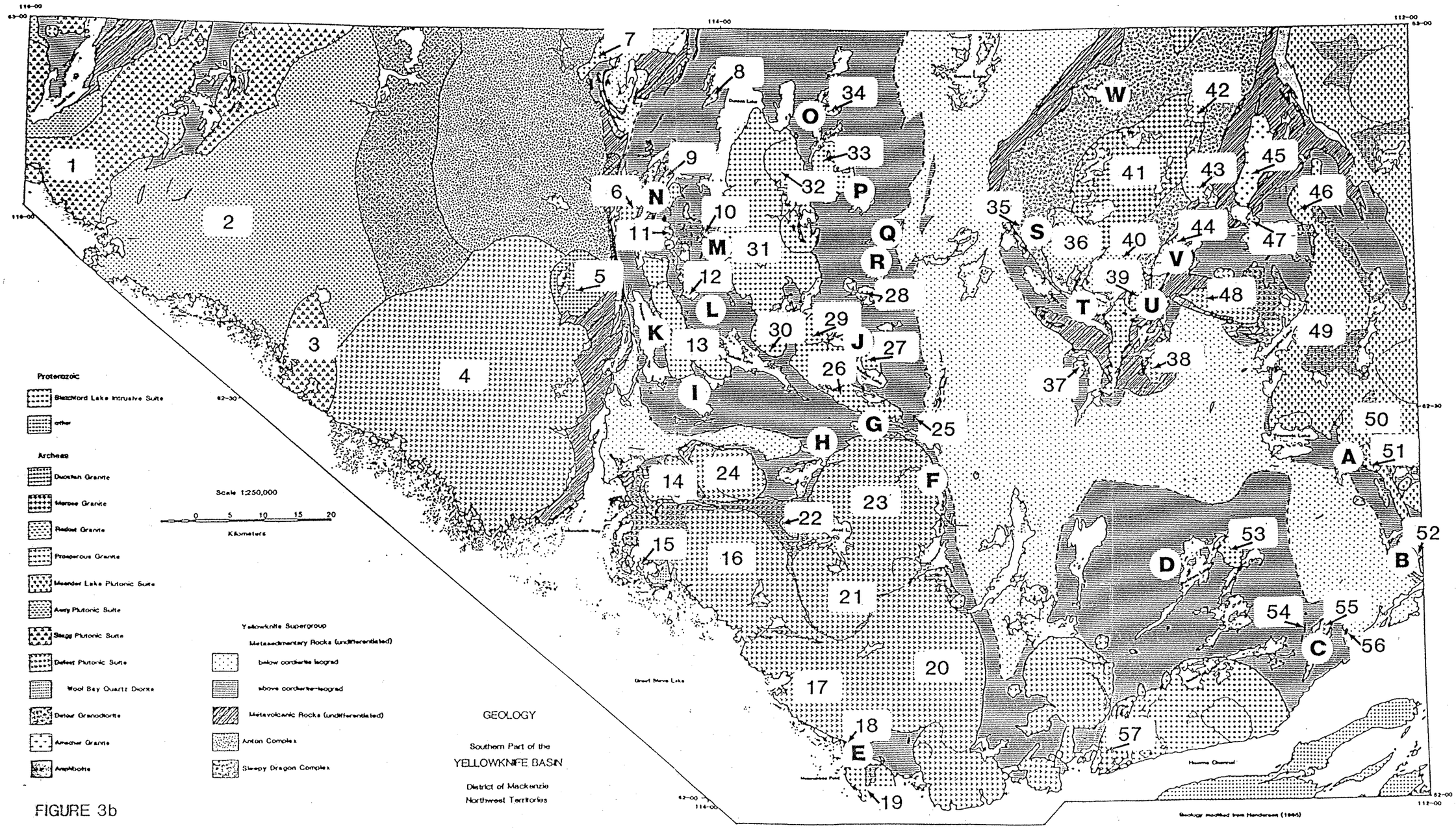
Proterozoic
Blatchford Lake Intrusive Suite
other
Archean
Duncan Granite
Marose Granite
Redout Granite
Prosperous Granite
Meander Lake Plutonic Suite
Avery Plutonic Suite
Stagg Plutonic Suite
Defeat Plutonic Suite
Wool Bay Quartz Diorite
Defeat Granodiorite
Amacher Granite
Amphibolite
Scale 1:250,000
0 5 10 15 20
Kilometers
Yellowknife Supergroup
Metasedimentary Rocks (undifferentiated)
below cordierite isograd
above cordierite-isograd
Metavolcanic Rocks (undifferentiated)
Anton Complex
Sleepy Dragon Complex
GEOLOGY
Southern Part of the
YELLOWKNIFE BASIN
District of Mackenzie
Northwest Territories
Great Slave Lake
Hearne Channel
Geology modified from Henderson (1946)

FIGURE 3b

PLUTONS (superscripts indicate lithodemic unit):

1. Frank Channel[4]
2. North Arm[5]
3. Trout Rock[4]
4. Western[3]
5. Duckfish[10]
6. Quyta[3]
7. Rocky[7]
8. Crapaud[3]
9. Neck[7]
10. Staple[7]
11. Drygeese[7]
12. Alexie[7]
13. Prosperous[7]
14. Mason[3]
15. Wool Bay[3]
16. Moose[3]
17. Black Fly[3]
18. Hare[7]
19. Matonabbee[7]
20. Hearne[3]
21. Defeat-South[3]
22. Defeat[3]
23. Harding[3]
24. Jennejohn[3]
25. Frog[7]
26. Cameron[7]
27. Hidden[7]
28. Scott[7]
29. Sparrow[7]
30. Prelude[7]
31. Duncan-West[7]
32. Duncan-East[7]
33. Wedge[7]
34. Prestige[7]
35. Ross Lake[1]
36. Redout[8]
37. Donor[7]
38. Beaulieu[3]
39. Horse Fly[8]
40. Ross River[8]
41. Morose[9]
42. Abediah[7]
43. Goon[7]
44. Turnback[8]
45. Amacher[2]
46. Old Grump[6]
47. Two Bug[7]
48. Birch[3]
49. Desperation[6]
50. Eastern[6]
51. McDade[7]
52. Doubling[3]
53. Buckham[7]
54. McDuff[7]
55. Faulkner[3]
56. Beaver[3]
57. Camp[9]

---

[1] - Sleepy Dragon Complex
[2] - Amacher Granite
[3] - Defeat Plutonic Suite
[4] - Stagg Plutonic Suite
[5] - Awry Plutonic Suite
[6] - Meander Lake Plutonic Suite
[7] - Prosperous Granite
[8] - Redout Granite
[9] - Morose Granite
[10] - Duckfish Granite

PEGMATITE GROUPS/SERIES:

A - Tanco Lake Group
B - Doulbling Lake Group
C - Faulkner Lake Series
D - Buckham Lake Group
E - Great Slave Lake Group
F - Harding Lake Series
G - Reid Lake Group
H - Upland Lake Series
I - Bighill Lake Group
J - Sparrow-Thompson-Hidden Lakes Group
K - Prosperous Lake Group
L - Petey Lake Series
M - Circle Lake Series
N - Short Point Lake Group
O - Lamoureux Lake Group
P - Blaisdell Lake Group
Q - Sproule Lake Series
R - Harald Lake Group
S - Upper Ross Lake Group
T - Detour Lake Series
U - Bug Group
V - Turnback Lake Group
W - Sleepy Dragon Lake Series

FIGURE 3: Geologic map of the Yellowknife - Hearne Lake map area. A) geologic map, B) index map for the geologic map, indicating individual plutons and pegmatite groups/series as indicated above. Geology modified after Henderson (1985)

metamorphic effects which were superimposed on earlier metamorphic assemblages, producing aureoles of cordierite, andalusite and sillimanite around the plutons. Several of the biotite-muscovite granite plutons contain pegmatitic phases, and are accompanied by pegmatite bodies which intrude the schists of the Yellowknife Supergroup within the contact aureole surrounding the pluton.

The pegmatite field is subdivided into four geographical areas for ease of discussion: southeastern, northeastern, northwestern and southwestern (Figure 4). These areas may be delineated by two imaginary lines: one originates at the western shore of Gordon Lake and extends southward to Hearne Channel, just west of Francois Bay; the second line extends westward from the south shore of Desperation Lake to the south shore of Harding Lake, onward to the mouth of Yellowknife Bay.

The areal distribution locally results in mineralogical and geochemical zoning of pegmatite bodies around their parent intrusion. Regional zonation of pegmatites around granites is suggested up to well-developed in different parts of the northeastern and northwestern parts of the field (e.g., Hutchinson, 1955a), but absent in the southeastern and southwestern regions.

The distribution of pegmatites within the immediate vicinity of granitic intrusions is controlled by many structural features including different types of fracture sets, bedding planes, foliation, schistosity and preexisting intrusive contacts (Kretz, 1968).

The pegmatites vary from narrow dikes to large, irregular shaped, homogeneous bodies lacking internal zonation, to complex dikes showing well-developed internal zonation, replacement units and extensive rare-element mineralization.

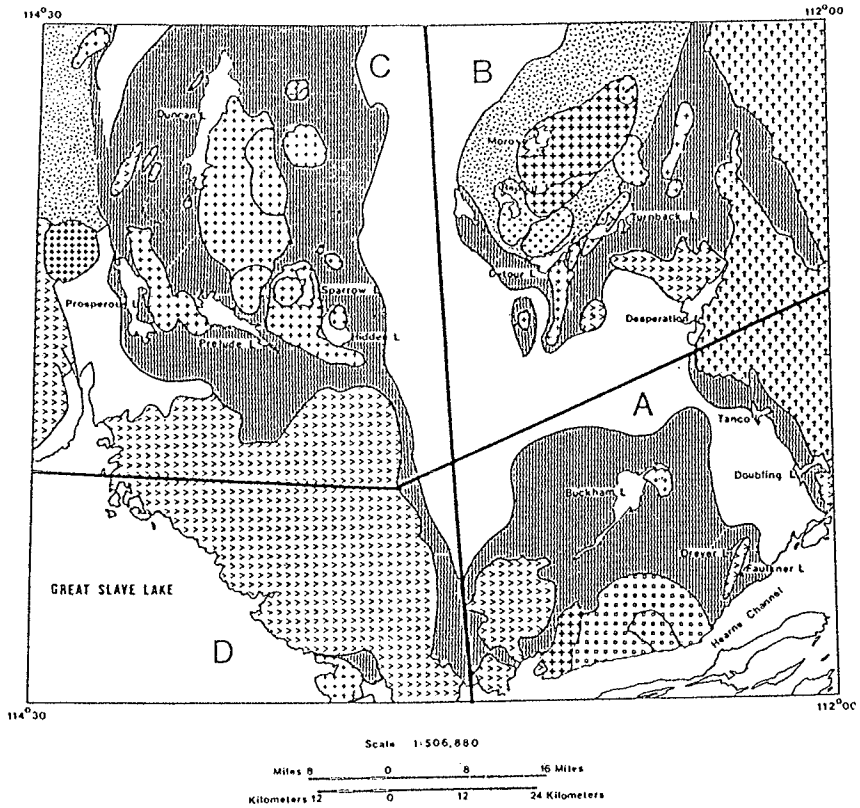

Figure 4: Geographical subdivision of the Yellowknife pegmatite field. Geographical areas for this study are designated by letters A-D. A) southeastern, B) northeastern, C) northwestern and D) southwestern.

Previous work

During World War II, limited access to foreign deposits and increased demand for tantalum led to intensive searches for domestic Ta deposits in the United States and Canada. This resulted in the exploration and subsequent discovery of Nb- and Ta-bearing pegmatites in the Yellowknife-Hearne Lake area. In addition, columbite-tantalite has been reported in other regions in the Northwest Territories (Lac de Gras, Aylmer Lake areas, Lord, 1951; Benjamin Lake area, Heywood and Davidson, 1969).

The first reported occurrence of Nb- and Ta-bearing minerals in the Yellowknife field was by Jolliffe (1944), who examined nearly 500 pegmatites and found 100 containing columbite-tantalite and 22 containing cassiterite. His report included compositional and physical data on samples from a selected number of pegmatite swarms. In an unpublished report, Jolliffe (1943) noted the occurrence of cassiterite and amblygonite in the Yellowknife field.

Between 1946 and 1948, three small mills operated on the properties of De Staffany Tantalum Beryllium Mines Limited, Peg Tantalum Lines Limited and the Freda No. 1 claim, during which time a total of less than 5 tons of tantalum concentrate was produced (Lord, 1951). Approximately 1,200 and 1,400 pounds of Ta concentrate were recovered from the Moose and Bet pegmatites, respectively by De Staffany Tantalum Beryllium Mines Limited. In addition, a small amount of Sn concentrate was produced at the Bet pegmatite by De Staffany Tantalum Beryllium Mines Limited. 500 pounds of concentrate was produced at the Freda pegmatite, whereas in less than 1 year, 3,750 pounds of concentrate was recovered from the Peg Tantalum claims (Lord, 1951). Between 1953 and 1954, Boreal Rare Metal recovered 39,100

pounds of concentrate from the Moose and Bet pegmatites (Department of Indian Affairs and Northern Development Mineral Claim sheet, 85-I-1).

Rowe (1952) described columbite-tantalite occurrences from selected pegmatites of the field. Hutchinson (1955b) noted an order-disorder relationship in tapiolites from the Peg swarm near Ross Lake, and examined the optical properties of columbites and tapiolites from the area, in addition to providing X-ray fluorescence analyses of some specimens. Descriptions of Nb, Ta and Sn minerals were made by Meintzer and Černý (1983) and Meintzer et al. (1984), whereas Wise et al. (1985a) provided detailed discussion on their geochemistry. The Tantalum Mining Company of Canada Limited (Tanco) staked claims in the area and collected several samples for assaying of the tantalum ore. At present, none of their data has been published.

CHAPTER 3

Experimental methods and procedures

Introduction

The chemical compositional data for this study were obtained by electron microprobe methods. X-ray powder and single-crystal diffraction methods were used to characterize order-disorder relationships of the minerals in their natural state, complemented by unit cell dimension refinement on heated specimens with increased order.

Sampling and Mineral Separation

Sampling

A total of 345 pegmatite bodies was examined for Nb, Ta and Sn minerals during the summer months of 1980-1983, with a two week follow-up period in the summer of 1985. Samples were collected *in situ* whenever possible, and from the rubble of previously blasted trenches and exploration pits. When present, samples were taken from all zones of pegmatites carrying Nb-Ta-Sn mineralization. In each pegmatite examined, sampling of Nb-, Ta- and Sn-oxide minerals was based primarily on color and was aimed at obtaining samples of various crystal morphologies and paragenetic associations. A total of 489 mineral samples was collected from the Yellowknife field. Descriptions of all samples collected and the extent of laboratory investigation done on each are given in Appendix A.

Separation

Samples were prepared for X-ray diffraction and electron microprobe studies by manually separating the mineral from its matrix under a binocular microscope. Samples selected for X-ray powder diffraction were hand-cleaned of any attached matrix material. Hand-cleaned samples were also mounted for preparation of polished sections. When mineral separation was found impossible due to extremely small grain size, rock slabs containing the sample were cut and made into 27 x 46 mm thin sections or 12 x 12 mm slabs, polished, and mounted for use in the electron microprobe.

X-ray diffraction methods

X-ray powder diffractometry

A total of 291 specimens selected on the basis of different crystal morphologies and paragenetic associations was prepared for X-ray powder diffraction study. Crystal fragments were crushed in a ceramic mortar and ground to a fine powder with a ceramic pestle. Acetone was added to the powder, which was then mixed to a slurry and mounted on a standard 27 x 46 mm microscope glass slide. The slide was then mounted on a Philips powder diffractometer (PW 1050) goniometer or on an automated Philips powder diffractometer system (PW 1710).[1] Operating conditions are listed in Table 3.

Samples were scanned once at 1° or 6° 2θ/minute for the purpose of qualitative mineral identification. Slower scans of 0.25° or 0.60° 2θ/minute were used in the refinement of the unit cell dimensions. Diffractograms collected on the PW 1050 goniometer were standardized with unann-

[1] Prior to the purchase of the automated PW 1710 system in 1982, all X-ray powder diffraction work was done on the PW 1050 instrument which accounted for only 15% of the total X-ray work performed.

Table 3: Operating conditions of X-ray powder diffraction study.

Model		PW 1050	PW 1710
Radiation		CuKα	CuKα
Filter/monochromator (PW 1710)		Ni	Graphite
Operating voltage		50 kV	40 kV
Operating current		20 ma	40 ma
Scanning speeds:	Identification	1° 2θ/min	3° 2θ/min
	Cell Refinement	0.25° 2θ/min	0.60° 2θ/min
Scanning range:	Columbite-tantalite	10° - 65°	10° - 65°
	Ixiolite	10° - 65°	10° - 65°
	Ferrotapiolite	10° - 96°	10° - 96°
	Cassiterite	10° - 96°	10° - 96°

ealed CaF_2 (a=5.4620 Å). Annealed CaF_2 (a=5.46379(4) Å) calibrated against a NBS silicon reference standard (batch 640a; a=5.430825 Å) was used as an internal standard in all slow scans collected on the PW 1710 system. Diffraction peak positions were measured manually at the half-width point at half-height (CuKα = 1.5418 Å) for the non-automated diffractometer. Peak positions and intensities were determined for the automated PW 1710 system using a computer hardware continuous scanning program (CSP) which searches for the tops of diffraction peaks. The gross peak positions were calculated to true $CuK\alpha_1$ positions ($CuK\alpha_1$= 1.54064 Å) and calibrated against the internal standard using the computer program FIX, which reduces systematic error in positional data to ± 0.01° 2θ (Ercit, 1986). The corrected 2θ angles were used for the unit cell refinement of 205 of the 291 samples examined using a modified version of the CELREF least-squares refinement computer program of Appleman and Evans (1973).

Single crystal X-ray diffractometry

A crystal of tapiolite ,0.1 - 0.2 mm in size, was selected for crystal structure analysis. The crystal was chosen because its powder diffraction pattern indicated a low degree of structural order. The crystal was mounted on a glass fiber, attached to a goniometer head and mounted on a Charles Supper Company precession camera to verify the degree of order. All precession photography used both unfiltered and Zr-filtered MoKα radiation at a crystal-to-film distance of 60 mm and precession angles of 10° and 25°. After precession photographs were taken, the goniometer head was mounted on a Nicolet R3m automated four-circle diffractometer. Intensity data were collected using graphite-monochromated MoKα radiation. Fifteen to twenty-five reflections were used to center the crystal. The setting angles of fifteen automatically aligned intense reflections were used in a least-squares refinement of the unit cell dimensions. Data collection was performed using the approach of Hawthorne (1985) as described below.

Intensity data were collected in the θ-2θ scan mode, using 96 steps with a scan range from [2θ(MoKα_1)-1]° to [2θ (MoKα_2)+1]° and a variable scan-rate between 4.0° and 29.3°/minute, depending on the intensity of an initial 1 s count at the center of the scan range. Backgrounds were measured for half the scan time at the beginning and end of each scan. Two standard reflections were monitored every 48 measurements to check for stability and constancy of crystal alignment. Reflections were measured over 1 asymmetric unit from 3° to 60° 2θ. Ten strong reflections were measured at 10° intervals of ψ (the azimuthal angle corresponding to rotation of the crystal about its diffraction vector) from 0° to 350°. These data were used to calculate an empirical ellipsoidal absorption-correction. The data

were also corrected for Lorentz, polarization and background effects, averaged and reduced to structure factors.

Scattering curves for neutral atoms, together with coefficients of anomalous dispersion were taken from Cromer and Mann (1968) and Cromer and Liberman (1970). The SHELXTL system of programs was used to carry out data reduction and refinement.

Heating Experiments

A total of 124 samples was chosen for heat-treatment of which 105 were used for unit cell refinement. Crystal fragments 2 to 5 mm in size were placed in silica boats lined with Ag-Pd foil and heated in a Fisher Isotemp muffle furnace (Model 186) in air at 1000° C/ 1 atm for 16 hours. Regulation of the furnace temperature was precise to ± 20°C. Care was taken to maintain an operating temperature of not more than 1050° C. At 1050° C, the Ag-Pd foil began to break down and reaction with the surface of the mineral occurred. X-ray diffractograms of samples heated to 1100° C contained additional reflections which corresponded to a mixture of an $AgTaO_3$-type and a $FeNbO_4$-type phase. Samples were cooled to room temperature and then X-rayed on the PW 1710 system. Refinement of the unit cell was obtained using the procedures described above for unheated samples.

Optical Examination

Polished mounts and thin sections containing small grains of Nb-, Ta- and Sn-oxide minerals were viewed under a reflecting microscope before being subjected to microanalysis. Samples were inspected for homogeneity, zoning, twinning and textural relationships among the different phases.

Nb-, Ta- and Sn-oxide mineral assemblages were initially identified by petrographic observation and later verified by microprobe analysis.

Electron Microprobe Analysis

Sample preparation

Crystal fragments were mounted in epoxy-filled Bakelite rings, with crystals displaying bladed or platy habits being mounted on end with their long axis normal to the surface of the mount. The surface of the mount was ground flat and polished successively with 600 grit, 3000 grit and 6 μm Pb polish. Thin sections were made from saccharoidal albite and fine-grained plagioclase-quartz pegmatite samples and polished as described above.

Microprobe analysis

Microprobe analyses were obtained using a Material Analysis Company, model MAC 5 electron microrprobe in the energy dispersive mode (ED). Operating conditions and standards used for microanalysis are given in Table 4. Energy dispersive spectra were collected with a KEVEX Micro-X 7000 ED spectrometer and reduced with KEVEX computer software utilizing the MAGIC V computer program of Colby (1980). Backscattered electron imagery was frequently used for examining textural features such as exsolution lamellae and inclusions, as well as for making routine checks for chemical inhomogeneity and compositional zoning. A minimum of two points of analysis (rim and core) were collected for each crystal. In most cases, however, 3 to 6 points of analysis were collected across the mineral grain.

Although the KEVEX software was equipped with a deconvolution routine for solving spectra peak overlap, it was found ineffective for most analysis of Nb,Ta,Sn-oxide minerals. Therefore, a semi-automated technique for solving peak overlap was devised by Dr. T.S. Ercit (pers. comm., 1982). The technique involves the use of the University of Manitoba microprobe lab's library spectra of individual elements which were stripped to make overlap-free standard spectra (Ercit, 1986).

Formula Calculation.

Electron microprobe analyses of columbite-tantalite, tapiolite, ixiolite and cassiterite occasionally showed cations sum in excess of structurally available sites when all the iron was calculated as Fe^{2+}. Recalculation of the unit-cell contents was adjusted by converting an adequate part of Fe^{2+} to Fe^{3+} to eliminate the cation surplus. Ferric iron for columbite-tantalite, tapiolite and cassiterite was calculated by normalizing on 24, 12 and 4 anions, respectively. Ixiolite unit-cell contents were calculated according to the crystallochemical assumptions applied to wodginite (Černý et al., 1985b; Ercit, 1986).

Table 4: Operating conditions and standards used for the MAC 5 electron microprobe.

Operating conditions	
Accelerating voltage	15 kV
Specimen current*	5 nA, 10 nA
Beam diameter	1-2 μm
Collection time	200 seconds
Filament current	2.6 amps
Standards	**X-ray spectral lines**
Chromite, fayalite	Fe$K\alpha$
$CaNb_2O_6$, $Ba_2NaNb_5O_{15}$	Nb$L\alpha$
Manganotantalite	Mn$K\alpha$, Ta$M\alpha$
Cassiterite	Sn$L\alpha$
Rutile, ilmenite	Ti$K\alpha$
Microlite	Na$K\alpha$
Uraninite	U$M\alpha$
PbTe	Pb$M\alpha$
$CaNb_2O_6$, microlite	Ca$K\alpha$
Scandium metal	Sc$K\alpha$

$CaNb_2O_6$ (Institut de Chemie Université de Fribourg, Suisse), ilmenite (Ilmen Mts.), microlite (Harding Mine), fayalite (Union Carbide Corp.), rutile, uraninite (University of Manitoba). All other standards obtained from Charles M. Taylor Co.

*Specimen current of 5 nA was measured on ZnS, whereas current at 10 nA was measured on fayalite.

CHAPTER 4

The Yellowknife pegmatite field

The Yellowknife pegmatite field is populated by pegmatites of the orogenic rare-element class and includes barren, beryl, complex and albite-spodumene types (Table 5). Within each area which constitutes the Yellowknife pegmatite field, pegmatites can be separated into spatially, mineralogically and geochemically related groups, henceforth referred to as pegmatite series or groups.[2] At present, the grouping of pegmatite bodies into series is based primarily on geographical distribution, and paragenetic or geochemical relationships with no intended genetic connotation. Final series or group designation will be made when the concurrent mineralogical and geochemical investigations of geographically related pegmatite bodies and granitoid plutons are concluded (Meintzer, 1987). Names of pegmatites and swarms are based on historical usage where established or on terms assigned by R.E. Meintzer and the author. A list of the pegmatite series/groups recognized at present is given in Table 6 and relative mineral abundances for each series/group is given in Table 7. Locations of pegmatite series/groups are shown in Figures 5 to 20.

Throughout this chapter, reference will be made to various assemblages constituting primary zones and replacement units. Usage of the term assemblage will be as defined by Černý et al. (1981), "the mineral composition of a given zone, replacement body or fracture filling". The assemblages

[2] The term "series" is used here as defined by Černý et al. (1981) and denotes a population of spatially close pegmatites whose assignment to a specific parent intrusion is unknown or undetermined. The term "group" is similar in definition, except that the parent intrusion is known.

refer only to the mineral content and do not imply specific textural relationships, unless specifically stated.

It is necessary at this time to comment on the metasomatic assemblages observed in the Yellowknife field. Our present understanding of the temporal relationships between metasomatic assemblages and the primary zone is obscure. Clearly, assemblages of lithium muscovite + quartz or albite + muscovite replacing feldspathic units are of secondary origin. However, large cleavelanditic albite and saccharoidal albite units may or may not represent primary crystallizing bodies, although Thomas and Spooner (1984) suggest that saccharoidal albite is largely primary in origin, formed as a result of continuous decreasing crystallization temperature of a localized supercritical fluid occurring contemporaneously with the residual melt. Furthermore, London (1986) documented the origin of saccharoidal albite units in a complex pegmatite from a residual, dense borosilicate medium reacting with pre-existing units but depositing the bulk of albite as a primary precipitate. However, London concedes that this origin does not necessarily apply to all albitic units in all pegmatite types. In the Yellowknife field, the albite-rich units show distinct reactions with the neighboring K-feldspar-bearing assemblages, but large-scale replacement of pre-existing lithologies is not evident; textural evidence of such a process may not be traceable at all. Consequently, the traditional classification of saccharoidal albite and cleavelandite units as metasomatic assemblages is applied here.

Of the 23 pegmatite series/groups studied, only 13 showed evidence of Nb-Ta-Sn mineralization. The following sections describing the pegmatite series/groups are restricted to those showing Nb-Ta-Sn mineralization. The

Table 5: Classification of rare-element pegmatites of orogenic affiliation. After Černý, in press.

Pegmatite type [feldspar + mica type]	Pegmatite subtype, geochemical signature	Typical minerals	Economic potential	Zoning	Replacement	Examples
RARE-EARTH [Kf>plg to ab; bi≥msc]	allanite-monazite REE (P,U,Th)	allanite monazite	(REE)	incipient to advanced	incipient to moderate	Upper Tura River, Ural Mts. West Portland, Quebec Kobe, Japan
	gadolinite Be,Y,REE,Nb≥Ta F(U,Th)	gadolinite fergusonite euxenite (topaz) (beryl)	Y,REE (Be,Nb-Ta)			Shatford Lake group, Manitoba Ytterby, Sweden* Evje-Iveland field, Norway Barringer Hill, Texas Pyörönmaa, Finland
BERYL [Kf>ab; msc>bi]	beryl-columbite Be,Nb≥Ta (Sn)	beryl columbite-tantalite	Be (Nb-Ta)	incipient to advanced	incipient to advanced	Meyers Ranch, Colorado Greer Lake group, Manitoba Donkerhoek, Namibia Ural Mts., USSR
	beryl-columbite-phosphate Be,Nb≥Ta,P (Sn,Li,F)	beryl, columbite-tantalite triplite triphylite				Hagendorf-Süd, Germany* Dan Patch, South Dakota Connecticut localities Crystal Mt. field, Colorado
COMPLEX [Kf≥ab; msc≥lep]	(high-P) spodumene Li,Rb,Cs,Be,Ta≥Nb (Sn,P,F)	spodumene beryl tantalite (amblygonite) (lepidolite) (pollucite)	Li,Rb, Cs,Be Ta, (Sn,Ga,Hf)	advanced, complex, partly obscured by meta-somatic units	advanced, complex, extensive	Harding, New Mexico Hugo, South Dakota* Mongolian Altai #3 Etta, South Dakota White Picacho district, Arizona Manono, Zaire
	(low-P) petalite Li,Rb,Cs,Be,Ta>Nb (Sn,P,F)	petalite beryl tantalite (amblygonite) (lepidolite) (pollucite)				Tanco, Manitoba* Bikita, Zimbabwe Varuträsk, Sweden Luolamäki, Finland Londonderry, Australia Hirvikallio, Finland
	lepidolite F,Li,Rb,Cs,Be Ta>Nb (Sn,P)	lepidolite topaz beryl microlite (pollucite)	Li,Rb, Cs,Ta, Be (Sn,Ga)			Brown Derby, Colorado* Pidlite, New Mexico Himalaya district, California Khukh-Del-Ula, Mongolia Wodgina, Australia
	amblygonite P,F,Li,Rb,Cs Be,Ta>Nb (Sn)	amblygonite beryl tantalite (lepidolite) (pollucite)	Li,Rb Cs,Ta Be (Sn,Ga)			Viitaniemi, Finland Peerless, South Dakota
ALBITE-SPODUMENE [ab>Kf; ((msc))]	Li (Sn,Be,Ta≥Nb)	spodumene (cassiterite) (beryl) (tantalite)	Li,Sn (Be,Ta)	rudimentary; near-homogeneous	incipient to moderate	Kings Mountain, North Carolina* Preissac-Lacorne, Quebec Peg Claims, Maine Volta Grande, Brazil
ALBITE [ab>>Kf; (msc,lep)]	Ta≥Nb,Be,Sn (Li)	tantalite beryl (cassiterite)	Ta (Sn)	advanced	moderate	Hengshan, China USSR

Boron may be negligible to highly enriched in the beryl to spodumene types, and is low in the rare-earth type.

* - see text for detailed description

Table 6: List of pegmatite series/groups of the Yellowknife field.

SOUTHEASTERN AREA

- Eastern Section
  - Doubling Lake Series
    - Usk pegmatite
    - Was pegmatite
  - Tanco Lake Group
    - Jo swarm
    - Stringbean pegmatite
    - Thor-Echo swarm
      - Peewee pegmatite
      - Snake pegmatite
      - West pegmatite
      - Tanco pegmatite
      - Central pegmatites
      - Eastern pegmatites
    - Archide swarm
      - Peanut
      - Archide pegmatite
      - Manoko pegmatite
      - Erdnuss pegmatite
- Western Section
  - Faulkner Lake Series
    - Big Hill pegmatite
    - Bet pegmatite
    - Moose pegmatites
    - Tan swarm
  - Buckham Lake Series
    - Bin pegmatite
    - Hid pegmatite
    - Lens pegmatite
    - Lit swarm
    - Mac pegmatite
    - Mut pegmatite

SOUTHWESTERN AREA

- Great Slave Lake Group
  - Slave swarm
  - Drybones pegmatite

NORTHWESTERN AREA

- Eastern Section
  - Lamoureux Lake Series
    - Fle pegmatite
  - Blaisdell Lake Group
    - Bill swarm
    - Melody swarm
    - Vo swarm
  - Sproule Lake Series
    - Cata swarm
    - Fly swarm
  - Harald Lake Series
    - Harald swarm
    - Moon swarm
  - Sparrow-Thompson-Hidden Lake Group
    - Casper swarm
    - Heidi swarm
    - Ekid swarm
    - Fi swarm
    - Freda swarm
    - Frog pegmatite
    - Greg swarm
    - Jolly pegmatite
    - Ki swarm
      - Ki pegmatite
      - Tom pegmatite
    - Lu swarm
    - Murky pegmatite
    - Qi swarm
    - Tadpole pegmatite
    - Tanya swarm
    - Waco swarm
- Southern Section
  - Harding Lake Series
    - Jake-Da swarm
    - Paint swarm
    - Sky pegmatite
  - Reid Lake Series
    - Ann & Boa swarm
    - Pancho Villa swarm
  - Upland Lake Series
    - Jenne swarm
    - Panono Pete swarm
  - Highill Lake Group
    - Anne Marie swarm
    - Big swarm
    - Bubo swarm
    - Fern swarm
    - Limo swarm
    - Mirt swarm
    - Nite swarm
    - Odin swarm
  - Prosperous Lake Group
    - Minipud swarm
  - Short Point Lake Series
    - Murphy swarm
  - Petey Lake Series
    - Alexie Lake East swarm
      - Cujo pegmatite
      - Fozzie pegmatite
      - Jumbo pegmatite
      - Miss Peggy pegmatite
      - Runt pegmatite
      - Spud pegmatite
      - Tiny Teddy pegmatite
      - Tittles pegmatite
      - Yassar pegmatite
    - Alexie Lake West swarm
      - Alex pegmatite
      - Gnat pegmatite
      - Hawk pegmatite
      - Magic pegmatite
      - Rainy Day pegmatite
      - Wetfoot pegmatite
    - Dike swarm
      - Lily pegmatite
      - Rose pegmatite
    - Geo swarm
      - Ace pegmatite
      - Hex pegmatite
      - Iva pegmatite
      - Seedy pegmatite
    - Lil' Rascals swarm
      - Alfalfa pegmatite
      - Barbalbo pegmatite
      - Buckwheat pegmatite
      - Chubby pegmatite
      - Darla pegmatite
      - Petey pegmatite
      - Porky pegmatite
      - Spanky pegmatite
      - Stymie pegmatite
      - Wheezer pegmatite
    - River swarm
      - Boffo pegmatite
      - Slash pegmatite
      - Splash pegmatite
      - Sweaty pegmatite
      - Whiskey pegmatite
  - Circle Lake Series
    - Dr. Bob pegmatite
    - Riber pegmatite

NORTHEASTERN AREA

- Bug Group
  - Ant
  - Beetle
  - Skeeter swarm
- Detour Lake Series
  - Demon swarm
  - Ptarmigan swarm
- Peg Group
- Sleepy Dragon Lake Series
- Turnback Lake Group
  - Eaglet swarm
  - Eyrie pegmatite
  - Talon pegmatite

Table 7: Relative mineral abundances for pegmatite series/groups of the Yellowknife pegmatite field.

PEGMATITE SERIES/GROUPS

MINERAL	FAULKNER	BUCKHAM	DOUBLING	TANCO	GREAT SLAVE	BUG	PEG	DETOUR	SLEEPY DRAGON	TURNBACK	LAMOUREUX	BLAISDELL	SPROULE	HARALD	SPARROW*	HARDING	REID	UPLAND	BIGHILL	PROSPEROUS	SHORT POINT	PETEY	CIRCLE
Microcline	A	A	A	A	A	A	A	A	A	A	A	A	A	A	A	A	A	A	A	A	A	A	A
Albite (± oligoclase)	A	A	A	A	A	A	A	A	A	A	A	A	A	A	A	A	A	A	A	A	A	A	A
Quartz	A	A	A	A	A	A	A	A	A	A	A	A	A	A	A	A	A	A	A	A	A	A	A
Biotite	R				R	R	L	R		R	R	R							R		R	R	
Muscovite	S	S	S	L	S	L	S	S	L	L	S	S	L	L	S	L	S	L	S	S	S	S	S
Lithian muscovite																							L
Lepidolite																			†				L
Spodumene	S	A	S	L			R					R	L	R	L	S	S	L	L				
Petalite	†																						
Cordierite																							
Garnet:												R	R	R									
Almandine						R	R	R		R					R				R		R	R	
Spessartine							R																
Tourmaline:	†																						
Schorl					R		R	R			R	R	R		R				R	R	R	R	L
Elbaite																			?				R
Beryl	R	R	R	R		R	L		R		R	R	R	R	R	R	R	R	R	R		R	L
Zircon	R	R																					
Hematite																							
Ilmenite																							
Magnetite																							
Gahnite							R				?	?			?			?				R	
Uraninite		?	?		?		?															?	
Cassiterite					R							R	R		R	†		R					
Columbite-tantalite:														R									
Ferrocolumbite	R	R	R	R			R					R	r		R	r	R	R	R				r
Ferrotantalite	r	r	r	r			r					r	R		r	r	r		r				r
Manganocolumbite		r	r	r			r					r	R		r	R			r				r
Manganotantalite	r						r					r	r						r				R
Ferrotapiolite	R	R	r	R			R					R	R		R	R	R		R				R
Ixiolite		R										R							R				
Microlite							R					R	R		R				R				R
Wodginite																							
Apatite	R	R	R	R		R	R					R	R	R	R	R	R		R		R	R	R
Amblygonite-montebrasite	R	R	R	R								R	R		R	†	R					R	R
Graftonite-beusite							R																
Triphylite-lithiophilite	R	R	R	R			R					R	R		R	R	R		R				
Ferrisicklerite-sicklerite	R	R	R	R			R					R	R		R	R	R		R				
Heterosite-purpurite	R																R						
Alluaudite-Ferroalluaudite											?	R				R							
Lazulite-scorzalite	†																				R		
Arsenopyrite							R					R	R	R	R		R		R				
Bornite							R																
Chalcopyrite												R							R				
Loellingite																			R				
Molybdenite							R								R				R				
Pyrite		R					R					R			R		R		R			R	
Sphalerite		R		R			R					R				R			R			R	

Sparrow* = Sparrow-Thompson-Hidden Series
A=abundant S=subordinate
L=low R,r=rare (r=lesser species of group)
†=reported ?=tentatively identified

descriptions are supplemented by the compositional data of Meintzer (1987) for K-feldspar, platy muscovite and beryl. The primary means of analysis for K-feldspar, muscovite and beryl was by atomic absorption spectroscopy or direct current-plasma emission spectroscopy as described by Meintzer (1987). For complete detailed descriptions of all examined pegmatite series and groups the reader is referred to Meintzer (1987).

Southeastern area

Faulkner Lake Series

This series is comprised of the Bet, Big Hill, Moose bodies and the Tan swarm, and surrounds the Faulkner tonalite intrusion (Figure 5). The McDuff granite sill is situated between the Bet body and Tan swarm. The pegmatites occur as concordant to slightly discordant dikes and sills hosted by quartz-biotite schist. All of the pegmatites strike generally N to NE with the exception of Tan #3 dike, which strikes NW and dips to the NE. Dips are generally steep and towards the W. The pegmatites show variable degrees of internal zonation ranging from patchy (Big Hill) to well-developed (Bet, Moose). Spodumene, montebrasite, beryl, and triphylite are among the rare-element minerals present. Nb-Ta-Sn mineralization is fairly extensive throughout the series.

As a group, pegmatites of the Faulkner Lake series rank as some of the most fractionated pegmatites in the entire Yellowknife field. A wide range of rare-alkali accumulation is evident in blocky K-feldspar and muscovite from the area (Table 8). The average geochemical indicators are typical of advanced fractionation, although they do not attain the degree of fraction-

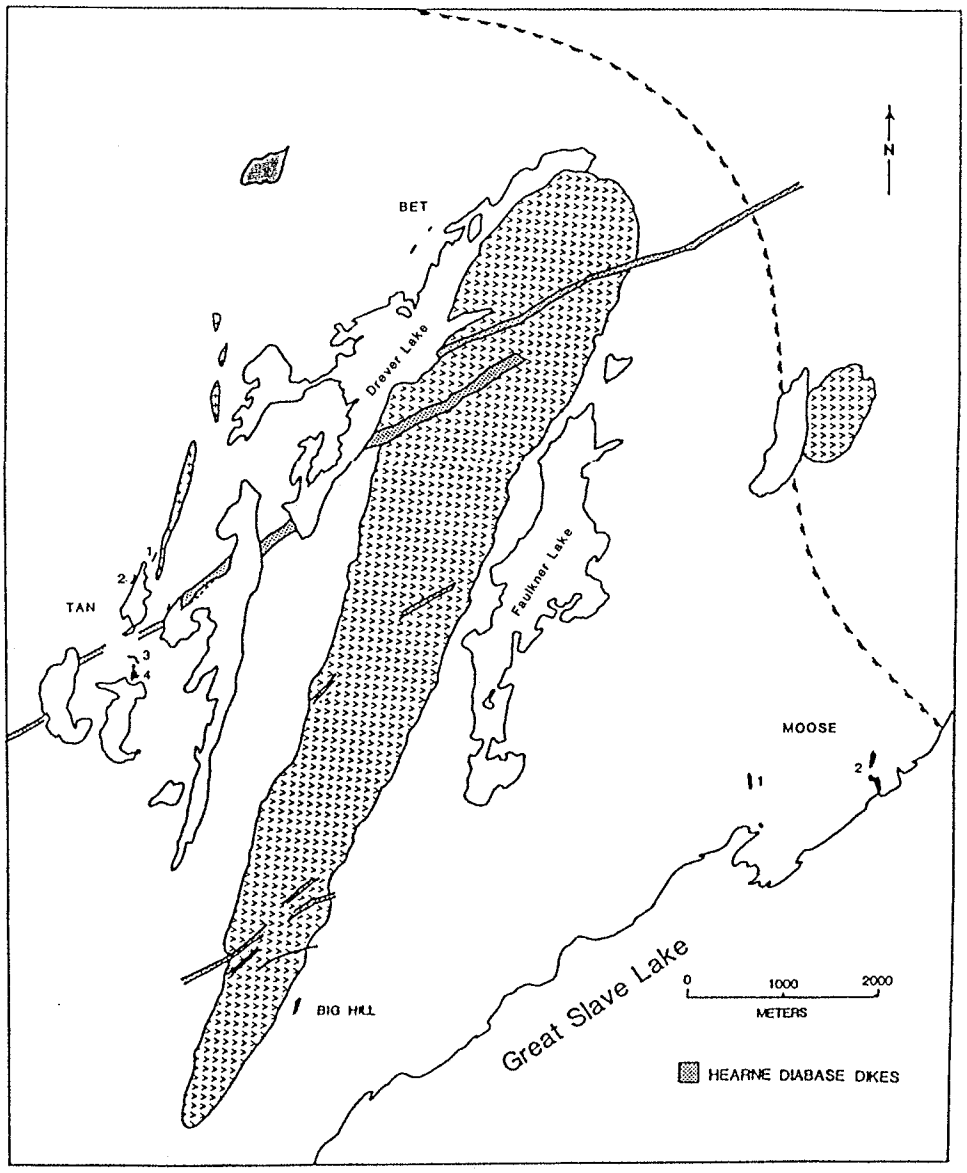

Figure 5: Location map of the Faulkner Lake pegmatite series. Symbols as shown in Figure 3.

ation typical of extremely fractionated, pollucite-bearing pegmatites such as the Tanco deposit at Bernic Lake, Manitoba (Černý, 1982b).

Table 8: Compositional characteristics of K-feldspar, muscovite and beryl for the Faulkner Lake pegmatite series.

		K/Rb	Rb	Cs	Ba	Sr	Pb		
Blocky K-feldspar	$\bar{x}$	13.8	8750	237	25	53	32		
	s	7.3	3180	436	21	18	23		
	range	6.92-35.1	2720-15700	46-1680	<1-58	28-74	8-74		
	n	13	13	13	6	6	6		
		Li_2O	K/Rb	Rb	Cs	Be	Nb	Ta	Nb/Ta
Platy muscovite	$\bar{x}$	0.032	15.9	5560	127	19	92	124	0.763
	s	0.011	7.1	2430	88	4	48	41	0.404
	range	0.018-0.052	7.1-322	2380-10200	40-310	11-25	40-170	78-207	0.377-1.44
	n	14	14	14	14	14	8	8	8
		Li	Na_2O	Na/Li	Cs				
Beryl	$\bar{x}$	1930	1.37	6.12	1400				
	s	790	0.09	2.86	430				
	range	882-3090	1.25-1.48	3.55-11.0	968-2030				
	n	5	5	5	5				

Elements - ppm, oxides - wt.%. Symbols: $\bar{x}$ = arithmetic mean, s = standard deviation, n = number of samples analyzed.

Big Hill pegmatite.

The Big Hill pegmatite consists of two subparallel bodies situated approximately 1.6 km N of the Hearne Channel and 4 km SE of the Tan swarm. The pegmatite is exposed in the two limbs of an anticline. The larger limb dips from 65° NW at the northern end, nearly vertical in the middle and 55°

SW at the southern end. The strike is generally N 30° E along the anticlinal axis. The main body is approximately 137 m long with patchy to poor internal zonation, whereas the smaller body is 35 m long and 1 m wide. In addition to Nb-Ta mineralization, other rare-element minerals include spodumene, montebrasite and minor beryl. Metasomatic assemblages include granular albite and secondary muscovite replacing K-feldspar and spodumene.

Historically, sampling of the pegmatite for Ta mineralization has been minimal. Lord (1951) reports the collection of a 20 kg pegmatite sample which contained 0.129% $(Ta,Nb)_2O_5$ and 0.12% SnO_2. Recent assaying of chip samples by Thomas (1980) showed Ta_2O_5 and SnO_2 contents ranging from 0.02-0.07%. Niobium contents were generally 0.01% Nb_2O_5 or less. Based on these results, Thomas reports the possible occurrence of wodginite along with tantalite and cassiterite. The present author has found no indication of wodginite in any of the collected material, and a large majority of the samples collected contained only cassiterite and ferrotapiolite. Crystals of ferrotapiolite and cassiterite, up to 2 cm but more typically near 0.5 cm, occur as platy and anhedral grains associated with cleavelandite + quartz ± spodumene. In most samples collected, the ferrotapiolite and cassiterite are intimately intergrown.

Tan swarm.

The Tan swarm consists of four separate bodies located E of Blatchford Lake. The bodies extend along strike with the McDuff granite sill to the NE, and dip steeply to the NE (75° - 90°). Saccharoidal albite, cleavelandite and secondary muscovite are common and host the majority of Nb and Ta minerals. The quartz + cleavelandite + muscovite assemblage also contains Nb and Ta minerals. A 10 kg sample from Tan #3 yielded 32.6 g of Ta concentrate that assayed 66.70% $(Ta,Nb)_2O_5$, 15.96% SnO_2 and 0.20% TiO_2.

Assays of chip samples showed Ta concentrates ranging from 0.006 - 0.107% Ta_2O_5 (Thomas, 1982). Jolliffe (1944) reports the sparse and irregular distribution of tabular columbite-tantalite crystals up to 2.5 cm long and equidimensional aggregates of cassiterite up to 0.64 cm across. Nb-Ta-Sn mineralization was found in the following assemblages: medium-grained quartz + cleavelandite + spodumene, medium-grained quartz + cleavelandite + muscovite and medium- to coarse-grained K-feldspar + spodumene + quartz + cleavelandite. Although Jolliffe reports the occurrence of abundant columbite-tantalite, the present author notes that ferrotapiolite is the dominant Nb, Ta mineral present. It occurs as short prismatic crystals or anhedral grains disseminated in muscovite replacing K-feldspar or as platy crystals in cleavelandite. Cassiterite, ferro- or manganotantalite are found as intergrowths in ferrotapiolite.

Bet pegmatite.

The Bet pegmatite lies 0.16 km W of Drever Lake and approximately 8 km N of Hearne Channel, near the NW margin of the Faulkner tonalite. The pegmatite is concordant in nodular quartz-biotite schist, strikes N 10° E and dips steeply to the W. The body is 100 m long and 9 m wide, and is moderately zoned with spodumene and montebrasite reaching 2 and 1 m in size, respectively. Beryl and Nb and Ta minerals are closely associated with metasomatic albitization. In 1947, the De Staffany Tantalum Beryllium Mines Ltd. treated about 1700 kg of ore from the Bet pegmatite. In 1948, almost 640 kg of concentrate of unspecified grade was recovered. A sample of concentrate analyzed by the Bureau of Mines, Ottawa gave the following results; 57.76% Ta_2O_5, 7.9% Nb_2O_5, 13.4% SnO_2 and 0.22% TiO_2 (Lord, 1951). Nb and Ta minerals were noted in the upper and central parts of the sill

(Lord, 1951); however, low Ta assay values of samples from the wall zone support the visual observation of low Ta mineralization in that zone (LeCouteur, 1980a). Fortier (1946) found large columbite-tantalite crystals 10.2 x 1.5 cm in size and a cassiterite 2.5 cm long. In addition, Fortier also noted 25.4 x 0.13 cm thin plates of ferrocolumbite. Ferrocolumbite and rare ferrotantalite occur as platy or blocky crystals in cleavelandite. Rare inclusions of ferrotapiolite or cassiterite occur in ferrotantalite.

Moose pegmatites.

The Moose pegmatites are two bodies emplaced along a fracture system and are found within 500 m of the shore along Hearne Channel. Only the Moose #2 body was visited during this study. The pegmatite strikes N for about 425 m with dips varying from moderate (30° - 55° W) in the southern section to steep (85° W) in the central and northern sections. Like the Bet pegmatite, the Moose #2 body is irregularly but well-zoned and contains abundant, large spodumene and montebrasite crystals. Patches of saccharoidal albite and secondary muscovite are scattered throughout the pegmatite.

Over the past 40 years, the Moose pegmatite has been the subject of several assessment programs for Ta and/or Li. Various samples collected by the Geological Survey of Canada were taken for concentration tests. The results indicated a predominantly Nb-rich concentrate with Ta_2O_5 contents ranging from 20 to 40% (Lord, 1951). Analysis of concentrations by Groves (1978, 1981) showed trace amounts of W, Hf and U. Detailed mapping of the pegmatite provided information on the zonal distribution of Nb and Ta minerals occurring in the body (Jolliffe, 1943; Rowe, 1952; Mosher, 1969). The following zones have been shown to host Nb-Ta mineralization:

1. border zone: fine-grained quartz-plagioclase-muscovite

2. wall zone: fine- to medium-grained cleavelandite-quartz-muscovite
3. first intermediate zone: plagioclase-cleavelandite-quartz
4. second intermediate zone: blocky perthite-quartz-spodumene-muscovite.

Nb-Ta mineralization is characterized by ferrocolumbite and rare cassiterite. Ferrocolumbite occurs as thin radiating plates up to 9 cm across (Jolliffe, 1944). Tabular or blocky crystals in cleavelandite ± lithian muscovite ± quartz occur with the greatest frequency.

Buckham Lake Group

Northwest of Buckham Lake, 4-13 km from the Buckham granite, lie the Lit swarm and the Hid and Mac pegmatites. A second group of pegmatites consisting of the Bin, Lens and Mut pegmatites, lie to the SE of Buckham Lake approximately 8 km SW of the Buckham granite (Figure 6). Zonation is poor (e.g.; Hid) to well-developed (Mac) in pegmatites of this series. Albitization is generally extensive and the mineralogy is quite diverse. Spodumene is uniformly distributed in all pegmatites whereas saccharoidal albite is present in all, but in variable quantities. Spodumene, 3 m long, and microcline crystals 1 m long are common in the Mac pegmatite. With respect to Nb-Ta mineralization, this series contains one of the most diverse pegmatites in the field - the Mac pegmatite. Rare-alkali accumulation in K-feldspar and muscovite indicate an advanced degree of fractionation comparable to, but less than that found in the Faulkner Lake series (Table 9). It is interesting to note that the geochemical indicators of the southern group show significantly lower degrees of fractionation than the pegmatites north of Buckham Lake, which are spatially closer to the Buckham granite.

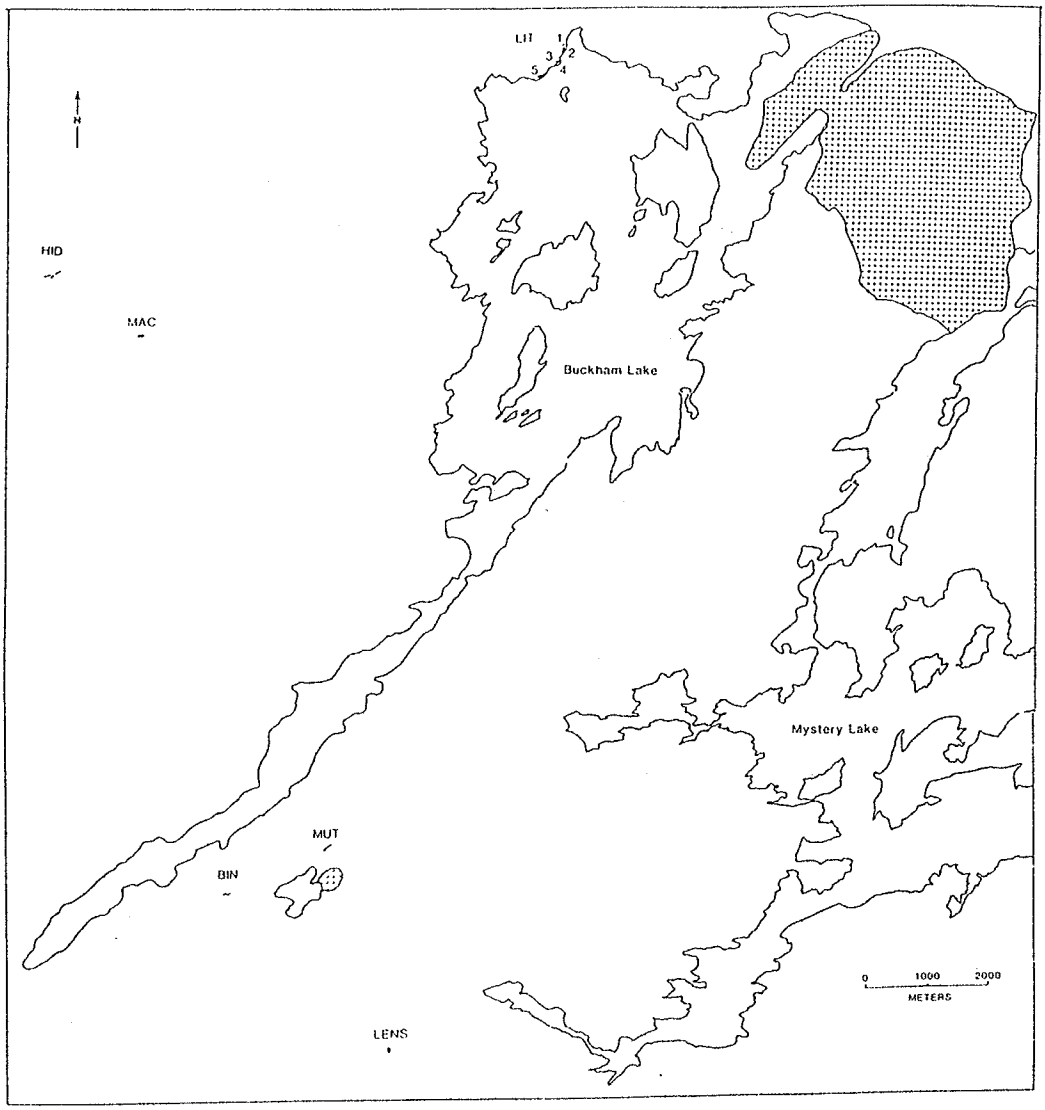

Figure 6: Location map of the Buckham Lake pegmatite group. Symbols as shown in Figure 3.

Table 9: Compositional characteristics of K-feldspar, muscovite and beryl for the Buckham Lake pegmatite group.

		K/Rb	Rb	Cs	Ba	Sr	Pb
Blocky K-feldspar	$\bar{x}$	24.9	5650	170	51	74	47
	s	11.5	3440	247	12	20	29
	range	6.63-57.6	1650-16400	11-840	38-61	52-92	20-78
	n	20	20	20	3	3	3

		Li_2O	K/Rb	Rb	Cs	Be	Nb	Ta	Nb/Ta
Platy muscovite	$\bar{x}$	0.078	15.5	5350	89	90	nd	nd	nd
	s	0.035	6.8	2170	61	200	nd	nd	nd
	range	0.039-0.150	7.5-27.2	2650-8830	33-230	20-623	nd	nd	nd
	n	9	9	9	9	9	0	0	0

		Li	Na_2O	Na/Li	Cs
Beryl	$\bar{x}$	1950	1.52	6.22	2110
	s	540	0.13	1.87	1400
	range	1270-2840	1.35-1.80	3.80-9.16	310-5130
	n	12	12	12	12

Elements - ppm, oxides - wt.%. Symbols: $\bar{x}$ = arithmetic mean, s = standard deviation, n = number of samples analyzed, nd = not determined.

Mac pegmatite.

The Mac pegmatite trends N 80° W with an average dip of 60° SW. It is a lens-shaped body 120 m long and on the average 8 m wide. Zoning is well-developed over the length of the body and includes a discontinuous quartz + muscovite core. Widespread metasomatism is conspicuous in the central parts of the pegmatite. Rare-element mineralization includes abundant spodumene, beryl, montebrasite and Nb and Ta minerals.

The Mac pegmatite contains several species of Nb- and Ta-bearing minerals which occur in medium-grained quartz + cleavelandite + spodumene + muscovite and medium-grained K-feldspar + quartz + spodumene + muscovite + montebrasite intermediate zones. Platy to tabular ferrocolumbite-ferrotantalite dominate over other Nb and Ta minerals present. Ferrotapiolite and cassiterite are rare and occur as inclusions in ferrotantalite or ixiolite. Crystals of columbite-tantalite measuring up to 5.7 x 3.2 x 2.5 cm were noted in the spodumene rich zone by Jolliffe (1944). Mn- and Fe-rich ixiolites are common and occur as massive anhedral grains up to 5 cm in diameter.

Lit swarm.

The Lit swarm consists of five bodies trending NE along the northern shore of Buckham Lake. Only the Lit #2, Lit #4 and Lit #5 bodies were examined in this study. Zoning in Lit #2 and Lit #4 is generally poor, consisting essentially of a quartz + cleavelandite + muscovite wall zone and a K-feldspar + spodumene + cleavelandite + quartz + muscovite core. Most of the zoning has been obscured by metasomatic albitization. In contrast, the Lit #5 dike displays better zoning, including a quartz core but containing less K-feldspar and montebrasite in the intermediate zone. Nb-Ta mineralization was found only in the intermediate zone or central parts of the pegmatite. Platy (up to 0.6 cm long) and blocky (up to 3.8 x 1.3 x 0.3 cm) crystals of ferrocolumbite are associated with cleavelandite + quartz ± muscovite.

Hid pegmatite.

The Hid pegmatite strikes N 80° E and dips steeply to the N. It has a total outcrop length of 280 m which averages 4 m wide. The body is poorly

zoned and spodumene-rich with minor Nb-Ta mineralization. Small platy crystals of columbite-tantalite occur in the plagioclase + quartz + muscovite assemblage.

Bin pegmatite.

The Bin pegmatite lies 0.8 km E of the SW arm of Buckham Lake. The pegmatite is crudely lens-shaped, striking N 80° E. It is 122 m long and averages 12 m wide. Abundant spodumene and subordinate montebrasite are conspicuous in the intermediate zones, whereas beryl occurs in only trace amounts. Nb-Ta mineralization consists of platy columbite-tantalite and anhedral grains of ferrotapiolite and cassiterite. Nb, Ta and Sn minerals occur in the quartz + plagioclase + muscovite + spodumene outer intermediate zone.

Lens pegmatite.

The Lens pegmatite outcrops approximately 3.6 km NNW of the western part of Blatchford Lake and 3.5 km SE of Bin. The lenticular body strikes N 15° W, dips vertically, is 91 m long and up to 18 m wide. Zoning is virtually nonexistent. With the exception of spodumene, rare-element mineralization is extremely poor. No montebrasite was found although small amounts of apatite and triphylite do occur. Nb-Ta mineralization occurs as rare crystals of columbite-tantalite and ferrotapiolite within a segregated quartz + spodumene + K-feldspar intermediate unit at the northernmost end of the dike.

Mut pegmatite.

The Mut pegmatite is a sill-like body located 1 km SE of Buckham Lake and 1.6 km ENE of the Bin pegmatite. The Mut dike strikes N 50° E with near vertical dips. The pegmatite is 91 m long, 4.5 m wide and is poorly zoned. Rare-element mineralization includes abundant spodumene, rare beryl

and triphylite and minor columbite-tantalite which is found in the quartz + K-feldspar + spodumene + plagioclase + muscovite assemblage.

Tanco Lake Group

The Tanco Lake group is located within 1 km of the northern and eastern shores of Tanco Lake and within 300-2500 m of the western margin of the Eastern granite (Figure 7). It consists of the Stringbean pegmatite, the Jo, Arachide and Thor-Echo swarms. Blocky K-feldspar and muscovite show relatively modest accumulations of rare-alkalis (Table 10).

Jo swarm.

The pegmatites of the Jo swarm trend northeasterly for abount 70 to 250 m. The dikes vary in texture and zonation from fine-grained homogeneous quartz + albite + muscovite ± K-feldspar ± beryl to medium- to coarse-grained blocky K-feldspar + spodumene + muscovite. Beryl and platy ferrocolumbite are concentrated along the margins of quartz.

Thor-Echo swarm.

The Thor-Echo swarm consists of numerous SE trending dikes which crop out over an area 2 km long and 0.5 km wide. Internal zonation within the individual pegmatites is variable and is commonly obscured by metasomatic albitization. Rare-element mineralization is also variable, although spodumene is conspicuously the most abundant rare-element mineral present.

The Nb and Ta minerals present within the series are ferrocolumbite, ferrotantalite and rare manganocolumbite (Thor-Echo). They occur as platy, bladed, tabular, blocky or anhedral grains within cleavelandite + quartz, K-feldspar + plagioclase + quartz, saccharoidal albite and rarely with spodumene or montebrasite. Cassiterite is rare and occurs intergrown with ferrotantalite in the Thor-Echo swarm.

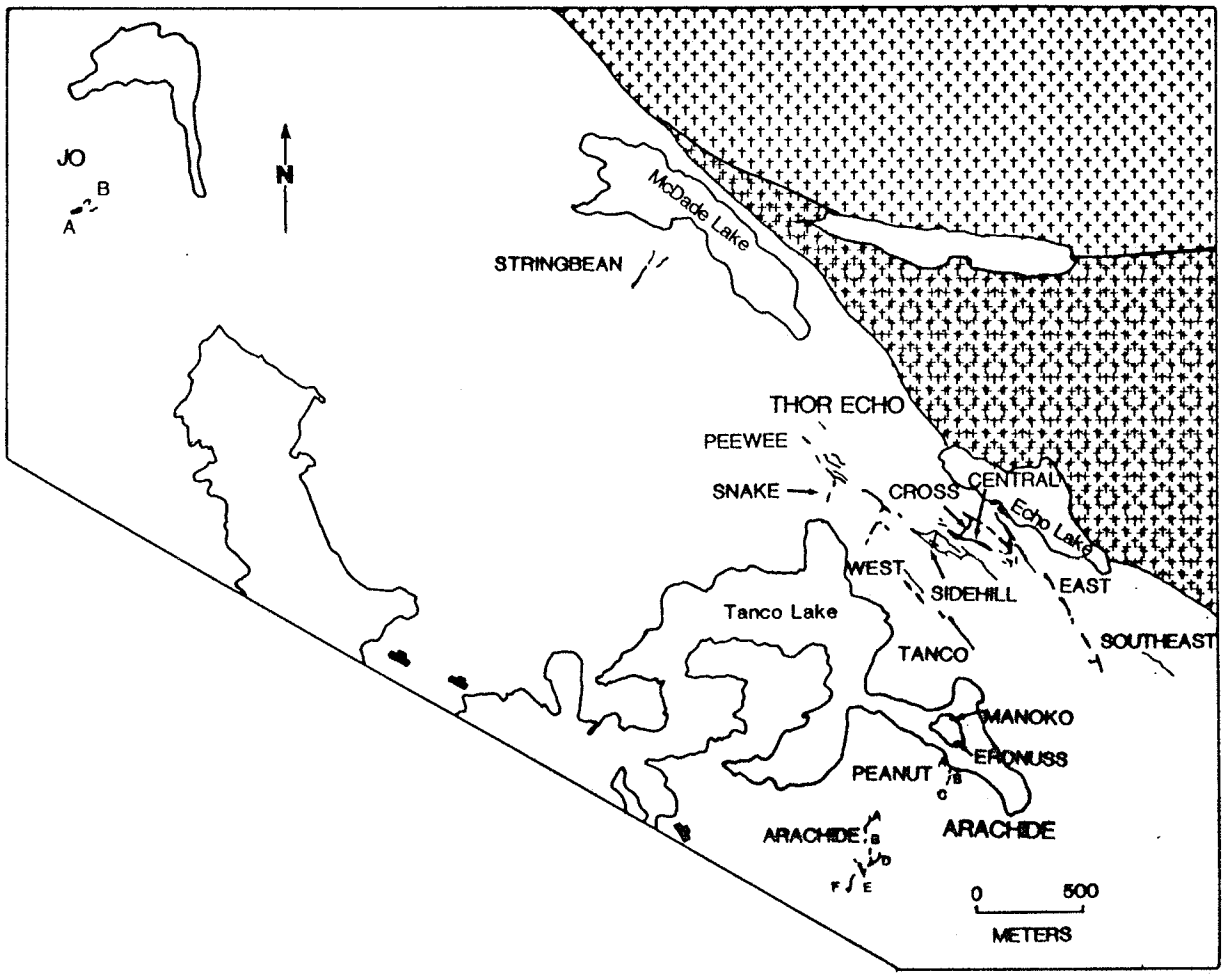

Figure 7: Location map of the Tanco Lake pegmatite group. Symbols as shown in Figure 3.

Table 10: Compositional characteristics of K-feldspar, muscovite and beryl for the Tanco Lake pegmatite group.

		K/Rb	Rb	Cs	Ba	Sr	Pb		
Blocky K-feldspar	$\bar{x}$	24.4	4940	100	nd	nd	nd		
	s	8.2	1710	87	nd	nd	nd		
	range	11.5-51.9	2010-9600	25-412	nd	nd	nd		
	n	37	37	37	0	0	0		
		Li_2O	K/Rb	Rb	Cs	Be	Nb	Ta	Nb/Ta
Platy muscovite	$\bar{x}$	0.074	19.6	4300	81	25	nd	nd	nd
	s	0.036	6.7	1850	47	5	nd	nd	nd
	range	0.012-0.151	10.3-31.7	2100-8500	27-195	20-44	nd	nd	nd
	n	21	21	21	21	21	0	0	0
		Li	Na_2O	Na/Li	Cs				
Beryl	$\bar{x}$	2160	1.24	5.35	1560				
	s	800	0.31	4.02	720				
	range	140-3220	0.38-1.77	3.40-21.2	370-3210				
	n	23	23	23	23				

Elements - ppm, oxides - wt.%. Symbols: $\bar{x}$ = arithmetic mean, s = standard deviation, n = number of samples analyzed, nd = not determined.

Arachide swarm.

The Arachide swarm consists of a group of pegmatites which outcrop on a small island in the eastern arm of Tanco Lake and continues on the southwestern shore. The pegmatites strike predominantly NE and NW, with westerly and easterly dips. The pegmatites are spodumene-bearing and generally lack well-developed internal zonation. Beryl, triphylite and ferrocolumbite occur as accessory minerals near the quartz core of the Peanut, Erdnuss and Arachide bodies.

Doubling Lake Series

This series consists of the spodumene-bearing Usk and Was pegmatites and is situated about 1 km W of the Doubling granodiorite and 2 km SE of Doubling Lake (Figure 8). The pegmatites strike northwesterly with near vertical dips. The Was pegmatite is fine-grained and homogeneous; the Usk dike is also homogeneous but with isolated patches of K-feldspar + quartz core development. One crystal of ferrotapiolite was found in a medium-grained part of the Usk pegmatite. Extensive albitization in the form of saccharoidal albite and fine-grained muscovite is common in Usk and hosts the majority of Nb and Ta minerals. Nb-Ta mineralization occurs as blades of ferrocolumbite in both pegmatites.

Overall, pegmatite fractionation in this series is very similar to the Tanco Lake group in terms of rare-alkali accumulations in K-feldspar (Table 11). In contrast, muscovite from the Doubling Lake series seems to be more fractionated, but this may be misleading because of the insufficient sampling. Compared to the Tanco Lake group, the muscovites of the Doubling series contain distinctly higher amounts of Cs.

Northeastern area

Upper Ross Lake Group

The Peg swarm is a cluster of over 500 pegmatites intruding an interbedded complex of the Ross granodiorite, amphibolite and biotite schist, and is located between the Upper Ross and Redout Lakes. The pegmatites vary from simple, concordant, unzoned bodies in the E near the granite to highly discordant, zoned, rare-element bearing in the W. The pegmatites extend westward from and show a regional zonation about the Redout granite.

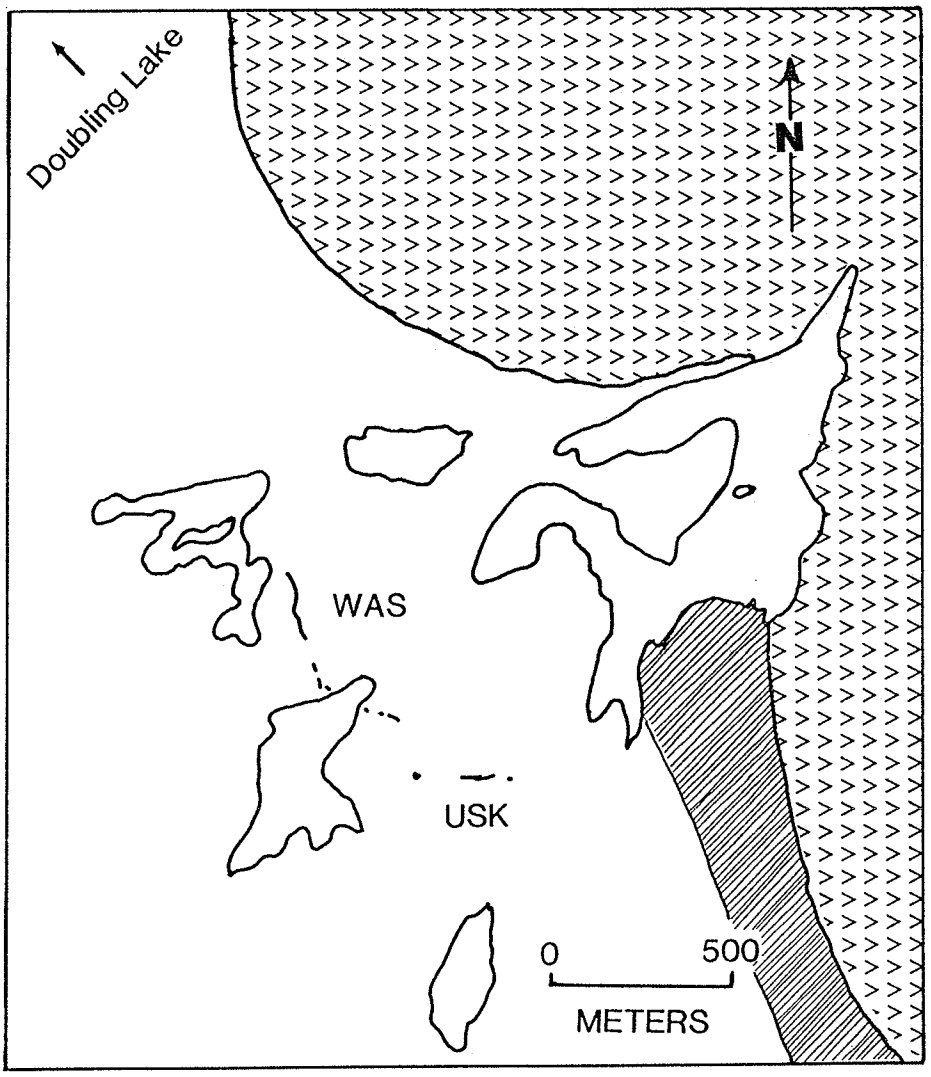

Figure 8: Location map of the Doubling Lake pegmatite series. Symbols as shown in Figure 3.

This regional distribution was first noted by Rowe (1952) and described in greater detail by Hutchinson (1955a). Five zones were identified, based largely on the regional distribution of the rare-element minerals beryl, columbite-tantalite, tapiolite and spodumene (Figure 9). As a result of this study and the concurrent study of Meintzer (1987), these zones have been greatly modified from those of Rowe and Hutchinson (Figure 10).

Table 11: Compositional characteristics of K-feldspar, muscovite and beryl for the Doubling Lake pegmatite series.

		K/Rb	Rb	Cs	Ba	Sr	Pb		
Blocky K-feldspar	$\bar{x}$	26.3	4350	135	<1	42	10		
	s	6.5	1380	66	nd	nd	nd		
	range	14.2-33.5	3020-7500	55-250	nd	nd	nd		
	n	9	9	9	1	1	1		
		Li_2O	K/Rb	Rb	Cs	Be	Nb	Ta	Nb/Ta
Platy muscovite	$\bar{x}$	0.070	12.1	5400	448	22	nd	nd	nd
	s	0.002	1.5	260	183	1	nd	nd	nd
	range	0.068-0.071	11.0-13.2	5210-5580	318-577	21-22	nd	nd	nd
	n	2	2	2	2	2	0	0	0
		Li	Na_2O	Na/Li	Cs				
Beryl	x	1900	1.70	6.64	2380				
	s	nd	nd	nd	nd				
	range	nd	nd	nd	nd				
	n	1	1	1	1				

Elements - ppm, oxides - wt.%. Symbols: $\bar{x}$ = arithmetic mean, s = standard deviation, n = number of samples analyzed, nd = not determined.

In general, however, rare-element mineralization as well as pegmatite fractionation increases westwards across the area. Table 12 summarizes some of the geochemical characteristics of the entire Peg swarm. The data indicate a low degree of fractionation for the swarm, but one must take into account that a large majority of the analyzed K-feldspars and muscovites were collected from the more primitive regional zones 1 and 2. A more realistic approach would be to note the ranges instead of the absolute means of the compositional parameters. For a more detailed review of the geochemical characteristics of each zone, the reader is referred to Meintzer (1987).

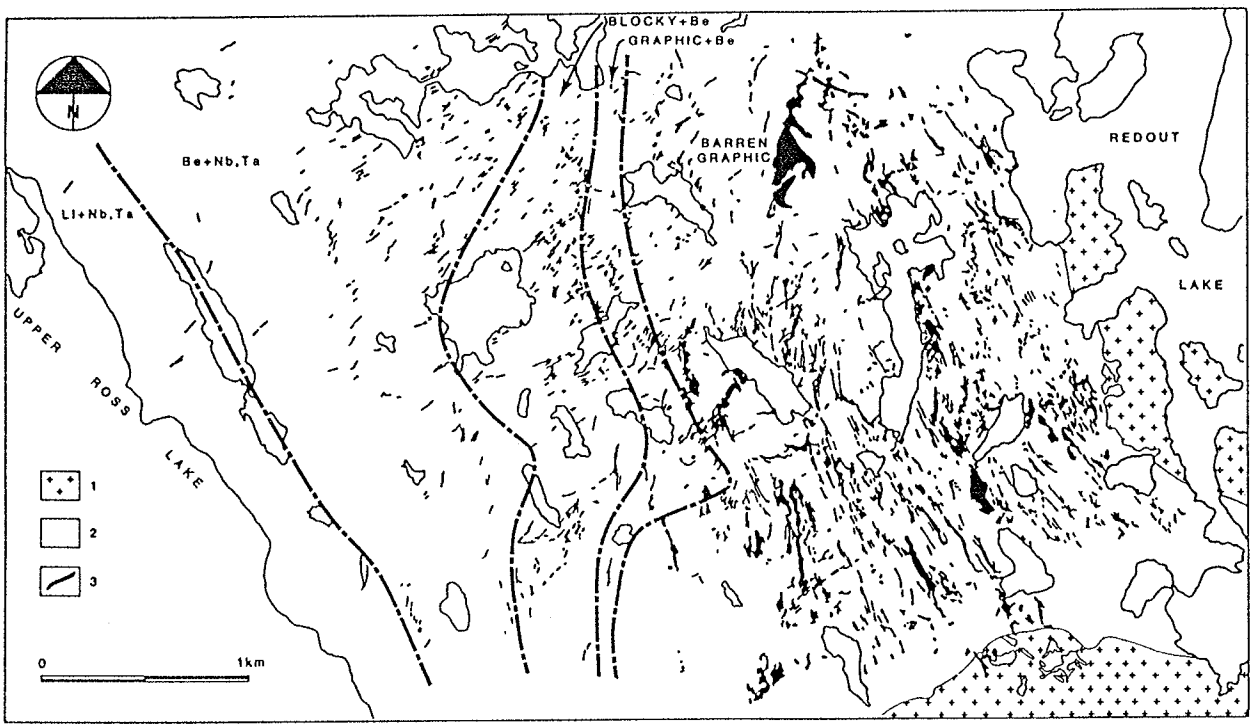

Figure 9: Regional zonation of pegmatites between the Upper Ross and Redout Lakes. Geology after Hutchinson (1955a). (1) Redout granite, (2) Interlayered granodiorite and amphibolite and (3) Pegmatites.

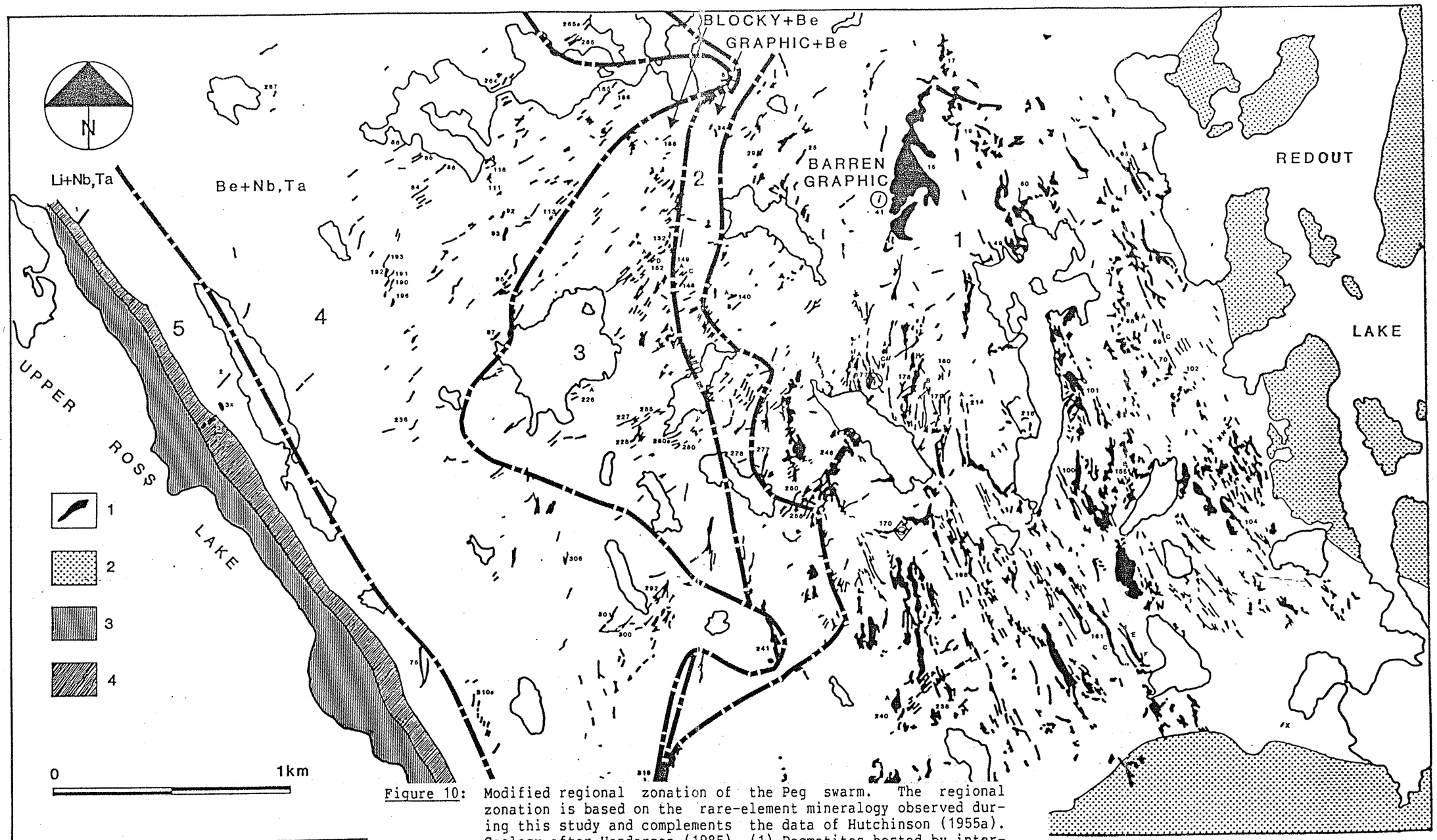

Figure 10: Modified regional zonation of the Peg swarm. The regional zonation is based on the rare-element mineralogy observed during this study and complements the data of Hutchinson (1955a). Geology after Henderson (1985). (1) Pegmatites hosted by interlayered granodiorite and amphibolite, (2) Redout granite, (3) Burwash Formation and (4) Cameron River mafic volcanics.

From 1943-1952, about 1700 kg of Ta concentrate was produced from the Peg claims (Lord, 1951), most of which seems to have been extracted from dike #3 (dike #92 of Hutchinson). Concentrate from the dike #1 assayed at 82.37% $(Ta,Nb)_2O_5$, 1.5% TiO_2, 13.91% FeO, 0.66% MnO and 0.14% SnO_2. Jolliffe (1944) observed that columbite-tantalite typically occurs in albite near quartz lenses, but also in perthite, quartz, muscovite and beryl. Rowe (1952) examined columbite-bearing pegmatites and observed the following: Nb and Ta minerals were found in the fine-grained plagioclase + quartz border zone, medium-grained cleavelandite + quartz + muscovite + perthite intermediate zone and perthite + quartz pods (cores ?). Hutchinson (1955a) found the highest concentrations and largest crystals near the margins of quartz + perthite cores and in perthite + plagioclase + quartz + muscovite wall zones of well-zoned pegmatites. Hutchinson (1955a) notes that ferrotapiolite occurs as the principal Nb, Ta mineral in the pegmatites of the Upper Ross area. He further states that both zones 4 and 5 contain pegmatites which carry Nb and Ta minerals, and although tiny plates of columbite-tantalite are rare in zone 5, ferrotapiolite is absent.

During this study, we have found that Nb-Ta mineralization occurs predominantly in Hutchinson's zone 4 and rarely in his zones 3 and 5. Electron microprobe analyses show that ferrocolumbite is the principal Nb-Ta mineral in the group and that ferrotapiolite is subordinate. Ferrotantalite, manganocolumbite, cassiterite and microlite are rare. The crystal morphology of columbite-tantalite varies greatly within the series, ranging from platy, bladed and tabular crystals to anhedral grains. Radiating aggregates of bladed crystals are commonly found, mainly in a medium-grained plagioclase + quartz + muscovite assemblage. Manganocolumbite occurs only in the spodumene-bearing dikes of zone 5.

Table 12: Compositional characteristics of K-feldspar, muscovite and beryl for the Peg swarm.

		K/Rb	Rb	Cs	Ba	Sr	Pb		
Blocky K-feldspar	$\bar{x}$	97.0	1670	54	66	33	30		
	s	58.1	1320	266	105	89	18		
	range	13.7-285	324-8290	1-2480	3-938	3-854	1-123		
	n	219	219	219	90	90	90		
		Li_2O	K/Rb	Rb	Cs	Be	Nb	Ta	Nb/Ta
Platy muscovite	$\bar{x}$	0.053	66.7	1990	54	18	264	26	8.80
	s	0.046	54.4	1320	88	13	131	45	8.62
	range	0.002-0.230	11.6-243	336-6180	<1-693	1-76	43-515	<8-175	0.921-38.3
	n	92	92	92	92	92	68	68	26
		Li	Na_2O	Na/Li	Cs				
Beryl	$\bar{x}$	433	0.66	16.4	314				
	s	367	0.41	12.1	511				
	range	54-2000	0.25-2.04	3.73-59.4	28-3850				
	n	68	68	68	68				

Elements - ppm, oxides - wt.%. Symbols: $\bar{x}$ = arithmetic mean, s = standard deviation, n = number of samples analyzed.

Ferrotapiolite is generally found as single, anhedral grains or as blebs included within ferrotantalite from zone 4 of the swarm. They are found in similar paragenetic associations as columbite-tantalite and rarely with beryl or biotite. Cassiterite is present only in the spodumene-bearing pegmatites (zone 5) as subhedral crystals in plagioclase + quartz. Microlite was found in dikes #84, #93 and #192 from zone 4 and occurs as rare anhedral blebs replacing ferrotantalite.

Northwestern area

Blaisdell Lake Group

The Blaisdell Lake group lies 3 km E and SE of the Wedge granite and Blaisdell Lake (Figure 11). The group consists of the Bill, Melody and Vo swarms. Pegmatite bodies of this area were first examined by Jolliffe (1944) who found small parts of them containing columbite-tantalite and/or cassiterite. Our examination of pegmatites within this area suggests a regional zonation of pegmatites about the Wedge granite. Zonation within individual pegmatites vary from homogeneous to well-developed. Rare-element mineralization is common whereas albitization is patchy and occurs only in the Melody and Vo swarms. Blocky K-feldspar and muscovite show a very wide range of rare-alkali concentrations (Table 13).

Bill swarm.

The Bill swarm lies N of Blaisdell Lake and along the eastern edge of the Wedge Lake granite, intruding both the granite and the adjacent quartz-biotite schist. Jolliffe (1944) found beryl in 32 of the 50 pegmatites examined. Of these, 12 contained columbite-tantalite and/or cassiterite. Tourmaline and minor occurrences of lithiophilite, pyrite, arsenopyrite, molybdenite and amblygonite were also reported. No molybdenite, lithiophilite or amblygonite was observed in this work. The pegmatites are medium to coarse-grained with well-developed internal zonation, and trend N to NW.

Ferrocolumbite is the dominant Nb, Ta mineral in the swarm and occurs as bladed, platy or tabular crystals in plagioclase, K-feldspar ± quartz or beryl. Rare cassiterite is associated with ferrocolumbite in dike #5.

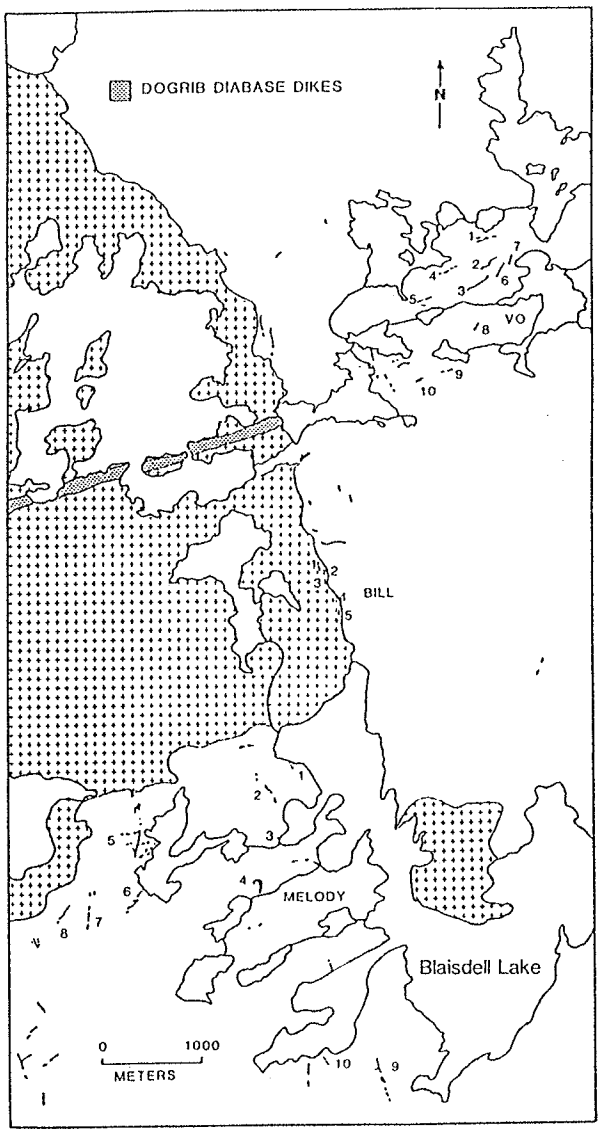

Figure 11: Location map of the Blaisdell Lake pegmatite group. Symbols as shown in Figure 3.

Table 13: Compositional characteristics of K-feldspar, muscovite and beryl for the Blaisdell Lake pegmatite group.

		K/Rb	Rb	Cs	Ba	Sr	Pb		
Blocky K-feldspar	$\bar{x}$	66.9	1930	45	55	41	29		
	s	31.7	1080	51	76	38	21		
	range	11.2-	414-	12-	1-	1-	<1-		
		233	7910	423	480	160	103		
	n	80	80	80	80	80	80		
		Li_2O	K/Rb	Rb	Cs	Be	Nb	Ta	Nb/Ta
Platy muscovite	$\bar{x}$	0.084	38.9	2390	90	25	216	7	19.2
	s	0.049	20.3	900	75	9	75	17	12.0
	range	0.010-	17.4-	693-	12-	8-	31-	<8-	2.80-
		0.195	112	4290	347	51	355	90	35.3
	n	34	34	34	34	34	34	34	10
		Li	Na_2O	Na/Li	Cs				
Beryl	$\bar{x}$	670	0.45	8.77	832				
	s	670	0.27	8.12	1020				
	range	48-	0.25-	3.34-	181-				
		2380	1.23	40.1	5070				
	n	25	25	25	25				

Elements - ppm, oxides - wt.%. Symbols: $\bar{x}$ = arithmetic mean, s = standard deviation, n = number of samples analyzed.

Melody swarm.

The Melody swarm is located nearly 3 km W of Blaisdell Lake. The pegmatites are medium-grained with generally poor internal zonation. Strikes are variable although most tend to trend northwesterly. Beryl, columbite-tantalite, ferrotapiolite and minor triphylite are the only rare element minerals present. Tourmaline is common in most of the bodies.

The Melody swarm contains ferrocolumbite-ferrotantalite and ferrotapiolite as the predominant Nb and Ta minerals. Ferrotapiolite occurs as large grains in K-feldspar (dike #9) surrounding a segregated quartz pod.

Ferrocolumbite-ferrotantalite forms platy crystals and granular masses associated with cleavelandite or K-feldspar ± beryl.

Vo swarm.

The Vo swarm is located about 2 km E of the Wedge granite. The dikes strike roughly N 40° E with near vertical dips. Outcrops of pegmatites vary between 122 - 244 m long and up to 12 m wide. Most of the dikes are medium-grained and nearly homogeneous, with poorly defined spodumene-rich bands. The spodumene occurs in a ladder-type arrangement and is commonly altered to fine-grained, greenish muscovite. Beryl, triphylite, columbite-tantalite, tourmaline and minor apatite and garnet occur in many of the bodies. Patches of albitization occur locally.

Columbite-tantalite, ferrotapiolite, cassiterite and microlite have been identified in the Vo swarm. The Nb-Ta-Sn mineralization is associated with cleavelandite or saccharoidal albite. Columbite-tantalite occurs as radiating blades to tabular crystals in cleavelandite. Cassiterite forms microscopic inclusions within ferrotapiolite, and microlite occurs as anhedral grains replacing manganotantalite.

Sproule Lake Series

The Fly and Cata swarms outcrop in nodular quartz-biotite schist near Sproule Lake approximately 5.5 km from the Wedge and Scott granites (Figure 12). The dikes are commonly albitized and show poor to moderate zonation. Spodumene, beryl and montebrasite are predominant among the rare-element minerals present. The rare-alkali concentrations of blocky K-feldspar and muscovite are generally high and indicative of advanced fractionation (Table 14).

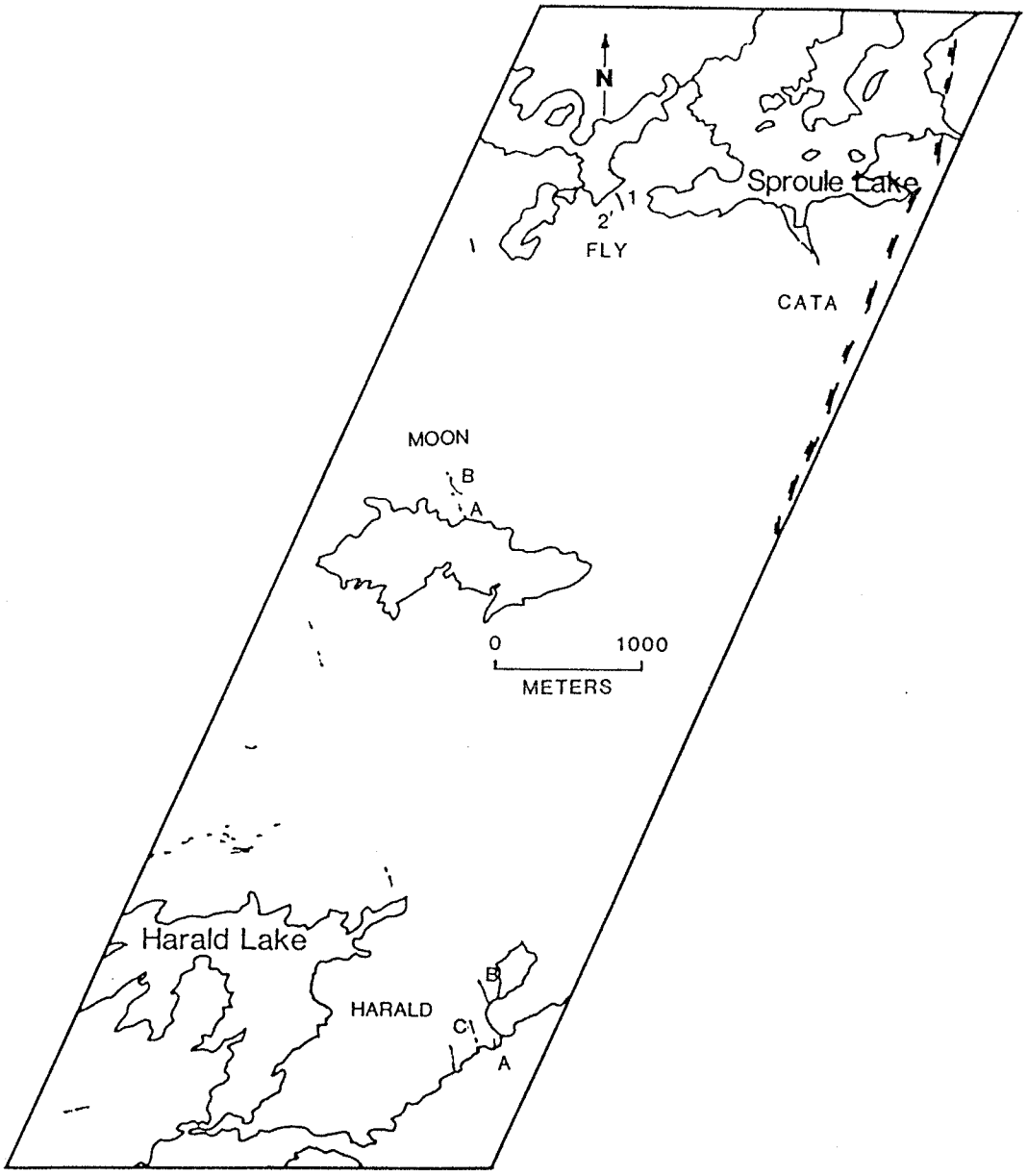

Figure 12: Location map of the Sproule Lake and Harald Lake pegmatite series. Symbols as shown in Figure 3.

Table 14: Compositional characteristics of K-feldspar, muscovite and beryl for the Sproule Lake pegmatite series.

		K/Rb	Rb	Cs	Ba	Sr	Pb		
Blocky K-feldspar	$\bar{x}$	13.1	8540	418	19	42	17		
	s	1.8	1320	154	9	11	8		
	range	12.0-15.1	7040-9480	240-518	9-26	34-55	12-26		
	n	3	3	3	3	3	3		
		Li_2O	K/Rb	Rb	Cs	Be	Nb	Ta	Nb/Ta
Platy muscovite	$\bar{x}$	0.079	6.37	11800	1430	15	47	62	1.33
	s	0.078	0.73	800	510	9	33	82	1.32
	range	0.030-0.169	5.58-7.02	11200-12700	954-1970	7-25	9-70	<8-155	0.40-2.26
	n	3	3	3	3	3	3	3	2
		Li	Na_2O	Na/Li	Cs				
Beryl	$\bar{x}$	2980	1.55	4.40	6890				
	s	1610	0.16	1.99	4680				
	range	1840-4120	1.44-1.66	2.99-5.81	3580-10200				
	n	2	2	2	2				

Elements - ppm, oxides - wt.%. Symbols: $\bar{x}$ = arithmetic mean, s = standard deviation, n = number of samples analyzed.

Fly swarm.

The pegmatites of the Fly swarm are located at the W end of Sproule Lake. Only the spodumene-bearing Fly #1 dike was observed during this study. The body strikes N 25° W and dips 45° SW. Spodumene is abundant but concentrations are scattered throughout the pegmatite. Ferrisicklerite is present locally, as is blue-green apatite which occurs in the border zone along the pegmatite-schist contact.

The Fly pegmatite contains thin blades of ferrocolumbite in a quartz + K-feldspar assemblage. Microscopic blades of manganocolumbite occur in fine-grained albite bodies. Several of these blades show alteration of their edges to an unknown Ca-, Nb-bearing mineral.

Cata swarm.

The Cata swarm consists of 10 bodies aligned in a belt situated on the S side of Sproule Lake (Figure 13). The pegmatites are discordant and cut nodular quartz-biotite schist. The pegmatite belt strikes NW and individual bodies dip between 30° and 60° to the SW. Internal zonation varies from body to body, ranging from nearly homogeneous to poorly developed zoning to well zoned. Rare element mineralization includes abundant spodumene, minor beryl, montebrasite, triphylite and apatite. The Nb-Ta-Sn mineralization is represented by abundant cassiterite and subordinate columbite-tantalite.

Nb-, Ta- and Sn-bearing minerals are particularly concentrated in the central and southernmost sections of the swarm. Columbite-tantalite becomes less abundant and is actually rare in the southernmost extension of the swarm. Cassiterite appears in relatively abundant quantities throughout, although its best concentration is in the southern part of the swarm. Cassiterite and columbite-tantalite occur chiefly in cleavelandite, along with montebrasite and blue-green apatite. Cassiterite has been reported in irregular aggregates up to 3.2 x 2.5 x 0.9 cm in size (Jolliffe, 1944). Manganocolumbite is the dominant member of the columbite-tantalite group present, occurring as blades or tabular crystals in cleavelandite ± muscovite (Jolliffe, 1944).

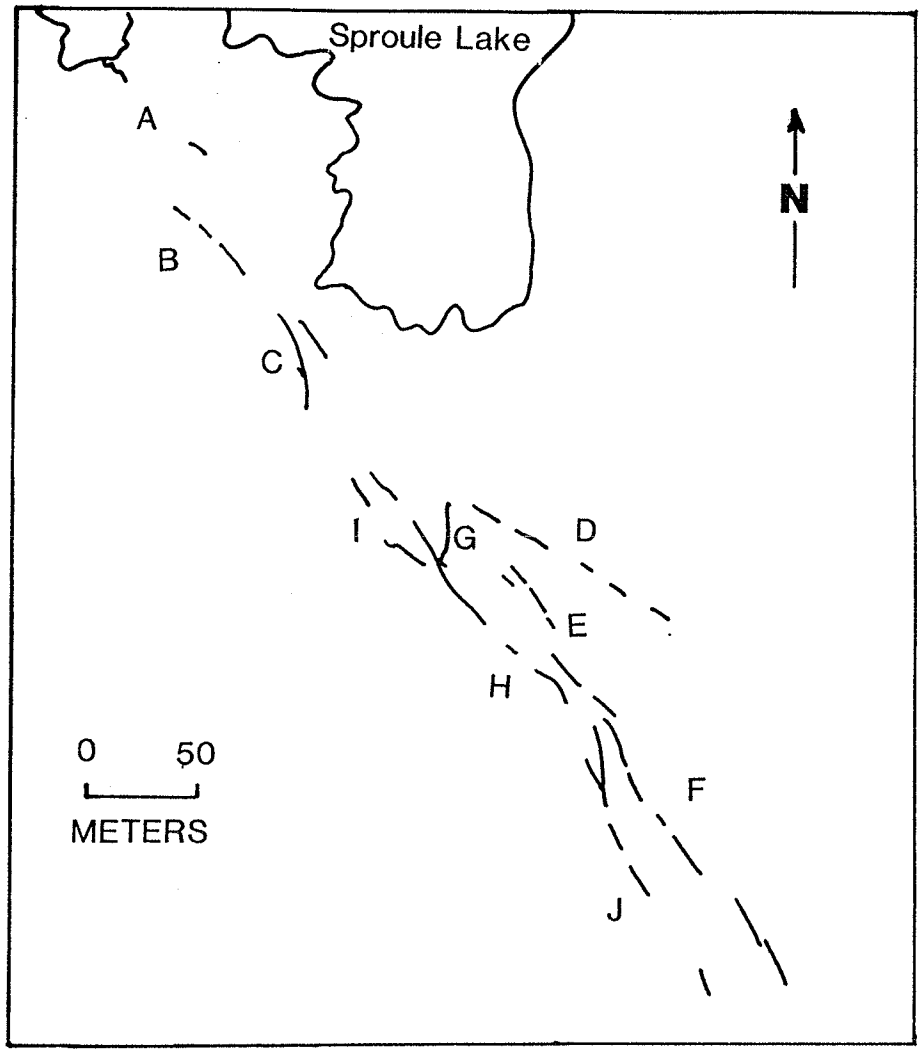

Figure 13: Detailed location map of the Cata swarm. Map modified after Jolliffe (1943).

Harald Lake Series

This series comprises a swarm of pegmatites along the N shore of Harald Lake (Harald swarm) and a swarm approximately 800 m SE of Halfmoon Lake (Moon swarm) (Figure 12). The nearest granite plutons are located 5.75 km (Blaisdell and Scott plutons) from the Moon swarm and 3.1 km (Scott pluton) from the Harald swarm. Rare-alkali concentrations for K-feldspar and beryl are given in Table 15.

Table 15: Compositional characteristics of K-feldspar, muscovite and beryl for the Harald Lake pegmatite series.

		K/Rb	Rb	Cs	Ba	Sr	Pb
Blocky K-feldspar	$\bar{x}$	58.2	2660	81	158	44	31
	s	34.8	2130	57	152	21	7
	range	18.6-104	1040-5800	39-165	20-316	18-66	20-36
	n	4	4	4	4	4	4

		Li	Na_2O	Na/Li	Cs
Beryl	$\bar{x}$	444	0.60	10.0	510
	s	nd	nd	nd	nd
	range	nd	nd	nd	nd
	n	1	1	1	1

Elements - ppm, oxides - wt.%. Symbols: $\bar{x}$ = arithmetic mean, s = standard deviation, n = number of samples analyzed, nd = not determined.

Harald swarm.

The Harald swarm consists of four dikes which strike to the NW across NE-trending nodular schist. Only one dike was sampled in detail. The pegmatite is largely homogeneous and consists of medium-grained quartz + pla-

gioclase + K-feldspar ± muscovite with pod-like core areas of quartz + K-feldspar. Rare element mineralization is minor and includes rare beryl and blades of columbite-tantalite.

Moon swarm.

The Moon swarm outcrops on the N shore of an unnamed lake SE of Half-moon Lake and S of Parr Lake, 2 km SW of the Fly swarm. Only one dike from the swarm was sampled. It strikes NW and outcrops over a length of approximately 170 m with a maximum width of 2.4 m.

The pegmatite is crudely zoned, consisting of a fine- to medium-grained quartz + plagioclase + K-feldspar + muscovite wall zone and a medium-grained quartz + K-feldspar ± spodumene core. Besides spodumene, a single microscopic blade of columbite-tantalite represents the only rare-element mineralization found thus far from this swarm.

Sparrow-Thompson-Hidden Lakes Group

This group consists of a large number of pegmatites which intrude the eastern margin of the Cameron granite and the schist surrounding the Cameron and Hidden plutons. Most of the pegmatite population is located to the E of Sparrow Lake and W of Hidden Lake with lesser occurrences S of Hidden Lake and along the southernmost lobe of the Cameron pluton (Figure 14). A crude regional zonation of pegmatites exists around the eastern margin of the Cameron granite. The pegmatites vary from generally simple with variable development of internal zonation to homogeneous bodies of albite + spodumene. Beryl, Nb and Ta minerals, spodumene, montebrasite and triphylite are the only rare-element minerals present. Spodumene + quartz intergrowths occur locally in the Waco swarm. Small patches of albitization units occur locally. The average K/Rb ratio for K-feldspar in this

series suggests a somewhat low degree of fractionation, but the K/Rb of the muscovites imply the opposite (Table 16).

Casper swarm.

The Casper swarm intrudes the northern lobe of the Cameron granite and extends eastwards into quartz-biotite schist towards Thompson Lake and N towards Scott Lake. Pegmatites intruding the granite occur as straight, tabular dikes, often showing sharp contacts with simple, but well-developed zonation. The dikes strike predominantly NNE to NE and vary from highly discordant to concordant. Schorl and beryl are abundant in these pegmatites. Pegmatites intruding the schist along the granite margins are generally large, homogeneous bodies with occasional pods of quartz which may contain subordinate beryl. Farther east, the pegmatites become smaller and more dike-like. Nb-Ta mineralization is evident in these pegmatites, along with beryl and minor triphylite.

In the Casper swarm, Nb-Ta mineralization is present in the form of ferrocolumbite-ferrotantalite and rare ferrotapiolite and microlite. Columbite-tantalite occurs as anhedral grains and veinlets in muscovite + perthite or plagioclase + quartz ± muscovite assemblages. Ferrotapiolite occurs as inclusions in ferrotantalite from only one dike in the swarm. Secondary microlite replacing ferrotapiolite was found in only one sample.

Heidi swarm.

The Heidi swarm lies just N of Hidden Lake and the Hidden granite pluton and consists of well-zoned, simple pegmatites with fairly abundant beryl. The Heidi dikes strike predominantly E-W but also trend NW to SE along probable fractures. Bladed ferrotantalite occurs in the K-feldspar + quartz ± muscovite assemblage and in rare fine-grained late muscovite replacing K-feldspar.

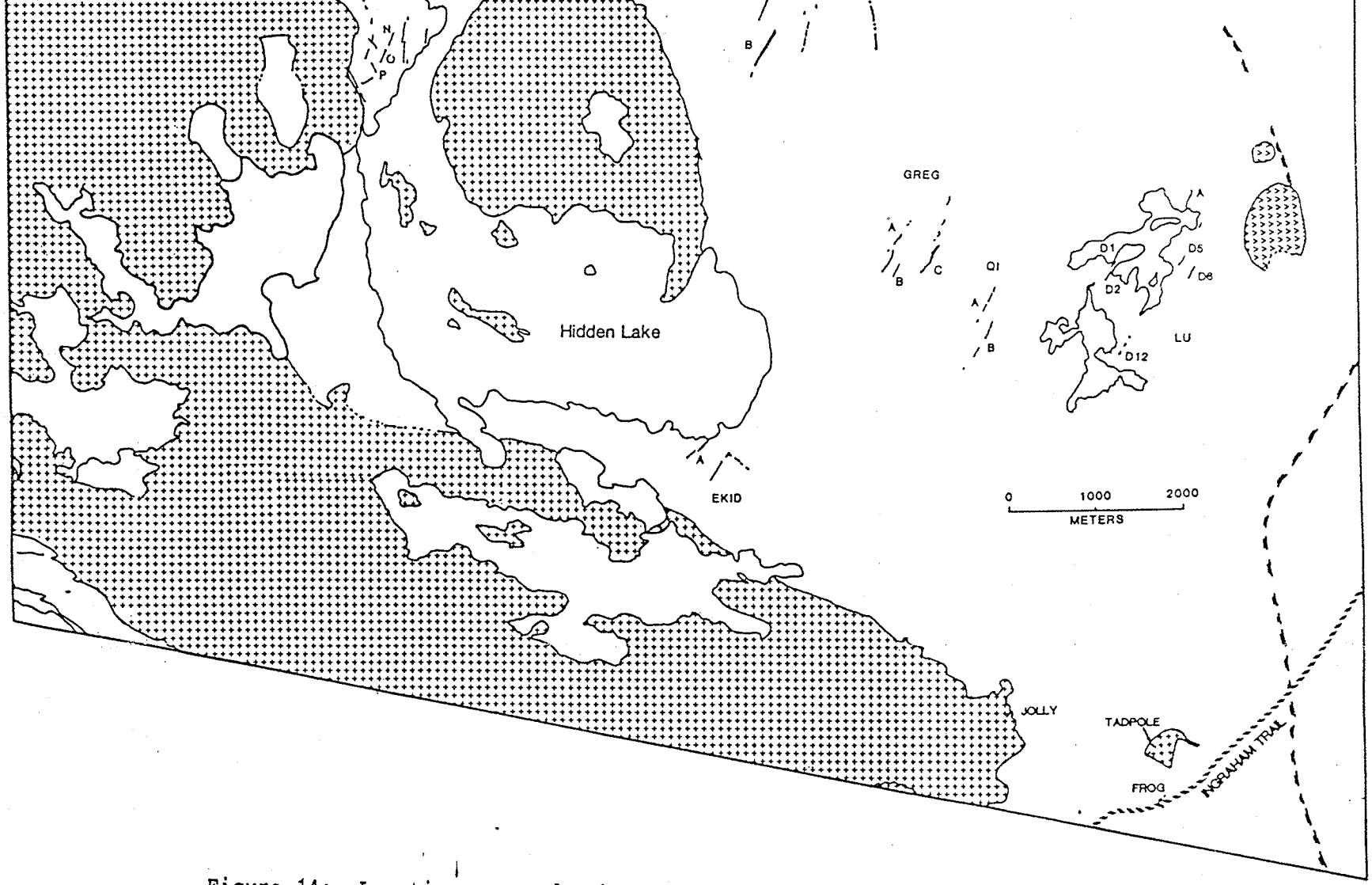

Figure 14: Location map of the Sparrow-Thompson-Hidden Lakes pegmatite group. Symbols as shown in Figure 3. Metamorphic isograds from Kamineni (1975).

Table 16: Compositional characteristics of K-feldspar, muscovite and beryl for the Sparrow-Thompson-Hidden Lake pegmatite group.

		K/Rb	Rb	Cs	Ba	Sr	Pb		
Blocky K-feldspar	$\bar{x}$	59.3	2460	88	111	54	24		
	s	37.8	1610	94	116	54	13		
	range	13.3-	330-	9-	5-	1-	0-		
		314	7860	548	481	290	91		
	n	89	89	89	85	85	85		
		Li_2O	K/Rb	Rb	Cs	Be	Nb	Ta	Nb/Ta
Platy muscovite	$\bar{x}$	0.042	31.2	3040	114	23	207	14	10.5
	s	0.033	17.2	1280	135	7	84	22	8.6
	range	0.002-	11.5-	767-	15-	10-	36-	<8-	0.34-
		0.129	99.5	6210	855	38	371	105	38.8
	n	43	43	43	43	43	42	42	20
		Li	Na_2O	Na/Li	Cs				
Beryl	$\bar{x}$	1020	0.81	9.5	1480				
	s	890	0.47	6.96	1260				
	range	62-	0.22-	2.56-	152-				
		3700	1.76	34.5	5570				
	n	52	52	52	52				

Elements - ppm, oxides - wt.%. Symbols: $\bar{x}$ = arithmetic mean, s = standard deviation, n = number of samples analyzed.

Murky pegmatite.

The Murky pegmatite is an isolated body which lies on the western shore of Thompson Lake. It is a partly-zoned body striking N 63° E and dips 60° SE. The internal zonation consists of a fine- to medium-grained quartz + plagioclase + K-feldspar + muscovite ± beryl wall/intermediate zone and a medium- to coarse-grained quartz + K-feldspar + beryl ± montebrasite core. Ferrocolumbite occurs as small veinlets 2.5 x 0.6 cm in the plagioclase + quartz + muscovite intermediate zone; and as platy crystals in blocky K-feldspar of the core.

Ki swarm.

The Ki swarm consists of a set of pegmatites extending for about 3 km SE of Thompson Lake. Only the northernmost Tom pegmatite showed any Nb-Ta mineralization. The pegmatite consists predominantly of medium-grained quartz + plagioclase + K-feldspar + muscovite and shows no evidence of internal zonation, except for alternating bands of aplite and coarse-grained pegmatite. Saccharoidal albite is relatively common and host rare grains of ferrocolumbite. Platy crystals of ferrocolumbite also occur in coarse-grained quartz + K-feldspar + muscovite units.

Waco swarm.

The NW trending Waco swarm to the N of Thompson Lake contains five bodies with varying degrees of zonation. Spodumene, beryl and columbite-tantalite are common. Ferrocolumbite is found as platy crystals or anhedral grains in blocky K-feldspar or cleavelandite. Ferrotapiolite and cassiterite occur as anhedral grains included within the ferrocolumbite.

Freda pegmatite.

The Freda pegmatite is the most fractionated body in this group, and contains beryl, montebrasite, spodumene, cassiterite, ferrocolumbite, ferrotapiolite amd microlite. The dike trends E to SE and dips 10° - 33° S. The outcrop has a length of 91 m and an average width of 3.5 m. The pegmatite is well-zoned with local patches of aplitic material. The core is typically coarse-grained K-feldspar + quartz ± spodumene ± montebrasite. Beryl, ferrocolumbite, ferrotantalite, microlite and cassiterite are also present. An assay of a grab sample by the Bureau of Mines, Ottawa showed 46.16% Ta_2O_5, 31.18% Nb_2O_5, 1.83% SnO_2 and 0.57% TiO_2 (Lord, 1951). Ferrocolumbite is associated with cassiterite, beryl, montebrasite or lithian muscovite in a K-feldspar or cleavelandite + quartz assemblage. The ferro-

columbite is commonly intergrown with massive cassiterite which is concentrated in the western end of the pegmatite with patches of replacement muscovite. Cassiterite is abundant throughout the pegmatite and occurs as anhedral grains up to 3.8 cm in size. One sample of ferrotapiolite, partly replaced by microlite, was found as anhedral blebs included within cassiterite.

Fi swarm.

The spodumene-bearing dikes of the Fi swarm lie 2.4 km S of Thompson Lake, less than 0.8 km E of the Hidden granite. Two large bodies measured approximately 610 m long, 37 m wide, and 3010 m long, 7.6 m wide respectively. They are homogeneous, with alternating bands of aplite and pegmatite occurring frequently. Pegmatitic phases contain the bulk of the spodumene mineralization, in which spodumene crystals show no preferred orientation. Nb-Ta mineralization is minor and occurs as bladed crystals of ferrocolumbite in isolated K-feldspar + quartz pods.

Ekid swarm.

The Ekid swarm is located on the SE shore of Hidden Lake, striking NE for about 840 m. Only one dike from this swarm was examined during this study. The pegmatite is medium- to coarse-grained and partly zoned. Beryl, triphylite and columbite-tantalite all occur within the K-feldspar + quartz + muscovite + plagioclase intermediate zone. Isolated quartz pods occur locally.

Greg swarm.

The Greg pegmatites (bodies A, B and C) are homogeneous spodumene-bearing dikes which generally trend NE and commonly dip steeply to the NW. The main dike extends over a length of 1180 m and has an average width of

18 m. All three bodies lack internal zonation and are comprised predominantly of medium-grained quartz + plagioclase + spodumene + muscovite. Medium-grained spodumene-rich bands commonly alternate with medium-grained pink aplitic bands. Bladed crystals of ferrocolumbite is associated with medium-grained cleavelandite + quartz + muscovite ± spodumene.

Qi swarm.

The Qi pegmatites, located less than 1 km SE of the Greg dikes, are identical texturally and mineralogically to the Greg pegmatites. In both swarms, rare-element mineralization is dominated by abundant spodumene, accompanied by minor quantites of triphylite and rare beryl (Qi). Small anhedral grains of ferrocolumbite represent the only Nb-Ta mineralization in the Qi pegmatites.

Lu swarm.

The Lu pegmatites lie 4.5 km E of Hidden Lake and about 3.2 km W of Tibbitt Lake. They strike approximately N 26° E to N 40° E with dips from 45° to 75° NW. The dikes range from 103 to 256 m long and average 6 m wide. The bodies are homogeneous, and mainly consist of medium- to coarse-grained quartz + K-feldspar + spodumene. Aplite bands frequently alternate with spodumene-rich pegmatitic bands. Bladed ferrocolumbite-ferrotantalite and blocky to subhedral crystals of cassiterite are common in the plagioclase ± quartz ± muscovite assemblage.

Jolly pegmatite.

The Jolly pegmatite is situated in the margin of the southernmost extension of the Cameron pluton, 4.25 km SE of Hidden Lake. The pegmatite is well-zoned, strikes about N 60° W and outcrops for about 60 m. The pegmatite is a fine- to medium-grained assemblage of quartz + plagioclase +

K-feldspar + muscovite with pods of quartz + K-feldspar which host rare white beryl. Platy crystals of columbite-tantalite were found in medium-grained muscovite replacing K-feldspar of the Jolly pegmatite.

Frog Granite

A small aplitic and locally muscovitic leucogranite intrusion (Frog Granite) contains rare columbite-tantalite. The single crystal of columbite-tantalite found in this study occurred in a 2 cm wide pegmatite vein crosscutting the pluton. K-feldspar within the vein is locally replaced by muscovite. Nearby, a 1 m wide dike (Tadpole pegmatite) also occurs in this pluton, but had no observable Nb-Ta mineralization. This is the only known occurrence of Nb and Ta minerals in a granite from the Yellowknife area.

Reid Lake Series

This series comprises the Ann & Boa swarm and the Pancho Villa swarm. All pegmatites outcrop within 2 km of the southeastern margin of the Cameron granite (Figure 15). The pegmatites are medium-grained, lack internal zonation and contains isolated pods of metasomatic albite. Spodumene commonly occurs nearly perpendicular to the wall and is often found in bands alternating with pink aplite (Ann). Rare triphylite, montebrasite and beryl also occur in the series. Rare-alkali concentrations of K-feldspar and muscovite are similar to those of the Sparrow-Thompson-Hidden Lake group (Table 17).

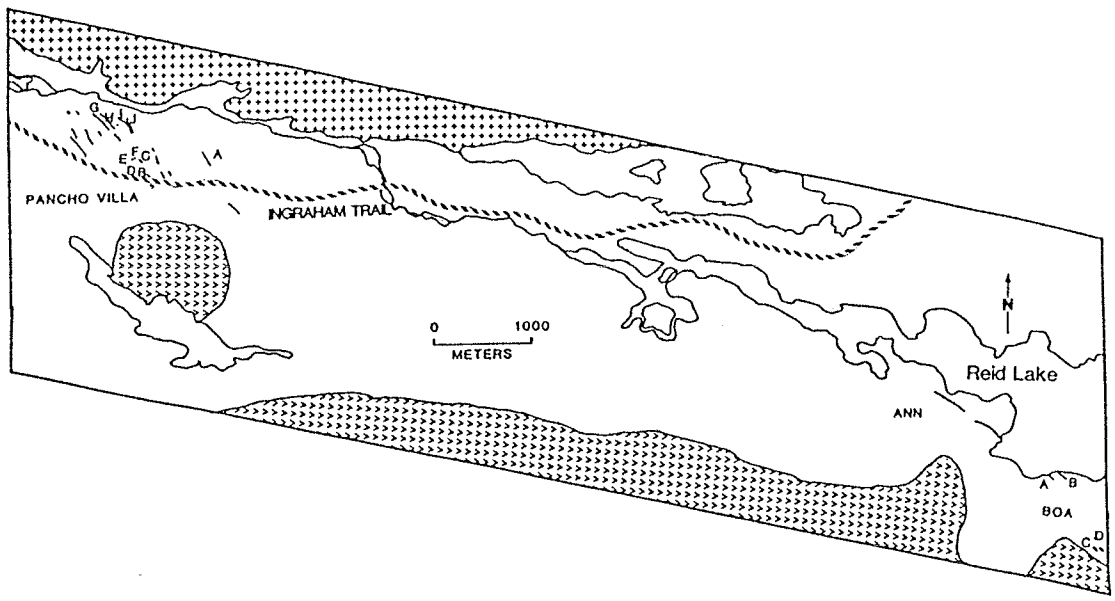

Figure 15: Location map of the Reid Lake pegmatite series. Symbols as shown in Figure 3.

Table 17: Compositional characteristics of K-feldspar, muscovite and beryl for the Reid Lake pegmatite series.

		K/Rb	Rb	Cs	Ba	Sr	Pb		
Blocky K-feldspar	$\bar{x}$	34.1	4280	129	286	73	53		
	s	18.4	2310	75	276	39	19		
	range	15.7-	1820-	33-	25-	31-	22-		
		58.1	6930	254	772	136	72		
	n	10	10	10	6	6	6		
		Li_2O	K/Rb	Rb	Cs	Be	Nb	Ta	Nb/Ta
Platy muscovite	$\bar{x}$	0.094	23.7	4740	357	20	152	33	2.74
	s	0.076	14.3	3660	567	6	105	23	2.14
	range	0.020-	7.89-	1780-	131-	89-	35-	<8-	0.673-
		0.210	44.3	10100	1460	26	278	52	4.95
	n	6	6	6	6	6	4	4	3
		Li	Na_2O	Na/Li	Cs				
Beryl	$\bar{x}$	1940	1.34	5.86	1280				
	s	920	0.41	2.32	640				
	range	740-	0.80-	3.32-	720-				
		3500	1.84	9.58	2550				
	n	7	7	7	7				

Elements - ppm, oxides - wt.%. Symbols: $\bar{x}$ = arithmetic mean, s = standard deviation, n = number of samples analyzed.

Ann & Boa swarm.

The Ann pegmatite is a spodumene-bearing body exposed for about 0.9 km, averaging 12 m wide and striking N 50° W. The texture of the pegmatite varies from an assemblage of coarse-grained K-feldspar + quartz + cleavelandite + spodumene to predominantly aplitic units. Saccharoidal albite occurs locally. Spodumene, beryl and ferrocolumbite were the only rare-element minerals observed, although amblygonite was previously reported by Mulligan (1965). Ferrocolumbite is found predominantly as fine-grained

blades associated with cleavelandite + muscovite + quartz. Occasionally veinlets of ferrocolumbite were noted.

Pancho Villa swarm.

The Pancho Villa swarm consists of several small pegmatite dikes which intrude nodular quartz-biotite schist 6 km NE of Upland Lake and 40 km E of Yellowknife. The pegmatites strike NW and are traceable for several hundred meters. Zonation in most of the bodies is poor; most are medium- to coarse-grained, homogeneous dikes with a well-developed wall zone of fine-grained muscovite + plagioclase + quartz pegmatite. Small pods of saccharoidal albite and quartz occur locally. Accessory rare-element minerals include beryl, columbite-tantalite, ferrotapiolite and triphylite.

Body C of the swarm is the largest and best developed in terms of internal zonation. In addition to the wall zone described above, this dike also contains a first intermediate zone consisting of medium- to coarse-grained spodumene + microcline + muscovite, a second intermediate zone of coarse-grained plagioclase + microcline + quartz ± beryl which grades into a quartz + microcline core.

Nb and Ta minerals are represented by ferrocolumbite, ferrotantalite and ferrotapiolite that occurs as platy to tabular crystals near the core margins. Very fine, disseminated grains are found in the pink aplitic parts and in medium-grained to saccharoidal albite parts of most of the dikes. A small crystal of ferrotapiolite was found in the western part of Body C associated with quartz + medium-grained muscovite.

Harding Lake Series

The Sky pegmatite and the Jake-Da and Paint swarms are located N and NW of Harding Lake and intrude the NW margin of the Defeat granodiorite (Figure 16). The nearest granite pluton is the Cameron granite, 10.5 km to the NW. The pegmatites are generally medium-grained and texturally homogeneous. Alternating aplite and fine-grained spodumene-rich bands are common in all pegmatites. Fractionation in this series seems to be very similar to that of the Reid Lake series (Table 18).

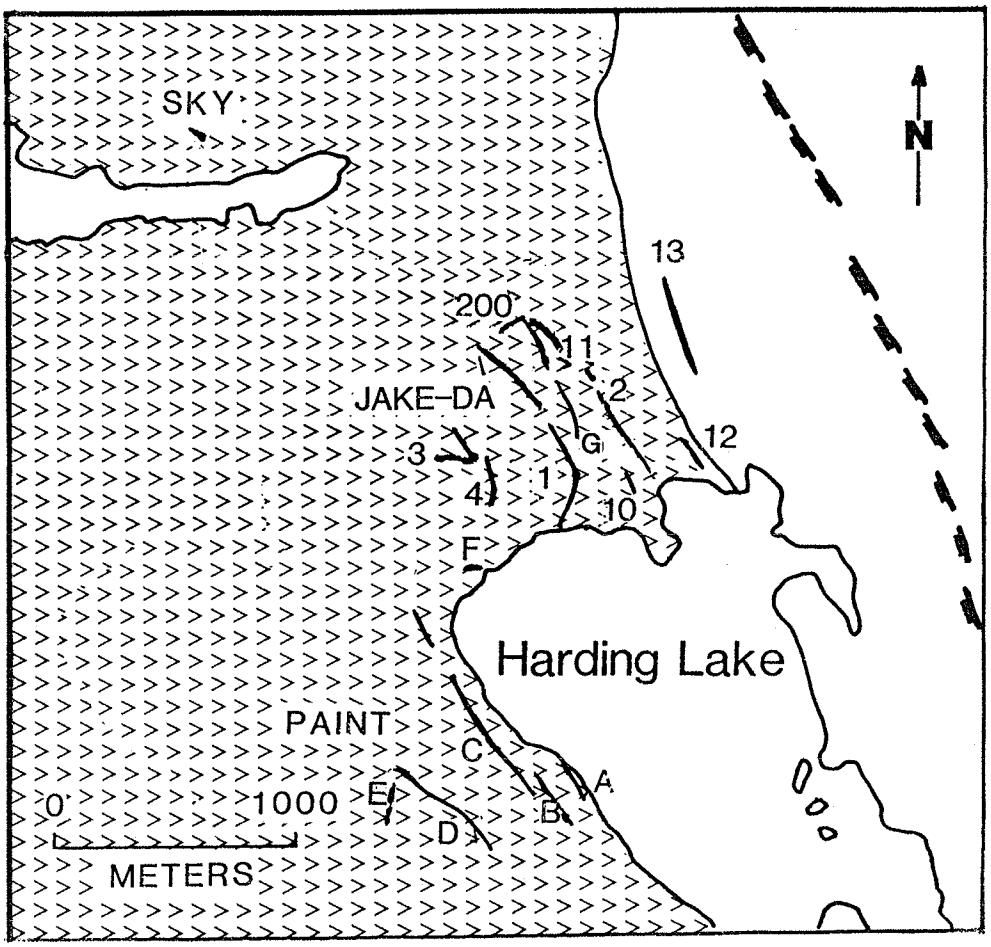

Figure 16: Location map of the Harding Lake pegmatite series. Symbols as shown in Figure 3.

Table 18: Compositional characteristics of K-feldspar and beryl for the Harding Lake pegmatite series.

		K/Rb	Rb	Cs	Ba	Sr	Pb
Blocky K-feldspar	$\bar{x}$	43.5	2380	92	200	58	20
	s	16.1	538	35	100	22	11
	range	22.5-65.7	1630-3000	66-156	73-342	25-94	9-42
	n	6	6	6	6	6	6

		Li	Na_2O	Na/Li	Cs
Beryl	$\bar{x}$	2070	1.56	6.55	1380
	s	990	0.18	2.81	793
	range	1400-3520	1.30-1.72	2.74-9.14	260-2020
	n	4	4	4	4

Elements - ppm, oxides - wt.%. Symbols: $\bar{x}$ = arithmetic mean, s = standard deviation, n = number of samples analyzed.

Sky pegmatite.

The Sky pegmatite is a small tabular body, hosted by the Defeat granodiorite. It is a simple, homogeneous medium-grained pegmatite which strikes N 80° W and dips 51° W. Although zonation is absent, segregations of coarse-grained quartz + K-feldspar pods do occur. Saccharoidal albite and aplitic units are present locally. Rare-element mineralization occurs as green and white spodumene accompanied by minor manganocolumbite, which occurs in local pods of saccharoidal albite.

Jake-Da swarm.

The Jake-Da swarm consists of 13 pegmatite dikes; however, only the main dike which, was previously explored, was examined in this study. The Jake pegmatite outcrops for about 275 m, N 25° E from the N shore of Harding Lake. Other dikes of the swarm trend between N 25° E and N 25° W.

Rare-element mineralization includes abundant spodumene and minor amounts of montebrasite, triphylite, beryl, zircon and columbite-tantalite.

Assaying of pegmatite samples showed local concentrations of Ta and Nb at 126 ppm and 260 ppm, respectively, although the average concentrations were 22 and 53 ppm. Blocky or platy ferro- and manganocolumbite occur in cleavelandite + quartz + muscovite assemblage or as thin blades in muscovite replacing spodumene.

Paint swarm.

Four major NNE trending dikes define the Paint swarm which is located on the NW shore of Harding Lake. The largest dike, Body C, was the only one sampled and it outcrops for about 1060 m. Green and white spodumene, minor triphylite, beryl and columbite-tantalite are the only rare-element minerals present. Nb-Ta mineralization is present only as tiny blades of manganocolumbite in a cleavelandite + quartz + muscovite assemblage.

Upland Lake Series

The Pancho Pete and Jenne swarms make up the Upland Lake series. The pegmatites are situated W of Upland Lake and E of Jennejohn Lake respectively, and the nearest granite is the Cameron granite, 6 km to the NE (Figure 17). The Jenne dikes are the only ones in which Nb and Ta minerals were found. The dikes strike N 45° E with dips between 78° and 85° NW. The average outcrop length is about 137 m and the width varies from 0.6 - 1.2 m. The Jenne dikes are homogeneous with no obvious zonation. Spodumene and tiny blades of columbite-tantalite and cassiterite are present in a plagioclase + muscovite + quartz assemblage.

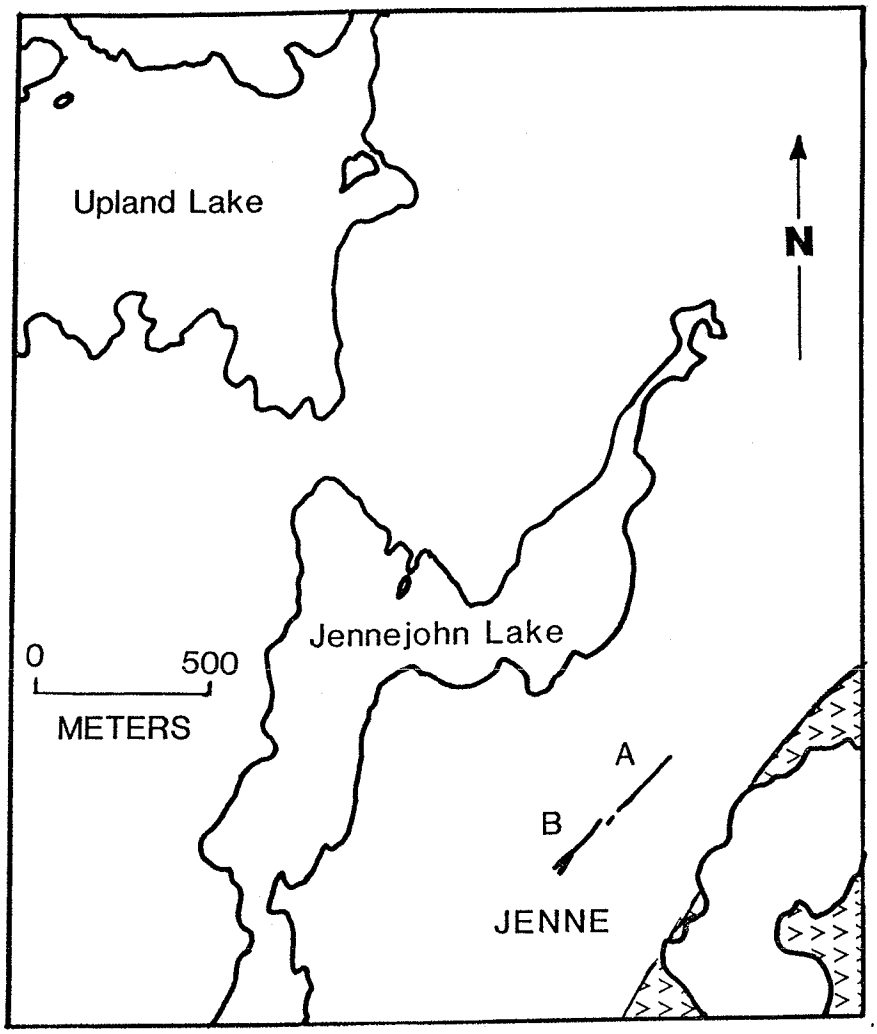

Figure 17: Location map of the Jenne pegmatite swarm. Symbols as shown in Figure 3.

Bighill Lake Group

This group includes the Big, Limo, Odin, Mint and Nite swarms, which occur within 3 km S of the Prosperous granite and N and SE of Bighill Lake (Figure 18). The pegmatites are typically spodumene-bearing with poor internal zonation and rare pods of albitization. Nb-Ta mineralization is scarce. The geochemical characteristics of the Bighill Lake group suggest a low degree of fractionation; however, the fractionation of pegmatites within the group spans a wide range (Table 19).

Big swarm.

The Big swarm lies immediately SE of Bighill Lake, approximately 19 km E of Yellowknife. Two systems of parallel dikes strike N 20° E across quartz-biotite schist which strikes N 70° E. The pegmatites dip steeply to the NW. The two pegmatite systems actually consist of smaller subparallel dikes which extend 1,280 and 1,067 m, respectively. Internal zoning is very poor to absent in most of the pegmatites; the texture varies from a medium-grained homogeneous assemblage of quartz + K-feldspar + plagioclase + muscovite to coarse-grained bodies displaying irregular banding of successive pink to white spodumene-poor aplitic units and spodumene-rich pegmatitic units.

Ferrocolumbite-manganocolumbite dominates the Nb-Ta mineralization and occurs as platy to tabular crystals in plagioclase + quartz ± muscovite. Ferrotapiolite and cassiterite occur as inclusions within columbite-tantalite. Rare uranium-bearing microlite is found replacing ferrotapiolite.

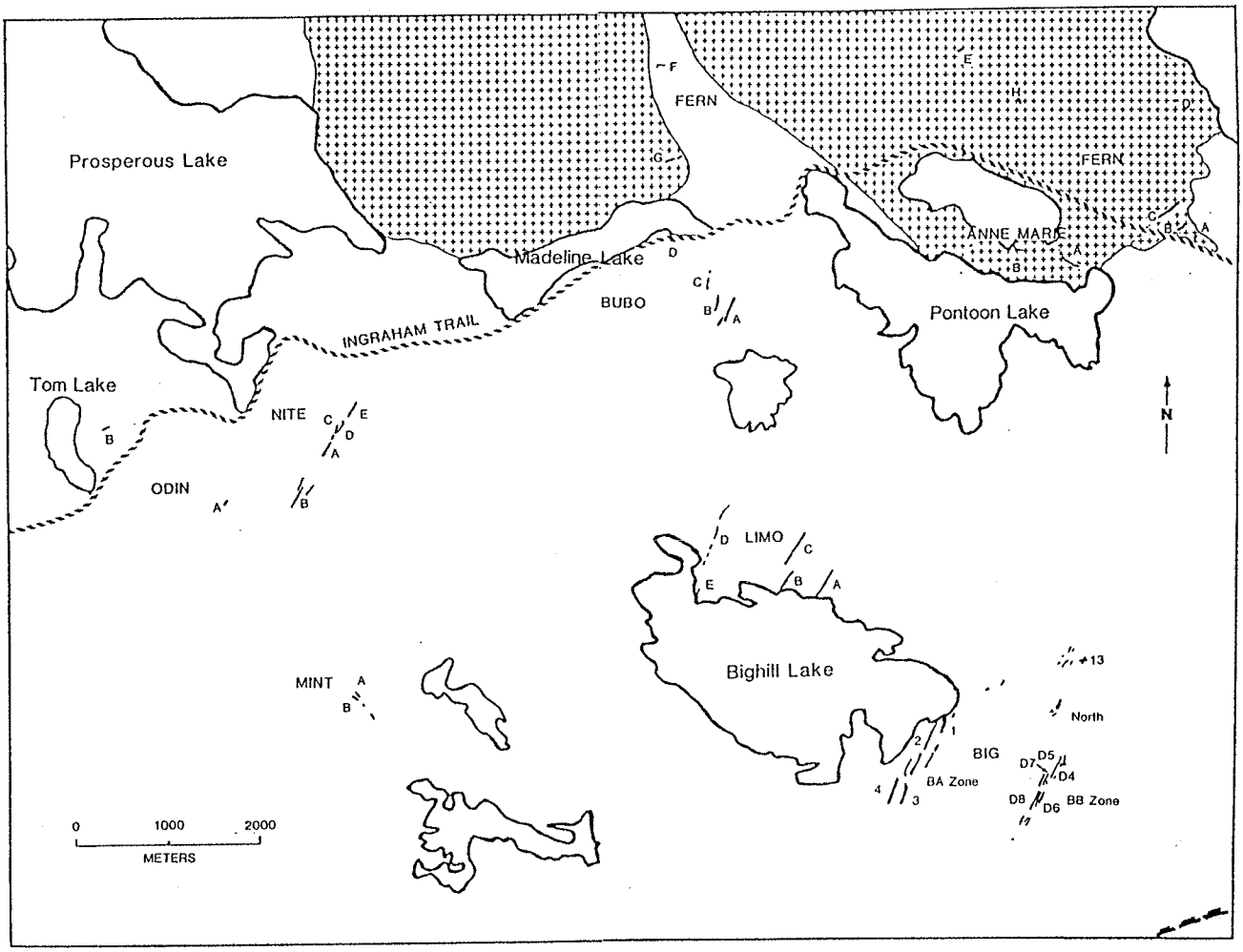

Figure 18: Location map of the Bighill Lake pegmatite group. Symbols as shown in Figure 3.

Table 19: Compositional characteristics of K-feldspar, muscovite and beryl for the Bighill Lake pegmatite group.

		K/Rb	Rb	Cs	Ba	Sr	Pb		
Blocky K-feldspar	$\bar{x}$	78.2	2590	111	87	34	25		
	s	71.8	2220	134	120	22	19		
	range	12.3-	286-	17-	<1-	6-	<1-		
		383	8760	650	485	85	75		
	n	33	33	33	33	33	33		
		Li_2O	K/Rb	Rb	Cs	Be	Nb	Ta	Nb/Ta
Platy muscovite	$\bar{x}$	0.075	27.0	4000	196	21	202	52	7.15
	s	0.047	15.3	2480	234	8	89	55	5.84
	range	0.007-	7.21-	1220-	43-	10-	22-	<8-	0.38-
		0.161	66.2	9600	1140	48	376	225	19.5
	n	28	28	28	28	28	27	27	24
		Li	Na_2O	Na/Li	Cs				
Beryl	$\bar{x}$	1190	1.00	9.87	2040				
	s	670	0.42	11.0	2480				
	range	54-	0.38-	1.79-	273-				
		2560	1.66	52.2	7800				
	n	19	19	19	19				

Elements - ppm, oxides - wt.%. Symbols: $\bar{x}$ = arithmetic mean, s = standard deviation, n = number of samples analyzed.

Limo swarm.

The Limo swarm lies to the N of Bighill Lake and like the Big swarm, it too is spodumene-bearing. The dikes generally trend NNE with bifurcation of the dikes occurring freguently. Dips vary greatly, but most dip steeply (70° - 85°) to the W. The largest dike outcrops for 550 m. However, in contrast to the Big swarm, the Limo dikes are conspicuously coarse-grained with more prominent internal zonation. Curiously enough, these dikes contain very little Nb-Ta mineralization, unlike the high con-

centrations found in the Bighill dikes. Rare fine-grained blades of columbite are found in saccharoidal albite.

Odin swarm.

The Odin A and Odin B pegmatites are small homogeneous bodies. Rare-element mineralization is poor, with spodumene occurring only in Body B and minor tantalite occurring in both bodies. Nb and Ta minerals occur disseminated in a cleavelandite + quartz ± muscovite assemblage and in the aplitic wall zone.

Mint swarm.

The Mint pegmatites (bodies A and B) are medium-grained spodumene-bearing dikes with essentially no internal zonation except for a local quartz + muscovite + spodumene core found in body B. In addition to spodumene, Nb and Ta minerals are the only other rare-element minerals found. The pegmatites strike N 35° E and N 40° E with near vertical dips. Nb-Ta mineralization is represented by columbite-tantalite, ferrotapiolite, ixiolite and minor microlite.

Nite swarm.

The Nite swarm is located 13 km NE of Yellowknife and 1.5 km S of Prosperous Lake. The pegmatites strike N 35° E and dip 50° to 85° SE. The main dike is 0.9 km long and averages 7.5 m wide. Minor en echelon pegmatitic and aplitic dikes occur along much of its length.

The Nite pegmatites are generally homogeneous with poor zonation. A minor aplitic wall zone consisting of fine-grained plagioclase + quartz + muscovite is discontinuous along its length. A medium-grained quartz + spodumene + plagioclase + muscovite intermediate zone comprises the bulk of the pegmatite. Saccharoidal albite occurs locally. Accessory minerals include beryl, spodumene, triphylite, apatite and columbite-tantalite.

Ixiolite with Mn > Fe and Ta > Nb, intergrown with manganotantalite and minor ferrotapiolite, occurs in the Mint as well as the Nite pegmatite.

Circle Lake Series

This series outcrops W of "Circle Lake", approximately 10 km W of the Duncan granite batholith (Figure 19). Only two pegmatites, Dr. Bob and Riber, comprise this series. They are the only bodies, within an area dominated by pegmatites of simple mineralogy, lacking internal zonation and rare-element mineralization, which contain Nb- and Ta-oxide minerals. The geochemical indicators show that the pegmatites of this series, particularly the Riber pegmatite, are among the more fractionated bodies in the entire field (Table 20).

Dr. Bob pegmatite.

The Dr. Bob pegmatite is a medium to coarse-grained, partly zoned pegmatite containing beryl, columbite-tantalite and cassiterite. The zonation consists of a fine- to medium-grained plagioclase + quartz + muscovite wall zone, a medium-grained K-feldspar + quartz + muscovite + cleavelandite intermediate zone which host the Nb, Ta and Sn minerals and a small quartz + K-feldspar ± beryl core. Albitization occurs locally in patches. Ferrocolumbite occurs as inclusions within anhedral grains of cassiterite. The cassiterite is associated with medium-grained cleavelandite.

Riber pegmatite.

The Riber pegmatite is the most fractionated and mineralogically diverse pegmatite in the series. It is emplaced in a quartz-biotite schist approximately 6 km N of Prelude Lake and 1.7 km W of the Duncan granite. The pegmatite strikes N 67° E and is exposed for 52 m with an average width

of 13 m. It is well-zoned and contains isolated pods of replacement lithian muscovite and albitization bodies. Rowe (1952) mapped and described in detail the zonation of the Riber pegmatite (Figure 20). The zones from the wall inward are:

1. fine- to medium-grained quartz + plagioclase ± muscovite wall zone,
2. coarse-grained quartz + plagioclase + muscovite ± schorl first intermediate zone,
3. medium- to coarse-grained quartz + plagioclase ± K-feldspar ± schorl ± second intermediate zone,
4. medium- to coarse-grained quartz + cleavelandite + muscovite ± beryl ± schorl ± elbaite ± apatite third intermediate zone,
5. medium- to coarse-grained quartz + cleavelandite + beryl + elbaite ± montebrasite fourth intermediate zone,
6. coarse-grained quartz ± elbaite core, and
7. coarse-grained K-feldspar ± quartz ± cleavelandite core.
8. Replacement unit

The diverse mineralogy of the Riber pegmatite exemplifies the complex nature of its zoning and high degree of fractionation. The list of rare-element minerals occurring in this pegmatite is impressive and includes amblygonite-montebrasite, triphylite, elbaite, beryl, zircon, columbite-tantalite, and rare lepidolite.

Nb-Ta mineralization occurs in zones 4 and 5 and is represented by blocky to prismatic manganotantalite along with subordinate platy ferrocolumbite enclosed in cleavelandite ± quartz ± muscovite or rarely amblygonite-montebrasite and tourmaline. Rare inclusions of ferrotapiolite and muscovite occur in manganotantalite. Uranium-bearing microlite occurs

as isolated subhedral grains or anhedral blebs replacing manganotantalite. The microlites show varying contents of U, Pb and Ca.

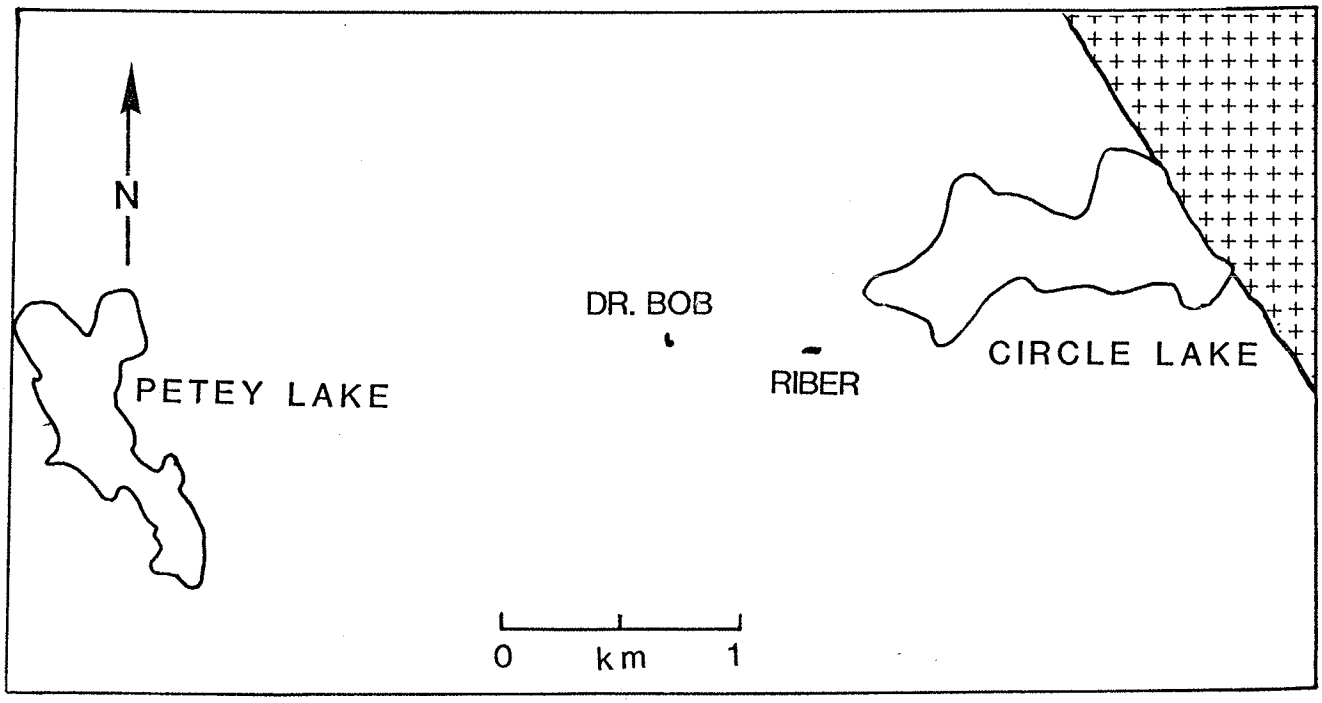

Figure 19: Location map of the Circle Lake pegmatite series. Symbols as shown in Figure 3.

Table 20: Compositional characteristics of K-feldspar, muscovite and beryl for the Circle series.

		K/Rb	Rb	Cs	Ba	Sr	Pb
Blocky K-feldspar	$\bar{x}$	37.4	5110	1680	195	76	3
	s	29.4	4160	990	223	13	4
	range	10.1-69.3	1530-10100	222-2350	10-494	58-87	<1-9
	n	4	4	4	4	4	4

		Li_2O	K/Rb	Rb	Cs	Be	Nb	Ta	Nb/Ta
Platy muscovite	$\bar{x}$	0.137	30.5	3400	100	21	159	23	6.91
	s	0.073	22.1	1960	64	3	nd	nd	nd
	range	0.081-0.220	14.2-55.8	1390-5300	38-166	18-24	nd	nd	nd
	n	3	3	3	3	3	1	1	1

		Li	Na_2O	Na/Li	Cs
Beryl	$\bar{x}$	778	0.98	9.93	7120
	s	391	0.39	3.46	9450
	range	407-1330	0.50-1.36	6.81-14.9	327-20900
	n	4	4	4	4

Elements - ppm, oxides - wt.%. Symbols: $\bar{x}$ = arithmetic mean, s = standard deviation, n = number of samples analyzed, nd = not determined.

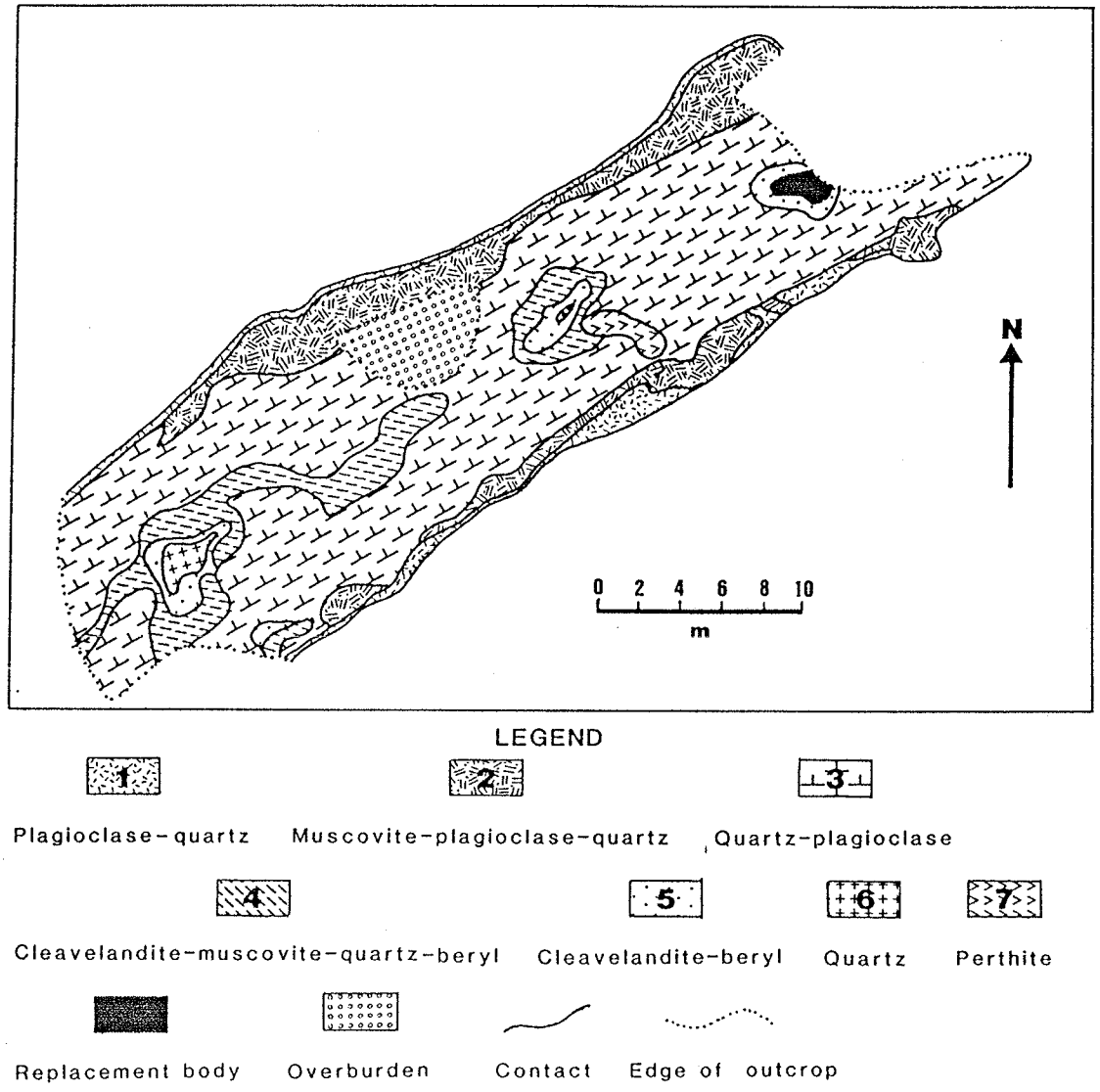

Figure 20: Geologic map of the Riber pegmatite. Modified after Rowe (1952).

CHAPTER 5

Mineralogy of Nb, Ta and Sn in the Yellowknife Pegmatite Field

Columbite-tantalite, ixiolite, ferrotapiolite, cassiterite and microlite are the only Nb-,Ta- and Sn-bearing minerals identified from the Yellowknife pegmatite field. They occur as rare accessory phases in pegmatites that are usually zoned and carry other rare-element minerals such as beryl, amblygonite-montebrasite and spodumene. The Nb-Ta-Sn mineralization is found in the border, wall, intermediate zones and core of the pegmatites. The Nb, Ta and Sn minerals are generally associated with the assemblage albite + quartz + muscovite , but they are also commonly found with late albitization and replacement muscovite bodies.

Columbite-tantalite group

Minerals of the columbite-tantalite group are the most abundant Nb- and Ta-bearing phases found in the Yellowknife pegmatite field and were identified in a large majority of the rare-element pegmatites examined. They are black with a submetallic luster and a black to dark greenish-gray to dark brown streak. In hand specimen, they are difficult to distinguish from ferrotapiolite or cassiterite. In transmitted light, columbite-tantalite is opaque, but shows a dark brown color in thin fragments. In reflected light, columbite-tantalite is bright pale gray. Many of the columbite-tantalites examined in polished sections were inhomogeneous, and contained inclusions of cassiterite, ferrotapiolite, microlite, albite, quartz, K-feldspar or pyrite. Zoning (Figure 21) and twinning is evident in several of the specimens but generally these features are absent.

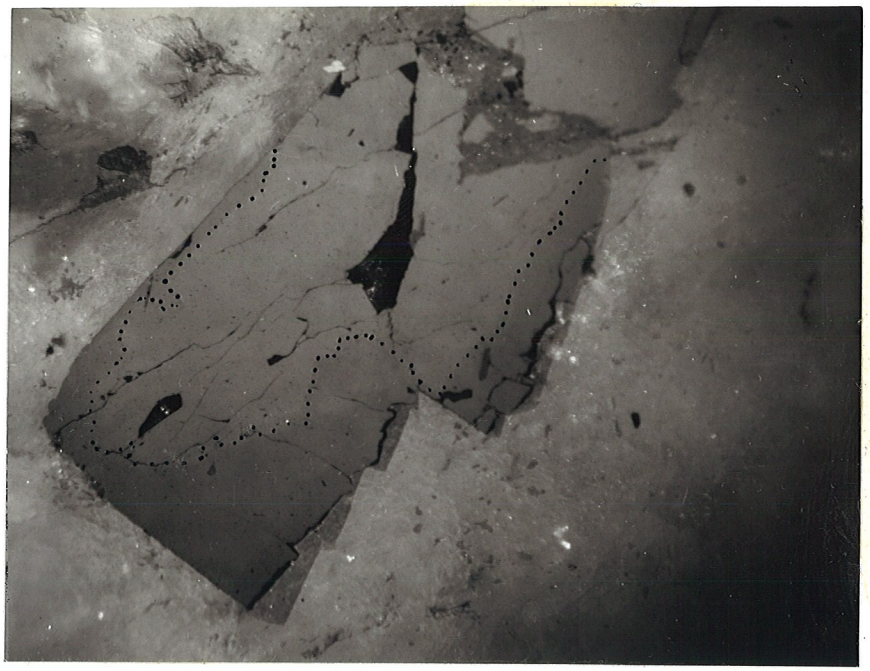

Figure 21: Compositionally zoned columbite-tantalite crystal from the Ann pegmatite. Dotted line denotes the boundary between zones. The Mn/(Mn + Fe) and Ta/(Ta + Nb) ratios of the zones are: light gray area - 0.32 and 0.27, respectively; dark gray area - 0.24 and 0.47, respectively. Magnification 10x.

The crystal morphology of columbite-tantalite varies from euhedral bladed, platy or tabular crystals to blocky, brick-shaped crystals and anhedral grains (Figures 22 - 26). Columnar crystals are present in some pegmatites, but their occurrence within the field is rare. Crystals may be found disseminated in saccharoidal albite (Figure 27), or as radiating tabular crystal aggregates associated with a medium-grained albite + quartz + muscovite assemblage (Figure 28), or as anhedral blebs included in ferrotapiolite or cassiterite (Figures 29, 30). In general, most columbite-tantalite is associated with medium-grained cleavelandite + quartz ± muscovite assemblages. Columbite-tantalite may also be associated with beryl, spodumene, amblygonite-montebrasite, triphylite or zircon.

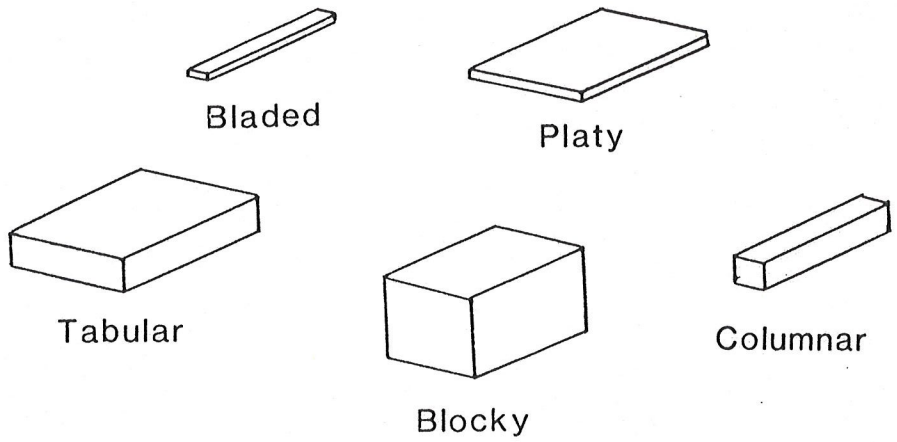

Figure 22: Diagrammatic representation of the crystal morphologies of columbite-tantalite observed in the Yellowknife pegmatite field.

Figure 23: Bladed crystals of columbite-tantalite from the Bin pegmatite.

Figure 24: Platy crystal of columbite-tantalite from the Lu pegmatite.

Figure 25: Blocky crystal of columbite-tantalite from the Moose pegmatite.

Figure 26: Anhedral crystals of columbite-tantalite in K-feldspar + lithium muscovite replacement pod from the Bet pegmatite.

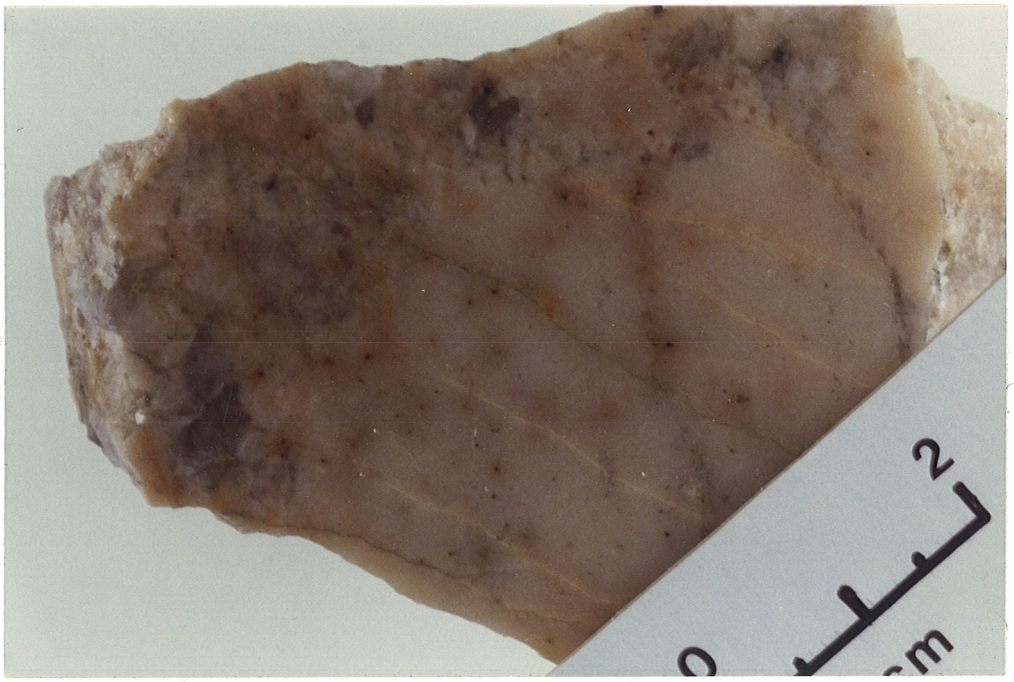

Figure 27: Crystals of columbite-tantalite in saccharoidal albite from the Moose pegmatite.

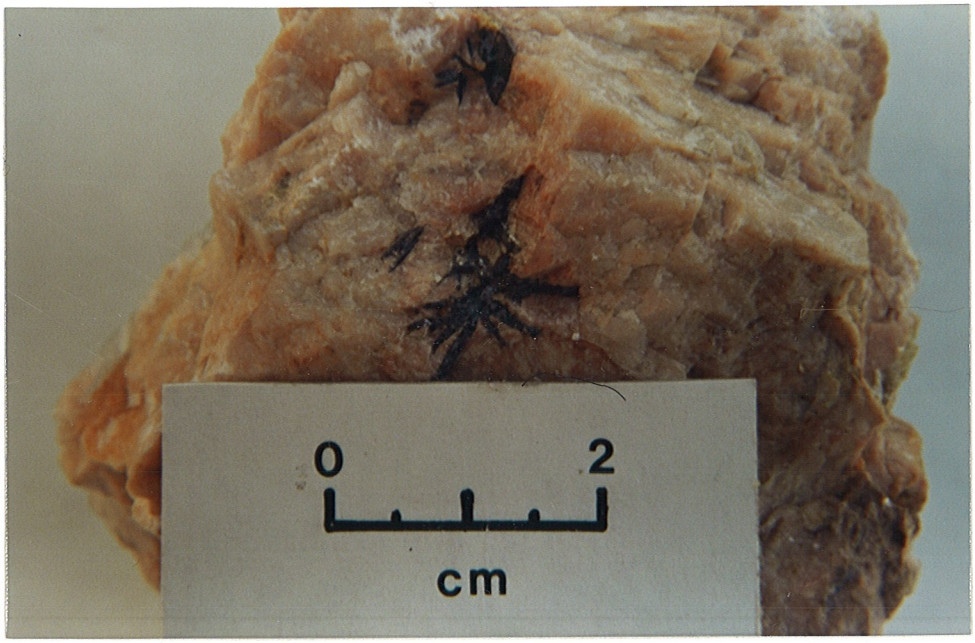

Figure 28: Radiating aggregate of tabular columbite-tantalite crystals from the Peg swarm dike # 93.

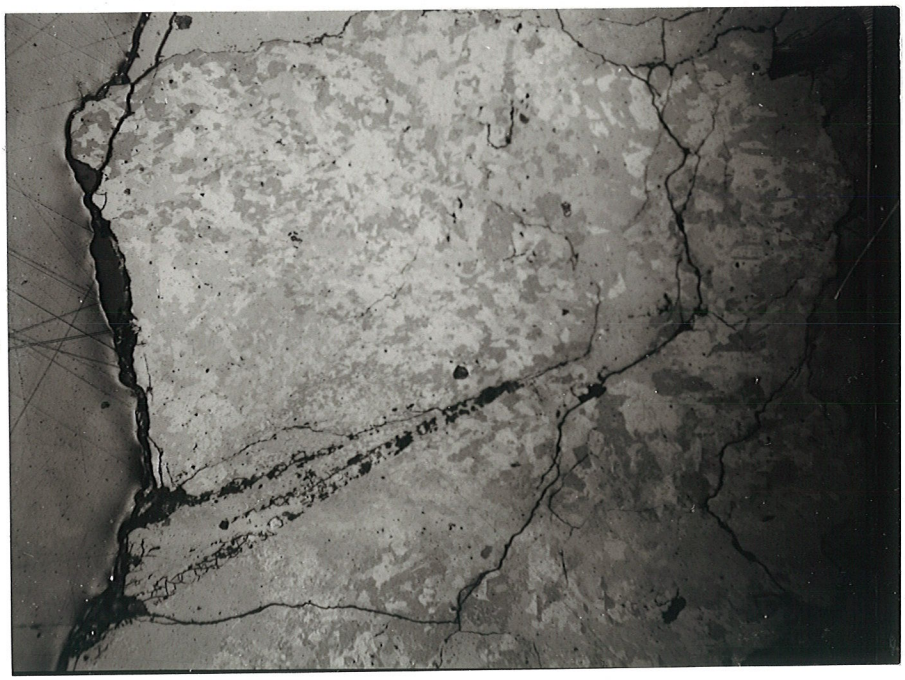

Figure 29: Ferrotantalite (light gray)-ferrotapiolite (dark gray) symplectite from the Casper "I" pegmatite. Magnification 10x.

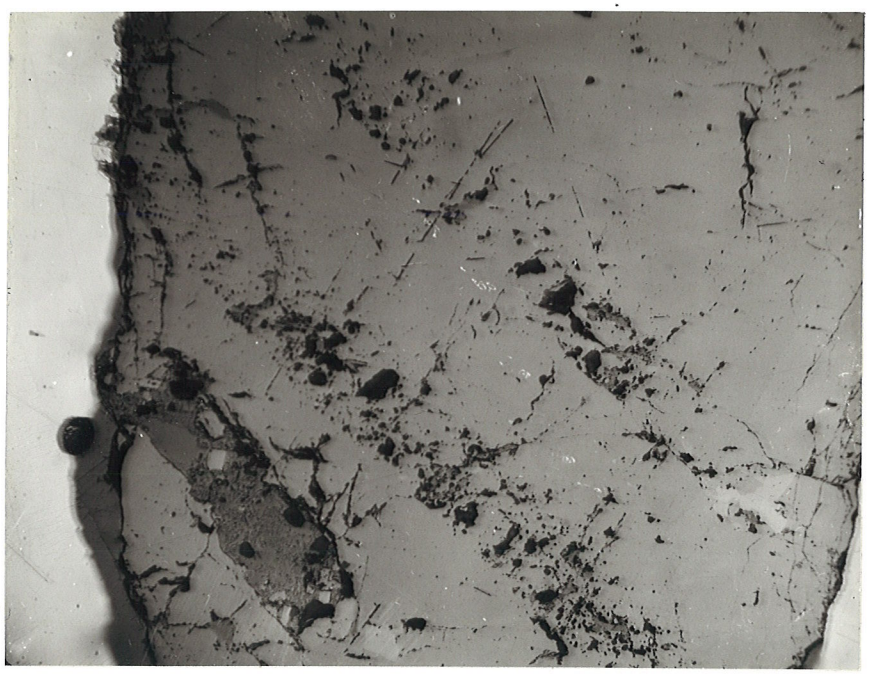

Figure 30: Inclusion of columbite-tantalite (light gray) in cassiterite (dark gray) from the Dr. Bob pegmatite. Magnification 10x.

Ixiolite

Ixiolite is rare in the Yellowknife field and occurs only in the Mac, Mint, Bin and Nite pegmatites. Its physical properties are very similar to those of columbite-tantalite, and a safe distinction between the two is possible only by X-ray diffraction methods and chemical analysis. Ixiolite from the Yellowknife field occurs only as anhedral grains in cleavelandite.

Tapiolite series

Ferrotapiolite is the second most abundant Nb- and Ta-bearing mineral in the Yellowknife field, occurring primarily in the Peg swarm located in the northeastern section of the field. Ferrotapiolite is found predominantly in lithium-poor pegmatites in a quartz + plagioclase assemblage and

occasionally with beryl or spodumene. It may be closely associated with columbite-tantalite and cassiterite, occurring as microscopic inclusions in either mineral. Epitaxial overgrowth by cassiterite is spectacular, but uncommon (Figure 31).

Ferrotapiolite is black with a submetallic luster and dark brown to black streak. It occurs most commonly as massive grains; rarely are crystal faces well-developed (Figures 32, 33). Twinned crystals were noted in several polished sections (Figure 34). Ferrotapiolite commonly contains inclusions of cassiterite or columbite-tantalite, along with various silicate minerals (Figure 35). Some ferrotapiolites contain inclusions of microgranular microlite, which may possibly be a product of ferrotapiolite alteration (Figure 36).

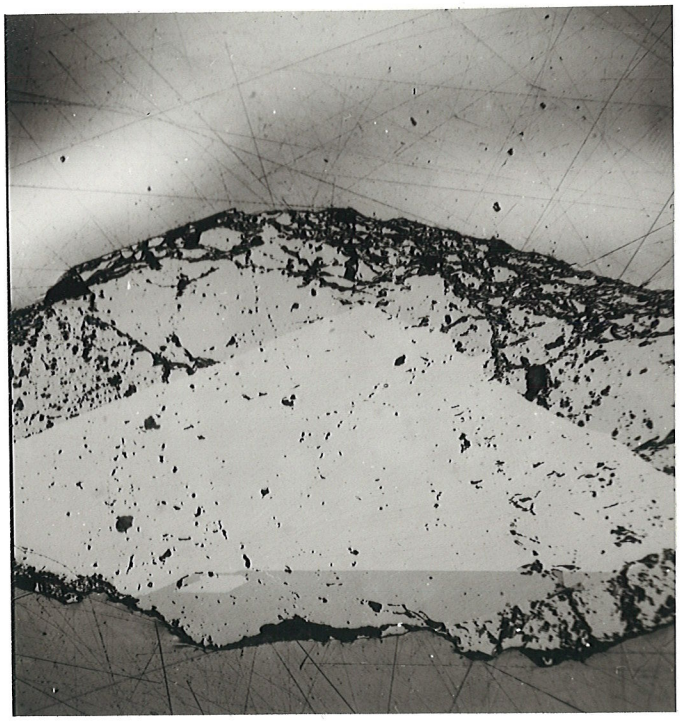

Figure 31: Cassiterite overgrowth on euhedral twinned ferrotapiolite crystal from the Tan #2 pegmatite. Magnification 10x.

Figure 32: Ferrotapiolite crystal from the Usk pegmatite.

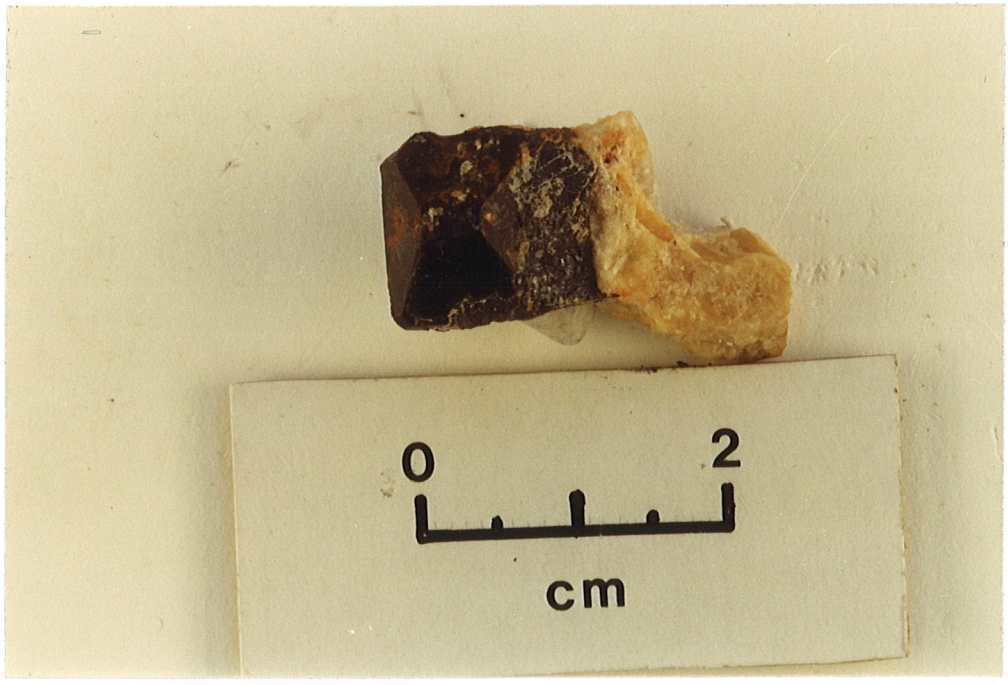

Figure 33: Ferrotapiolite crystal from the Peg #170 dike.

Figure 34: Twinned ferrotapiolite crystal from the Tan #2 pegmatite. Magnification 10x.

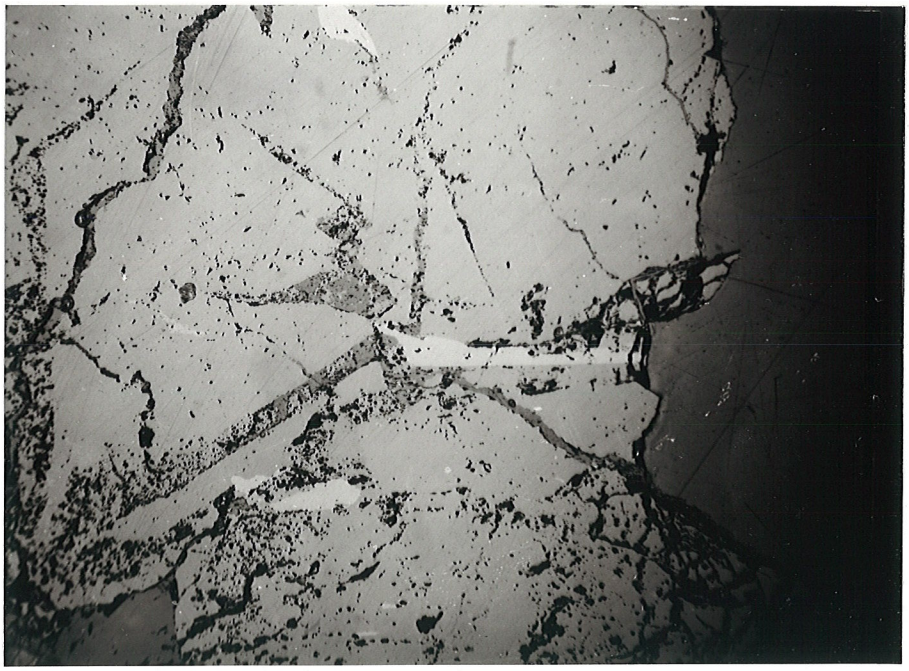

Figure 35: Cassiterite (white) inclusion in ferrotapiolite (gray) from the Tan #2 pegmatite. Magnification 10x.

Figure 36: Microlite (dark gray) - ferrotapiolite (light gray) symplectite from the Mint pegmatite. Magnification 10x.

Cassiterite

Cassiterite is common in many of the rare-element pegmatites, particularly those which contain spodumene. It is usually subordinate to columbite-tantalite or ferrotapiolite, although in some pegmatites it exists as the dominant phase. Cassiterite occurs primarily as massive anhedral grains, rarely showing crystal forms, or as veinlets in quartz + muscovite + plagioclase assemblages. It is black and is easily distinguishable from other Nb- and Ta-oxide minerals by its light brown streak.

Cassiterite may contain inclusions of columbite-tantalite, ferrotapiolite, quartz and feldspars. In polished sections, cassiterite may be observed as anhedral grains in columbite-tantalite, ferrotapiolite and ixiolite or as epitaxial overgrowths on ferrotapiolite (Figure 37). Twinning is common and present in many samples (Figure 38).

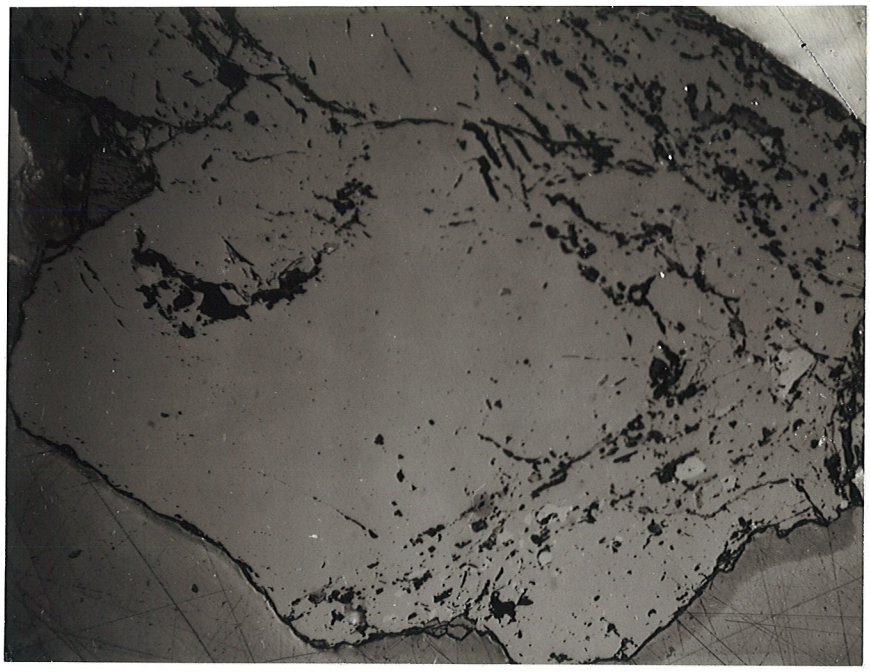

Figure 37:. Cassiterite overgrowth on ferrotapiolite from the Lu pegmatite. Note the inclusions of columbite-tantalite (light gray) in the cassiterite. Magnification 10x.

Figure 38: Twinned cassiterite crystal from the Jenne pegmatite. Magnification 10x.

Microlite

Microlite is rare in the Yellowknife pegmatite field and has been found primarily in the northwestern section of the field. It is inconspicuous in hand specimen and is only observable under a microscope as anhedral blebs replacing ferrotapiolite (Figure 36) or less commonly manganotantalite. Uranium-bearing microlite has been found in only a few localities, most notably the Riber pegmatite near Circle Lake. There it occurs not only as anhedral blebs in manganotantalite, but also as rare isolated subhedral crystals (Figures 39, 40).

Figure 39: Anhedral microlite inclusions (dark gray) in manganotantalite (light gray) from the Riber pegmatite. Magnification 10x.

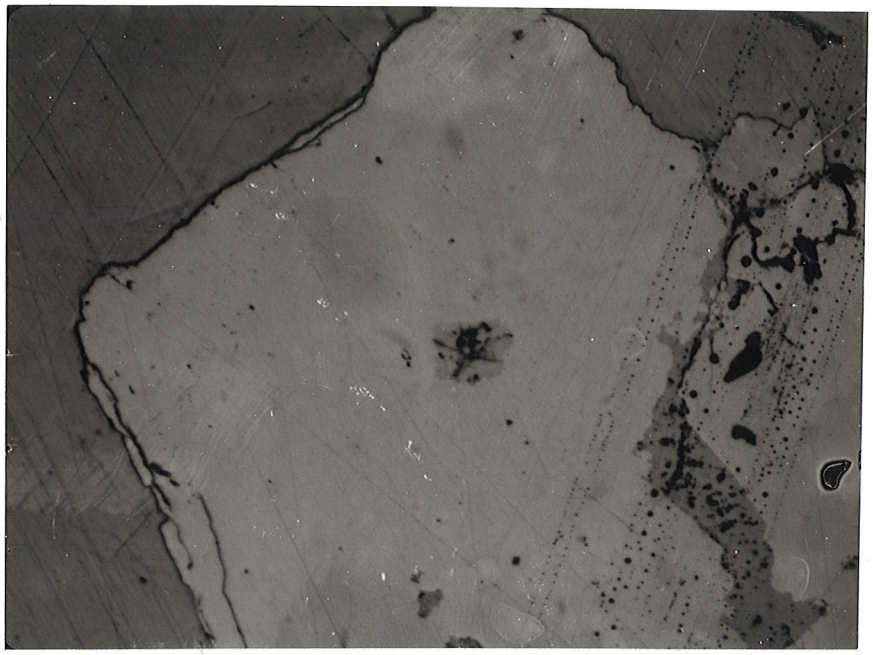

Figure 40: Subhedral crystal of uranmicrolite (dark gray) in manganotantalite from the Riber pegmatite. Magnification 36x.

CHAPTER 6

Columbite-tantalite Group

Introduction

The chemically and structurally diverse columbite-tantalite group dominates the Nb-, Ta- and Sn-oxide mineralogy of the Yellowknife pegmatite field and has, in the past, been the subject of much economic interest (cf. Chapter 1). The columbite-tantalite structure is closely related to that of ixiolite and the two will be discussed together along with the wodginite structure. Chemically, the columbite-tantalite group is quite variable, showing extensive isomorphous substitution among divalent, trivalent, quadrivalent and pentavalent cations.

α-PbO_2 related structures

The crystal structure of ixiolite is of truly orthorhombic α-PbO_2 type, with a completely random distribution of cations resulting in a completely disordered structure. The structure crystallizes in the space group Pbcn, Z=1, and forms the basic sub-structure of the ordered columbite-tantalite and wodginite structures. Figure 41 shows a comparison of the ixiolite, columbite-tantalite and wodginite unit cells. Grice et al. (1976) solved the ixiolite structure and verified it as being the columbite substructure proposed by Nickel et al. (1963a).

The α-PbO_2 structure, henceforth referred to as the ixiolite structure, is characterized by zig-zagged chains of edge-sharing distorted

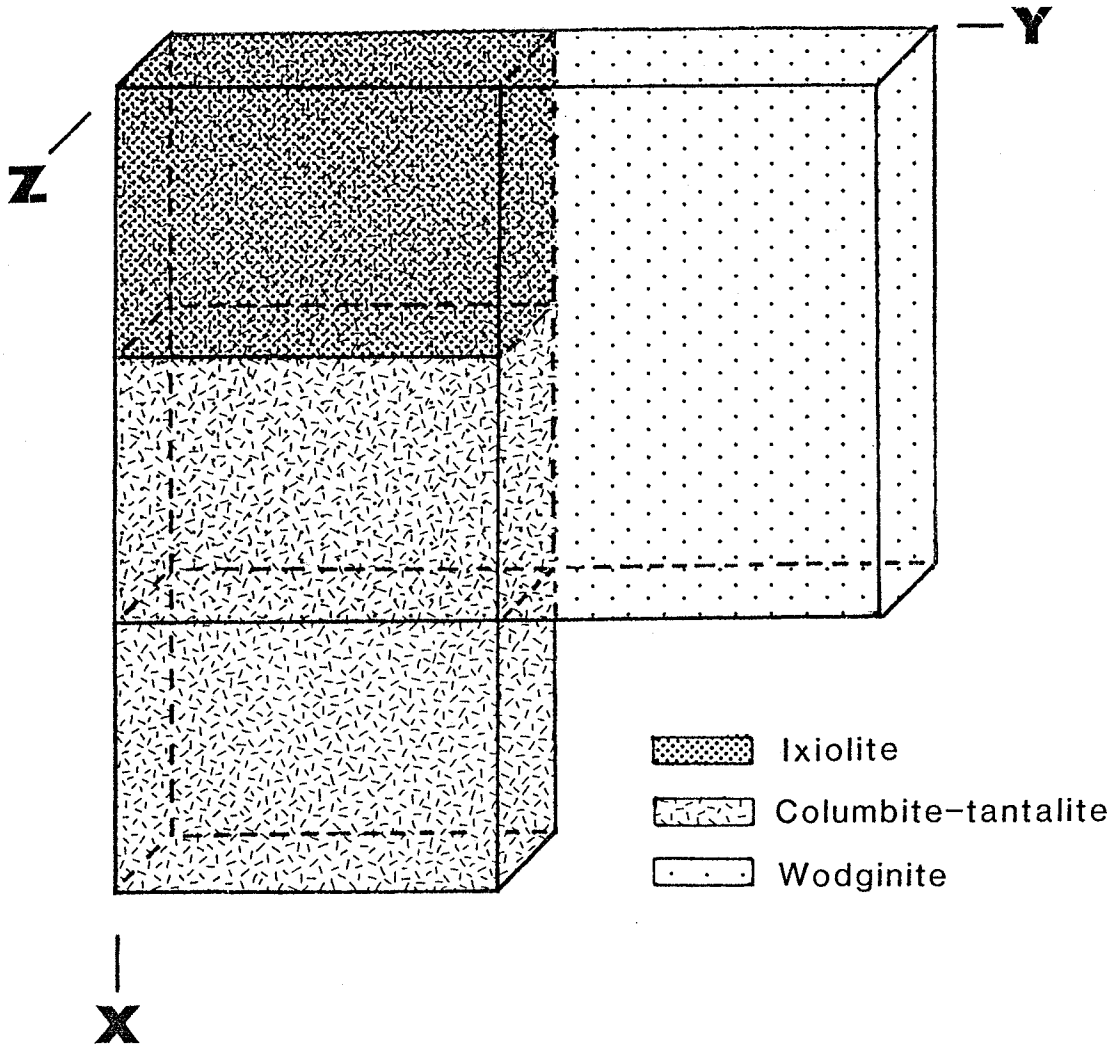

Figure 41: Comparison of the ixiolite, columbite-tantalite and wodginite unit cells. After Grice et al. (1976).

octahedra (Figure 42). The oxygens form a pseudo-hexagonal close-packed layer parallel to (100). The chains run parallel to the c axis and are linked together by shared octahedral corners of the adjacent chains. Each oxygen is coordinated by three cations.

Columbite-tantalite group minerals have the general formula AB_2O_6 in which A = Mn, Fe^{2+},Mg and Ca and B = Nb, Ta, space group Pbcn with Z=4. The columbite structure, first solved by Sturdivant (1930) and later refined by Foord (1976), Grice et al. (1976) and Weitzel (1976), is also characterized by the same close-packed arrangement and octahedral linkage that occurs in the ixiolite structure. Nickel et al. (1963a) were the first to observe that the columbite structure was actually an ordered derivative of the ixiolite structure. The A- and B-cations order into two distinct sites in layers parallel to (100) with one layer of A-bearing chains followed by two layers of B-bearing chains along the a axis. This results in a tripling of the the a unit cell dimension of ixiolite (Figure 43).

The similarity between the ixiolite and the wodginite structures was first inferred by Nickel et al. (1963b). Their findings suggested that wodginite was a superstructure of ixiolite. The details of the wodginite structure were first published by Grice (1973) and his data were re-refined to the currently accepted model by Ferguson et al. (1976).

The wodginite structure is monoclinic, space group C 2/c, Z=4 with a general formula corresponding to ABC_2O_8. As in columbite, oxygens form hexagonal close-packed layers perpendicular to (100), and the structure also contains chains of staggered edge-sharing octahedra which run parallel to the c axis. However, in wodginite, cations order into three distinct

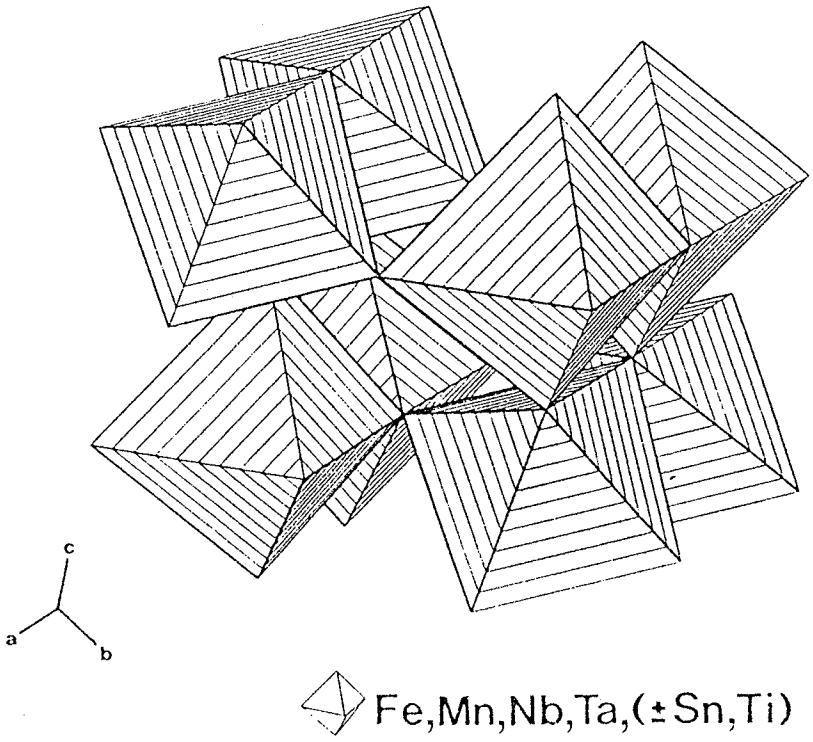

Figure 42: Crystal structure of ixiolite. All cations are randomly distributed over all cation sites resulting in statistically identical cation polyhedra throughout the structure.

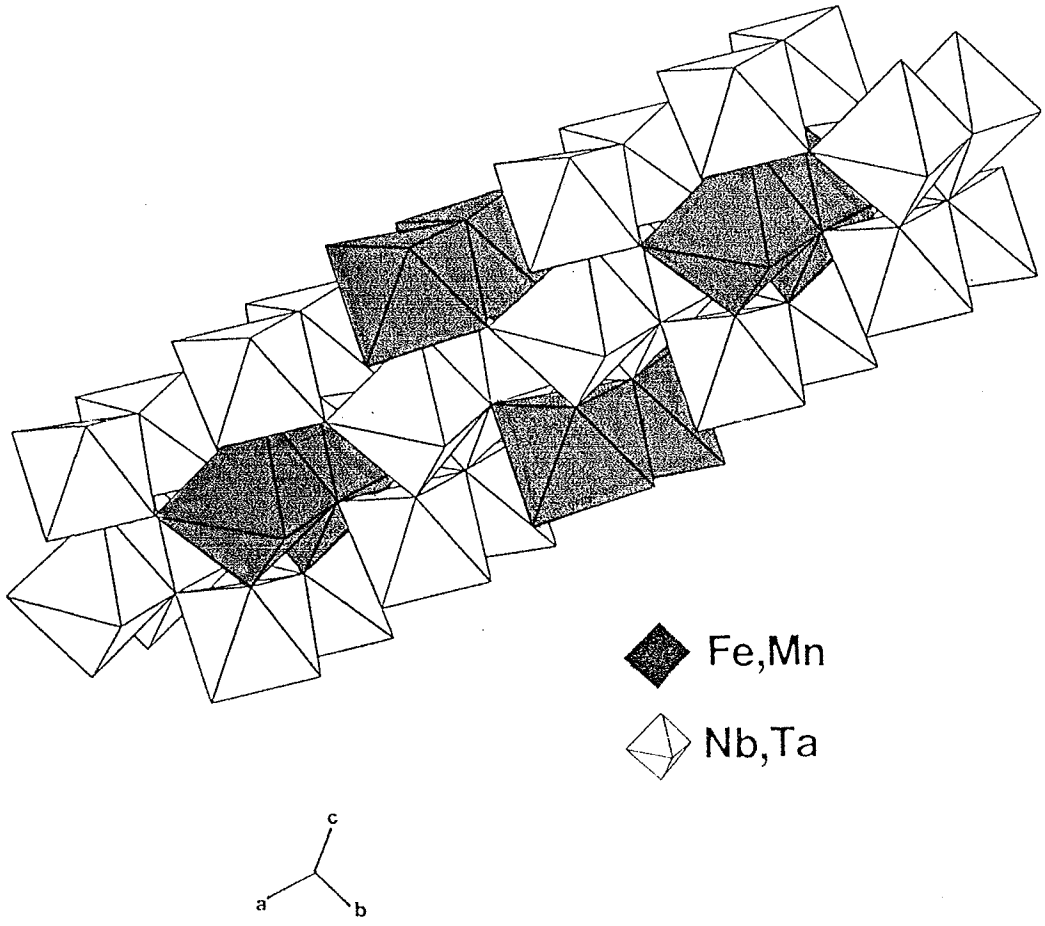

Figure 43: Crystal structure of ordered columbite-tantalite. Two unique cation sites, A and B, are occupied by (Fe, Mn) and (Nb, Ta), respectively.

sites instead of the two found in the columbite structure. The A-site is dominated by Mn and Fe^{2+}, the B-site by Sn, Ti, Ta and the C-site by Ta and Nb. This ordering scheme results in a doubling of both the a and the b dimensions of the ixiolite subcell.

The wodginite structure consists of two types of chains; one consisting of A- and B-site coordination polyhedra and the second type consisting only of C-site coordination polyhedra (Figure 44). In any given layer, only one of these two types of chains exists such that layers of A + B chains alternate with layers of C chains.

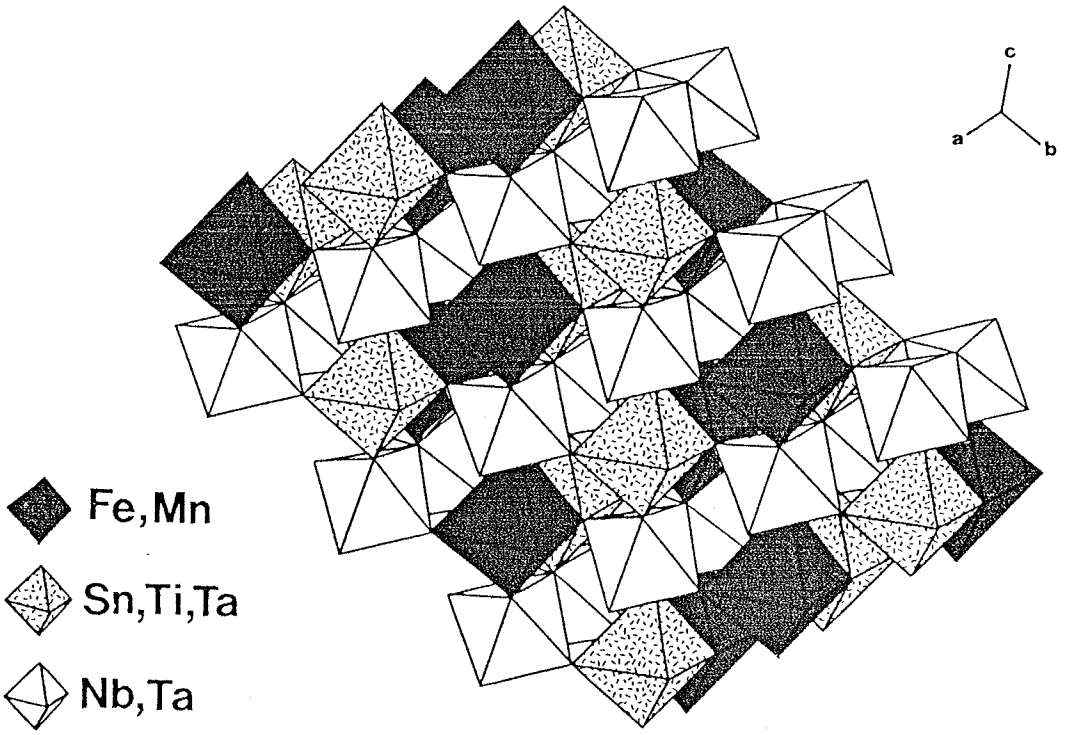

Figure 44: Crystal structure of ordered wodginite.

X-ray crystallography

Order-disorder relationships

The crystal structure of naturally occurring columbite-tantalite typically shows varying degrees of cation ordering. The structure may vary from fully ordered (columbite-tantalite of Sturdivant, 1930) through various stages of intermediate ordering up to nearly fully disordered ("pseudo-ixiolite" of Nickel *et al.*, 1963a).

These structural variations have created much confusion concerning the nomenclature of this mineral group. The names columbite and tantalite are customarily assigned to members of the group which have the fully ordered columbite structure. Nickel *et al.* (1963a) assigned the name "pseudo-ixiolite" to the disordered columbite structure. However, the name "pseudo-ixiolite" is not recognized by the IMA as a legitimate mineral species and thus the name ixiolite is commonly used to describe any disordered structure. It is true that the disordered structures of columbite and wodginite are nearly identical and that the true structure type can only be ascertained by ordering the disordered structure by heat treatment. It is this aspect which led to the definition of "pseudo-ixiolite"; upon heating it reverts to the columbite structure, whereas, ixiolite reverts to the wodginite structure. Obviously closer comparison of the disordered structure types is neccessary to avoid future confusion. For the moment, only the name of the species modified by the adjectives "ordered" (76 - 100% order), "partially ordered" (26 - 75% order) and "disordered" (0 - 25% order) will be used to describe columbite-tantalite structures. The use of the name ixiolite will be restricted to minerals with highly disordered structures which transform into wodginite after heating.

Presently, the exact cause of cation disorder is poorly understood. Two different interpretations have been proposed for ordering in columbite-tantalite. Graham and Thornber (1974b) proposed a unique "metamictization" which leads to the breakdown of initially homogeneous, but complex, non-stoichiometric phases into submicroscopic intergrowths of several phases of simple stoichiometry. The resulting mixture generates disordered columbite-tantalite X-ray diffraction patterns (cf. Ewing, 1975 and Graham, 1975). However, experimental studies indicate that the initial growth of synthetic columbite-tantalite occurs in a disordered state and only attains partial to complete ordering upon extended subsolidus heating (Moreau and Tramasure, 1965; Komkov and Dubik, 1974). The metastable high-energy disordered structure apparently forms within the stability field of the ordered structure; ordering evolves from the disordered structure in solid state. At low PT conditions the disordered state is more persistent than at higher PT conditions where the disorder-order transition is more rapid.

Variation in structural states may have been controlled by factors related to the pegmatite crystallization history or pegmatite fluid composition. Rapid cooling would tend to favor the preservation of disordered structures, whereas slower cooling at high temperatures would tend to promote ordering. Electrostatic energy calculations by Giese (1975) suggest that columbite-tantalite of different structural states should form with equal ease. Clearly other factors are involved, and the most obvious is compositional variations, particularly the presence of "impurity" cations such as Ti, Sn and Sc. The presence of these trivalent and quadrivalent cations in the structure may disrupt the stoichiometry and contribute to the growth in the disordered state. With the exception of Ti, variation

diagrams of composition versus degree of order in the Yellowknife columbite-tantalites showed little correlation. A slight correlation is observed when (Ti+Sn+Sc)/(Ta+Nb) is plotted against the degree of order of natural specimens (Figure 45). It is apparent from the cation-order plots that Ti, and not Sn or Sc, contributes the most to the trend. As Ti is generally concentrated in the early crystallizing columbite-tantalite, the above trend suggests that the degree of order might be indirectly related to the degree of pegmatite fractionation.

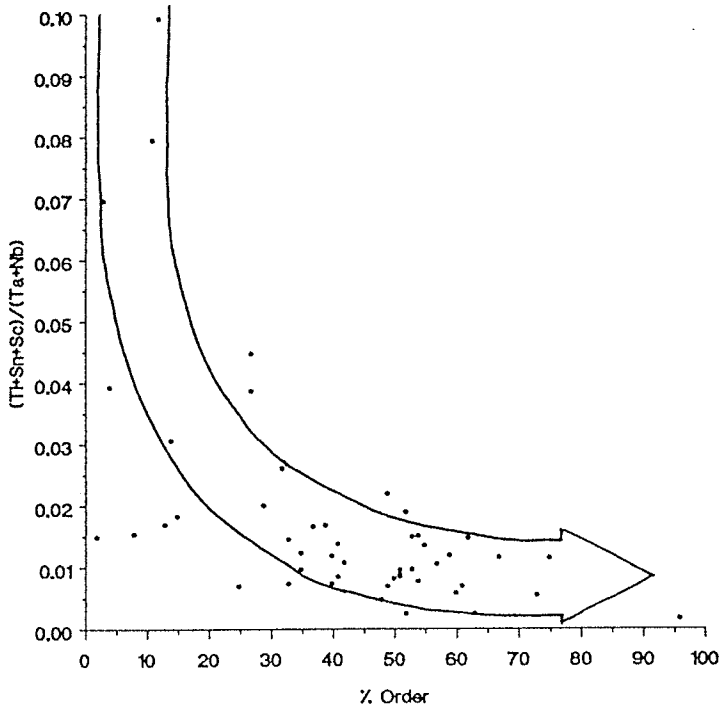

Figure 45: Plot of (Ti+Sn+Sc)/(Ta+Nb) versus percent order in columbite-tantalite from the Yellowknife field.

Structural state variations in columbite-tantalite

An extensive data base of columbite-tantalite unit cell dimensions has been collected by Černý and Ercit (1985) and their results show a wide range of structural states. At present, there is no accurate means of quantifying the degree of order in columbite-tantalite, except by crystal structure refinement. Early attempts by Nickel et al. (1963a) were based on the comparison of the intensities of the (200) and (110) supercell reflections. In the columbite structure, reflections with $h \neq 3$ may show diminished intensities or become absent as disorder increases.

Because the a and c unit cell dimensions are strongly sensitive to structural changes, Komkov (1970) suggested the use of the a/c ratio, in the space group setting Pbcn, as an indicator of degree of order. The unit cell expands along c and contracts along a with increasing disorder, and consequently the a/c ratio decreases with increasing disorder. However, this method does not take into account the chemical variability in the series which also influences the unit cell dimensions. The a/c ratio also varies with chemical composition: e.g., 2.825 to 2.839 for ordered states in ferrocolumbite and manganotantalite, respectively. The a/c ratio of disordered states is more restricted (2.76 - 2.77) and not as sensitive to compositional changes.

Černý and Turnock (1971) devised a graphical method of representing the degree of order. Their a vs. c plot proved useful in illustrating structural variations in the columbite-tantalite group. For direct comparison of ordered and disordered unit cells, the a dimension of the disordered phase is multiplied 3x. The plot is also quite useful in estimating the Fe/Mn ratio, yet it is relatively insensitive to changes in the Nb/Ta ratio.

Presently the a-c plot is based on synthetic ordered $FeNb_2O_6$, $MnNb_2O_6$ and $MnTa_2O_6$ of Wise et al., (1985b) (Figure 46). The data of disordered $(Mn,Ta)O_2$ were selected from the extreme values of naturally occurring samples approaching this composition. The values of disordered $(Fe,Nb)O_2$ is approximated as the "intersection of the empirical borderline for $(Fe<>Mn,Nb<>Ta)_4O_8$ compositions with the average slope of tielines drawn from the ordered $FeNb_2O_6$ corner" (Černý and Ercit, 1985).

As stated previously, disordered phases convert to ordered phases upon heating. When cell dimensions from both the natural and heated samples are plotted on the a-c diagram, tie-lines joining the two points may be drawn to represent a heating vector or path of ordering. Heating vectors are typically parallel to subparallel; however, crossing tie-lines are occasionally observed. Possible causes of deviant tie-line slopes will be discussed in following sections.

Recently Ercit (1986) improved the a-c plot and derived equations for calculating the degree of order and mole fraction of Mn from the unit cell dimensions. Assuming that all lines of equal order are parallel, he calculated the average slope of a line drawn through the data of Wise et al., (1985b) which represented 100% order. A line of identical slope was extrapolated from the most fully disordered natural sample of columbite-tantalite to represent 0% order. The degree of order is found through the linear interpolation between the ordinate intercepts of the 0% and 100% lines. From this, Ercit derived the following equations:

$$y=c-0.2329 * a$$

$$\% \text{ order}=1727-941.6 * y,$$

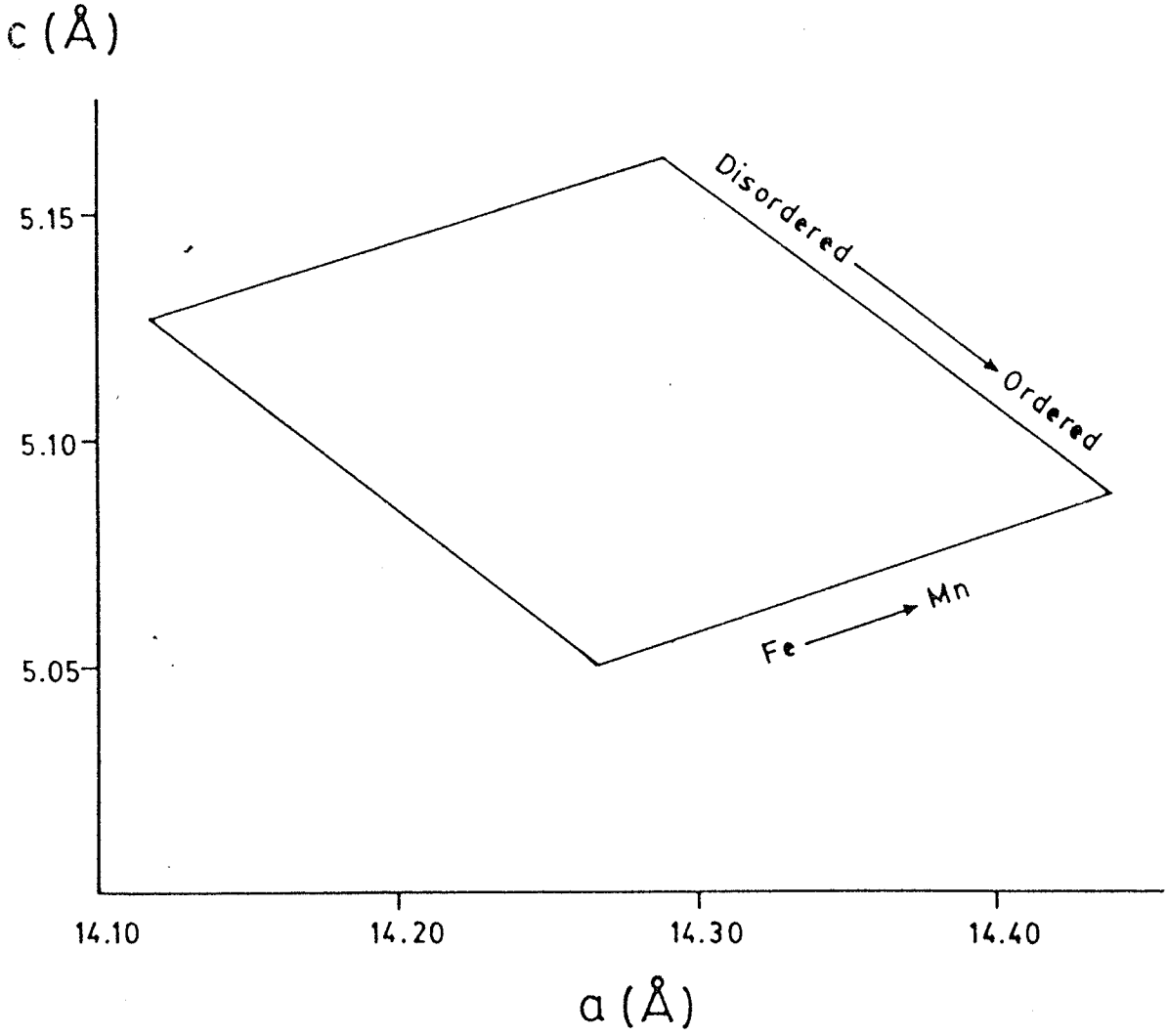

Figure 46: Order-disorder diagram for the columbite-tantalite group. The a cell dimension is expressed for all phases using the ordered cell size. After Ercit (1986).

where a and c are the unit cell dimensions. The accuracy was determined to be ±5%, which is acceptable considering allowances were not made for the "contamination" of the sample by impurity elements (Ca, Mg, Sc, Fe^{3+}, Ti, Sn, W).

The unit cell dimensions of the Yellowknife columbite-tantalites determined by X-ray powder diffractometry are given in Appendix B along with the calculated degree of order. Although the percent order of the Yellowknife specimens extend over a large range, most specimens fall between 40 - 50% order.

Heating vectors

Comparison of the disordered and ordered state in columbite-tantalite can be made by plotting the a and c cell dimensions on an a-c diagram and connecting the points with a tie-line. An examination of the tie-line slopes from the Yellowknife data shows that most slopes fall in the range between -0.5 and -0.8 with the ideal average slope calculated at -0.666 (Figure 47). However, quite frequently tie-lines deviate from the ideal slope and on occasion cross one another. The reason for crossing tie-lines is not apparent and may be due to a number of factors. Several causes of deviated tie-lines are presented for discussion:

1. Chemical inhomogeneity in the crystal,
2. Substitution by R^{3+} R^{4+} cations,
3. New mineral phases produced as a result of heating.

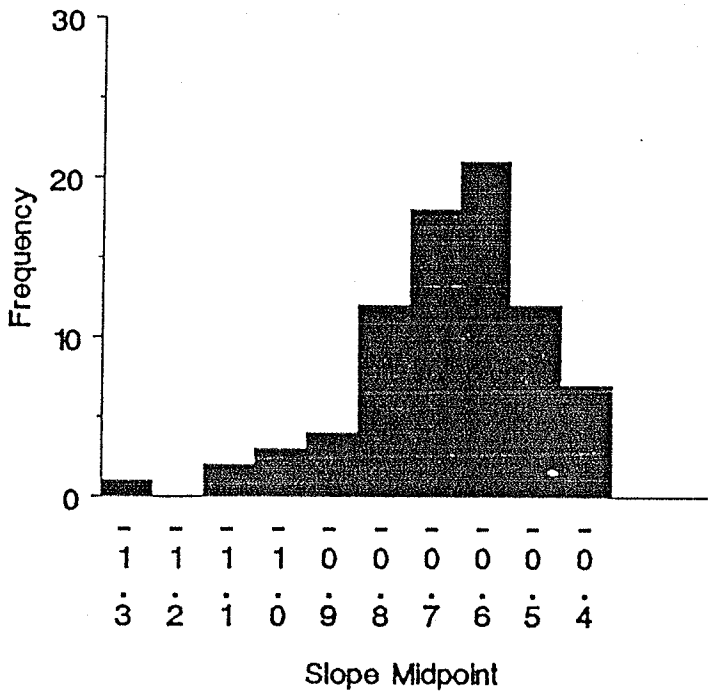

Figure 47: Histogram of Yellowknife columbite-tantalite tie-line slopes.

Chemical inhomogeneity

Electron microprobe analyses of the Yellowknife columbite-tantalites show widespread chemical inhomogeneity within a single crystal. Occasionally, large areas of varying chemistry are present within a crystal and fragments may be selected from one grain with remarkable differences in chemistry and unit cell dimensions. Tie-lines drawn between unit cell dimensions derived from fragments of such chemical diversity may result in slopes noticeably divergent from the ideal.

Content of R^{3+} and R^{4+} cations

Wise et al. (1985b) observed that the columbite-tantalite unit cell parameters are strongly influenced by Fe-Mn substitution and to a lesser degree by Nb-Ta substitution. This implies that the A-site chemistry is primarily responsible for the variations observed in the unit cell dimensions. Substitution of significant quantities of R^{3+} and/or R^{4+} cations into the columbite-tantalite structure might also cause noticeable effects on the a and c unit cell dimensions. Incorporation of Fe^{3+} or Ti at the A or B site should result in lower a and c dimensions, the decrease being a consequence of the smaller size of the substituent cation. The substitution of Sn at the A site might have a similar effect as Fe^{3+} and Ti, but concentration at the B site would result in an increase in cell size due to the larger radius of Sn relative to Nb or Ta. However, as the substitution of Sn into the columbite-tantalite structure involves both sites, it is probable that the overall effect would be a shrinkage of the unit cell.

In the disordered phase, the site occupancies of R^{3+} and R^{4+} cations would not require any special considerations, as all cations are statisti-

cally distributed and hence the calculated unit cell dimensions would be a true measure of the overall structure. Upon ordering, the R^{3+} and R^{4+} cations must occupy definite positions within the structure, according to strict substitution schemes. Thus it is the ordered phase which would deviate from the ideal structure due to cation substitution. As a result, the observed unit cell dimensions of ordered phases containing substantial R^{3+} or R^{4+} cations tend to be smaller than ordered phases lacking these cations. Thus the general slope of the tie-lines of "contaminated" ordered phases may be considerably steeper than the ideal.

New mineral phases produced by heat treatment

The heating of disordered phases often results in the formation of other Nb, Ta and Sn phases, either by (i) ordering of R^{3+} and R^{4+} cations, (ii) exsolution of mineral constituents, or (iii) reaction with contaminating minerals. The formation of new phases will greatly affect the unit cell dimension of the heated ordered columbite-tantalite primarily because of partitioning effects between the coexisting phases.

Ordering of isomorphous R^{3+} and R^{4+} cations during subsolidus heating, may result in the formation of minor Nb- or Ta-rich phases, depending on the bulk composition of the natural specimen. Most of the concern in heating experiments centers around the oxidation of Fe^{2+} to Fe^{3+} and its resultant products, $FeNbO_4$ or $FeTaO_4$. Athough it has been shown by Grice (1970) that the oxidation of Fe^{2+} is negligible under the heating conditions described previously (cf. Chapter 3), there are occasions when considerable $FeNbO_4$ or $FeTaO_4$ is produced. This is dependent largely on the Fe:Nb or Fe:Ta ratio of the bulk composition. If these ratios deviate significantly

from the normal columbite stoichiometry, either as a result of Fe oxidation or due to isomorphously incorporated Fe^{3+}, then some $FeNbO_4$ or $FeTaO_4$ phase will be created during heating.

The occurrence of these phases coexisting with columbite-tantalite suggests that the limits of $Fe^{3+}(Nb,Ta)O_4$ - $(Fe,Mn)(Nb,Ta)_2O_6$ solid solution has been reached; at 1180° C, approximately 15 mol. % $FeNbO_4$ can occur in columbite isomorphously (Turnock, 1966). This incorporation of Fe^{3+} into the columbite structure will cause a decrease in the unit cell dimensions due to the much smaller ionic radii of Fe^{3+} compared to Fe^{2+} or Mn.

Similarly, substantial quantities of Sn in the columbite structure may result in the formation of a wodginite phase in addition to ordered columbite-tantalite. Komkov (1970) suggested that a wodginite phase would form on heating if more than 1-2% SnO_2 was incorporated into the columbite structure. The solid solution of $(Fe,Mn)(Nb,Ta)_2O_6$ - SnO_2 has not been accurately determined experimentally, although Schröcke (1966) estimates that at 1000° C, about 5 mol % SnO_2 will enter the columbite structure isomorphously.

When a wodginite phase does form under favorable stoichiometry, preferential partitioning of Mn and Ta into the wodginite phase will result in an Fe- and Nb-enriched columbite. The net result would be to create a columbite with a unit cell smaller than the unheated disordered sample.

Ferrotapiolite might also occur in the heated patterns due to exsolution. For example, given a homogeneous ferrotantalite phase, the following exsolution reaction might occur:

$$(Fe,Mn)_2(Ta,Nb)_4O_{12} \longrightarrow MnNb_2O_6 + FeTa_2O_6,$$

The presence of a ferrotapiolite phase would result in an increase in the slope from the ideal due to the preferential partitioning of Fe and Ta into the tapiolite phase. This in turn results in Mn- and Nb-enrichment in the remaining orthorhombic phase; hence, larger unit cell dimensions are attained than determined for the unheated phase of intermediate composition.

Reaction with associated Nb, Ta and Sn minerals may produce unwanted phases which will affect the bulk composition of the ordered columbite-tantalite. The most conspicuous reaction is between columbite-tantalite and cassiterite to form wodginite. The effect of wodginite formation on the composition of columbite has been discussed above, and as a precaution, the unheated pattern should be carefully checked for cassiterite admixture before heating. Reactions with adjacent silicate minerals seem to be negligible, but should be avoided nonetheless. Minerals with Ca-rich compositions may allow for the production of fersmitic phases.

To summarize, the presence of Nb, Ta and Sn phases other than columbite-tantalite will greatly affect its unit cell dimensions. Care should be exercised when selecting mineral grains for heat treatment, and if possible, only homogeneous phases should be used. In most instances, however, this is not always possible and the researcher should be wary of the possible production of contaminant phases.

Chemistry

The mineral chemistry of the columbite-tantalite group may be represented diagrammatically on the "columbite quadrilateral", which is bounded by the end-members $FeNb_2O_6$, $FeTa_2O_6$, $MnNb_2O_6$ and $MnTa_2O_6$ (Figure 48). A

two-phase compositional gap lies between the fields of tapiolite solid solution and columbite solid solution. The compositional fields had been originally outlined by synthetic experiments of Moreau and Tramasure (1965) and Schröcke (1966), and later examined by Komkov and Dubik (1974). The experimentally derived two-phase regions do not correspond well with the fields defined by natural compositions and by coexisting ferrotantalite-ferrotapiolite pairs (Figure 48). Metastability plagues most experimental data and the question of true equilibria in the experimental data or natural assemblages remains unanswered. For example, the few tapiolite analyses which cross the compositional boundary into the two-phase region (Lahti et al., 1983) are thought to represent metastable phases within the system possibly as a result of rapid nucleation due to quenching (Černý and Ercit, 1985).

The chemistry of columbite-tantalite from the Yellowknife pegmatite field is quite variable. Fe, Mn, Nb, and Ta are typically the major elements found in these minerals with Ti and Sn occurring as major to minor constituents. Trace amounts of Ca and Sc were found in only a few samples. Electron microprobe analyses of all Yellowknife columbite-tantalites are given in Appendix C.

The stoichiometry of the Yellowknife columbite-tantalite minerals approaches the ideal formula, despite the near ubiquitous substitution of the major elements by Sn, Ti and Fe^{3+}. Although Fe^{2+} and Nb typically dominate the mineral chemistry relative to Mn and Ta, appreciable quantities of Ti, Sn and Fe^{3+} are frequently found (Figure 49). Sn and Ti contents are generally low, typically $< 1.0\%$ ($SnO_2 + TiO_2$) (Figure 50), although local enrichments do occur, where the maximum values of SnO_2 and TiO_2 reach

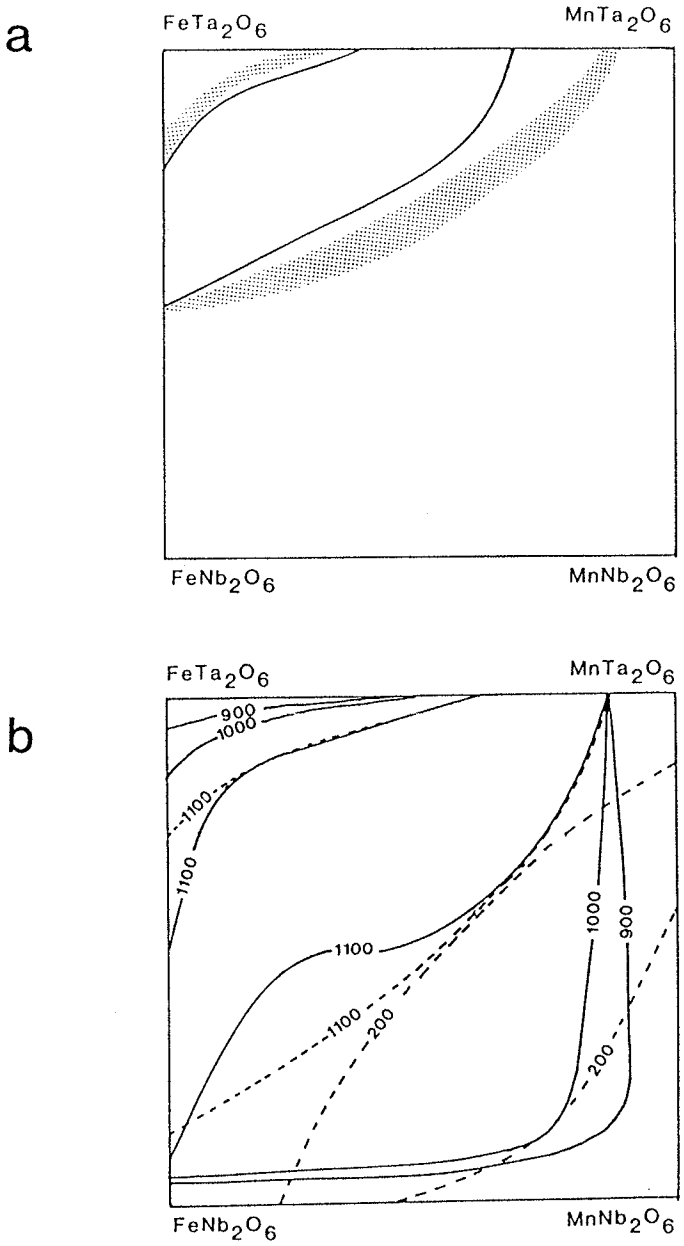

Figure 48: The columbite quadrilateral. (a) Solid lines denote compositional fields defined by natural samples, dotted belts denote boundaries indicated by coexisting tapiolite-tantalite pairs (Černý et al., 1986a). (b) Experimentally determined compositional fields for various temperatures (C°). Data taken from Schröcke (1966) - solid lines and Komkov & Dubik (1974) - dashed lines.

1.70% and 3.81%, respectively. Trivalent Fe contents are typically less than 0.5% Fe_2O_3, and high values (2.5 to 4.33 %) are rarely found.

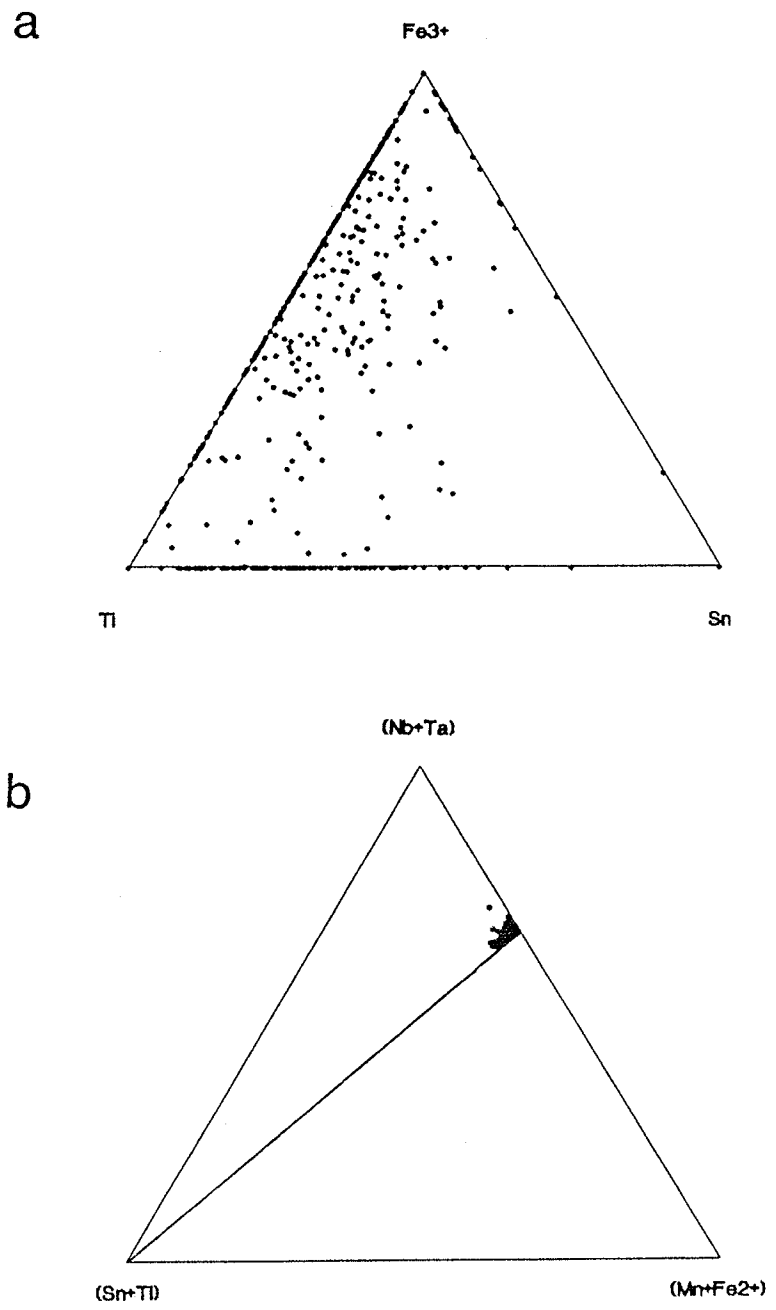

Figure 49: Bulk composition (atomic) of the Yellowknife columbite-tantalites. (a) Compositions in the Ti-Fe^{3+}-Sn triangle, and (b) the (Nb,Ta) - (Sn,Ti) - (Fe,Mn) triangle.

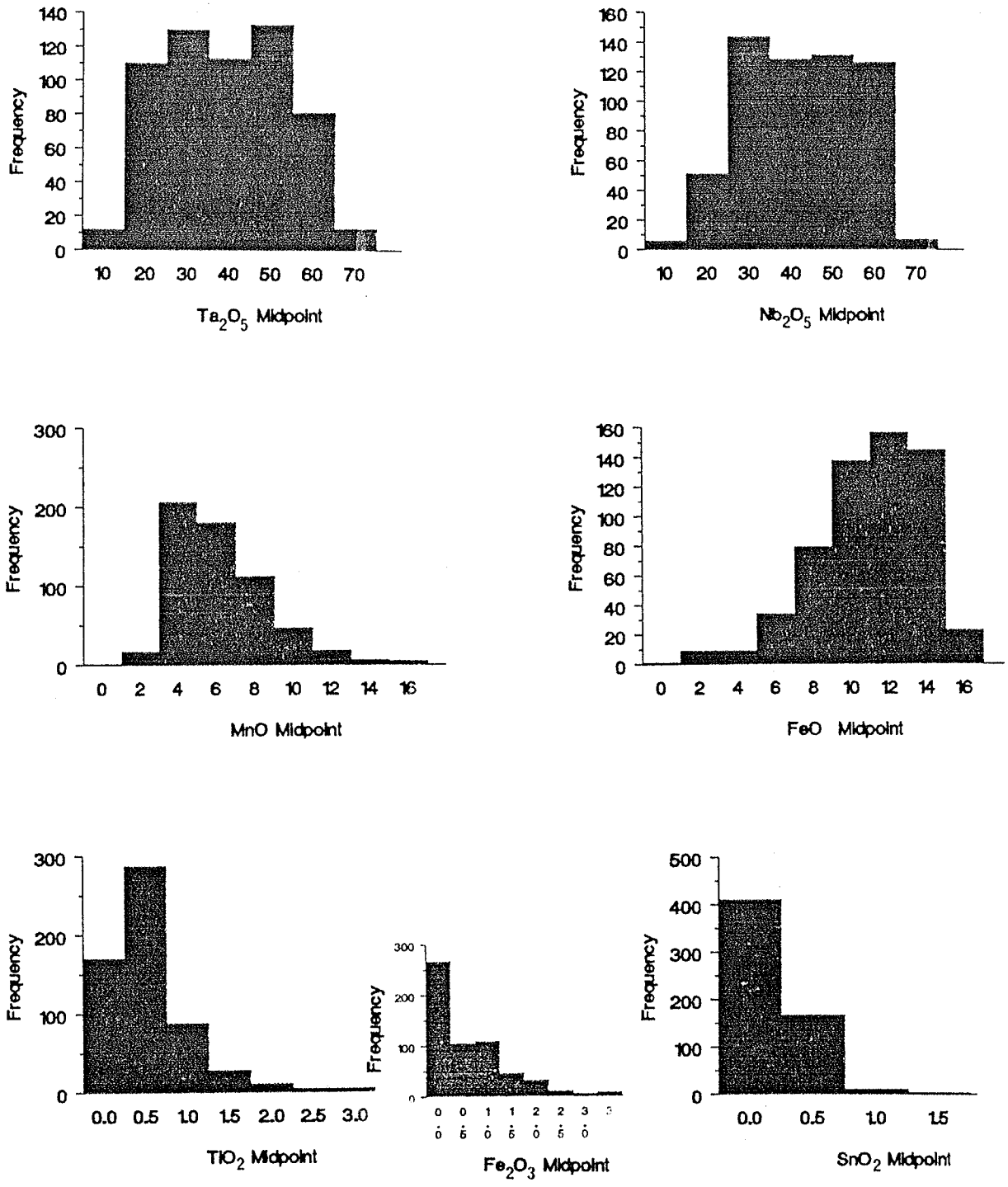

Figure 50: Compositional histograms of Yellowknife columbite-tantalites based on 592 microprobe analyses.

Isomorphous substitution

Figure 51 shows cation-cation plots for the Yellowknife columbite-tantalites. Figure 51a is a plot of total Fe (as Fe^{2+}) versus Mn, and shows a strong negative correlation between Fe and Mn (R=-0.97) thus indicating that the presence of most Mn in columbite-tantalite is due to Fe-Mn substitution. Scattering along this trend is due to the substitution of minor amounts of Ti,Sn and Fe^{3+} at the A-site.

Figure 51b is a plot of Nb versus Ta, and unlike Fe and Mn, isomorphism between Nb and Ta is more extensive. A strong negative correlation exists between Nb and Ta (R=-0.99) and the small amount of scatter is also due to the presence of Sn and Ti at the B-site. Despite the apparent accumulation of Sn and Ti at both the A- and B-sites, correlation of these cations with the other major cations is very weak to nonexistent. Their presence in columbite-tantalite seems to be geochemically, rather than crystallochemically controlled.

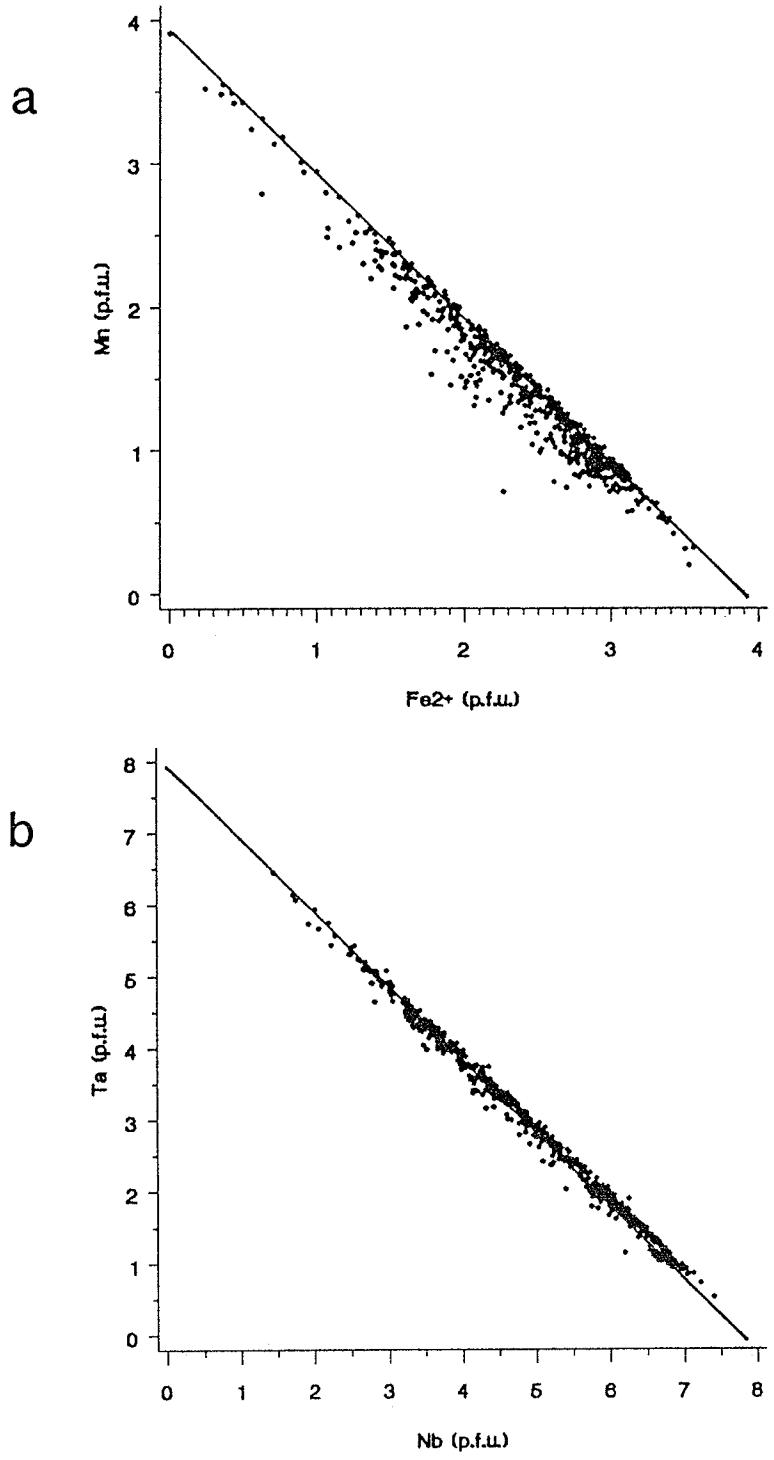

Figure 51: Yellowknife columbite-tantalite group mineral cation-cation plots. (a) Fe^{2+} versus Mn, (b) Nb versus Ta.

CHAPTER 7

Ixiolite

Introduction

Since its discovery in 1857 by Nordenskiöld and its formal acceptance as a re-defined mineral species in 1963, ixiolite has been the subject of an ongoing debate. Traditionally, ixiolite is described as being orthorhombic with a unit cell equivalent to the columbite subcell: a=4.74 Å, b=5.73 Å, c=5.15 Å. Recent studies have shown structures transitional from orthorhombic ixiolite to monoclinic wodginite in which a strong ixiolite subcell with ß only slightly greater than 90° is observed (Polyakov and Cherepivskaya, 1981; Lahti, 1982; Wise and Černý, 1986; Ercit, 1986; Foord et al., 1987). These "monoclinic ixiolites" or "pseudo-orthorhombic wodginites" all apparently revert to a monoclinic wodginite structure after heating, thus suggesting the presence of an order-disorder relationship between ixiolite and wodginite.

Chemically, ixiolite is also similar to wodginite, consisting of appreciable R^{3+}, R^{4+} and/or R^{6+} cations and giving a general formula of $(Fe^{2+},Mn^{2+},Fe^{3+},Sc^{3+},Sn^{4+},Ti^{4+},Nb^{5+},Ta^{5+},W^{6+})O_2$. The stannian ixiolite described by Nickel et al.(1963a) seems to be the most common variety, with Sn as the dominant substituent for (Fe^{2+},Mn) and (Nb,Ta). Titanian, scandian and tungstenian varieties are less common and will not be discussed in detail in this thesis. However, it is important to note that these varieties do show structural characteristics similar to those of the stannian

type. In view of the compositional and general structural similarity to wodginite, the status of ixiolite as a valid mineral species is still questioned. This chapter of the thesis will not only describe the chemistry of the Yellowknife ixiolites, but will also critically address the ixiolite problem with particular emphasis on the stannian variety.

X-ray crystallography

One of the first indications that ixiolite was similar to wodginite was through comparison of their respective X-ray powder diffraction patterns (Nickel et al., 1963b; Table 21, Figure 52). On close inspection, one notes the obvious decreased diffraction intensities of ixiolite relative to wodginite and columbite-tantalite. Broad diffraction peaks and diminished intensities of supercell reflections are characteristic of the ixiolite phase. The nearly identical X-ray diffraction patterns of ixiolite, wodginite and columbite-tantalite reveal their structural similarity (Nickel et al., 1963a). With nearly complete disorder, the intensities of supercell reflections are very low and all diffractograms, regardless of composition, appear identical. However, on closer examination, minor to weak wodginite-like supercell reflections may still be observed in ixiolite diffraction patterns. In the past, X-ray diffraction equipment may not have been sensitive enough to detect these low-angle low-intensity reflections now observed in the pattern of type ixiolite as well as those for other ixiolites. The PW 1710 system was able to detect these reflections and they have subsequently been identified in ixiolite from several localities, including the Yellowknife pegmatite field. These reflections are equivalent to the $(\bar{1}11,111)$ and (021) supercell reflections of wodginite.

These reflections violate the orthorhombic Pbcn space group and can be indexed only on a monoclinic cell. The unit cell dimensions of 14 natural ixiolites of varying compositions are given in Table 22. For direct comparison to wodginite, the unit cells of the stannian and titanian varieties are calculated on a monoclinic wodginite cell. The unit cell of the scandian variety does not transform to wodginite upon heating, therefore the subcell dimensions are reported.

The conversion of ixiolite to wodginite after heating has in the past been thought to represent an ixiolite-wodginite order-disorder transition, but up until now, has not been adequately documented. It is now known that wodginites show a wide spectrum of structural states varying from fully ordered to very disordered (Ercit, 1986). A plot of $\underline{V}$ versus β is used to show changes due to order-disorder effects in wodginite and may also serve to illustrate similar effects in ixiolite. The heating vectors of ixiolite plotted on the $\underline{V}$-β plot are generally subparallel to those of wodginite (Figure 53), which suggests a gradual transition from ixiolite to wodginite with progressive ordering. In general, the β angle approaches 90° with increasing disorder of ixiolite as well as for wodginite.

Table 21: X-ray powder diffraction data for natural ixiolite, wodginite and columbite-tantalite.

	Ixiolite Skogböle	Ixiolite YKF-1	Wodginite Wodgina		Columbite YKF-189
hkl	d(obs)Å	d(obs)Å	d(obs)Å	hkl	d(obs)Å
110	---	---	7.216	200	7.124
020	---	---	5.740	110	5.334
$\bar{2}00$	---	4.742	4.764	-	---
$\bar{1}11$	---	---	4.230	-	---
111	---	---	4.172	-	---
021	3.785	3.819	3.821	-	---
220	3.661	3.660	3.670	111	3.677
$\bar{1}30$	3.506	3.545	---	400	3.588
$\bar{2}21$	2.988	2.986	3.003	311	2.976
221	---	---	2.961	-	---
040	2.878	2.869	2.872	020	2.874
$\bar{3}11$	---	---	2.652	220	2.669
311	---	---	2.611	-	---
002	2.586	2.577	2.558	002	2.536
041	2.506	2.507	2.504	021	2.499
240	---	---	2.457	-	---
$\bar{4}00$	2.371	2.373	2.383	600	2.390
$\bar{2}02$	2.269	2.269	2.273	420	2.241
$\bar{2}41$	2.218	2.218	2.207	321	2.216
$\bar{2}22$	2.109	2.110	2.112	-	---
222	---	---	2.082	312	2.087
-	---	---	---	402	2.070
421	2.005	---	2.009	421	2.050
042	---	1.917	1.911	502	1.900
440	1.828	1.827	1.833	620	1.838
$\bar{2}60$	1.773	1.773	1.776	330	1.778
$\bar{4}02$	---	1.751	1.761	-	---
$\bar{4}41$	1.722	1.724	1.735	231	1.738
441	---	---	1.718	621	1.728

-Philips PW 1710 diffractometer, automatic divergent slit with Cu$K\alpha_1$ radiation and a graphite monochromator.
-Ixiolite samples are fully disordered; wodginite and columbite samples are fully ordered.

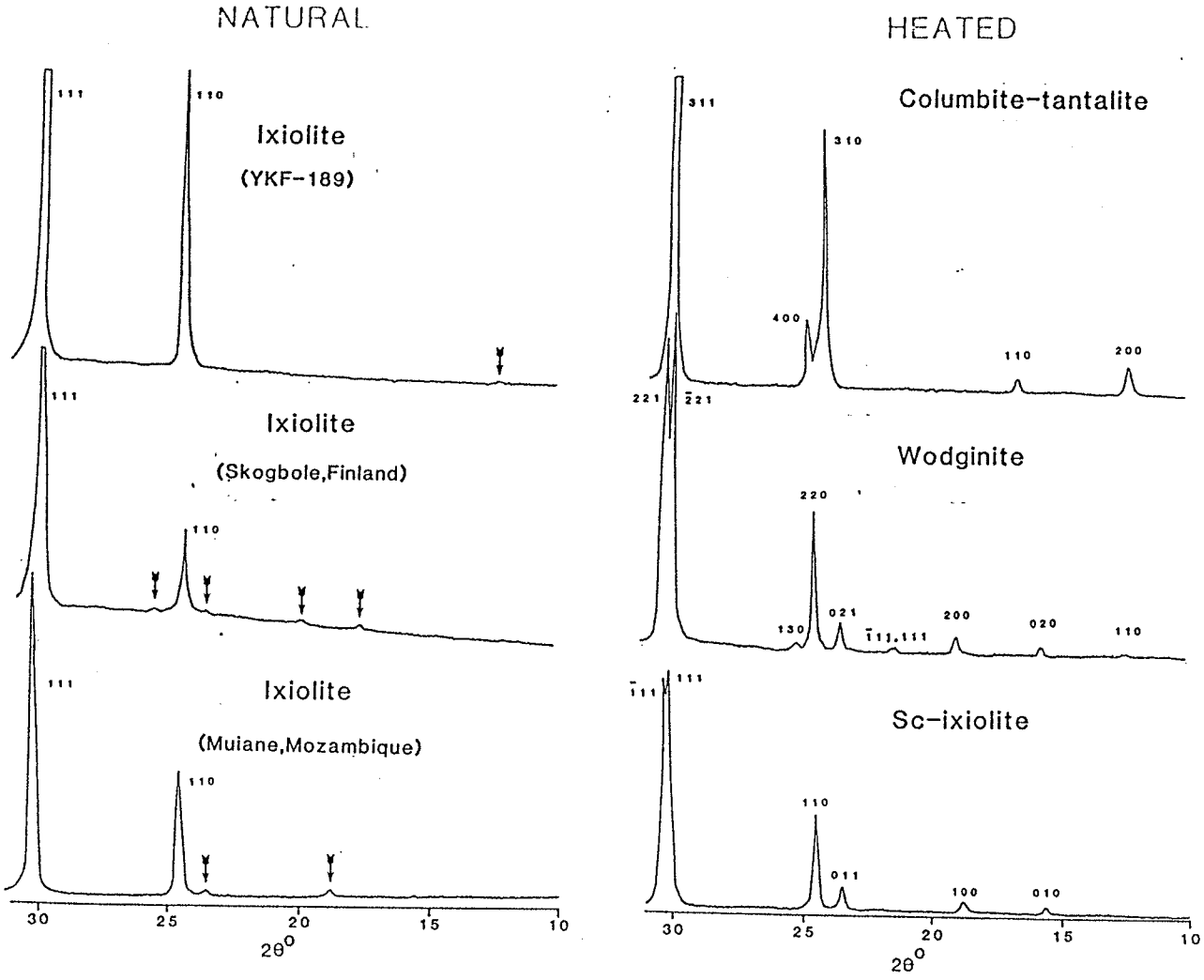

Figure 52: Comparison of x-ray powder diffractograms of natural ixiolite and its heated equivalents, columbite-tantalite, wodginite and Sc-ixiolite. Arrows in ixiolite patterns mark position of supercell reflections.

Table 22: Unit cell dimensions of ixiolite.

	a(Å)	b (Å)	c(Å)	ß(°)	V(Å³)
Stannian					
Skogböle (holotype)	9.481(3)	11.494(5)	5.158(2)	90.13(3)	562.1(2)
Skogböle, Finland	9.514(3)	11.448(3)	5.151(2)	90.32(3)	561.0(2)
Mac-9 Yellowknife	9.489(3)	11.469(3)	5.154(2)	90.13(3)	560.9(3)
Mac-11 Yellowknife	9.505(4)	11.461(3)	5.138(2)	90.57(3)	559.7(2)
Nite-317 Yellowknife	9.491(2)	11.466(3)	5.163(1)	90.15(2)	561.8(2)
Kapparberg, Sweden	9.496(3)	11.432(3)	5.164(2)	90.78(3)	560.6(3)
Lower Tanco, Manitoba	9.471(3)	11.426(2)	5.122(2)	90.28(3)	554.3(2)
Cross Lake, Manitoba	9.505(3)	11.483(3)	5.147(2)	90.13(7)	561.8(3)
Helen Beryl, S. D.	9.435(3)	11.405(3)	5.124(1)	90.07(2)	551.4(2)
Helen Beryl, S. D.	9.436(3)	11.404(2)	5.127(1)	90.07(3)	551.7(2)
Titanian					
Tanco, Manitoba	9.443(12)	11.438(3)	5.129(1)	90.08(2)	554.5(2)
Scandian					
Muiane, Mozambique	4.7292(7)	5.6916(8)	5.102(1)	90.42(2)	135.34(5)
Muiane, Mozambique	4.7028(5)	5.6822(9)	5.1010(6)	90.03(2)	136.30(2)
Naquissupa, Madagascar	4.7023(5)	5.6855(6)	5.1025(4)	90.03(2)	136.41(2)

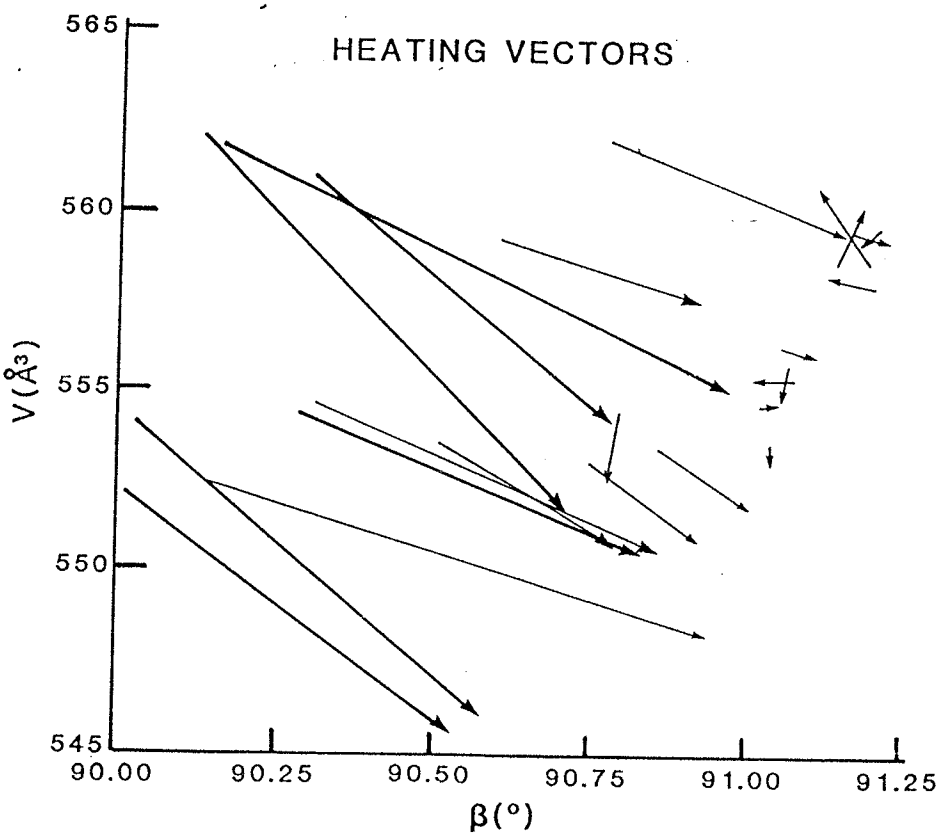

Figure 53: Ixiolite plotted on the wodginite V versus ß plot. Thin arrows - wodginite specimens of Ercit (1986). Heavy arrows - ixiolite. Arrowheads mark the plot of heated phases. Modified after Ercit (1986).

Single crystal studies: Buerger precession photography

The original Buerger precession photographs of ixiolite were reported by Nickel et al. (1963a) as having orthorhombic symmetry with space group Pcan (Pbcn). Re-examination of the type material from Skogböle, Finland (M-6591) gave different results. Precession photographs of a spherical-shaped single crystal were taken for long exposure times (72 hours) and the results indicate monoclinic symmetry. Long exposures made very weak super-cell reflections more visible which allowed their usage in determining the true symmetry of the mineral. Examination of the zero-level photographs shows pseudo-orthorhombic symmetry with apparent mirror planes perpendicular to the principal axes a, b, c (Figure 54). Although the orientation of diffraction spots on the photographs is symmetrical, closer examination of the relative intensities indicate that this symmetry is only apparent. The relative intensities of any given pair of reflections are vastly different and are not identical across the "pseudo-mirror planes", clearly indicating that orthorhombic symmetry is not present in the mineral. Only in orientations with a or c as the precession axis (b-c or a-b planes), does one find a valid mirror plane perpendicular to b. These observations are further verified in the 1st-level photographs of the same orientations (Figure 55). Measurement of the angle between the principal axes a and c (β angle) gives a value slightly larger than 90°.

The apparent orthorhombic symmetry observed in the precession photographs by Nickel et al. (1963a) may be the result of twinning on a microscopic scale. If ixiolite is actually a fully disordered wodginite, then twinning is quite likely. Ercit (1986) examined numerous wodginites showing varying degrees of structural order from several localities and found

most to be twinned. Until now, twinning has yet to be observed and documented in ixiolite. Figure 56 illustrates how twinning in wodginite could produce pseudo-orthorhombic symmetry.

In precession photographs of wodginite oriented such that b is the precession axis, the point group symmetry is shown to be 2. Twinning of two individual lattices produces a composite lattice with point group symmetry of 2mm. If ß is notably greater than 90°, then splitting of the diffraction spots will occur along (100) and (001). On the other hand, if ß is equal to or very close to 90°, then splitting will not be observed, as in the case of ixiolite. Differences in diffraction intensities show that the point group symmetry is not 2mm, but instead, remains 2. Based on these observations, the true symmetry of the Skogböle ixiolite seems to be monoclinic with space group C 2/c and not orthorhombic (Pbcn) as proposed by Nickel et al. (1963a).

Chemical composition

In contrast to columbite-tantalite, the Yellowknife ixiolites are always Ta-rich relative to Nb. Interestingly enough, the Yellowknife ixiolites are Nb-richer than most of the global ixiolite samples (unpubl. data of P. Černý). In the Yellowknife samples, Fe contents are slightly higher than Mn (Appendix C, Figure 57), but tend to cluster near the Fe:Mn ratio of 1:1. SnO_2 contents are highly variable (13.2 - 17.9 wt. %) whereas TiO_2 is less so (0.1 - 2.25 wt. %).

Overall, ixiolite is compositionally very similar to wodginite. Until now, crystallochemical studies of ixiolite have been non-existent. Examination of data collected by P. Černý shows that the geochemical and crys-

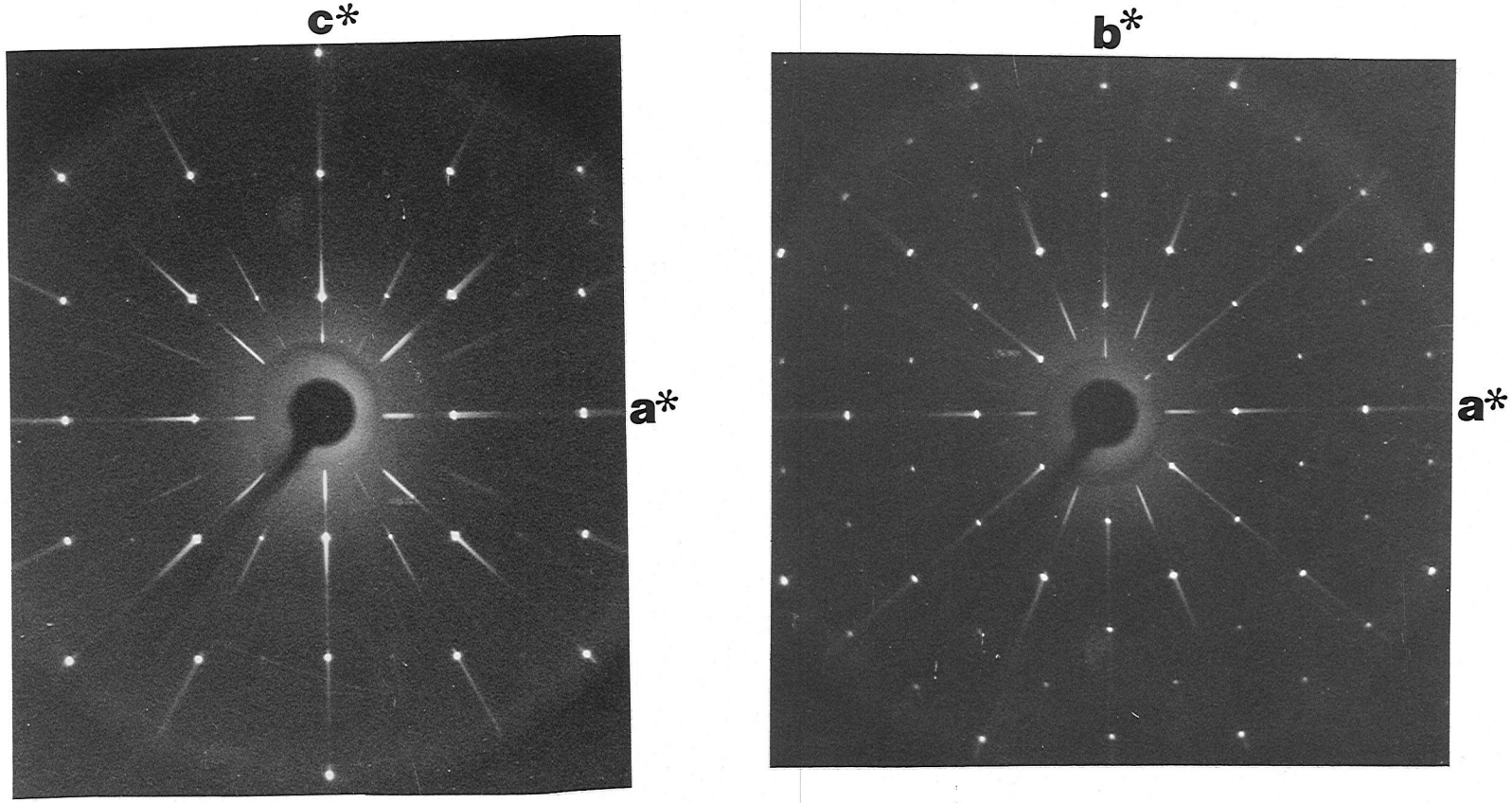

Figure 54: Zero level precession photographs of Skogböle ixiolite.

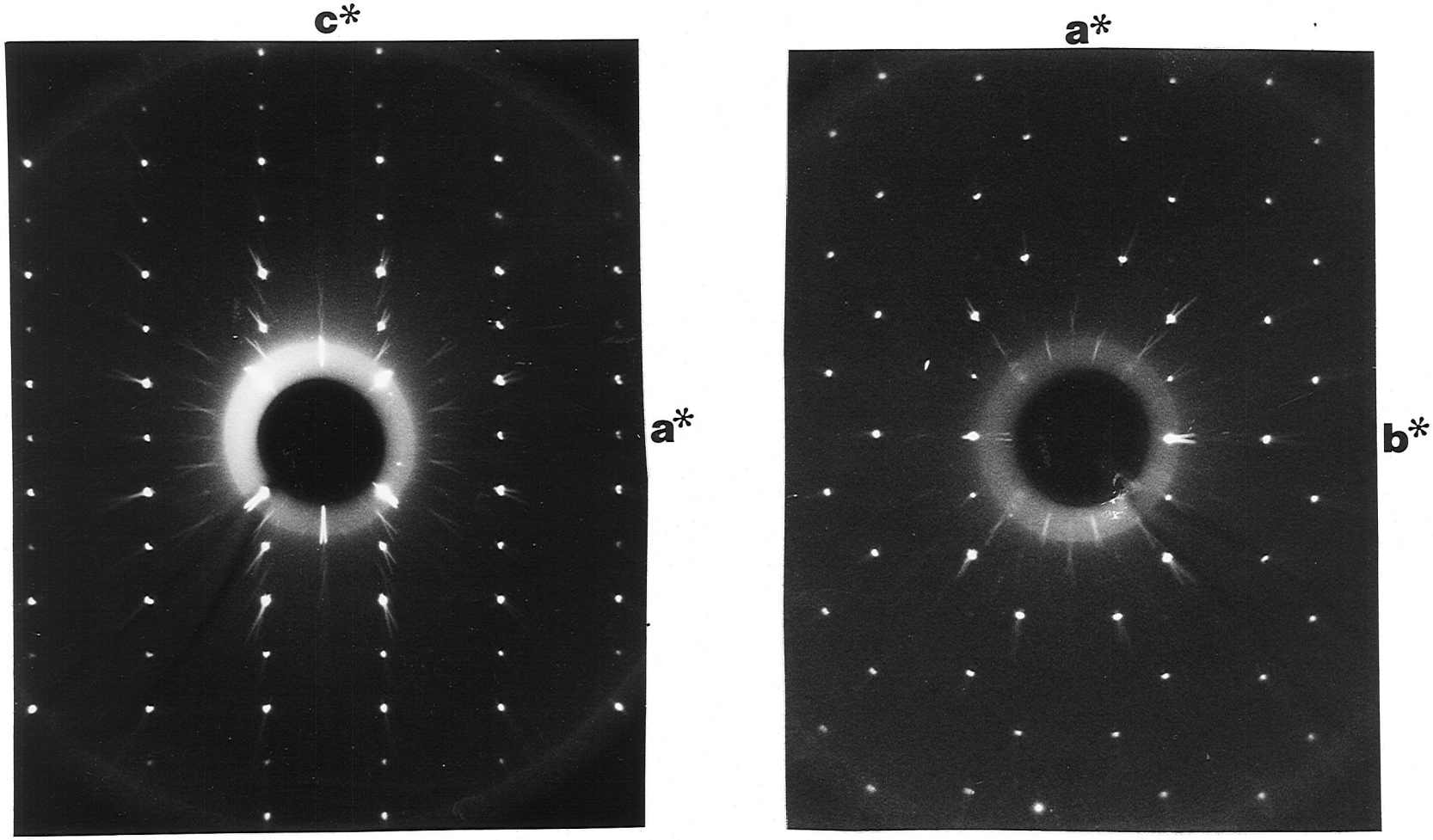

Figure 55: First level precession photographs of Skogböle ixiolite.

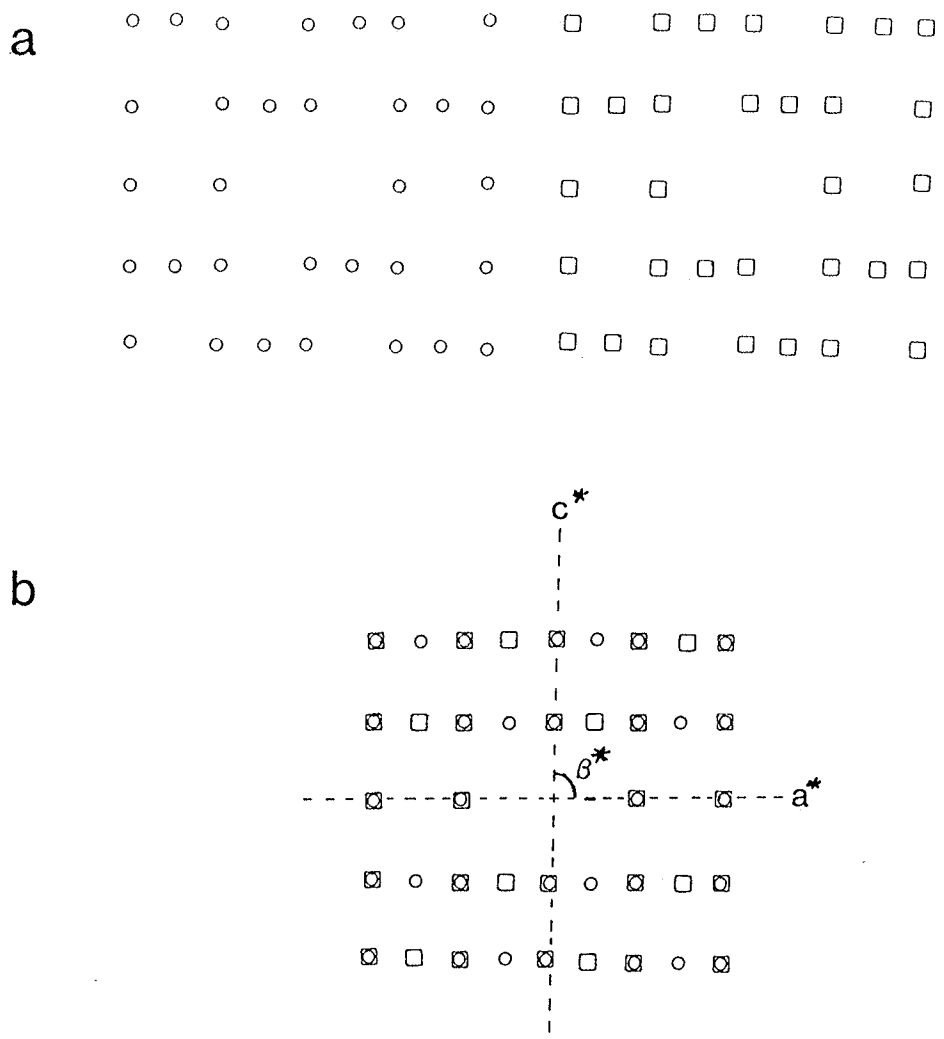

Figure 56: Schematic diagram of a zero-level precession photograph showing pseudo-orthorhombic symmetry produced by twinning. (a) Lattices of two individual monoclinic wodginite crystals. Beta is slightly greater than 90°. (b) Composite lattice of twinned crystal. Dashed lines denote pseudo-mirror planes.

tallochemical features of ixiolite are remarkably similar to those of wodginite. The Yellowknife ixiolites agree well with this conclusion; compositions plotted on the (Nb,Ta) - (Sn,Ti) - (Fe,Mn) triangle plot along the $(Fe,Mn)(Nb,Ta)_2O_6$ - SnO_2 join close to the ideal wodginite stoichiometry (Figure 58).

Isomorphous substitution

Figure 59 shows cation-cation plots representing the major substitutions occurring in the Yellowknife ixiolites. A plot of Fe^{2+} versus Mn (Figure 59b) shows a relatively good negative correlation (R=-0.71) despite the limited substitution. The main trend of Nb-Ta substitution (Figure 59b) is not so well-defined and is characterized by considerable scatter which suggests additional substitution for Nb or Ta by another cation. The minor scatter observed in Figure 60 indicates that the incorporation of Sn into ixiolite is strongly influenced by the presence of Nb and Ta. The joint effect of these correlations is shown in Figure 58, indicating that the dominant substitution is that of $3(Ti,Sn)^{4+} \longrightarrow 2(Ta,Nb)^{5+} + (Fe,Mn)^{2+}$.

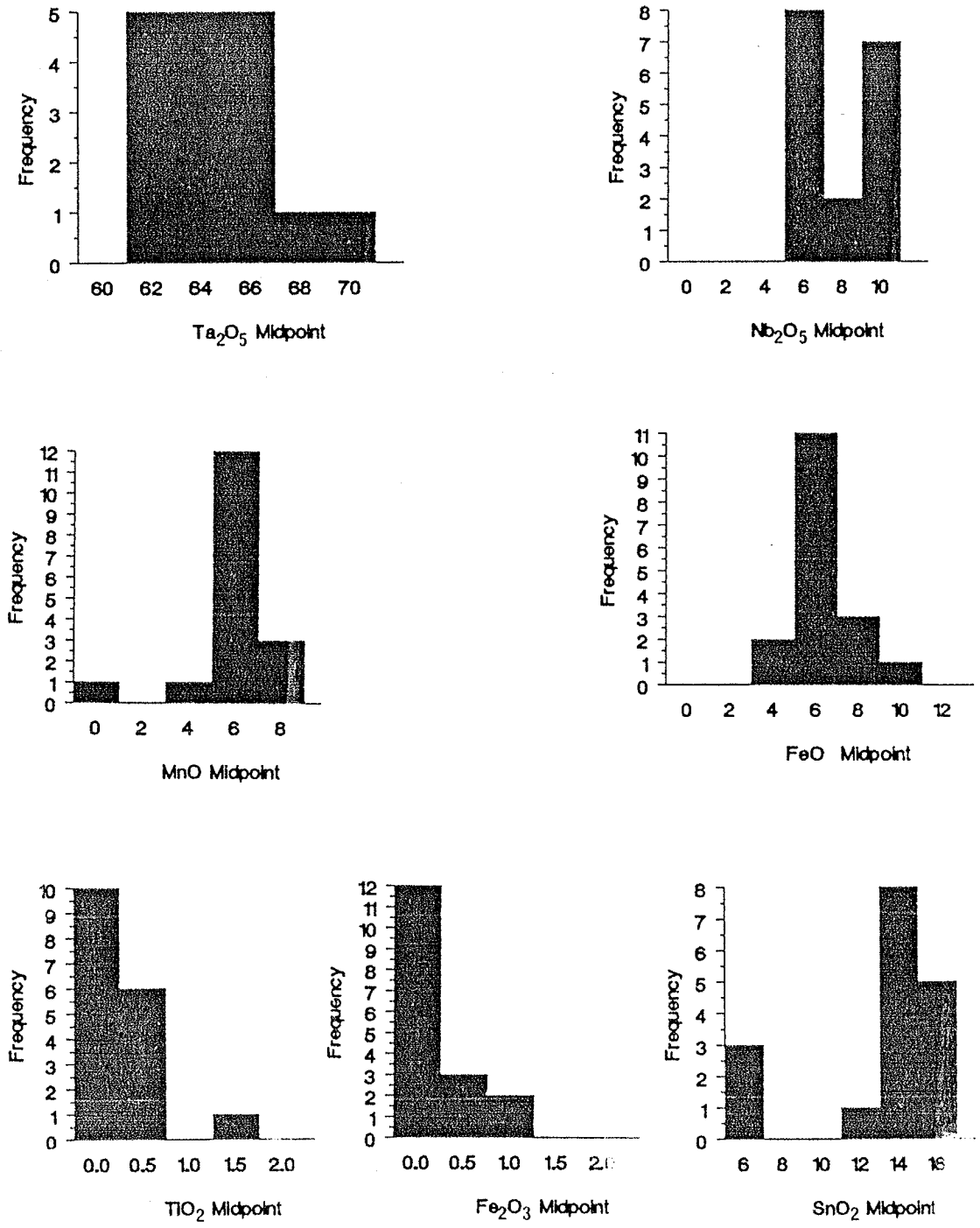

Figure 57: Compositional histograms for Yellowknife ixiolite based on a total of 17 electron microprobe analyses.

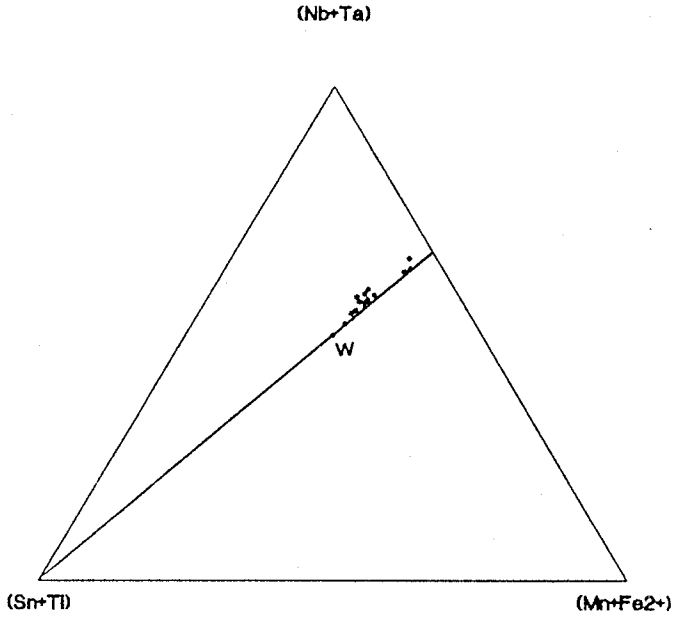

Figure 58: Yellowknife ixiolite compositions plotted on the (Nb,Ta) - (Sn,Ti) - (Fe,Mn) triangle. (W) marks ideal wodginite composition. Ixiolite compositions lie above the ideal line due to some Fe being present as Fe^{3+}.

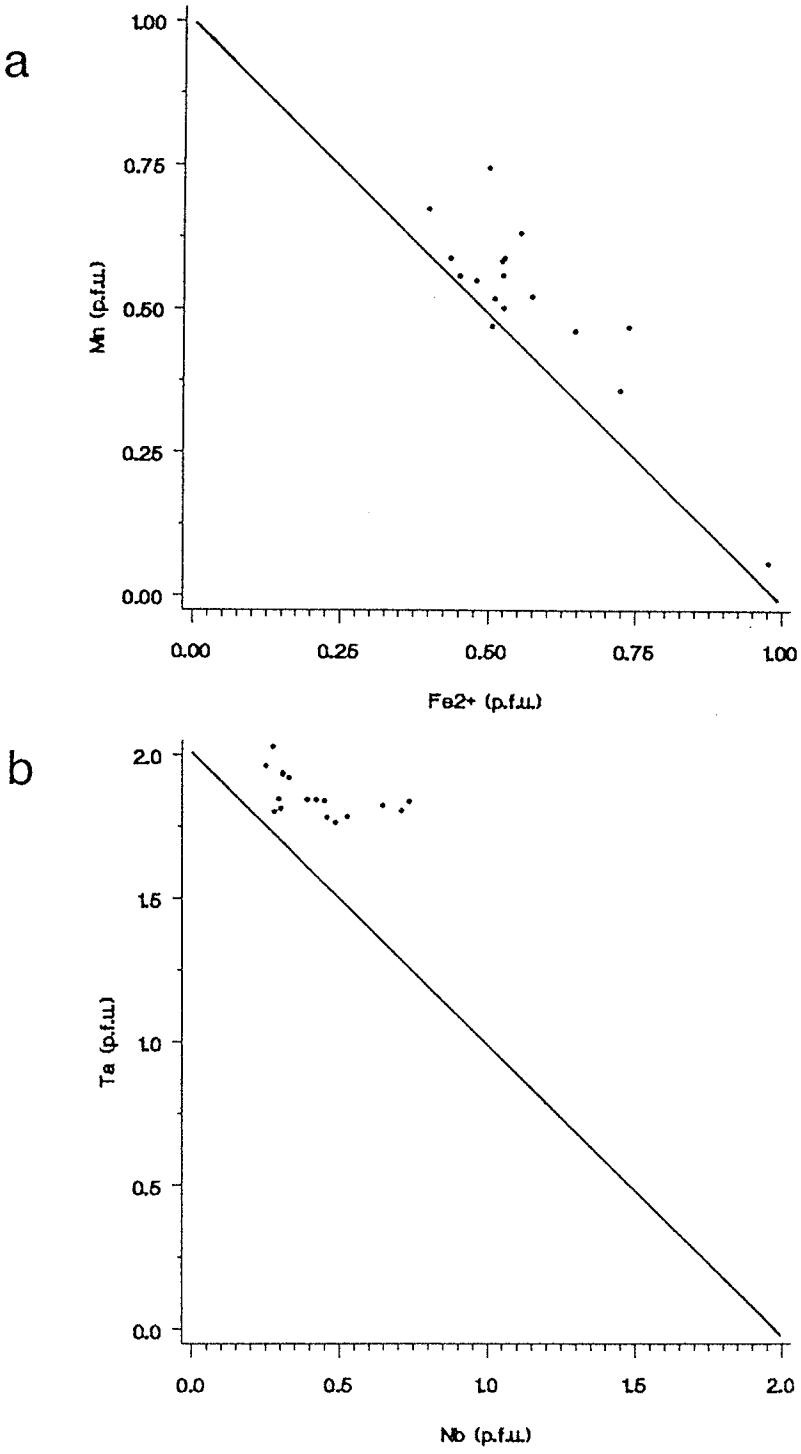

Figure 59: Cation-cation plots for Yellowknife ixiolites: (a) Fe^{2+} versus Mn, (b) Nb versus Ta.

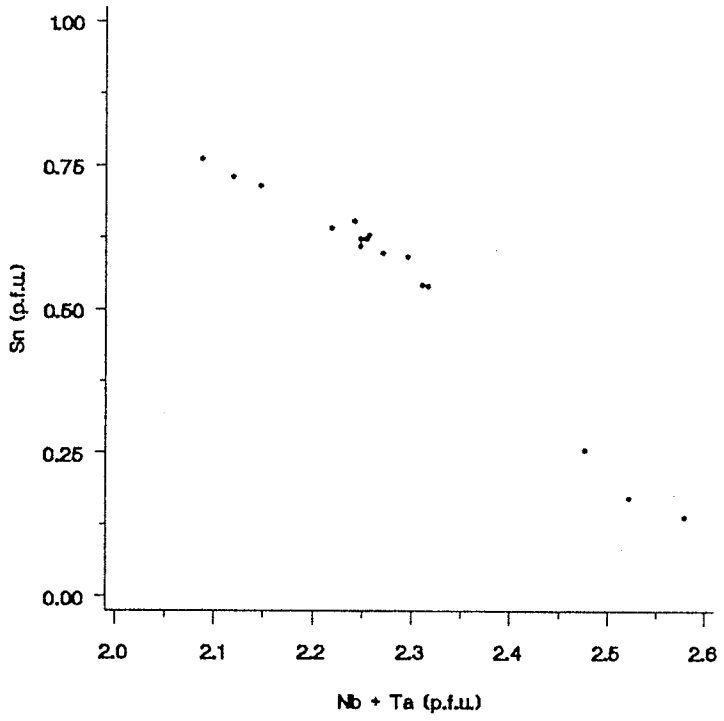

Figure 60: Sn versus (Nb+Ta) plot of Yellowknife ixiolites.

CHAPTER 8

Tapiolite Series

Introduction

The relatively abundant occurrence of the tapiolite series minerals (ferrotapiolite-manganotapiolite) in the Yellowknife pegmatite field presents an excellent opportunity to examine the crystallochemical and geochemical characteristics of this mineral series that are poorly represented in the literature. Although tapiolite series minerals are subordinate to columbite-tantalite in abundance, they do occur with surprising frequency in many areas of the pegmatite field. This wide regional distribution coupled with ubiquitous structural and chemical variations provides material for substantially advancing the characterization of this important mineral series.

Rutile-related structures

The tapiolite series minerals are tetragonal, crystallize in the space group $P4_2/mnm$, Z=2, and are structurally related to rutile. The AO_2 rutile structure (TiO_2) was first solved by Goldschmidt (1926), and consists of edge-sharing distorted octahedra. The oxygens are in a hexagonal close-packed arrangement parallel to (001); each oxygen is coordinated by 3 cations. The distorted octahedra form straight chains which run parallel to the c axis. Adjacent chains are linked together by shared octahedral corners.

As in the rutile structure, chains of edge-sharing octahedra running parallel to the c axis occur in the tapiolite structure (Figure 61). However, an ordered arrangement of cations into two distinct sites distinguishes between the two structure types. In tapiolite, (Fe,Mn) and (Ta,Nb) occupy unique cation positions (Figure 61c), such that the cation octahedra are arranged in the trend ...-AO_6-BO_6-BO_6-AO_6-... along c , where A=(Fe,Mn) and B=(Ta,Nb). As a result, the periodicity of the rutile c axis is tripled, whereas the a dimension remains virtually unchanged. Goldschmidt (1926) referred to this structure as the trirutile structure.

The trirutile structure of tapiolite is strongly affected by changes in cation ordering. A random distribution of cations over the A and B sites reduces the trirutile unit cell (Figure 61b) to that of rutile (disordered tapiolite with monorutile structure). This order-disorder relationship is frequently observed in natural tapiolite samples and will be discussed in greater detail later in this chapter.

X-ray crystallography

Variability of structural state in tapiolite

As in the columbite-tantalite series minerals, the unit cell dimensions of the tapiolite group are strongly affected by order-disorder and compositional variations, particularly Nb, Ti, Mn and Fe^{3+} (Clark and Fejer, 1978; unpub. data of Wise). The existence of disordered tapiolite and intermediate states transitional to ordered tapiolite was first reported by Hutton (1958). His single crystal studies revealed the presence of small domains of varying degrees of order occurring within one single crys-

tal. The data of Clark and Fejer (1978) confirmed the large variations in structural state present in the tapiolite series. With increasing disorder, both the a and c dimensions increase, c increasing at a much faster rate than a. A typical disordered tapiolite may show unit cell dimensions of a=4.75 Å and c=9.25 Å. The unit cell dimensions of the Yellowknife tapiolites cover a wide range of structural order and are given in Table 23. Contrary to the columbite-tantalite series, order-disorder relationships in the tapiolite group have not been adequately documented, partly because of the limited number of tapiolite samples available for study and the lack of heating experiments on natural samples.

The first attempt to quantify order-disorder in the tapiolite series was by Komkov (1974), who noted that the intensities of the (002) and (101) reflections diminished with increasing disorder. In general, all hkl reflections in which $l \neq 3$ show diminished intensities with disorder. Because of their great sensitivity to structural changes, the I (002)/ I (101) ratio of tapiolite was used as an indicator of order. However, the present author has found this method to be unsatisfactory, due to the strong positive influence of Mn on the intensity of the (002) reflection. Clark and Fejer (1978) noted that the c dimension of disordered tapiolite was significantly larger than for ordered tapiolite. Tapiolites were considered disordered if their c dimension was greater than 9.24 Å. However, examination of numerous tapiolite unit cell dimensions showed this conclusion to be erroneous. High Mn contents can also produce large c values in tapiolite that have fully ordered structures. In view of the strong chemical influence on the unit cell dimensions, an a-c plot similar to the one used for columbite-tantalite can not be used to estimate order-disorder in the tapiolite group (Figure 62). The bounding cell dimensions of the

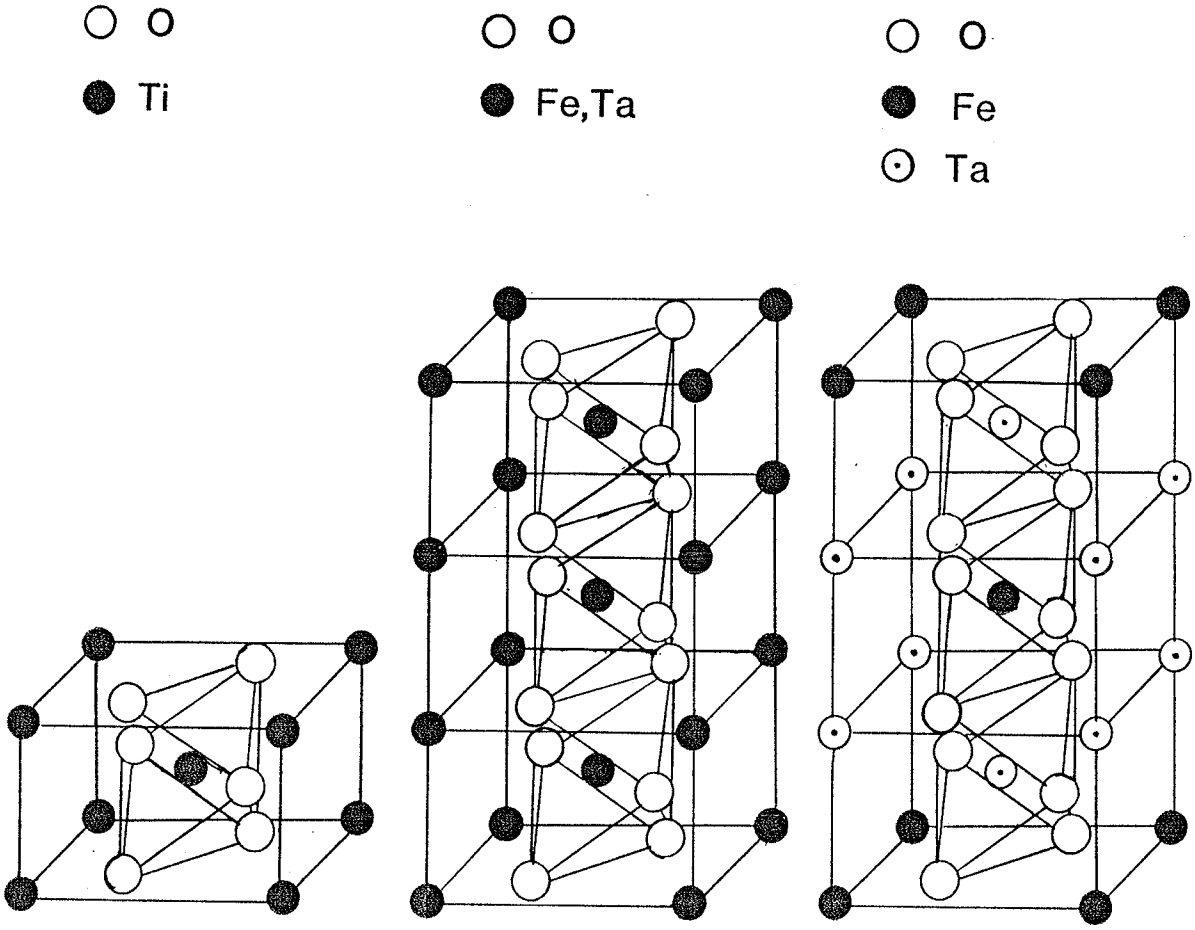

Figure 61: Comparison of rutile related structures. (a) Rutile structure, (b) disordered tapiolite, (c) ordered tapiolite. After Moreau and Tramasure, (1965).

Table 23: Unit cell dimensions for Yellowknife tapiolites.

Natural

Sample No.	a	c	V
Bet-4	4.7610(5)	9.217(5)	208.92(9)
Big-B-8	4.7565(4)	9.255(2)	209.40(5)
Big Hill-Cs-1	4.7546(7)	9.226(3)	208.57(7)
Big Hill-12	4.757(1)	9.230(2)	208.9(1)
Big Hill-16	4.7574(5)	9.233(4)	208.97(8)
Big Hill-17	4.7570(7)	9.238(3)	209.06(7)
Big Hill-23	4.7576(2)	9.225(1)	208.80(2)
Big Hill-24	4.750(2)	9.25(1)	208.6(2)
Big Hill-25	4.7409(4)	9.2386(9)	207.65(4)
Big Hill-30	4.7587(3)	9.257(3)	209.63(6)
Big Hill-31	4.7581(3)	9.2541(2)	209.51(5)
Big Hill-33	4.7581(5)	9.254(3)	209.50(6)
Big Hill-34	4.7567(2)	9.232(1)	208.88(3)
Bin-19	4.7570(9)	9.248(7)	209.3(1)
Bin-20	4.7580(2)	9.269(3)	209.84(6)
Cas-I-1	4.7486(6)	9.239(3)	208.32(6)
Cas-I-2	4.7488(8)	9.246(6)	208.5(1)
Lens-10	4.7545(4)	9.2355(9)	208.77(2)
Mel-9-11	4.7571(3)	9.222(2)	208.70(5)
Mint-A-3	4.7540(2)	9.241(1)	208.86(3)
Mint-A-6	4.7566(5)	9.224(3)	208.70(6)
Nite-A-3	4.7599(4)	9.243(2)	209.41(4)
Nite-A-6	4.7548(4)	9.218(3)	208.40(7)
Nite-A-8	4.758(1)	9.224(4)	208.8(1)
Nite-A-10	4.7570(4)	9.236(2)	209.00(4)
Nite-C-8	4.7598(3)	9.249(20	209.55(4)
Nite-C-12	4.7591(3)	9.254(3)	209.59(7)
Peg-8-4	4.7511(8)	9.228(3)	208.31(7)
Peg-88-2	4.7515(4)	9.248(4)	208.79(7)
Peg-93-35	4.7527(3)	9.259(2)	209.15(4)
Peg-93-37A	4.7509(4)	9.259(1)	208.98(4)
Peg-170-4	4.7508(4)	9.247(4)	208.70(8)
Peg-191-2	4.7543(5)	9.270(5)	209.52(9)
Peg-196-4	4.7553(3)	9.275(4)	209.72(8)
Peg-319-1	4.7560(3)	9.281(1)	209.94(3)
Peg-319-2	4.7565(5)	9.276(2)	209.86(6)
Pvilla-C-12	4.7554(5)	9.254(1)	209.27(4)
Pvilla-C-15	4.719(1)	9.252(5)	206.0(1)
Rib-26	4.7381(4)	9.2367(9)	207.36(3)
Tan-4-1	4.7550(4)	9.254(2)	209.24(5)
Tan-2-19	4.7573(3)	9.246(3)	209.25(7)
Tan-2-20	4.7561(5)	9.252(2)	209.28(4)
Tan-4-3	4.759(1)	9.228(3)	209.0(1)
Usk-15	4.7528(5)	9.252(5)	209.0(1)
Waco-B-1	4.7486(6)	9.221(2)	207.92(5)

Heated

Sample No.	a	c	V
Bet-4	4.754(5)	9.16(2)	207.0(5)
Big-B-8	4.7480(5)	9.191(2)	207.21(5)
Mint-A-3	4.7419(9)	9.168(3)	206.2(1)
Nite-A-3	4.7487(4)	9.203(1)	207.53(3)
Peg-8-4	4.743(1)	9.177(4)	206.4(1)
Peg-88-2	4.7510(2)	9.1908(6)	207.46(2)
Peg-93-35	4.7439(3)	9.182(1)	206.64(3)
Peg-93-37A	4.7437(6)	9.182(2)	206.63(5)
Peg-170-4	4.7470(3)	9.1799(9)	206.86(2)
Peg-170-8	4.7476(5)	9.170(1)	206.25(4)
Peg-191-2	4.7520(3)	9.196(1)	207.66(3)
Peg-196-4	4.7510(3)	9.2044(9)	207.76(3)
Peg-319-1	4.7506(3)	9.185(2)	207.28(4)
Peg-319-2	4.7480(2)	9.1892(7)	207.16(2)
Pvilla-C-12	4.7438(9)	9.184(2)	206.67(8)
Tan-2-20	4.7537(9)	9.200(2)	207.89(6)
Tan-4-3	4.7520(3)	9.201(3)	207.78(5)
Usk-15	4.7469(5)	9.195(2)	207.18(5)
Tan-2-20	4.7388(3)	3.1758(6)	71.32(1)

ordered Mn- and Fe^{3+}-rich tapiolites were determined from synthetic members produced by Turnock (1966). Turnock's synthetic material was X-rayed on the PW 1710 powder diffraction system and the unit cell dimensions were refined using the CELREF program. Table 24 gives the new, improved unit cell parameters for synthetic end-member tapiolites.

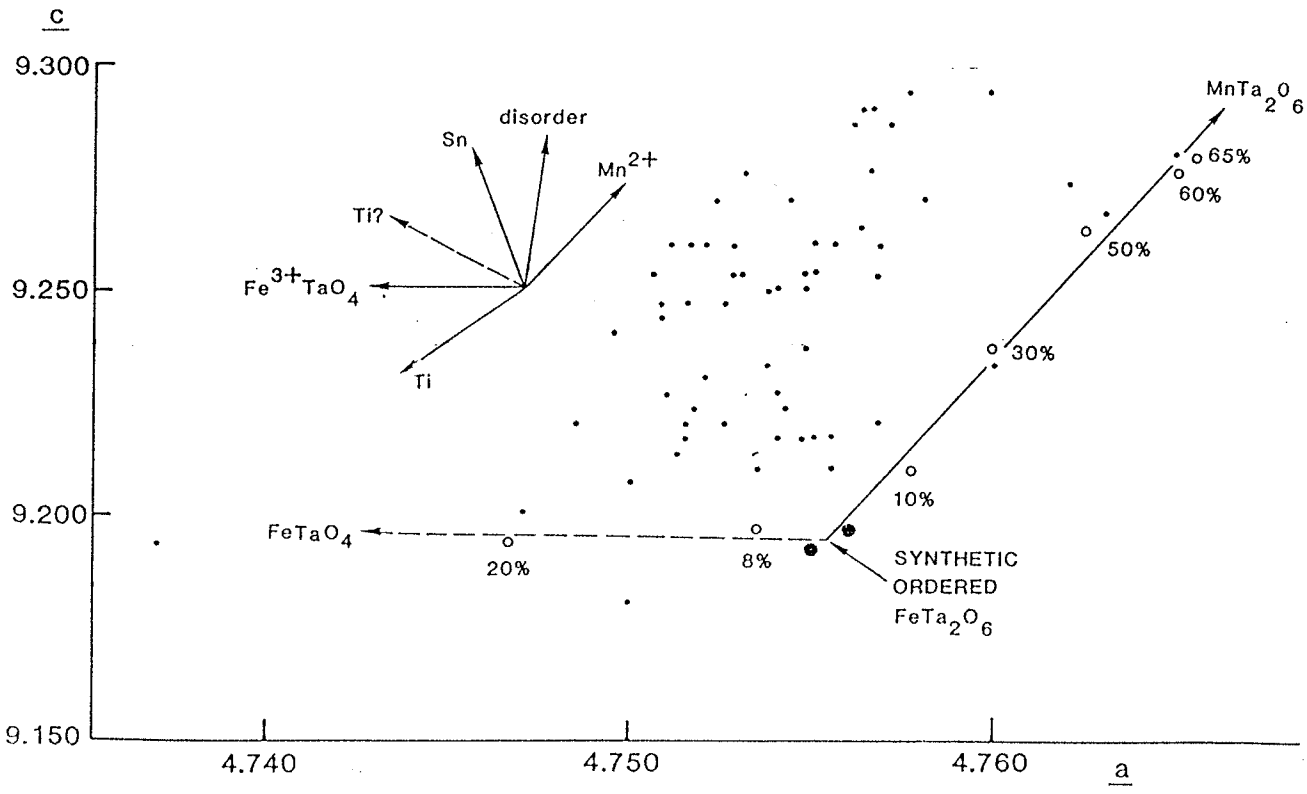

Figure 62: Tapiolite series a-c order-disorder plot for Yellowknife. Data for Mn and Fe^{3+} trends taken from the refined data of Turnock (1966).

Table 24: Improved unit cell dimensions for synthetic end-member ordered tapiolites.

Mn-Tapiolites	a(Å)	c(Å)	V(Å^3)
$FeTa_2O_6$	4.7570(4)	9.1992(9)	208.17(3)
$(Fe._9Mn._1)Ta_2O_6$	4.7587(3)	9.2122(9)	208.61(2)
$(Fe._7Mn._3)Ta_2O_6$	4.7611(2)	9.2393(6)	209.44(2)
$(Fe._5Mn._5)Ta_2O_6$	4.7637(3)	9.2660(8)	210.28(2)
$(Fe._{65}Mn._{35})Ta_2O_6$	4.7665(2)	9.2817(7)	210.87(2)
Fe^{3+}-Tapiolites			
$(Fe^{2+}._{92}Fe^{3+}._{08})Ta_2O_6$	4.7548(4)	9.1996(10)	207.99(3)
$(Fe^{2+}._8Fe^{3+}._2)Ta_2O_6$	4.7478(3)	9.1942(7)	207.26(2)

Structure refinement of partially disordered ferrotapiolite

As part of a concurrent study on the crystal chemistry of the tapiolite series, a crystal of ferrotapiolite from the Yellowknife field was chosen for crystal structure analysis. The crystal was selected on the basis of its low degree of order as ascertained by X-ray powder diffractometry. A crystal fragment was taken from sample YKF-303 (collected from the Nite-A pegmatite) and shaped into a sphere with an average radius of 0.11 mm. A set of 25 reflections were collected with the centering routine of the four-circle diffractometer and used for calculating the unit cell parameters. The calculated unit cell dimensions from the four-circle diffractometer are: a=4.7487(9)Å, c=9.218(2)Å, V=207.87(9)Å^3, which are significantly different from those obtained by X-ray powder diffractometry (a=4.7599(4)Å, c=9.243(2)Å, V=209.41(4)Å^3. The difference between the two sets of unit cell dimensions is probably a result of varying degrees of order within the bulk sample used in the powder method. A total of 240 reflections were measured over one asymmetric unit of the tapiolite cell.

Structure refinement.

The structure was refined using a starting model of fully ordered tapiolite with the structural formula AB_2O_6. Starting atomic positions were those of Weitzel and Klein (1974). Compositional differences were minimized by using the average of three electron microprobe analyses in the refinement (Table 25). In the refinement of the starting model, cations were assigned to crystallographic sites according to the structural formula, with Ti and Sn assigned to the A- and B-sites in proportions which satisfied charge balance requirements. Refinement of the structure was constrained, such that both sites were mixed according to the disordered model with a structural formula of $(Fe._{33},Ta._{67})(Fe._{67},Ta_{1.33})O_6$.

Table 25: Average microprobe analysis for structure refinement of sample YKF-303.

Oxide	wt. %	Cations per 12(O)	
FeO	13.4	Fe^{2+}	1.87
MnO	1.4	Mn^{2+}	0.20
TiO_2	0.1	Ti^{4+}	0.01
SnO_2	0.5	Sn^{4+}	0.03
Nb_2O_5	3.4	Nb^{5+}	0.26
Ta_2O_5	81.0	Ta^{5+}	3.68
	99.8		6.05

Refinement of the starting model (fully isotropic) resulted in R-indices of R=9.7%, wR=8.6%. Subsequent refinements involved extensive cation mixing between the A- and B-site which produced lower R-indices. Least-squares refinement of all variables with anisotropic temperature factors resulted in convergence at R=8.1% and wR=7.8%. The final refined model gave a degree of order of 74(3)%.

Final atomic positions and anisotropic temperature factors are given in Table 26. Selected interatomic distances and angles are given in Table 27. Observed and calculated structure factors for the final model are given in Appendix D.

At the time of this study, the author was unaware of a previous structure analysis conducted by von Heidenstam (1968). He studied a tapiolite crystal with compositition of $Fe(Ta_{1.8},Nb_{.2})O_6$ and a degree of order of 50%. The results found in this study compare favorably with that of von Heidenstam (1968). The mean metal-oxygen distance for the A-octahedron of the Yellowknife sample is significantly larger than the sample examined by v. Heidenstam (Yellowknife - 2.13Å; v. Heidenstam - 2.07Å). On the other hand, the mean metal-oxygen distance for the B-octahedron is very similar for both samples (Yellowknife - 1.98Å; v. Heidenstam - 2.02Å). Differences in the mean bond length reflect the combined effect of larger Mn contents and higher degree of cation ordering observed in the Yellowknife sample.

Chemistry

Ferrotapiolite compositions from the Yellowknife field are not as variable as columbite-tantalite. Electron microprobe analyses for all Yellowknife tapiolites are given in Appendix C. In the Yellowknife samples, Fe and Ta dominate this species chemically with Fe/(Fe + Mn) ratios varying from 0.83 to 1.00, and Ta/(Ta + Nb) ratios ranging from 0.79 to 1.00. Although Nb may occur in substantial quantities, up to a maximum of 14.5% Nb_2O_5, the contents of Mn, Ti and Sn are generally low; the sum of their oxides is typically less than 2.0% (Figure 63). Manganese contents of the Yellowknife tapiolites rarely exceed 1.0% MnO, although a maximum of

2.5% was observed in one analysis. Both TiO_2 and SnO_2 contents are typically less than 1.0% with maximum values of 4.9% and 3.9%, respectively. Fe_2O_3 contents vary considerably from 0.0 to 4.6%.

As a general rule, the A-site chemistry of the Yellowknife tapiolites is fairly restricted. Although both Mn and Fe^{3+} are found, their substitution is limited (Figure 64a). The Yellowknife specimens lie predominantly along the Fe^{2+}-Fe^{3+} join and rarely show any indication of extensive Mn enrichment. The uniform chemistry of the Yellowknife tapiolites is further typified by the B-site chemistry. Tantalum-rich compositions dominate the mineral chemistry, showing only minor enrichment in Nb and ($Ti+Sn+Fe^{3+}$) (Figure 64b).

Although limited in overall abundance (Figure 65a), the relative accumulation of the minor elements, Ti, Sn and Fe^{3+} in the Yellowknife tapiolites is restricted, but it offers some insight into the geochemistry of the tapiolite series in general. Trivalent Fe is by far the most common substituent of the major elements, with Ti and Sn showing more restricted accumulations (Figure 65b).

Table 26: Atomic positional and thermal parameters for tapiolite.

Atomic positions

Atom	x	y	z	*U(equiv.)
M(1)	0	0	0	2.1(2)
M(2)	0	0	0.3315(3)	2.56(6)
O(1)	0.3192(82)	0.3192(82)	0	3.6(1)
O(2)	0.3025(55)	0.3025(55)	0.3209(29)	3.2(7)

*U(equiv.)=U(equiv.) x 10^2

Anisotropic temperature factors

Atom	U_{11}	U_{22}	U_{33}	U_{23}	U_{13}	U_{12}
M(1)	200 (35)	200 (35)	216 (43)	0 (0)	0 (0)	134 (80)
M(2)	262 (10)	262 (10)	243 (13)	0 (0)	0 (0)	-27 (21)
O(1)	268 (164)	268 (164)	542 (279)	0 (0)	0 (0)	118 (224)
O(2)	373 (119)	373 (119)	221 (131)	14 (113)	14 (113)	118 (167)

Uij = Uij x 10^4

Table 27: Selected interatomic distances (Å) and angles (°) for tapiolite.

Bond Lengths

A-O distances			B-O distances		
A-O(1)	x2	2.14(6)	B-O(1)b	x2	1.97(4)
A-O(2)d	x4	2.12(3)	B-O(2)	x2	2.03(4)
			B-O(2)e	x2	1.93(3)

O-O distances around A		O-O distances around B	
O(1)a-O(2)g	3.01(6)	O(1)b-O(1)c	2.43(5)
O(2)d-O(2)g	3.30(5)	O(1)b-O(2)	2.87(5)
O(2)e-O(2)g	2.65(5)	O(1)b-O(2)e	2.96(5)
		O(2)e-O(2)a	2.76(5)

---

a: -x, -y, z; b: 1/2-x, y-1/2, z+1/2;
c: x-1/2, 1/2-y, z+1/2; d: 1/2-x, y-1/2, z-1/2;
e: x-1/2, 1/2-y, 1/2-z; f: x-1/2, 1/2-y, z-1/2;
g: 1/2-x, y-1/2, 1/2-z.

Bond Angles

O(1)d-A-O(2)f	77(2)	O(1)b-B-O(6)c	76(3)
O(2)e-A-O(2)f	103(2)	O(1)c-B-O(2)e	99(2)
		O(1)b-B-O(2)	92(6)
		O(2)b-B-O(2)g	88(5)
		O(2)e-B-O(2)g	87(2)
<O-A-O>	90(2)	<O-B-O>	88(4)

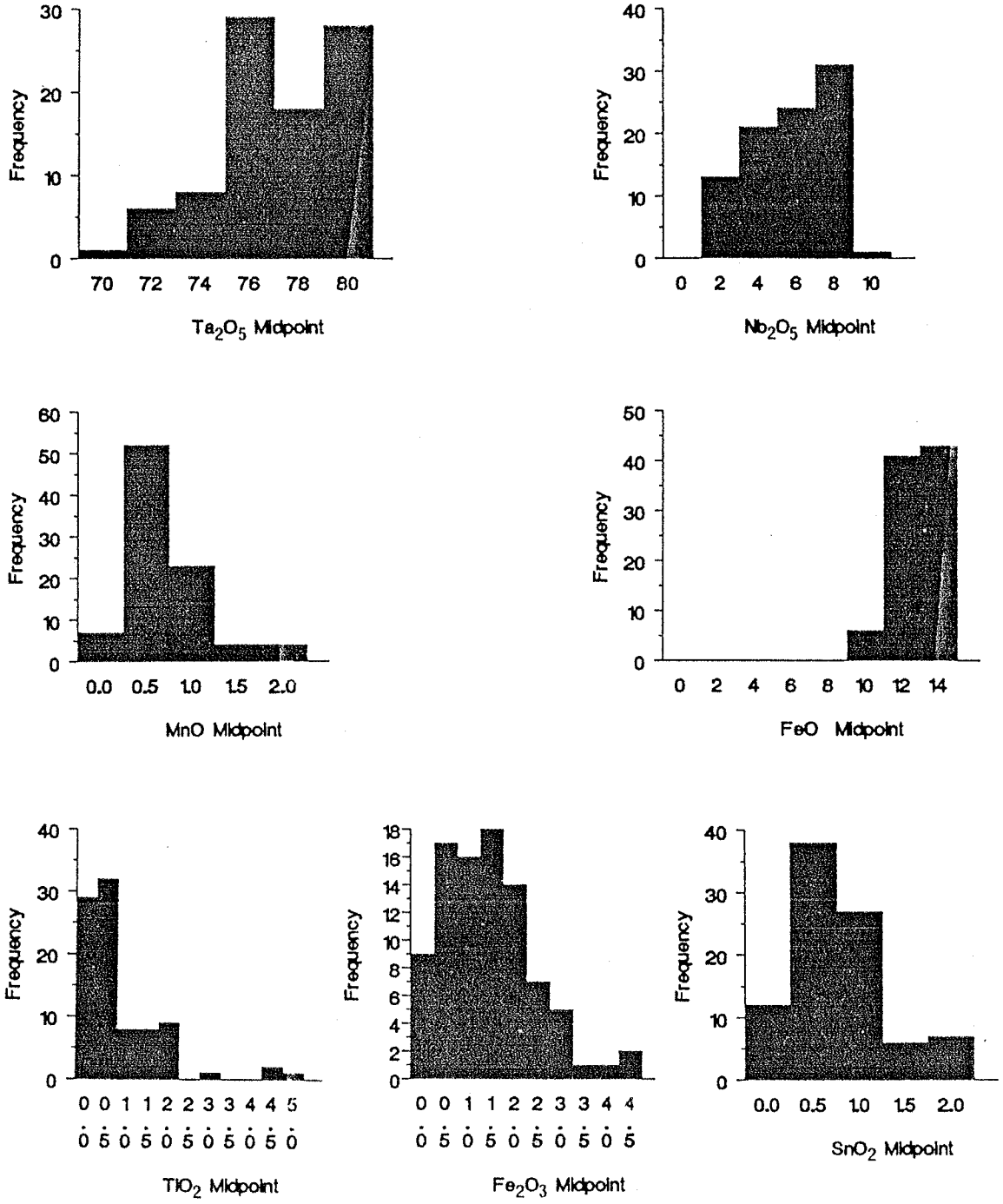

Figure 63: Compositional histograms for Yellowknife tapiolites based on a total of 90 electron microprobe analyses.

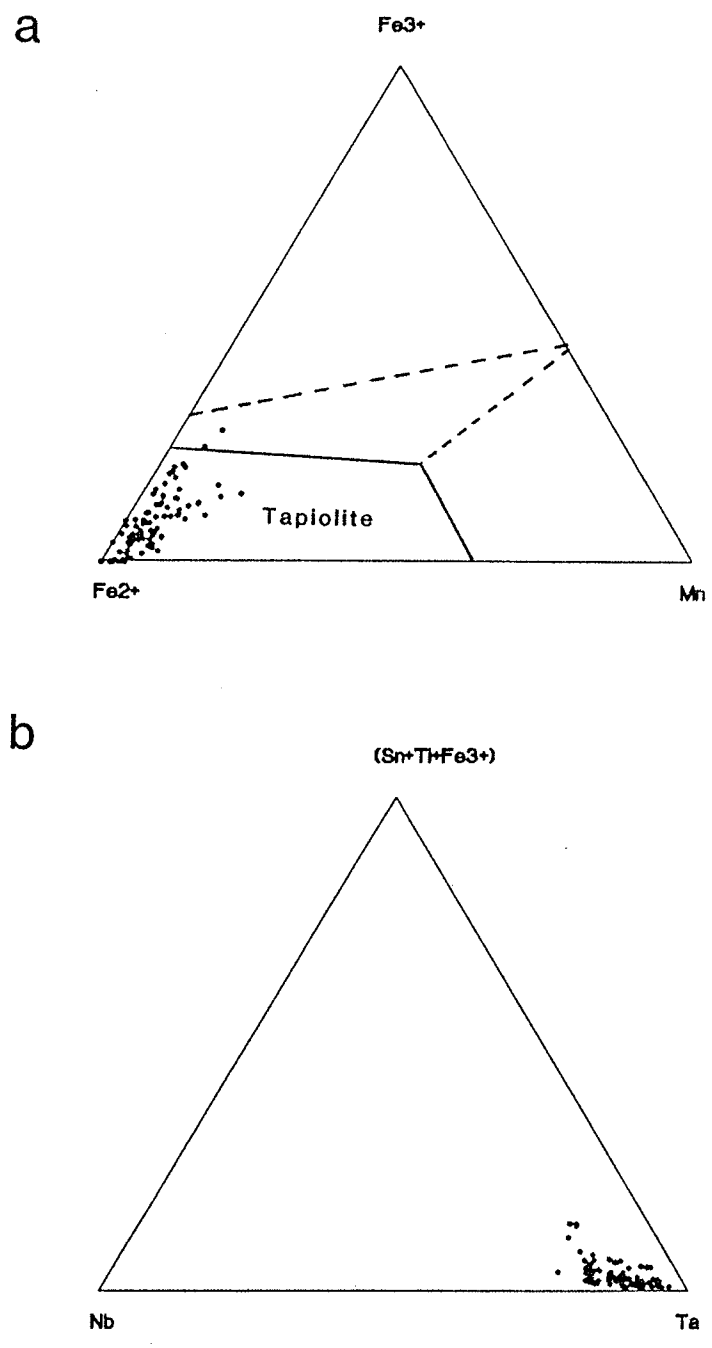

Figure 64: Bulk composition (atomic) of main cations in the Yellowknife tapiolites. (a) A-site and (b) B-site chemistry. Diagram (a) modified after Turnock (1966).

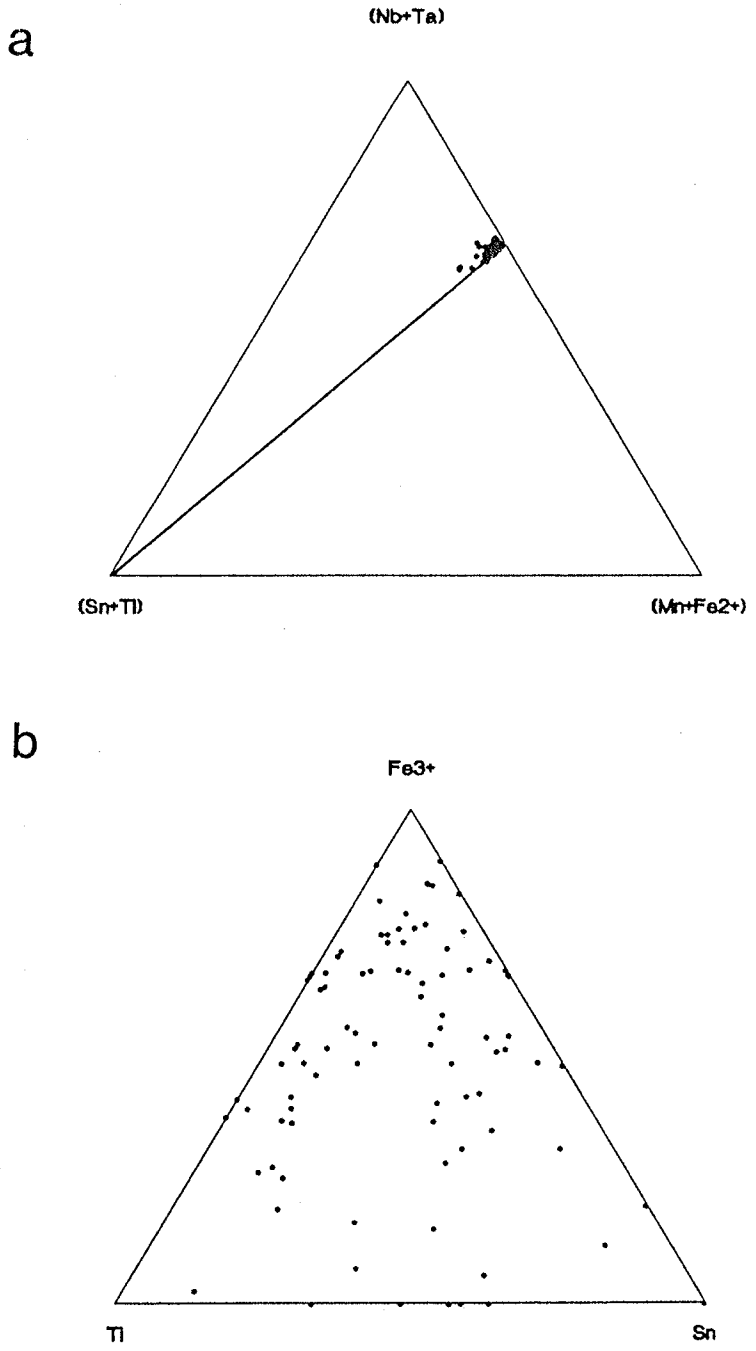

Figure 65: Bulk composition (atomic) of the Yellowknife tapiolites. (a) (Nb,Ta) - (Sn,Ti) - (Fe,Mn) and (b) Ti - Fe^{3+} - Sn triangles Tapiolite compositions plot above the ideal line in Figure (a) due to the presence of Fe^{3+}.

Isomorphous substitution

The tapiolite series minerals of the Yellowknife field show similar isomorphism trends between Fe-Mn and Nb-Ta as the columbite-tantalite group (Figures 66 and 67). However, the extent of Fe-Mn and Nb-Ta substitution is considerably less than that of columbite-tantalite. The variation in the Fe content of the Yellowknife tapiolites is controlled predominantly by the substitution of Mn. However, considerable scatter is observed in the main trend of the A-site cations and this is due to one of two factors. First, most Yellowknife tapiolites contain appreciable quantities of Fe^{3+} which apparently substitutes for Fe^{2+} (Figure 66b). Although substitution of Fe^{2+} by Fe^{3+} is not extensive, as shown by Turnock (1966), there is a strong negative correlation (R=-0.85) which suggests that this substitution scheme plays a significant role in defining tapiolite chemistry.

A somewhat less obvious substitution occurring at the A-site is that of Fe^{2+} by Ti. In this case the negative trend is not so well-defined as considerable scatter occurs along the trend.

Isomorphous substitution of cations at the B-site is dominated by the Nb-Ta pair (Figure 67a) with significant substitution by Ti also occurring. As mentioned previously, Nb-Ta substitution shows a strong negative correlation (R=-0.87) despite its limited extent. Beugnies and Mozafari (1968) found that the substitution of $FeNb_2O_6$ in natural tapiolites is limited to 36 mol %. Scatter among the data points is most likely due to substitution of (Ta+Nb) by Ti (Figure 67b) and to a minor degree by Mn (Figure 68).

Two substitution schemes acting independently or jointly dominate the tapiolite series:

$$3(Ti,Sn)^{4+} \longrightarrow 2(Nb,Ta)^{5+} + (Fe,Mn)^{2+}$$

$$Fe^{2+} + Nb^{5+} \longrightarrow Fe^{3+} + Ti^{4+}.$$

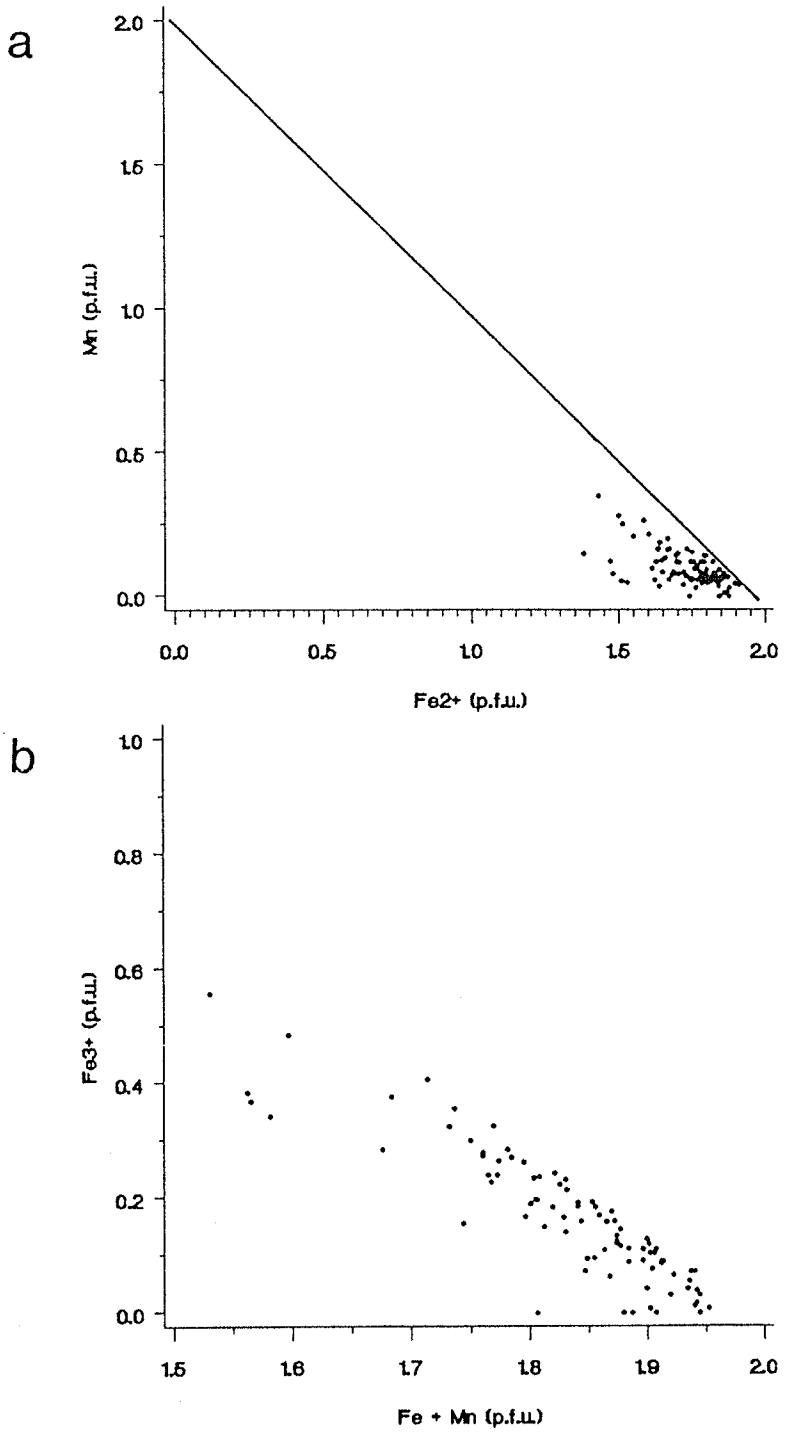

Figure 66: Cation-cation plots for Yellowknife tapiolite: (a) Fe^{2+} versus Mn, (b) Fe^{3+} versus (Fe^{2+} + Mn).

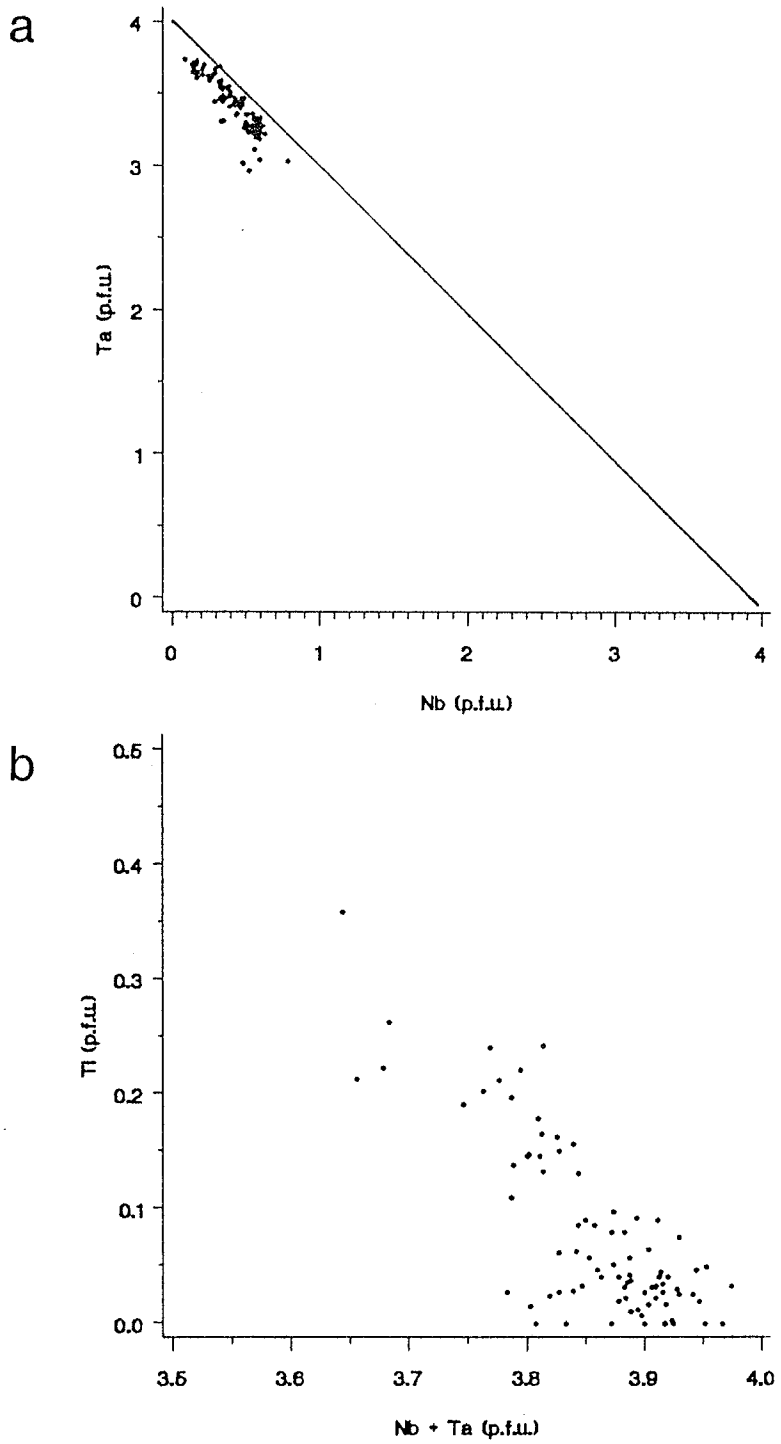

Figure 67: Cation-cation plots for Yellowknife tapiolite: (a) Nb versus Ta, (b) Ti versus (Nb + Ta).

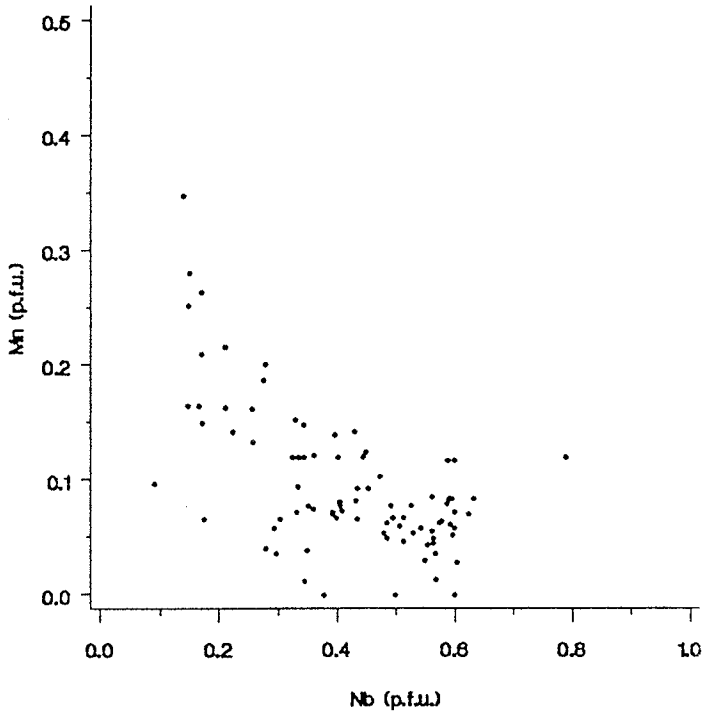

Figure 68: Cation-cation plot for Yellowknife tapiolite: Nb versus Mn.

CHAPTER 9

Cassiterite

Introduction

Cassiterite, like tapiolite, crystallizes in the tetragonal space group $P4_2/mnm$, Z=2. It is isostructural with rutile, with Sn occupying the identical atomic position as Ti. Unlike tapiolite, the cassiterite structure shows no tendency towards order-disorder and any significant changes within the crystal structure are probably due to compositional changes.

X-ray crystallography

The unit cell dimensions of the Yellowknife cassiterites determined by X-ray powder diffractometry are given in Table 28; they agree well with the values for synthetic SnO_2 and show only slight to moderate deviations from the ideal. As order-disorder effects in cassiterite are nonexistent, the variations in unit cell dimensions are most likely due to compositional differences. Clark *et al.* (1976) showed that the unit cell dimension of cassiterites, in particularly *c*, were inversely proportional to the sum to Fe, Ti, Nb and Ta. With the exception of two samples from the Tan swarm, the Yellowknife cassiterites agree well with their results (Figure 69). A plot of the cell volume versus the sum of Fe, Ti, Nb and Ta from the Yellowknife cassiterites, also shows a negative correlation, but not to the same degree as the *c* dimension. The deviation of the Tan samples from the trends is inexplicable at the moment.

Table 28: Unit cell dimensions of 31 natural Yellowknife cassiterites.

Sample No.	a(Å)	c(Å)	V(Å^3)
Bet-114	4.7367(6)	3.1837(6)	71.43(2)
Big Hill-Cs-1	4.7386(5)	3.1826(6)	71.46(1)
Big Hill-12	4.7398(4)	3.1834(5)	71.52(1)
Big Hill-16	4.740(1)	3.180(1)	71.46(4)
Big Hill-17	4.740(1)	3.184(2)	71.54(5)
Big Hill-23	4.7401(3)	3.1852(3)	71.57(1)
Big Hill-24	4.7401(2)	3.1854(3)	71.571(7)
Big Hill-25	4.7408(5)	3.1854(5)	71.59(1)
Bin-4	4.7378(2)	3.1825(3)	71.436(7)
Bin-18	4.7394(3)	3.1860(5)	71.57(1)
Bin-19	4.743(1)	3.178(5)	71.47(5)
Cata-T-2	4.7359(3)	3.1829(3)	71.39(1)
Cata-U-1	4.7373(3)	3.1840(3)	71.456(9)
Dr.Bob-3	4.7380(2)	3.1846(3)	71.490(9)
Dr.Bob-5	4.7385(3)	3.1847(3)	71.507(9)
Freda-10	4.7358(3)	3.1825(4)	71.38(1)
Freda-18	4.7361(3)	3.1840(4)	71.421(1)
Jim-Lit-A-1	4.7400(4)	3.1840(5)	71.54(1)
Jim-Lit-A-4	4.7371(3)	3.1831(4)	71.430(9)
Lu-B-4	4.7391(3)	3.1853(3)	71.539(8)
Lu-B-5	4.7364(2)	3.1841(2)	71.431(7)
Lu-B-8	4.7377(3)	3.1804(4)	71.387(9)
Lu-C-3	4.7390(3)	3.1841(3)	71.511(8)
Lu-C-5	4.7370(5)	3.1846(7)	71.46(2)
Mac-109	4.7414(5)	3.1839(4)	71.58(1)
Peg-1-3	4.7370(2)	3.1824(3)	71.410(8)
Peg-1-4	4.7368(2)	3.1820(3)	71.394(7)
Tan-2-20	4.7387(3)	3.1757(4)	71.310(8)
Tan-2-19	4.7435(5)	3.1766(5)	71.48(1)
Tan-4-3	4.7432(8)	3.184(1)	71.64(3)
Vo-5-20	4.7378(3)	3.1830(4)	71.45(1)

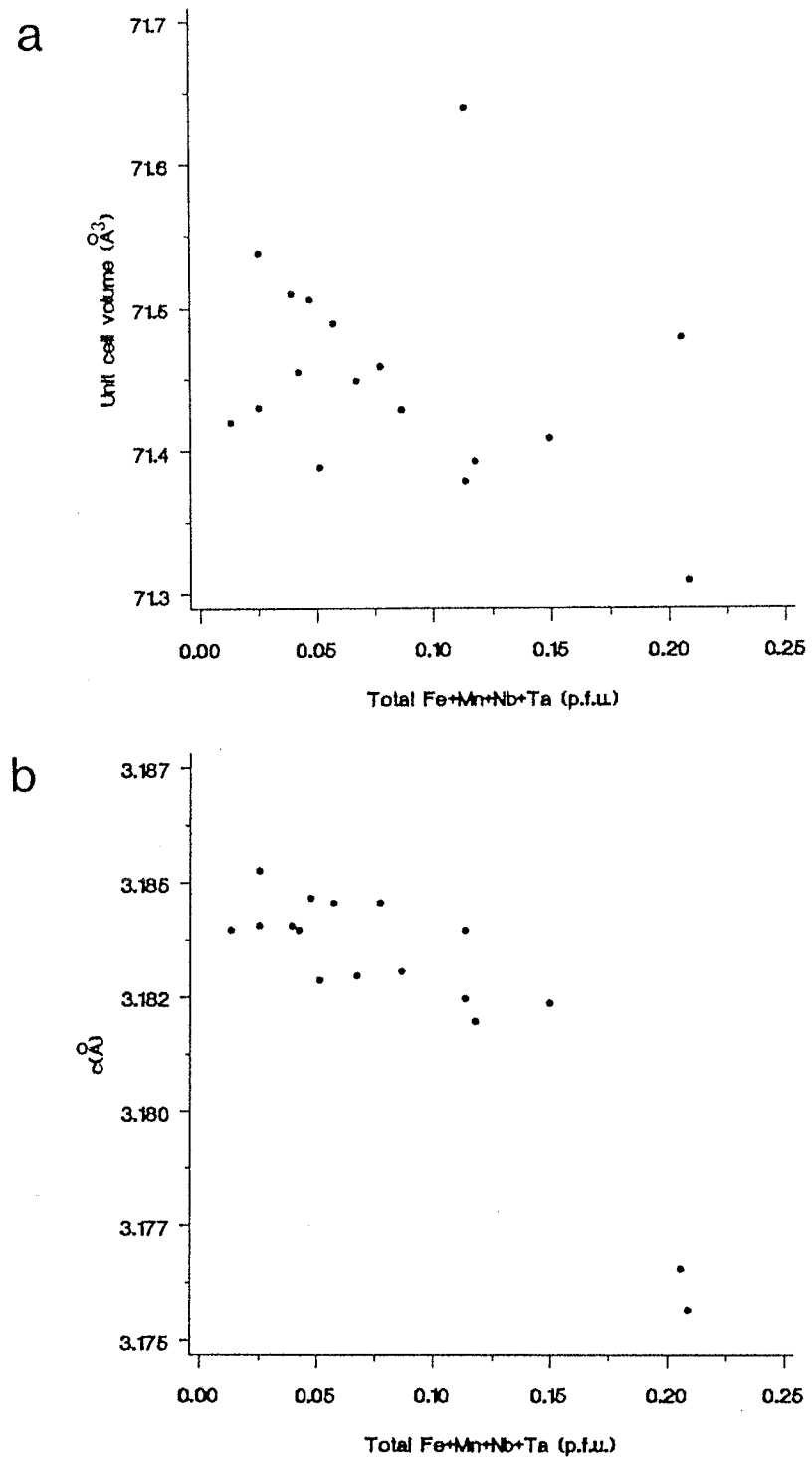

Figure 69: Composition versus unit cell dimensions for Yellowknife cassiterites. (a) Unit cell volume versus sum of Fe,Ti,Nb, and Ta, (b) c unit cell dimension versus sum of Fe,Ti,Nb, and Ta.

Chemistry

The chemistry of cassiterite, ideally SnO_2, in granitic pegmatites is often characterized by the presence of significant quantities of Fe, Ta, Nb and Mn (Foord, 1982). Cassiterite from the Yellowknife pegmatite field frequently contains elevated concentrations of these elements, which are incorporated into the cassiterite structure by substituting for Sn. Overall, as much as 16 wt.% of Fe, Ta, Nb, Ti and Mn oxides substitute for Sn (Appendix C). Typically, the Yellowknife cassiterites show considerable accumulations of Fe and Ta with only minor to trace concentrations of Nb, Ti and Mn (Figure 70). Calculated Fe_2O_3 contents of the Yellowknife cassiterites range from 0.0 to 3.6%, whereas FeO varies from 0.0 to 2.3%. The Ta_2O_5 content of most Yellowknife cassiterite falls within the range 0 to 2%, although cassiterites with Ta_2O_3 in excess of 5% do occur locally.

The Ti content of most cassiterite, including those of pegmatitic origin, is typically low (< 0.10% TiO_2). Analyses of cassiterite from the Yellowknife pegmatite field generally show no detectable Ti or very minor amounts. Local accumulations are observed in a few pegmatites and values reach a maximum of only 0.6% TiO_2.

Isomorphous substitution

Limited substitution of Sn by Fe^{2+}, Fe^{3+}, Nb and Ta is common in the Yellowknife cassiterites and all show negative correlations (Figures 71 and 72). The incorporation of Fe^{2+} into cassiterite seems to occur more easily than Fe^{3+}. Tantalum is more likely to occur in cassiterite than Nb, which may be a reflection of the extreme fractionation achieved by the pegmatite at the time of cassiterite crystallization.

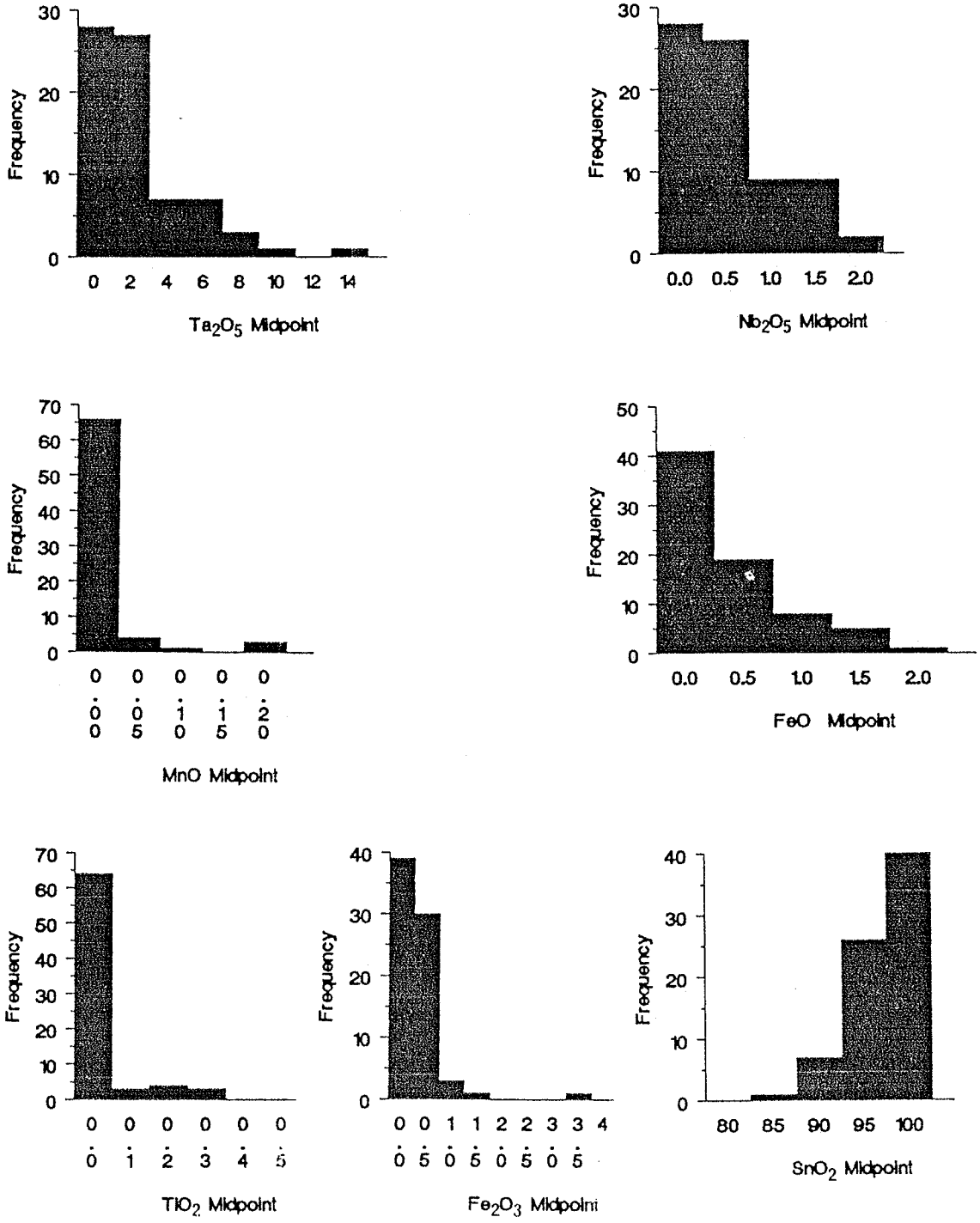

Figure 70: Compositional histograms for Yellowknife cassiterite based on a total of 99 microprobe analyses.

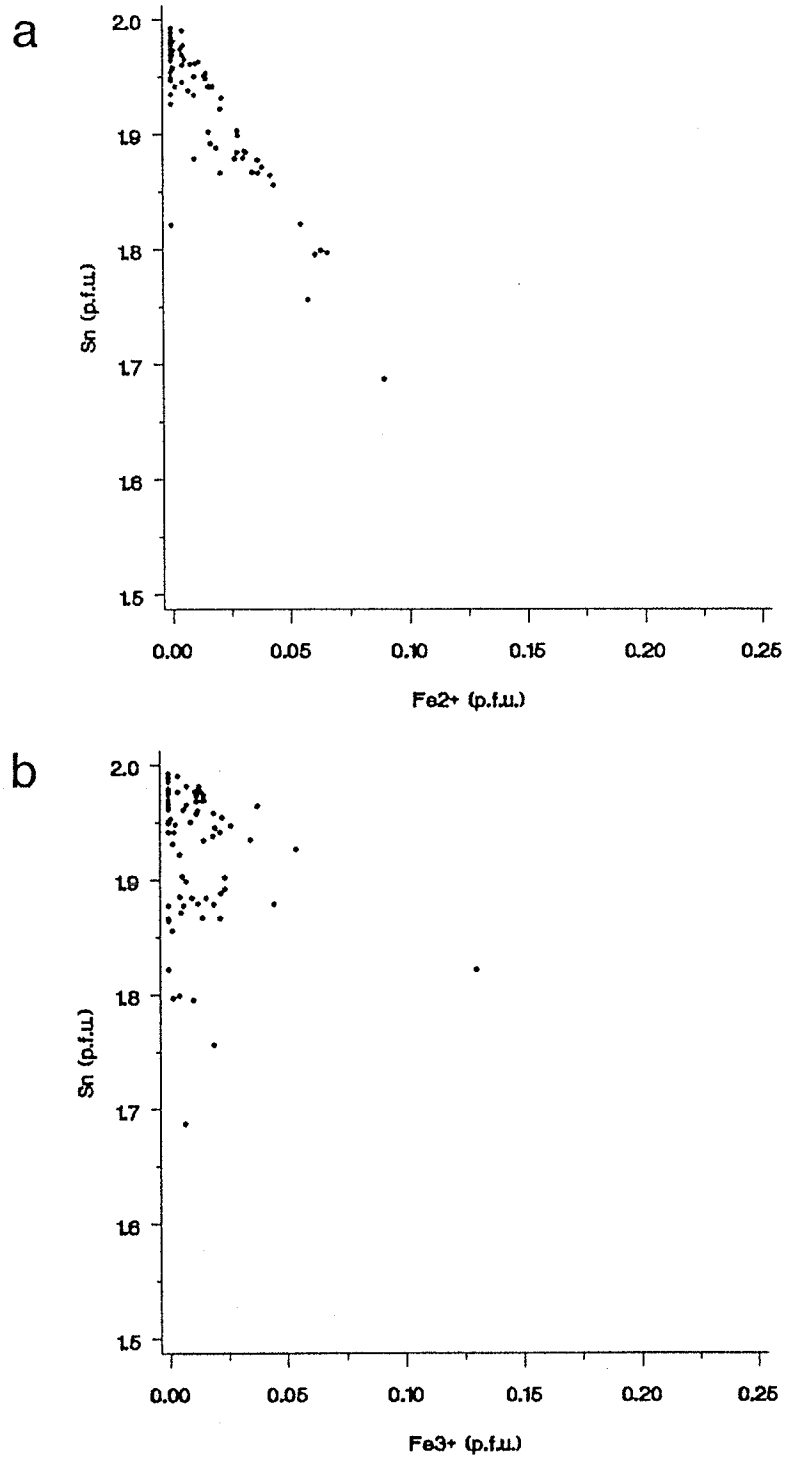

Figure 71: Cation-cation plots for Yellowknife cassiterites: (a) Sn versus Fe^{2+} and (b) Sn versus Fe^{3+}.

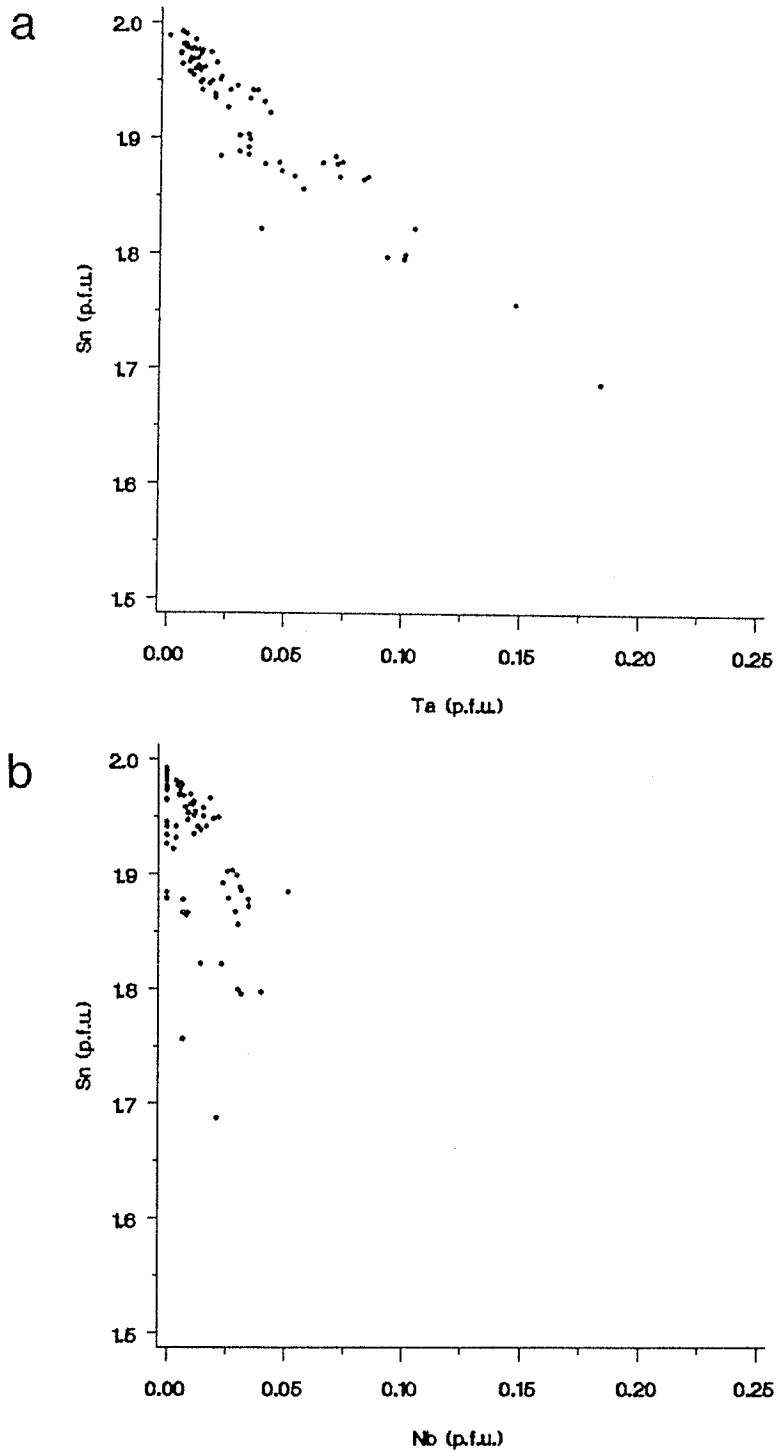

Figure 72: Cation-cation plots for Yellowknife cassiterites: (a) Sn versus Ta and (b) Sn versus Nb.

Compositionally, the Yellowknife cassiterites may be interpreted as solid solutions of SnO_2 and a "tapiolite component" $(Fe>Mn)(Ta>Nb)_2O_6$ as compositions plot close to the $Sn-(Fe,Mn)-(Ta,Nb)_2$ join (Figure 73a). Although cassiterite compositions vary widely in their Ta/(Ta + Nb) ratios, they always show Ta > Nb (Figure 73b).

The form of Fe in cassiterite has been the subject of much debate and at present no conclusive answer has been provided. Most Fe present in cassiterite is thought to occur in the form of Fe-hydroxy-stannate and Fe-stannate inclusions, with only a limited amount being isomorphously incorporated into the cassiterite structure (Grubb and Hannaford, 1966; Voronina et al., 1978). Iron in cassiterite can occur both as Fe^{2+} and Fe^{3+} as discovered by Mössbauer studies (Grubb and Hannaford, 1966; Banerjee et al., 1970).

Figure 74 suggests the possibility of two mechanisms by which Fe may enter the cassiterite structure. A plot of $Fe^{2+}-Fe^{3+}-(Ta,Nb)$ better illustrates this point (Figure 74a). Note that the majority of the analyses plot along the $FeTa_2O_6-FeTaO_4$ join, suggesting extensive $Fe^{2+}-Fe^{3+}$ solid solution. A strong positive correlation (R=0.93) is found between Fe^{2+} and Ta, with a trend extending along a Fe:Ta slope of 1:2 (Figure 74b). In contrast, a plot of Fe^{3+} versus Ta shows no correlation.

Synthetic studies show limited isomorphous substitution between SnO_2 and TiO_2 (Schröcke, 1972). The few Yellowknife samples which contain detectable Ti do not show any significant correlation between Sn and Ti. The lack of a significant correlation between these cations may be due to the low Ti contents, caused by the relatively low availability of Ti at the time of cassiterite formation (i.e. a geochemical rather than a crystal chemical consequence).

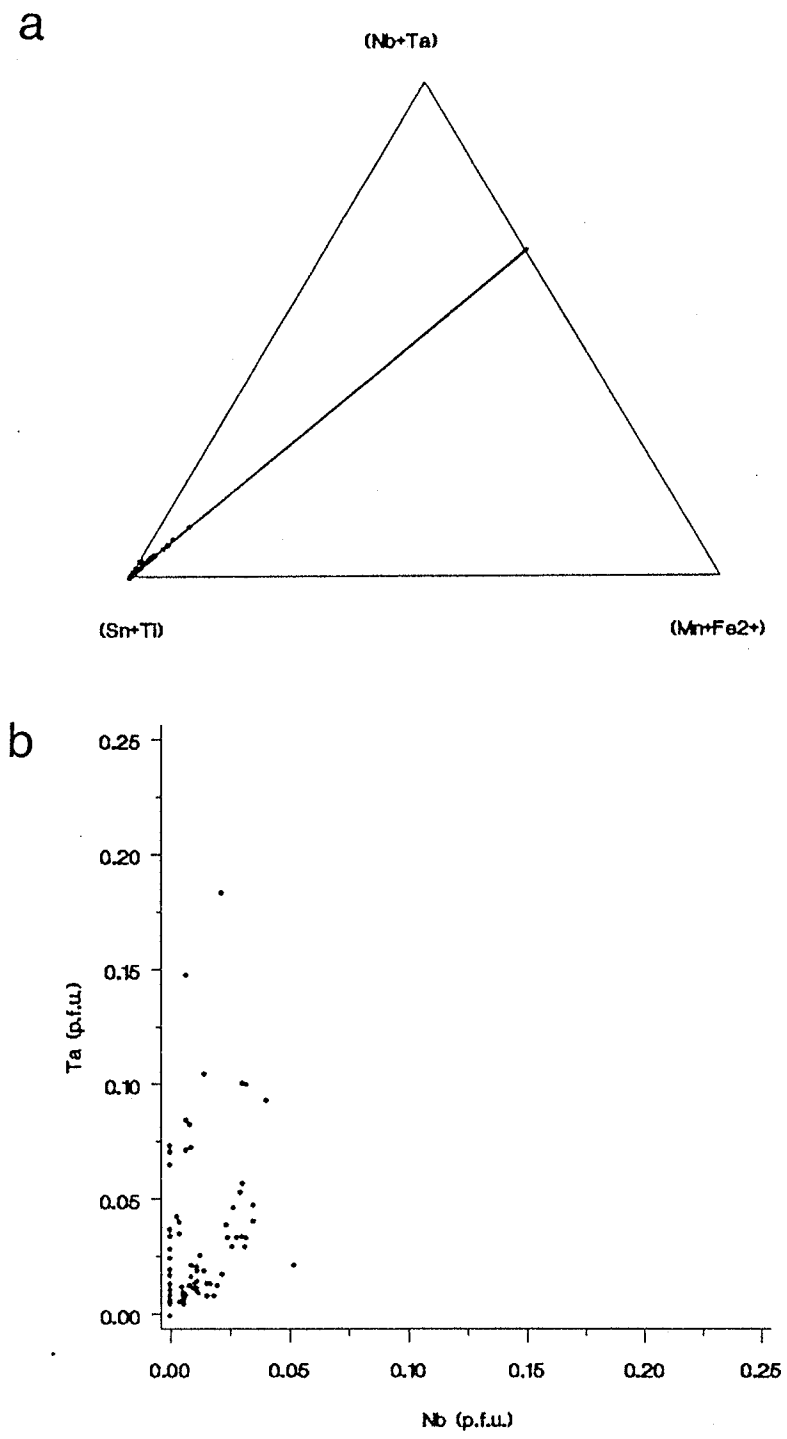

Figure 73: Bulk composition (atomic) for Yellowknife cassiterites. (a) R^{2+}-R^{4+}-R^{5+} triangle, (b) plot of Nb versus Ta.

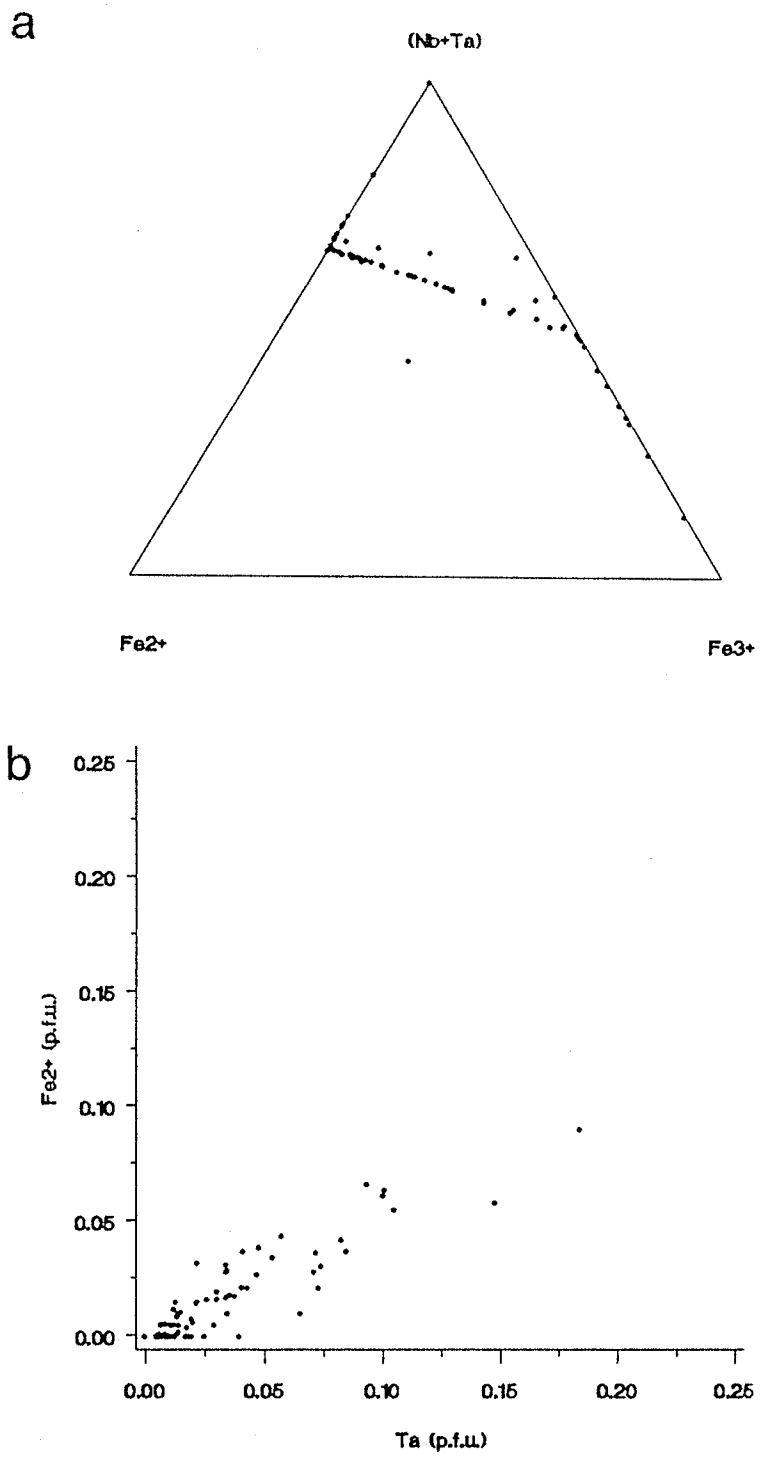

Figure 74: Bulk composition (atomic) for Yellowknife cassiterites in the Fe^{2+}-Fe^{3+}-(Ta+Nb) triangle. (a) Fe^{2+}-Fe^{3+}-(Ta+Nb) triangle, (b) plot of Fe^{2+} versus Ta.

CHAPTER 10

Pyrochlore Group

Introduction

Members of the pyrochlore group are probably the second most abundant Nb- and Ta-oxide mineral in granitic pegmatites after columbite-tantalite. The majority of the known species restricted to granitic pegmatites are Ta- and Ti-rich, of which, microlite and uranmicrolite are the most common. The occurrence of Nb-dominant members is very limited in pegmatitic environments; they are typically found in carbonatites and alkalic rocks.

Minerals of the pyrochlore group crystallize in the cubic space group Fd3m, Z=8 and have the general formula $A_{2-n}B_2X_6Y_{1-m}\,pH_2O$, in which A=Na, Ca, K, Sb^{3+}, U, Pb, Sr, Th, REE, Bi, Sn^{2+}, Ba, Mn, Cs, Fe^{2+}; B=Ta, Nb, Ti, Zr, Fe^{3+}, Sn^{4+}, W; X=O; Y=O, OH, F; m=0-2; n=0-1 and p=0-1(?) (Foord, 1982; Groult et al., 1982). The pyrochlore group is divided into three subgroups on the basis of the dominant cation (Nb, Ta or Ti) occupying the B-site. The subgroups as defined in Hogarth (1977) and approved by the International Mineralogical Association Commission on New Minerals and New Mineral Names are: pyrochlore subgroup = (Nb+Ta)>2Ti and Nb>Ta; microlite subgroup = (Nb+Ta)>2Ti and Ta≥Nb; betafite subgroup = 2Ti≥(Nb+Ta). Individual species occurring within each subgroup are further defined by the chemistry of the dominant A-site cation other than Ca and Na (Table 29).

Table 29: Classification of the Pyrochlore Group Minerals. Modified after Hogarth (1977), Černý et al. (1979), and Groat et al. (1987).

SUBGROUP:		PYROCHLORE Nb+Ta>2Ti & Nb>Ta	MICROLITE Nb+Ta>2Ti & Ta≥Nb	BETAFITE 2Ti≥Nb+Ta
No A-cation other than Na or Ca >20% total A-cations		pyrochlore	microlite	calciobetafite (Ca>Na)
Any A-cation, other than Na or Ca, >20% of total A-cations. Name is for the dominant non-(Na,Ca) cation.	K	kalipyrochlore		
	Sr		stannomicrolite	
	Ba	bariopyrochlore	bariomicrolite	
	Pb	plumbopyrochlore	plumbomicrolite	plumbobetafite
	Sb		stibiobmicrolite	stibiobetafite
	Bi		bismutomicrolite	
	Y*	yttropyrochlore		yttrobetafite
	Ce*	ceriopyrochlore		
	U	uranpyrochlore	uranmicrolite	betafite

Ce* + La → Eu , Y* + Y + Gd → Lu

* the prefixes "cerio" or "yttro" are applied if Y* + Ce* >20% total A-cations, not just if Y* >20% or if Ce* >20%.

Crystal structure of pyrochlore group minerals

The crystal structure of the pyrochlore group was first described by von Gaertner (1930). The structure is derived from the fluorite structure (Fm3m) by removing 1/8 of the anions in an ordered manner. In fluorite, all of the cubes share their edges with adjacent cubes (Figure 75a). Removal of 1/8 of the anions such that 1/2 of the cubes lack two opposing vertices, results in the formation of octahedra (Figure 75b). Thus in the pyrochlore (defect fluorite) structure, 1/2 of the polyhedra are cubes and 1/2 are octahedra. All of the cubes share their edges; half with other cubes and half with octahedra. In contrast, octahedra not only share edges with cubes, but also share two of their corners with neighboring octahedra. The large A-cations occupy the cubes and the smaller B-cations typically fill the octahedral positions.

The stoichiometry of the pyrochlore group is typically non-ideal, with vacancies occuring at the A-site and the Y-site. Recent structure refinements by Groult et al. (1982) have also shown the existence of vacancies at the X-site. In contrast, the B-site of natural and synthetic pyrochlore group minerals is always fully occupied.

Chemistry

Electron microprobe analyses for all Yellowknife microlites are given in Appendix C. Oxide totals vary between 85.7 and 99.2, and low sums suggest substantial incorporation of H_2O and/or F. Because of the possible occurrence of vacancies at the X-site, formula calculations are based on the normalization of the fully occupied B-site to 2 cations per formula unit.

a

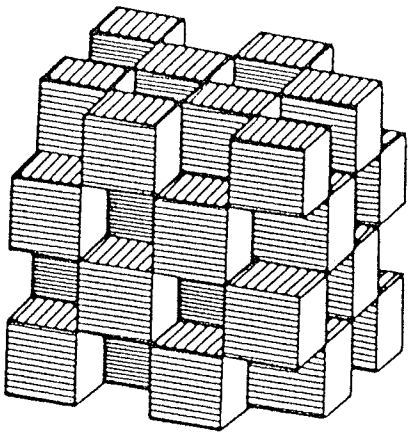

b

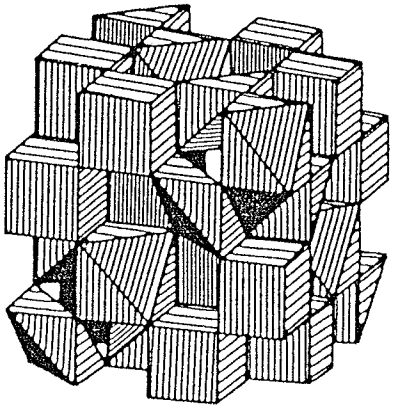

Figure 75: Derivation of the pyrochlore structure from the fluorite structure. (a) Fluorite structure, (b) ideal pyrochlore structure. Figures after Ercit (1986).

The major element chemistry of the Yellowknife microlites is quite comparable to microlite compositions from other localities (von Knorring and Fadipe, 1981; von Knorring and Condliffe, 1984; Lumpkin et al., 1986). The major cations occurring at the A-site are Ca and Na, with Ca typically ranging from 0.07 to 1.67 cations per formula unit and Na from 0.0 to 0.50 cations per formula unit (Figure 76a). Of the numerous cations capable of substituting for Ca and/or Na at the A-site, Fe is typically the most common substituent. Total Fe calculated as FeO ranges from 0.0 to 6.0 wt.% in the Yellowknife specimens. Many microlite analyses show enrichment in U (up to 14 wt. % UO_2) and Pb (up to 4 wt. % PbO). Enrichment in these elements invariably results in a decreased Ca content.

The B-site chemistry is dominated by Ta and Nb with limited substitution by Ti, but all contain Ta > Nb and 2Ti < (Nb+Ta) (Figure 76b) and therefore are classified as microlites. Tin is conspicuously absent in all Yellowknife microlite analyses.

Isomorphous substitution

The complex mineral chemistry and the presence of cation and anion vacancies make it difficult to adequately characterize the substitution schemes present in the microlite subgroup. Isomorphism between Nb and Ta is evident within the Yellowknife samples and the correlation is strongly negative (R= -0.94). Any scatter within the trend is due to substitution by Ti in the B-site (Figure 77).

Characterization of the A-site chemistry is more difficult; however, plots of Na versus A-site vacancies and Ca versus A-site vacancies do suggest some structural control on their occurrence (Figure 78). A plot of Ca

a

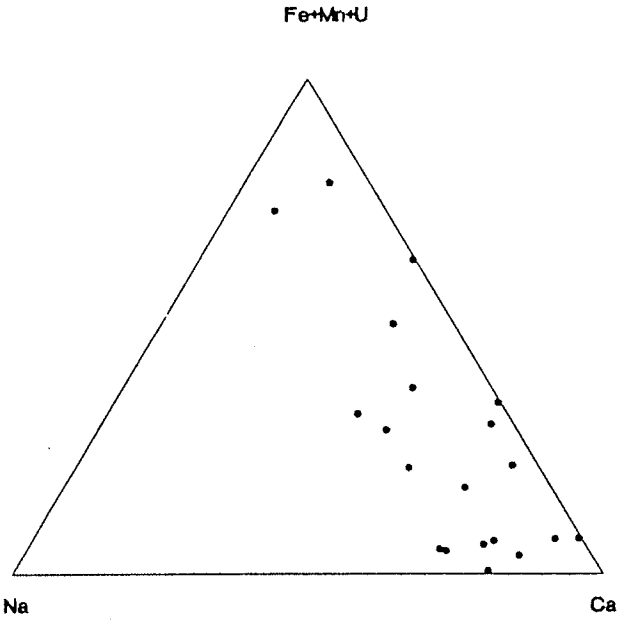

b

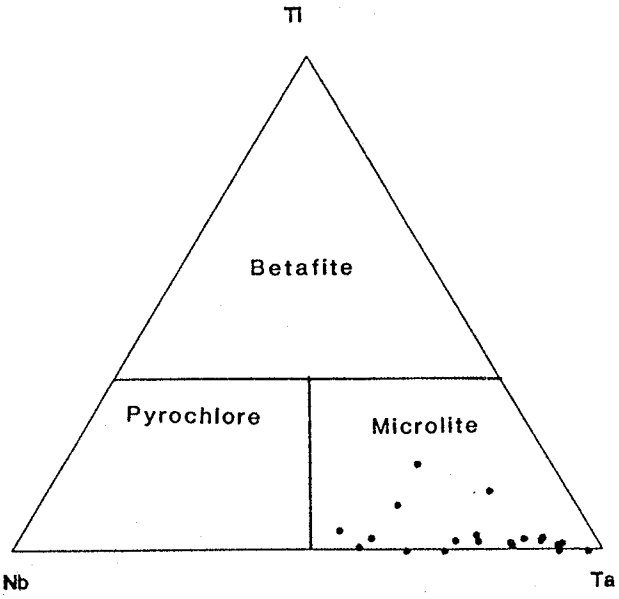

Figure 76: Populations of cations in the Yellowknife pyrochlore group minerals. (a) A-site and (b) B-site chemistry.

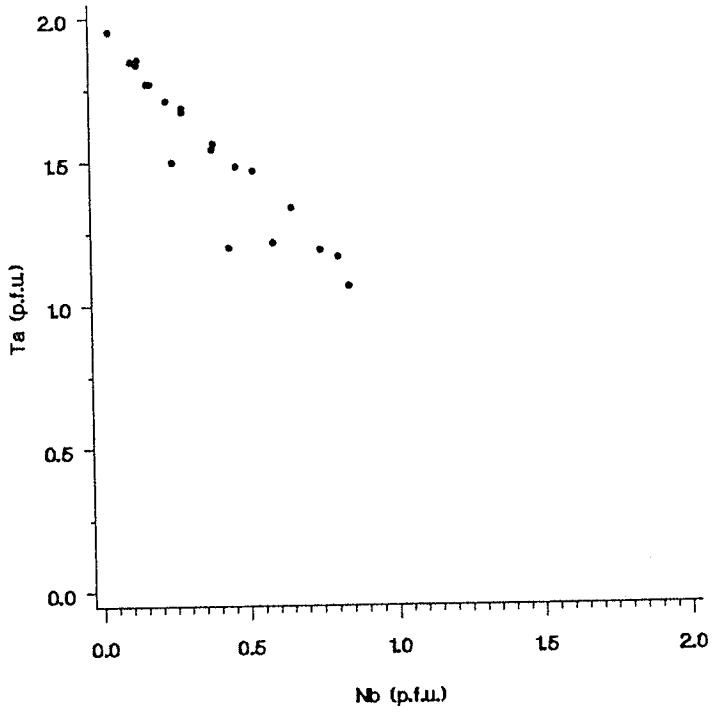

Figure 77: Nb versus Ta plot for Yellowknife microlites.

versus U shows very little correlation between the two cations; however, the plot is somewhat useful in separating microlites of different paragenesis (Figure 79a). Microlites associated with columbite-tantalite tend to have a different U signature than those found with tapiolite. Iron-bearing microlites show a negative correlation with Ca and a positive correlation with Mn; however this does not hold true of all microlite specimens (Figure 79b).

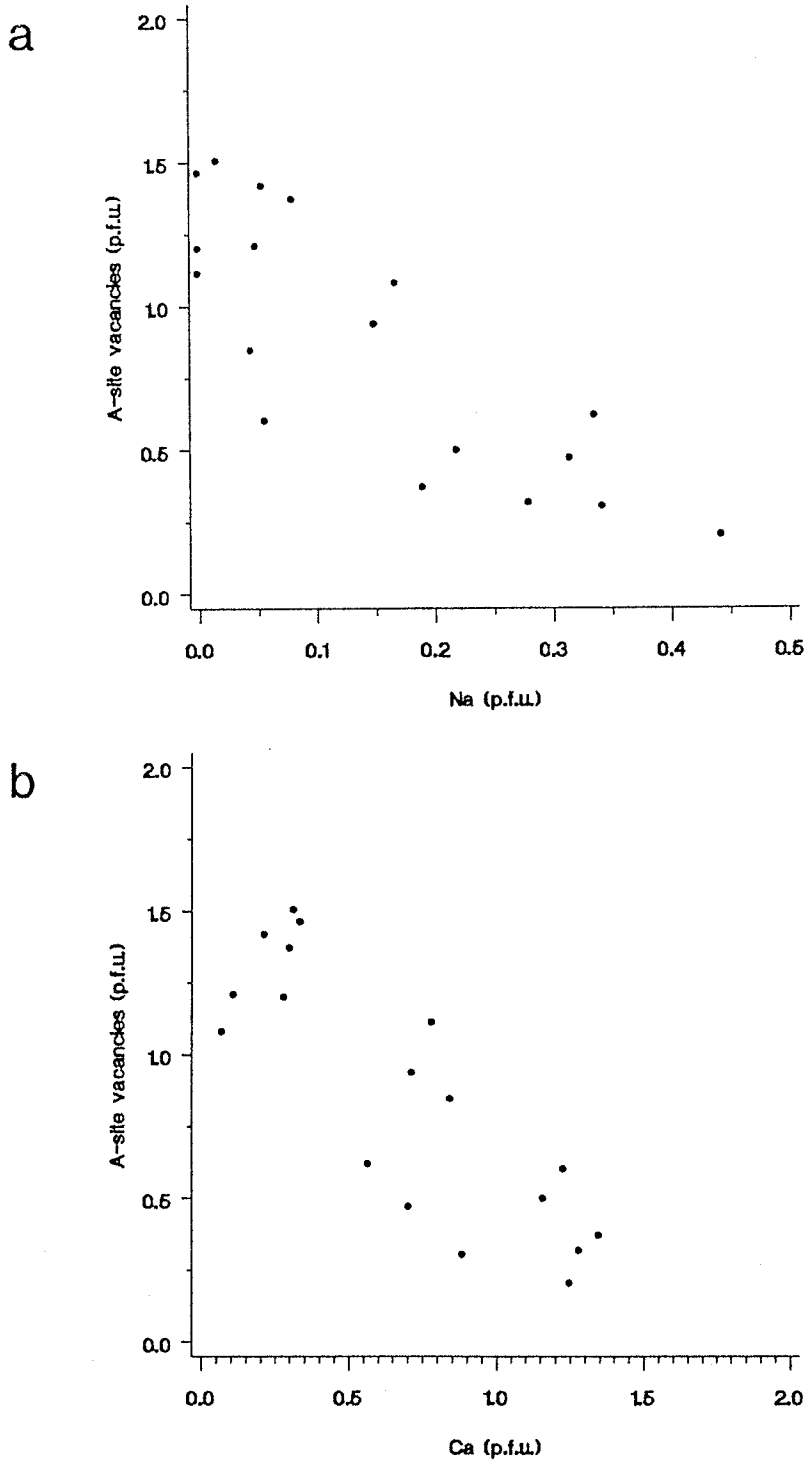

Figure 78: Cation-cation plots for Yellowknife microlites. (a) Na versus A-site vacancies, (b) Ca versus A-site vacancies.

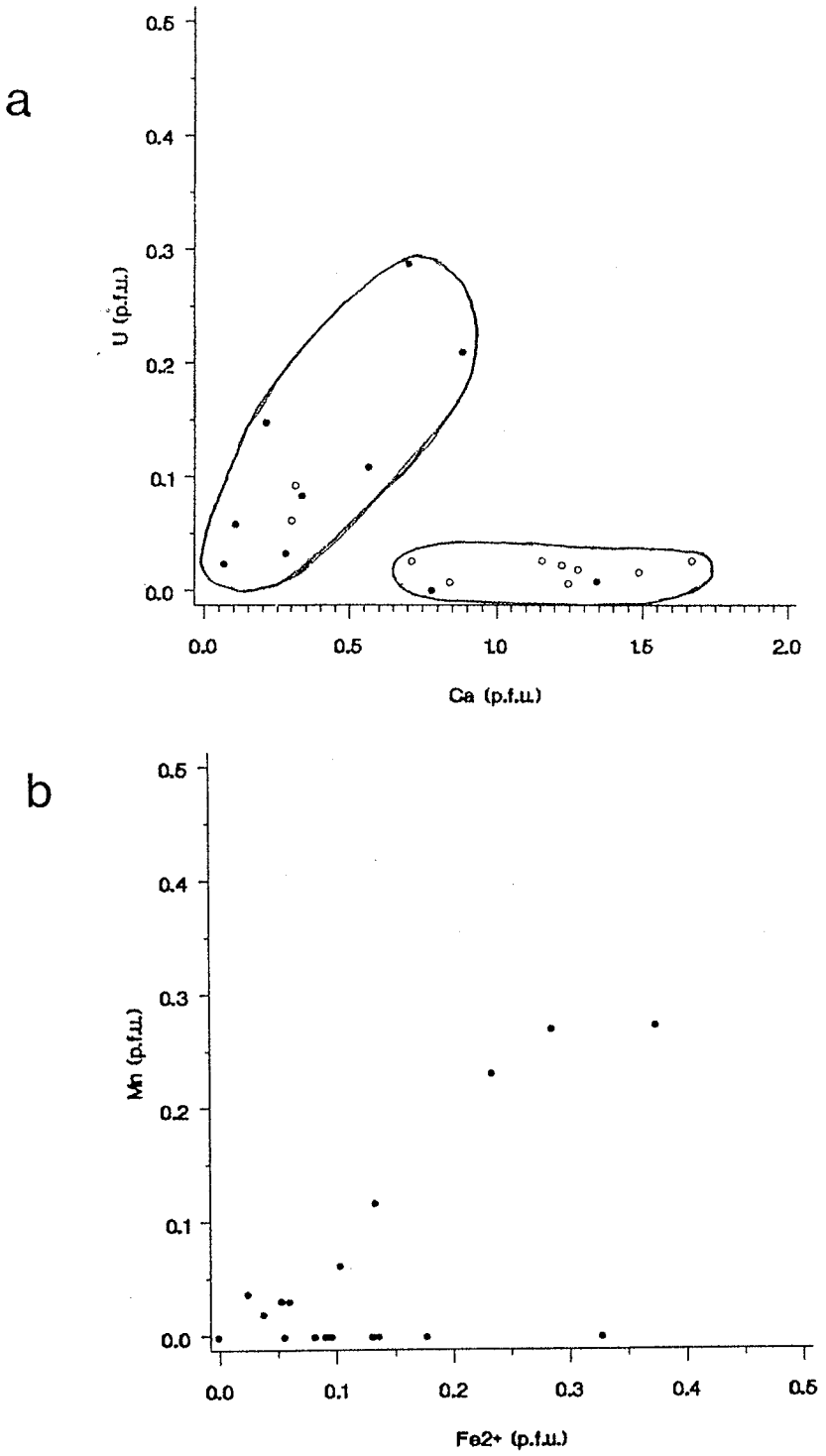

Figure 79: Cation-cation plots for Yellowknife microlites. (a) Ca versus U; Open circles - microlites associated with ferrotapiolite, dots - microlites associated with columbite-tantalite. (b) Mn versus Fe (All Fe as Fe^{2+}).

CHAPTER 11

Element partitioning

Introduction

The distribution of elements among coexisting phases is dependent upon their individual crystallochemical preferences and stabilities under given PT conditions within the parent system. The partitioning of Fe,Mn,Nb,Ta,Ti and Sn in Nb,Ta mineral associations is not well understood and studies of this type are extremely rare (Ginzburg, 1956; Černý et al., 1981; Černy and Ercit, 1985; Černý et al., 1985b; Černý et al., 1986b). Thus, it is desirable to characterize the behavior of the major elements among coexisting Nb-, Ta- and Sn-oxide minerals. To augment the present data, the major element preference of coexisting Nb, Ta and Sn minerals from the Yellowknife field is critically examined here.

Columbite-tantalite vs. ferrotapiolite

Ferrotapiolite is always conspicuously enriched in Ta and Fe when compared to coexisting columbite-tantalite. In most cases, tie-line slopes of all ferrotapiolite + columbite-tantalite pairs are generally regular, suggesting near equilibrium conditions. Compositional data for ferrotapiolite + columbite-tantalite pairs show very restricted Mn substitution in ferrotapiolite and only slightly greater substitution of Nb (Figure 80a). In contrast, the coexisting orthorhombic phase shows a narrow range of Mn/(Mn + Fe) ratios along with very limited Ta/(Ta + Nb) ratios. Reasons for the

preference of Fe and Ta in the tetragonal phase relative to the orthorhombic phases have been suggested by Weitzel (1976). Evidently, the difference in polarizing effect of Ta^{5+} and Nb^{5+} results in the preference of Ta for tetragonal rather than orthorhombic structures. In addition, the difference in ionic radii between Mn^{2+} and Fe^{2+} (0.83 and 0.78Å for Mn and Fe respectively; Shannon, 1976) apparently controls their preference for a particular structure type. The larger Mn cation is too big to be accomodated by the tapiolite structure and therefore enters the orthorhombic columbite structure (the average A-O distances for ferrotapiolite and manganotantalite are 2.07 Å, v. Heidenstam, 1968; and 2.18 Å, Grice et al., 1976, respectively).

Columbite-tantalite vs. cassiterite

Columbite-tantalite + cassiterite pairs follow a similar partitioning effect as columbite-tantalite + ferrotapiolite pairs. The cassiterite contains little or no Mn and strongly prefers Fe and Ta relative to Mn and Nb (Figure 80b). However, unlike ferrotapiolite, the amount of Nb which accumulates into cassiterite is much greater. The coexisting columbite-tantalite shows a slightly larger range of Mn/(Mn + Fe) ratios than those found in the ferrotapiolite + columbite-tantalite pairs. Tie-line slopes are quite erratic and irregular, indicating nonequilibrium among the coexsisting mineral pairs.

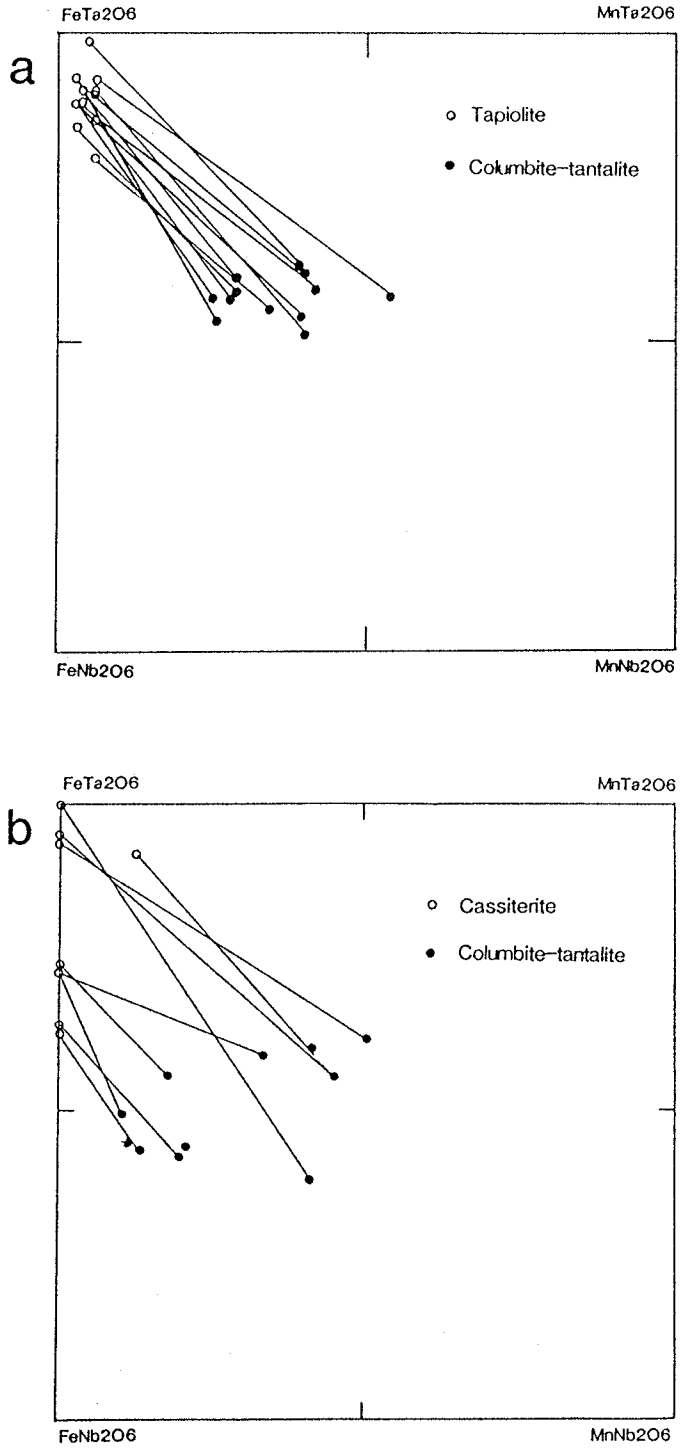

Figure 80: Composition of coexisting mineral pairs in the columbite quadrilateral. Atomic ratios with all Fe as Fe^{2+}. Tie-lines connect coexisting phases. (a) columbite-tantalite + ferrotapiolite, (b) columbite-tantalite + cassiterite.

Ferrotapiolite vs. cassiterite

Ferrotapiolite + cassiterite pairs are not only scarce in the Yellowknife field, but in other pegmatite districts as well (unpubl. data of Wise). In general, Fe is concentrated in cassiterite relative to ferrotapiolite, whereas the behavior of Ta and Nb is quite erratic (Figure 81a). In pairs of this type, Sn is conspicuously absent or occurs in minor quantities in ferrotapiolite.

Ferrotapiolite vs. ixiolite

This mineral pair is also scarce and the available data indicates a strong preference for Mn of ixiolite (Figure 81b). Partitioning of Ta between the two phases is essentially equal.

Ixiolite vs. cassiterite

The only available analysis of ixiolite coexisting with cassiterite shows a preference for Ta by cassiterite relative to ixiolite.

Microlite vs. columbite-tantalite and ferrotapiolite

Compared to coexisting (or replaced) columbite-tantalite, microlite is always enriched in Ta relative to Nb (Figure 82a). In contrast, the Ta content is slightly lower in microlite coexisting with ferrotapiolite (Figure 82b). However, some microlite + ferrotapiolite pairs show nearly equal Ta distribution.

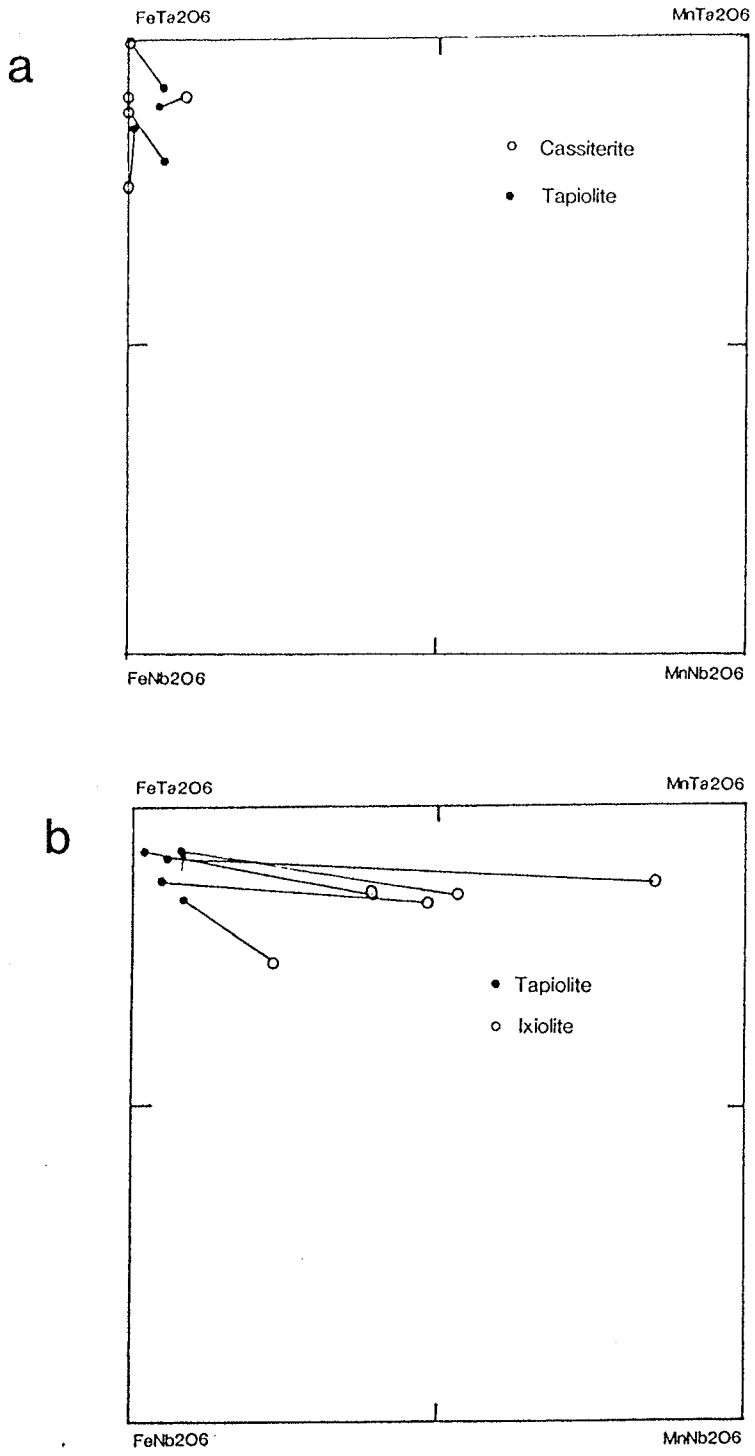

Figure 81: Composition of coexisting mineral pairs in the columbite quadrilateral. Atomic ratios with all Fe as Fe^{2+}. Tie-lines connect coexisting phases. (a) ferrotapiolite + cassiterite, (b) tapiolite + ixiolite.

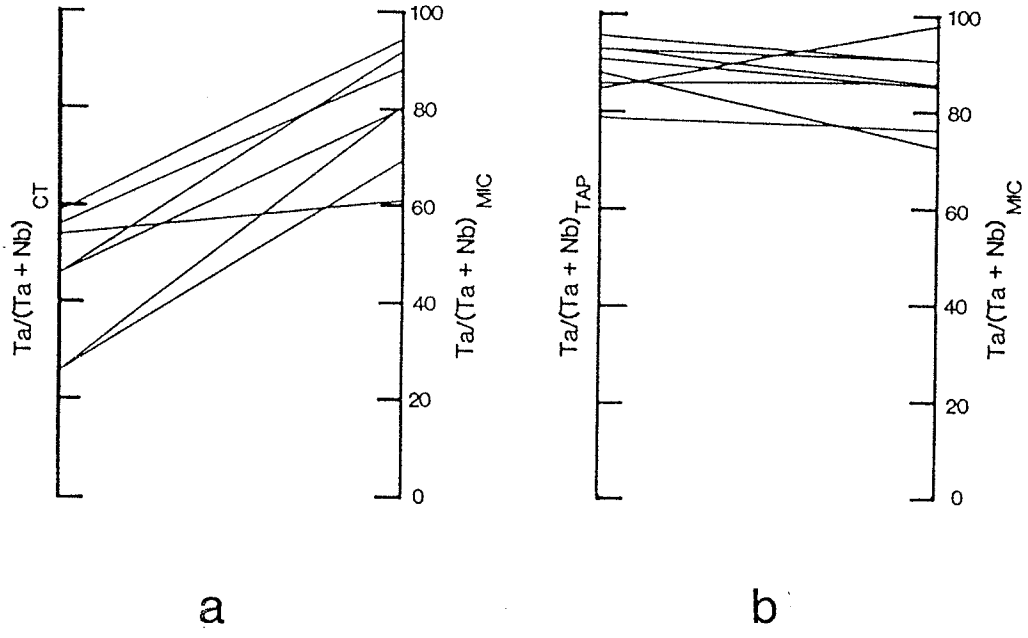

Figure 82: Composition of coexisting (a) microlite + columbite-tantalite, and (b) microlite + ferrotapiolite.. Tie-lines connect coexisting phases.

CHAPTER 12

Regional chemical and structural variations of Nb, Ta and Sn minerals

Introduction

Poorly documented geochemical and paragenetic relationships among Nb-,Ta- and Sn-bearing oxide minerals from granitic pegmatites have greatly hindered our basic understanding of this mineral family (Černý et al., 1981; von Knorring and Condliffe, 1984; Lumpkin et al., 1986). Only a small number of studies have addressed the topic of regional mineralogy and geochemistry of Nb and Ta, and even so, the available information is still relatively incomplete (Černý et al., 1981; Anderson, 1984; Černý et al., 1986b). Although studies of these types are of great importance, their scope rarely extends beyond discussion of individual pegmatites or groups of cogenetic origin. Regional studies are, to say the least, important but scarce.

The Yellowknife pegmatite field study presents an excellent opportunity to examine the geochemical evolution and paragenetic relationships of Nb- and Ta-bearing minerals from a large area of geologically and chemically diverse pegmatite types. In this chapter, the geochemical, structural and paragenetic aspects of Nb-,Ta- and Sn-bearing minerals from individual pegmatites, pegmatite series and/or groups and the entire pegmatite field as a whole are systematically examined.

Chemical and structural variations in pegmatites and pegmatite swarms

Southeastern area

Faulkner Lake Series.

The Moose pegmatite belongs to the spodumene subtype of complex pegmatites. It is well-zoned and contains abundant spodumene and montebrasite. Columbite-tantalite occurs in three morphological varieties and paragenetic associations. Crystals of columbite-tantalite may show platy, tabular or blocky habits and occur in cleavelandite + quartz, cleavelandite + montebrasite and sporadic cleavelandite + lithian muscovite assemblages. Correlation between crystal habit, paragenesis and position within the pegmatite was not observed.

Despite the variations in morphology and paragenesis, the chemistry and structural state of columbite-tantalite from this pegmatite are essentially uniform. Ferrocolumbite compositions show very limited ranges of Mn/(Mn + Fe) ratios (0.18-0.27) and generally narrow ranges of Ta/(Ta + Nb) ratios (0.14-0.32) (Figure 83). High Ta/(Ta + Nb) ratios are rare. Similarly, the variation in structural state is also very limited. All specimens, regardless of morphology and association, show intermediate structural states, with the degree of order for all specimens examined ranging between 37 and 62 % (Figure 84).

The Bet pegmatite is also a well-zoned body with abundant spodumene and montebrasite. With a few exceptions, the chemistry and structural state of columbite-tantalite from the Bet pegmatite closely coincides with those found in the Moose pegmatite, with Mn/(Mn + Fe) ratios of 0.16-0.26 and Ta/(Ta + Nb) ratios of 0.23-0.34 (Figure 83). The degree of order for

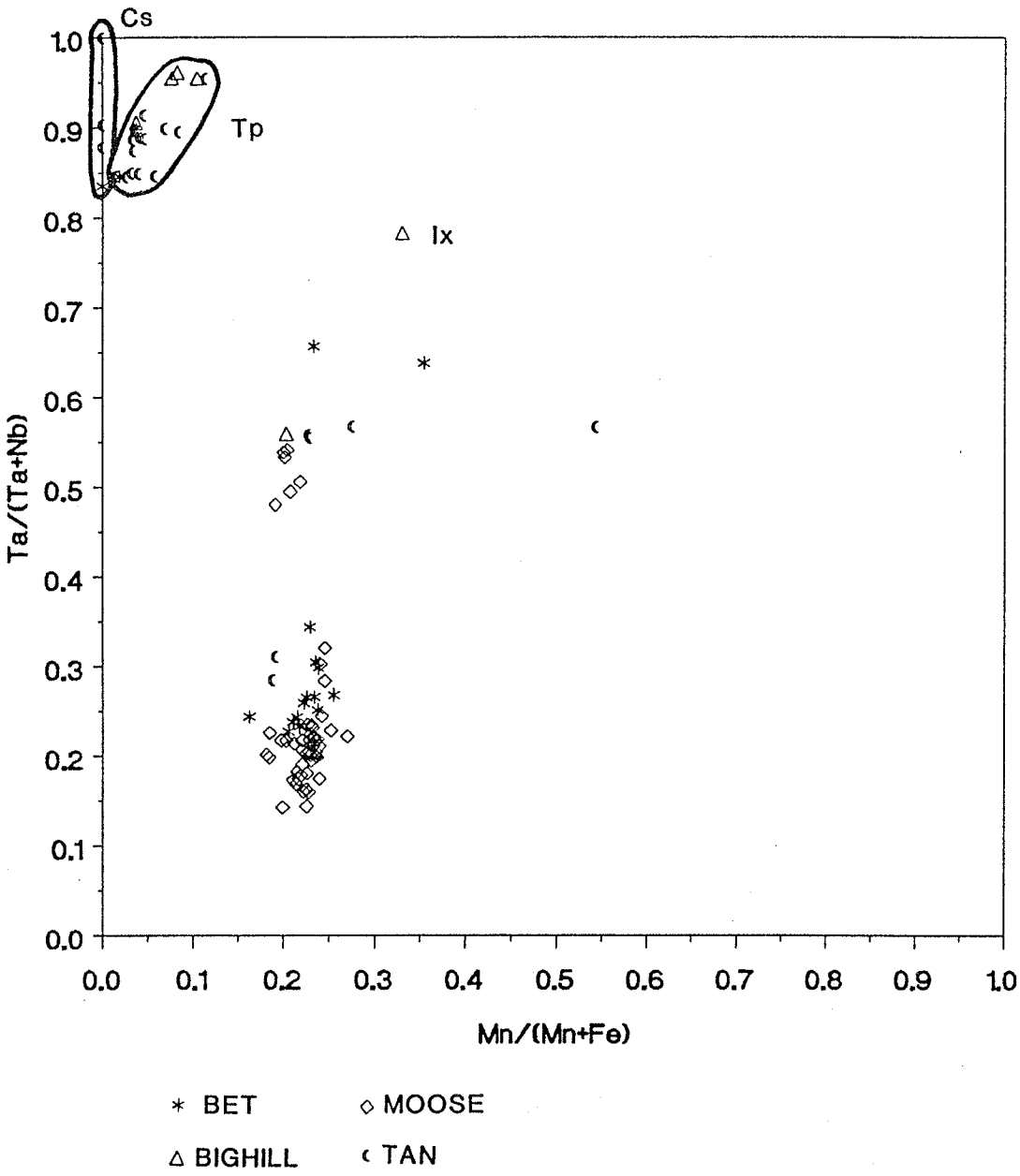

Figure 83: Chemistry of Nb,Ta-oxide minerals from the Faulkner Lake pegmatite series. Compositional fields are marked for ixiolite (Ix), tapiolite (Tp) and cassiterite (Cs); the remaining symbols are for columbite-tantalite minerals.

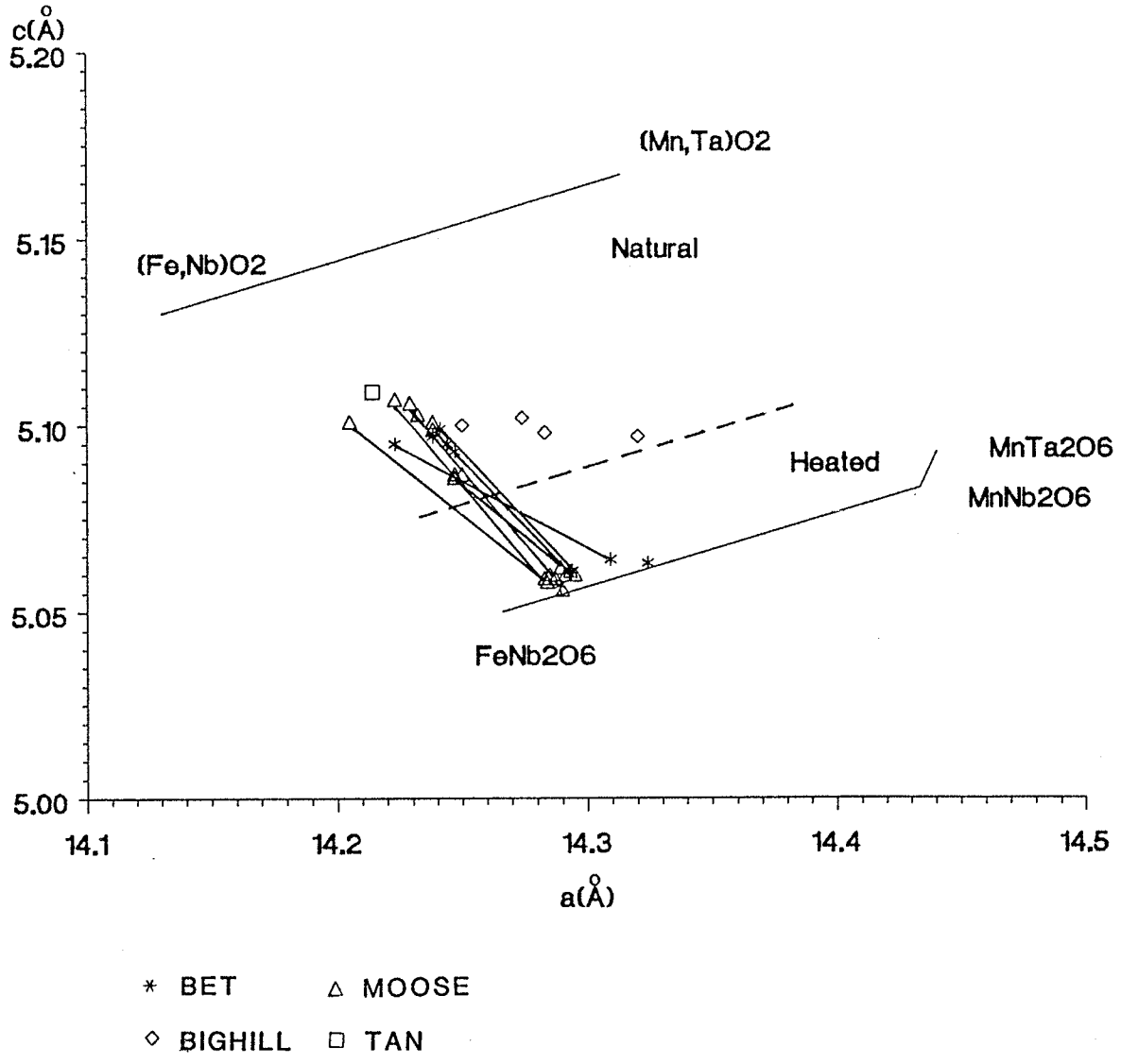

Figure 84: The a-c plot illustrating the structural state of columbite-tantalites from the Faulkner Lake pegmatite series. Dashed line separates natural and heated samples.

the columbite-tantalite minerals of the Bet pegmatite varies between 49 and 56 % (Figure 84). A single sample coexisting with ferrotapiolite shows a lower degree of order along with higher Mn/(Mn + Fe) and Ta/(Ta + Nb) ratios than other Bet samples. The associated ferrotapiolite from this pegmatite has Mn/Mn + Fe) and Ta/(Ta + Nb) ratios of 0-0.02 and 0.83-0.85 respectively.

The Tan swarm seems to contain very little columbite-tantalite, with ferrotapiolite being the dominant Nb- and Ta-oxide mineral present. Only one sample of columbite-tantalite was available for X-ray powder diffraction study and it showed a slightly lower degree of order (33 %) than the Moose and Bet samples (Figure 84). In addition, the composition of columbite-tantalite is highly variable. Mn/(Mn + Fe) ratios range from 0.19 to 0.23 and Ta/(Ta + Nb) ratios range from 0.30 to 0.56 (Figure 83). Crystals of ferrotapiolite from the Tan swarm are quite homogeneous, with ratios for Mn/(Mn + Fe) and Ta/(Ta + Nb) ranging from 0-0.07 and 0.85-0.93 respectively. Tantalian cassiterite, with Ta_2O_5 and FeO contents as much as 13.5% and 2.3% respectively, was found in trace amounts in bodies #2 and #4.

Chemically, the Big Hill samples fall within the ferrotantalite field of the columbite quadrilateral, with Mn/(Mn + Fe) and Ta/(Ta + Nb) ratios of 0.49 and 0.54, respectively. Ferrotapiolite has Mn/(Mn + Fe) ratios of 0.04-0.08 and Ta/(Ta + Nb) ratios of 0.91-9.96. Cassiterite is notably tantalian, containing up to 4.7% Ta_2O_5. Rare ixiolite with 15% SnO_2 has a Mn/(Mn + Fe) ratio of 0.33 and a Ta/(Ta + Nb) ratio of 0.78. Columbite-tantalite from the Big Hill pegmatite is quite ordered compared to columbite-tantalite from the pegmatites discussed above. The degree of order varies from 50 to 68 % (Figure 84).

Buckham Lake Group.

Samples collected from dike #2 of the Lit swarm showed minor variations in their chemsitry and structural state. Compositionally, the columbite-tantalite minerals vary from ferrocolumbite to ferrotantalite with Mn/(Mn + Fe) ratios 0.39-0.42 and Ta/(Ta + Nb) ratios of 0.46-0.58 (Figure 85). The crystals display two predominant habits; platy - generally ferrocolumbite in composition, and blocky - ferrotantalite. Correlation with paragenetic association was not possible. Intermediate degrees of order (33 to 48 %) is typical of columbite-tantalite from this body (Figure 86). A single ferrotapiolite analysis revealed chemistry typical of other tapiolites in the area. Columbite-tantalite compositions from the #4 body were significantly greater in their Mn and Ta contents. Both Mn/(Mn + Fe) and Ta/(Ta + Nb) ratios are extremely homogeneous, with values ranging from 0.25-0.27 and 0.43-0.50 respectively.

The highly fractionated Mac pegmatite contains abundant spodumene and subordinate fluorian montebrasite (Wise et al., 1987). Columbite-tantalite from this pegmatite shows the lowest degree of order in this part of the field, ranging from 2 to 12 % (Figure 86). The specimens occur as platy or tabular crystals in a plagioclase + quartz assemblage of the intermediate zone. The range of Mn/(Mn + Fe) ratios is narrow (0.40 - 0.46) whereas the Ta/(Ta + Nb) ratio is slightly more variable (0.34 - 0.63) (Figure 85). In any case, the composition of the columbite-tantalite does not seem to correlate with the structural state.

Ixiolite is conspicuous in the Mac pegmatite, occurring as massive grains up to 5 cm across. As expected, ixiolite shows an extremely low

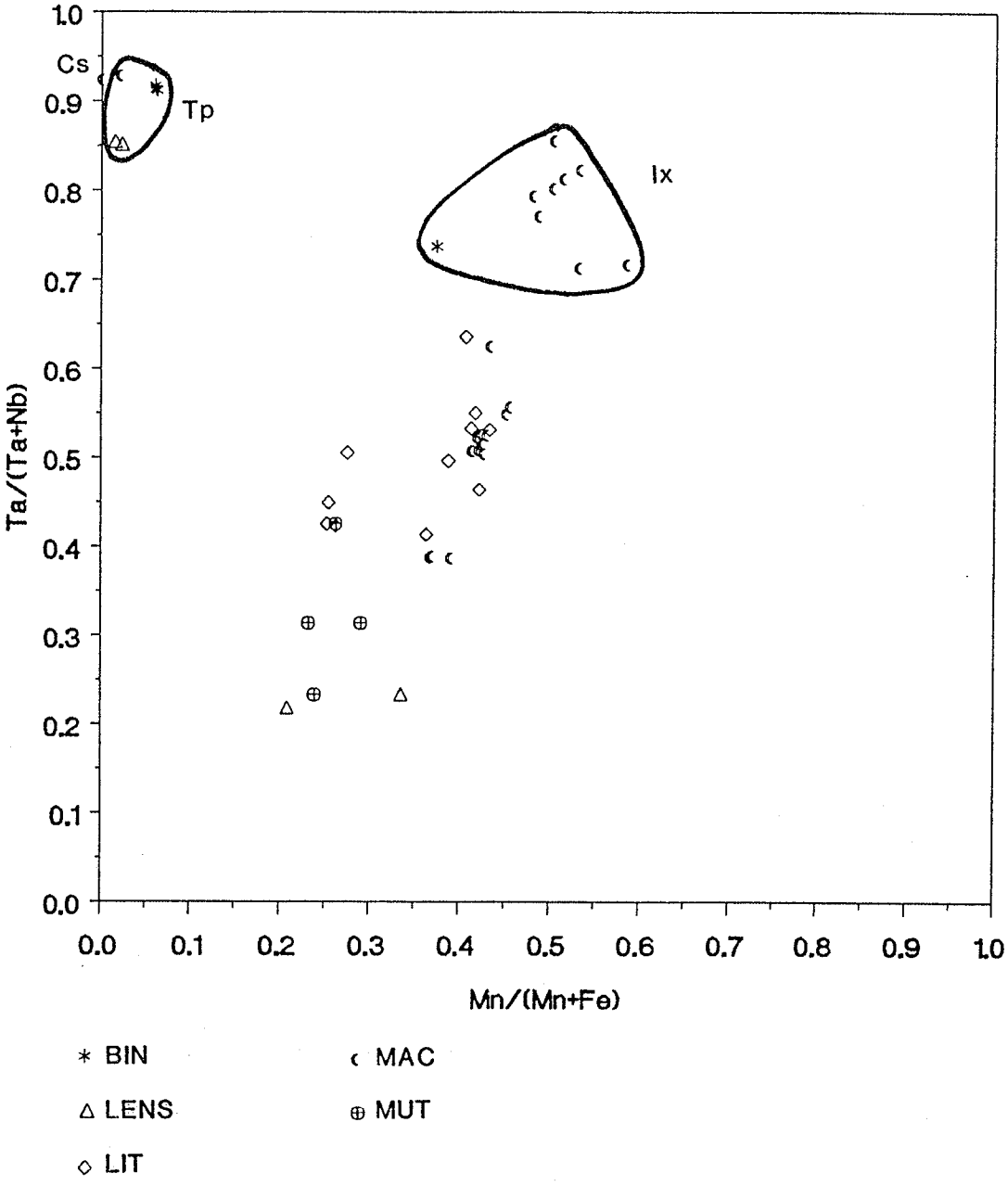

Figure 85: Chemistry of Nb,Ta-oxide minerals from the Buckham Lake pegmatite group. Compositional fields are marked for ixiolite (Ix), tapiolite (Tp) and cassiterite (Cs); the remaining symbols are for columbite-tantalite minerals.

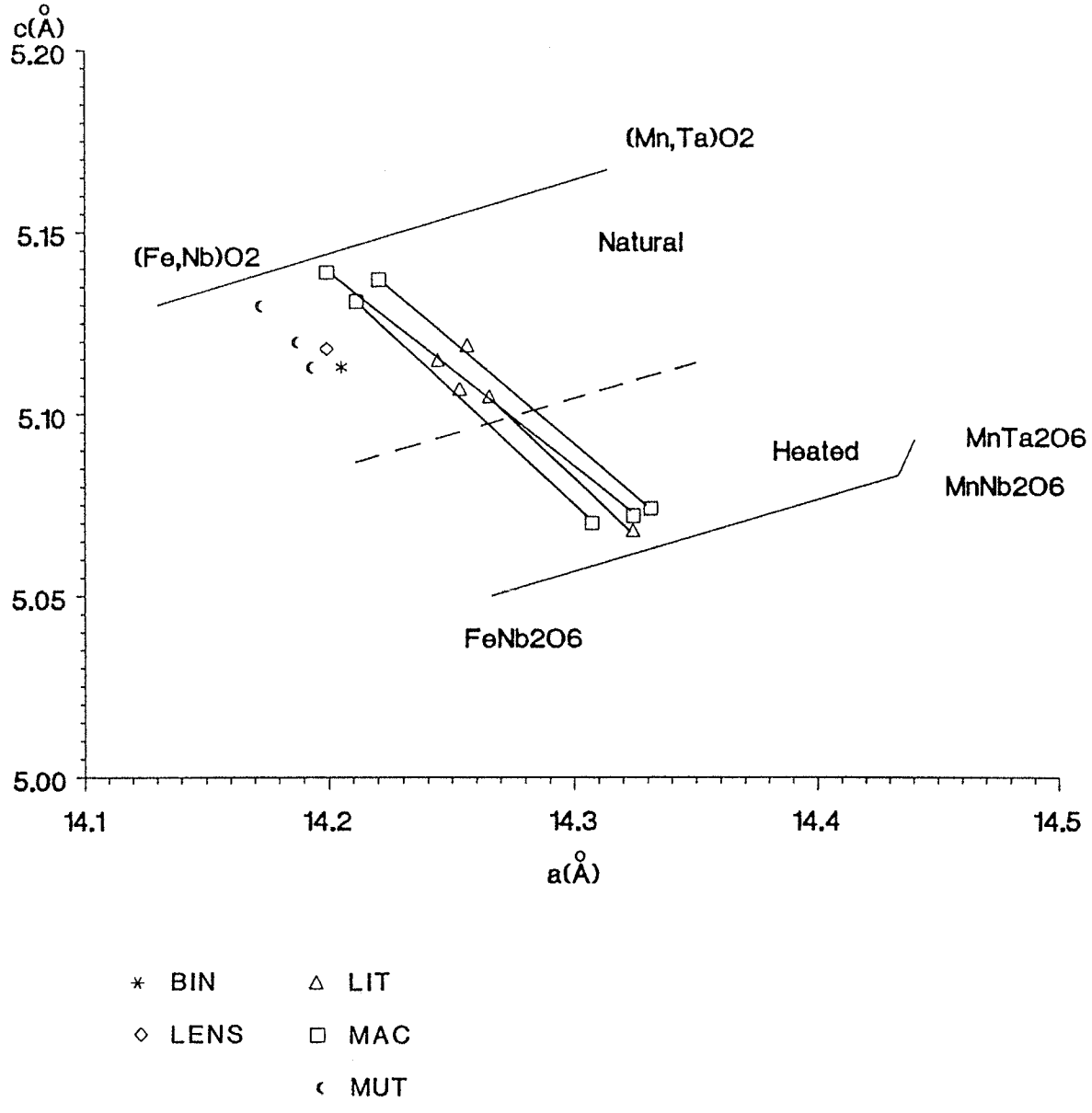

Figure 86: The a-c plot illustrating the structural state of columbite-tantalites from the Buckham Lake pegmatite group. Dashed line separates natural and heated samples.

degree of order, with slight variations in Mn/(Mn + Fe) and Ta/(Ta + Nb) ratios (0.34 - 0.59 and 0.72 - 0.87 respectively) (Figure 85). The Sn content is typical of most stannian ixiolites, reaching a maximum of 16.5 wt. % SnO_2. Cassiterite is notably Ta-rich (up to 6.2% Ta_2O_5) with traces of Fe and Nb.

Columbite-tantalite from the spodumene-bearing Bin, Lens and Mut pegmatites all show low degrees of order within the range of 4 to 28 % (Figure 86). The range of Mn/(Mn + Fe) and Ta/(Ta + Nb) ratios for the Mut pegmatite varies from 0.23 to 0.29 and 0.30 to 0.47, respectively. Sn generally occurs in minor quantities, whereas Ti may reach values of 2.0% TiO_2.

The Lens pegmatite has Mn/(Mn + Fe) ratios of 0.21 to 0.34 and Ta/(Ta + Nb) ratios of 0.22 to 0.23. Ferrotapiolite analyses are typically Mn-poor: (Mn/(Mn + Fe) = 0.02), whereas Nb substitution is more extensive: (Ta/(Ta + Nb) = 0.85).

In contrast, ferrotapiolite from the Bin pegmatite is richer in Mn and Ta than those from the Lens pegmatite. Ixiolite with 6.3% SnO_2 was observed coexisting with ferrotapiolite.

Tanco Lake Group.

In the eastern part of the southeastern area, one sample of columbite-tantalite occurring as a platy crystal with plagioclase, quartz and montebrasite was collected and studied from the Jo swarm. It plots within the ferrocolumbite field, with Mn/(Mn + Fe) and Ta/(Ta + Nb) ratios similar to those found in samples from the Moose pegmatite (Figure 87). The sample also shows an intermediate degree of order (53 %), comparable to samples from the Moose pegmatite (Figure 88).

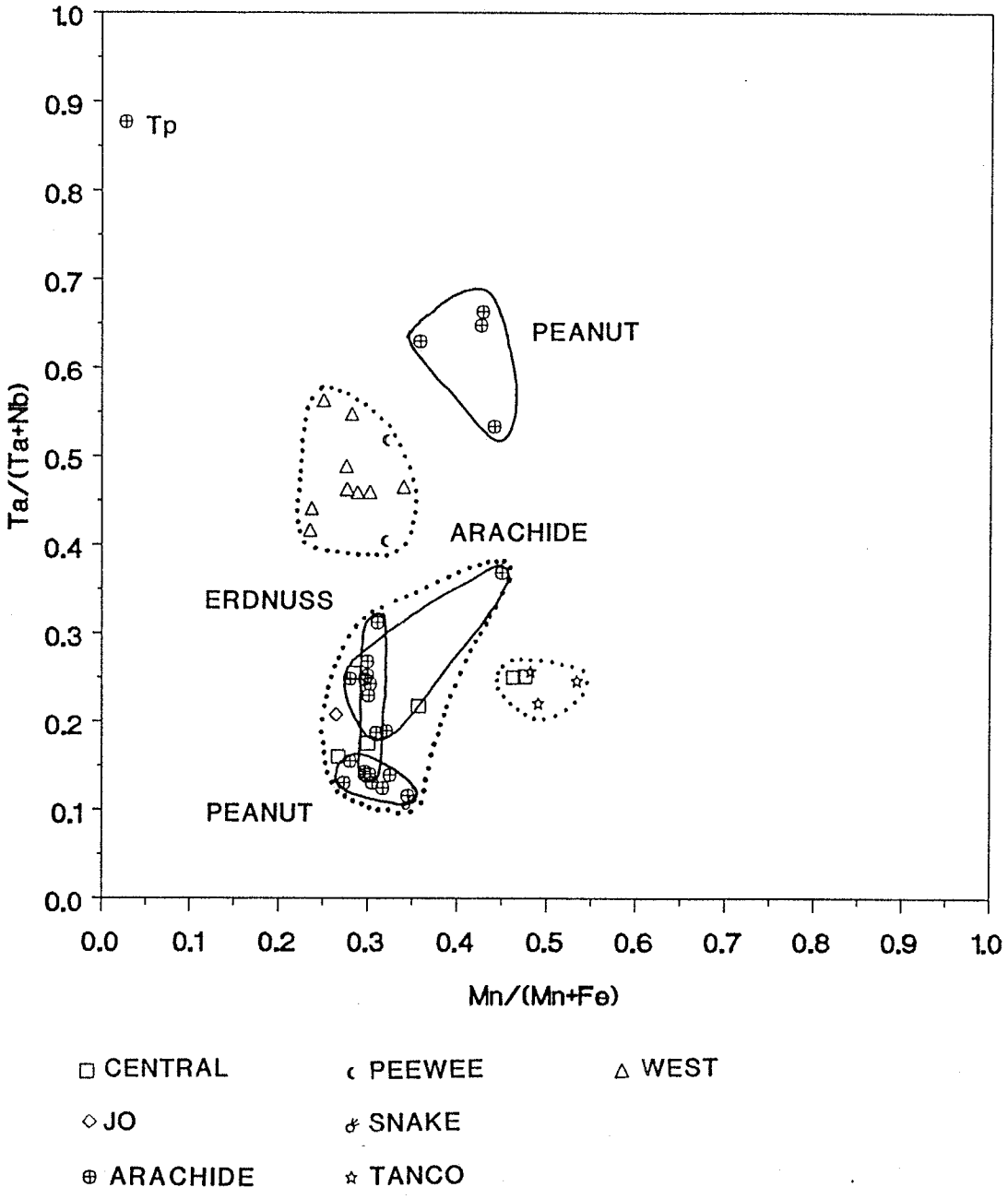

Figure 87: Chemistry of Nb,Ta-oxide minerals from the Tanco Lake pegmatite group. Fields (dotted line) mark the compositions of the three columbite-tantalite populations of the Thor-Echo swarm discussed in the text.

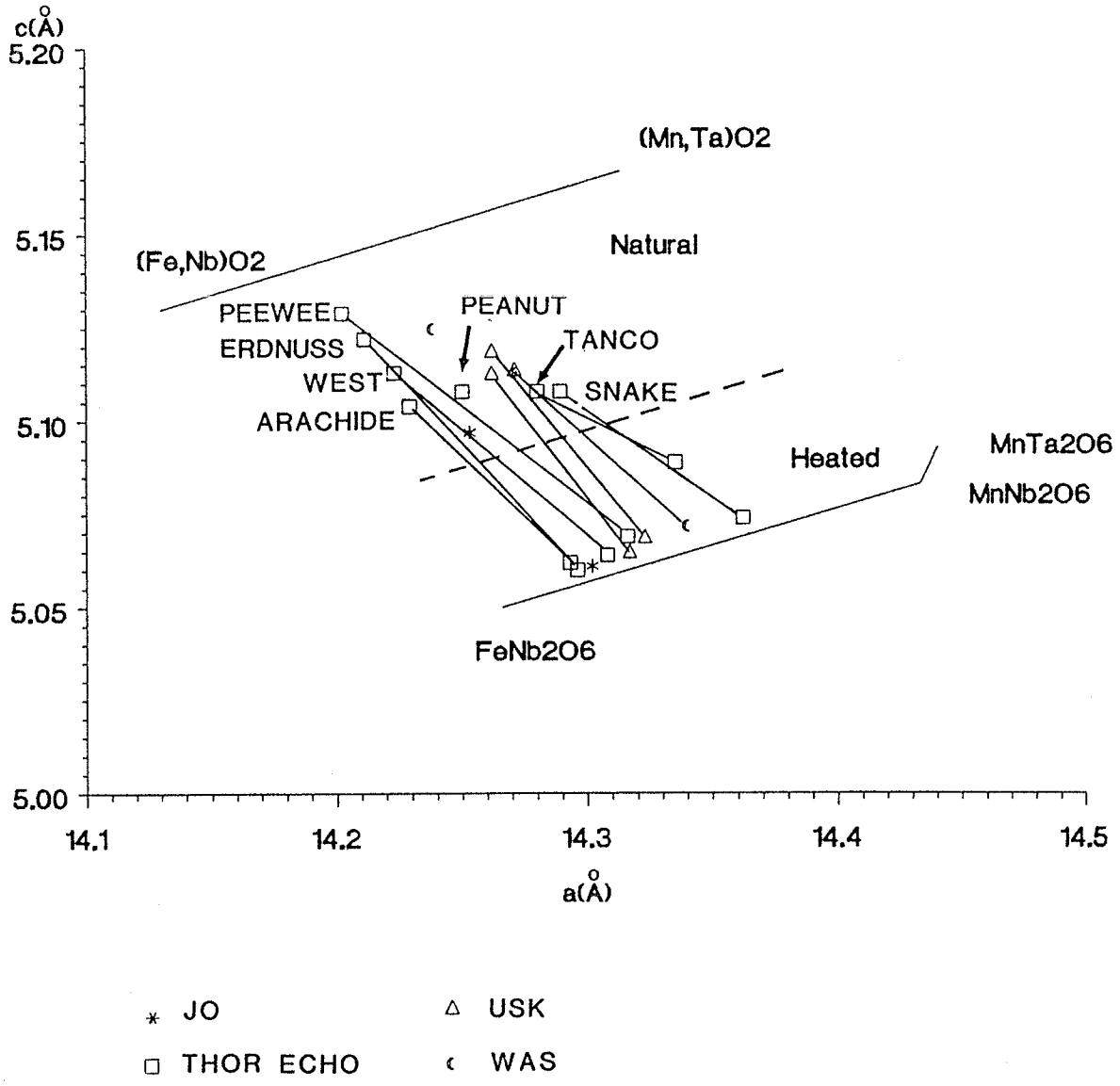

Figure 88: The a-c plot illustrating the structural state of columbite-tantalites from the Tanco Lake pegmatite group and the Doubling Lake pegmatite series. Dashed line separates natural and heated samples.

All columbite-tantalites collected from the Thor Echo swarm show tabular habits regardless of their paragenetic association. The structural state of the samples varies from highly disordered (THE-PW-3) to intermediate order (THE-SN-B-1) (Figure 88). Analyses of columbite-tantalite from the Peanut body show a strong bimodal distribution in terms of their Ta/(Ta + Nb) ratios (Figure 87). The two populations may be correlated with their relative time of origin. The low Ta population were collected from the K-feldspar + quartz + spodumene + muscovite intermediate zone. In contrast, the high Ta population was found as tiny blades in saccharoidal albite. The conspicuous difference in Ta content between the two populations suggests that the saccharoidal albite body may have formed well after consolidation of the intermediate zone.

In contrast to the Peanut body, analyzed columbite-tantalite from saccharoidal albite in the West pegmatite has a major element signature very similar to columbite-tantalite from the plagioclase + K-feldspar + muscovite + quartz + spodumene intermediate zone.

Disregarding the columbite-tantalite compositions from saccharoidal albite bodies, microprobe analyses indicate a trimodal distribution of compositions for the Thor-Echo swarm; two of the three populations are separated from each other by their distinct Ta/(Ta + Nb) ratios, whereas their Mn/(Mn + Fe) ratios are essentially identical:

(i) The Peewee and West dike samples typically show intermediate Ta/(Ta + Nb) ratios (0.41 - 0.52) and restricted Mn/(Mn + Fe) ratios (0.24 - 0.32).

(ii) The second population includes the Peanut, Erdnuss, Arachide, Central and Snake bodies. Columbite-tantalites from these dikes are significantly Nb-richer with Mn/(Mn + Fe) ratios ranging from 0.29 - 0.36.

(iii) The third population, consisting of minerals from the Tanco body and a few analyses from the Central body, has a Mn/(Mn + Fe) ratio near 0.50.

The only ferrotapiolite analysis from the Thor-Echo swarm (THE-PN-A-3B) is typical of most ferrotapiolites from the SE area of the Yellowknife field, with Mn/(Mn + Fe) = 0.03, Ta/(Ta + Nb) = 0.88.

Doubling Lake Series.

Specimens from the Usk and Was pegmatites show nearly identical chemistries and structural states (Figures 88 and 89). Columbite-tantalite from both bodies show platy habits and intermediate degrees of order (Usk: 35-42 %, Was: 23-42 %). The Mn/(Mn + Fe) value of the Was pegmatite columbite-tantalites is slightly higher than those of the Usk body; 0.50 compared to a maximum of 0.45 in the Usk dike, but the Usk pegmatite samples show higher Ta/(Ta + Nb) ratios than the Was samples; 0.65 compared to 0.40 for the Was dike. Ferrotapiolite from the Usk pegmatite shows a very high Ta/(Ta + Nb) ratio (0.96) and low Mn/(Mn + Fe) ratio (0.08).

Northeastern area

Upper Ross Lake Group.

The ranges of Mn/(Mn + Fe) and Ta/(Ta + Nb) ratios for columbite-tantalite from the Peg swarm are very close to those found in samples from the southeastern area of the field (Table 30, Figure 90). In most instances, columbite-tantalite compositions from individual bodies follow the general trend of narrow Ta/(Ta + Nb) ratios with very limited Mn/(Mn + Fe) ratios. Exceptions are observed in dikes #93, #95, #97 and #75, in which both Mn/Fe and Ta/Nb fractionation is more extensive.

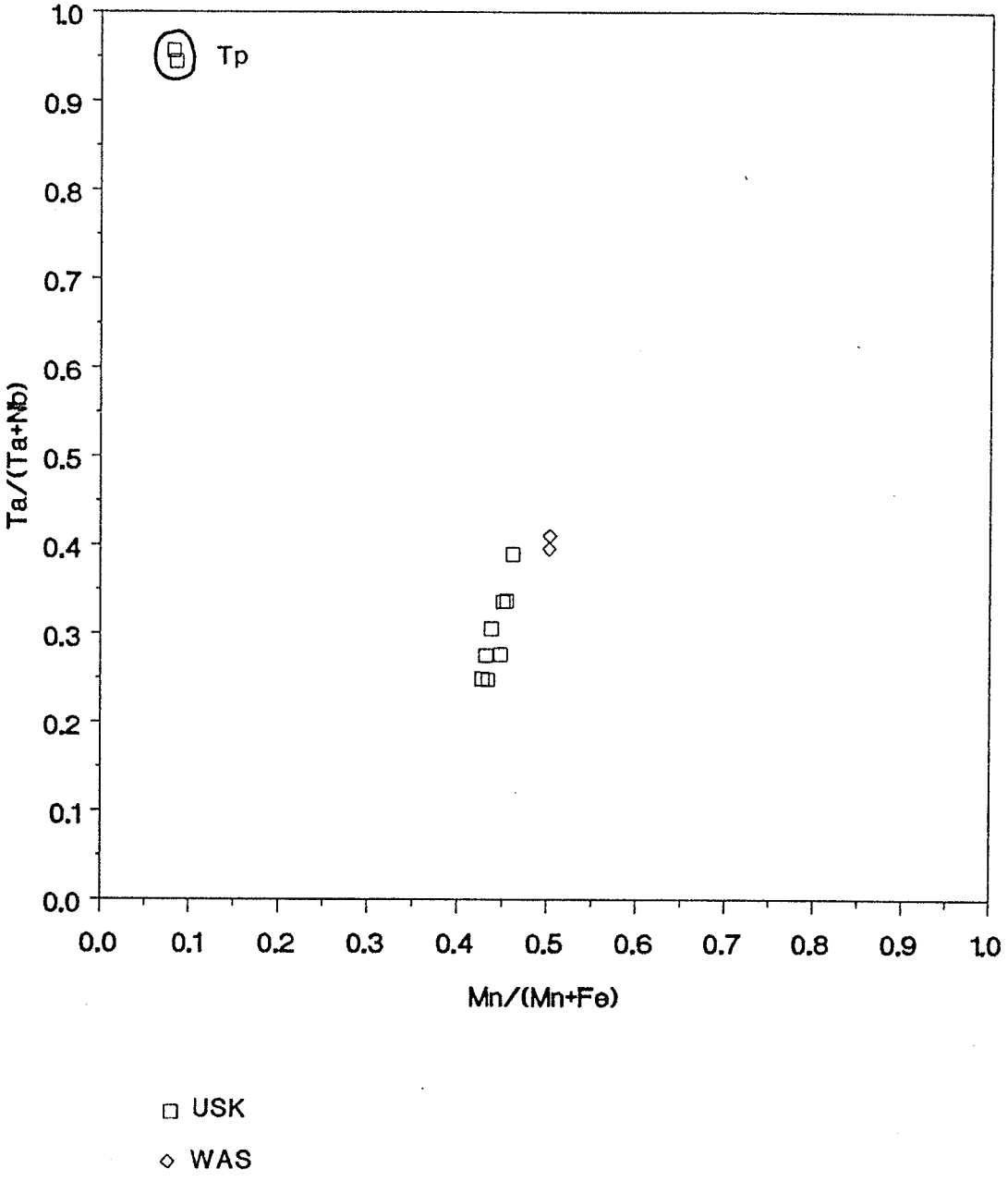

Figure 89: Chemistry of Nb,Ta-oxide minerals from the Doubling Lake pegmatite series. Compositional field is marked for tapiolite (Tp); the remaining symbols are for columbite-tantalite minerals.

Table 30: Average Mn/(Mn + Fe) and Ta/(Ta + Nb) ratios of columbite-tantalite for sampled pegmatites of the Peg swarm.

Pegmatite	Mn/(Mn + Fe)	Ta/(Ta + Nb)
Peg-8	0.342	0.136
Peg-75	0.294	0.241
Peg-84	0.308	0.577
Peg-86	0.351	0.449
Peg-93	0.308	0.445
Peg-95	0.373	0.293
Peg-97	0.298	0.176
Peg-113	0.332	0.226
Peg-118	0.430	0.295
Peg-170	0.158	0.396
Peg-190	0.408	0.383
Peg-191	0.400	0.443
Peg-192	0.406	0.556
Peg-196	0.556	0.575
Peg-241	0.180	0.325
Peg-285	0.342	0.136
Peg-292	0.203	0.565
Peg-300	0.350	0.396

Ferrotapiolite occurs in dikes #8, #84, 88, #93, #196 and #319. Ferrotapiolite from dike #196 shows considerable Mn enrichment: (Mn/(Mn + Fe) = 0.12-0.17) as well as greater Ta fractionation than other tapiolites in the group. Cassiterite was found only in the spodumene-bearing dike #1. Ta contents are low, although 5.8 wt% Ta_2O_5 was observed in one analysis.

The structural state of the Peg swarm columbite-tantalite varies from low order (6% in dike #92) to intermediate order (54% in dike #75) (Figure 91). As noted previously, decreased Ta contents seem to be proportionally related to increased degrees of order.

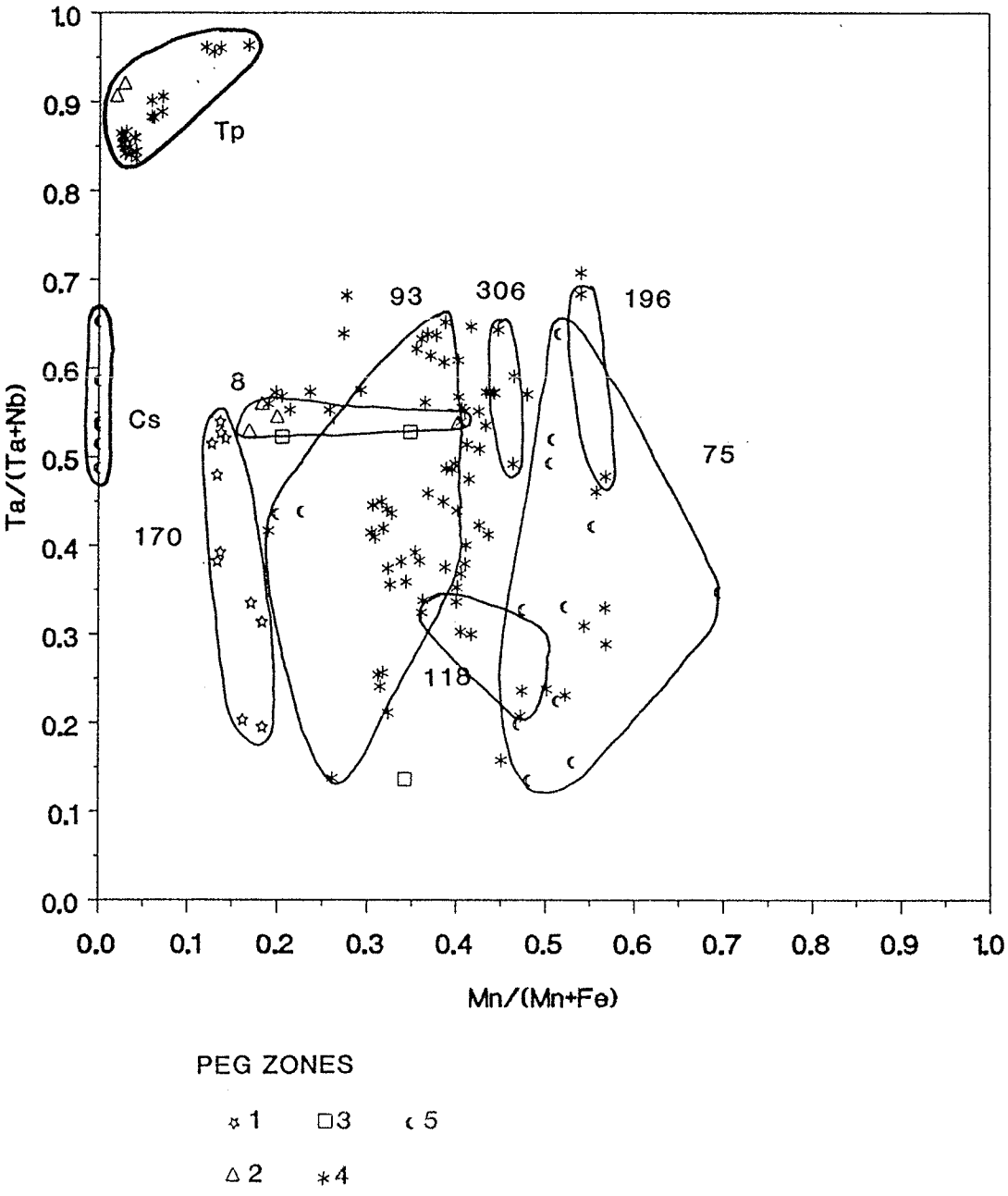

Figure 90: Chemistry of Nb,Ta-oxide minerals from the Peg swarm. Compositional fields are marked for tapiolite (Tp) and cassiterite (Cs); the remaining symbols are for columbite-tantalite minerals. Numbered fields represent the columbite-tantalite compositions of selected individual pegmatite bodies.

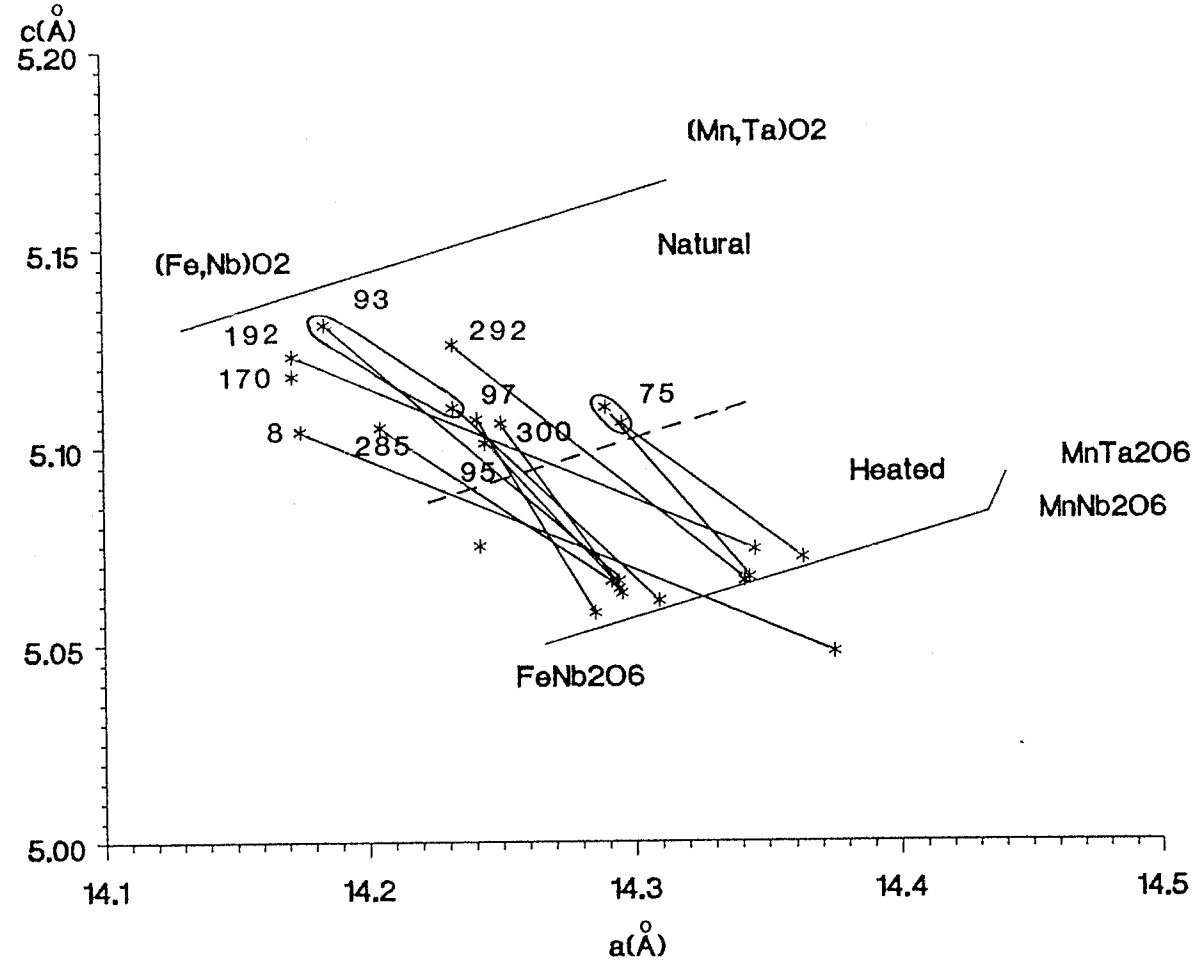

Figure 91: The a-c plot illustrating the structural state of columbite-tantalites from the Peg swarm. Dashed line separates natural and heated samples. Numbers designate individual pegmatite bodies.

Northwestern area

Blaisdell Lake Group.

Columbite-tantalite from the Bill swarm shows uniform chemical composition and variable structural states. All samples are ferrocolumbite with small variations in Mn/(Mn + Fe) and Ta/(Ta + Nb) ratios (Figure 92). The three bodies sampled had columbite-tantalite with similar Mn/(Mn + Fe) ratios (Bill #2: 0.19-0.21, Bill #4: 0.23-0.26, Bill #5: 0.21-0.39). For all bodies, Ta/(Ta + Nb) ratios fall within the range of 0.12-0.24. A sample taken from a saccharoidal albite pod in Bill #4 showed ratios only slightly higher than those from primary zones. Six specimens from the swarm show variable degrees of order (Figure 93) which range from low (12%) to intermediate (47%).

The Melody swarm contains columbite-tantalite of similar structural state as found in the Bill swarm (Figure 93). The degree of order varies from 14 to 55%. Samples from the Melody swarm show a significant increase in the Ta/(Ta + Nb) ratio, compared to samples from the Bill swarm, while maintaining a comparable Mn/(Mn + Fe) ratio (Figure 92). The Mn/(Mn + Fe) ratio of the Melody bodies #5, #6, #8 and #9 all fall within the narrow range of 0.17-0.30. However, each body has a distinct Ta signature. Body #9 shows the greatest enrichment of Ta, with a Ta/(Ta + Nb) ratio of 0.55 as well as having subordinate ferrotapiolite. The ferrotapiolite is low in Mn: (Mn/(Mn + Fe) = 0.02), and has a Ta/(Ta + Nb) ratio of 0.85, comparable to other tapiolites previously described from the field.

The spodumene-bearing Vo swarm minerals also show a similar range in order-disorder values (15-54%) as minerals from the Bill and Melody swarms (Figure 93). The pegmatites of the Vo swarm show evidence of considerable

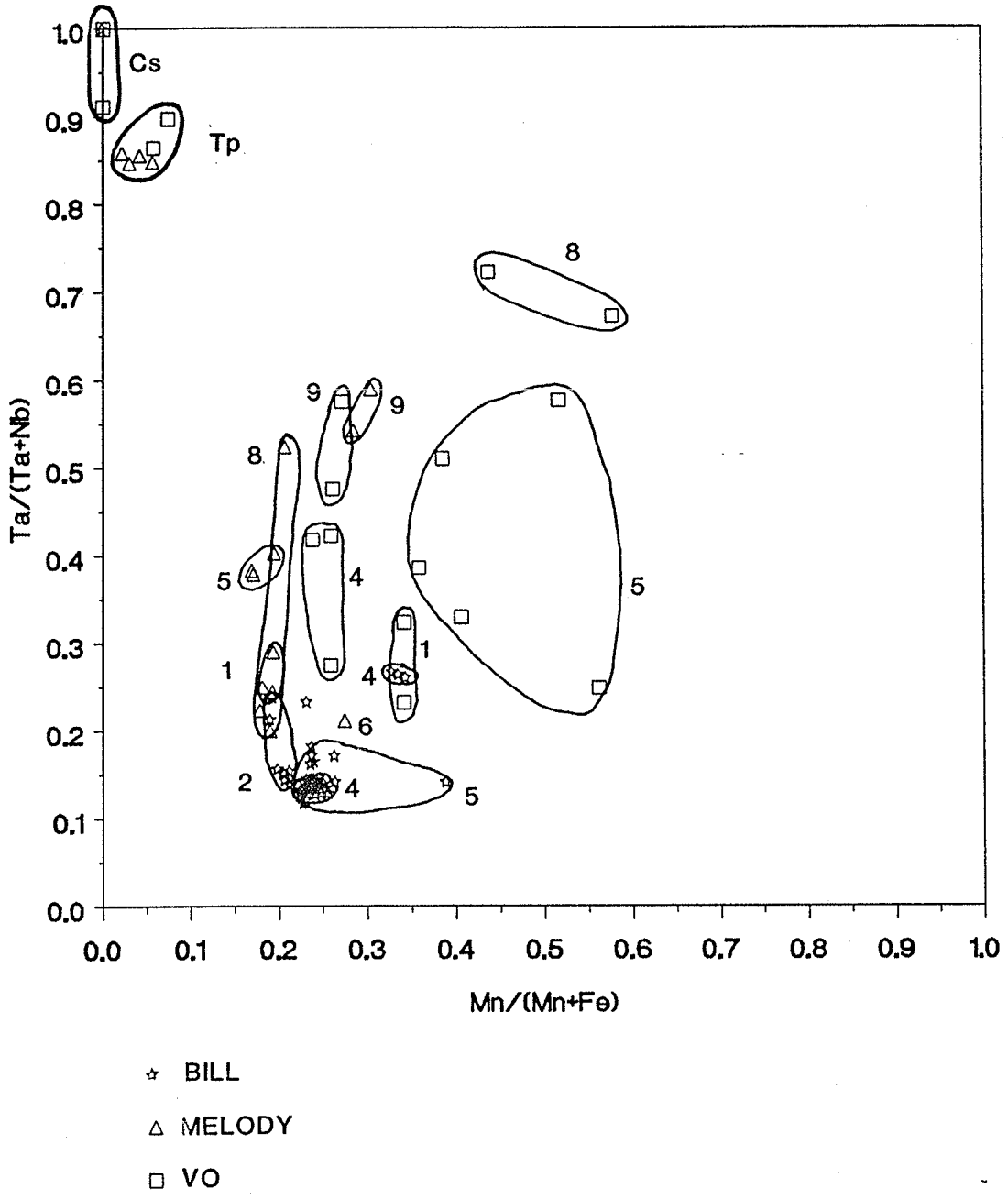

Figure 92: Chemistry of Nb,Ta-oxide minerals from the Blaisdell Lake pegmatite group. Compositional fields are marked for tapiolite (Tp) and cassiterite (Cs); the remaining symbols are for columbite-tantalite minerals. Numbered fields represent the columbite-tantalite compositions of individual pegmatite bodies.

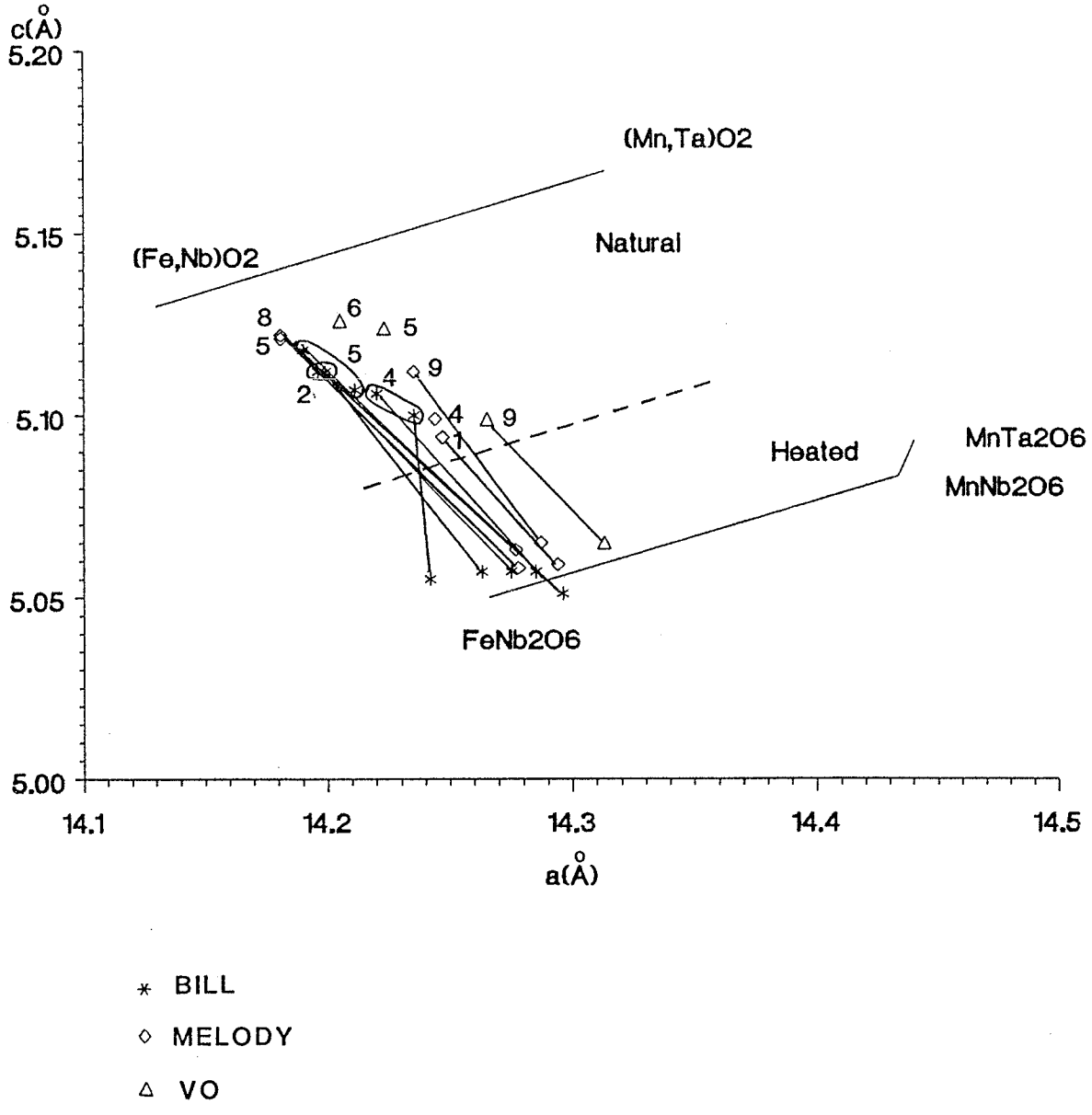

Figure 93: The a-c plot illustrating the structural state of columbite-tantalites from the Blaisdell Lake pegmatite group. Dashed line separates natural and heated samples. Numbers designate individual pegmatite bodies.

metasomatism. Most of the columbite-tantalites collected were obtained from saccharoidal albite bodies, with only a few exceptions. In general, samples associated with the saccharoidal albite were more enriched in Mn than columbite-tantalite from primary zones. In all cases however, all columbite-tantalites show restricted Mn/(Mn + Fe) ratios and narrow Ta/(Ta + Nb) ratios (Figure 92).

Sproule Lake Series.

The majority of the columbite-tantalite compositional data from the Fly pegmatite was obtained from microscopic blades occurring in saccharoidal albite. Considerable differences in the Ta/(Ta + Nb) ratios were observed in several grains in close proximity to one another (Figure 94). The fractionation of Mn and Ta in these specimens is much more extensive than in samples from the plagioclase + quartz + muscovite intermediate zone of the pegmatite. The degree of order is typically intermediate (25 - 64%; Figure 95). Ferrotapiolite analyses approach end-member compositions with Ta/(Ta + Nb) = 0.92-0.98 and Mn/(Mn + Fe) = 0.03-0.05.

Unlike the Fly samples, massive grains, tabular and columnar crystals of columbite-tantalite are present in the nearby Cata pegmatites. Although the Ta/(Ta + Nb) ratios remain somewhat uniform throughout the pegmatite swarm, different sections show divergent Mn/(Mn + Fe) ratios (Figure 94). In general, Mn enrichment increases towards the southern end of the swarm, where the Mn/(Mn + Fe) ratio reaches a value of 0.75. Ta fractionation also increases to the south, but to a lesser degree than Mn. This higher fractionated part of the swarm is characterized by abundant cassiterite, which is typically tantalian and niobian, but lacks significant accumulations of Fe, Mn and Ti.

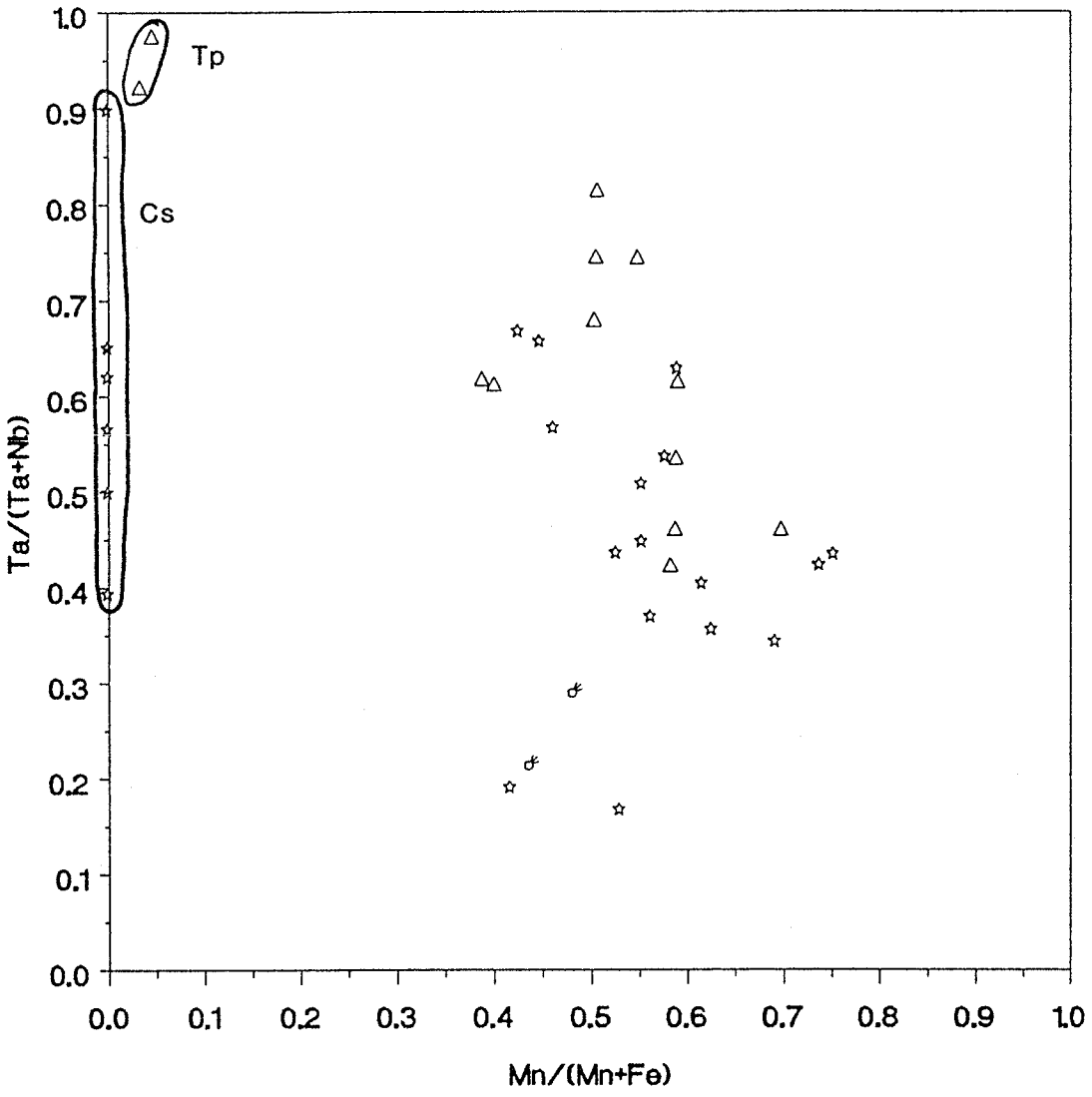

Figure 94: Chemistry of Nb,Ta-oxide minerals from the Sproule Lake and Harald Lake pegmatite series. Compositional fields are marked for tapiolite (Tp) and cassiterite (Cs); the remaining symbols are for columbite-tantalite minerals.

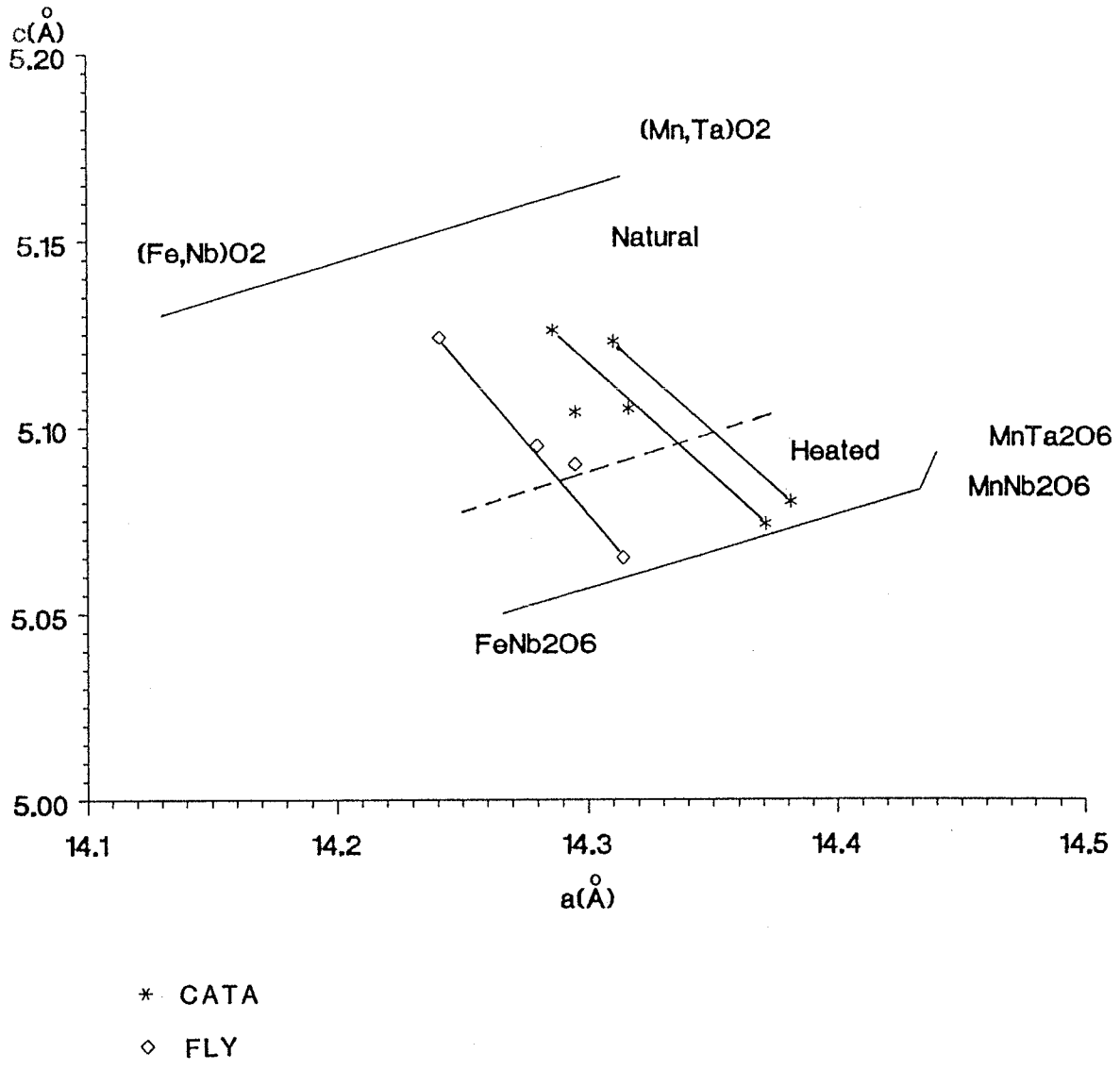

Figure 95: The a-c plot illustrating the structural state of columbite-tantalites from the Sproule Lake pegmatite series. Dashed line separates natural and heated samples.

In comparison to the Fly pegmatite, columbites-tantalites from the Cata swarm are ordered to a similar degree, despite their morphological and chemical differences (Figure 95). All types are moderately ordered with degrees of order in the range of 33-60%.

Harald Lake Series.

Two analyses of columbite-tantalite from the Moon pegmatite gave Mn/(Mn + Fe) and Ta/(Ta + Nb) ratios of 0.44 to 0.49 and 0.22 to 0.29, respectively.

Sparrow-Thompson-Hidden Lakes group.

With the exception of dike "A", all dikes of the Casper swarm containing Nb and Ta minerals show a characteristic narrow range of Mn/(Mn + Fe) ratios with more extensive Ta/(Ta + Nb) ratios (Figure 96). Samples from a saccharoidal albite body in the "I" dike show the highest Mn/(Mn + Fe) ratio at 0.45. Ferrotapiolite compositions are high in Ta: (Ta/(Ta + Nb) = 0.87-0.94) with moderate Mn enrichment.

With one prominent exception, the structural state of columbite-tantalite from the Casper swarm shows an intermediate degree of order. The unit cell dimensions of a single sample from dike "S" indicate extremely low structural order (6%) (Figure 97). Omitting this point, the *a* and *c* cell dimensions of the Casper swarm cluster into two separate populations, each representative of a single pegmatite body. Those from dike "I" are of particular interest; their separation is apparently a consequence of coexisting ferrotapiolite which preferentially incorporates Fe and Ta, thereby resulting in a Mn- and Nb-rich columbite which, in turn, shifts the columbite unit cell dimensions further to the right on the *a*-*c* plot. Samples from this dike are of intermediate order (41%).

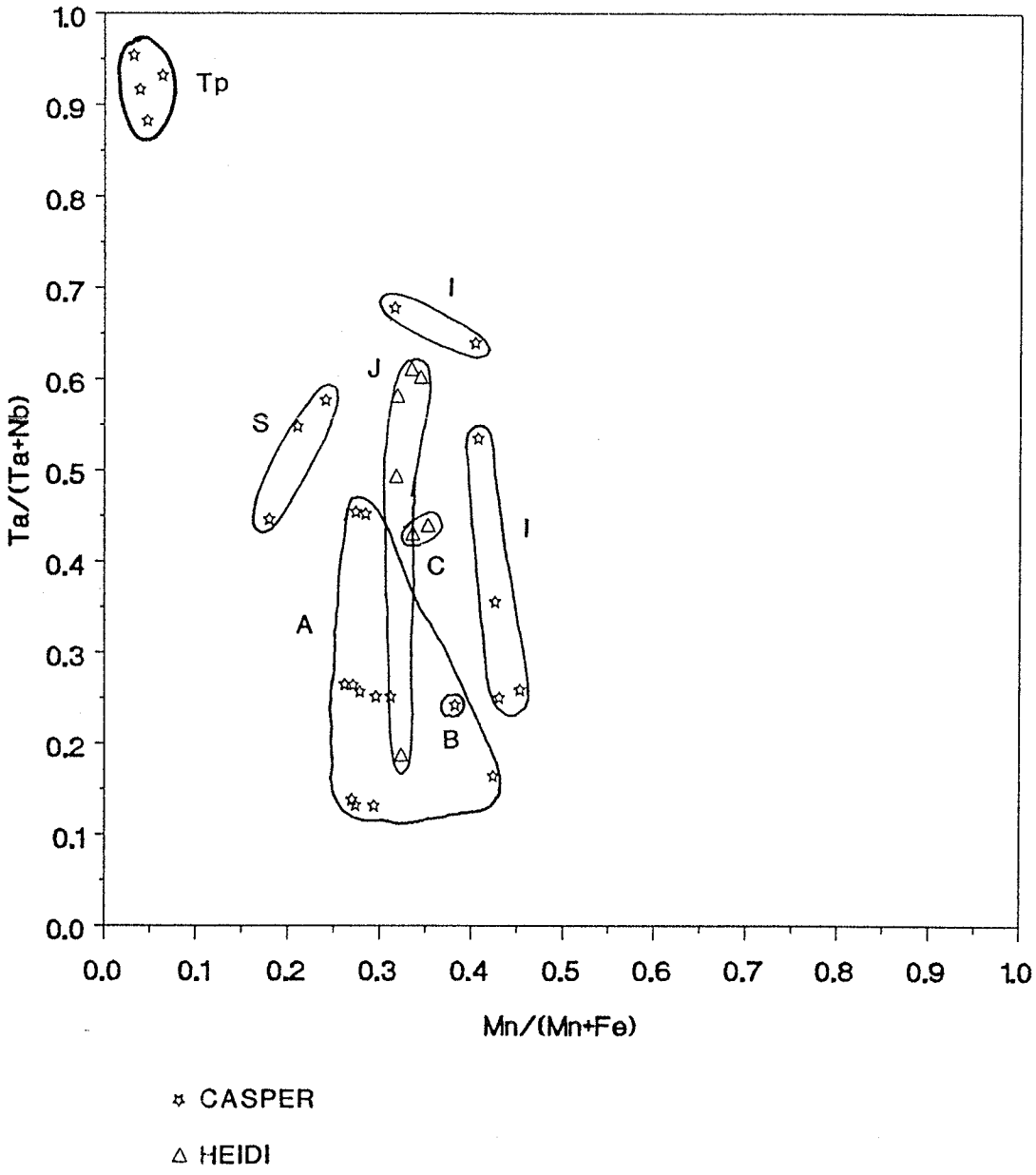

Figure 96: Chemistry of Nb,Ta-oxide minerals from the Casper and Heidi pegmatite swarms. Compositional field is marked for tapiolite (Tp); the remaining symbols are for columbite-tantalite minerals. Lettered fields represent the columbite-tantalite compositions of individual pegmatite bodies.

The other population represented by dike "A" is also of intermediate order but is significantly more ordered than samples from either dike "I" or "S". The degree of order in dike "A" ranges from 51 to 62%.

The Heidi pegmatites, located to the immediate SE of the Casper swarm, are mineralogically simple but well-zoned bodies which occur in the aureole surrounding the northern margin of the Hidden Granite. Only two pegmatites (dikes #3 and #10) contained Nb and Ta minerals. Restricted Mn/(Mn + Fe) ratios (0.32-0.35) and very large Ta/(Ta + Nb) variations (0.19-0.61) are characteristic of dike #10, whereas in dike #3 both ratios are very limited (Figure 96). Columbite-tantalites from the Heidi dikes are more disordered, with more uniform chemistry than most of the Casper columbite-tantalites (Figure 97).

Although spatially separated by a considerable distance, the Tom and Murky pegmatites show restricted Mn/(Mn + Fe) ratios and generally low Ta fractionation (Figure 98). Platy ferrocolumbite crystals of intermediate order (56-60%) is typical of both dikes (Figure 99). In contrast, the Waco swarm farther to the N is characterized by low to moderate Ta fractionation and moderate Mn fractionation. The Ta/(Ta + Nb) ratios range from 0.23 to 0.62, and the Mn/(Mn + Fe) ratios vary from 0.22 to 0.64. With few exceptions, columbite-tantalite chemistry of the Waco swarm is relatively uniform.

An a-c plot of the Waco columbites-tantalites indicates low to intermediate degrees of order. Specimens from body "A" are, as a group, more ordered than those from body "B" (Figure 99).

The Freda pegmatite shows moderate to very high degrees of order (42-96%) with compositions of Ta-rich ferrocolumbite (Figure 99). In gen-

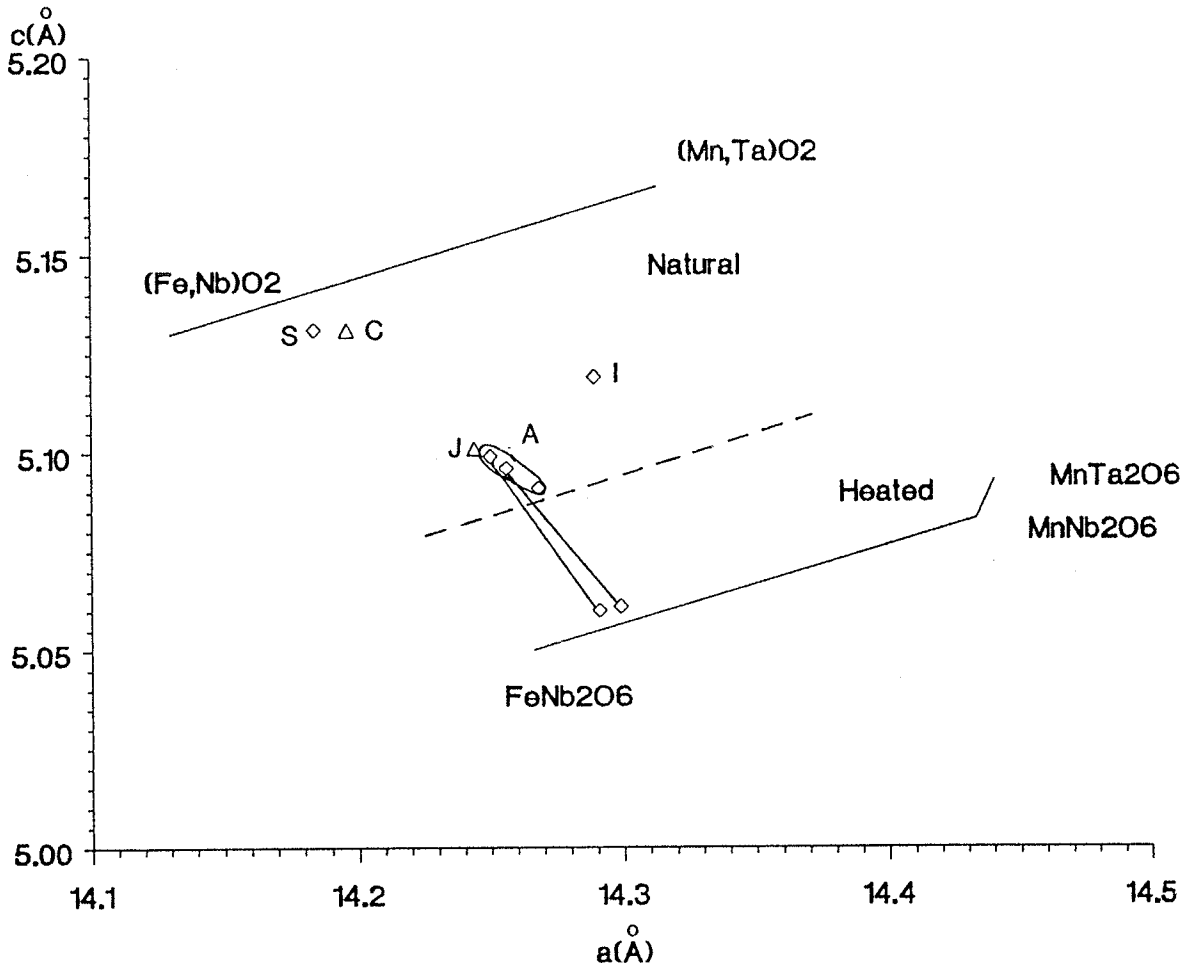

Figure 97: The a-c plot illustrating the structural state of columbite-tantalites from the Casper and Heidi pegmatite swarms. Dashed line separates natural and heated samples. Letters designate individual pegmatite bodies.

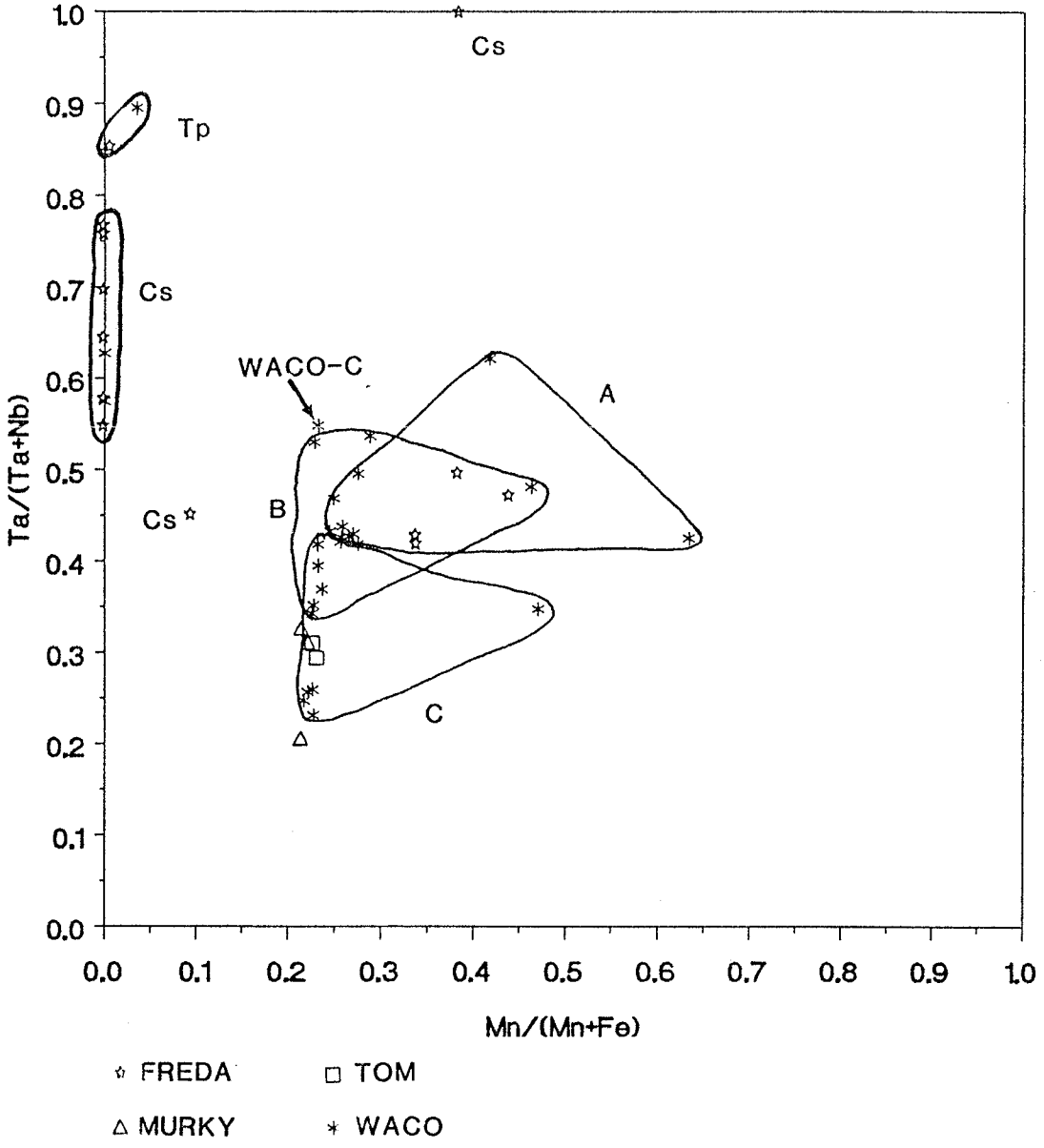

Figure 98: Chemistry of Nb,Ta-oxide minerals from the Tom, Murky, Waco and Freda pegmatites. Compositional fields are marked for tapiolite (Tp) and cassiterite (Cs). Lettered fields represent the columbite-tantalite compositions of individual pegmatite bodies.

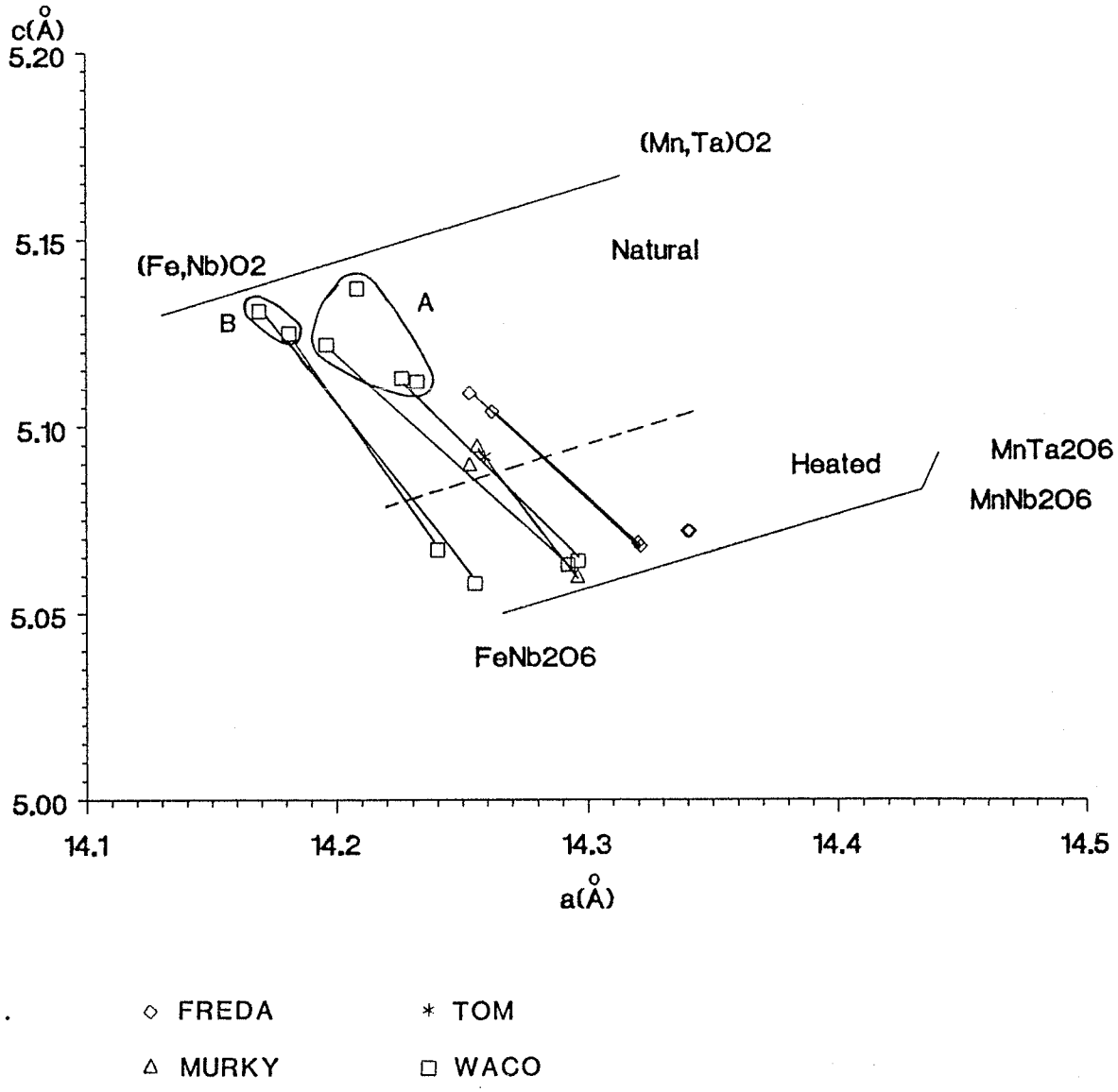

Figure 99: The a-c plot illustrating the structrual state of columbite-tantalites from the Tom, Murky, Waco and Freda pegmatites. Dashed line separates natural and heated samples. Letters designate individual pegmatite bodies.

eral, the Freda samples show degrees of Mn and Ta fractionation comparable to that of the Waco swarm (Figure 98). This highly fractionated body also contains abundant cassiterite which is notably Ta rich (up to 7% Ta_2O_5). Like most other cassiterites from the Yellowknife field, samples from the Freda dike do not contain significant Ti and Mn.

Two platy crystals of ferrocolumbite in blocky K-feldspar ± quartz assemblages from the "A" dike of the Fi pegmatites have nearly identical Mn/(Mn + Fe) and Ta/(Ta + Nb) ratios (Figure 100). A third sample from the "B" dike was analyzed and contains significantly higher Ta contents, but with similar Mn/(Mn + Fe) ratios as the "A" dike. Structurally, samples from the "A" dike plot in the region of intermediate order (Figure 101). Only two samples from the "A" dike were available, yet the range of order between them is quite large (59-71%).

One massive grain of ferrocolumbite from the Qi pegmatite gave a degree of order value of 66% with a Mn/(Mn + Fe) ratio of 0.26 and a Ta/(Ta + Nb) ratio of 0.33, and a single specimen from the Greg pegmatite showed a Mn/(Mn + Fe) ratio of 0.41 and a Ta/(Ta + Nb) ratio of 0.20 (Figures 100 and 101). X-ray powder diffraction data was unattainable for the Greg sample due to the very small size of the crystal.

The composition of columbite-tantalites from the Lu swarm cluster into three large populations (Figure 100). The smallest group consists of ferrocolumbites from body "D5", with Mn/(Mn + Fe) ratios from 0.17 to 0.20 and Ta/(Ta + Nb) ratios from 0.41 to 0.47.

The second largest population (body "D6") consists of ferrocolumbite, with minor ferrotantalite and shows a wide variation in Mn/(Mn + Fe) and Ta/(Ta + Nb) ratios. In this body, the rates of Mn/Fe and Ta/Nb fractiona-

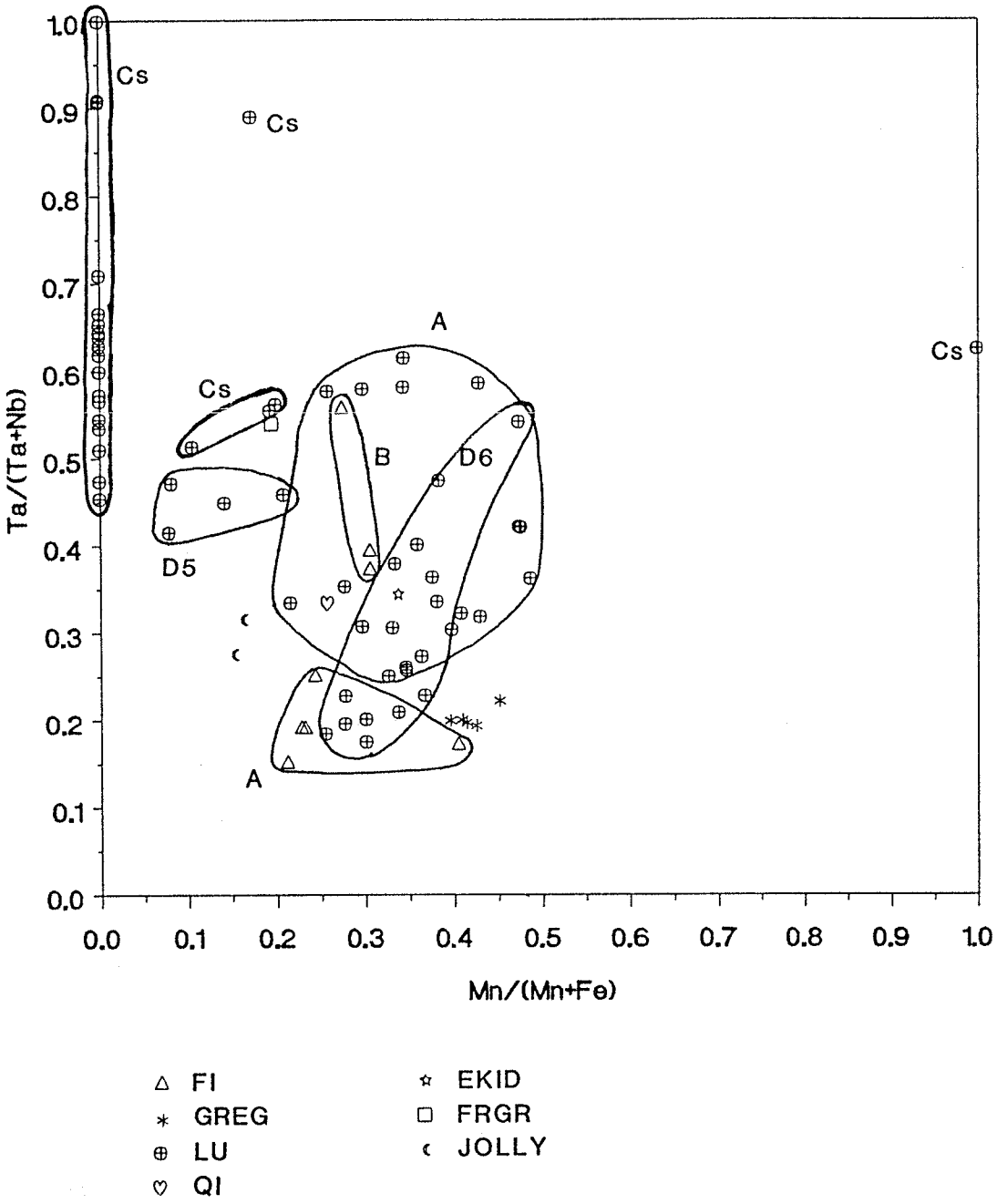

Figure 100: Chemistry of Nb,Ta-oxide minerals from Fi, Qi, Greg, Lu, Ekid, Jolly and Frog granite pegmatites. Compositional field is marked for cassiterite (Cs). Numbered and lettered fields represent the columbite-tantalite compositions of individual pegmatite bodies.

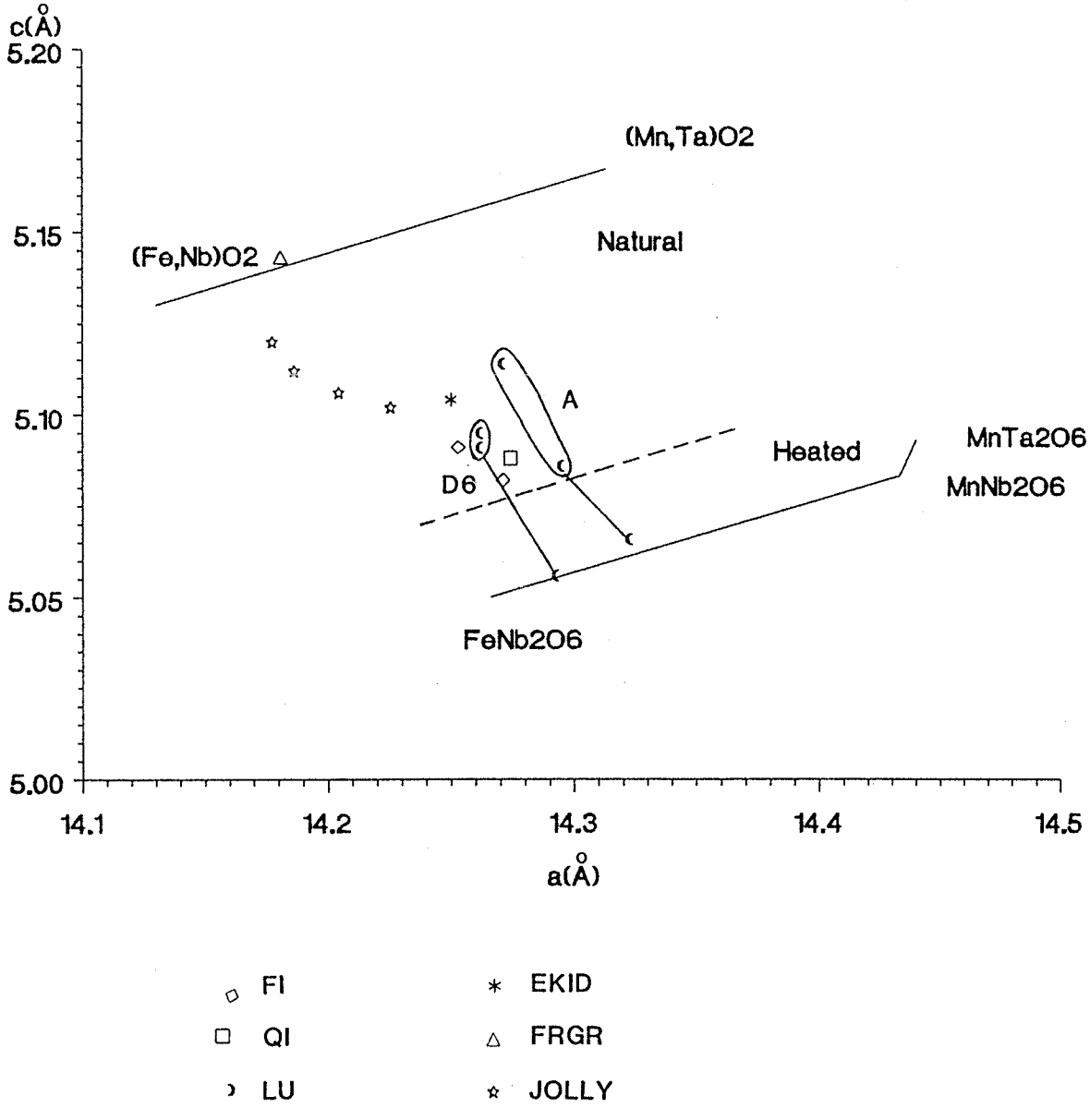

Figure 101: The a-c plot illustrating the structural state of columbite-tantalites from the Fi, Qi, Lu, Ekid, Jolly and Frog granite pegmatites. Dashed line separates natural and heated samples. Letters designate individual pegmatite bodies.

tion are nearly equal, in contrast to the steep gradients observed in the previously discussed pegmatite bodies of the field. Columbite-tantalite analyses from body "A" comprises the largest and most variable population. Mn/(Mn + Fe) ratios vary greatly from 0.22-0.48 along with large variations in Ta/(Ta + Nb) ratios (0.26-0.62).

Cassiterite occurs in great abundance in the Lu pegmatites and generally speaking, compositions from all bodies are fairly uniform. Ti, Fe and Mn contents are generally minor, although local enrichments do occur. Ta/(Ta + Nb) ratios range from 0.46-1.00.

Two pegmatites (Ekid and Jolly) located near the southernmost extension of the Cameron Granite, and a third pegmatite vein within the Frog Granite (Frgr), contained columbite-tantalite with near fully disordered structural states (Frgr) to intermediate structural state (Jolly and Ekid) (Figure 100).

The columbite-tantalites of the Jolly and Ekid pegmatites plot within the ferrocolumbite field of the columbite quadrilateral (Figure 100). High Ti contents (1.5% TiO_2) were observed in the Jolly ferrocolumbite. In contrast, the columbite-tantalite from the Frog granite (Frgr) shows variable composition ranging from ferrocolumbite to ferrotantalite

Reid Lake Series.

Columbite-tantalite collected from the spodumene-bearing Ann pegmatite is predominantly ferrocolumbite in composition, with the exception of one ferrotantalite sample (Figure 102). Narrow Mn/(Mn + Fe) ratios (0.26 - 0.39) with variable Ta/(Ta + Nb) ratios (0.12 - 0.55) are evident. A single sample from a pod of saccharoidal albite has Ta/(Ta + Nb) ratios comparable to specimens from the main pegmatite body, but shows a significantly

lesser degree of Mn enrichment (Mn/(Mn + Fe) = 0.23-0.28). The structural state is of intermediate order (Figure 103).

Samples from the Pancho Villa swarm show high to intermediate degrees of order varying from 23 to 52% (Figure 103). Samples from body "C" are the most disordered in this swarm. The columbite-tantalite varies from ferrocolumbite to ferrotantalite with very restricted Mn/(Mn + Fe) and Ta/(Ta + Nb) ratios (Figure 102).

Harding Lake Series.

Only one specimen from the Paint swarm was available for microprobe study, and the analysis shows that it is Mn and Nb rich (Figure 104). X-ray powder diffraction data for 3 samples show variable but intermediate to high degrees of order (Figure 105).

Samples from the spatially related Jake-Da swarm show a lower degree of order than the Paint specimens (Figure 105). The composition of columbite-tantalite from the main dike varies from ferrocolumbite to manganocolumbite (Figure 106). The samples as a group show a wide range of Mn/(Mn + Fe) ratios (0.43-0.97) and somewhat limited Ta/(Ta + Nb) ratios (0.07-0.33).

Two crystals occurring in saccharoidal albite from the Sky pegmatite each show uniform Mn/(Mn + Fe) and Ta/(Ta + Nb) ratios comparable to the Jake-Da specimens.

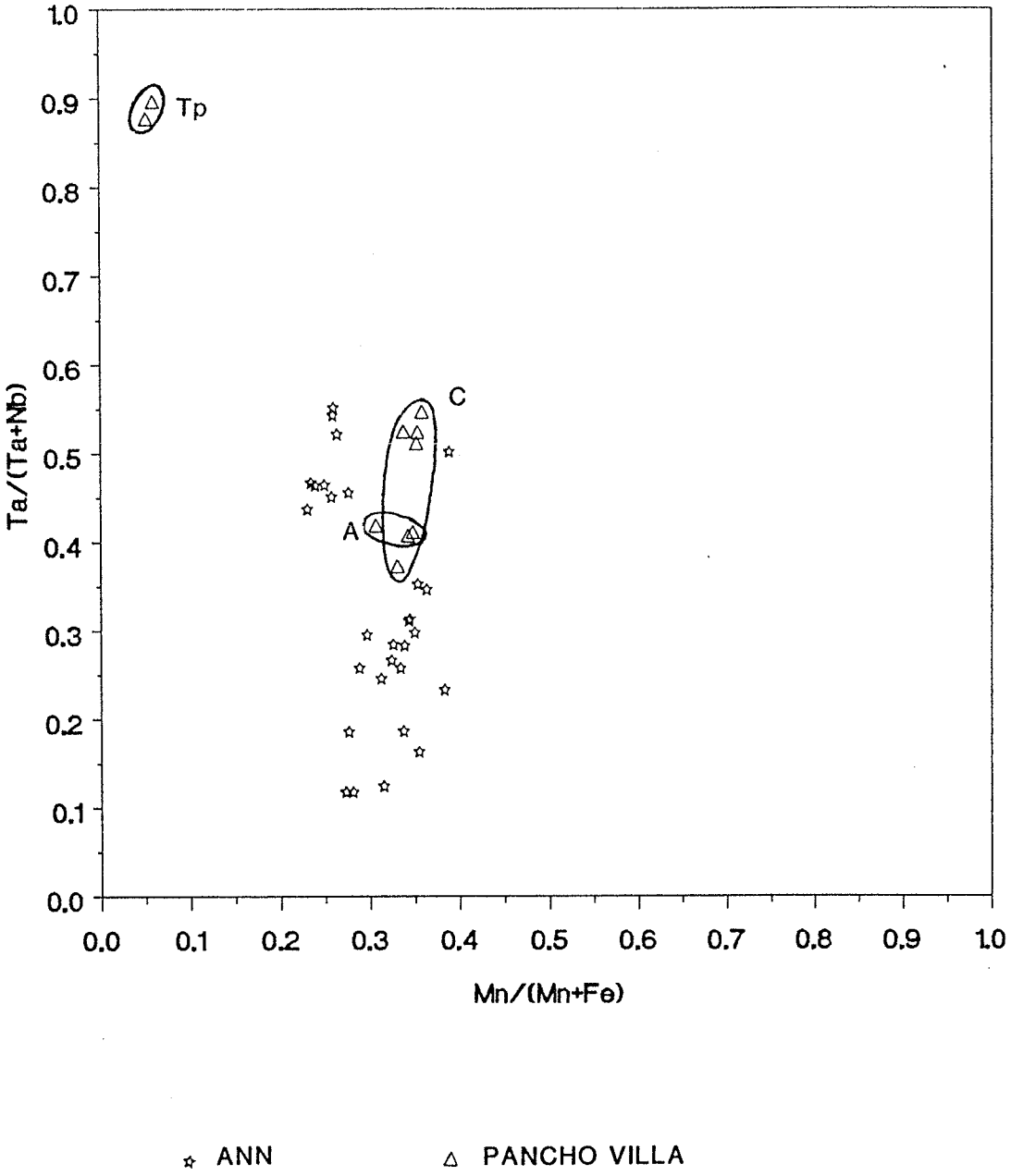

Figure 102: Chemistry of Nb,Ta-oxide minerals from the Reid Lake pegmatite series. Compositional field is marked for tapiolite (Tp). Lettered fields represent the columbite-tantalite compositions of individual pegmatite bodies.

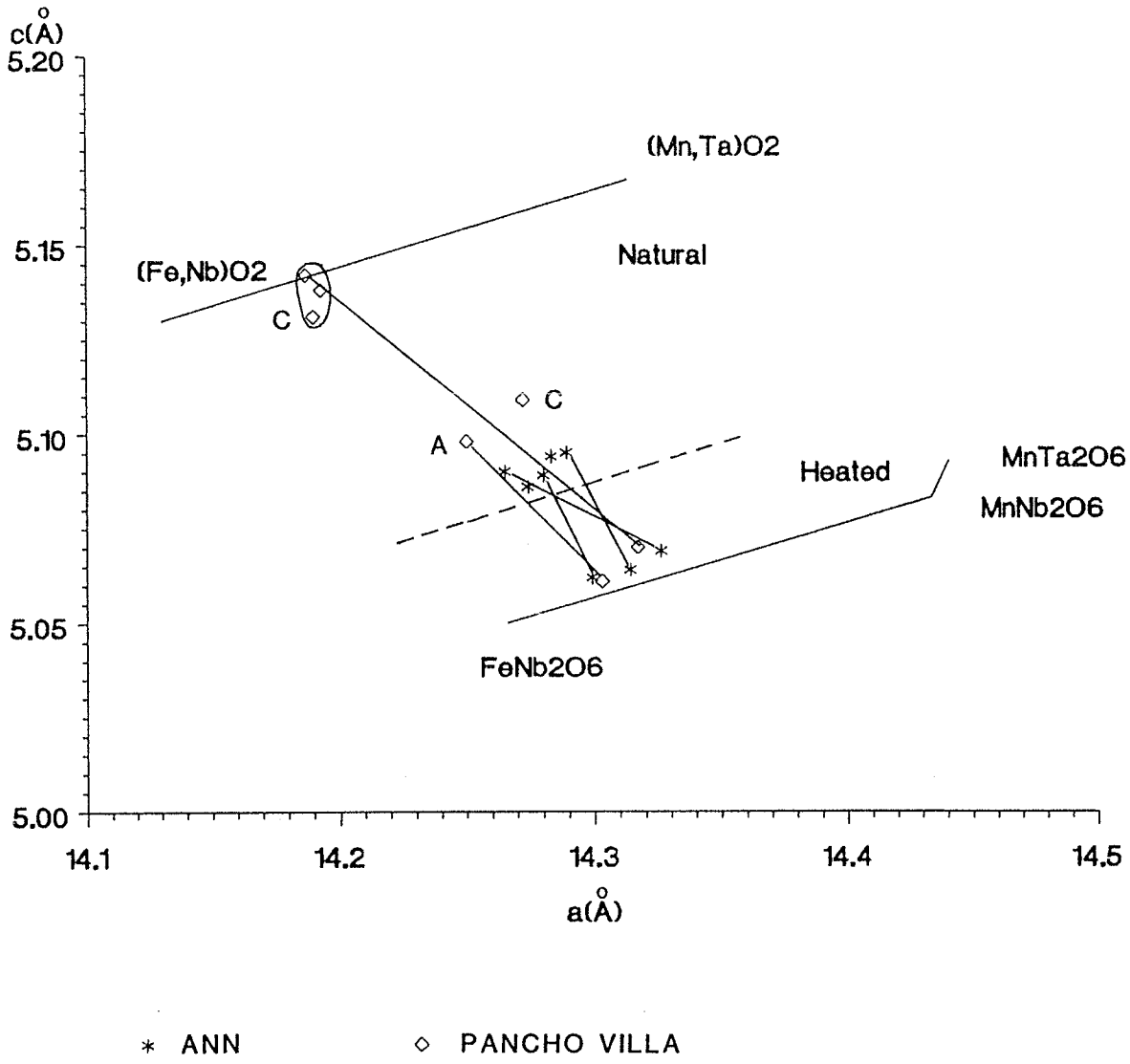

Figure 103: The a-c plot illustrating the structural state of columbite-tantalites from the Reid Lake pegmatite series. Dashed line separates natural and heated samples. Letters designate individual pegmatite bodies.

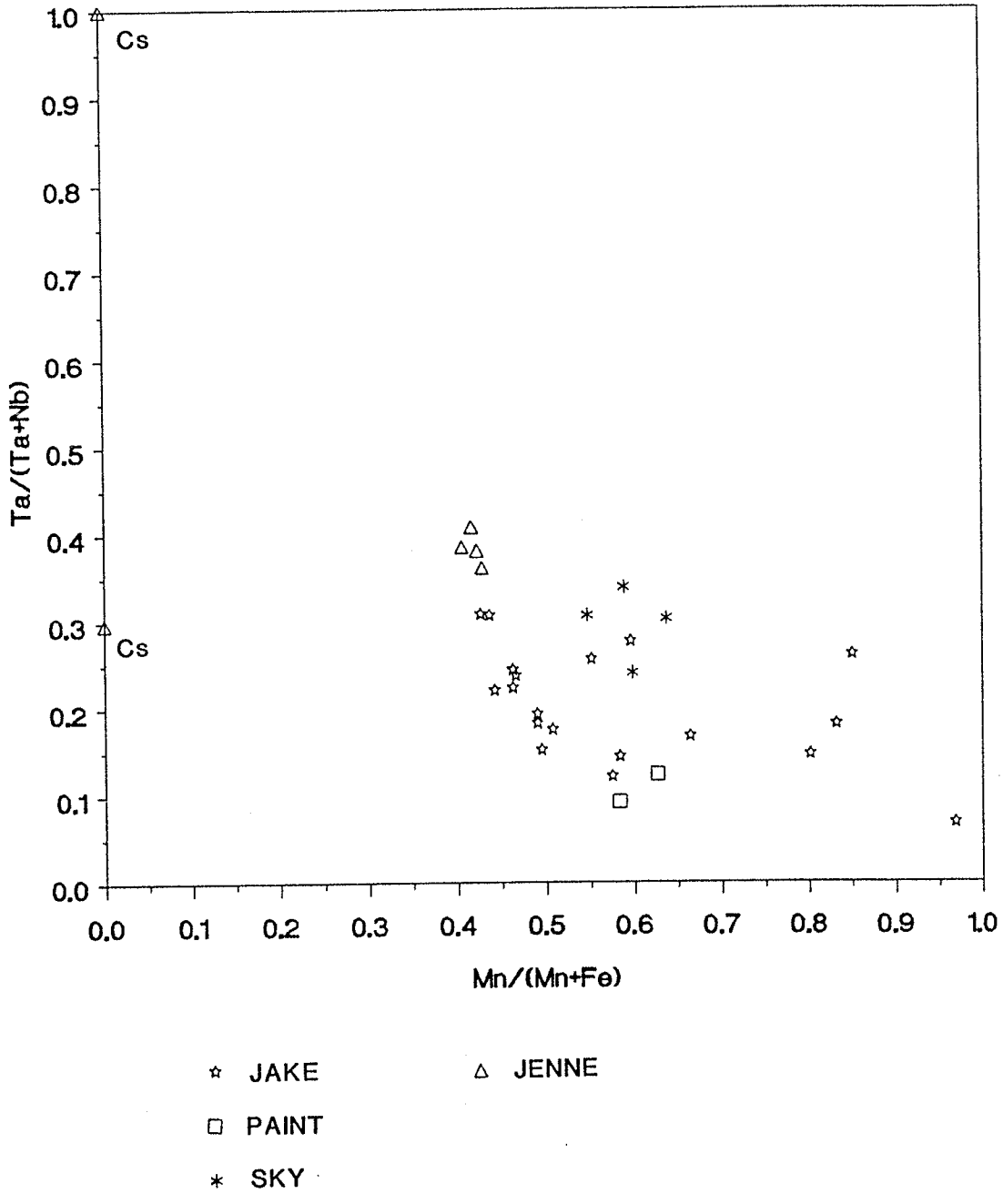

Figure 104: Chemistry of Nb,Ta-oxide minerals from the Harding Lake pegmatite series and the Jenne pegmatite.

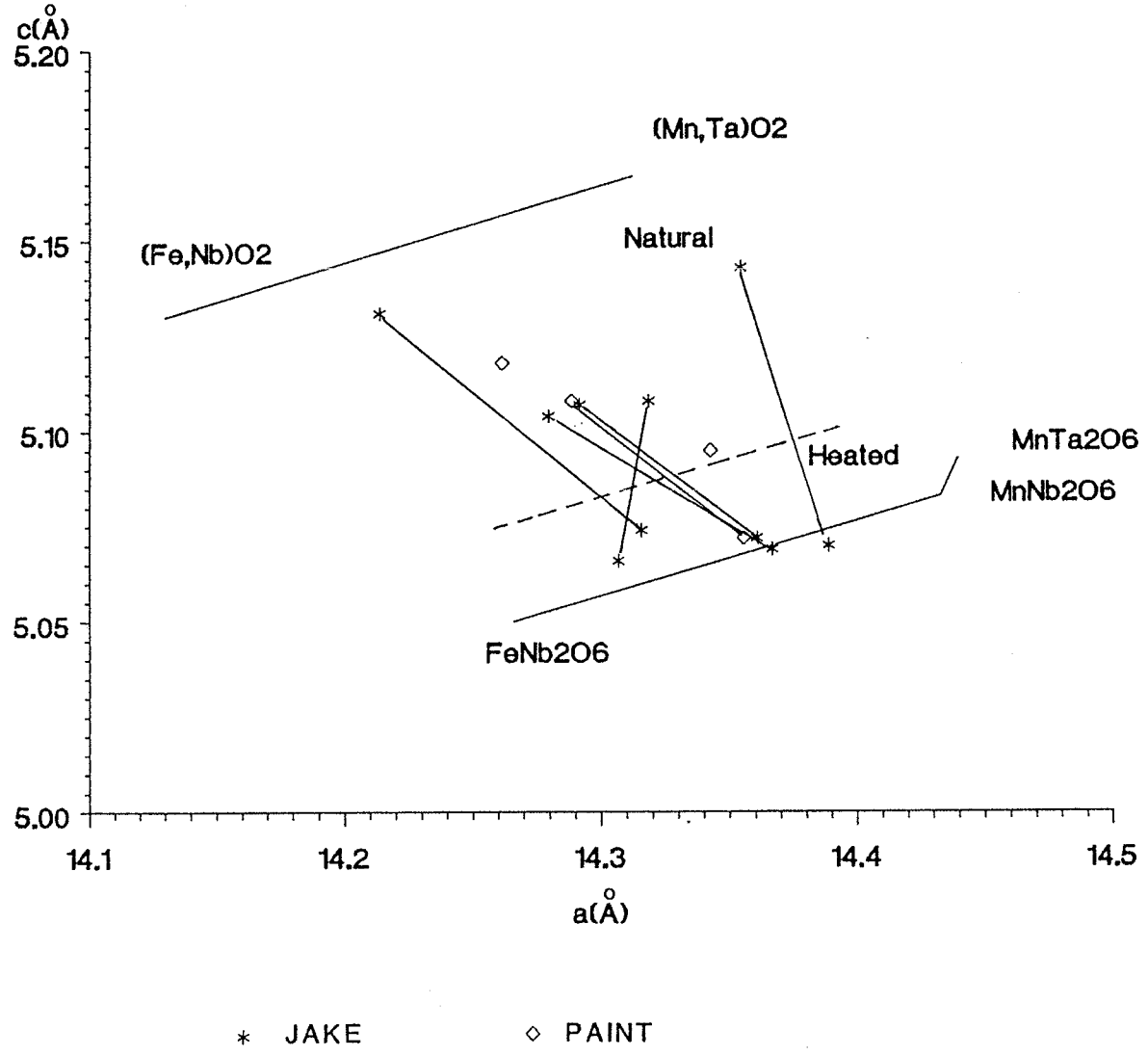

Figure 105: The a-c plot illustrating the structural state of columbite-tantalites from the Harding Lake pegmatite series. Dashed line separates natural and heated samples.

Upland Lake Series.

Columbite-tantalite compositions from the Jenne pegmatite show slightly higher Ta fractionation but comparable Mn/(Mn + Fe) ratios than the Jake-Da, Paint or Sky pegmatites (Figure 104). Rare cassiterite contains only minor traces of Ta, Nb, Fe, Ti and Mn.

Bighill Lake Group.

Columbite-tantalite is scarce from the Limo swarm. The only X-ray powder diffraction data available indicate a somewhat low degree of order (Figure 107). Chemical data for columbite-tantalite occurring as microscopic blades in a saccharoidal albite unit show compositions within the ferrocolumbite field of the columbite quadrilateral (Figure 106).

The Big swarm to the E of the Limo swarm contains platy to tabular crystals of ferrocolumbite, ferrotantalite and minor manganocolumbite. Columbite-tantalite compositions from the "BA" and "BB" zones, are notably separated in the columbite quadrilateral (Figure 106). Specimens from the "BA zone" are strongly enriched in Mn and Nb, whereas samples from the "BB zone" typically show compositions of ferrocolumbite with minor ferrotantalite. Unlike specimens from the "BA zone", those from the "BB zone" show a large variation in their Ta/(Ta + Nb) ratios (0.13-0.59) while maintaining a limited Mn/(Mn + Fe) ratio. Ferrotapiolite analyses are, for the most part, very uniform with very little variation in major element chemistry.

The bimodal columbite-tantalite population produced by compositional differences are not evident in the X-ray powder diffraction data. All samples, regardless of their provenance, show intermediate degrees of order (Figure 107).

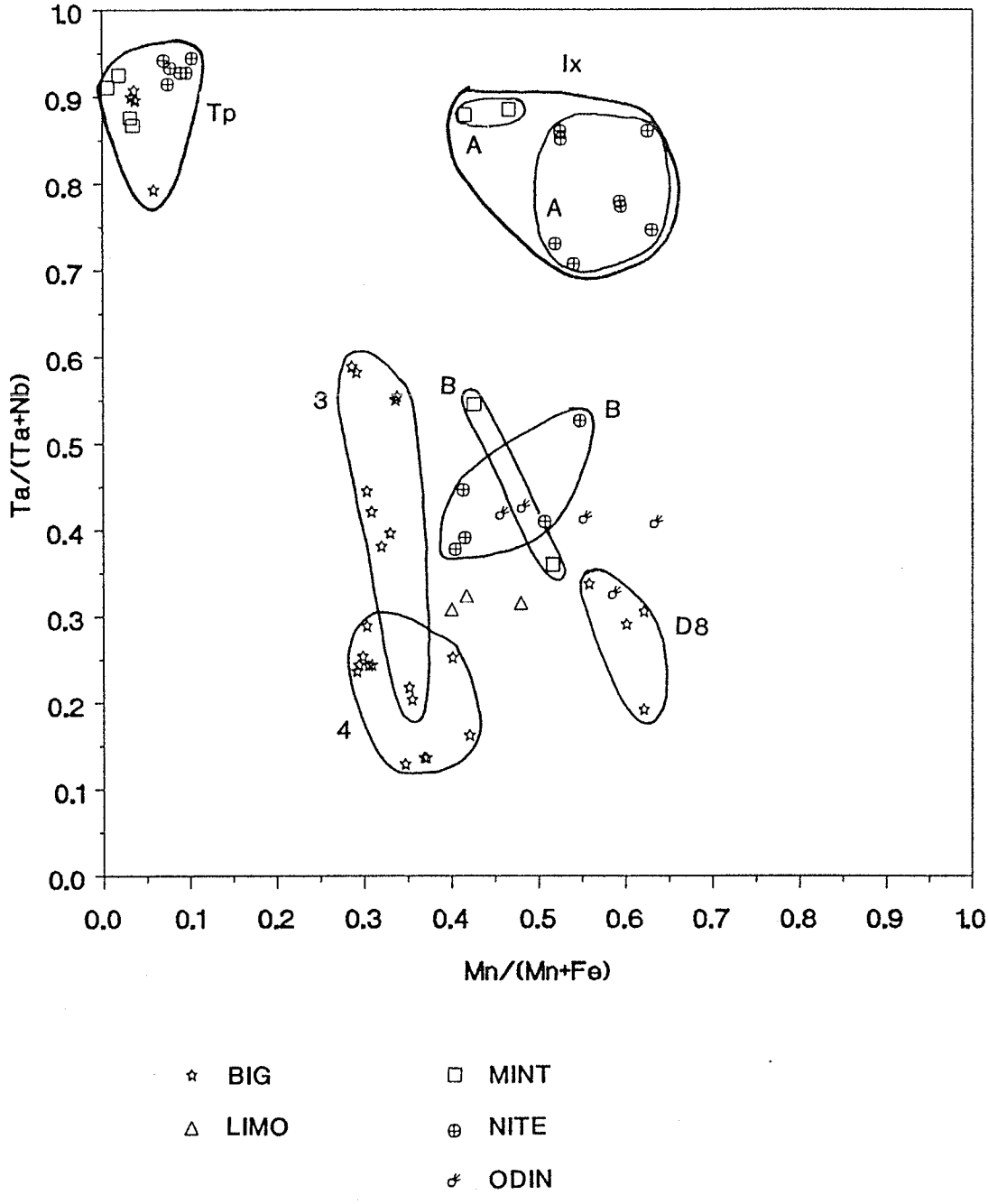

Figure 106: Chemistry of Nb,Ta-oxide minerals from the Bighill Lake pegmatite group. Compositional fields are marked for ixiolite (Ix) and tapiolite (Tp). Numbered and lettered fields represent the columbite-tantalite compositions of individual pegmatite bodies.

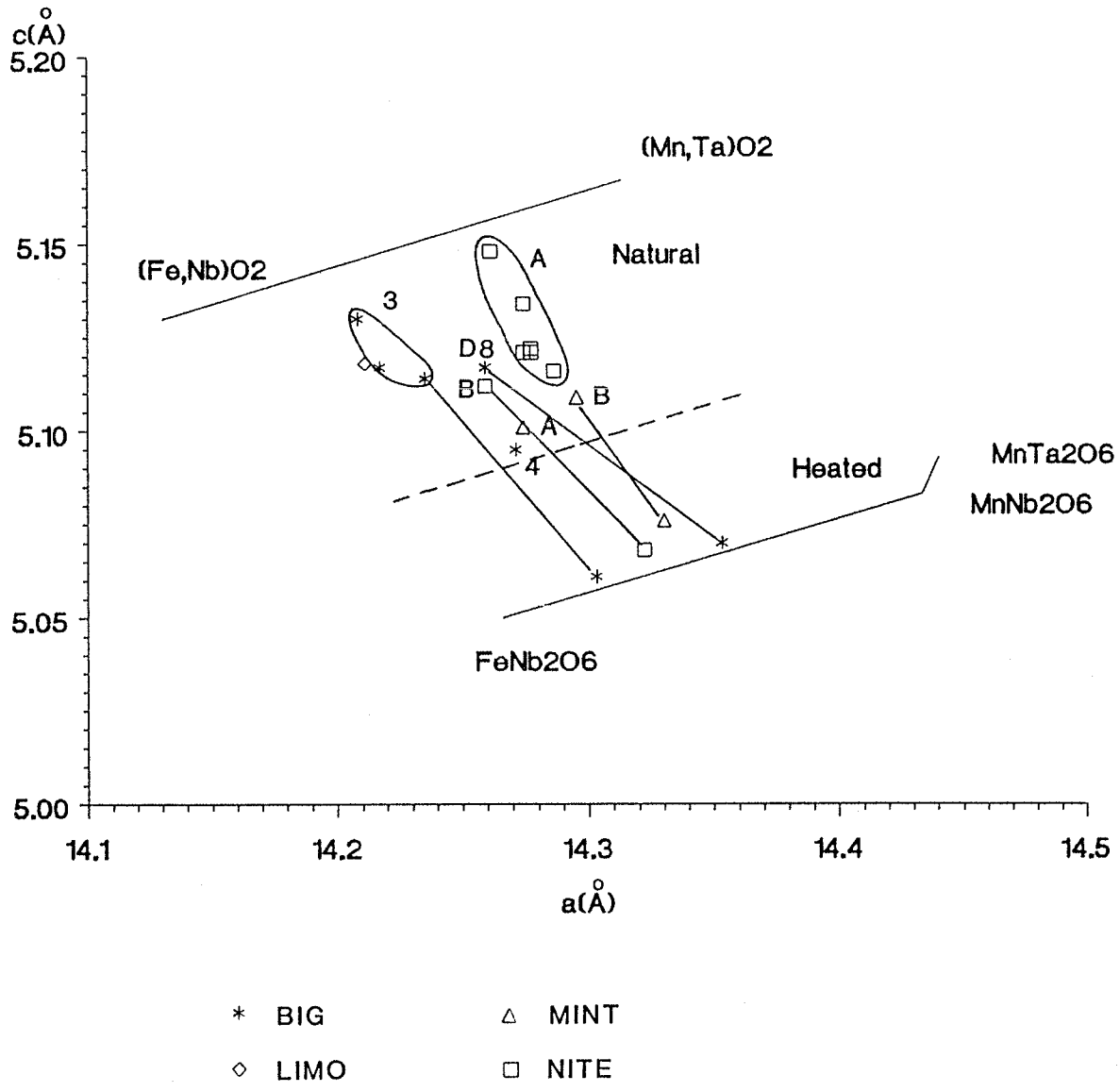

Figure 107: The a-c plot illustrating the structural state of columbite-tantalites from the Bighill Lake pegmatite group. Dashed line separates natural and heated samples. Numbers and letters designate individual pegmatite bodies.

The structural state of columbite-tantalite from the Nite swarm can be described as intermediate with little variation within the swarm (Figure 107). The degree of order ranges from 7 to 43% over the entire swarm. This feature is of particular interest because of the considerable difference in chemistry between the "A" and "B" bodies (Figure 105). Samples collected from body "A" are stannian ixiolites with Mn/(Mn + Fe) ratios of 0.53-0.63 and Ta/(Ta + Nb) ratios of 0.74-0.86, whereas those from body "B" are ferrocolumbites.

Stannian ixiolite from the Mint pegmatite (body "A") is slightly richer in Fe and Ta than the Nite ixiolite (Figure 105). Body "B" contains ferrocolumbite with uniform chemistry. Only one columbite-tantalite was available for X-ray powder diffraction study and its unit cell dimensions indicate an intermediate degree of order (Figure 107). Ferrotapiolites from both the Nite and Mint pegmatites are Ta rich, with the Nite samples showing slightly greater Mn enrichment.

The columbite-tantalite compositions of the Odin pegmatite fall within the ferrocolumbite field (saccharoidal albite association) and the manganocolumbite field (cleavelandite association) of the quadrilateral.

Circle Lake Series.

The Dr. Bob pegmatite is characterized by the occurrence of cassiterite and minor ferrocolumbite and ferrotapiolite (Figure 108). The cassiterite has Ta>>Nb and contains very little Ti, Fe^{3+} or Mn. Coexisting ferrocolumbite has a narrow range of Mn/(Mn + Fe) ratios (0.05-0.15) and marginally variable Ta/(Ta + Nb) ratio (0.52-0.54). Ferrotapiolite is typically depleted in Mn, but enriched in Ti (up to 2% TiO_2).

The highly fractionated Riber pegmatite shows columbite-tantalite with considerable variation in structural state and chemistry, which is none too surprising for a pegmatite with extensive and well-developed internal zonation and enrichment in Li, B and F.

Two kinds of crystal habits dominate the Riber columbite-tantalite morphology; their crystal forms are typically restricted to a particular paragenetic assemblage.

Platy columbite-tantalite generally occurs in a cleavelandite + muscovite + quartz + beryl assemblage of the intermediate zone. Schorl and zircon also occur as common accessory phases of this zone. Invariably, the composition of the platy crystals is ferrocolumbite with a low Ta/(Ta + Nb) ratio (0.11) and low Mn/(Mn + Fe) ratios (0.24-0.28) (Figure 109).

The second major morphological type are the tabular crystals associated with the cleavelandite + beryl zone. Beryl and green tourmaline (elbaite) are locally present. Columbite-tantalite of this type shows a wide range of structural states, varying from moderately disordered to moderately ordered (Figure 109). Chemically, they are manganotantalite and manganocolumbite which often contain inclusions of microlite. The crystallization of microlite seems to be responsible for a reversal in the Ta fractionation, as indicated by the "boomerang" trend shown on the columbite quadrilateral (Figure 108). Preferential partitioning of Ta by the microlite lowers the Ta/(Ta + Nb) ratio of the coexisting columbite-tantalite, thus resulting in the reversal shown by sample number RIB-A-7. It is interesting to note that this sample also shows the highest degree of order (75%) of any Riber sample.

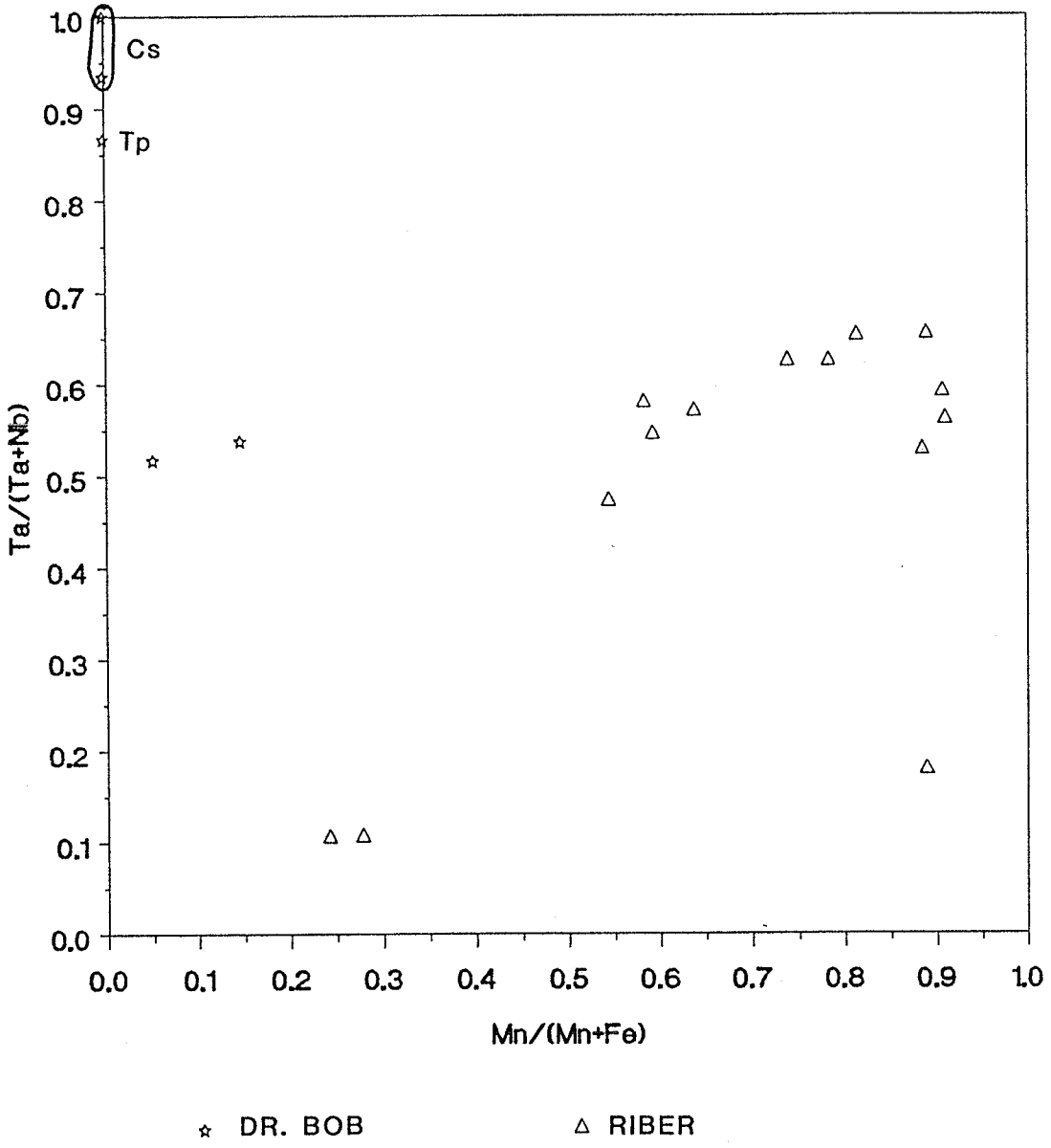

Figure 108: Chemistry of Nb,Ta-oxide minerals from the Circle Lake pegmatite series. Compositional fields are marked for tapiolite (Tp) and cassiterite (Cs); the remaining symbols are for columbite-tantalite minerals.

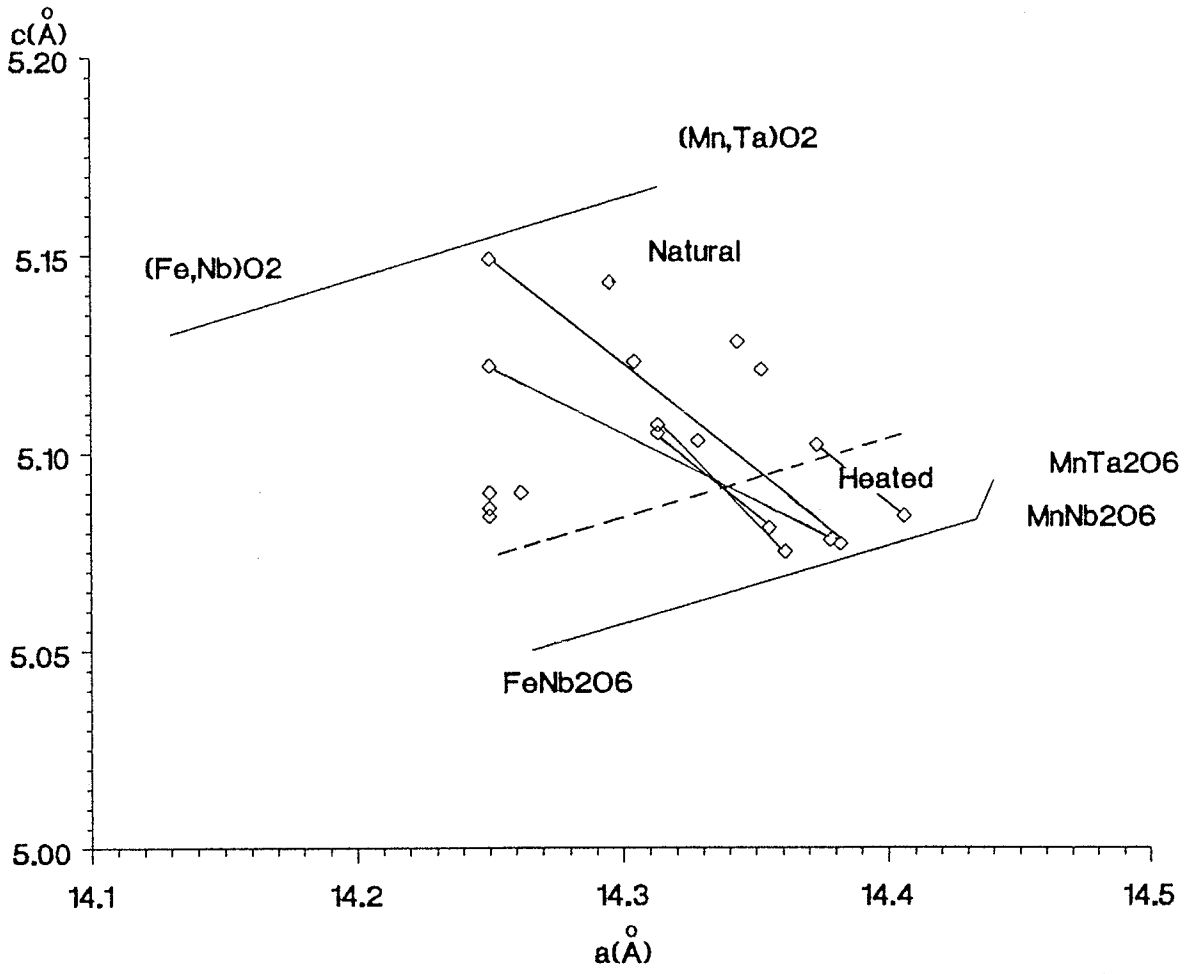

Figure 109: The a-c plot illustrating the structural state of columbite-tantalites from the Riber pegmatite (Circle Lake series). Dashed line separates natural and heated samples.

Chemical and structural variations in pegmatite series

Southeastern area

Compositions of columbite-tantalite from the Faulkner Lake series show highly variable Ta/(Ta + Nb) ratios with limited Mn/(Mn + Fe) values (Figure 110). The compositional varieties of the series are predominantly ferrocolumbite, which occur extensively in the Li- and F-enriched Moose and Bet pegmatites, grading into subordinate ferrotantalite in the Bet pegmatite and Tan swarm. The Nb/Ta fractionation proceeds at a faster rate than Fe/Mn fractionation, as evident from the steep compositional gradient (Figure 110).

The most fractionated pegmatite of this series (Tan #4 dike) contains, in addition to ferrotantalite, manganotantalite, ferrotapiolite and cassiterite. The Nb,Ta mineral assemblage suggests that this pegmatite represents the maximum degree of fractionation in the immediate vicinity surrounding the Faulkner tonalite.

The structural state of columbite-tantalite from the Faulkner Lake series is predominantly intermediate (Figure 111). Structural state data for columbite-tantalite from individual pegmatite bodies and swarms shift with their respective chemistries; the fields for the Moose and Bet pegmatites overlap one another both structurally and chemically, whereas the lower degree of order in the Tan swarm coincides with its higher content of Ta.

Compositional data for the Buckham Lake group columbite-tantalite show a similar steep gradient of Nb/Ta fractionation as observed in the Faulkner Lake series (Figure 110). In contrast to the aforementioned series, the

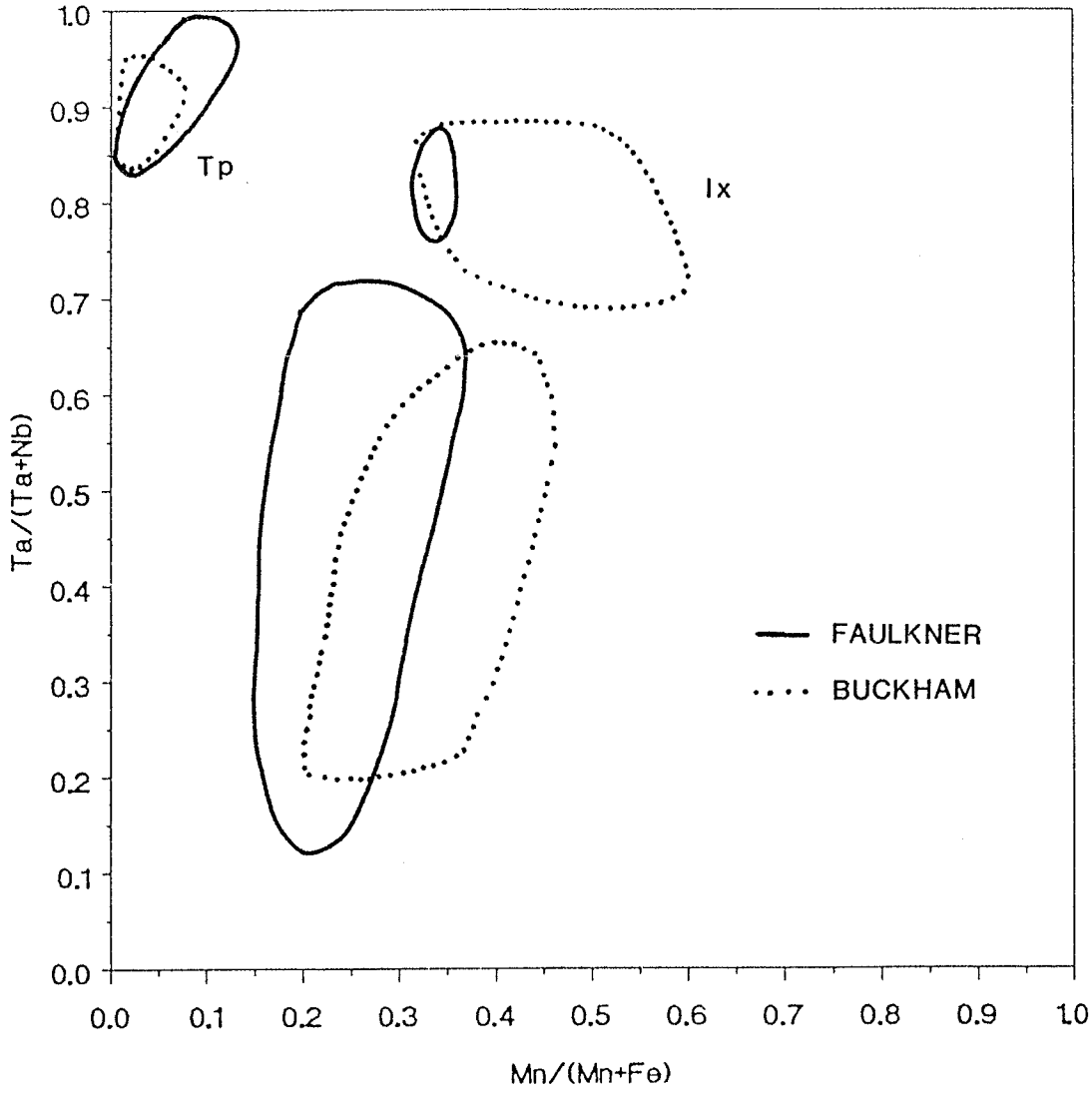

Figure 110: Chemistry of Nb,Ta-oxide minerals from the Faulkner pegmatite series and Buckham pegmatite group.

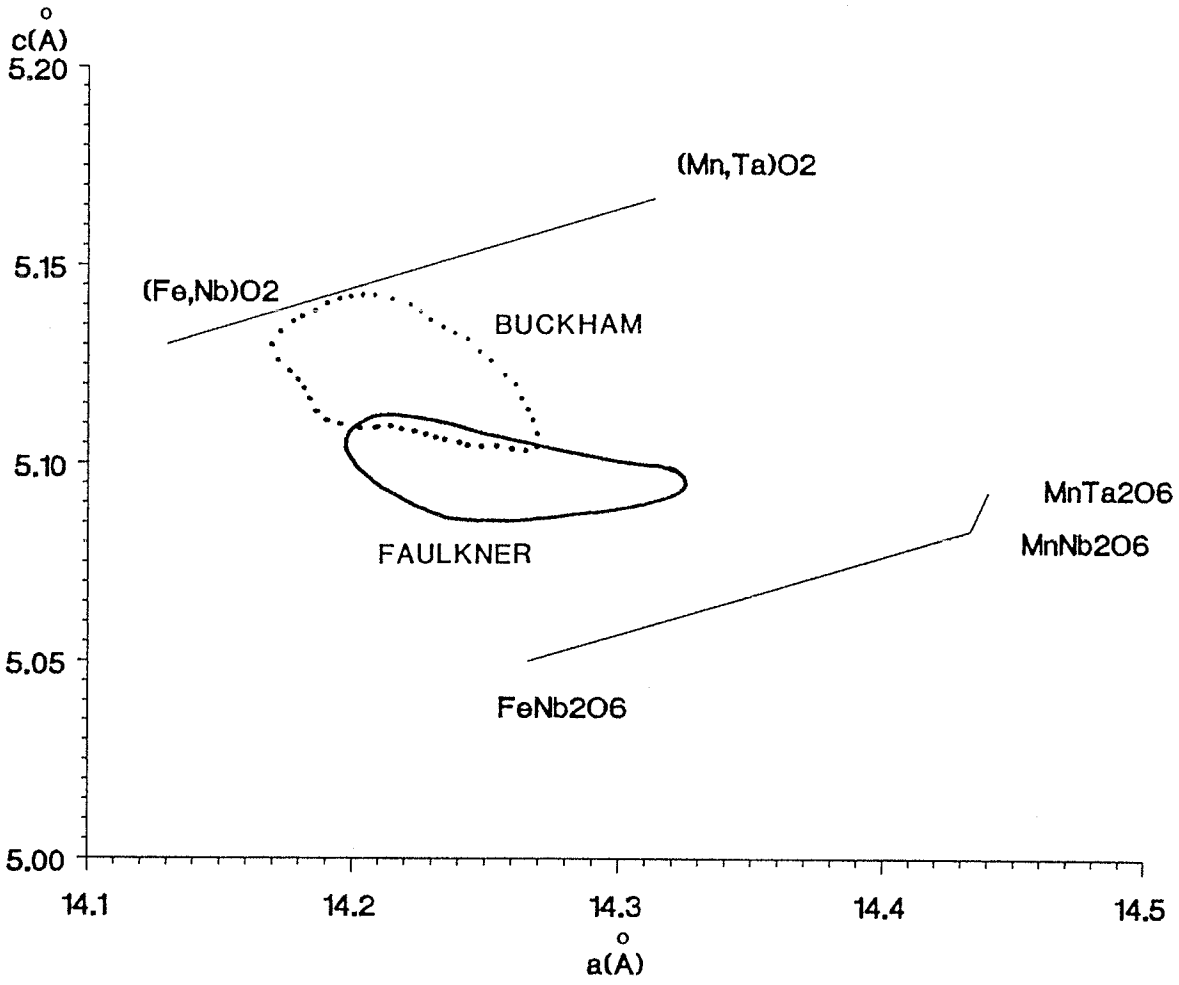

Figure 111: The a-c plot illustrating the structural state of columbite-tantalites from the Faulkner pegmatite series and Buckham pegmatite group.

Buckham Lake group shows a much higher degree of Nb/Ta and Fe/Mn fractionation. Compositions vary distinctly from Ta-rich ferrocolumbite through ferrotantalite to stannian ixiolite.

Structurally, the data from this series show a bimodal distribution, in effect coinciding with the compositional data (Figure 111). One population is formed by ixiolites, which show extreme disorder, and is related to the Ta- and Sn-rich, Fe=Mn type chemistry. A second population consists of columbite-tantalite of low to intermediate degrees of order. The variation in structural state of the columbite-tantalite can be correlated with the Ta content of the mineral; samples showing low states of order are richer in Ta than those of intermediate structural states.

The Usk and Was pegmatites of the Doubling Lake series are populated by platy ferrocolumbite crystals, locally grading into manganocolumbite compositions (Figure 112). Fe/Mn fractionation seems to be slightly more developed than in the Faulkner Lake series or Buckham Lake group, although the Nb/Ta fractionation is less extensive.

The structural aspects of the columbite-tantalite group minerals are characteristic of the southeastern portion of the field; generally moderate variations of intermediate order (Figure 113). As noted in other series of the Yellowknife field, increased disorder seems to be linked to increased Ta contents.

The Tanco Lake group consists of the Jo, Arachide and Thor-Echo swarms, which chemically show wide variations in Mn/(Mn + Fe) and Ta/(Ta + Nb) ratios (Figure 112). As with other series of the southeastern area, the Tanco Lake series shows a steep Nb/Ta fractionation gradient.

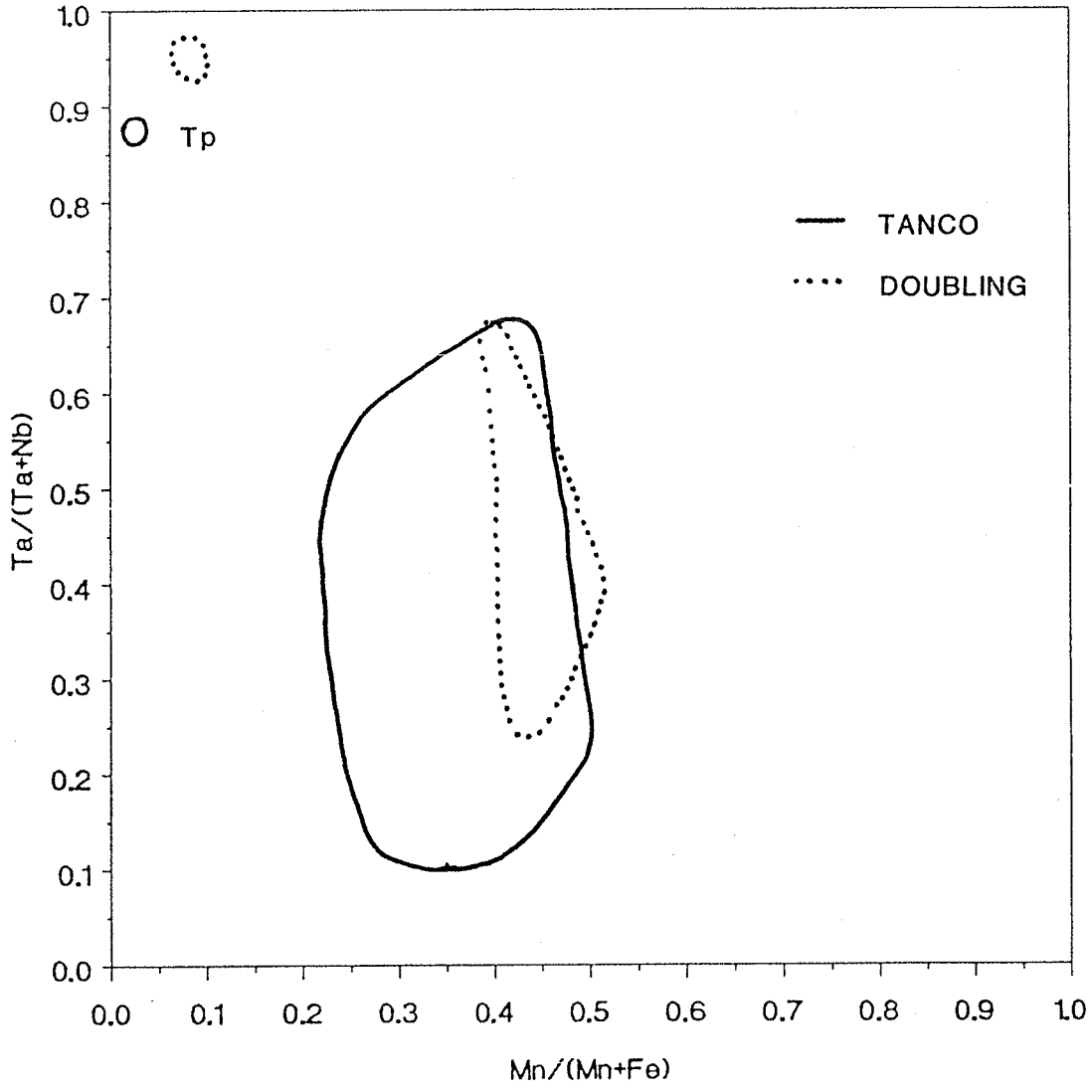

Figure 112: Chemistry of Nb,Ta-oxide minerals from the Doubling pegmatite series and Tanco pegmatite group.

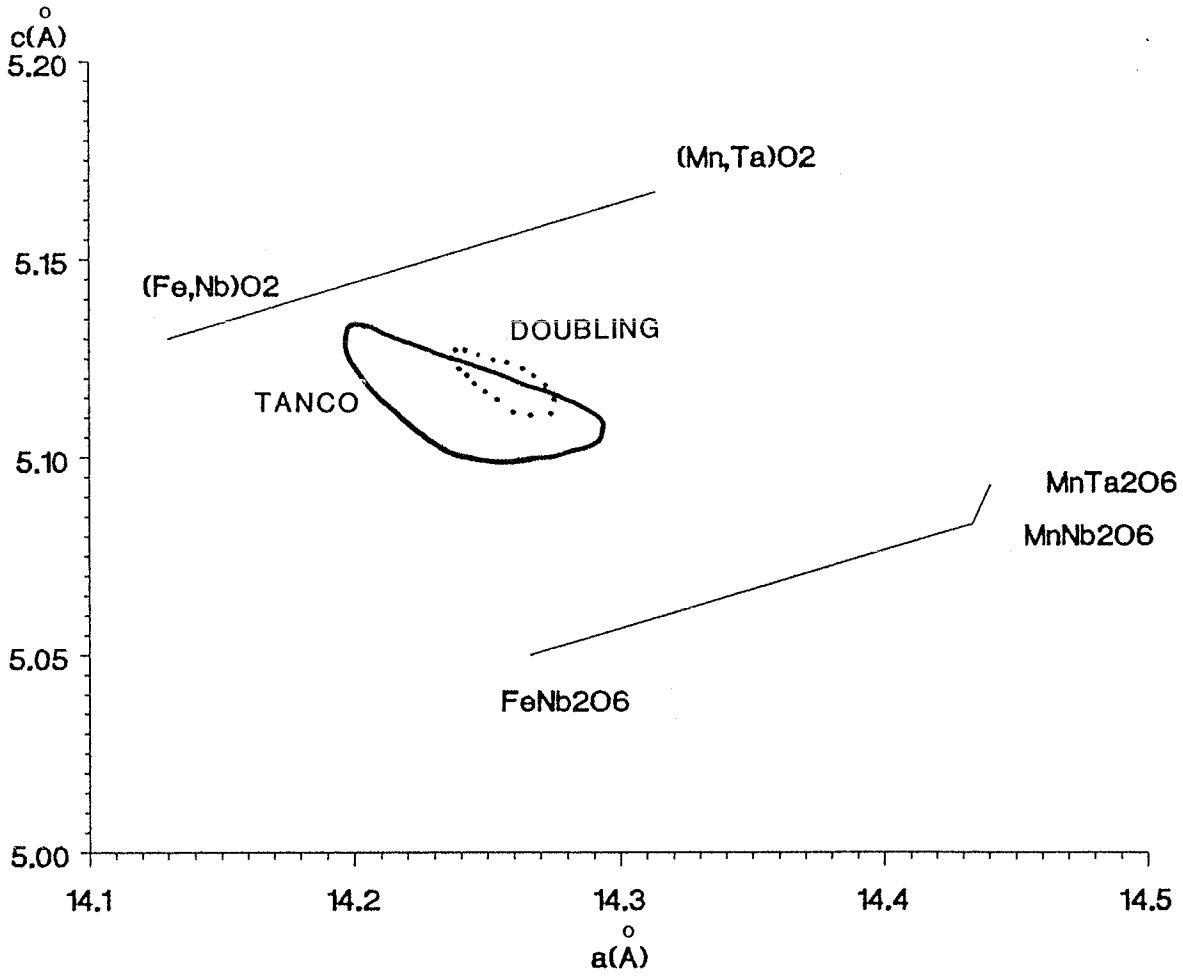

Figure 113: The a-c plot illustrating the structural state of columbite-tantalites from the Doubling pegmatite series and Tanco pegmatite group.

The structural state of the Tanco Lake series columbite-tantalites show widely variable degrees of order-disorder (Figure 113). Degrees of order vary from largely disordered to intermediate, and unlike the previously discussed series, there is no apparent correlation between the Ta content and degree of order.

Northeastern area

The regionally zoned Peg swarm represents the only known Ta-producing area occurring in the northeastern portion of the field. The zonation previously described by Hutchinson (1955a) and subsequently modified by Wise et al. (1985a) is currently based on changes in rare-element mineralization across the region. The chemistry and structural state of columbite-tantalite from the Peg swarm are strongly correlated with the regional zonation of the area. The crystal morphology of columbite-tantalite crudely follows the regional zonation, varying from massive grains in zone 1, to tabular or platy crystals in zone 4 to strictly platy crystals in zone 5. The change in morphology seems to progress with changes in the composition of the mineral. Massive grains are strongly enriched in Fe and Nb, whereas crystals become more platy with increasing Mn and Ta.

The regional chemistry of the Nb,Ta mineral assemblages shows a distinct predominance of Nb relative to Ta and Fe relative to Mn (Figure 114). Extending westward from the Redout Granite, the Mn/(Mn + Fe) ratio increases in columbite-tantalite from zone 1 to zone 5. The Mn/(Mn + Fe) ratio in columbite-tantaltite of individual pegmatites from zones 1 - 4 is very restricted, yet the range is quite extensive within any particular zone. In contrast, the trend of Ta-enrichment in the region is quite irregular.

The Ta/(Ta + Nb) ratio in columbite-tantalite of individual pegmatites is somewhat more extensive. On the whole, the Nb/Ta fractionation of specific zones and over the entire region is quite variable and does not parallel Fe/Mn fractionation. zone 4, which contains the bulk of the Nb-Ta mineralization, particularly illustrates the irregular behavior of Ta fractionation relative to Mn fractionation.

In addition to the zoning of Fe/Mn, the area also shows a crude zoning in Ti contents with Ti decreasing from zone 3 to zone 5. The zonation of Sn contents is not observed despite the occurrence of cassiterite in zone 5. In any case, the area is Ti-enriched compared to other regions in the field. In addition to columbite-tantalite, ferrotapiolite and cassiterite are also enriched in Ti.

The segregation of structural state indicators of columbite-tantalite into the respective zones is less clear due to the limited number of samples available from zones 1 - 3 (Figure 115). However, samples from zones 4 and 5 show excellent clustering. Material from zone 4 shows variable degrees of order, ranging from nearly fully ordered to moderately high disorder. zone 5 samples also show moderately high degrees of order. In comparison to samples from the southeastern region, the Peg swarm specimens also show a correlation of increasing Ta content with decreasing degree of order.

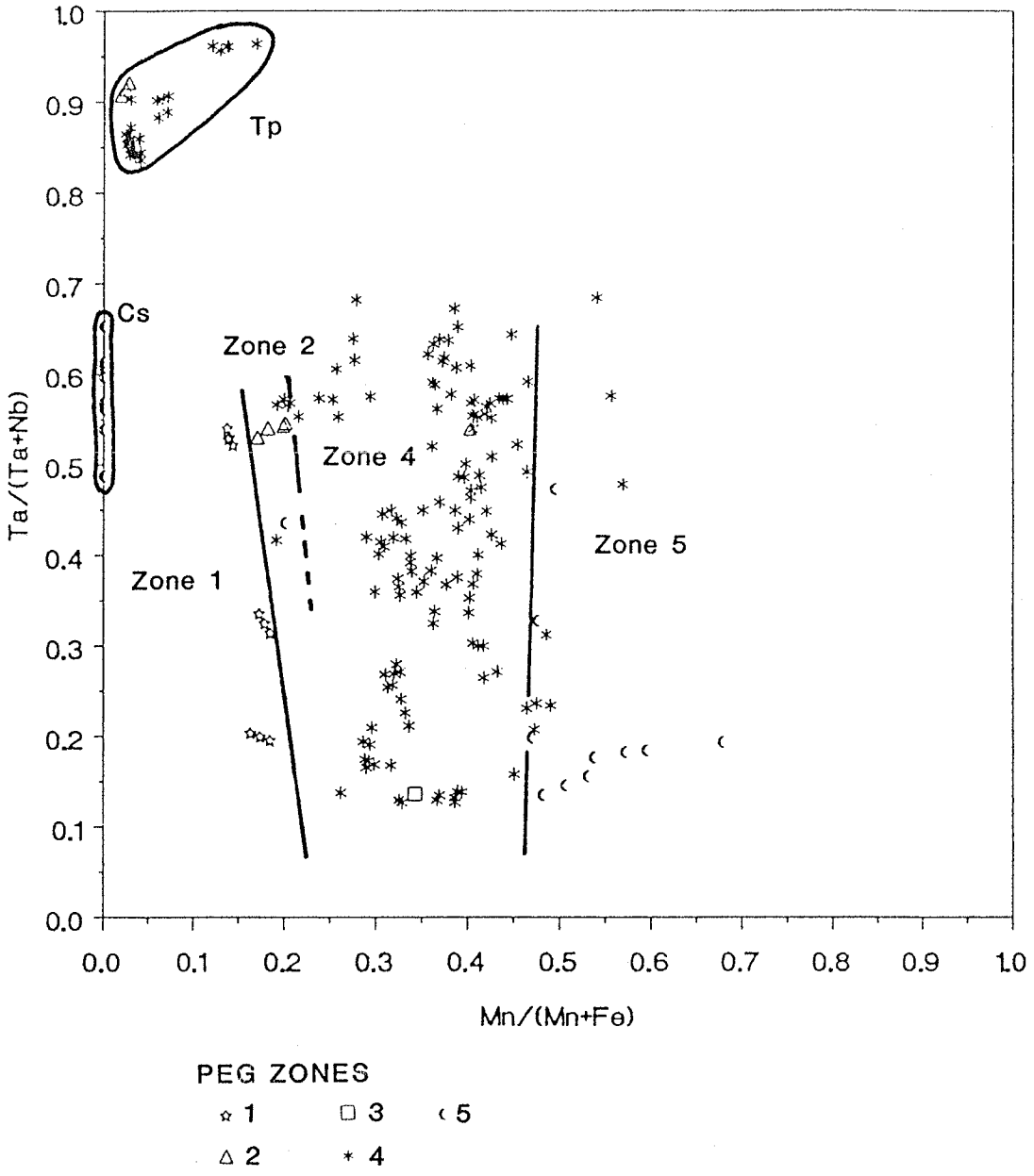

Figure 114: Chemistry of Nb,Ta-oxide minerals from the Peg swarm.

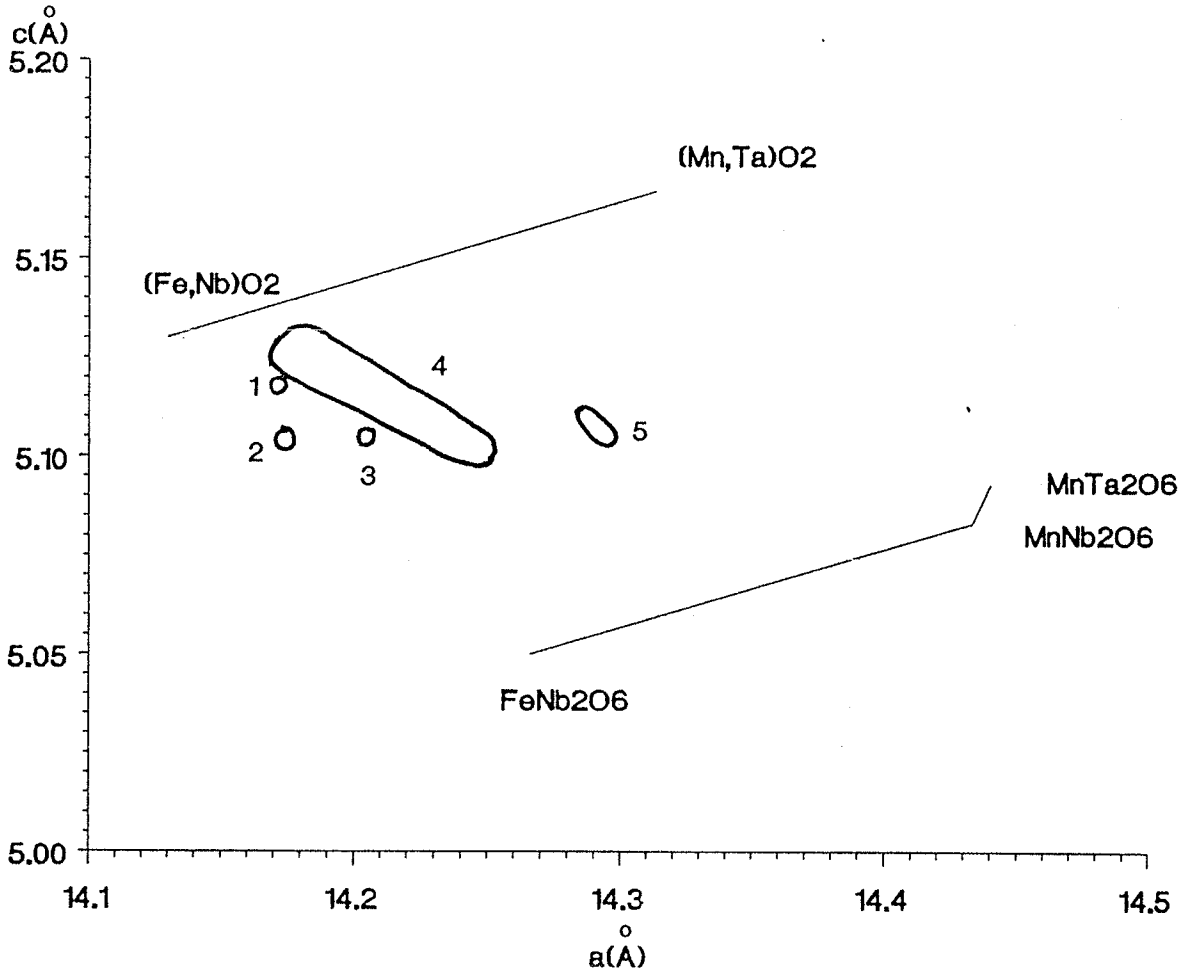

Figure 115: The a-c plot illustrating the structural state of the columbite-tantalites from the Peg swarm. Numbers refer to each of the five main zones.

Northwestern area

Columbite-tantalite from the Blaisdell Lake group shows the limited Mn/(Mn + Fe) and variable Ta/(Ta + Nb) ratios which apparently is characteristic of the Yellowknife pegmatite field. Ferrocolumbite dominates the mineral chemistry with rare ferrotantalite occurring locally (Figure 116). Based on the chemical data presented earlier, the three pegmatite swarms which form the Blaisdell Lake group seem to occur in zones surrounding the Wedge Granite. This regional zonation is suggested by field observations of locally increased rare-element mineral concentrations in the pegmatites across the area away from the Wedge Granite. The chemistry of columbite-tantalite strongly supports the field observations. The least fractionated Bill swarm lies near the margins of the granite-schist contact and shows the lowest Ta/(Ta + Nb) ratio of the three swarms. Further out from the granite lies the Melody swarm which shows increased Ta contents relative to the Bill swarm. The spodumene-bearing Vo swarm, found at the greatest distance from the granite pluton, shows the highest Ta/(Ta + Nb) ratio, in addition to greater Mn-fractionation. Structurally, the columbite-tantalites of the Blaisdell Lake series show a wide range of degree of order varying from moderate to low (Figure 117).

The Sproule Lake series consists of some of the most Mn-rich columbite-tantalites in the entire field. Manganocolumbite-manganotantalite dominate the Nb- and Ta-oxide chemistry, and ferrocolumbite-ferrotantalite is rare (Figure 116). Wide ranges of Mn/(Mn + Fe) and Ta/(Ta + Nb) ratios are typical of this series. The Mn-rich bulk chemistry of this series agrees well with the general fractionation trends extending southeastward from the Wedge Granite. It is possible that the

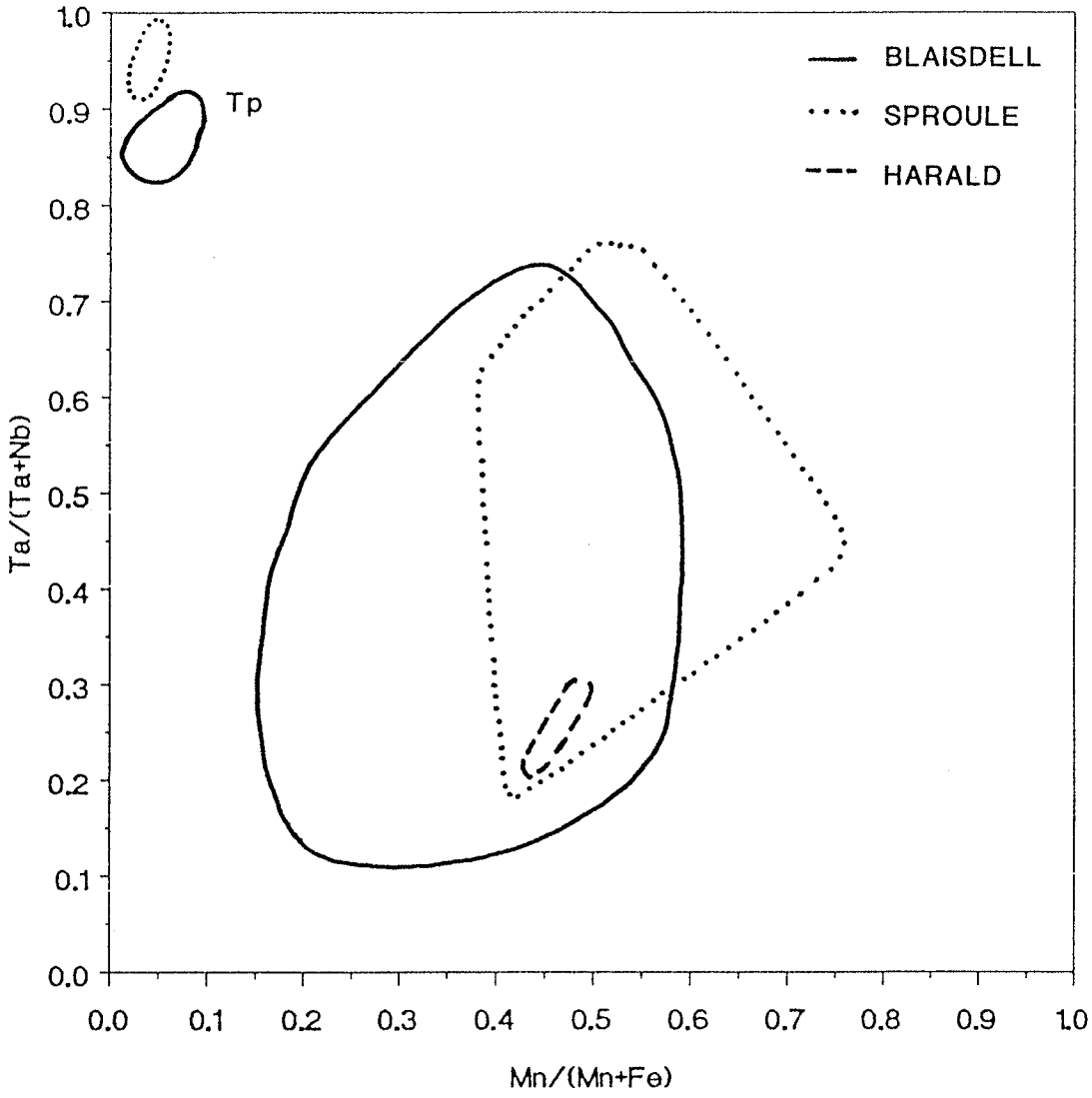

Figure 116: Chemistry of Nb,Ta-oxide minerals from the Blaisdell Lake pegmatite group and Sproule Lake pegmatite series.

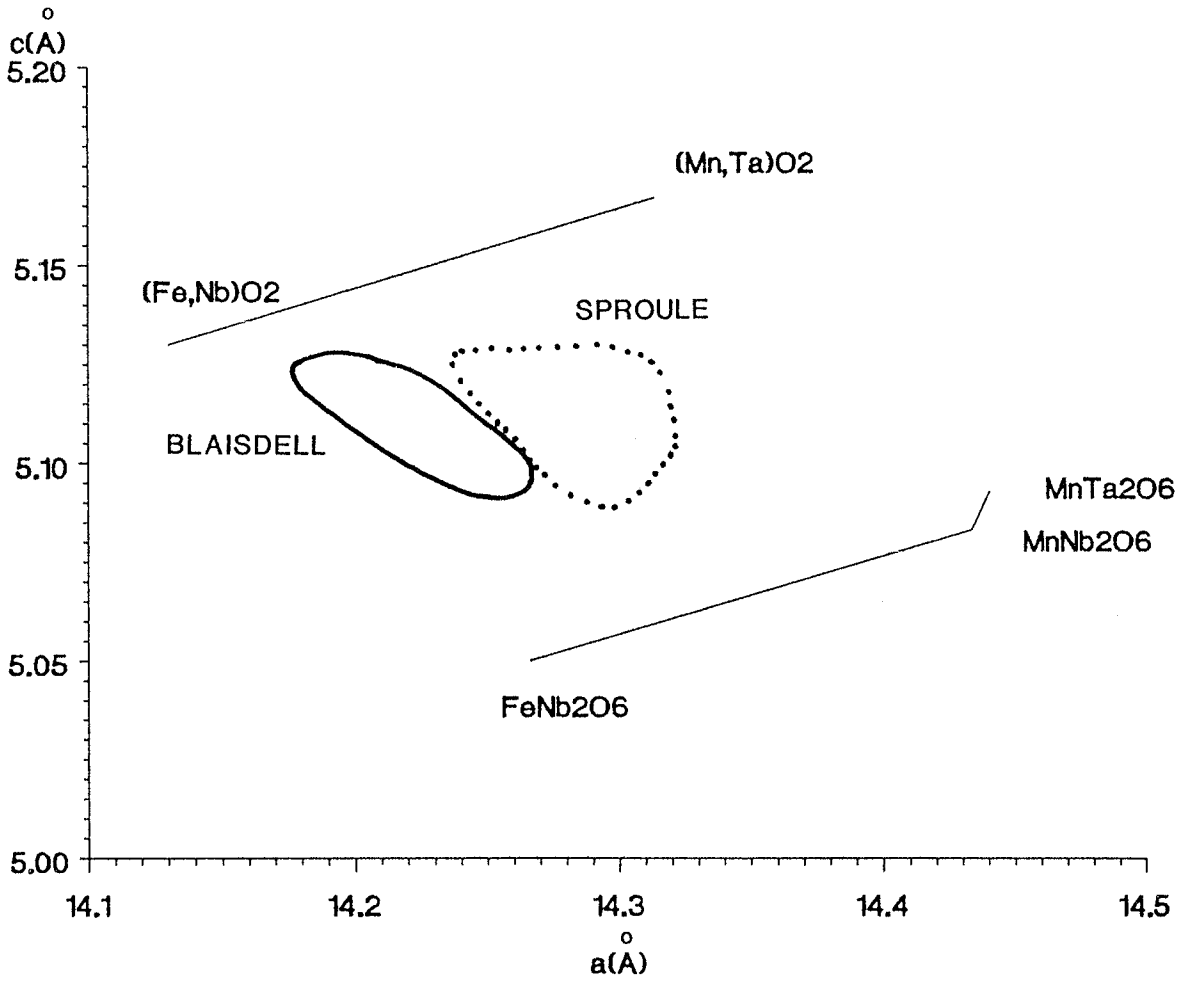

Figure 117: The a-c plot illustrating the structural state of columbite-tantalites from the Blaisdell Lake pegmatite group and Sproule Lake series.

Sproule Lake series represents the extreme margin of a pegmatite group extending from the Wedge Granite.

The structural state of the minerals from this series is slightly different from those found in the Blaisdell Lake group, showing predominantly intermediate degrees of order, but also with high degrees of order (Figure 117). Structural state is not correlated with Ta contents, as evidenced by the intermediate degrees of order in Ta-rich species compared to the Ta-poorer samples showing lower degrees of order by the Blaisdell Lake group.

The Sparrow-Thompson-Hidden pegmatite group is characterized by columbite-tantalite compositions which plot within the ferrocolumbite field of the columbite quadrilateral (Figure 118). Locally, cassiterite and ferrotapiolite are present. Restricted Mn/(Mn + Fe) ratios are accompanied by steep increases in the Ta/(Ta + Nb) ratio with increasing pegmatite fractionation; this seems to increase eastward from the Sparrow/Cameron granite plutons and northward from the southern shores of Thompson Lake for approximately 4 km.

Structurally, columbite-tantalite shows highly variable degrees of order (Figure 119), typically ranging from intermediate to low. Order generally decreases in pegmatites from south of Thompson Lake northward, and increases eastward from the Sparrow/Cameron plutons.

Restricted ranges of the Mn/(Mn + Fe) ratios and steeply increasing Ta/(Ta + Nb) ratios are typical of the Reid Lake series (Figure 120). Compositions are predominantly ferrocolumbite with minor ferrotantalite. Structural data show variable degrees of order-disorder, extending from fully disordered to nearly ordered (Figure 121). Order decreases with increasing distance from the Cameron Granite.

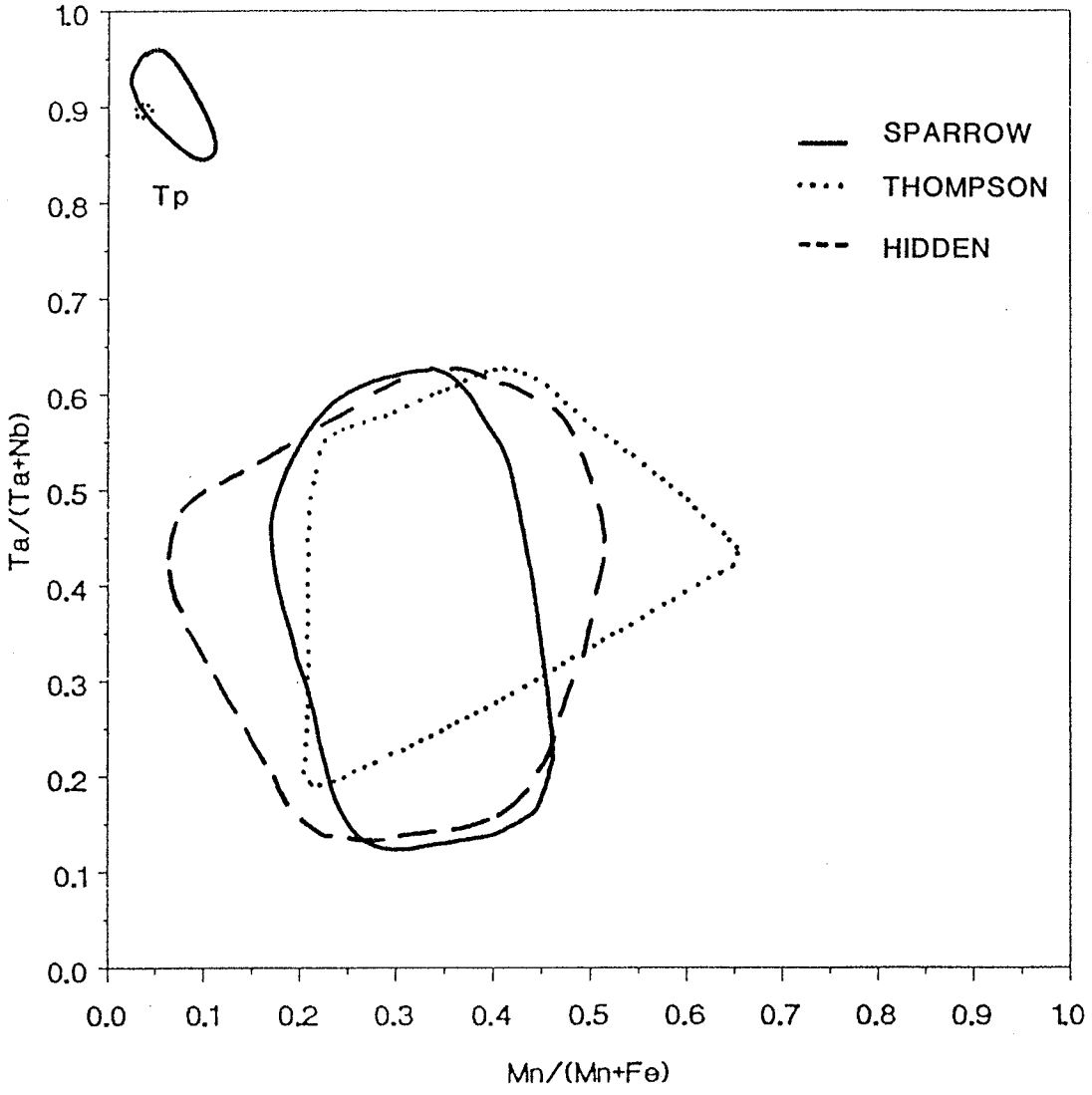

Figure 118: Chemistry of Nb,Ta-oxide minerals from the Sparrow-Thompson-Hidden Lakes group.

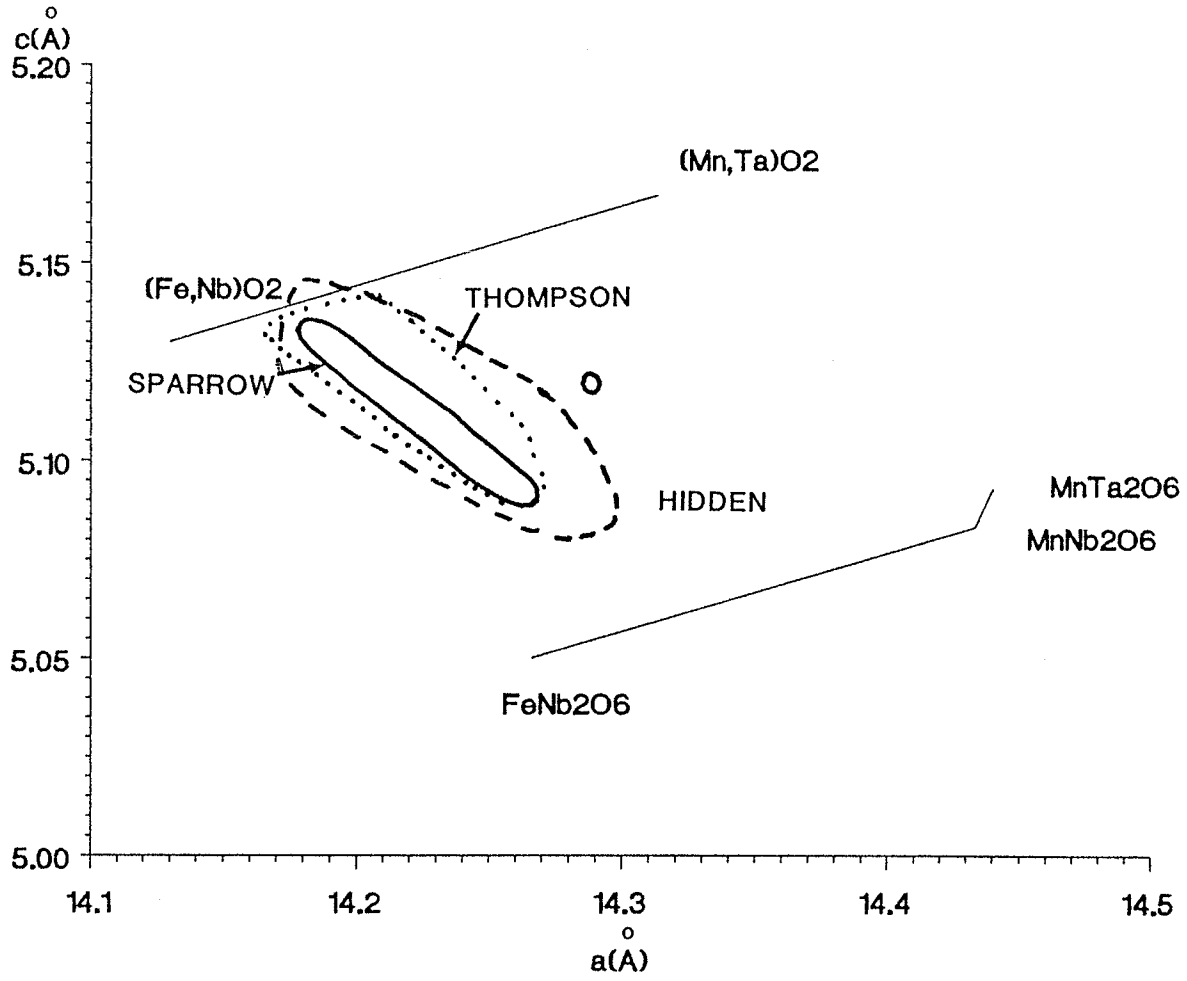

Figure 119: The a-c plot illustrating the structural state of the columbite-tantalites from the Sparrow-Thompson-Hidden Lakes group.

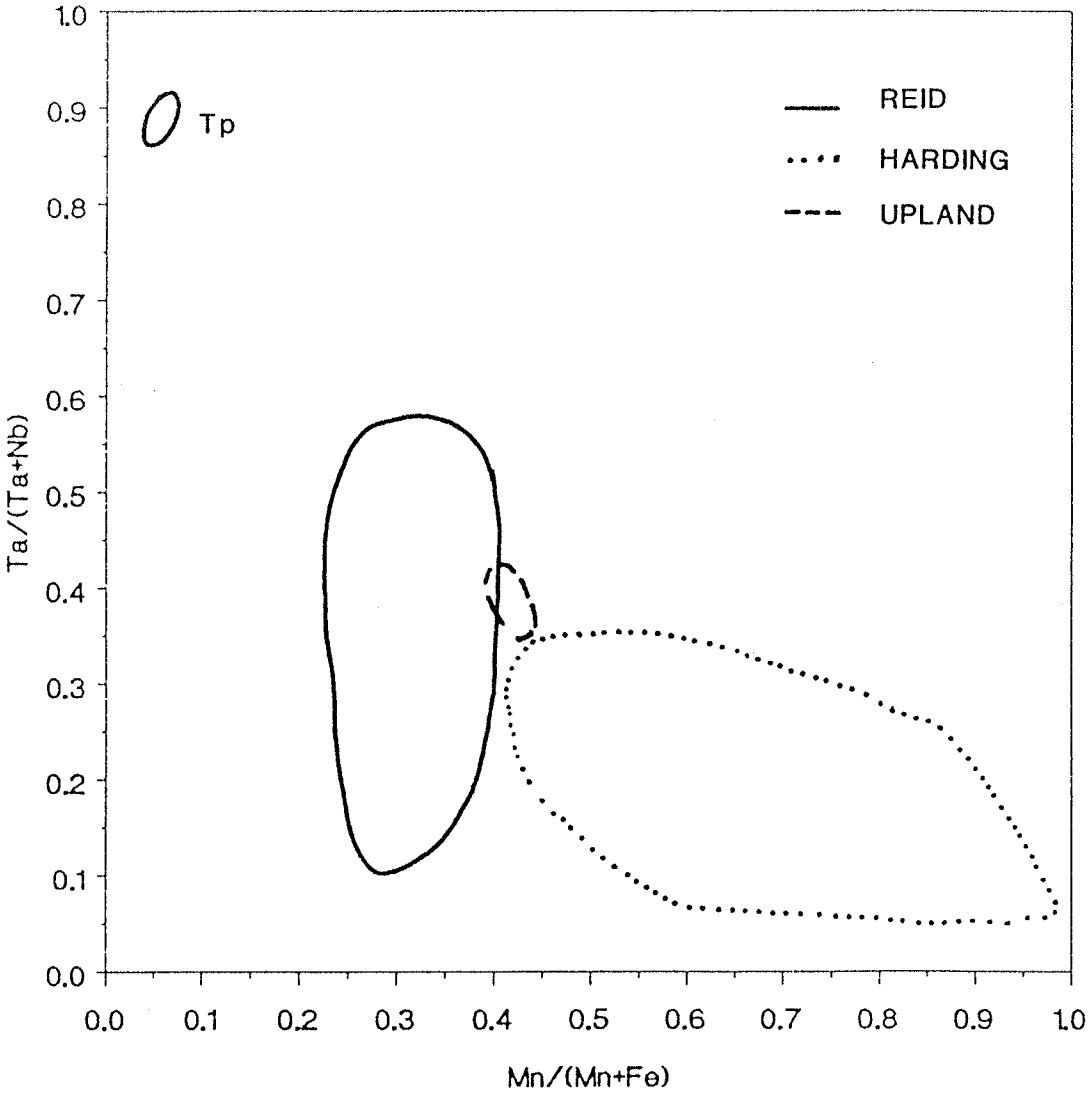

Figure 120: Chemistry of Nb,Ta-oxide minerals from the Reid Lake and Harding Lake pegmatite series.

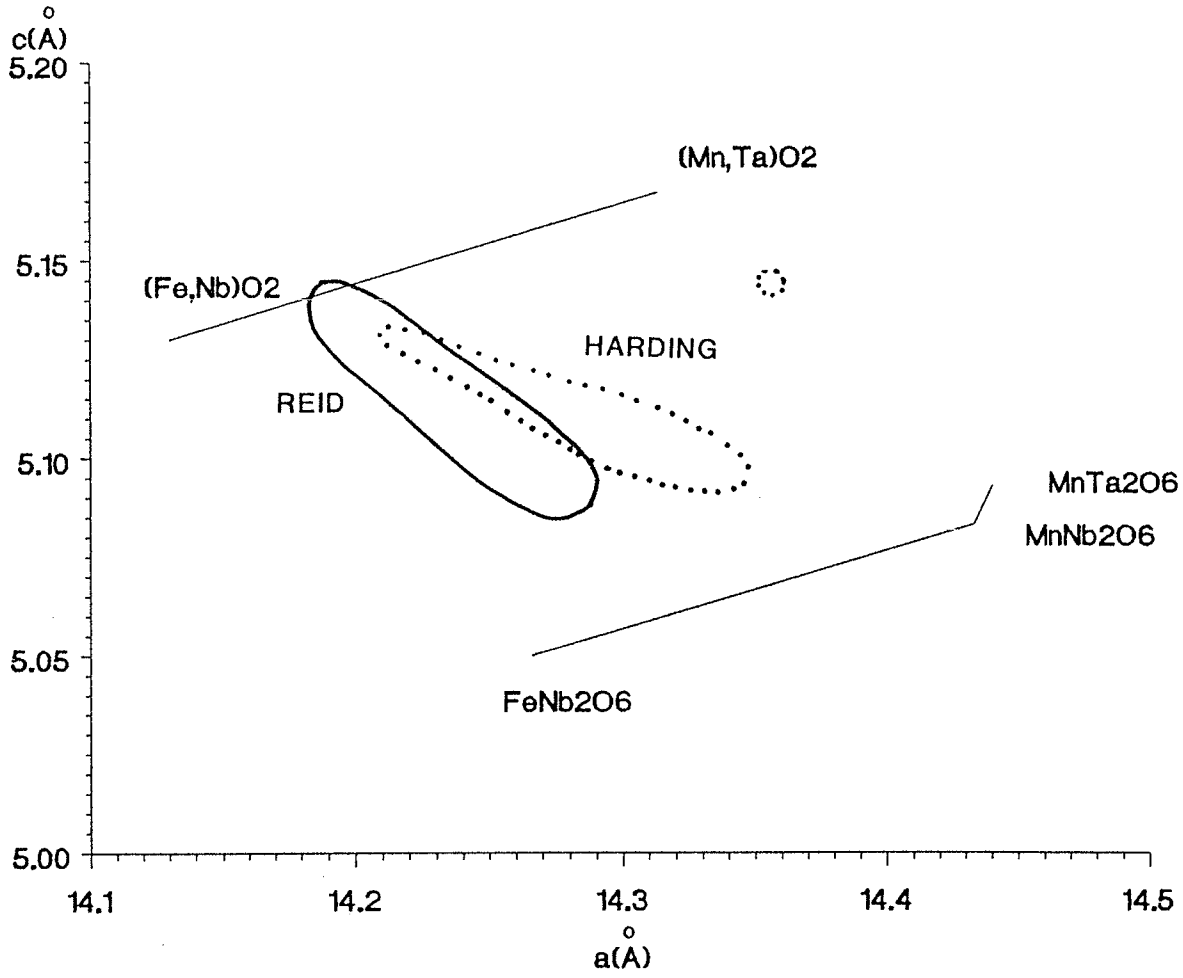

Figure 121: The a-c plot illustrating the structural state of columbite-tantalites from the Reid Lake and Harding Lake pegmatite series.

Columbite-tantalites from the Harding Lake series are characterized by high Nb contents and extreme Mn fractionation. Moderate ranges of Mn/(Mn + Fe) and Ta/(Ta + Nb) ratios are typical of the Jake-Da swarm but not of the Paint and Sky pegmatites (Figure 120). The high Mn but low Ta fractionation contrasts sharply with the pegmatite series to the north. The distinct difference in composition suggests that these pegmatites may not be genetically related to the pegmatites of the Sparrow-Thompson-Hidden group or Reid Lakes series.

An extensive range of order-disorder is typical of the Harding Lake series columbite-tantalites, varying from highly disordered specimens from the Jake-Da swarm to the nearly ordered Paint samples (Figure 121). Degrees of order-disorder seem to be crudely related to the distance from the Defeat Granodiorite, with order decreasing further away from the pluton.

The Bighill Lake group shows widely variable Ta/(Ta + Nb) and moderately limited Mn/(Mn + Fe) ratios (Figure 122). Compositions grade imperceptibly from ferrocolumbite into stannian ixiolite which seems to represent the culmination of Ta fractionation in this group. The typical NW-SE order-disorder trend of columbite-tantalites is not apparent in this series, but may simply be the result of scarcity of samples. Columbite-tantalites of this series all show moderate degrees of disorder (Figure 123).

Adequate characterization of the Circle Lake pegmatite series is not possible at present, due to the scarcity of pegmatites bearing Nb-, and Ta-oxide minerals. As a result, the majority of columbite-tantalite data for this series is represented by the highly evolved and well-zoned Riber

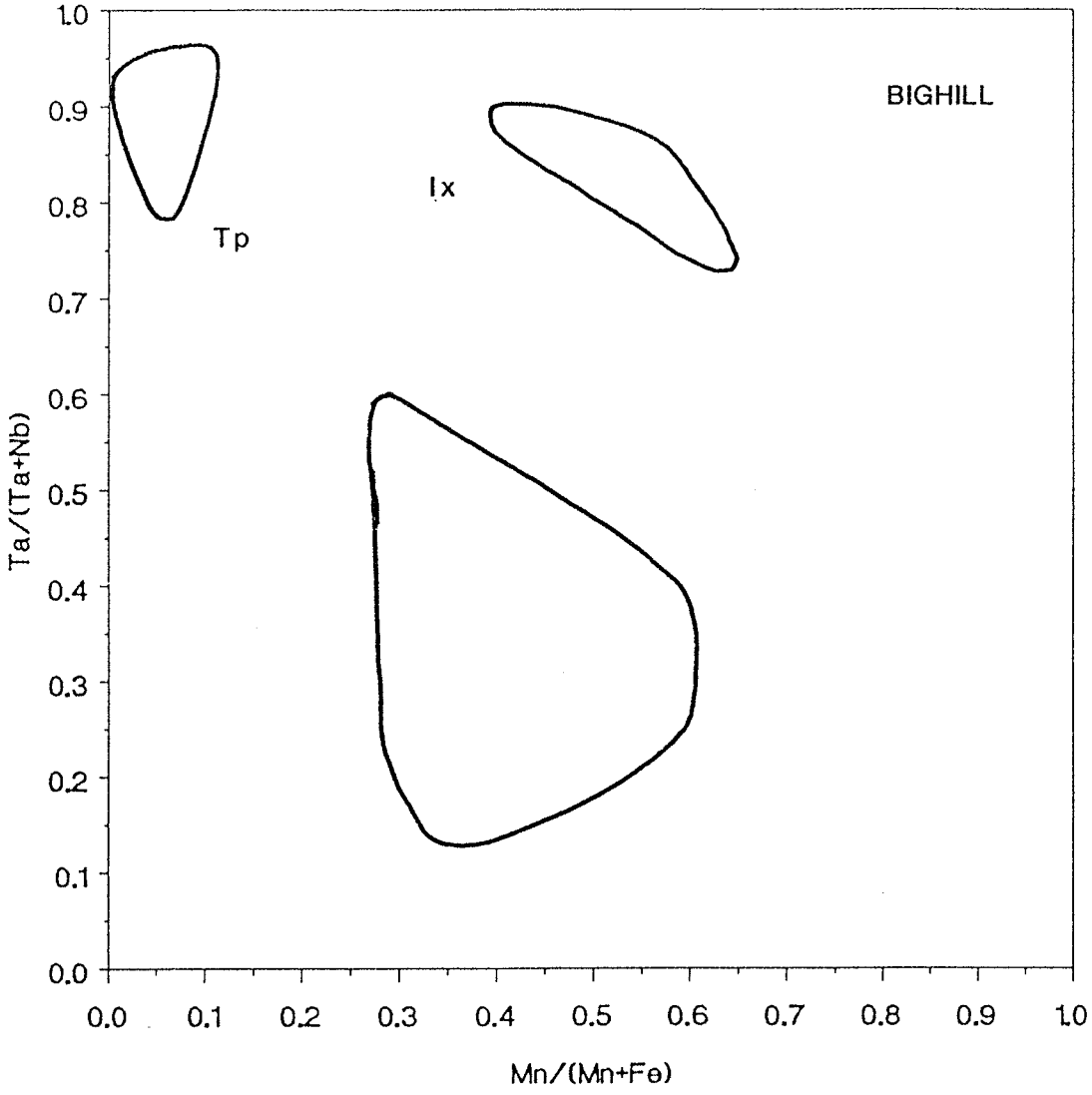

Figure 122: Chemistry of Nb,Ta-oxide minerals from the Bighill Lake pegmatite group.

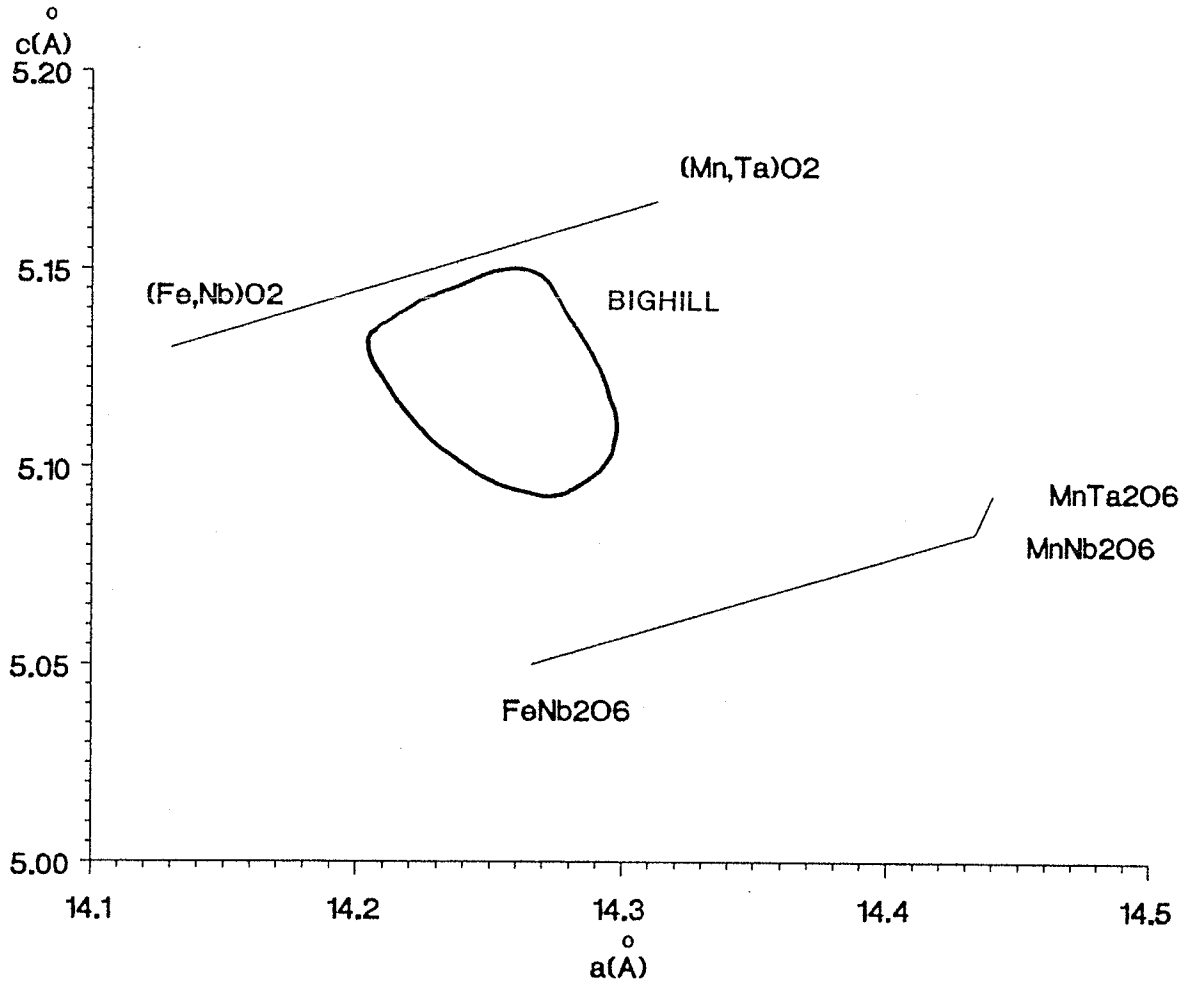

Figure 123: The a-c plot illustrating the structural state of columbite-tantalites from the Bighill Lake pegmatite group.

pegmatite. A single ferrotantalite analysis from the Dr. Bob pegmatite represents the only other columbite-tantalite data available for this series (Figure 124). Mn/(Mn + Fe) ratios are variable with Mn generally greater than Fe (Figure 124). The fractionation of Nb/Ta and Fe/Mn proceeds normally, i.e. increasing Ta/Nb with increasing Mn/Fe, with a reversal in the Nb-Ta fractionation occurring in the later stages of the Riber pegmatite consolidation.

The structural state of columbite-tantalite from the Riber pegmatite has been discussed previously. However, it is appropriate to re-emphasize the extreme variation in order-disorder (Figure 125). In comparison to the Bighill Lake group, the order-disorder variation of columbite-tantalite in the Riber pegmatite is obviously controlled by the crystallization history of the pegmatite, whereas the observed variations of the Bighill Lake group may be controlled by their spatial relationship to the Prosperous Granite. It is unlikely that the Riber pegmatite is related to pegmatites from these series owing to their distinct differences in chemistry and widely disparate structural degrees.

Chemical and structural variations in the pegmatite field

The Yellowknife pegmatite field consists of numerous pegmatites belonging to the barren, beryl + columbite and complex spodumene subtypes of the rare-element class of orogenic association. These pegmatites contain abundant minerals of the columbite-tantalite group, as well as ferrotapiolite, ixiolite, cassiterite and microlite.

The overall chemical signature of the entire pegmatite field shows an enrichment in Fe and Nb, with local enrichment in Mn, Ta, Sn and Ti. The

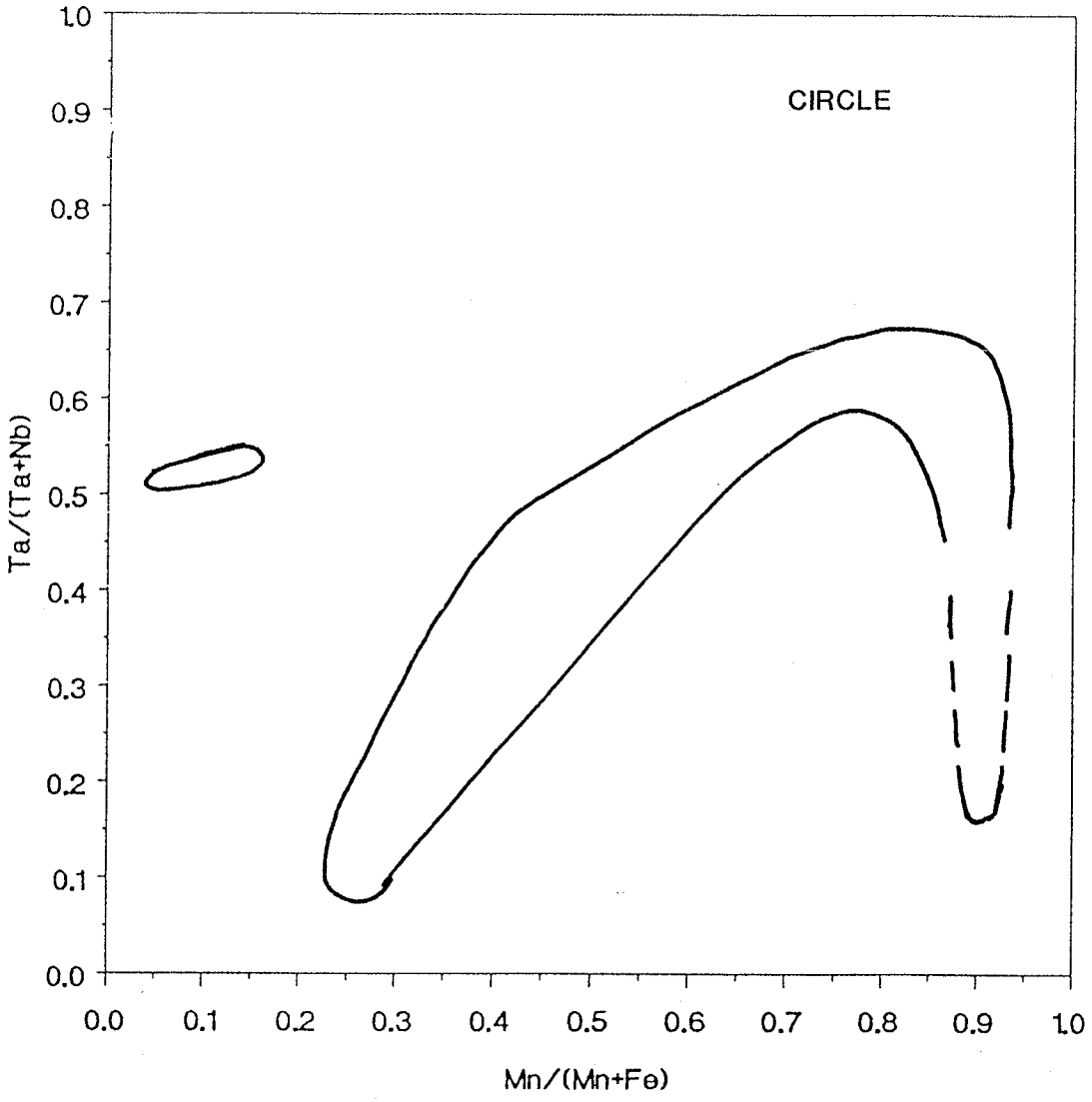

Figure 124: Chemistry of Nb,Ta-oxide minerals from the Circle Lake pegmatite series.

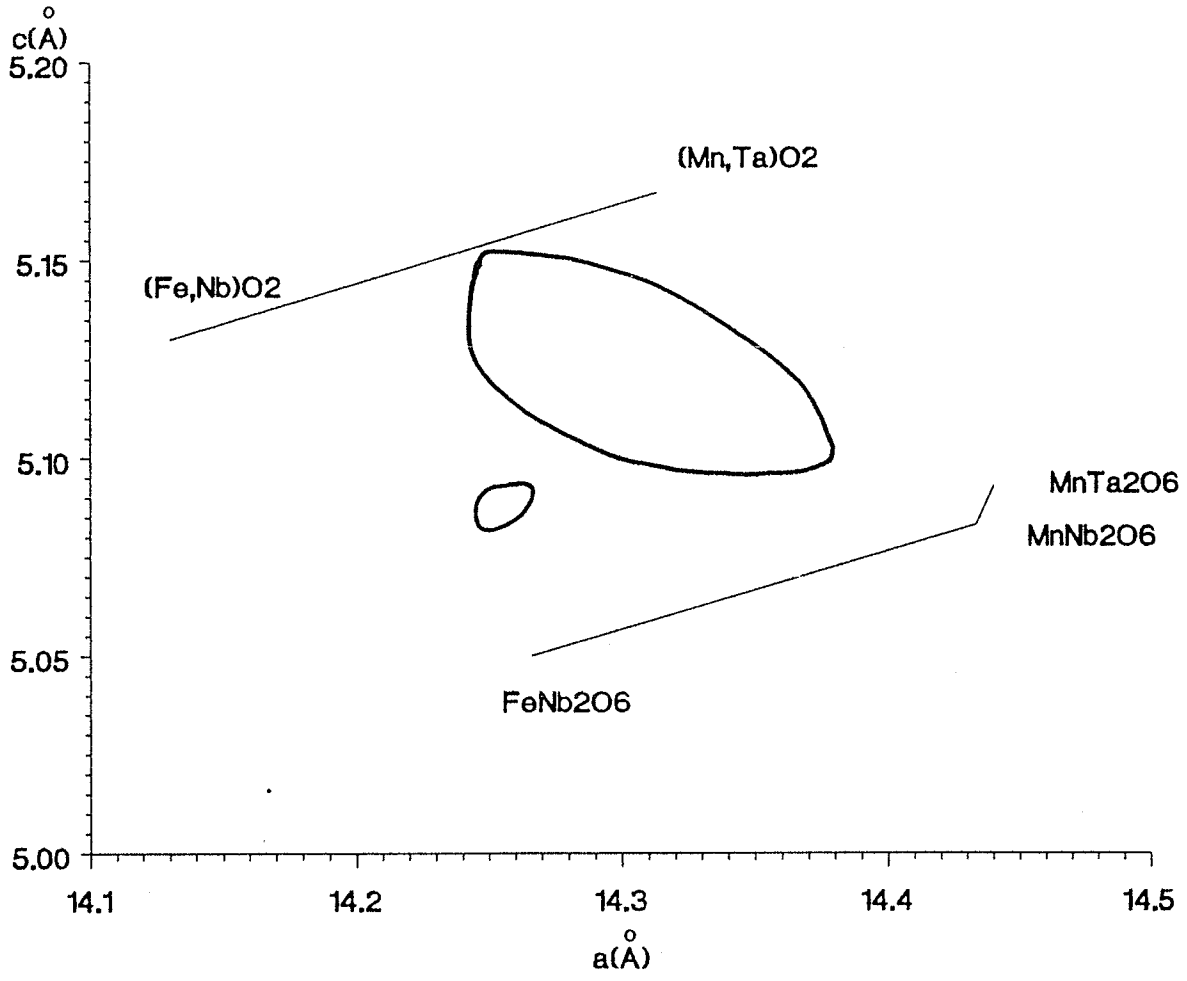

Figure 125: The a-c plot illustrating the structural state of columbite-tantalites from the Riber pegmatite (Circle Lake series).

fractionation of Mn is generally low with the exception of the Riber pegmatite and the Harding Lake pegmatite series. The compositional data collected for the field populates the Fe-rich half of the quadrilateral (Figure 126). The majority of Mn/(Mn + Fe) ratios fall within a restricted range (0.05 - 0.45), although local enrichment expands this range to a maximum of 0.88.

Nb/Ta fractionation in the field is extensive; Ta/(Ta + Nb) ratios range from 0.10 - 0.97. The extreme enrichment in Ta is documented by the progressive crystallization of Ta-rich mineral species which commonly proceeds from ferrocolumbite to ferrotantalite, ferrotapiolite and ixiolite. The degree of Ta fractionation is erratic across the field, and as in the case of Mn, extreme Ta enrichment is restricted to small areas (Buckham, Circle and Bighill groups). Locally, Ta fractionation proceeds to the extent that abundant ferrotapiolite crystallizes (Peg swarm).

The accumulation of Ti, Fe^{3+} and Sn in Nb- and Ta-oxide minerals is conspicuously low for most of the pegmatite series, but local enrichment is observed (Table 31). Areas of Ti enrichment include the Blaisdell Lake group, the Waco swarm and the Dr. Bob pegmatite. Significant Ti enrichment also occurs in the pegmatites of the Peg swarm. In these pegmatites, columbite-tantalite, ferrotapiolite and cassiterite are all enriched in Ti relative to the remainder of the pegmatites of the field. Calculated Fe_2O_3 contents in columbite-tantalite for the field show a maximum value of 4.3 % occurring in the Tanco Lake group; however, average abundances in columbite-tantalites of the Peg swarm, Dr. Bob and Bill pegmatites indicate that they are more enriched in Fe^{3+} than the other dikes of the field. Enrichment in Sn is generally restricted to pegmatites in the southeastern

area and in the vicinity of Sproule, Sparrow, Thompson and Hidden Lakes where abundant cassiterite is found. A second isolated area of Sn and Ta enrichment occurs in the Bighill Lake group, south of Prosperous Lake, where stannian ixiolite is common.

Columbite-tantalite and ferrotapiolite typically show intermediate degrees of order (Figure 127). Although the ranges of order may differ significantly among individual pegmatites or pegmatite swarms, there is only moderate variation in the average degree of order from series to series across the field.

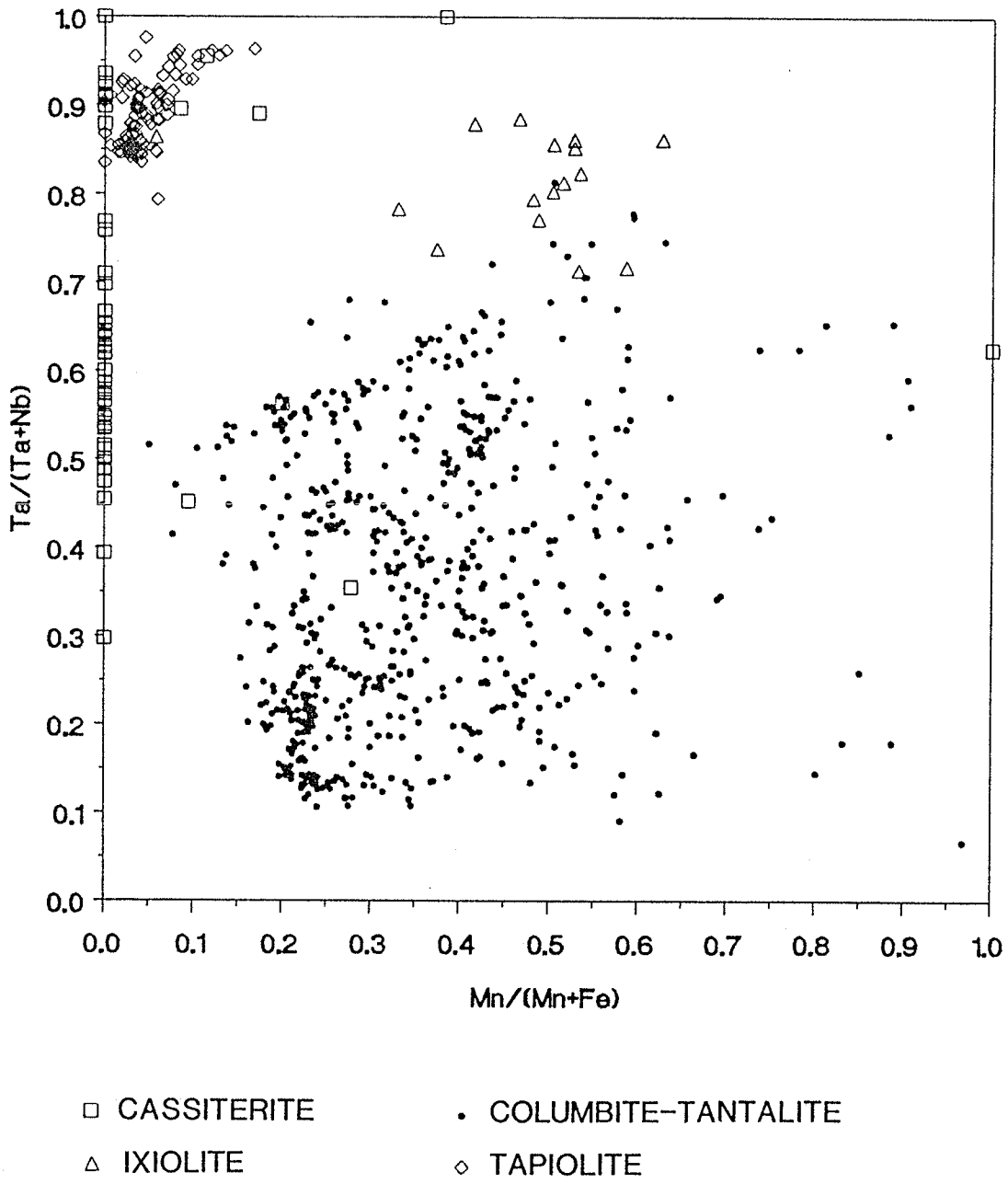

Figure 126: Columbite-tantalite, tapiolite and cassiterite compositions plotted on the columbite quadrilateral of the Yellowknife pegmatite field.

Table 31: Average abundances of minor elements in columbite-tantalites of the Yellowknife pegmatite field.

Pegmatites	n	TiO_2	SnO_2	Fe_2O_3
Ann	38	0.29	0.15	0.30
Bet	23	0.41	0.30	0.59
Big	30	0.40	0.10	0.74
Bill	44	1.24	0.16	1.10
Casper	28	0.39	0.11	0.81
Cata	8	0.16	0.33	0.28
Dr. Bob	2	0.93	0.77	1.19
Fi	11	0.29	0.23	0.26
Fly	7	0.15	0.17	0.15
Freda	6	0.06	0.34	0.01
Greg	1	0.16	0.17	0.34
Heidi	9	0.73	0.16	0.53
Jake	19	0.56	0.03	0.62
Jo	1	0.65	0.00	0.00
Limo	4	0.42	0.27	0.59
Lit	10	0.20	0.21	0.27
Lu	48	0.11	0.24	0.18
Mac	20	0.55	0.88	0.13
Melody	12	0.76	0.05	0.42
Mint	3	0.22	0.25	0.03
Moose	82	0.47	0.16	0.25
Murky	4	0.10	0.10	0.60
Nite	5	0.20	0.53	0.45
Odin	4	0.12	0.04	0.09
Paint	3	0.44	0.00	0.29
Peg	159	0.67	0.06	1.03
Pancho Villa	11	0.46	0.29	0.49
Qi	1	0.00	0.00	0.00
Riber	20	0.54	0.14	0.52
Tan	7	0.87	0.36	0.28
Thor-Echo	51	0.40	0.10	0.65
Tom	3	0.11	0.00	0.50
Usk	16	0.21	0.13	0.72
Vo	21	1.33	0.29	0.69
Waco	32	1.28	0.49	0.43

n = number of analyses.

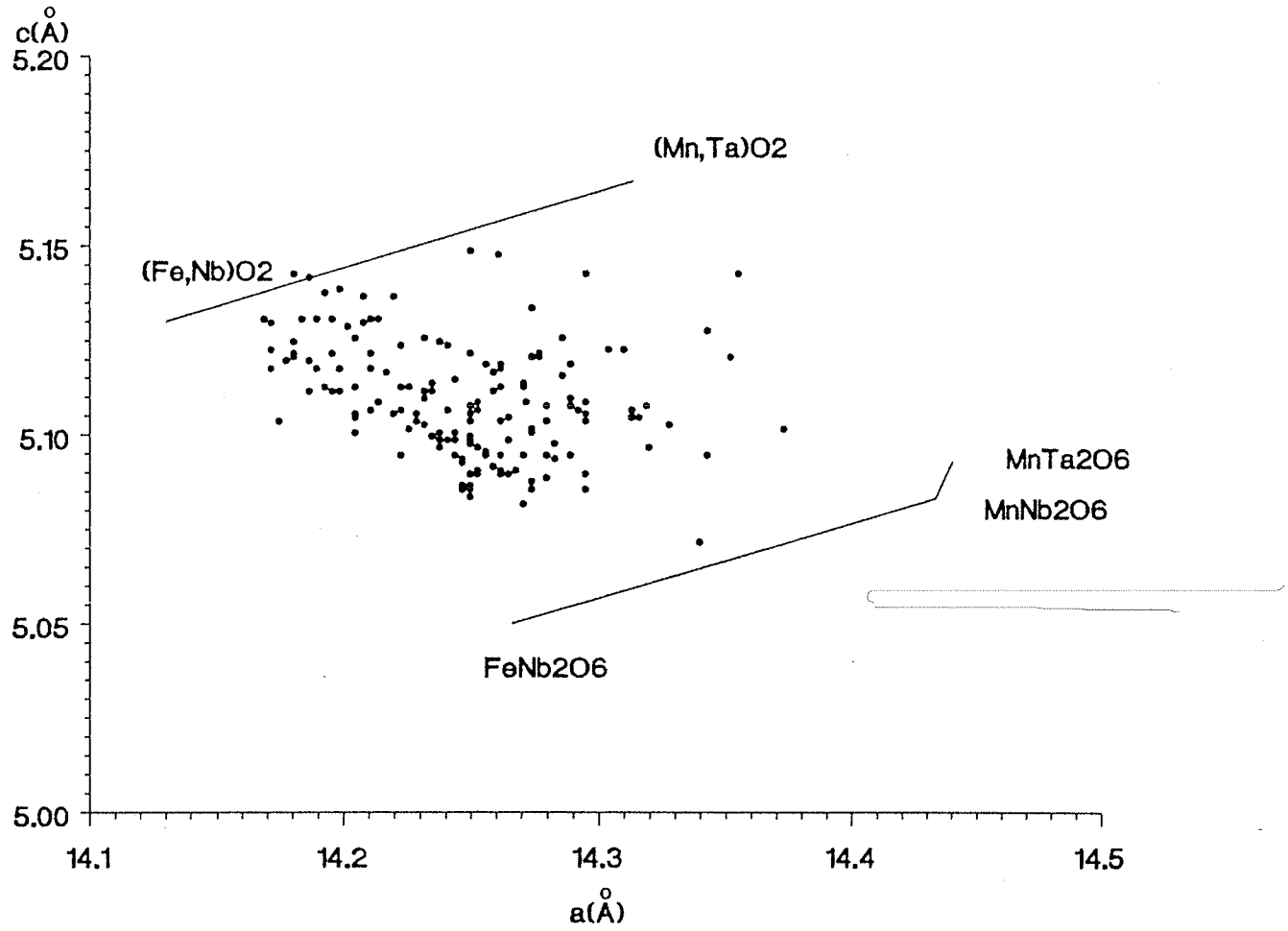

Figure 127: The a-c plot illustrating the structural state of columbite-tantalites from the Yellowknife pegmatite field.

CHAPTER 13

Discussion

In the following sections, geochemically and petrochemically important aspects of the present study are examined, as they apply to the pegmatite, series/group and/or field scale of interpretation.

Columbite-tantalite in saccharoidal albite units

Much of the attention concerning columbite-tantalite from the Yellowknife pegmatite field has been focused on specimens occurring in coarse-grained primary units and zones. However, on the worldwide scale of economic pegmatite deposits, Nb-, and Ta-oxide minerals are concentrated mainly in late units of saccharoidal albite, commonly showing advanced fractionation levels relative to the early generations (Černý, 1982a; Černý, 1987).

In the Yellowknife field, local units of saccharoidal albite are found in many of the pegmatites of the southeastern region and in a few pegmatites scattered across the remainder of the field. The saccharoidal albite bodies which carry Nb-Ta mineralization are restricted primarily to the pegmatites of the beryl-columbite and complex spodumene subtypes. Nb-Ta mineralization in saccharoidal albite bodies is characterized by the presence of columbite-tantalite group minerals and rare ferrotapiolite and microlite. Columbite-tantalite commonly occurs as black, fine-grained euhedral to subhedral bladed crystals, typically less than 1 mm long. Most are homogeneous, although some do contain ferrotapiolite and microlite inclusions.

The compositions of columbite-tantalite from saccharoidal albite units extend over much of the same ranges as columbite-tantalite in other units (Figure 128a). Individual crystals generally show restricted Mn/(Mn + Fe) ratios with more extensive Ta/(Ta + Nb) ratios, varying from 0.20 to 0.70 and 0.14 to 0.75, respectively. Concentrations of Ti and Sn are the same order of magnitude as in the primary units.

Within individual pegmatites, columbite-tantalite from saccharoidal albite shows extremely variable degrees of fractionation compared to other units of the pegmatite. Locally, columbite-tantalite from saccharoidal albite units shows advanced Mn fractionation with uniform Ta/Nb ratios compared to intermediate zones, whereas in other cases, Ta fractionation is more advanced in the saccharoidal albite unit than in the intermediate zones (Figure 128b). In the Peanut pegmatites, Ta fractionation is more advanced in the saccharoidal albite unit relative to the intermdeiate zone, whereas columbite-tantalite from saccharoidal albite of the Casper "I" pegmatite shows a lesser degree of Ta fractionation relative to columbite-tantalite from the intermediate zone. Columbite-tantalites from saccharoidal albite of the West, Ann and Odin "B" pegmatites are notably Mn-poorer than those from other zones. In contrast, columbite-tantalite from the saccharoidal albite unit of the Fly pegmatite is significantly Mn-richer than columbite-tantalite from its primary zones, whereas columbite-tantalite from the intermediate zone and saccharoidal albite units of the Moose and Big pegmatites show near identical Mn/(Mn + Fe) and Ta/(Ta + Nb) ratios.

The extremely variable chemistry of these samples suggests that the saccharoidal albite units were derived from localized fluids of the solidifying pegmatite melt in a non-systematic manner across the field. As a

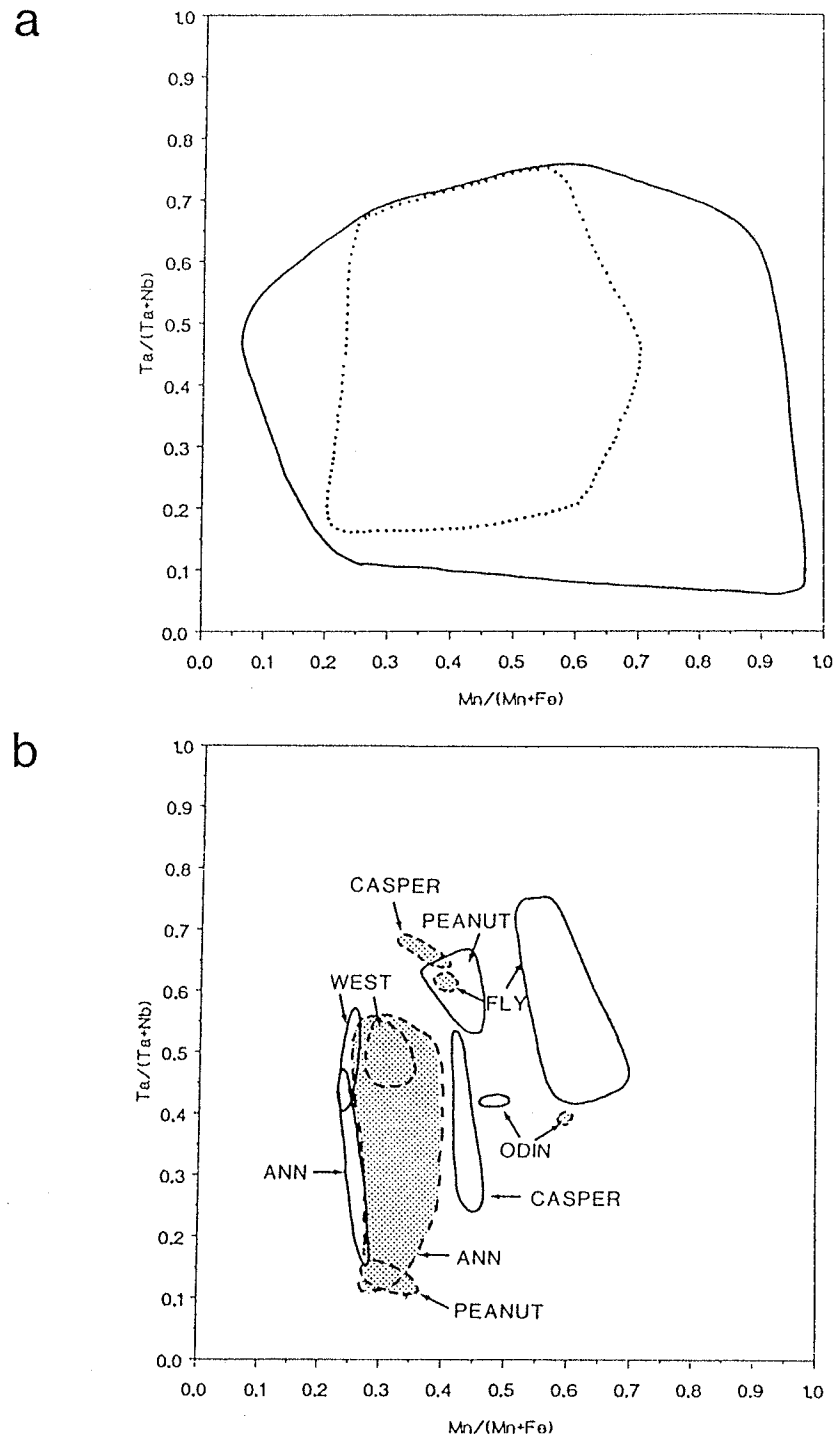

Figure 128: Compositional fields for columbite-tantalite associated with saccharoidal albite. (a) Solid line defines the compositional boundary of all Yellowknife columbite-tantalite, exclusive of saccharoidal albite association. Dotted line outlines the compositions of saccharoidal albite-associated columbite-tantalite. (b) Compositional fields for columbite-tantalite from primary zones (dotted pattern) and saccharoidal albite units (open) of selected Yellowknife pegmatites.

gross generalization, these fluids were locally more fractionated than previously consolidated zones; however, some of the columbite-tantalite compositions are suggestive of origin pre-dating or consanguineous with other primary zones.

Fractionation of Fe/Mn

The fractionation of Fe/Mn is not well understood in granite magma systems. Volatile transfer in granitic magma chambers (Shaw, 1974; Hildreth, 1979,1981) and Mn-F complexes (Shawe, 1968; Bailey, 1977) have been proposed to explain the separation of Mn from Fe.

During progressive pegmatite fractionation, the Fe/Mn ratio gradually decreases as Fe accumulates in the early formed mineral phases. Fractionation may proceed to the point where Fe is virtually exhausted from the melt, leaving the residual melt Mn-enriched. The extreme fractionation of Mn is typically associated with F-rich lepidolite- and microlite-bearing zones. The accessory mineralogy of these zones typically includes manganocolumbite, manganotantalite, Mn-rich wodginite, spessartine, lithiophilite and other Mn-rich phosphates, all with very low Fe/Mn ratios (Černý et al., 1985a; Černý and Ercit, 1985). The conspicuous association of Mn-rich minerals with F-rich lepidolite- and microlite-bearing zones seems to support the conclusion proposed by Shawe (1968) and Bailey (1977) that Mn may preferentially form complexes with F in granitic magmas.

The influence of F on the fractionation of Mn was demonstrated by the evolution of Nb- and Ta-oxide minerals from the Greer Lake pegmatitic granite and its pegmatite aureole (Černý et al., 1986b). In the primitive potassic pegmatite phases of the pegmatitic granite and of the less frac-

tionated pegmatites, ferrocolumbite, and ferrotantalite with Mn/(Mn + Fe) < 0.5, occur with rare ferroan ixiolite. Localized pegmatititc pods within the Greer Lake granite and its related pegmatites carry Li,Rb,Cs and F-rich assemblages which contain manganotantalite and Mn-rich wodginite.

The strong tendency for Mn to selectively accumulate in F-rich lepidolite zones has also been observed at other pegmatite localities. The beryl-columbite-type Plex pegmatite, Baffin Island, N.W.T., contains ferrocolumbite in its quartz core, evolving to manganocolumbite in late pods of Li- and F-enriched muscovites (Černý and Ercit, 1985). Samples collected from the lepidolite-type Himalaya dike system of southern California show extreme manganocolumbite compositions (Foord, 1976). Manganotantalite and Mn-rich wodginite occur in the Li,Rb,Cs,Be,Ta,F-rich Tanco pegmatite (Ercit, 1986). In contrast, the F-poor Lower Tanco pegmatite which underlies the Tanco body lacks significant lepidolite and carries columbite-tantalite with significantly higher Fe/Mn ratios (Ferreira, 1984).

One of the more conspicuous characteristics of columbite-tantalite from the Yellowknife field is its notable enrichment in Fe relative to Mn. On the whole, extreme Mn fractionation is not observed in the pegmatites of the Yellowknife field, although areas of local Mn enrichment do occur. Columbite-tantalite from the Riber pegmatite and pegmatites of the Harding Lake series all show more advanced Mn fractionation than columbite-tantalite occurring elsewhere in the field.

Manganese enrichment in the Riber pegmatite.

The Riber pegmatite is of the complex amblygonite subtype and contains abundant elbaite in addition to rare lepidolite and microlite. The development of Nb- and Ta-oxides from this pegmatite follows the general evolutionary path of concomitantly increasing Mn and Ta:

(i) Ferrocolumbite grading into ferroan manganotantalite and manganocolumbite occurs in the third intermediate zone, which also contains lepidolite, apatite and microlite. Ferrocolumbite crystallizes with what seems to be the earliest assemblage of this zone, an assemblage which contains schorl, zircon and lithian muscovite. The mineralogy of this most primitive assemblage of the third intermediate zone attests to a relatively low level of F enrichment.

(ii) A later assemblage of the third intermediate zone marks a notable increase in F activity. Schorl grades into elbaite and is associated with beryl, apatite and the first seemance of lepidolite.

(iii) The Nb-Ta mineralization of the fourth intermediate zone occurs predominantly in Li- and F-rich assemblages which carry manganotantalite with rare manganocolumbite and microlite. This zone also hosts elbaite, beryl, lepidolite and the only occurrence of amblygonite from the entire field.

Manganese enrichment in the Harding Lake Series.

The Mn enrichment observed in the pegmatites of the Harding Lake series is more difficult to explain. In two separate visits to the Jake-Da and Paint pegmatites, extensive sampling failed to produce mineral species which would suggest high F activity. Micas are virtually absent in these pegmatites and although amblygonite was reported by Groves (1980) and Stacey (1981a), none was found by the author. Montebrasite is widespread in the field (Wise et al., 1987), and the presence of amblygonite is suspect. With regard to other carriers of F in these pegmatites, only apatite is found in accessory quantites, but is absent in the Sky pegmatite, rare in the Paint pegmatite and only marginally abundant in the Jake-Da pegmatite.

The probable absence of amblygonite and the lack of significant Li- and F-enriched micas in these pegmatites leads me to speculate that some other mechanism may be responsible for the prominent Mn enrichment shown by these pegmatites. Triphylite occurs as the principal Fe-dominant mineral phase, and although a green variety of spodumene contains considerable quantities of Fe (up to 1.37 wt. % Fe_2O_3), the partitioning behavior of Fe between coexisting columbite-tantalite and triphylite or spodumene is unknown.

The possibility of contamination of the pegmatite magma by possible passage through Mn-enriched lithologies should also be considered; however, this too seems unlikely. The pegmatites of the Harding Lake series are hosted by the Defeat ganodiorite, evidently emplaced along a pre-existing fracture system. Chemical analyses of this pluton show no indication of Mn enrichment (R.E. Meintzer, pers. comm.), nor does the pegmatite contain any xenoliths of granodiorite or the underlying metamorphic rocks that might suggest the presence of Mn-enriched rocks.

Fractionation of Nb/Ta

The fractionation of Nb/Ta during pegmatite evolution is well-documented in many pegmatites, but the processes responsible for Nb,Ta fractionation remains unclear (Černý et al., 1985a; Černý and Ercit, 1985). Wang et al. (1982) suggested that differences in the relative thermal stabilites of F-based Nb,Ta complexes may be the principal factor determining the separation of Nb and Ta. The Ta- and F-bearing complexes are generally stable to lower temperatures than is the case for Nb- and F-complexes, and thus Nb is removed from the system at higher temperature regimes in the early stages of pegmatite consolidation.

The pronounced trend of Ta enrichment with progressive pegmatite fractionation can occur with equal ease in most pegmatite environments (Černý and Ercit, 1985). F-poor magmas are just as capable of crystallizing Ta-dominant mineral species as highly fractionated Li and F-rich melts. However, it is only in the latter case that the highest levels of Ta accumulation is attained. The geochemically primitive beryl-columbite type Plex pegmatite of Baffin Island, N.W.T., for example, carries ferrocolumbite, locally evolving to manganocolumbite in Li,F-enriched muscovite pods (Černý and Ercit, 1985). In contrast, the cogenetic Tanco and Lower Tanco pegmatites provide even stronger evidence for F-induced Nb/Ta fractionation.

The Li,Rb,Cs-enriched Lower Tanco body is notably poor in F-rich mineral assemblages, and is considerably less-fractionated than the Tanco deposit which overlies it. The Nb-Ta mineralization of the Lower Tanco body is characterized by ixiolite and manganocolumbite-manganotantalite (Ferreira, 1984). Tapiolite, wodginite and microlite are extremely rare. In contrast, the highly fractionated Li,Rb,Cs,,Be,Ta,F,P-rich Tanco deposit displays a great diversity of Ta-dominant mineral species, including manganotantalite, wodginite, Nb-poor ferrotapiolite, several species of microlite (including cesstibtantite and Sb,Sn,U and Pb-enriched microlites) and simpsonite (Ercit, 1986).

Extensive Nb/Ta fractionation in the Yellowknife field does not reach the level attained by the Tanco deposit; on the contrary, the bulk of Nb,Ta mineral compositions in the Yellowknife field is Nb-enriched. However, in some areas of the field, Nb/Ta fractionation does progress to the point of significant Ta enrichment.

Although ixiolite is common in some pegmatites of the Buckham and Bighill Lake groups, ferrotapiolite is the most common Ta-dominant mineral species present in the field, with notable concentrations occurring in the Peg swarm, Tan swarm and the Bighill group. Most of these pegmatites are generally low in F. On the other hand, the F-enriched Riber pegmatite contains appreciable manganotantalite, microlite and uranmicrolite.

Regional variation of Mn and Ta

The mobility of Mn and Ta in granitic magmas depends to a large degree on the relative thermal stabilities of their complexes and their affinity for transport in a hydrous phase by volatile components. This transport typically operates during the differentiation of the magma and is enhanced by the upward diffusion of H_2O and other volatile components through the melt from the solidifying magma chamber (Hildreth, 1981). Typically, Mn and Ta tend to accumulate in the hydrous phase of the pegmatite melt and are then transported away from the granitic source. They become enriched in thermally stable, fluid and mobile fractionated melts, enriched in H_2O, B and F (Černý, 1987). Thus, an increase in Mn and Ta concentrations away from the granite pluton is expected in cogenetic granite-pegmatite associations. This relationship is observed in some areas of the Yellowknife field; however, most of the trends are ill-defined.

The best example of increasing Mn and Ta contents away from a pluton, occurs in the Blaisdell Lake series. Increasing Mn and Ta with increasing distance from the Wedge granite is conspicuous (Figure 129). In contrast, in the pegmatites of the Peg swarm, the Mn/(Mn + Fe) ratio varies from 0.16 in the principally barren pegmatites of zone 1, to 0.45 in the spodumene-

bearing zone 5, but the Ta/(Ta + Nb) ratios of columbite-tantalite bearing pegmatites show a very erratic progression across the area (Figure 130).

The Mn/(Mn + Fe) and Ta/(Ta + Nb) ratios in the pegmatites surrounding the Buckham granite indicate increasing Mn and Ta contents away from the pluton (Figure 131). In contrast, the pegmatites surrounding the Faulkner granodiorite intrusion show little variation in Ta and no variation at all in Mn contents away from the pluton. Farther east, two divergent SE-NW trends of increasing Mn and Ta is observed in the pegmatites situated in the aureole adjacent to the Eastern granite (Figure 132). On the other hand, the pegmatites surrounding the southernmost extension of the Prosperous granite show decreasing Mn/(Mn + Fe) ratios with increasing distance from the pluton, along with irregular Ta trends (Figure 133).

The distribution of Mn and Ta in the pegmatite aureole of the Cameron, Sparrow and Hidden plutons is very irregular. Trends of increasing Mn/(Mn + Fe) extend northward towards the Scott granite, westward towards the Sparrow granite and southward towards the Cameron pluton, each trend originating from a source near Thompson Lake (Figure 134). The Mn contours of the area show that an E-W trending Mn trough is present (Figure 135); the reason for this anomaly is not apparent. The pattern of Mn distribution may be affected by the effects of overlapping Mn migration from the Scott, Sparrow, Hidden and Cameron granites. The distribution pattern observed may represent a local erosion surface. Further detailed study is obviously needed.

The irregular fractionation trends of Mn and Ta observed in the Yellowknife field do not support their use in defining parent-product relationships amongst granites and pegmatites. The Fe/Mn and Nb/Ta trends

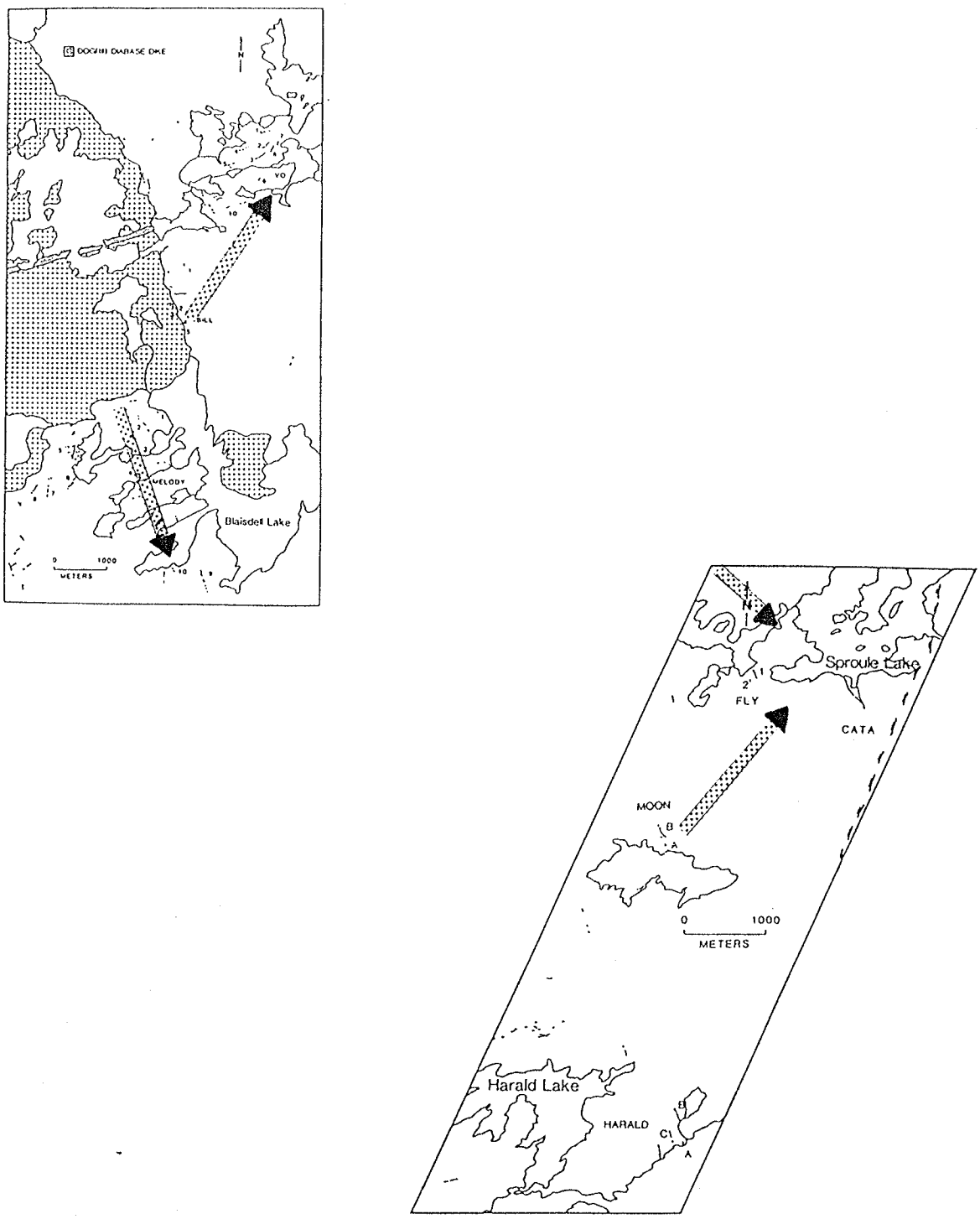

Figure 129: Distribution of Mn and Ta in columbite-tantalite around the Wedge granite. Arrows point towards increasing Mn and/or Ta. Black arrows - Ta, stippled arrows - Mn, stippled arrow with black arrowhead - Ta and Mn.

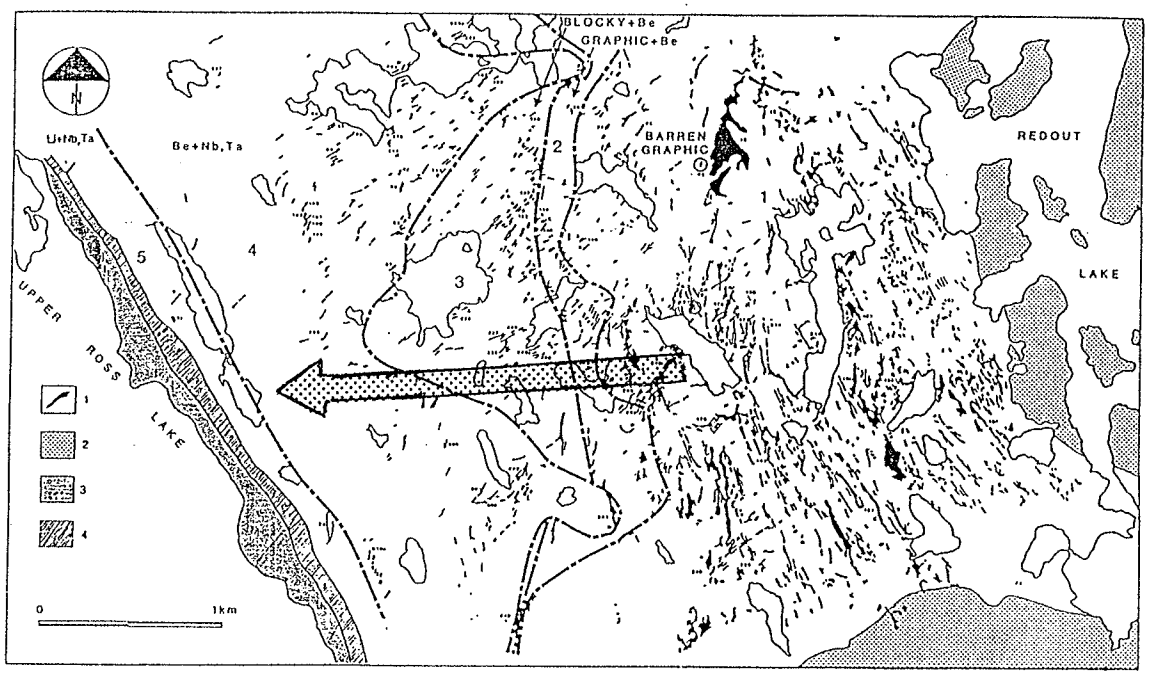

Figure 130: Distribution of Mn in columbite-tantalite in the Peg swarm. Arrows point towards increasing Mn content.

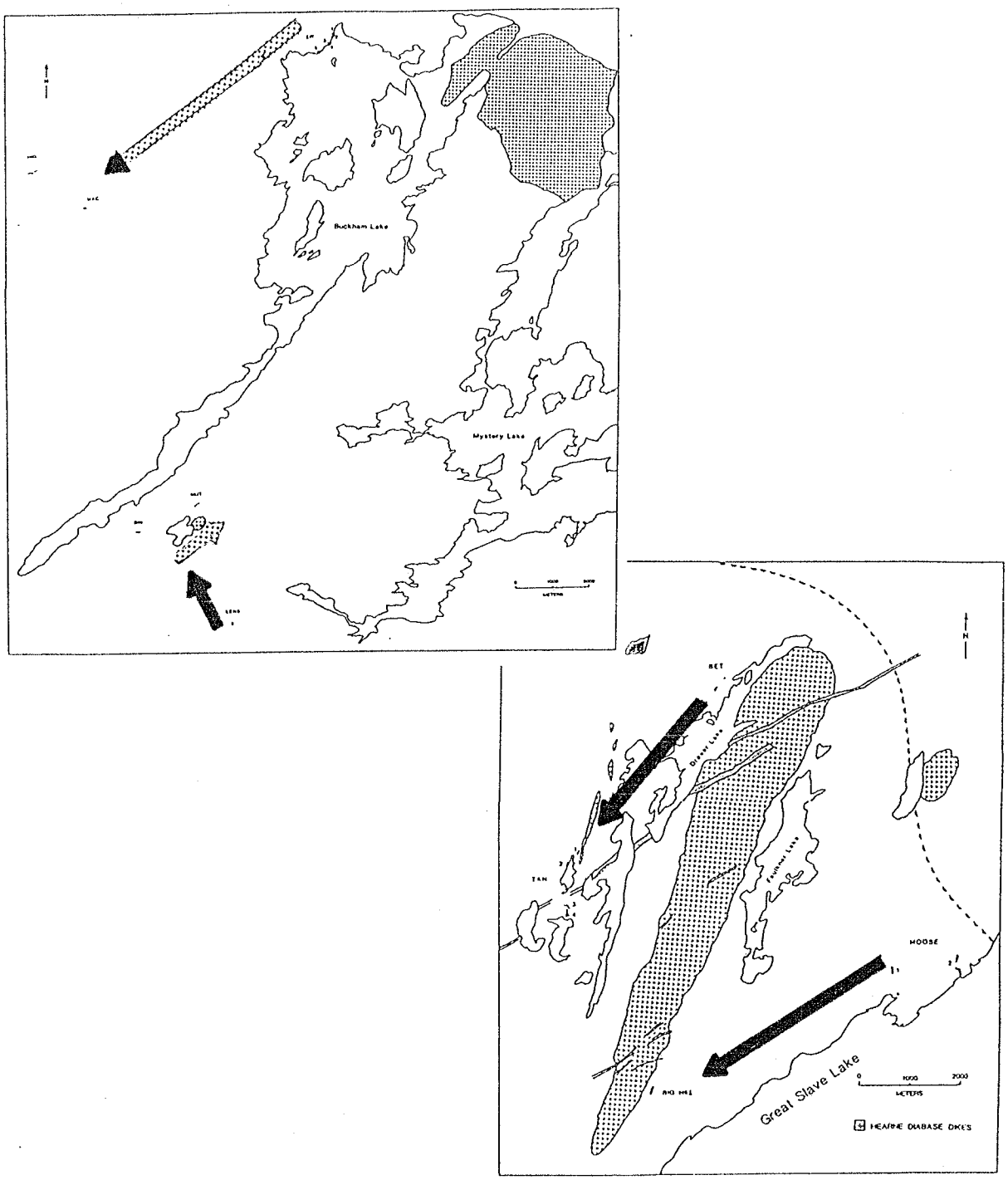

Figure 131: Distribution of Mn and Ta in columbite-tantalite surrounding the Buckham and Faulkner intrusions. Arrows point towards increasing Mn and Ta contents. Black arrow - Ta, stippled arrow - Mn, stippled arrow with black arrowhead - Mn and Ta.

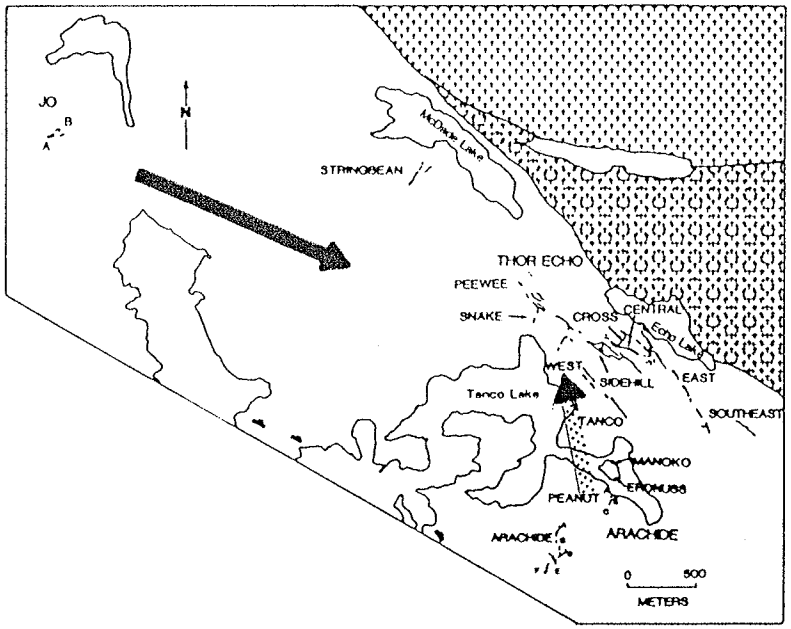

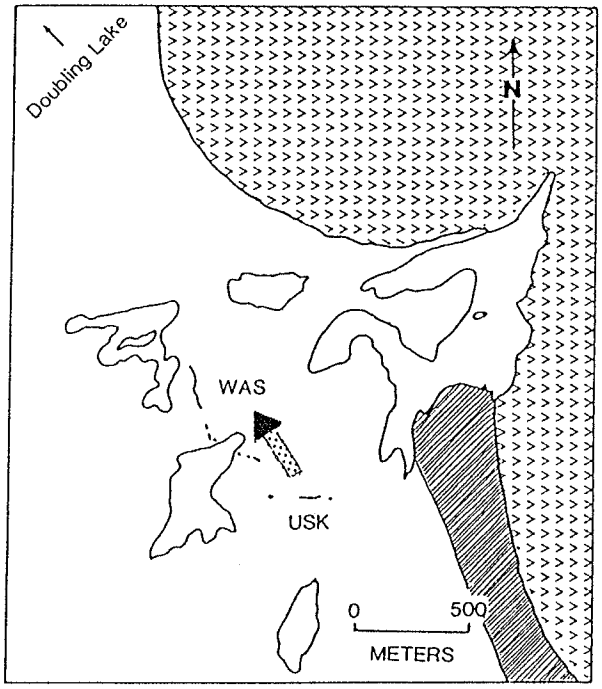

Figure 132: Distribution of Mn and Ta in columbite-tantalite adjacent to the Eastern granite. Arrows point towards increasing Mn and Ta contents. Black arrow - Ta, stippled arrow with black arrowhead - Mn and Ta.

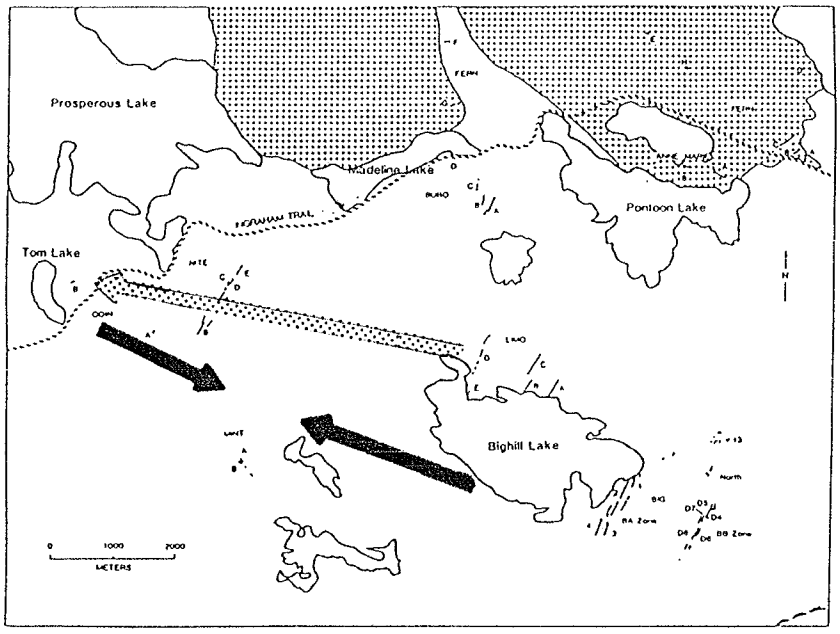

Figure 133: Distribution of Mn and Ta in columbite-tantalite south of the Prosperous granite. Arrows point towards increasing Mn and Ta contents. Black arrows - Ta, stippled arrow - Mn.

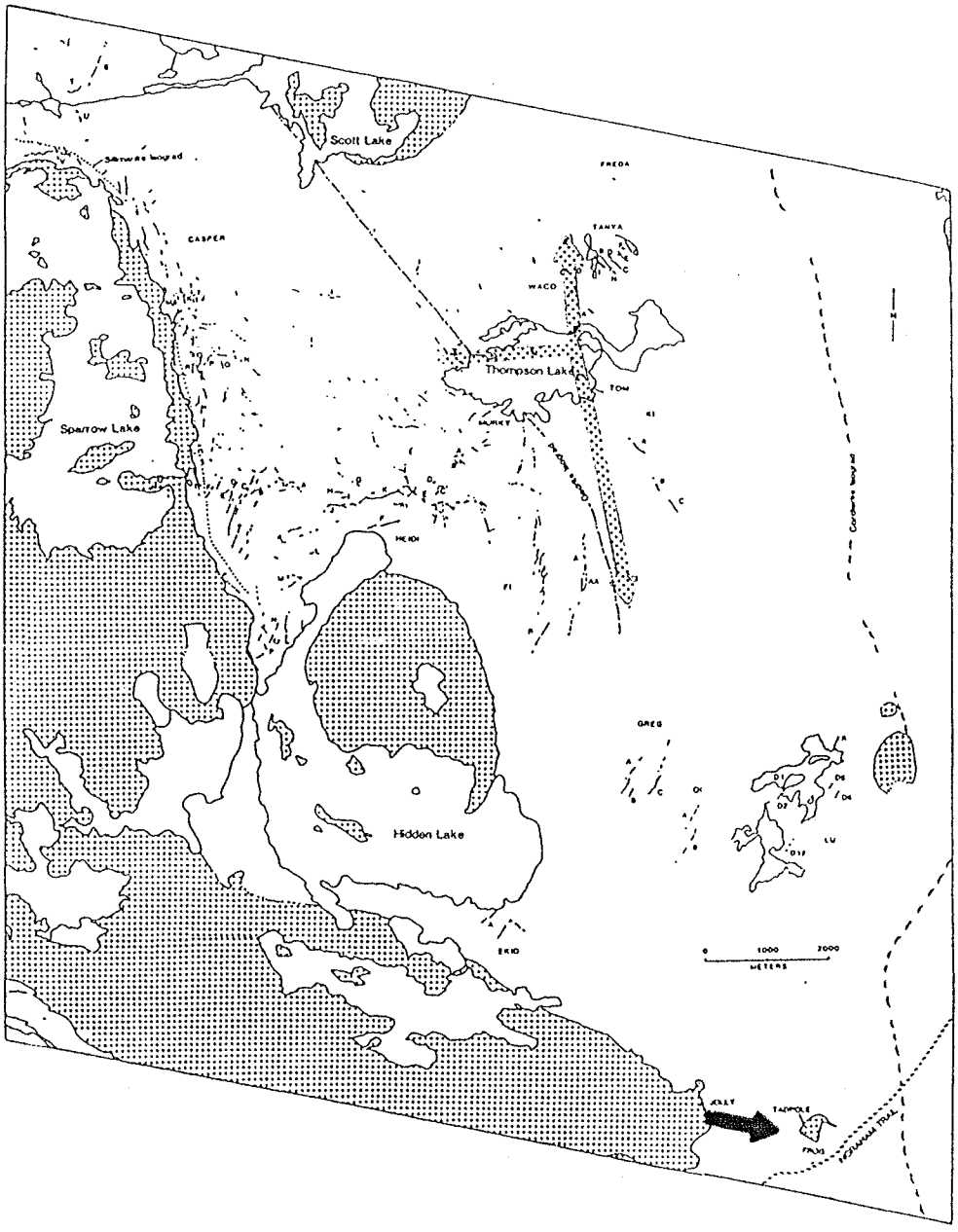

Figure 134: Distribution of Mn and Ta in columbite-tantalite in the vicinity of the Cameron granite. Arrows point towards increasing Mn and Ta contents. Black arrow - Ta, stippled arrows - Mn.

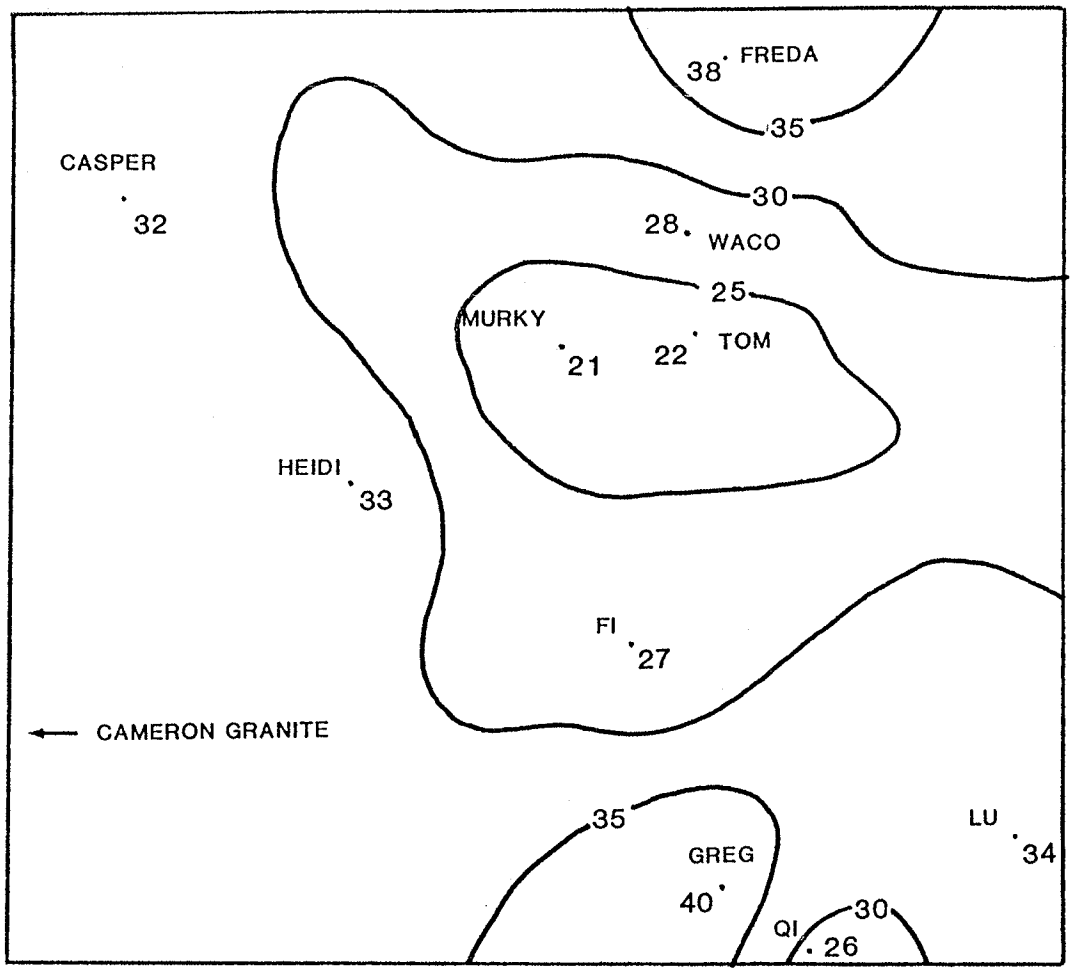

Figure 135: Contour map of Mn/(Mn + Fe) ratios in columbite-tantalite from pegmatites of the Sparrow-Thompson-Hidden series.

within columbite-tantalite are strongly influenced by the presence of coexisting mineral phases, particularly ferrotapiolite and ixiolite. Their presence would greatly alter the Fe/Mn and Nb/Ta ratios of columbite-tantalite, leading to deceiving results and erroneous interpretations.

Regional differences in Ti and Sn

The occurrence of Ti and Sn in Nb- and Ta-oxide minerals of the Yellowknife pegmatite field is generally low, typically in amounts less than 0.5 oxide wt. %. However, local enrichment of Ti and Sn is observed in some areas.

In pegmatites of the Sparrow-Thompson-Hidden Lake and Blaisdell Lake series and the Peg swarm, TiO_2 reaches maximum values in columbite-tantalite of 2.7, 3.8 and 2.4 wt. % , respectively. The Wedge granite, which seems to be parental to the Blaisdell Lake series pegmatites, carries the highest Ti content of all granites examined in the field (R.E. Meintzer, pers. comm.). Similarly, the Cameron and Sparrow plutons also have high Ti concentrations, and their cogenetic pegmatites contain Ti-enriched columbite-tantalite. The Ti-enrichment of columbite-tantalite, ferrotapiolite and cassiterite of the Peg swarm possibly reflects not only the increased accumulation of Ti within the Redout granite, but may also be a consequence of contamination from the amphibolite component of the interlayered granodiorite-amphibolite host rocks.

Compared to the localized enrichment of Ti, enrichment in Sn is more extensive. Whereas the field lacks Ti-based mineral species such as niobian or tantalian rutile and ilmenite, Sn minerals are common and include tantalian cassiterite and ixiolite. Tin-enriched areas include the Buckham

Lake series, Sparrow-Thompson-Hidden Lake series and the Sproule Lake series. Cassiterite and/or ixiolite is abundant in these series, and the concentrations of Sn in columbite-tantalite are significantly above the average found in the field. Significantly, pegmatites of these series are the most fractionated in the whole pegmatite field.

Thus the distribution of Ti and Sn in Nb- and Ta-bearing oxide minerals of the Yellowknife field seems to be the result of normal fractionation of Ti- and Sn- enriched granite magmas. Ti is mainly inherited from Ti-rich parental granites, and is typical of geochemically primitive pegmatites, although locally, elevated concentrations do occur in highly fractionated series. Sn seems to be accumulated mainly in highly evolved series. Assimilation of Ti from host rocks may have played only a neglible role.

Regional variation of structural state

The structural state data for the Yellowknife columbite-tantalite presented in the previous chapter show that intermediate degrees of order are typical of the whole field, with largely disordered and largely ordered phases comprising only a small percentage of the sample population. A strong relationship between the degree of order and the (Ti+Sn+Sc)/(Ta+Nb) ratio exists for the Yellowknife samples (cf. Chapter 6), a relationship which suggests the possible influence of "contaminant" R^{3+} and R^{4+} elements on the structural state.

Trends in distribution of degrees of order around pegmatitic granite intrusions are variable across the Yellowknife field. A relationship of decreasing degree of order with distance from the pluton, as observed in

the Greer Lake columbite- tantalite (Černý et al., 1986b), varies from well-defined to absent.

The structural state of columbite-tantalite in pegmatites surrounding the Faulkner tonalite shows a decrease in degree of order away from the intrusion (Figure 136). Likewise, a similar relationship is observed for the Defeat granodiorite-Harding Lake series association (Figure 137) and for the Wedge granite-Blaisdell Lake series association (Figure 138). In contrast to these examples, pegmatites of the Bighill and Tom Lake series show reversed trends, i.e. decreasing order towards the Prosperous granite intrusion (Figure 139). The pegmatites of the Sparrow-Thompson series also show a generally inverse trend (Figure 137).

Other regions tend to show more complex patterns; the Buckham Lake series displays both "normal" and "reversed" trends (Figure 136), and the Peg swarm shows well-developed mineral and chemical zoning, but no correlation between degree of order and distance from the pluton (Figure 140).

The large variations in structural state in columbite-tantalite of the Yellowknife field may have been controlled by variable rates of subsolidus cooling. If it is assumed that the intitial crystallization of columbite-tantalite occurs in the disordered state, rapid cooling would tend to favor the metastable preservation of the disordered phase. In contrast, under conditions of slow cooling, the ordered state evolves from the disordered state. The implication of this interpretation is that small dikes would tend to crystallize disordered columbite-tantalite, whereas large bodies undergoing slow cooling would allow the crystallization of ordered phases. This interpretation does not seem to apply to the Yellowknife pegmatites, as highly variable degrees of order exist in pegmatites of similar physical

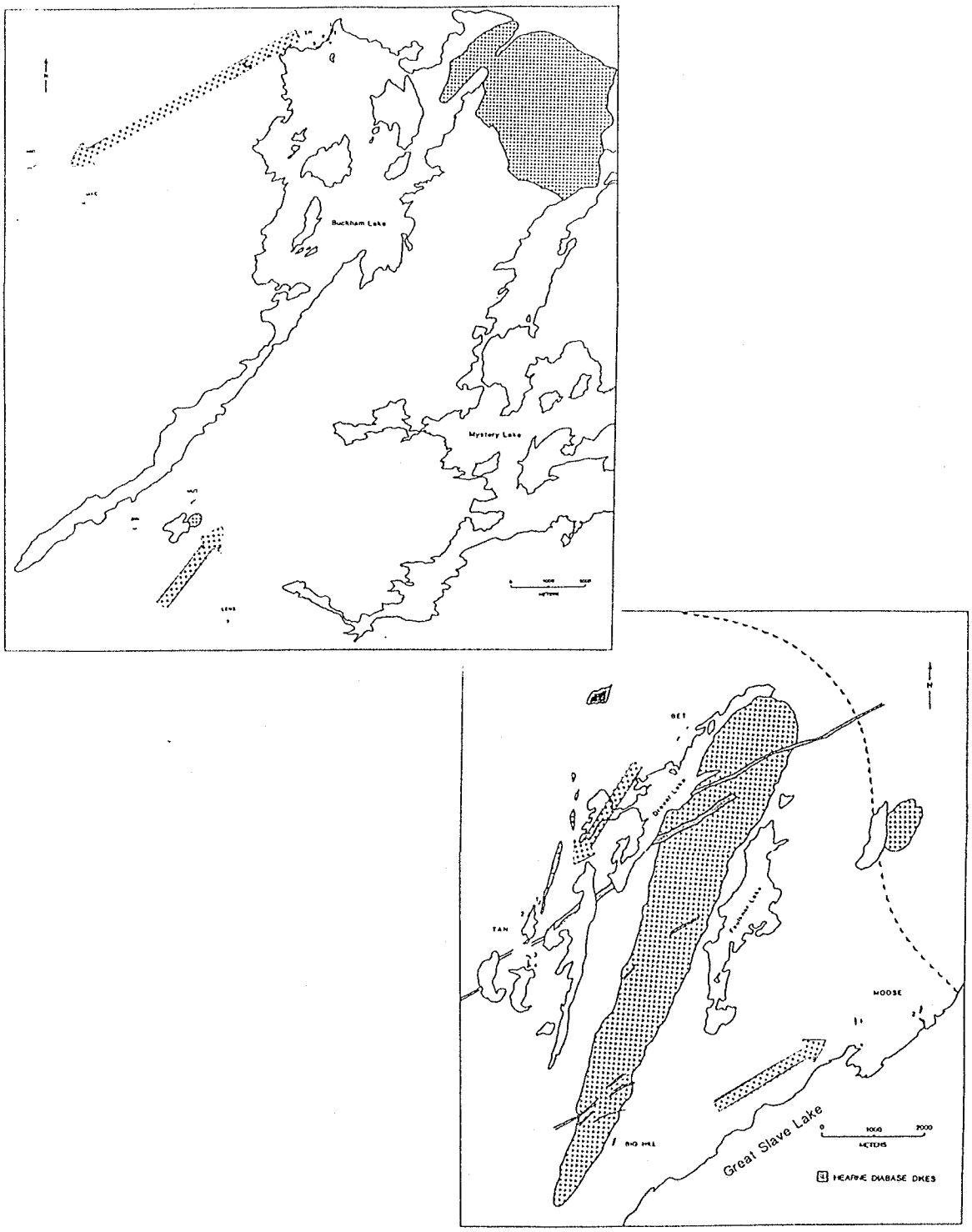

Figure 136: Distribution of degree of order in columbite-tantalite around the Buckham granite and Faulkner granodiorite. Stippled arrows point towards lower degree of order.

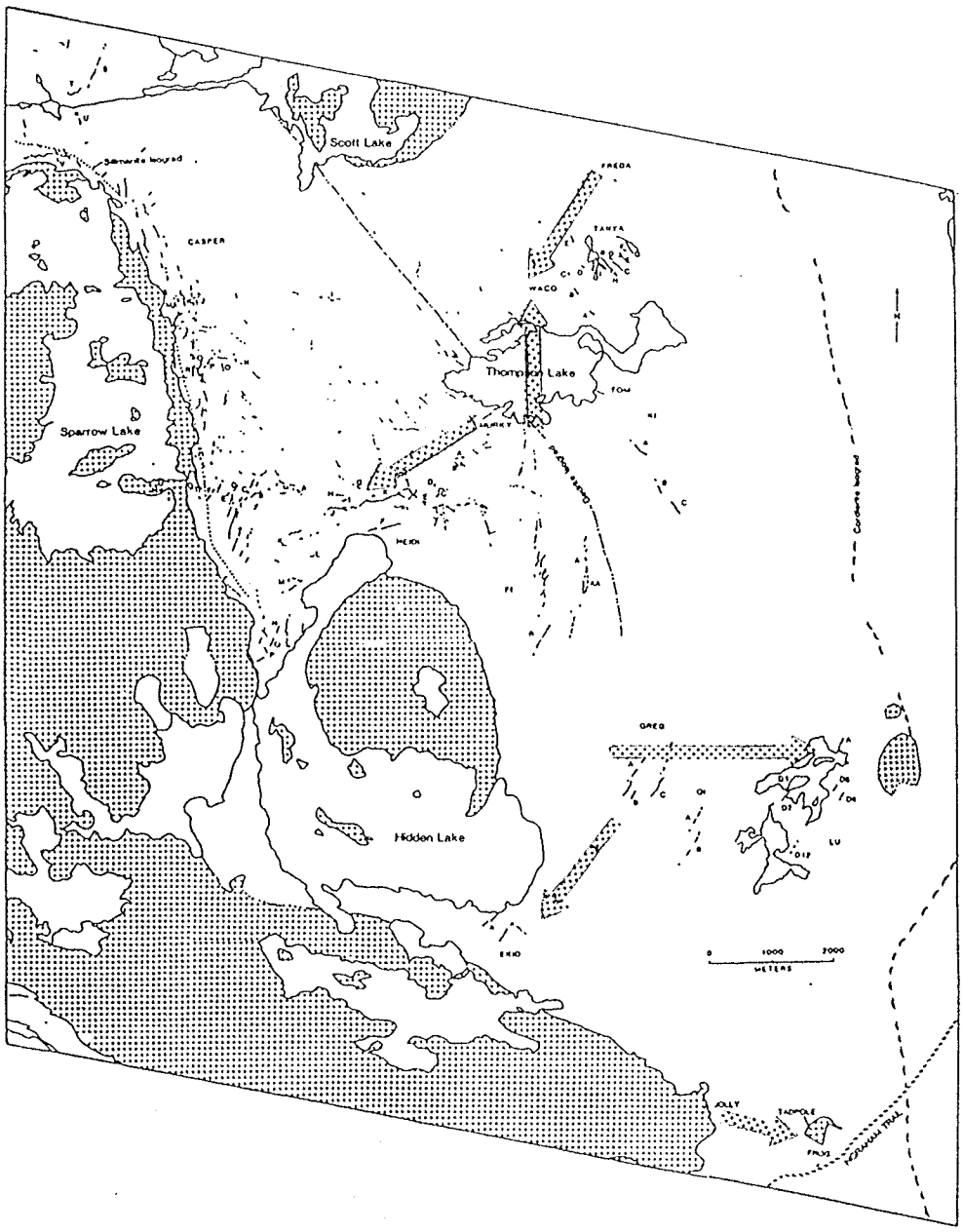

Figure 137: Distibution of degree of order in columbite-tantalite near the Cameron granite. Stippled arrows point towards lower degree of order.

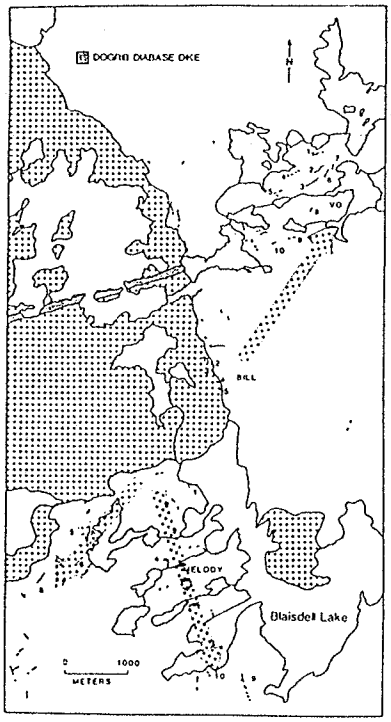

Figure 138: Distribution of degree of order in columbite-tantalite near the Wedge granite. Stippled arrows point towards lower degree of order.

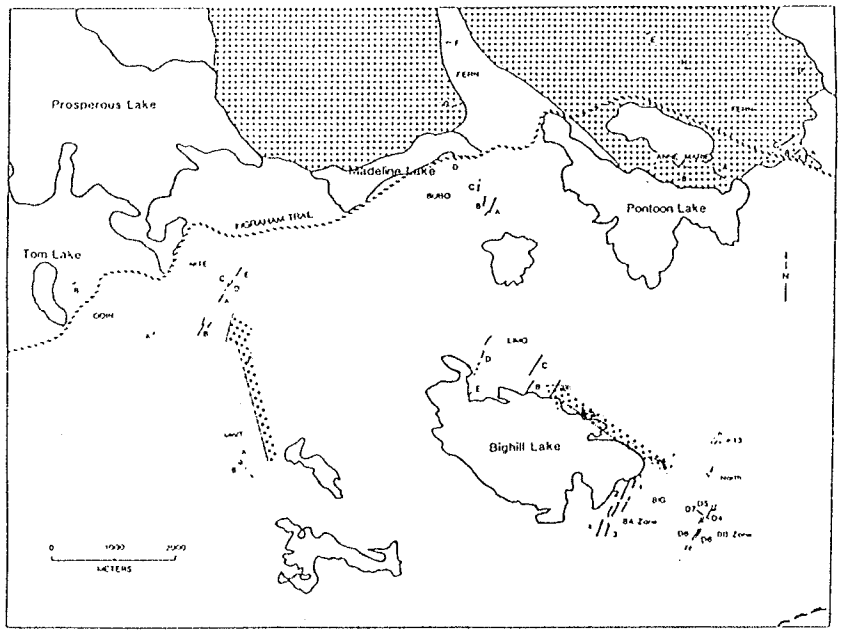

Figure 139: Distribution of degree of order in columbite-tantalite near the southern margin of the Prosperous granite. Stippled arrows point towards lower degree of order.

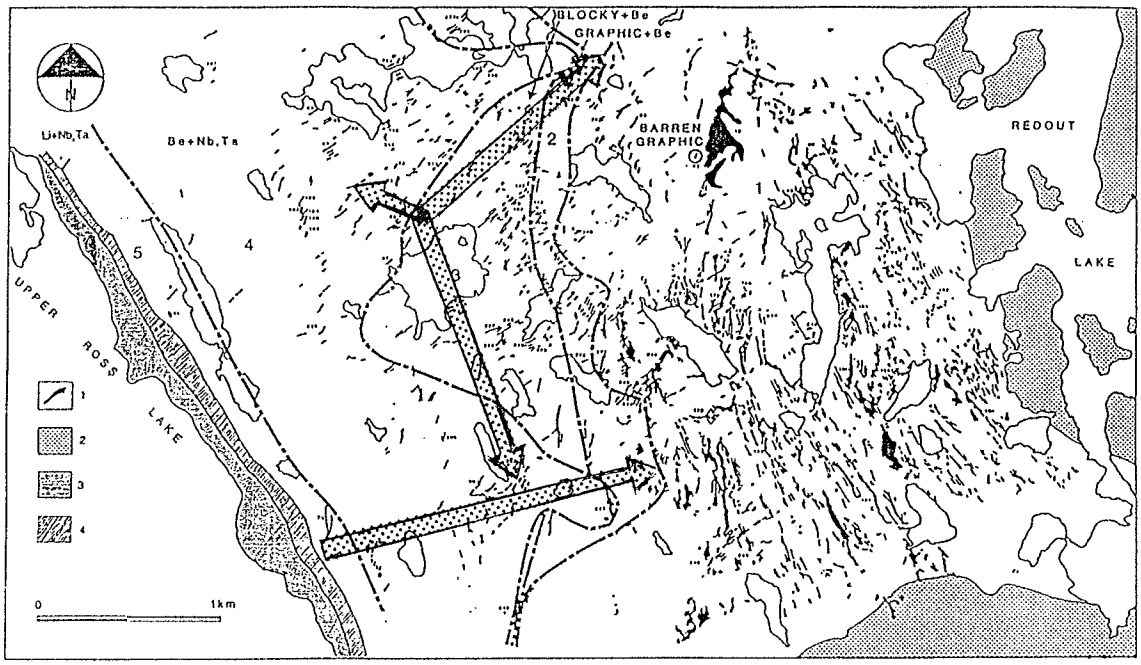

Figure 140: Distribution of degree of order in columbite-tantalite in the Peg swarm. Stippled arrows point towards lower degree of order.

dimensions. Also, this interpretation would be valid only if the temperature level of the host rocks was uniform across the field. This is an unlikely condition, and the thermal conditions of the metamorphic rocks at the time of pegmatite intrusion and consolidation are unknown.

The influence of Ti and Sn on the structural state of columbite-tantalite from the Yellowknife field is quite strong (cf. Figure 45, Chapter 6). The substitution of Ti and Sn for Nb and Ta in the structure disrupts the stoichiometry and inhibits ordering. The Ti and Sn contents may be the main factor responsible for the variable distribution patterns observed in the field.

With progressive fractionation, Ti is expected to decrease whereas Sn will generally increase. Early formed columbite-tantalite will be enriched in Ti (assuming no Ti-based mineral species are also crystallizing). The substitution $2(Nb,Ta) + (Fe,Mn) \longrightarrow 3Ti$ causes a disruption of the local stoichiometry and consequently inhibits ordering. As fractionation progresses, the Ti content of the melt gradually decreases and less Ti is available for the crystallizing columbite-tantalite. Lower Ti contents mean less substitution of Nb and Ta, and hence higher degrees of ordering can be attained. This sequence of events may explain the gradual increase in order away from parent intrusions in some areas of the Yellowknife field.

Similarly, as Sn contents gradually increase with fractionation, columbite-tantalite accumulate increasing amounts of Sn (until the activity is so high that cassiterite or ixiolite-wodginite will crystallize). As a result, the structural state of columbite-tantalite evolves from ordered to disordered states with progressive Sn fractionation. Thus, a trend of

decreasing order away from the intrusion is expected. Applying this premise to the Greer Lake columbite-tantalite, samples showing the lowest degree of order are significantly richer in Ti and Sn than those of high order (Černý et al., 1986b).

It is obvious that the hypothesis presented here requires more field and experimental work. However, it should be stressed that based on the findings of this study, the influence of Ti and Sn on the structural state of columbite-tantalite is definitely confirmed.

The Fe/Mn signature of the Yellowknife field

Ignoring for the moment the two anomalous areas of the Yellowknife field, the Riber pegmatite and the Harding Lake series, it is relatively easy to explain the restricted Mn factionation within the whole field. The field consists mainly of beryl-columbite type and complex spodumene subtype pegmatites which are poor in Li- and F-enriched micas. The accessory mineralogy shows no indication of appreciable activity of F in the residual melts and fluids of the consolidating pegmatites. With the exception of the Riber pegmatite, lepidolite is absent from the field, whereas F-dominant amblygonite and microlite occur only locally; even the distribution of fluorapatite throughout the field is quite sporadic.

The Black Hills pegmatite field of South Dakota contains pegmatites of similar types. These pegmatites also carry Fe-rich Nb and Ta minerals, and manganocolumbite, manganotantalite plus wodginite are found in considerable quantities only in the Li- and F-enriched Peerless, Bob Ingersoll No.1 and Tin Mountain pegmatites, where considerable concentrations of lithia micas and/or amblygonite are present (Černý et al., 1985b; Černý and Ercit, 1985;

Papike et al., 1986). In the Mongolian Altai pegmatite field all pegmatites carry manganocolumbite and manganotantalite. Pegmatites of this field evolve into highly fractionated lepidolite-rich, pollucite-beaing complex bodies which also carry microlite, uranmicrolite and bismutomicrolite (Wang et al., 1981; Černý and Ercit, 1985).

Thus it is likely that the general lack of appreciable Fe/Mn fractionation in the Yellowknife field is due to the overall F-poor composition of the granite-pegmatite sequences.

The evolution of the Nb, Ta, and Sn mineral paragenesis in the Yellowknife field

The evolution of Nb-, Ta- and Sn-oxide minerals in the Yellowknife field reflects the general fractionation trend of Fe/Mn and Nb/Ta observed in other fields (Černý and Ercit, 1985; Černý et al., 1986b). In granite-pegmatite sequences of the Yellowknife field, the composition of Nb and Ta minerals evolves from predominantly Fe- and Nb-rich mineral species to Fe- and Ta-rich or rare Mn-rich phases (Figure 141).

The evolutionary trend of Nb-, Ta- and Sn-oxide minerals of the Yellowknife field may be generalized as follows:

i) Ferrocolumbite is typically the first Nb,Ta mineral species to crystallize, with primitive Fe/Mn and Nb/Ta ratios. As fractionation progresses (decreasing Fe/Mn and Nb/Ta ratios), the composition of columbite-tantalite grades imperceptibly from ferrocolumbite to ferrotantalite, manganocolumbite or manganotantalite, depending on the relative rates and degree of Mn and Ta fractionation. If the rate of Ta fractionation greatly exceeds that of Mn, then the evolutionary trend of Nb- and Ta-oxide minerals proceeds from ferrocolumbite to ferrotantalite. However, if Mn frac-

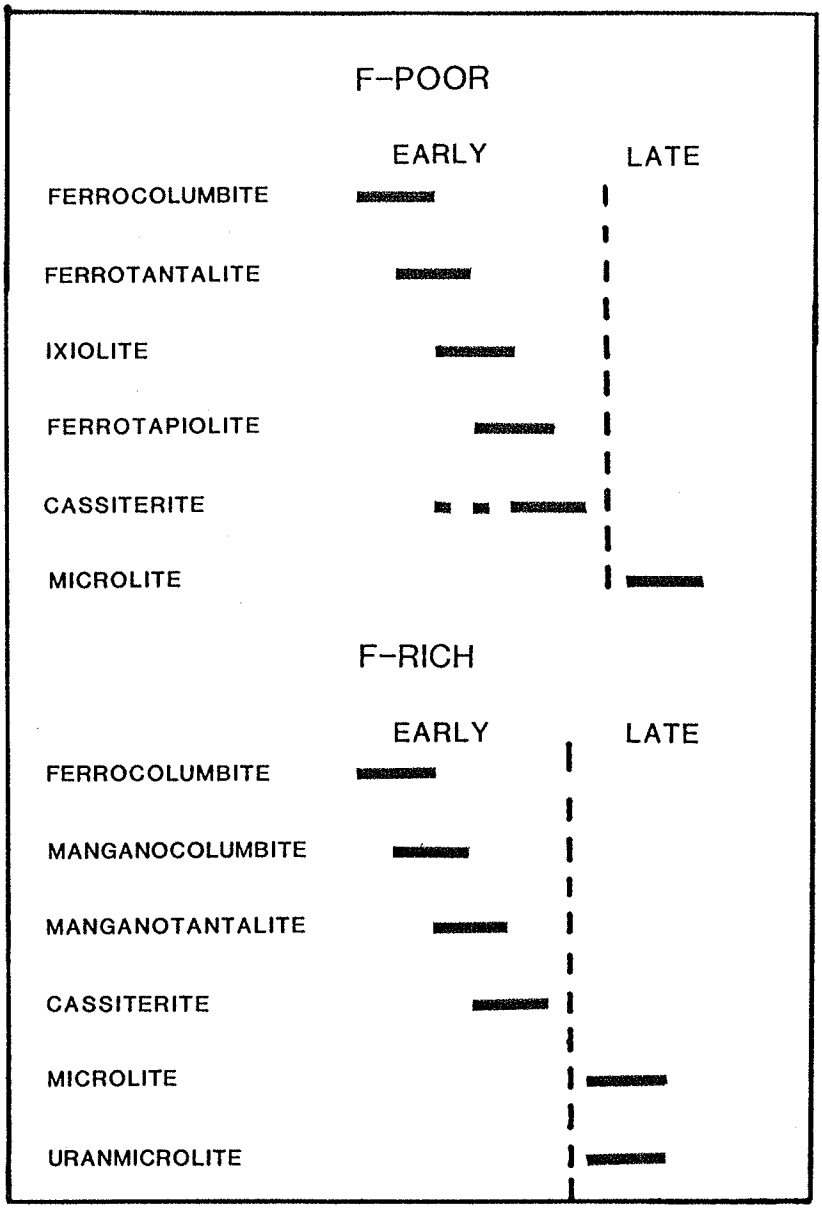

Figure 141: Generalized crystallization history of Nb,Ta,Sn parageneses in the F-poor and F-enriched pegmatites of the Yellowknife pegmatite field.

tionation is faster than Ta, then ferrocolumbite evolves to manganocolumbite or manganotantalite. In this trend, ferrotapiolite does not occur.

(ii) Ferrotapiolite typically crystallizes after or with ferrotantalite, but only when the Ta/(Ta + Nb) ratio is greater than 0.5 and the Mn/(Mn + Fe) is typically low (< 0.4).

(iii) With progressive fractionation of Fe/Mn and Nb/Ta, Ti contents decrease whereas Sn contents increase. Ixiolite will form when the melt has a Mn/(Mn + Fe) ratio of 0.35 to 0.65, provided the activities of Ta and Sn are also high.

(iv) Cassiterite typically crystallizes as the last Nb-,Ta- and Sn-bearing oxide mineral, particularly when the melt is depleted in Fe,Mn,Nb and Ta. However, cassiterite may form at any stage of the Nb, Ta, and Sn mineral paragenesis, either as a result of direct primary crystallization under conditions of very high Sn activity or as a result of exsolution from columbite-tantalite or ferrotapiolite.

(v) Microlite occurs as a replacement of pre-existing Nb- and Ta-bearing phases subjected to hydrothermal alteration. The processes of microlite alteration are generally divided into 2 types; primary or hydrothermal, and secondary or weathering (Van Wambeke, 1970). In an examination of altered microlite from the Harding pegmatite, New Mexico, Lumpkin et al. (1986) characterized the geochemical behavior of the A-site cations, H_2O and F during microlite alteration. Their results showed minor increases in Fe and Mn, decreases in Na and variable changes in Ca, F, H_2O and A-site vacancies as a result of hydrothermal alteration. Typically, Na, Ca and F are leached out and extensive hydration occurs in microlite subjected to secondary alteration.

The chemical analyses of the Yellowknife microlites suggest that hydrothermal alteration played a major role in defining the chemistry of microlite. A general increase in Fe and Mn coupled with a decrease in Na content agrees well with the findings of Lumpkin et al.(1986). However, the concentration of Fe and Mn may simply be a consequence of the bulk composition of the parent mineral which the microlite replaced. The concomitant decrease in Ca is apparently due to the substitution of U which apparently becomes more concentrated in the pegmatitic fluid as fractionation progresses.

The evolution of Nb-, Ta- and Sn-oxide minerals in the Yellowknife pegmatite field agrees well with the general trends presented by Černý et al. (1986a) (Figure 142). The predominant F-poor beryl-columbite and complex spodumene type pegmatites of the Yellowknife field show the typical development of Fe-rich species, evolving with progressive fractionation into ferrotapiolite or ixiolite. The strong vertical to subvertical segments of pronounced Nb/Ta fractionation at relatively constant Mn/(Mn + Fe) are quite evident. The rare F-rich pegmatites of the area show Mn increasing with fractionation, its path being typically subhorizontal and indicating prominent Fe/Mn fractionation at a more or less constant Ta/(Ta + Nb) ratio. It thus seems that not only the geochemical evolution but also the paragenesis of the Nb- and Ta-bearing oxide minerals for the Yellowknife field is strongly dependent on the relative activity of F within the pegmatite melt.

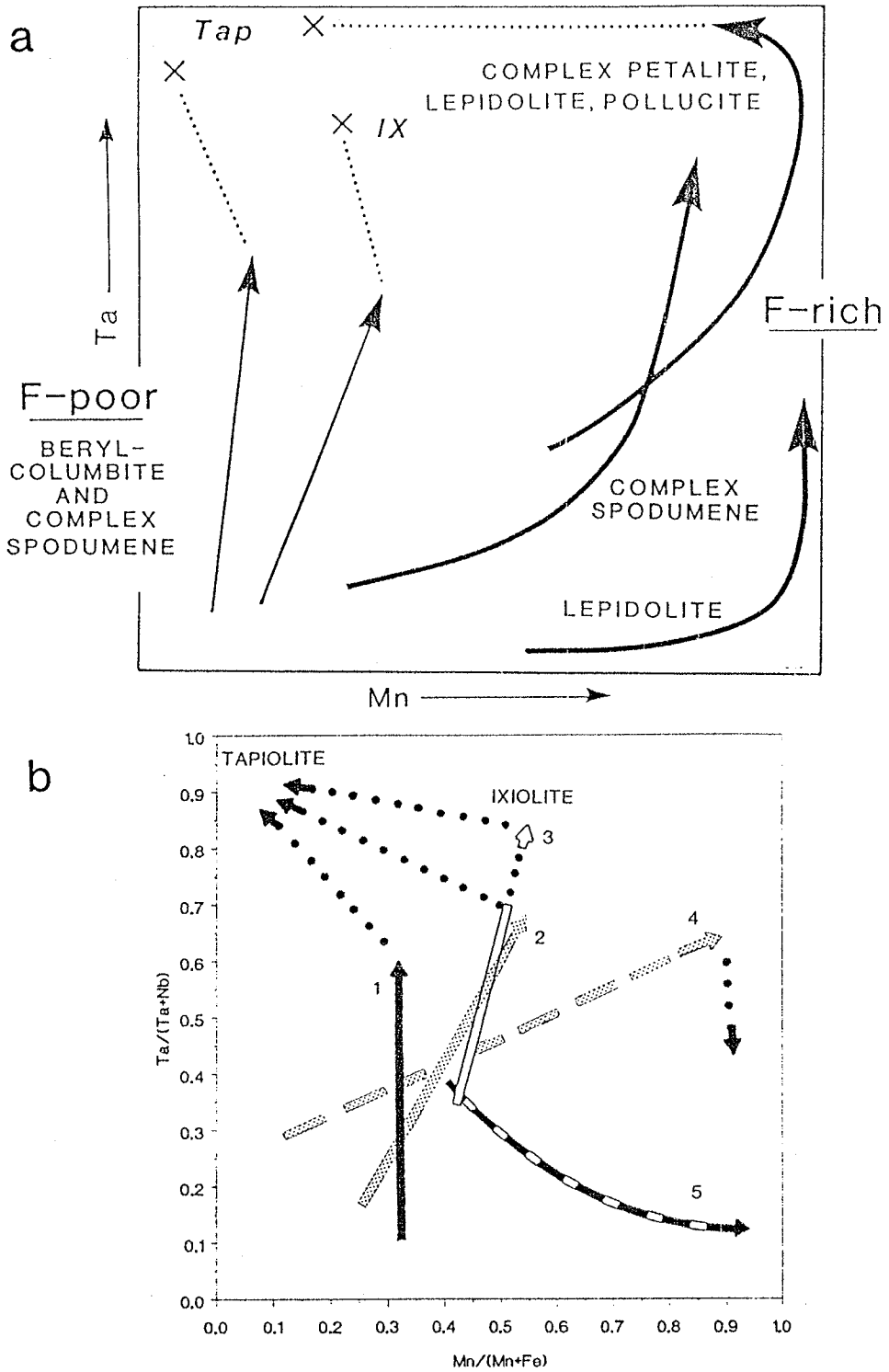

Figure 142: Generalized fractionation trends of Nb-, and Ta-oxide minerals. (a) General trend of global pegmatite populations (after Černý et al., 1986a). b) General and some specific trends for the Yellowknife field. 1) - General trend for the majority of the Yellowknife field, 2) - Blaisdell Lake group and Sproule Lake series, 3) - Buckham and Bighill Lakes groups, 4) - Riber pegmatite, 5) - Harding Lake series.

CHAPTER 14

Economic Evaluation

Rare-element granitic pegmatites are the primary source of commercial tantalum, and to a much lesser degree niobium and tin. In addition, pegmatites are also an important source of feldspar, mica, beryllium, lithium, rubidium, cesium, uranium, thorium, rare earth elements and gem materials. The economic potential of Ta in the Yellowknife pegmatite field has long been under scrutiny, and assessment of several properties has been made.

In evaluating the economic potential of any pegmatite-bearing area, several factors must be taken into consideration. First, prospective economic pegmatite deposits require the determination of the fractionation level attained by the pegmatite, which may be reflected by its rare-element mineralization or rare-alkali concentrations. Such qualitative geochemical indicators of fractionation as K/Rb and K/Cs ratios in K-feldspar and mica, Na/Li ratio in beryl and Nb/Ta ratio in Nb- and Ta-bearing minerals may be used as a measure of the overall degree of fractionation in individual pegmatite, and hence as an indirect measure of its economic potential:. second, the viability of economic exploitation depends on the absolute concentrations (quantitative indicators) of the desired element and the distribution of the minerals bearing that element. The size and accessibility of the pegmatite is also important, as well as the ease in which the potential ore mineral(s) can be extracted.

Qualitative indicators

Although progressive enrichment of Ta had previously been correlated with increasing rare-alkali fractionation by several workers (Ginzburg, 1960; Beus et al., 1968; Solodov, 1971), quantitative characterization of this relationship has only recently been realized. Plots of K/Rb ratio for core-margin, blocky K-feldspar versus the Ta/(Ta + Nb) ratio in columbite-tantalite from three pegmatite groups in Manitoba show well-defined linear relationships between the two parameters (Anderson, 1984; Černý et al., 1985a, 1986b). Typically, advanced fractionation of Ta is achieved only at low K/Rb ratios. A similar but somewhat less definitive relationship exists between K/Cs in K-feldspar and Nb-Ta fractionation (Anderson, 1984), although data are at present scarce.

Figure 143 shows the average Ta/(Ta + Nb) ratio for columbite-tantalite versus the average K/Rb and K/Cs ratios for blocky core-margin K-feldspar in individual pegmatites of the Yellowknife pegmatite field. The paucity of data points is due to the scarcity of core-margin K-feldspar in columbite-bearing pegmatites. Correlation between the fractionation trends of columbite-tantalite and core-margin K-feldspar shows considerable spread among the data. Nevertheless, the data do show a general trend of increasing Ta enrichment with increasing rare-alkali content. The scatter within the trend seems to be related to the overall composition of the pegmatite. Beryl + columbite type pegmatites typically show higher K/Rb and K/Cs ratios with generally low to moderate Ta/(Ta + Nb) ratios. A linear trend among this type of pegmatite is not well-defined. In contrast, individual spodumene-bearing pegmatites show a good linear trend for K/Rb versus Ta/Nb, and in general show lower K/Rb and K/Cs ratios than the beryl + columbite types.

Similar relationships are observed for K/Rb and K/Cs in muscovites versus Nb/Ta fractionation, although trends are not as well-defined as those observed for K-feldspar (Figure 144).

Perhaps the most useful geochemical indicator of Ta mineralization potential is the Nb/Ta ratio in muscovites. According to Beus (1966), the Nb/Ta ratio of muscovite derived from Ta-enriched pegmatites is significantly higher than those originating from Ta-poor pegmatites. A plot of Nb/Ta ratio of muscovite versus Ta/(Ta + Nb) in columbite-tantalite from the Yellowknife field is shown in Figure 145. Although more data would be desirable, the available analyses are aligned in a well-defined negative trend, confirming the findings of Beus (1966).

Quantitative indicators

The Yellowknife pegmatite field has been examined for its Ta potential on numerous occasions, often in conjunction with Be and/or Li assessment. As noted in Chapter 1, small-scale mining operations existed during the mid-1940's through the mid-1950's, yet resulted in only meager productions of Ta concentrates. Recent assaying of various pegmatites, particularly spodumene-bearing bodies, shows low Ta, Nb and Sn values (Table 32). The observed assay values are not perfectly comparable because of the different sampling methods and analytical procedures used by different authors. Nevertheless, the overall results are not encouraging, and the data are restricted to only a few pegmatites. A better geochemical indicator for Ta mineralization is the Ta content in primary muscovites (Odikaze, 1958; Heinrich, 1962; Beus, 1966; Gordiyenko, 1970).

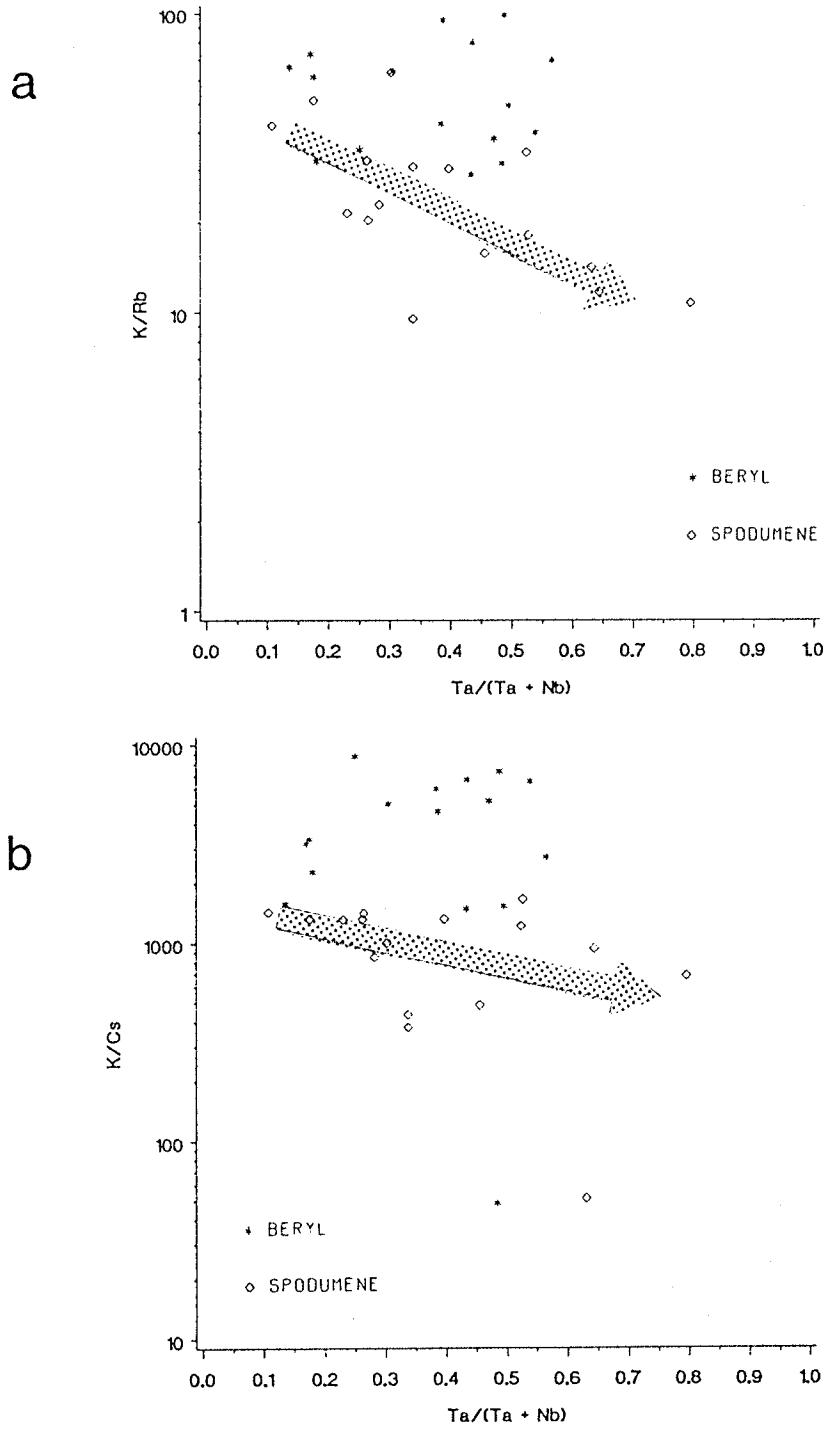

Figure 143: Plot of average Ta/(Ta + Nb) (atomic) of columbite-tantalite versus the average (a) K/Rb and (b) K/Cs for core-margin K-feldspar in individual pegmatites.

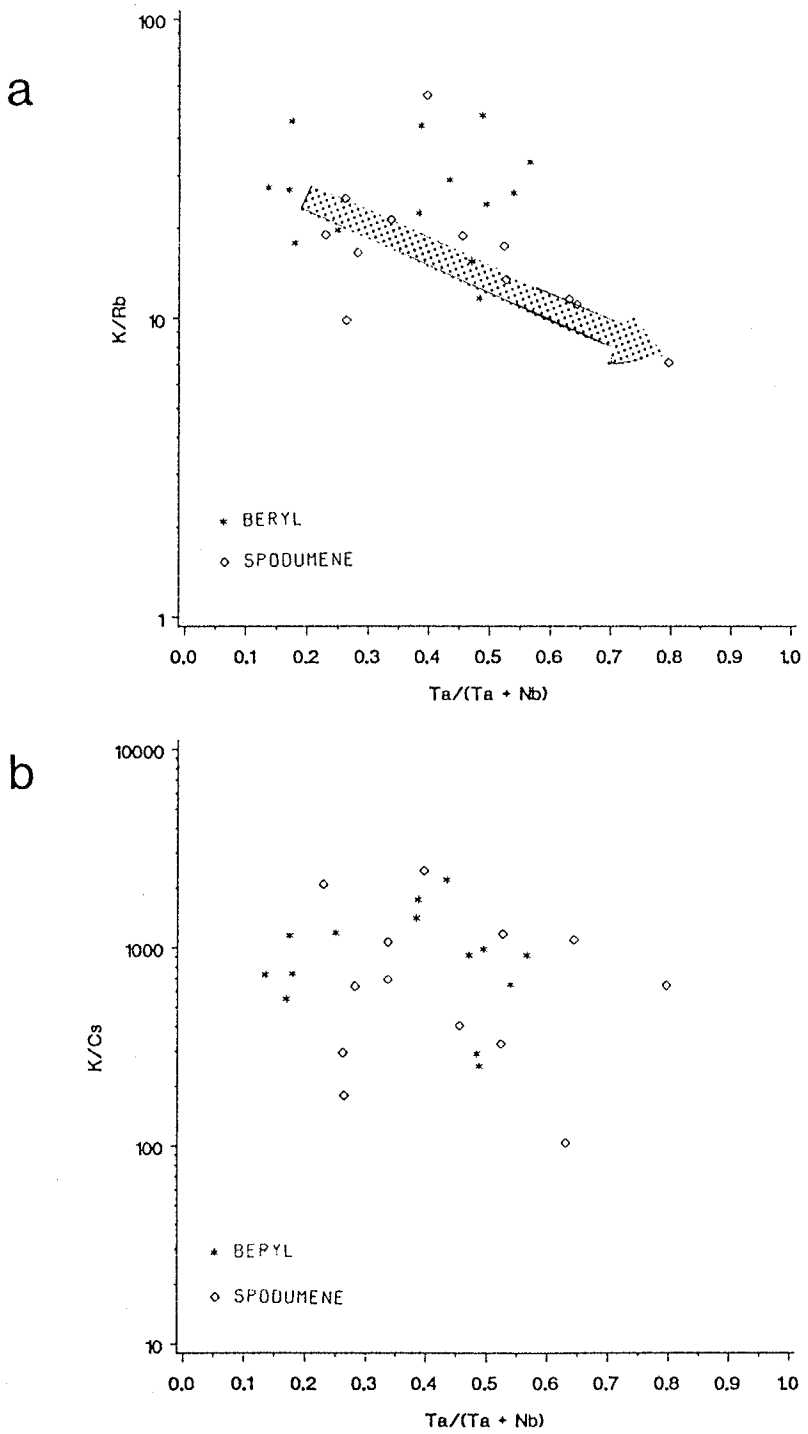

Figure 144: Plot of average Ta/(Ta + Nb) (atomic) of columbite-tantalite versus the average (a) K/Rb and (b) K/Cs in platy muscovite in individual pegmatites.

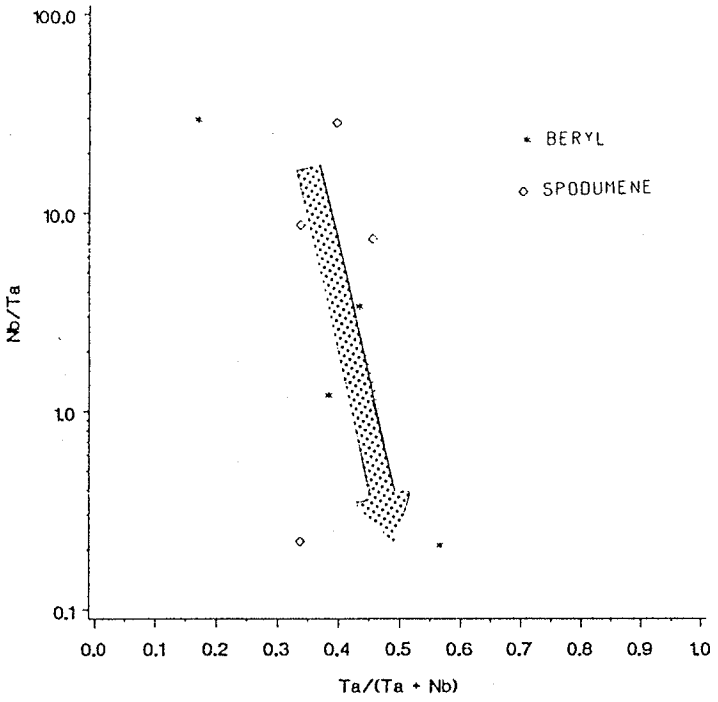

Figure 145: Plot of average Ta/(Ta + Nb) (atomic) in columbite-tantalite versus the average Nb/Ta ratio (weight percent) in platy muscovite in individual pegmatites.

Muscovite is one of the principal "carriers" of Ta, and its chemistry reflects the geochemical evolution of the pegmatite melt at the time of its crystallization. Nb,Ta,Rb and Cs contents increase in muscovite with progressive pegmatite fractionation, and are indicative of the accumulation of these rare elements in the bulk pegmatite composition. However, it is the absolute Ta and Cs contents which seem to be the most useful indicator of Ta mineralization (Gaupp et al., 1984).

Figure 146 shows the diagram of Ta and Cs in primary muscovites for pegmatites of the Yellowknife field. The Yellowknife data show considerable scatter, extending well into the field represented by secondary muscovite. This scatter may be caused in some cases, by unclear distinction between primary and secondary muscovite generations. However, it must be pointed out that micas from relatively few pegmatites were used for the diagram of Gaupp et al. (1984), and most of them come from pegmatite fields of distinctly different geochemical signature (enriched in F, P, B relative to the Yellowknife field). It is also known that some data available to the above authors were omitted to "streamline" the trend (P. Černý, pers. comm. 1984). The omitted data fall into the high-Ta, low-Cs area "violated" by most of the Yellowknife data that deviate from the trend of primary micas. It must also be pointed out that the present results are the first ones used to test the Ta versus Cs indicator; more data from diverse pegmatite fields must be collected before a better assessment of the indicator can be made.

Table 32: Average niobium, tantalum and tin assay values of some pegmatite(s) of the Yellowknife pegmatite field.

Pegmatite(s)	Nb	Ta	Sn
Ann[2]	-	0.004	-
Bet[9]	0.01	Tr.	0.016
Big[3]	-	0.002	-
Big Hill[13]	0.01	0.045	0.035
Fi[4]	-	0.002	-
Fly[10]	0.01	0.01	-
Freda[12]	0.01	0.01	-
Greg[1]	-	0.003	-
Jake[14]	0.006	0.003	-
Moose[8]	0.04	0.02	-
Nite[5]	-	0.007	0.006
Pancho Villa[15]	0.003	0.006	-
Tan[16]	-	0.07	-
Thor Echo[6]	-	0.003	-
Usk[11]	Tr.	Tr.	-
Vo[7]	-	0.002	-
Was[11]	0.01	Tr.	-

All values are in elemental weight percent. Data taken from: 1 - Canadian Superior (1975), 2 - Morrison (1975a), 3 - Morrison (1975b), 4 - Morrison (1975c), 5 - Morrison (1975d), 6 - Morrison (1975e), 7 - Groves (1978), 8 - Morrison (1978), 9 - LeCouteur (1980a), 10 - LeCouteur (1980b), 11 - LeCouteur (1980c), 12 - LeCouteur (1980d), 13 - Thomas (1980), 14 - Stacey (1981a), 15 - Stacey (1981b), 16 - Thomas (1982).

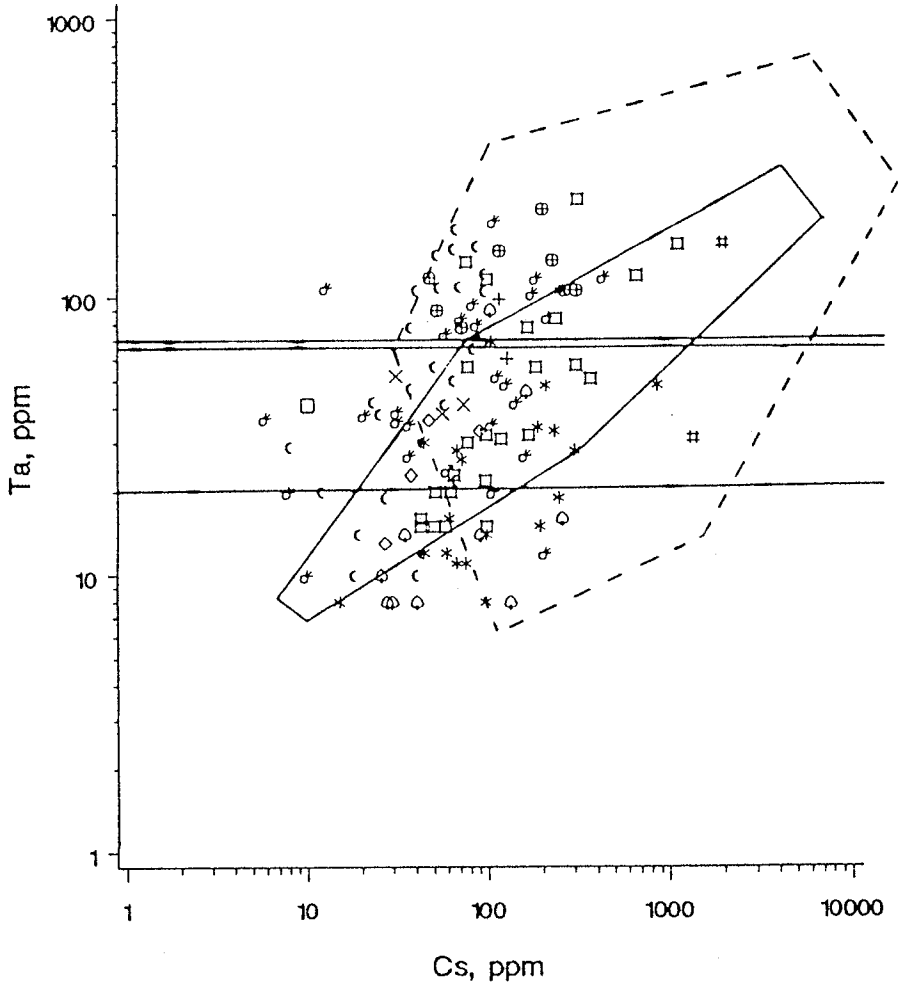

Figure 146: Plot of Ta versus Cs in platy muscovite for individual pegmatites of the Yellowknife pegmatite field. Double line marks the lower limit of Ta-prospective localities after Gordiyenko (1970), the single line denotes the same according to Beus (1966). Solid line denotes field of primary muscovites, dashed line denotes field of secondary muscovites (From Gaupp et al., 1984).

Concluding Remarks

The mineralogical, geochemical and paragenetic observations made in this study show that the overall fractionation levels of pegmatites from the Yellowknife field vary from poor to moderate. In terms of Ta fractionation, the field is predominantly poor, showing typically high Nb/Ta ratios across most of the field. The Ta-bearing pegmatites of the field are generally small dikes whose concentration of Ta minerals is often low. The Ta- and Nb-oxide minerals are conspicuously chemically inhomogeneous, containing locally significant quantities of Ti and Sn, and Nb dominant over Ta in a large majority of cases.

Certain geochemical indicators may be used to aid in the location of pegmatites with potential Ta mineralization. The most promising indicator seems to be the absolute Ta content in primary muscovite, which reflects the Ta content in the bulk pegmatite composition. The value of the Ta versus Cs indicator is rather uncertain. The Nb/Ta ratio in muscovite decreases with increasing Nb/Ta fractionation in columbite-tantalite; however, more data is required in order to fully define such a trend.

At present, the depressed state of the Ta market, coupled with a dismal outlook for the near future, makes it obvious that exploitation of the Yellowknife pegmatite field solely for Ta would be highly uneconomical. The absence of a developed road system extending to areas of potentially minable pegmatites, and the relatively long distance from pegmatites to markets are also unattractive factors. The concentrations of Ta in most pegmatites are too low to be considered for mining purposes, and most of the Ta-rich pegmatites are small. In addition, the consistent presence of Sn and Ti as impurities would make the ore minerals unfavorable for processing. Concentration of Ta-minerals as a by-product along with perhaps

K-feldspar, beryl or spodumene might be considered a profitable venture, but even so, the number of pegmatites suitable for such a scale of operation seems to be limited.

CHAPTER 15

Summary and conclusions

The Archean Yellowknife pegmatite field of central Northwest Territories is populated by numerous pegmatites which have intruded large granite and granodiorite bodies and metasedimentary rocks within the aureoles of these plutons. The pegmatite population belongs to the rare-element class, ranging from predominantly barren bodies through beryl-columbite subtype to the less common spodumene subtype. Except for the barren pegmatites, most bodies of the mineralized subtypes contain concentrations of Nb,Ta and Sn. The Nb-, Ta- and Sn-oxide minerals constitute only a small fraction of the parent pegmatite, yet their chemistry is strongly indicative of the overall degree of fractionation attained by the pegmatite, and it directly reflects some overall geochemical features of the parent pegmatite melts/fluids.

The gross geochemical signature of the Yellowknife field as depicted by the Nb-, Ta- and Sn-oxide minerals is one of Fe and Nb dominance, with local enrichment in Ta, Sn and Ti . The clustering of columbite-tantalite compositions in the Fe-Nb quadrant of the columbite quadrilateral is overwhelming and reflects the primitive nature of the pegmatitic melt/fluid at the time of pegmatite consolidation. Mn-rich mineral species are rare, and ferrocolumbite, ferrotapiolite and Fe-rich ixiolite occur with the greatest frequency in both beryl-columbite and complex spodumene pegmatites.

Beryl-columbite subtype pegmatites always carry Fe- and Nb-dominant Nb,Ta mineral species except in the rare case where Ta enrichment proceeds to the point of ferrotantalite or ferrotapiolite crystallization. The Li-rich pegmatites of the Yellowknife field typically carry Nb- and Ta-oxide

minerals with Fe > Mn, quite unlike the Mn-rich compositions found in the Li-rich pegmatites of most fields of the world (e.g., Wang et al., 1981; von Knorring and Fadipe, 1981; Anderson,1984; Černý and Ercit, 1985). Closer examination of the accessory mineralogy of the Yellowknife pegmatites shows the absence of late F-rich minerals such as amblygonite, lepidolite and topaz, which is indicative of low F activity in the consolidating pegmatitic melt/fluid. This may be the primary cause of the poor Fe/Mn fractionation, although the evidence is only empirical and experimental confirmation is not available at present (Černý and Ercit, 1985).

In contrast to Fe/Mn fractionation, Nb/Ta fractionation within the Yellowknife pegmatites is much more extensive. The fractionation of Nb/Ta ideally proceeds towards Ta enrichment with progressive pegmatite fractionation. In the Yellowknife pegmatite field, this trend is well-illustrated by successively more Ta-rich mineral species with increasing fractionation. The progressive enrichment of Ta commonly proceeds from ferrocolumbite to ferrotantalite, ferrotapiolite and rare ixiolite. Like Mn enrichment, Ta enrichment is apparently also controlled by the activity of F (Černý et al., 1985a), but based on the Yellowknife data, other geochemical factors may play a major role. Extreme Nb/Ta fractionation seems to proceed with equal ease in both F-poor and F-enriched environments of the Yellowknife pegmatites. The Nb/Ta ratio decreasing without appreciable Fe/Mn reduction exhibited by the Yellowknife field is somewhat unique among other documented cases of otherwise well-fractionated and Li-enriched pegmatite fields (Černý and Ercit, 1985).

The Yellowknife pegmatite field never contains sufficient quantities of Ti to form Ti-based mineral species such as rutile or ilmenite, although

Nb and Ta minerals do concentrate significant quantities of Ti in their structures. Enrichment in Ti is typical of pegmatite series related to Ti-rich granites. On the other hand, Sn contents within columbite-tantalite and ferrotapiolite are generally low, and Sn-minerals such as cassiterite and ixiolite do occur frequently, but are generally restricted to highly fractionated spodumene-bearing pegmatites.

Structurally, Nb and Ta minerals of the Yellowknife field tend to show intermediate degrees of order rather than largely ordered or largely disordered. This uniform degree of structural state mimics the uniform character of the geochemistry of this mineral family, suggesting relatively similar conditions of crystallization for all pegmatites of the field. The primary control of the ordering is the disturbance of stoichiometery by Ti and Sn substitution; differential cooling histories might have played some role but cannot be documented.

From the economic viewpoint, the geochemical features of the Yellowknife pegmatite field preclude the occurrences of complex pegmatite subtypes carrying extensive Ta mineralization, such as the Tanco or Greenbushes deposits. Any significant concentrations of Ta that may be encountered in this field would be represented by high accumulations of oxide minerals with intermediate to high values of Nb/Ta, similar to those exploited from the Peg group in the past. The only chances of finding additional (and most probably hidden) deposits with low Nb/Ta ratios may be in the areas populated by the Buckham Lake and Bighill Lake series.

Recommendations for future research

The results of this study have not only added to the existing world-wide data base of Nb-, and Ta-oxide mineral analyses and unit cell dimensions, but has also greatly improved our basic understanding of Nb and Ta minerals in general. However, much work remains to be done in three respects.

(i) Follow-up regional studies in the Yellowknife field are desirable in areas showing particularly "anomalous" chemistries (e.g. Harding Lake series, Peg Group, Riber pegmatite). Particular emphasis should be placed on the role of F (and possibly Li and B) on Fe/Mn and Nb/Ta fractionation. More Ta and rare-alkali data is needed for muscovites in order to develop an adequate tool for the prospection of Ta-rich pegmatites.

(ii) Detailed studies of natural Nb- and Ta-mineral assemblages should focus on the geochemical evolution and paragenesis of coexisting phases, in order to establish the crystallization history of Nb and Ta minerals in geochemically different pegmatite types. Information gained from natural assemblages should be supplemented by extensive laboratory phase equilibria work.

(iii) Additional crystallochemical studies are desirable for columbite-tantalite, ixiolite and the tapiolite series, focusing primarily on order-disorder relationships; this would require systematic structure refinements on specimens of various compositions and structural states.

REFERENCES

Aleksandrov, I.V. and Trusikova, T.A. (1973): On the relations among structural types of tin, niobium and tantalum minerals according to geological and experimental data. Geochemistry International, 10, 604-608.

_____, Trusikova, T.A. and Tupitsin, B.P. (1969): Niobium and tantalum in carbon dioxide solutions. Geochemistry International, 6, 558-566.

Anderson, A.J. (1984): The geochemistry, mineralogy and petrology of the Cross Lake pegmatite field, central Manitoba. M.Sc. thesis, University of Manitoba, Winnipeg, Manitoba.

Appleman, D.E. and Evans, H.T. Jr. (1973): Job 9214: Indexing and least-squares refinement of powder diffraction data. U.S. Geological Survey, Computer Contributions 20; NTIS Document PB2-16188.

Bailey, J.C. (1977): Fluorine in granitic rocks and melts: a review. Chemical Geology, 19, 1-42.

Banerjee, S.K., Johnson, C.E. and Krs, M. (1970): Mössbauer study to find the origin of weak ferromagnetism in cassiterite. Nature 225, 173-175.

Beugnies, A. and Mozafari, Ch. (1968): Contribution a l'étude des propriétés des columbotantalites et des tapiolites. Annales de la Société Géologique de Belgique, 91, 35-91.

Beus, A.A. (1966): Distribution of tantalum and niobium in muscovites from granitic pegmatites. Geokhimiya, 1216-1220 (in Russian).

_____, Berengilova, V.V., Grabovskaya, L.I., Kotchemasov, G.G., Leontyneva, L.A. and Sitnin, A.A. (1968): Geochemical Exploration for Endo-

genic Deposits of Rare Elements. Nedra, Moscow; English translation: Geological Survey of Canada Library, Ottawa.

Brandt, K. (1943): X-ray studies on ABO_4 compounds of rutile type and AB_2O_6 compounds of columbite type. Arkiv för Kemi, Mineralogi och Geologi, 17A, no. 158., 1-8.

Cameron, E.N., Jahns, R.H., McNair, A.H. and Page, L.R. (1949): Internal structure of granitic pegmatites. Economic Geology Monograph, v. 2, 115 p.

Canadian Superior Exploration, Ltd. (1975), Index map - Best Bet claim: unpublished map, Vancouver, B.C., Drawing I-7, scale 1:21600, 1 sheet.

_____ (1975), Index map - Greg Dykes & QI claims: unpublished map, Vancouver, B.C., Drawing I-7, scale 1:21600, 1 sheet.

Černý, P. (1982a): Anatomy and classification of granitic pegmatites. In Granitic Pegmatites in Science and Industry (P. Černý, ed.). Mineralogical Association of Canada, Short Course Handbook, 8, 1-39.

_____ (1982b): The Tanco pegmatite at Bernic Lake, southeastern Manitoba. In Granitic Pegmatites in Science and Industry (P. Černý, ed.). Mineralogical Association of Canada, Short Course Handbook, 8, 527-543.

_____ (1987): Rare-Element Granitic Pegmatites. Geological Association of Canada, Monograph Series on Mineral Deposits Geology, A.C. Brown, ed., (in press).

_____ and Ercit, T.S. (1985): Some recent advances in the mineralogy and geochemistry of Nb and Ta in rare-element granitic pegmatites. Bulletin de Minéralogie, 108, 499-532.

_____, Ercit, T.S. and Wise, M.A. (1986a) Mineralogy, paragenesis and geochemical evolution of Nb-, and Ta-oxide minerals in granitic pegmatites. 14th General Meeting of the International Mineralogical Association Programs with Abstracts, 71.

_____, Goad, B.E., Hawthorne, F.C. and Chapman, R. (1986b): Fractionation trends of the Nb- and Ta-oxide minerals in the Greer Lake pegmatitic granite and its pegmatite aureole, southeastern Manitoba. American Mineralogist, 71, 501-517.

_____, Hawthorne, F.C., LaFlamme, J.H.G. and Hinthorne, J.R. (1979): Stibiobetafite, a new member of the pyrochlore group from Vezná, Czechoslovakia. Canadian Mineralogist, 17, 583-588.

_____, Meintzer, R.E. and Anderson, A.J. (1985a): Extreme fractionation in rare-element granitic pegmatites: selected examples of data and mechanisms. Canadian Mineralogist, 23, 381-421.

_____, Roberts, W.L., Ercit, T.S. and Chapman, R. (1985b): Wodginite and associated oxide minerals from the Peerless pegmatite, Pennington County, South Dakota. American Mineralogist, 70, 1044-1049.

_____, Trueman, D.L., Zeihlke, D.V., Goad, B.E. and Paul, B.J. (1981): The Cat Lake-Winnipeg River and Wekusko Lake pegmatite fields, Manitoba. Manitoba Department Mines Economic Geology Report ER80-1, 230 p.

_____ and Turnock, A.C. (1971): Niobium-tantalum minerals from granitic pegmatites at Greer Lake, southeastern Manitoba. Canadian Mineralogist, 10, 755-772.

Clark, A.M. and Fejer, E.E. (1978): Tapiolite, its chemistry and cell dimensions. Mineralogical Magazine, 43, 477-480.

_____, Fejer, E.E., Donaldson, J.D. and Silver, J. (1976): The ^{119}Sn Mössbauer spectra, cell dimensions and minor element contents of some cassiterites. Mineralogical Magazine, 40, 895-898.

Colby, J.W. (1980): MAGIC V - a computer program for quantitative electron-excited energy dispersive analysis. In QUANTEX-Ray Instruction Manual, Kevex Corporation, Foster City, California.

Cromer, D.T. and Liberman, D. (1970): Relativistic calculation of anomalous scattering factors for X-rays. Journal of Chemical Physics, 53, 1891-1898.

_____ and Mann, J.B. (1968): X-ray scattering factors computed from numerical Hartree-Fock wave functions. Acta Crystallographica, A24, 321-324.

Ercit, T.S. (1986): The simpsonite paragenesis: the crystal chemistry and geochemistry of extreme tantalum fractionation: Ph.D. thesis, University of Manitoba, Winnipeg, Manitoba.

Eskova, E.M. (1964): Niobium, in Geochemistry, mineralogy and genetic types of deposits of rare elements, v. 1 of Geochemistry of rare elements. Moscow, Izdatel'stovo "Nauka," p. 342-372 (in Russian).

Ewing, R.C. (1975): The crystal chemistry of complex niobium and tantalum oxides: IV. The metamict state. Discussion. American Mineralogist 60, 728-733.

Ferguson, R.B., Hawthorne, F.C. and Grice, J.D. (1976): The crystal structures of tantalite, ixiolite and wodginite from Bernic Lake, Manitoba. II. Wodginite. Canadian Mineralogist, 14, 550-560.

Ferreira, K.J. (1984): The mineralogy and geochemistry of the Lower Tanco pegmatite, Bernic Lake, Manitoba, Canada. M.Sc. thesis, University of Manitoba, Winnipeg, Manitoba.

Fersman, A.E. (1940): Pegmatites: In: Selected Works, v. 4, Moscow 1960 Acad. Sci. U.S.S.R., Moscow (in Russian).

Flörke, O.W., Gebert, W. and Wedepohl, K.H. (1974): Tantalum. In Handbook of Geochemistry 73, Springer-Verlag, Berlin.

Foord, E.E. (1976): Mineralogy and petrogenesis of layered pegmatite-aplite dikes in the Mesa Grande district, San Diego County, California. Ph.D. thesis, Stanford University, Stanford, California.

_____ (1982): Minerals of tin, titanium, niobium and tantalum in granitic pegmatites. In Granitic Pegmatites in Sciences and Industry (P. Černý, ed.). Mineralogical Association of Canada, Short Course Handbook 8, 187-238.

_____ and Cook, R.B. (1987): Mineralogy and paragenesis of the McAllister Sn-Ta pegmatite deposit, Coosa County, Alabama. Submitted to Canadian Mineralogist.

Fortier, Y.O. (1946): Preliminary Map, Yellowknife-Beaulieu Region, Northwest Territories. Geological Survey of Canada, Paper 46-23, scale 1:253440, 1 sheet.

von Gaertner, H.R. (1930): The crystal structure of loparite and pyrochlore. Neues Jahrbuch für Mineralogie Geol., Bd. 61, 1-30., (in German).

Gaupp, R., Möller, P., and Morteani, G. (1984): Tantal-Pegmatite: Geologische, petrologische und geochemische Untersuchungen. Monograph Series on Mineral Deposits, 23, Borntraeger Berlin-Stuggart, 124.

Giese, R.F. (1975): Electrostatic energy of columbite/ixiolite. Nature, 256, 31-32.

Ginzburg, A.I. (1956): On some characteristics of tantalum goechemistry and on the types of tantalum mineralization. Geokhimiya, 74-83 (in Russian).

_____ (1960): Specific geochemical features of the pegmatite process. Report of the 21st International Geological Congress, 17, 111-121.

Goldschmidt, V.M. (1926): Geochemische Verteilungsgesetze der Elemente. VI. Uber die Kristallstrukturen vom Rutiltypus mit bermerkukngen zur Geochemie Zweiwertigen und Vierwiertigen Elemente. Vidensk. Akad. i Oslo I, Math-Nat. Kl., skr. 1 paper 1, 5-21.

Gordiyenko, V.V. (1970): Mineralogy, geochemistry and genesis of the spodumene pegmatites. Nedra Leningrad 237 pp. (in Russian).

Gorzhevskaya, S.A., Sidorenko, G.A. and Ginzburg, A.I. (1974): Titano-tantalo-niobates. Moscow, 344 p. (in Russian).

Graham, J. (1975): The crystal chemistry of complex niobium and tantalum oxides: IV. The metamict state. Reply. American Mineralogist, 60, 734.

_____ and Thornber, M.R. (1974a): The crystal chemistry of complex niobium and tantalum oxides. I. Structural classification of MO_2 phases American Mineralogist, 59, 1026-1039.

_____ and Thornber, M.R. (1974b): The crystal chemistry of complex niobium and tantalum oxides: IV. The metamict state. American Mineralogist, 59, 1047-1050.

Grice, J.D. (1970): The nature and distribution of the tantalum minerals in the Tanco Mine pegmatite at Bernic Lake, Manitoba: Unpublished M.Sc. thesis, University of Manitoba, Winnipeg, Manitoba.

_____ (1973): Crystal structures of the tantalum oxide minerals tantalite and wodginite, and of millerite NiS. Ph.D. thesis, University of Manitoba, Winnipeg, Manitoba.

_____, Ferguson, R.B. and Hawthorne, F.C. (1976): The crystal structures of tantalite, ixiolite and wodginite from Bernic Lake, Manitoba. I. Tantalite and ixiolite. Canadian Mineralogist, 14, 540-549.

Groat, L.A., Černý, P. and Ercit, T.S. (1987): Reinstatement of stibiomicrolite as a valid species. Geologiska Foreningen i Stockholm Forhandlingar v. 109 (in press).

Groult, D., Pannetier, J. and Raveau, B. (1982): Neutron diffraction study of the defect pyrochlores $TaWO_{5.5}$, $H_2Ta_2O_6$, and $HTaWO_6 \cdot H_2O$. Journal of Solid State Chemistry, 41, 277-285.

Groves, W.D. (1978): Report on the Elk #1 mineral property, Hearne Channel, Great Slave Lake, N.W.T., for Hemisphere Development Corporation. Unpublished report (Document #080948, Geology Division, Yellowknife, Canada Department of Indian Affairs and Northern Development).

_____ (1980): Geological evaluation report on the Jake #1 mineral claim, Harding Lake, N.W.T., for Amhawk Resource Croporation. Unpublished report (Document #081139, Geology Division, Yellowknife, Canada Department of Indian Affairs and Northern Development).

_____ (1981): Geological evaluation report on Elk lithium-columbite tantalite pegmatite property and adjoining Beck 1, Beck 2, and Beck 3 claims. unpublished report, vancouver, B.C., Archean Resources Corp. (Document #081389), Geology Division, Yellowknife, Canada Department of Indian Affairs and Northern Development).

Grubb, P.L.C. and Hannaford, P. (1966): Ferromagnetism and colour zoning in some Malayan cassiterite. Nature, 209, 677-678.

Hawthorne, F.C. (1985): Refinement of the crystal structure of bloedite: Structural similarities in the $[\,^{VI}M(^{IV}T\Phi_4)_2\Phi_n]$ finite-cluster minerals. Canadian Mineralogist 23, 669-674.

von Heidenstam, O. (1968): Neutron and X-ray diffraction studies on tapiolite and some synthetic substances of trirutile structure. Arkiv För Kemi, Band 28, 375-387.

Heinrich, E.Wm. (1962): Geochemical prospecting for beryl and columbite. Economic Geology, 57, 616-619.

Henderson, J.B. (1985): Geology of the Yellowknife - Herne Lake Area, District of Mackenzie: A segment across an Archean basin. Geological Survey of Canada Memoir 414, 135 p.

Heywood, W.W. and Davidson, A. (1969): Geology of the Benjamin Lake Map Area, District of Mackenzie (75M/2). Geological Survey of Canada Memoir 361, 35 p.

Hildreth, W. (1979): The Bishop Tuff: evidence for the origin of compositional zonation in silicic magma chambers. Geological Society of America, Special Paper 180, 43-75.

_____ (1981): Gradients in silicic magma chambers: implications for lithospheric magmatism. Journal of Geophysical Research, 86, 10153-10192.

Hogarth, D.D. (1977): Classification and nomenclature of the pyrochlore group. American Mineralogist, 62, 403-410.

Hutchinson, R.W. (1955a): Regional zonation of pegmatites near Ross Lake, District of Mackenzie, Northwest Territories. Geological Survey of Canada, Bulletin 34, 50 p.

_____ (1955b): Preliminary report on investigations of minerals of columbium and tantalum and of certain associated minerals. American Mineralogist, 40, 432-452.

Hutton, C.O. (1958): Notes on tapiolite, with special reference to tapiolite from southern Westland, New Zealand. American Mineralogist, 43, 112-119.

Jolliffe, A.W. (1943): Tin and Tantalum Deposits, Sproule Lake, Ross Lake area, Northwest Territories. unpublished report, Geological Survey of Canada, 3 p.

_____ (1944): Rare element minerals in pegmatites, Yellowknife-Beaulieu area, Northwest Territories. Geological Survey of Canada, Paper 44-12, 24 p.

von Knorring, O. and Condliffe, E. (1984): On the occurrence of niobium, tantalum, and other rare element minerals in Meldon aplite, Devonshire. Mineralogical Magazine, 48, 443-448.

_____ and Fadipe, A. (1981): On the mineralogy and geochemistry of niobium and tantalum in some granite pegmatites and alkali granites of Africa. Bulletin de Minéralogie, 104, 496-507.

Kamineni, D.C. (1975): Chemical mineralogy of some cordierite-bearing rocks near Yellowknife, Northwest Territories, Canada. Contributions to Mineralogy and Petrology, 53, 293-310.

Komkov, A.I. (1970): Relationship between the X-ray constants of columbite and composition. Academy of Sciences USSR Doklady, 195, 434-436 (in Russian).

_____ (1974): Quantitative criteria for evaluating the degree of order of columbite and tapiolite. In "Kristallokhimiya i Strukturnaya Mineralogiya"., V.A. Frank-Kamentskiy, ed., Nauka Leningrad, 75-82 (in Russian).

_____ and Dubik, O,Yu. (1974): On the conditions of stability of columbite $FeNb_2O_6$ and tapiolite $FeTa_2O_6$ In "Kristallokhimiya i Struktunaya Mineralogiya", V.A. Frank-Kamenetskyi, ed., Nauka Leningrad, 25-30 (in Russian).

Kornetova, V.A. (1961): Some observations on the columbite-tantalite mineral group. Trudy Mineralogicheskogo Museya Akademii Nauk SSSR, 12, 65-69 (in Russian).

Kretz, R. (1968): Study of pegmatite bodies and enclosing rocks, Yellowknife-Beaulieu region, District of Mackenzie. Geological Survey of Canada, Bulletin 159, 109 p.

Kuzmenko, M.V. (1959): The geochemisty of tantalum and niobium. Akademii Nauk SSSR Instituta Mineralogogiya, Geokhimiya i Kristallokhimiya Redkikh Elementov Trudy, v. 3, p. 3-25 (in Russian); translation in International Geology Review (1961): v. 3, no. 1,p. 9-25.

_____ (1964): Tantalum, in Geochemistry, mineralogy and genetic types of deposits of rare elements. v.1 of Geochemistry of rare elements. Moscow, Izdatelstvo "Nauka", p. 373-402 (in Russian); translations, New York, Daniel Davey and Co., 1966.

Lahti, S.I. (1982): A new pseudo-orthorhombic wodginite variety from the Eräjärvi pegmatite area. Geologi, 34, No. 1, 6-7 (in Finnish).

_____, Johanson, B. and Virkkunen, M. (1983): Contributions to the chemistry of tapiolite - manganotapiolite, a new mineral. Bulletin of the Geological Society of Finland, 55, 101-109.

LeCouteur, P.C. (1980a): Assessment report, geochemical survey on Bet #1 and #2 claims, Yellowknife-Beaulieu River area, N.W.T., Mackenzie Mining District (85-I-1); unpublished report, vancouver, B.C., Cominco Ltd.

(Document #081132, Geology Division, Yellowknife, Canada Department of Indian Affairs and Northern Development).

_____ (1980b): Assessment report, geochemical survey on LITA claim, Yellowknife - Beaulieu River area, N.W.T., Mackenzie Mining District (85-I-1; 62°44'N, 113°30'W): unpublished report, Vancouver, B.C., Cominco, Ltd. (Document #081123, Geology Division, Yellowknife, Canada Department of Indian Affairs and Northern Development).

_____ (1980c): Assessment report, geochemical survey on MOSK and TIP claims, Yellowknife-Beaulieu River area, N.W.T., Mackenzie Mining District: unpublished report, Vancouver, B.C., Cominco Ltd. (Document #081125, Geology Division, Yellowknife, Canada Department of Indian Affairs and Northern Development).

_____ (1980d): Assessment report, geochemical survey on TABE claim, Yellowknife - Beaulieu River area, N.W.T., Mackenzie Mining District (85-I-1; 62°38'N, 113°29'W): unpublished report, Vancouver, B.C., Cominco, Ltd. (Document #081134, Geology Division, Yellowknife, Canada Department of Indian Affairs and Northern Development).

London, D. (1986): The magmatic-hydrothermal transition in the Tanco rare-element pegmatite: evidence from fluid inclusions and phase equilibrium experiments. American Mineralogist, 71, 376-395.

Lord, C.S. (1951): Mineral Industry of District of Mackenzie, Northwest Territories. Geological Survey of Canada, Memoir 261, 336 p.

Lumpkin, G.R., Chakoumakos, B.C. and Ewing, R.C. (1986): Mineralogy and radiation effects of microlite from the Harding pegmatite, Taos County, New Mexico. American Mineralogist, 71, 569-588.

McGlynn, J.C. (1977): Geology of Bear-Slave structural provinces, District of Mackenzie, Northwest Territories. Geological Survey of Canada, Open File 445.

_____ and Henderson, J.B. (1972): The Slave Province, in Price, R.A., and Douglas, R.J.W., eds., Variations in Tectonic Styles in Canada. Geological Associations of Canada Special Paper 11, 505-526.

Meintzer, R.E. (1987): The Mineralogy and Geochemistry of the Granitoid Rocks and Related Pegmatites of the Yellowknife Pegmatite Field, Northwest Territories. Unpublished Ph.D. thesis, University of Manitoba, Winnipeg, Manitoba.

_____ and Černy, P. (1983): Geological studies of rare element pegmatites in the Yellowknife basin of N.W.T. in Mineral Industry Report, 1978, Northwest Territories. Canada Department of Indian Affairs and Northern Development, EGS 1983-2, 189-202.

_____, Wise, M.A. and Černý, P. (1984): Distribution and structural setting of fertile granites and related pegmatites in the Yellowknife pegmatite field, District of Mackenze: in Current Research, Part A, Geological Survey of Canada, Paper 84-1A, 373-381.

Moreau, J. and Tramasure, G. (1965): Contribution a l'étude des séries columbite-tantalite et tapiolite-mossite. Annales de la Société Géologique de Belgique, 88, 301-391.

Morrison, M. (1975a): ANN pegmatite, District of Mackenzie, N.W.T.: unpublished map, Vancouver, B.C., Canadian Superior Exploration Ltd., Drawing 75-10, scale 1:960, 1 sheet.

_____ (1975b): Report on a geological survey of the BIG 1-13 mineral claims, Yellowknife area, District of Mackenzie, N.W.T.: unpublished report, Vancouver, B.C., Canadian Superior Exploration, Ltd.

(Document #080273, Geology Division, Yellowknife, Canada Department of Indian Affairs and Northern Development).

_____ (1975c): Report on a geological survey of the FI 2-7, 9-14 mineral claims, Yellowknife area, District of Mackenzie, N.W.T.: unpublished report, Vancouver, B.C., Canadian Superior Exploration, Ltd. (Document #080282, Geology Division, Yellowknife, Canada Department of Indian Affairs and Northern Development).

_____ (1975d): Report on a geological survey of the NITE 1-3 and 5-7 mineral claims, Yellowknife area, District of Mackenzie, N.W.T.: unpublished report, Vancouver, B.C., Canadian Superior Exploration, Ltd. (Document #080290, Geology Division, Yellowknife, Canada Department of Indian Affairs and Northern Development).

_____ (1975e): Report on a geological survey of the THOR 1-13 mineral claims, Yellowknife area, District of Mackenzie, N.W.T.: unpublished report, Vancouver, B.C., Canadian Superior Exploration, Ltd. (Document #080478, Geology Division, Yellowknife, Canada Department of Indian Affairs and Northern Development).

_____ (1978): A report on the 1978 drilling programme performed on the VO 1-9 mineral claims, Yellowknife area, District of Mackenzie, N.W.T.: unpublished report, Vancouver, B.C., Canadian Superior Exploration, Ltd. (Document #080833, Geology Division, Yellowknife, Canada Department of Indian Affairs and Northern Development).

Mosher, D.V. (1969): Report on pegmatite bodies occurring in the Yellowknife-Beaulieu region, District of Mackenzie, N.W.T., for Tantalum Mining Corporation of Canada, Limited, Toronto, Ont., A.C.A. Howe International, Ltd., Report #248 (Document #060386, Geology Division, Yellowknife, Canada Department of Indian Affairs and Northern Development).

Mulligan, R. (1965): Geology of Canadian lithium deposits. Geological Survey of Canada Economic Report, 21, 131 p.

Nickel, E.H., Rowland, J.F. and McAdam, R.C. (1963a): Ixiolite, a columbite substructure. American Mineralogist, 48, 961-979.

_____, Rowland, J.F. and McAdam, R.C. (1963b): Wodginite, a new tin-manganese tantalite from Wodgina, Australia and Bernic Lake, Manitoba. Canadian Mineralogist, 7, 390-402.

Odikaze, G.L. (1958): On the presence of niobium and tantalum in muscovites from pegmatites of the Dzirula crystalline massif. Geokhimiya, 479-485 (in Russian).

Padgham, W.A. (1985): Observations and speculations on supracrustal sucessions in the Slave Structural Province, in Ayres, L.D., Thurston, P.C., Card, K.D., and Weber, W., eds., Evolution of Archean Supracrustal Sequences. Geological Association of Canada Special Paper 28, 133-151.

Page, L.R. and others (1953): Pegmatite Investigations 1942-1945, Black Hills, South Dakota. U.S. Geological Survey Professional Paper 247, 228 p.

Papike, J.J., Shearer, C.K., Jolliff, B.L., Duke, E.F., Redden, J.A., Walker, R.J. and Laul, J.C. (1986): Proterozoic granite/pegmatite systems of the Black Hills, S.D.. 14th General Meeting of the International Mineralogical Association Programs with Abstracts, 195.

Parker, R.L. and Fleischer, M. (1968): Geochemistry of niobium and tantalum. U.S. Geological Survey Professional Paper 612, 43 p.

Polyakov, V.O. and Cherepivskaya, G.E. (1981): Ixiolite from the Ilmen Mountains. Mineralogicheskii Zhurnal, 1, 67-75 (in Russian).

Rankama, K. (1944): On the geochemistry of tantalum. Findlande Comm. Géol. Bulletin, no. 133, p. 1-78.

_____ (1948): On the geochemistry of niobium. Acad. Sci. Fennicae Annales, ser. A, III, Geological-Geog., no. 13, p. 1-57.

Rowe, R.B. (1952): Pegmatite deposits of the Yellowknife-Beaulieu region, District of Mackenzie. Geological Survey of Canada, Paper 52-8.

Schröcke, H. (1966): Solid equilibria within the columbite-tapiolite group, and of the columbite-tapiolite group with $YTi(Nb,Ta)O_6$, euxenite, and $FeNbO_4$. Neues Jahrbuch für Mineralogie Abhandlungen, 106, 1-54. (in German).

_____ (1972): Zur Kenntnis des Systems SnO_2 - TiO_2. Neues Jahrbuch für Mineralogie Monatshefte, 181-185. (in German).

Shannon, R.D. (1976): Revised effective ionic radii and systematic studies of interatomic distances in halides and chalcogenides. Acta Crystallographica, A32, 751-767.

Shaw, H.R. (1974): Diffusion of H_2O in granitic liquids. In Geochemical Transport and Kinetics (A.W. Hofmann, B.J. Giletti, H.S. Yoder, Jr. and R.A. Yund, eds.). Carnegie Institute of Washington Publication 634, 139-170.

Shawe, D.R. (1968): Geology of the Spor Mountain beryllium district, Utah. In Ore Deposits of the United States, 1933-1967, 2 (J.D. Ridge, ed.). AIMMPE, New York, 1148-1161.

Solodov, N.A. (1971): Scientific Principles of Perspective Evaluation of Rare-element Pegmatites. Nauka, Moscow, (in Russian).

Stacey, N.W. (1981a): Report on the phase one field programme on the Jake #1 and Jake #2 mineral claims, for Anhawk Resource Corporation. Unpub-

lished report (Document #081352, Geology Division, Yellowknife, Canada Department of Indian Affairs and Northern Development).

_____ (1981b): Report on phase one of the field programme on Pancho #1 and Pancho Villa mineral claims, Mackenzie mining distict, N.W.T., Canada for Powergem Resources Corp.: unpublished report (Document #081462, Geology Division, Yellowknife, Canada Department of Indian Affairs and Northern Development).

Sturdivant, J.H. (1930): The crystal structure of columbite. Zeitschrift für Kristallographie, 75, 88-108.

Thomas, D.G. (1980): Big Hill #1 claim, Hearne Channel, N.W.T.: unpublished report, Calgary, Alta., Highwood Resources, Ltd. Document #081266, Geology Division, Yellowknife, Canada Department of Indian Affairs and Northern Development).

_____ (1982): Tan Group, Blatchford Lake area, Northwest Territories: unpublished report, Calgary, Alta., for Kappa Resources, Ltd. (Document #062140, Geology Division, Yellowknife, Canada Department of Indian Affairs and Northern Development).

Thomas, A.V. and Spooner, E.T.C. (1984): Petrological evidence for downward and upward non-replacive crystallization in the growth sequence lower wall zone, Ta(-Sn) bearing banded albitite, beryl fringe to quartz core, Tanco pegmatite, Manitoba. Geological Association of Canada-Mineralogical Association of Canada Programs with Abstracts, 9, 111.

Turnock, A.C. (1966): Synthetic wodginite, tapiolite and tantalite. Canadian Mineralogist, 8, 461-470.

Vlasov, K.A., ed. (1966a): Geochemistry and mineralogy of rare elements and genetic types of their deposits, Niobium, in v.1, Geochemistry of

rare elements. Israel Program for Scientific Translations, Jerusalem, (1966), p. 335-367.

_____ (1966b): Geochemistry and mineralogy of rare elements and genetic types of their deposits, Tantalum, in v.1, Geochemistry of rare elements. Israel Program for Scientific Translations, Jerusalem, (1966), p. 368-396.

Voronina, L.B., Gaydukova, V.S., Dobrovolskaya, N.V. and Korovushkin, V.V. (1978): Forms of occurrence of iron in cassiterite. Geochemistry International, 15, 128-143.

Van Wambeke, L. (1970): The alteration processes of the complex titano-niobo-tantalates and their consequences. Neues Jahrbuch für Mineralogie, 112, 117-149.

Wang, X.-J., Zou, T.-R., Xu, X.-Y. and Qiu, Y.-Zh. (1981): Study of pegmatite minerals of the Altai region. Science Publishing House, Beijing, 140 p. (in Chinese).

Wang, Y.-R., Li, J.-T., Lu, J.-L. and Fan, W.-L. (1982): Geochemical mechanism of Nb-, and Ta-mineralization during the late stage of granite crystallization. Geochemistry Bejing 1, 175-185.

Weast, R.C., Astle, M.J. and Beyers, W.H. (eds.) (1986): CRC Handbook of Chemistry and Physics, 67th ed.. CRC Press Inc., Boca Raton, Florida.

Weitzel, H. (1976): Crystal structure refinement of wolframite and columbite. Zeitschrift für Kristrallographie, 144, 238-258 (in German).

_____ and Klein, S. (1974): Magnetic structure of the trirutile $FeTa_2O_6$. Acta Crystallographica, A30, 380-384 (in German).

Wise, M.A. and Černý, P. (1986): The status of ixiolite. 14th General Meeting of the International Mineralogical Association Programs with Abstracts, 265.

_____, Meintzer, R.E. and Černý, P. (1985a): Final report on the geological field study YK 83-84/008, the Yellowknife pegmatite field: Mineralogy and geochemistry of Nb, Ta, Sn oxide minerals, in Contributions to the Geology of the Northwest Territories, v. 2: Geology Division, Yellowknife, Canada Department of Indian Affairs and Northern Development EGS 1985-6, 15-25.

_____, Meintzer, R.E. and Černý, P. (1987): in press, Phosphate mineralogy of the Yellowknife pegmatite field, in Contributions to the Geology of the Northwest Territories, v. 3: Geology Division, Yellowknife, Canada Department of Indian Affairs and Northern Development.

_____, Turnock, A.C. and Černý, P. (1985b): Improved unit cell dimesions for ordered columbite-tantalite end members. Neues Jahrbuch für Mineralogie Monatshefte, 372-378.

Appendix A

MISCELLANEOUS INFORMATION FOR YELLOWKNIFE SAMPLES

Table 33: Miscellaneous information for Yellowknife samples.

Probe No.	Sample No.	Oxide Minerals	Habit	Association	XRD	Probe
YKF-1	Mac-9	Ct,Ix,Cs	Mas	Clv	H	x
YKF-2	Mac-11	Ct,Ix	Mas	Clv,Brl	H	x
YKF-3	Moose-7	Ct	Tab	Qtz,Clv,Mus	H	x
YKF-4	Moose-9	Ct	Tab	Qtz,Clv,Mus	H	x
YKF-5	Moose-12	Ct	Bld	Clv,Qtz,Amb	H	x
YKF-6	Moose-16	Ct	Pty	Clv,Qtz	H	x
YKF-7	Jo-17	U			X	
YKF-8	Jo-18	Ct	Pty	Clv,Qtz,Amb	H	x
YKF-9	Bet-4	Ct,Tp	Pty	Qtz	H	x
YKF-10	Bet-15	Ct	Bld	Clv,Amb	H	x
YKF-11	The-Ar-A-2	Ct	Bld	Plg,Qtz,Mus		x
YKF-12	The-Ar-G-3	Ct	Tab	Qtz,Plg,Mus	H	x
YKF-13	The-C-A-1					
YKF-14	The-C-E-2					
YKF-15	The-C-F-1-1	Ct	Bld	Clv,Qtz,Spd		x
YKF-16	The-En-4	Ct	Tab	Qtz	H	x
YKF-17	The-En-22-1					
YKF-18	The-Pn-A-4	Ct	Pty	Kfs,Qtz,Spd	N	x
YKF-19	The-Pn-A-10	Ct	Bld	Qtz,Kfs,Mus		x
YKF-20	The-Pw-3	Ct	Tab	Kfs	H	x
YKF-21	The-Pw-4	Ct	Bld	Kfs,Spd,Qtz		x
YKF-22	The-Sn-B-1	Ct	Tab	Clv,Qtz,Mus	H	x
YKF-23	The-T-7	Ct	Mas	Kfs,Plg,Qtz	H	x
YKF-24	The-W-1	Ct	Tab	Kfs,Qtz	H	x
YKF-25	The-W-10	P				
YKF-26	Usk-14-2	P				
YKF-27	Lit-2-2	Ct	Pty	Qtz,Mus	H	x
YKF-28	Lit-4-4	Ct	Mas	Clv	X	x
YKF-29	Mac-109	Ct	Col	Clv	H	x
YKF-30	Mac-111	Ct	Tab	Clv,Spd	H	x
YKF-31	Mac-112	Ct,Ix	Pty	Clv,Mus	H	x
YKF-32	Mac-115	Ct	Pty	Clv	H	x
YKF-33	Ann-T-5					
YKF-34	Ann-R-2	Ct	Pty	Qtz		x
YKF-35	Ann-P-1		Pty	Clv	H	x
YKF-36	Ann-O-3	Ct	Pty	Clv		x
YKF-37	Ann-N-1	Ct	Pty	Clv	H	x
YKF-38	Rib-A-7-A	Ct,Mc	Tab	Clv,Qtz	H	x
YKF-40	Waco-A-3	Ct,Cs	Tab	Kfs	X	x
YKF-41	Waco-A-4	Ct	Tab	Kfs		x
YKF-42	Waco-A-5	Ct	Mas		X	x
YKF-43	Waco-A-8	Zir,U	Pty	Qtz	H	x
YKF-44	Waco-A-9	Ct	Mas	Qtz	H	x
YKF-45	Bet-104	Ct	Pty	Clv	H	x
YKF-46	Bet-105	Ct	Pty	Clv	H	x
YKF-47	Bet-106	Ct	Pty	Clv	X	x
YKF-48	Bet-107	Ct	Pty	Clv	H	x
YKF-49	Tan-3-1	Ct	Pty	Kfs		x
YKF-50	Tan-4-1	Ct,Tp	Col	Kfs	N	x
YKF-51	Tan-4-2	Zir,U				x
YKF-52	Tan-4-3	Tp,Cs,Ct	Mas	Mus,Qtz,Plg	H	x
YKF-53	Moose-100	Ct	Pty	Qtz,Clv	X	x
YKF-54	Moose-101	Ct	Pty	Qtz	N	x
YKF-55	Moose-102	Ct	Pty	Amb,Clv	H	x
YKF-56	Moose-103	Ct	Bld	Qtz	X	x
YKF-57	Moose-104	Ct	Bld	Qtz,Amb	H	x
YKF-58	Moose-105	Ct	Tab	Amb	X	x
YKF-59	Cata-I-10	Ct	Pty	Clv	X	x
YKF-60	Cata-I-2	Ct	Col	Clv	H	x
YKF-61	Cata-G-1					
YKF-62	Tan-1-1	Ct	Pty	Clv		x
YKF-63	Tan-1-2					
YKF-64	Tan-2-1					
YKF-65	Tan-2-2	Tp	Pty	Qtz		x
YKF-66	Freda-3	Ct	Mas		H	x
YKF-67	Freda-4		Mas		H	
YKF-68	Freda-8	Cs	Mas		X	x
YKF-69	Cata-T-2	Ct,Cs	Mas	Plg,Qtz,Mus	N	x
YKF-70	Cata-S-1	U				x
YKF-71	Cata-U-1	Cs	Mas	Plg,Mus,Qtz	N	x
YKF-72	Peg-95-8					
YKF-73	Peg-93-3		Pty	Qtz	X	x
YKF-74	Peg-93-20	Ct	Tab	Plg	H	x
YKF-75	Peg-93-27	Ct	Tab	Plg	X	x
YKF-76	Peg-93-35	Tp,Cs,Mc	Tab	Qtz,Plg	H	x
YKF-77	Peg-93-43	Ct	Tab	Plg	X	x
YKF-78	Peg-M-1	Ct	Mas	Plg		x
YKF-79	Peg-1-3	Cs,Ct	Pty	Plg	N	x
YKF-80	Peg-1-12	Cs	Tab			x
YKF-81	Peg-1-4	Cs,Ct	Pty	Plg,Qtz,Mus	N	x
YKF-82	Peg-8-1-A	Ct	Mas	Plg		x
YKF-83	Peg-8-3					
YKF-84	Peg-8-4	Tp,Ct	Mas	Qtz,Mus,Plg	H	x
YKF-85	Peg-75-11	Ct	Pty	Plg,Spd	H	x
YKF-86	Peg-93-42	Ct	Tab	Plg	X	x
YKF-87	Peg-93-30		Tab	Plg	H	x
YKF-88	Peg-93-31	Ct	Pty	Mus,Plg	X	x
YKF-89	Peg-95-20	Ct	Pty	Mus,Qtz	H	x
YKF-90	Peg-95-16	Sph				x
YKF-91	Peg-97-9					
YKF-92	Peg-97-14	Ct	Pty	Spd,Plg		x
YKF-93	Peg-97-16	Ct	Pty	Kfs	H	x
YKF-94	Peg-65-2A	Gar				
YKF-95	Peg-170-16	Ct	Mas	Qtz		x
YKF-96	Peg-170-8	Ct	Mas	Plg	H	x
YKF-97	Peg-186-1				x	
YKF-98	Peg-264-6	Gah				
YKF-99	Peg-285-4	Ct	Pty	Plg,Qtz	H	x
YKF-100	Peg-310A-4					
YKF-101	Peg-319-1	Tp	Mas	Plg	H	x
YKF-102	Peg-319-2	Tp	Mas	Brl	H	x
YKF-103	Peg-97-17					
YKF-104	Peg-170-4	Ct,Tp	Mas	Qtz,Plg	H	x

YKF-105	Bet-111	Ct	Pty	Clv	H	x
YKF-106	Bet-114		Mas	Clv	X	x
YKF-107	Rib-9	Ct	Mas	Plg,Qtz	H	x
YKF-108	Waco-B-1	Tp,Ct	Mas	Kfs,Brl	H	x
YKF-109	Moose-112	Ct	Pty	Clv	X	
YKF-110	Moose-113	Ct	Tab	Clv	X	x
YKF-111	Moose-114	Ct	Tab	Clv	H	x
YKF-112	Moose-116	Ct	Tab	Clv	X	x
YKF-113	Moose-117	Ct	Pty	Clv	X	x
YKF-114	Moose-118	Ct	Pty	Clv	H	x
YKF-115	Moose-119		Pty	Clv		
YKF-116	Moose-120	Ct	Pty	Clv	X	x
YKF-117	Moose-121	Ct	Pty	Clv	X	x
YKF-118	Moose-122	Ct	Pty	Clv	H	x
YKF-119	Peg-192-8	Ct	Tab	Plg,Mus	X	x
YKF-120	Peg-113-1	Ct	Pty	Kfs,Brl		x
YKF-121	Peg-190-6					
YKF-122	Peg-191-2		Mas	Qtz,Plg	H	x
YKF-123	Peg-191-12	Ct		Plg		x
YKF-124	Peg-192-7	Ct	Pty	Plg		x
YKF-125	Peg-192-11	Ct	Tab	Plg	X	x
YKF-126	Peg-192-12	Ct,Mc	Pty	Plg,Mus	x	x
YKF-127	Peg-192-13	Ct	Tab	Plg	X	x
YKF-128	Peg-193-1					
YKF-129	Peg-193-5					
YKF-130	Peg-196-4	Tp		Qtz,Plg	H	x
YKF-131	Peg-88-1	Tp,Ct	Mas	Plg	H	x
YKF-132	Peg-84-1					
YKF-133	Peg-86-2	Ct	Pty	Plg		x
YKF-134	Peg-113-10					
YKF-135	Peg-113-9					
YKF-136	Peg-92-2					
YKF-137	Peg-300-3	Ct	Pty	Plg		x
YKF-138	Peg-300-13	Ct	Pty	Plg,Brl		x
YKF-139	Peg-300-14	Ct	Tab	Plg,Brl	H	x
YKF-140	Peg-267-5					
YKF-141	Peg-300-9					
YKF-142	Peg-241-10	Ct	Pty	Kfs		x
YKF-143	Peg-93-37A	Tp	Mas	Bt	H	x
YKF-144	Peg-285-5A					
YKF-145	Peg-292-9	Ct	Tab	Plg	H	x
YKF-146	Peg-236-8					
YKF-147	Peg-236-9					
YKF-148	Peg-236-5A					
YKF-149	Mel-9-11	Tp,Ct	Pty	Qtz	N	x
YKF-150	Mel-9-20	Ct	Mas		H	x
YKF-151	Mel-9-21	Tp	Mas		X	x
YKF-152	Vo-5-23				X	
YKF-153	Vo-5-20	Ct,Cs	Mas	Plg	x	x
YKF-154	Vo-6-7			Plg	x	
YKF-155	Vo-9-9	Ct	Tab	Plg	H	x
YKF-156	Fly-1-11	Ct,Tp		Qtz,Mus,Plg	H	x
YKF-157	Fly-1-4	P	Mas	Spd,Mus,Plg	x	x
YKF-158	Fly-1-14				X	x
YKF-159	Fly-1-17				X	x
YKF-160	Fly-1-3		Mas		N	
YKF-161	Fly-1-15					
YKF-162	Cata-C-2					
YKF-163	Cata-C-4	Ct	Pty	Plg		x
YKF-164	Cata-G-2					
YKF-165	Cata-G-3		Mas	Plg		
YKF-166	Cata-1-7	Ct	Tab	Plg,Mus	N	x
YKF-167	Cata-1-9	Ct,Cs	Tab	Brl	H	x
YKF-168	Cata-1-5		Mas	Plg		
YKF-169	Cata-K-1	Ct	Mas	Plg,Qtz,Mus	N	
YKF-170	Cata-2-1	Ct	Pty	Plg		x
YKF-171	Cata-B-1	Cs	Mas	Plg,Qtz	X	x
YKF-172	Bill-2-13	Ct	Tab	Plg	H	x
YKF-173	Bill-2-9	Ct	Pty	Plg	H	x
YKF-174	Bill-5-11	Ct	Pty	Qtz		x
YKF-175	Bill-5-8	Ct	Pty	Plg		x
YKF-176	Bill-5-9	Ct	Tab	Plg	H	x
YKF-177	Bill-5-12	Ct,Cs	Tab	Plg	H	x
YKF-178	Mel-1-12	Ct,Tp	Tab	Qtz	H	x
YKF-179	Mel-4-4					
YKF-180	Mel-4-11		Mas	Plg	N	
YKF-181	Mel-5-3	Ct	Pty	Plg	H	x
YKF-182	Mel-6-8	Ct	Pty	Plg		x
YKF-183	Mel-8-5	Ct	Tab	Kfs	H	x
YKF-184	Mel-10-4					
YKF-185	Peg-95-9	Ct	Pty	Plg	X	x
YKF-186	Peg-180-13	Gar				
YKF-187	Beetle-11	Gar				
YKF-188	Freda-12	Tp,Cs,Mc	Mas	Qtz,Kfs	X	x
YKF-189	Freda-14	Ct	Mas	Plg,Qtz,Amb	H	x
YKF-190	Freda-18	Cs	Pty	Qtz,Amb,Kfs	N	x
YKF-191	Waco-B-3	Ct	Mas	Clv	H	x
YKF-192	Waco-E-1					x
YKF-193	Waco-E-3				X	x
YKF-194	Tanya-C-2					
YKF-195	Murky-4					
YKF-196	Murky-8	Ct	Pty	Kfs	H	
YKF-197	Murky-9	Ct	Pty	Kfs	N	x
YKF-198	Tom-2	U				x
YKF-199	Tom-3	Ct	Bld	Qtz,Mus	N	x
YKF-200	Tom-4	U			X	x
YKF-201	Cas-A-4	Ct	Bld	Kfs,Qtz	H	x
YKF-202	Cas-A-5	Ct	Bld	Qtz,Mus	X	x
YKF-203	Cas-A-6	Ct	Bld	Kfs,Mus	N	x
YKF-204	Cas-A-10	Ct	Mas	Brl	H	x
YKF-205	Cas-A-11	Ct	Mas	Qtz,Plg	X	x
YKF-206	Cas-A-13					
YKF-207	Cas-A-14					
YKF-208	Cas-A-15				X	x
YKF-209	Cas-B-3	Ct			X	x
YKF-210	Cas-B-4	Gar				x
YKF-211	Cas-C-1	U				x
YKF-212	Cas-C-2	U				x

YKF-213	Cas-C-3	U				x
YKF-214	Cas-C-4		Mas	Kfs,Qtz,Mus		
YKF-215	Cas-C-6					
YKF-216	Cas-I-1	Tp,Ct,Mc	Mas	Kfs,Qtz	N	x
YKF-217	Cas-I-2	Tp,Mc	Mas	Kfs,Qtz	N	x
YKF-218	Cas-I-4					
YKF-219	Cas-L-4	U				x
YKF-220	Tanya-C-3	P			X	x
YKF-221	Qi-A-3	Ct	Mas	Qtz,Spd	N	x
YKF-222	Greg-C-3		Bld	Plg		
YKF-223	Greg-C-5		Bld	Plg		
YKF-224	Greg-C-7	Ct	Bld	Qtz,Plg		x
YKF-225	Greg-C-8					
YKF-226	Fi-A-3	P			X	x
YKF-227	Fi-A-4				X	x
YKF-228	Fi-A-5		Bld	Kfs,Qtz		
YKF-229	Fi-A-6	Ct	Bld	Kfs,Qtz,Spd	N	x
YKF-230	Fi-A-9	Ct	Bld	Kfs,Qtz	N	x
YKF-231	Fi-B-2	Ct	Bld	Kfs,Mus		x
YKF-232	Heidi-A-2		Mas	Kfs		
YKF-233	Heidi-C-1	Ct	Bld	Qtz,Kfs,Mus	N	x
YKF-234	Heidi-C-4					
YKF-235	Heidi-C-5	U			X	x
YKF-236	Heidi-C-7	U			X	x
YKF-237	Heidi-D-1		Mas	Kfs		
YKF-238	Heidi-I-3					
YKF-239	Heidi-J-1	U				x
YKF-240	Heidi-J-18	Ct	Pty	Mus,Qtz	N	x
YKF-241	Heidi-N-2	U				x
YKF-242	Bill-4-13	Ct	Bld	Brl,Qtz,Kfs	N	x
YKF-243	Bill-4-14	Ct	Bld	Kfs	X	x
YKF-244	Bill-4-15	Ct	Bld	Kfs	H	x
YKF-245	Bill-4-16		Bld	Kfs	X	x
YKF-246	Ann-Q-2	Ct	Bld	Plg,Mus,Qtz		
YKF-247	Ann-M-2	Ct	Pty	Plg,Mus	X	x
YKF-248	Ann-M-3	Ct	Bld	Plg,Mus	X	x
YKF-249	Ann-M-4	Ct	Bld	Plg,Mus,Qtz		x
YKF-250	Ann-M-5	Ct	Mas	Plg	N	x
YKF-251	Ann-M-6	Ct	Pty	Plg,Qtz	H	x
YKF-252	Ann-M-7	Ct	Pty	Plg,Mus	X	x
YKF-253	Ann-M-8	Ct	Pty	Plg,Mus	N	x
YKF-254	Ann-M-9	Ct	Pty	Sacc		x
YKF-255	Ann-N-2		Bld	Plg	X	
YKF-256	Paint-2	Ct	Bld	Plg	H	x
YKF-257	Jake-A-3			Qtz,Plg		
YKF-258	Jake-G-2	Ct	Pty	Plg,Spd	x	x
YKF-259	Jake-G-3	Ct	Blk	Plg	H	x
YKF-260	Jake-G-4	Ct	Pty	Mus		x
YKF-261	Jake-G-5	Ct	Pty	Plg,Mus	x	x
YKF-262	Jake-G-6	Ct	Bld	Plg,Mus,Spd	X	x
YKF-263	Jake-H-1	Ct	Pty	Plg,Brl		x
YKF-264	Lu-A-2	Ct	Bld	Qtz	X	x
YKF-265	Lu-A-3	Cs	Mas			x
YKF-266	Lu-A-4	Cs	Mas	Qtz	X	x
YKF-267	Lu-A-5	Ct	Pty	Qtz,Kfs	H	x
YKF-268	Lu-A-6	Ct	Pty	Plg	N	x
YKF-269	Lu-A-7	Ct	Pty	Qtz,Spd	X	x
YKF-270	Lu-A-9	Ct,Cs	Mas	Plg,Spd		x
YKF-271	Lu-A-10	Ct	Mas	Qtz,Plg	X	x
YKF-272	Lu-A-11	Ct	Mas	Plg,Qtz		x
YKF-273	Lu-A-15	Ct	Blk	Plg,Spd	X	x
YKF-274	Lu-D5-3	Ct,Cs	Mas	Plg,Mus		x
YKF-275	Lu-D5-4	Ct,Cs	Blk	Plg	N	x
YKF-276	Lu-D5-5	Ct,Cs	Mas	Plg,Qtz	N	x
YKF-277	Lu-D5-6	Cs,Ct	Mas	Plg	X	x
YKF-278	Lu-D5-8	Cs,Ct	Mas	Kfs,Mus,Qtz	N	x
YKF-279	Lu-D6-3	Ct,Cs	Mas	Plg,Qtz	N	x
YKF-280	Lu-D6-4	Ct,Cs	Mas	Plg,Qtz	X	x
YKF-281	Lu-D6-5	Cs	Mas	Clv	N	x
YKF-282	Lu-D6-6	Ct,Cs	Mas	Plg,Qtz	X	x
YKF-283	Lu-D6-7	Cs	Mas	Qtz,Plg	X	x
YKF-284	Lu-D6-10	Cs,Ct	Sub	Clv	X	x
YKF-285	Lu-D6-11	Cs	Mas	Kfs	X	x
YKF-286	Lu-D6-12	Ct	Pty	Plg,Mus,Qtz	N	x
YKF-287	Lu-D6-16	Ct,Cs	Pty	Clv	X	x
YKF-288	Lu-D6-18	Ct	Pty	Clv	X	x
YKF-289	Lu-D6-19	Ct	Pty	Clv,Mus	H	x
YKF-290	Lu-D6-21	Ct,Cs	Pty	Plg,Sph	X	x
YKF-291	Lu-D6-22					
YKF-292	Lu-D1-1		Mas	Plg	N	
YKF-293	Lu-D1-2	Cs	Mas	Qtz	X	x
YKF-294	Lu-D1-4	Ct,Cs	Blk	Plg	N	x
YKF-295	Lu-D2-1					
YKF-296	Pvilla-A-2		Pty	Plg,Mus	H	
YKF-297	Pvilla-A-7	Ct	Bld	Plg		x
YKF-298	Pvilla-C-4	Ct	Mas	Plg,Spd	H	x
YKF-299	Pvilla-C-7	Ct	Blk	Qtz,Plg	N	x
YKF-300	Pvilla-C-11	Ct	Blk	Qtz,Mus		
YKF-301	Pvilla-C-12	Tp	Mas	Qtz,Mus	H	x
YKF-302	Limo-C-4		Mas	Kfs		
YKF-303	Nite-A-3	Tp	Blk	Spd,Qtz	H	x
YKF-304	Nite-A-5		Mas	Kfs,Qtz,Spd		
YKF-305	Nite-A-6	Tp,Ct	Mas	Plg	N	x
YKF-306	Nite-A-7	Ct	Mas	Plg,Mus	N	x
YKF-307	Nite-A-8	Ct,Tp,Ix	Mas	Plg	X	x
YKF-308	Nite-A-10	Tp,Ct,Ix	Mas	Plg	N	x
YKF-309	Nite-A-11		Mas	Mus,Plg		
YKF-310	Nite-B-1	Ct	Bld	Spd,Qtz		x
YKF-311	Nite-B-4	Ct	Pty	Kfs	H	x
YKF-312	Odin-A-1		Mas	Mus,Clv		
YKF-313	Odin-A-2		Bld	Clv		
YKF-314	Odin-B-1	Ct	Pty	Plg,Qtz		x
YKF-315	Odin-B-2	U	Mas	Plg	X	x
YKF-316	Odin-B-3	U,Zir	Mas	Plg,Mus		x
YKF-317	Odin-B-10	Ct	Pty	Plg	X	x
YKF-318	Mint-A-2	Ct,Ix	Mas	Clv	X	x
YKF-319	Mint-A-3	Tp	Mas	Plg	H	x
YKF-320	Mint-A-6	Tp,Mc	Mas	Clv	N	x

YKF-321	Mint-B-4	Ct	Mas	Qtz,Clv	H	x
YKF-322	Lily-A-2	U	Mas	Plg		x
YKF-323	Lily-A-4	U	Mas	Plg	X	x
YKF-324	Rose-A-3		Bld	Brl		
YKF-325	Freda-10	Cs	Mas	Qtz,Mus,Plg	N	x
YKF-326	Freda-11	Cs	Mas	Qtz,Mus,Plg	X	x
YKF-327	Peg-75-25	U	Mas	Qtz,Plg,Mus	X	x
YKF-328	Peg-75-30	Ct	Pty	Qtz,Plg,Mus	H	x
YKF-329	Peg-75-31	Ct	Pty	Clv,Spd,Qtz		x
YKF-330	Lit-5-6		Bld	Clv,Qtz		
YKF-331	Lit-2-6		Pty	Spd		
YKF-332	Lit-2-7	P	Pty	Plg	N	x
YKF-333	Lit-2-8	P	Pty	Plg,Qtz	X	x
YKF-334	Lit-2-9	Ct	Blk	Kfs,Mus	N	x
YKF-335	Lit-2-10	Tp,Ct	Blk	Spd,Plg	N	x
YKF-336	Tan-2-10		Bld	Plg,Qtz		
YKF-337	Tan-2-12	Tp	Mas	Li-Mus,Plg		x
YKF-338	Tan-2-17		---	----		
YKF-339	Tan-2-18	Tp	Mas	Qtz		x
YKF-340	Tan-2-19	Tp,Cs	Pty	Kfs,Qtz	N	x
YKF-341	Tan-2-20	Tp,Cs	---	----	H	x
YKF-342	Tan-1-5		Pty	Li-Mus,Plg	N	
YKF-343	Was-17	Gar				
YKF-344	Was-20	Ct	Pty	Spd,Qtz,Mus	N	x
YKF-345	Was-21		Pty	Kfs,Qtz	H	
YKF-346	Usk-15	Tp	Blk	Qtz,Ap,Spd,B	H	x
YKF-347	Usk-16	Ct	Pty	Clv		x
YKF-348	Usk-17	Sph	Pty	Clv,Qtz,Mus		x
YKF-349	Usk-18	Ct	Pty	Mus,Qtz,Plg	N	
YKF-350	Usk-19	Ct	Pty	Kfs	H	x
YKF-351	Usk-20	Ct	Pty	Spd,Clv,Qtz	H	x
YKF-352	Usk-23		Mas	Plg,Srl	X	
YKF-353	Rib-15	Ct	Blk	Plg,Qtz	H	x
YKF-354	Rib-16		Pty	Plg,Srl	N	
YKF-355	Rib-17	Ct	Tab	Clv	H	x
YKF-356	Rib-18	Ct	Mas	Amb,Li-Mus	H	x
YKF-357	Rib-19	Ct	Pty	Plg	N	x
YKF-358	Rib-20	Zir	Bld	Zir,Clv	N	x
YKF-359	Rib-21		---	----		
YKF-360	Rib-22		---	----		
YKF-361	Dr.Bob-3	Tp,Cs	Mas	Plg,Clv	N	x
YKF-362	Dr.Bob-4		Mas	Mus,Kfs		
YKF-363	Dr.Bob-5	Ct,Cs	Mas	Qtz,Kfs	N	x
YKF-364	Big-D8-1	Ct,Cs	Pty	Plg,Qtz,Mus	H	x
YKF-365	Big-4-1	Ct	Pty	Qtz,Spd,Plg	N	x
YKF-366	Big-4-3	Ct	Pty	Spd,Qtz,Plg		x
YKF-367	Big-4-4	Ct,Cs	Pty	Plg,Qtz,Mus	X	x
YKF-368	Big-3-8	Tp,Ct	Mas	Plg,Mus,Qtz	H	x
YKF-369	Big-3-9	U	Mas	Plg,Qtz,Mus	X	x
YKF-370	Big-3-14	Ct	Pty	Plg	X	x
YKF-371	Big-3-15	Ct	Tab	Plg,Mus,Qtz	H	x
YKF-372	Big-3-16	Ct	Pty	Mus,Brl	X	x
YKF-373	Jenne-A-2	Ct	Mas	Clv,Qtz,Mus		x
YKF-374	Jenne-A-4	Cs	Mas	Plg,Qtz		x
YKF-375	Jenne-B-1	P	Mas	Mus,Qtz		x
YKF-376	Jake-C-4	Ct	Blk	Qtz,Plg,Mus	H	x
YKF-377	Jake-C-5	Ct	Tab	Qtz,Mus	H	x
YKF-378	Jake-C-6		Pty	Qtz		
YKF-379	Jake-B-2	Ct	Pty	Plg,Qtz	H	x
YKF-380	Cas-S-8	Ct	Mas	Qtz	N	x
YKF-381	Big-3-20	Ct	Pty	Plg		x
YKF-382	Big-3-25	Tp,Ct	Blk	Kfs,Qtz,Mus	N	x
YKF-383	Big-3-26	Tp,Ct,Mc	Tab	Kfs	N	x
YKF-384	Bin-4	Cs	Blk	Plg	N	x
YKF-385	Bighill-CS-	Tp,Cs	Blk	Qtz,Spd		
YKF-386	Rib-24	Ct	Tab	Elb,Clv	N	
YKF-387	Rib-26	Tp	Pty	Brl	X	
YKF-388	Rib-30	Ct	Blk	Qtz,Mus,Elb	N	
YKF-389	Rib-31	Ct	Pty	Plg,Zir	N	
YKF-390	Rib-34	Ct	Tab	Clv,Qtz	N	
YKF-391	Rib-35		Pty	Brl		
YKF-392	Rib-36	Ct	Tab	Clv	N	
YKF-393	Rib-37	Ct	Pty	Clv,Elb,Qtz,	N	
YKF-394	Limo-D-9	Ct	Pty	Plg,Qtz	N	
YKF-395	Limo-D-10		Pty	Plg,Qtz,Mus		
YKF-396	Nite-A-17	Ct	Tab	Plg,Spd	N	
YKF-397	Nite-A-18	Ct	Tab	Plg	N	
YKF-398	Nite-A-19	Ct,Tp	Tab	Plg	N	
YKF-399	Nite-C-8	Tp	Blk	Spd,Qtz	X	
YKF-400	Nite-C-9		Blk	Spd,Qtz		
YKF-401	Nite-C-10		Tab	Qtz,Plg		
YKF-402	Nite-C-11		Pty	Qtz,Mus		
YKF-403	Nite-C-12	Tp	Blk	Qtz,Spd	N	
YKF-404	Pvilla-B-4		Pty	Plg		
YKF-405	Pvilla-C-13	Ct	Pty	Qtz,Mus	N	
YKF-406	Pvilla-C-14		Pty	Mus,Qtz		
YKF-407	Pvilla-C-15	Ct,Tp	Tab	Mus,Qtz	X	
YKF-408	Pvilla-F-1					
YKF-409	Pvilla-F-2		Mas	Mus,Clv		
YKF-410	Pvilla-F-3		Mas	Clv,Mus		
YKF-411	Pvilla-H-1		Mas	Plg,Mus		
YKF-412	Pvilla-H-2		Pty	Mus,Qtz		
YKF-413	Bin-11	U	Mas	Qtz,Mus,Kfs	X	
YKF-414	Bin-15		Pty	Mus,Plg,Brl		
YKF-415	Bin-17	Ct	Pty	Mus,Qtz	N	
YKF-416	Bin-18	Cs	Mas	Qtz,Mus	N	
YKF-417	Bin-19	Tp,Cs	Mas	Mus,Qtz	X	x
YKF-418	Bin-20	Tp,Ix	Pty	Qtz,Clv	N	x
YKF-419	Lens-10	Tp	Mas	Qtz	N	x
YKF-420	Lens-11	Ct	Pty	Spd,Mus,Qtz	N	x
YKF-421	Mut-9	Ct	Tab	Spd,Kfs,Qtz	N	
YKF-422	Mut-10	Ct	Tab	Plg,Qtz	N	x
YKF-423	Mut-13	Ct	Tab	Plg	N	x
YKF-424	Hid-9		Pty	Plg,Qtz		
YKF-425	Hid-11		Pty	Plg,Mus,Qtz		
YKF-426	Bighill-11					
YKF-427	Bighill-12	Cs,Tp,Ct	Mas	Qtz,Plg	N	
YKF-428	Bighill-13		Pty	Qtz,Spd		

YKF-429	Bighill-16	Tp,Cs,Ct	Mas	Qtz,Clv	N	
YKF-430	Bighill-17	Cs,Tp,Ct	Mas	Spd,Plg	X	
YKF-431	Bighill-19					
YKF-432	Bighill-20		Pty	Mus,Qtz		
YKF-433	Bighill-21		Mas	Mus,Plg		
YKF-434	Bighill-23	Cs,Tp	Tab	Brl,Plg,Qtz	N	
YKF-435	Bighill-24	Cs,Tp	Mas	Qtz,Brl	N	
YKF-436	Bighill-25	Cs,Tp	Mas	Qtz,Clv,Mus	N	
YKF-437	Bighill-26	Tp,Ct	Pty	Plg,Qtz	N	x
YKF-438	Bighill-30	Tp	Mas	Qtz,Plg	N	x
YKF-439	Bighill-31	Tp	Mas	Qtz,Plg	X	
YKF-440	Bighill-32	Tp,Cs	Tab	Clv,Qtz		x
YKF-441	Bighill-33	Tp	Mas	Qtz	N	x
YKF-442	Bighill-34	Tp	Pty	Mus,Srl	N	x
YKF-443	Frgr-Pg-1	Ct	Tab	Mus,Kfs,Qtz	N	x
YKF-444	Jolly-6	Ct	Pty	Mus	N	
YKF-445	Jolly-7	Ct	Pty	Mus	N	
YKF-446	Jolly-8	Ct	Tab	Qtz,Mus	N	
YKF-447	Jolly-9	Ct	Tab	Qtz,Plg	N	x
YKF-448	Moon-3	Ct	Bld	Kfs,Qtz,Mus		x
YKF-449	Moon-4		Pty	Qtz,Kfs		
YKF-450	Harold-4		Mas	Plg,Qtz,Sacc		
YKF-451	Ekid-5	Ct	Pty	Qtz,Brl	N	x
YKF-452	Ekid-9	Srl	Mas	Plg,Qtz,Mus		
YKF-453	Paint-10	Ct	Pty	Plg,Spd,Qtz	N	
YKF-454	Paint-11		Pty	Kfs		
YKF-455	Paint-12		Mas	Plg		
YKF-456	Paint-13	Ct	Pty	Qtz,Kfs,Spd	N	
	Fly-1-7	Ct,Mc	Bld	Sacc		x
	Vo-5-24	Ct	Bld	Sacc		x
	Vo-8-3	Ct	Bld	Sacc		x
	Usk-7	Ct,Tp	Bld	Sacc		x
	Vo-4-2	Ct	Bld	Sacc		x
	Peg-84-2	Tp	Bld	Sacc		x
	Peg-84-4	Tp	Bld	Sacc		x
	Bet-112	Ct	Bld	Sacc		x
	Vo-1-10	Ct	Bld	Sacc		x
	Peg-306-9	Ct	Bld	Sacc		x
	Peg-95-12	Ct	Bld	Sacc		x
	Peg-95-17	Ct	Bld	Sacc		x
	Peg-75-3	Ct	Bld	Sacc		x
	Peg-191-6	Ct	Bld	Sacc		x
	Peg-85-1	Ct	Bld	Sacc		x
	Peg-75-4	Ct	Bld	Sacc		x
	Moose-115	Ct	Bld	Sacc		x
	Waco-C-11	Ct	Bld	Sacc		x
	The-Pn-A-3	Ct	Bld	Sacc		x
	Peg-191-7	Ct	Bld	Sacc		x
	Peg-196-3	Ct	Bld	Sacc		x
	Peg-196-10	Ct	Bld	Sacc		x
	Peg-190-7	Ct	Bld	Sacc		x
	Peg-191-4	Ct	Bld	Sacc		x
	The-W-17	Ct	Bld	Sacc		x
	Peg-84-3	Ct	Bld	Sacc		x
	Peg-118-9	Ct	Bld	Sacc		x
	Limo-C-1	Ct	Bld	Sacc		x
	Cas-1-6	Ct	Bld	Sacc		x
	Odin-B-8	Ct	Bld	Sacc		x
	Big-D6-4	Ct	Bld	Sacc		x
	Sky-6	Ct	Bld	Sacc		x

Abbreviations

Nb,Ta,Sn oxide minerals*

Ct - Columbite-tantalite
Tp - Tapiolite
Ix - Ixiolite
Cs - Cassiterite
Mc - Microlite
U - Uraninite
Zir - Zircon
P - Phosphate mineral
Gah - Gahnite
Sph - Sphalerite
Gar - Garnet

*List includes minerals which were identified by XRD or microprobe methods as non-Nb,Ta,Sn oxide minerals.

Crystal Habit

Pty - Platy
Bld - Bladed
Tab - Tabular
Blk - Blocky
Col - Columnar
Mas - Massive

Mineral Association

Qtz - Quartz
Kfs - K-feldspar
Plg - Plagioclase
Clv - Cleavelandite
Mus - Muscovite
Brl - Beryl
Spd - Spodumene
Sch - Srlorl
Elb - Elbaite
Zir - Zircon
Amb - Amblygonite-montebrasite
Ap - Apatite
Sph - Sphalerite
Sacc - Saccharoidal albite

XRD

X - denotes identification run of natural material only.
N - denotes identification run and unit cell refinement of natural material.
H - denotes identification run, heat treatment and unit cell refinement of heated material.

Probe

x - denotes analysis by electron microprobe, except in the case of non-Nb,Ta,Sn oxide minerals.

Appendix B

UNIT CELL DIMENSIONS FOR YELLOWKNIFE COLUMBITE-TANTALITES

Table 34: Unit cell dimensions for Yellowknife columbite-tantalites.

Sample No.	a(Å)	b(Å)	c(Å)	V(Å³)	% Order
		Natural			
Ann-M-5	4.7613(9)	5.7367(9)	5.0935(8)	139.13(3)	63
Ann-M-6	4.760(1)	5.736(1)	5.0892(9)	138.94(3)	67
Ann-M-8	4.755(1)	5.735(1)	5.090(2)	138.78(5)	63
Ann-N-1	4.7632(7)	5.7364(8)	5.0954(8)	139.23(3)	63
Ann-P-1	4.758(1)	5.737(1)	5.086(1)	138.85(3)	68
Bet-15	4.741(2)	5.729(2)	5.095(1)	138.38(5)	49
Bet-104	4.749(1)	5.733(1)	5.093(1)	138.66(4)	56
Bet-105	4.7463(9)	5.7313(9)	5.097(1)	138.65(3)	50
Bet-107	4.747(1)	5.729(1)	5.099(1)	138.68(4)	49
Bet-111	4.7475(9)	5.7283(9)	5.0947(9)	138.55(3)	53
Big-DB-1	4.753(2)	5.740(2)	5.117(2)	139.61(5)	36
Big-4-1	4.757(1)	5.735(1)	5.095(1)	159.02(3)	39
Big-3-15	4.745(2)	5.728(2)	5.114(2)	138.99(7)	33
Big-3-25	4.739(2)	5.732(2)	5.117(2)	138.99(5)	27
Big-3-26	4.736(2)	5.730(1)	5.130(2)	139.20(5)	12
Big Hill-12	4.761(3)	5.740(1)	5.098(3)	139.27(7)	59
Big Hill-16	4.773(1)	5.737(1)	5.097(5)	139.6(1)	68
Big Hill-17	4.750(3)	5.737(5)	5.10(1)	139.0(3)	50
Big Hill-26	4.758(6)	5.737(3)	5.102(3)	139.3(2)	53
Bill-2-9	4.733(1)	5.723(1)	5.112(1)	138.48(3)	27
Bill-2-13	4.732(1)	5.722(1)	5.112(1)	138.42(4)	27
Bill-4-13	4.7365(6)	5.7235(6)	5.1070(9)	138.45(2)	35
Bill-4-15	4.745(1)	5.725(1)	5.100(1)	138.53(3)	47
Bill-5-9	4.730(1)	5.7251(8)	5.118(1)	138.61(3)	20
Bill-5-12	4.740(1)	5.728(1)	5.106(1)	138.64(3)	38
Bin-17	4.7352(8)	5.7240(8)	5.1129(8)	138.58(3)	28
Cas-A-4	4.752(2)	5.733(2)	5.096(2)	138.83(6)	55
Cas-A-6	4.756(2)	5.733(1)	5.091(2)	138.81(5)	62
Cas-A-10	4.750(1)	5.731(1)	5.099(1)	138.80(4)	51
Cas-I-1	4.763(8)	5.734(3)	5.12(1)	139.8(3)	41
Cas-I-2	4.763(3)	5.734(2)	5.119(3)	139.8(1)	41
Cas-S-8	4.728(2)	5.722(2)	5.131(2)	138.81(7)	6
Cata-I-2	4.7697(8)	5.7447(9)	5.1227(9)	140.36(3)	41
Cata-I-7	4.765(1)	5.744(1)	5.104(1)	139.70(3)	56
Cata-I-9	4.772(1)	5.747(1)	5.105(1)	140.00(4)	60
Cata-K-1	4.762(1)	5.743(1)	5.126(1)	140.18(5)	33
Ekid-5	4.750(1)	5.733(1)	5.104(1)	139.01(4)	46
Fi-A-6	4.757(2)	5.732(2)	5.082(4)	138.6(1)	71
Fi-A-9	4.751(1)	5.731(1)	5.091(2)	138.61(5)	59
Fly-1-3	4.765(3)	5.740(3)	5.090(3)	139.20(9)	69
Fly-1-4	4.760(2)	5.739(2)	5.095(2)	139.19(7)	61
Fly-1-11	4.747(2)	5.731(2)	5.124(3)	139.40(6)	25
Freda-3	4.751(1)	5.732(1)	5.109(1)	139.13(4)	42
Freda-4	4.754(1)	5.734(1)	5.104(1)	139.12(5)	49
Freda-14	4.780(2)	5.747(2)	5.072(2)	139.35(5)	96
Frgr-Pg-1	4.727(1)	5.721(1)	5.1238(9)	138.57(3)	12
Heidi-C-1	4.732(1)	5.724(1)	5.131(1)	138.96(4)	9
Heidi-J-18	4.748(2)	5.730(2)	5.101(3)	138.77(8)	48
Jake-B-2	4.764(1)	5.744(1)	5.107(2)	139.74(5)	52
Jake-C-4	4.773(1)	5.742(1)	5.108(1)	140.01(4)	57
Jake-C-5	4.760(1)	5.741(1)	5.104(1)	139.46(5)	53
Jake-G-3	4.738(2)	5.730(2)	5.131(2)	139.33(6)	13
Jake-G-5	4.785(1)	5.768(1)	5.143(1)	141.92(5)	32
Jo-18	4.751(2)	5.733(2)	5.097(2)	138.83(5)	53
Jolly-6	4.7353(8)	5.7241(9)	5.1061(9)	138.40(3)	34
Jolly-7	4.742(1)	5.728(1)	5.102(1)	138.61(3)	43
Jolly-8	4.726(1)	5.719(1)	5.1198(9)	138.37(3)	15
Jolly-9	4.729(1)	5.720(1)	5.112(1)	138.30(4)	25
Lens-11	4.733(1)	5.726(1)	5.118(1)	138.67(4)	22
Limo-D-9	4.737(2)	5.727(2)	5.118(2)	138.85(5)	24
Lit-2-2	4.755(1)	5.738(1)	5.105(3)	139.30(6)	48
Lit-2-7	4.751(1)	5.731(1)	5.107(2)	139.08(5)	44
Lit-2-9	4.752(1)	5.736(1)	5.119(1)	139.53(4)	33
Lit-2-10	4.748(1)	5.736(1)	5.115(1)	139.32(4)	34
Lu-A-5	4.7650(9)	5.737(1)	5.0860(8)	139.04(3)	73
Lu-A-6	4.757(2)	5.741(2)	5.114(1)	139.68(5)	41
Lu-D6-12	4.754(1)	5.733(1)	5.095(1)	138.88(4)	57
Lu-D6-19	4.754(1)	5.735(1)	5.091(1)	138.81(3)	61
Mac-111	4.733(1)	5.732(1)	5.139(1)	139.40(4)	2
Mac-112	4.7370(8)	5.7295(9)	5.1311(9)	139.26(3)	12
Mac-115	4.740(1)	5.734(1)	5.137(1)	139.61(4)	8
Mel-1-12	4.749(2)	5.730(2)	5.094(3)	138.63(7)	55
Mel-4-11	4.748(1)	5.729(1)	5.099(1)	138.69(4)	49
Mel-5-3	4.7271(7)	5.7209(8)	5.1211(9)	138.49(3)	15
Mel-8-5	4.727(2)	5.722(2)	5.122(2)	138.53(7)	14
Mel-9-20	4.745(2)	5.727(1)	5.112(3)	138.90(6)	35
Mint-A-6	4.758(3)	5.739(2)	5.101(4)	139.3(1)	54
Mint-B-4	4.765(1)	5.740(2)	5.109(1)	139.77(5)	51
Moose-7	4.741(1)	5.719(2)	5.107(2)	138.48(4)	37
Moose-9	4.7425(9)	5.729(1)	5.106(1)	138.75(3)	39
Moose-12	4.735(1)	5.728(2)	5.101(1)	138.34(5)	39
Moose-16	4.750(2)	5.736(2)	5.087(1)	138.60(5)	62
Moose-101	4.744(1)	5.727(2)	5.103(1)	138.66(5)	43
Moose-102	4.7462(6)	5.7281(6)	5.1005(6)	138.66(2)	46
Moose-104	4.746(2)	5.730(1)	5.101(1)	138.70(5)	46
Moose-114	4.7461(8)	5.7300(9)	5.0988(8)	138.66(3)	48
Moose-118	4.7492(9)	5.733(1)	5.0867(9)	138.49(3)	61
Moose-122	4.7487(8)	5.7342(8)	5.0864(8)	138.50(3)	62
Murky-8	4.7510(7)	5.7320(7)	5.0902(8)	138.62(2)	60
Murky-9	4.752(1)	5.729(1)	5.095(1)	138.71(4)	56
Mut-9	4.724(1)	5.725(1)	5.1297(8)	138.72(3)	4
Mut-10	4.729(1)	5.726(1)	5.1203(9)	138.66(3)	17
Mut-13	4.731(1)	5.728(1)	5.113(1)	138.57(4)	25
Nite-A-6	4.758(1)	5.737(2)	5.121(2)	139.78(7)	35
Nite-A-7	4.762(1)	5.741(1)	5.1157(9)	139.85(3)	43
Nite-A-8	4.752(1)	5.723(2)	5.132(2)	139.71(6)	21
Nite-A-10	4.7537(7)	5.740(2)	5.148(3)	140.47(7)	7
Nite-A-17	4.759(1)	5.739(1)	5.121(1)	139.86(3)	36
Nite-A-18	4.759(2)	5.737(2)	5.122(2)	139.85(6)	35

Nite-A-19	4.758(4)	5.730(3)	5.134(5)	134(1)	23
Nite-B-4	4.753(1)	5.736(1)	5.112(1)	139.37(5)	41
Paint-2	4.763(1)	5.7396(7)	5.1080(6)	139.63(3)	51
Paint-10	4.7807(7)	5.7485(6)	5.0951(5)	140.02(2)	75
Paint-13	4.754(1)	5.741(1)	5.118(1)	139.69(3)	36
Peg-8-4	4.725(1)	5.714(1)	5.104(1)	137.83(4)	30
Peg-75-11	4.765(1)	5.743(1)	5.106(1)	139.73(3)	54
Peg-75-30	4.763(1)	5.739(1)	5.110(2)	139.69(5)	49
Peg-93-20	4.744(3)	5.727(3)	5.110(4)	138.83(9)	36
Peg-93-30	4.728(1)	5.726(1)	5.131(1)	138.91(4)	6
Peg-95-20	4.748(2)	5.743(1)	5.101(2)	138.87(4)	48
Peg-97-16	4.747(1)	5.731(1)	5.107(1)	138.91(4)	41
Peg-170-8	4.724(2)	5.722(2)	5.118(2)	138.34(5)	16
Peg-192-12	4.744(1)	5.731(1)	5.126(2)	139.34(5)	21
Peg-285-4	4.7353(8)	5.7252(8)	5.1048(9)	138.39(3)	35
Peg-292-9	4.724(2)	5.719(1)	5.123(2)	138.40(6)	11
Peg-300-14	4.750(1)	5.732(1)	5.106(2)	139.01(5)	44
Pvilla-A-2	4.750(1)	5.733(1)	5.098(1)	138.82(4)	52
Pvilla-C-4	4.7293(7)	5.7281(8)	5.1423(7)	139.30(2)	-4
Pvilla-C-7	4.730(1)	5.726(1)	5.131(1)	138.97(4)	7
Pvilla-C-13	4.7314(7)	5.7281(8)	5.1384(6)	139.26(2)	2
Pvilla-C-15	4.757(3)	5.728(3)	5.109(9)	139.2(2)	46
Qi-A-3	4.758(1)	5.735(1)	5.088(2)	138.85(5)	66
Rib-A-7-A	4.791(2)	5.749(1)	5.102(2)	140.51(6)	75
Rib-9	4.771(1)	5.746(1)	5.105(1)	139.96(4)	59
Rib-15	4.750(2)	5.747(2)	5.149(2)	140.55(6)	4
Rib-16	4.750(1)	5.731(1)	5.086(2)	138.48(5)	63
Rib-17	4.771(1)	5.742(1)	5.107(1)	139.90(4)	57
Rib-18	4.750(1)	5.743(2)	5.122(1)	139.74(4)	29
Rib-19	4.754(1)	5.732(1)	5.090(1)	138.71(4)	62
Rib-20	4.750(1)	5.732(1)	5.090(1)	138.61(4)	59
Rib-24	4.765(1)	5.749(1)	5.143(1)	140.88(5)	19
Rib-30	4.768(2)	5.745(2)	5.123(1)	140.30(5)	40
Rib-31	4.776(1)	5.748(1)	5.1032(9)	140.10(3)	64
Rib-34	4.7811(9)	5.7512(9)	5.128(1)	140.99(3)	44
Rib-36	4.784(1)	5.756(2)	5.121(1)	141.01(5)	52
Rib-37	4.7504(6)	5.7324(6)	5.0842(5)	138.45(2)	65
Tan-1-5	4.738(2)	5.730(2)	5.109(2)	138.70(8)	33
The-Ar-G-3	4.743(1)	5.726(2)	5.104(1)	138.64(5)	41
The-En-4	4.737(2)	5.724(3)	5.122(5)	138.87(8)	21
The-Pn-A-4	4.750(1)	5.735(1)	5.108(1)	139.15(4)	42
The-Pw-3	4.7343(8)	5.726(1)	5.1294(7)	139.05(3)	12
The-Sn-B-1	4.763(2)	5.742(2)	5.108(2)	139.69(5)	51
The-T-7	4.7598(9)	5.740(1)	5.108(1)	139.56(4)	49
The-W-1	4.7421(6)	5.7278(6)	5.1128(6)	138.87(2)	32
Tom-3	4.7525(8)	5.7340(8)	5.092(1)	138.75(3)	59
Usk-18	4.757(2)	5.738(2)	5.114(2)	139.60(6)	41
Usk-19	4.754(1)	5.734(2)	5.119(2)	139.53(5)	35
Usk-20	4.754(2)	5.735(2)	5.113(2)	139.39(5)	40
Vo-5-20	4.741(3)	5.730(3)	5.124(2)	139.20(9)	21
Vo-6-7	4.735(1)	5.727(2)	5.126(1)	139.01(4)	15
Vo-9-9	4.755(2)	5.732(2)	5.099(3)	138.96(7)	54
Waco-A-3	4.736(1)	5.732(1)	5.137(1)	139.45(5)	6
Waco-A-5	4.744(1)	5.726(2)	5.112(2)	138.85(5)	35
Waco-A-8	4.732(2)	5.722(2)	5.122(3)	138.66(7)	17
Waco-A-9	4.7416(8)	5.7284(8)	5.1133(8)	138.89(3)	32
Waco-B-1	4.727(3)	5.720(2)	5.125(3)	138.56(8)	11
Waco-B-3	4.723(1)	5.721(1)	5.131(1)	138.63(4)	3
Was-20	4.7456(6)	5.7355(6)	5.1251(7)	139.50(2)	24
Was-21	4.757(1)	5.740(1)	5.113(1)	139.62(5)	42

Heated

Sample No.	a(Å)	b(Å)	c(Å)	V(Å³)	% Order
Ann-M-6	14.299(3)	5.7376(8)	5.0624(9)	415.34(9)	96
Ann-N-1	14.326(3)	5.7432(9)	5.069(1)	417.04(9)	96
Ann-P-1	14.314(1)	5.7422(5)	5.0635(5)	416.19(5)	98
Bet-4	14.324(6)	5.733(1)	5.063(1)	415.7(1)	101
Bet-15	14.309(2)	5.7374(6)	5.0639(7)	415.73(7)	97
Bet-105	14.289(2)	5.7340(8)	5.0574(8)	414.37(8)	99
Bet-107	14.293(2)	5.7380(8)	5.0607(8)	415.06(7)	96
Bet-111	14.294(2)	5.7366(7)	5.0608(7)	414.98(7)	96
Big-A-1	14.353(3)	5.746(1)	5.070(1)	418.2(1)	101
Big-B-15	14.303(3)	5.7323(8)	5.0612(9)	414.95(9)	98
Bill-2-9	14.263(4)	5.730(1)	5.057(2)	413.3(2)	93
Bill-2-13	14.30(1)	5.726(2)	5.051(2)	413.5(3)	106
Bill-4-15	14.242(8)	5.730(1)	5.055(2)	412.5(2)	90
Bill-5-9	14.275(2)	5.7299(7)	5.0565(8)	413.60(7)	96
Bill-5-12	14.285(4)	5.732(1)	5.057(1)	414.0(1)	98
Cas-A-4	14.299(3)	5.735(1)	5.0611(9)	415.01(9)	97
Cas-A-10	14.291(2)	5.7351(9)	5.060(1)	414.72(9)	96
Cata-1-2	14.381(1)	5.7532(7)	5.0801(7)	420.32(6)	97
Cata-K-1	14.371(2)	5.7510(8)	5.0743(9)	419.39(8)	101
Fly-1-11	14.314(2)	5.7382(5)	5.0652(6)	416.03(6)	97
Freda-3	14.320(3)	5.7419(9)	5.069(1)	416.82(9)	94
Freda-4	14.321(2)	5.7421(5)	5.0675(6)	416.72(6)	96
Freda-14	14.341(2)	5.7468(7)	5.072(1)	418.02(9)	96
Jake-B-2	14.361(2)	5.7489(6)	5.0723(7)	418.76(6)	101
Jake-C-4	14.307(3)	5.7388(9)	5.066(1)	415.9(1)	94
Jake-C-5	14.367(5)	5.750(1)	5.069(1)	418.7(1)	105
Jake-G-3	14.316(8)	5.743(2)	5.074(2)	417.1(2)	89
Jake-G-5	14.389(4)	5.750(1)	5.070(1)	419.5(1)	109
Jo-18	14.302(1)	5.7375(4)	5.0605(4)	415.25(4)	98
Lit-2-2	14.324(2)	5.7422(7)	5.0676(7)	416.81(6)	96
Lu-A-5	14.323(1)	5.7402(4)	5.0664(6)	416.56(5)	98
Lu-D6-19	14.293(4)	5.735(1)	5.056(3)	414.4(2)	101
Mac-109	14.320(2)	5.7389(6)	5.0694(6)	416.62(6)	94
Mac-111	14.324(3)	5.7408(7)	5.072(1)	417.07(9)	92
Mac-112	14.307(4)	5.738(1)	5.070(1)	416.2(1)	91
Mac-115	14.331(3)	5.7430(9)	5.074(1)	417.6(1)	92
Mel-1-12	14.294(2)	5.7370(6)	5.0592(6)	414.89(6)	98
Mel-5-3	14.278(1)	5.7309(5)	5.0582(6)	413.90(5)	96
Mel-8-5	14.277(4)	5.727(1)	5.063(1)	413.9(1)	91
Mel-9-20	14.287(5)	5.730(1)	5.065(2)	414.7(2)	91
Mint-B-4	14.330(4)	5.738(1)	5.076(2)	417.4(2)	90
Moose-7	14.284(2)	5.7332(7)	5.0584(7)	414.24(7)	90
Moose-9	14.285(3)	5.7330(8)	5.060(1)	414.4(1)	95
Moose-12	14.283(2)	5.7345(8)	5.0585(8)	414.32(8)	96
Moose-16	14.287(3)	5.735(1)	5.059(1)	414.5(1)	97
Moose-102	14.293(2)	5.7363(7)	5.0607(7)	414.93(7)	96
Moose-104	14.291(1)	5.7364(5)	5.0597(5)	414.77(5)	97
Moose-114	14.295(3)	5.736(1)	5.0598(9)	414.84(9)	97
Moose-118	14.289(2)	5.7326(6)	5.0616(7)	414.62(7)	94
Moose-122	14.290(2)	5.7360(7)	5.0560(8)	414.42(7)	100
Murky-8	14.296(3)	5.7399(8)	5.060(1)	415.23(9)	98
Nite-B-4	14.322(1)	5.7402(5)	5.0676(5)	416.60(5)	96
Paint-2	14.356(4)	5.750(1)	5.072(1)	418.7(1)	99
Peg-8-4	14.375(5)	5.734(2)	5.048(2)	416.1(2)	126
Peg-93-20	14.295(2)	5.7365(7)	5.0634(7)	415.22(7)	95
Peg-93-30	14.294(1)	5.7310(4)	5.0659(4)	414.99(4)	92
Peg-93-37A	14.242(5)	5.722(2)	5.075(2)	413.6(2)	72
Peg-75-11	14.363(3)	5.7493(9)	5.072(1)	418.79(9)	101
Peg-75-30	14.343(4)	5.747(1)	5.067(1)	417.6(1)	101
Peg-95-20	14.309(2)	5.7398(9)	5.0611(8)	415.69(9)	100
Peg-97-16	14.285(2)	5.7348(7)	5.0581(7)	414.38(6)	97
Peg-192-12	14.341(3)	5.742(1)	5.066(1)	417.2(1)	102
Peg-285-4	14.291(7)	5.728(2)	5.066(2)	414.7(2)	91
Peg-292-9	14.345(3)	5.746(1)	5.074(1)	418.2(1)	95
Peg-300-14	14.294(3)	5.7419(8)	5.064(1)	415.6(1)	93
Pvilla-A-2	14.304(3)	5.7346(8)	5.0613(8)	415.17(9)	98
Pvilla-C-4	14.317(2)	5.7400(9)	5.0698(9)	416.6(1)	93
Rib-A-7-A	14.406(2)	5.7552(9)	5.0842(9)	421.53(9)	99
Rib-9	14.361(3)	5.749(1)	5.075(1)	419.0(1)	98
Rib-15	14.382(3)	5.749(1)	5.077(1)	419.8(1)	100
Rib-17	14.355(4)	5.747(1)	5.081(1)	419.2(1)	91
Rib-18	14.378(1)	5.7498(7)	5.0784(7)	419.84(7)	99
The-Ar-G-3	14.293(2)	5.7354(7)	5.0618(7)	414.95(7)	95
The-En-4	14.296(5)	5.7354(9)	5.0600(9)	414.9(1)	98
The-Pw-3	14.316(1)	5.7387(5)	5.0693(5)	416.46(5)	94
The-Sn-B-1	14.362(2)	5.7512(5)	5.0741(6)	419.11(6)	99
The-T-7	14.335(3)	5.743(1)	5.089(1)	417.4(1)	79
The-W-1	14.308(2)	5.7384(7)	5.0641(8)	415.78(8)	96
Usk-19	14.323(5)	5.741(1)	5.069(1)	417.0(1)	95
Usk-20	14.317(3)	5.7398(9)	5.0651(8)	416.23(9)	97
Vo-9-9	14.313(3)	5.741(1)	5.065(1)	416.2(1)	97
Waco-A-8	14.292(4)	5.732(1)	5.063(1)	414.8(1)	94
Waco-B-1	14.240(4)	5.708(1)	5.067(2)	411.9(1)	79
Waco-B-3	14.255(2)	5.7203(7)	5.0584(6)	412.59(7)	90
Waco-A-9	14.296(1)	5.7333(4)	5.0641(5)	415.09(5)	94
Was-21	14.340(3)	5.745(1)	5.072(1)	417.8(1)	96

Appendix C

ELECTRON MICROPROBE ANALYSES FOR YELLOWKNIFE NB-,TA-,SN-OXIDE MINERALS

Table 35:

Columbite-tantalite Analyses

Cations based on 24(O)

Sample no.	Ta_2O_5	Nb_2O_5	TiO_2	SnO_2	Fe_2O_3	FeO	MnO	CaO	Total	Ta^{5+}	Nb^{5+}	Ti^{4+}	Sn^{4+}	Fe^{3+}	Fe^{2+}	Mn^{2+}	Ca^{2+}	Total
ANN-M-2/1	30.2	52.1	0.0	0.0	0.0	12.6	6.3	0.0	101.1	2.07	5.93	0.00	0.00	0.00	2.65	1.34	0.00	11.99
ANN-M-2/2	33.0	50.1	0.0	0.0	0.0	12.3	6.3	0.0	101.6	2.27	5.74	0.01	0.00	0.00	2.61	1.34	0.00	11.97
ANN-M-3/1	51.3	30.6	0.6	0.0	0.0	10.0	6.3	0.0	98.7	3.99	3.95	0.12	0.00	0.00	2.38	1.52	0.00	11.97
ANN-M-3/2	55.5	27.1	0.4	0.2	0.0	12.1	4.2	0.0	99.4	4.38	3.55	0.09	0.02	0.00	2.93	1.03	0.00	12.00
ANN-M-4/1	14.7	66.1	0.1	0.0	0.0	14.7	5.5	0.0	101.0	0.94	7.05	0.01	0.00	0.00	2.89	1.09	0.00	11.99
ANN-M-4/2	14.6	65.5	0.3	0.3	0.0	14.3	5.5	0.0	100.4	0.94	7.02	0.04	0.03	0.00	2.83	1.11	0.00	11.98
ANN-M-5/1	38.9	44.1	0.0	0.0	0.0	11.5	6.5	0.0	101.0	2.78	5.23	0.00	0.00	0.00	2.52	1.45	0.00	11.98
ANN-M-5/2	35.5	47.2	0.2	0.4	0.4	11.9	6.4	0.0	101.9	2.47	5.45	0.03	0.04	0.09	2.54	1.38	0.00	12.00
ANN-M-6/1	54.2	27.4	0.3	0.0	0.4	11.8	4.2	0.0	98.3	4.31	3.62	0.07	0.00	0.08	2.88	1.04	0.00	12.00
ANN-M-6/2	33.9	48.0	0.2	0.0	0.0	11.8	6.3	0.0	100.2	2.38	5.62	0.03	0.00	0.00	2.55	1.38	0.00	11.97
ANN-M-6/3	28.8	53.0	0.3	0.4	0.1	13.0	5.9	0.0	101.5	1.95	5.97	0.06	0.04	0.02	2.71	1.24	0.00	12.00
ANN-M-6/4	35.3	46.5	0.0	0.0	1.4	11.1	6.5	0.0	100.8	2.48	5.43	0.00	0.00	0.27	2.41	1.42	0.00	12.00
ANN-M-6/5	53.4	29.4	0.4	0.0	2.1	11.1	4.6	0.0	100.9	4.07	3.73	0.08	0.00	0.43	2.59	1.09	0.00	12.00
ANN-M-6/6	47.6	33.0	1.0	0.6	1.0	11.9	4.2	0.0	99.3	3.60	4.15	0.21	0.06	0.22	2.77	1.00	0.00	12.00
ANN-M-7/1	47.3	32.4	0.9	0.5	1.4	11.8	4.0	0.0	98.3	3.61	4.12	0.19	0.06	0.30	2.77	0.94	0.00	12.00
ANN-M-7/2	30.3	50.2	0.0	0.1	0.6	12.1	6.0	0.0	99.4	2.12	5.83	0.00	0.01	0.12	2.60	1.31	0.00	12.00
ANN-M-7/3	45.6	33.4	1.5	0.5	2.6	10.7	4.5	0.0	98.8	3.42	4.16	0.30	0.06	0.54	2.47	1.05	0.00	12.00
ANN-M-8/1	26.9	53.1	0.1	0.0	0.6	11.1	7.2	0.0	99.2	1.85	6.09	0.03	0.00	0.12	2.36	1.55	0.00	12.00
ANN-M-8/3	47.3	33.9	0.1	0.3	0.4	11.9	4.7	0.0	98.6	3.62	4.31	0.02	0.03	0.09	2.81	1.11	0.00	12.00
ANN-M-9/1	22.5	59.2	0.2	0.0	0.2	14.1	5.4	0.0	101.6	1.48	6.48	0.03	0.00	0.03	2.86	1.11	0.00	12.00
ANN-M-9/2	45.5	35.2	1.3	0.7	0.0	12.9	3.8	0.0	99.4	3.40	4.37	0.28	0.07	0.00	2.97	0.89	0.00	11.99
ANN-M-9/4	48.0	33.4	1.5	0.8	0.5	12.5	4.0	0.0	100.7	3.57	4.13	0.31	0.09	0.11	2.86	0.94	0.00	12.00
ANN-N-1/2	32.7	49.5	0.0	0.2	0.3	12.4	6.1	0.0	101.3	2.27	5.70	0.00	0.02	0.06	2.64	1.31	0.00	12.00
ANN-N-1/3	39.4	43.4	0.0	0.0	0.4	11.5	6.4	0.0	101.1	2.82	5.16	0.00	0.00	0.07	2.52	1.43	0.00	12.00
ANN-O-3/1	33.3	47.8	0.0	0.0	0.0	12.8	5.4	0.0	99.2	2.37	5.64	0.00	0.00	0.00	2.80	1.19	0.00	11.99
ANN-O-3/2	22.4	58.4	0.0	0.0	0.0	12.7	6.4	0.0	100.0	1.50	6.51	0.00	0.00	0.00	2.63	1.34	0.00	11.98
ANN-O-3/3	19.8	60.7	0.0	0.0	0.0	12.6	6.9	0.0	100.1	1.31	6.69	0.00	0.00	0.00	2.57	1.42	0.00	12.00
ANN-R-2/1	15.5	65.3	0.3	0.0	0.0	13.6	6.3	0.0	101.0	1.00	6.98	0.05	0.00	0.00	2.70	1.25	0.00	11.98
ANN-R-2/2	29.8	51.5	0.2	0.0	0.0	13.3	5.3	0.0	100.1	2.06	5.92	0.04	0.00	0.00	2.83	1.15	0.00	12.00
BET-104/1	29.4	50.6	0.5	0.0	0.0	14.3	4.0	0.0	99.0	2.05	5.88	0.10	0.00	0.00	3.08	0.88	0.00	11.99
BET-104/2	26.1	53.5	0.3	0.0	0.8	14.4	3.9	0.0	98.9	1.80	6.12	0.05	0.00	0.14	3.06	0.83	0.00	12.00
BET-105/1	26.8	53.3	0.4	0.0	0.4	14.4	4.1	0.0	99.3	1.84	6.09	0.07	0.00	0.08	3.05	0.87	0.00	12.00
BET-105/2	27.5	53.1	0.3	0.0	0.0	14.8	3.9	0.0	99.6	1.89	6.07	0.06	0.00	0.00	3.13	0.83	0.00	11.99
BET-106/1	28.2	52.8	0.4	0.5	0.0	14.7	4.0	0.0	100.6	1.93	5.99	0.08	0.05	0.00	3.09	0.85	0.00	11.99
BET-106/2	28.2	52.5	0.4	0.4	0.0	15.7	3.0	0.0	100.2	1.93	5.99	0.07	0.04	0.00	3.32	0.64	0.00	12.00
BET-107/1	33.9	46.5	0.3	0.0	0.0	13.7	4.1	0.0	98.5	2.43	5.54	0.06	0.00	0.00	3.01	0.93	0.00	11.97
BET-107/2	33.2	47.0	0.2	0.3	0.0	13.8	4.3	0.0	98.8	2.37	5.57	0.04	0.03	0.00	3.02	0.95	0.00	12.00
BET-111/1	30.5	50.0	0.3	0.1	0.7	13.4	4.7	0.0	99.8	2.12	5.78	0.07	0.01	0.14	2.86	1.03	0.00	12.00
BET-111/2	30.2	50.3	0.4	0.0	0.8	13.9	4.2	0.0	99.8	2.10	5.80	0.07	0.00	0.15	2.97	0.91	0.00	12.00
BET-112A/A	63.3	19.9	0.7	0.5	0.8	11.6	3.7	0.0	100.4	5.12	2.68	0.15	0.06	0.17	2.89	0.93	0.00	12.00
BET-112A/B	38.2	43.8	0.2	0.0	0.2	13.7	4.1	0.1	100.3	2.74	5.22	0.04	0.00	0.05	3.01	0.91	0.03	12.00
BET-15/1	28.8	51.5	0.5	0.0	3.6	12.2	4.7	0.0	101.3	1.94	5.77	0.10	0.00	0.68	2.52	1.00	0.00	12.00
BET-15/6	30.1	50.0	0.6	0.0	1.8	13.1	4.4	0.0	100.1	2.08	5.73	0.11	0.00	0.34	2.78	0.95	0.00	12.00
BET-4/A	62.3	21.3	0.5	1.0	0.0	9.9	5.4	0.0	100.4	5.04	2.86	0.10	0.12	0.00	2.45	1.35	0.00	11.93
BIG-A-1/1	37.2	43.8	0.0	0.1	0.9	7.2	10.1	0.0	99.4	2.68	5.25	0.00	0.01	0.19	1.60	2.27	0.00	12.00
BIG-A-1/2	32.7	47.8	0.2	0.0	0.0	7.2	10.8	0.0	98.7	2.33	5.66	0.04	0.00	0.00	1.57	2.38	0.00	11.98
BIG-A-4-A	34.0	46.4	0.0	0.0	0.0	6.8	11.1	0.0	98.3	2.45	5.56	0.00	0.00	0.00	1.50	2.48	0.00	11.99
BIG-A-4-B	22.5	56.7	0.0	0.0	0.4	6.7	11.6	0.3	98.2	1.54	6.44	0.00	0.00	0.07	1.42	2.46	0.07	12.00
BIG-B-1/2	15.6	63.3	0.3	0.1	1.1	12.1	6.9	0.0	99.5	1.02	6.87	0.06	0.01	0.19	2.44	1.41	0.00	12.00
BIG-B-1/3	16.5	62.5	0.3	0.0	0.8	11.8	7.3	0.0	99.1	1.08	6.84	0.05	0.00	0.14	2.38	1.51	0.00	12.00
BIG-B-14/1	25.6	55.4	0.2	0.4	1.2	11.7	6.9	0.0	101.3	1.72	6.17	0.03	0.04	0.22	2.40	1.43	0.00	12.00
BIG-B-14/2	23.7	55.6	0.2	0.1	1.1	11.4	6.8	0.0	99.0	1.61	6.29	0.04	0.01	0.22	2.39	1.45	0.00	12.00
BIG-B-15/1	33.1	48.8	0.4	0.3	0.0	12.7	5.5	0.0	100.7	2.30	5.66	0.07	0.03	0.00	2.71	1.19	0.00	11.96
BIG-B-15/2	44.9	37.1	0.6	0.0	0.5	11.7	5.4	0.0	100.1	3.32	4.56	0.13	0.00	0.10	2.65	1.24	0.00	12.00
BIG-B-16/1	41.7	40.7	0.5	0.1	0.0	12.0	5.6	0.0	100.6	3.03	4.91	0.09	0.01	0.00	2.68	1.27	0.00	11.98
BIG-B-16/2	42.9	39.3	0.4	0.1	0.0	11.7	5.7	0.0	100.1	3.15	4.79	0.09	0.01	0.00	2.63	1.30	0.00	11.98
BIG-B-20/1	28.1	52.3	1.1	0.0	0.9	12.7	5.6	0.0	100.6	1.90	5.90	0.20	0.00	0.17	2.64	1.18	0.00	12.00
BIG-B-20/2	28.1	52.4	0.5	0.0	0.8	12.5	5.8	0.0	100.1	1.92	5.96	0.10	0.00	0.15	2.64	1.23	0.00	12.00
BIG-B-20/3	27.8	51.9	0.2	0.0	0.8	12.3	5.8	0.0	98.8	1.93	5.99	0.04	0.00	0.14	2.64	1.25	0.00	12.00
BIG-B-25/2	57.9	24.3	0.5	0.3	0.5	11.1	4.6	0.0	99.3	4.63	3.23	0.11	0.04	0.12	2.72	1.15	0.00	12.00
BIG-B-25/4	57.5	24.8	0.5	0.0	1.9	10.3	4.9	0.0	99.9	4.54	3.25	0.11	0.00	0.41	2.49	1.20	0.00	12.00
BIG-B-26/1	55.6	26.8	0.8	0.0	1.2	10.0	5.6	0.0	100.1	4.32	3.47	0.18	0.00	0.26	2.40	1.36	0.00	11.99

Sample no.	Ta_2O_5	Nb_2O_5	TiO_2	SnO_2	Fe_2O_3	FeO	MnO	CaO	Total
BIG-B-26/2	55.0	27.0	0.8	0.5	1.3	10.0	5.6	0.0	100.3
BIG-B-26/3	46.2	34.6	0.4	0.0	1.3	11.0	5.2	0.0	98.7
BIG-B-3/1	29.5	52.5	0.3	0.0	1.2	10.6	7.8	0.0	101.9
BIG-B-3/2	19.8	61.4	0.3	0.0	1.0	10.8	8.5	0.0	101.8
BIG-B-3/3	16.7	63.5	0.2	0.3	1.0	11.9	7.4	0.0	101.0
BIG-B-4/1	27.8	54.0	0.4	0.0	0.4	13.3	5.6	0.0	101.5
BIG-B-4/2	29.6	52.5	0.3	0.0	0.8	12.8	5.7	0.0	101.8
BIGHILL-26/1	54.8	26.0	0.0	0.3	2.3	11.4	3.5	0.0	98.3
BILL-2-13/1	25.0	55.7	0.7	0.0	1.2	14.8	3.7	0.0	101.2
BILL-2-13/2	18.3	60.7	1.4	0.4	1.1	14.7	4.2	0.0	100.8
BILL-2-13/3	26.7	51.4	2.6	0.0	1.7	13.8	3.6	0.0	99.9
BILL-2-9/1	18.0	60.4	1.1	0.1	1.7	14.4	4.1	0.0	99.9
BILL-2-9/2	18.0	61.3	1.3	0.0	0.7	15.1	4.0	0.0	100.4
BILL-2-9/3	17.4	61.9	1.6	0.0	1.8	14.4	4.3	0.0	101.4
BILL-2-9/4	17.3	62.0	1.7	0.0	0.6	15.2	4.1	0.0	100.9
BILL-2-9/5	17.9	58.1	3.8	0.0	3.1	13.2	3.9	0.0	100.0
BILL-4-13/1	17.0	62.0	1.4	0.0	2.0	13.2	5.3	0.0	100.8
BILL-4-13/2	17.2	62.9	1.0	0.4	1.2	14.6	4.6	0.0	101.9
BILL-4-13/3	17.1	62.7	0.9	0.1	0.8	14.6	4.7	0.0	101.0
BILL-4-14/1	17.4	61.9	0.9	0.0	0.1	14.9	4.5	0.0	99.8
BILL-4-14/2	16.0	63.3	0.8	0.0	1.4	14.5	4.5	0.0	100.6
BILL-4-14/3	15.4	63.0	0.8	0.0	1.5	13.7	5.1	0.0	99.5
BILL-4-15/1	16.2	63.5	0.9	0.0	1.2	14.7	4.6	0.0	100.9
BILL-4-15/2	17.1	61.1	1.0	0.0	1.3	14.0	4.7	0.0	99.1
BILL-4-15/3	16.9	61.6	0.9	0.0	0.7	14.3	4.7	0.0	99.1
BILL-4-16/1	29.8	49.3	1.0	0.4	1.2	11.5	6.1	0.0	99.2
BILL-4-16/2	26.4	52.3	0.8	0.0	0.8	13.7	4.3	0.0	98.4
BILL-5-11/1	16.9	62.9	0.8	1.1	0.0	14.9	4.0	0.0	100.6
BILL-5-11/2	16.4	63.2	1.4	0.0	2.3	13.4	5.2	0.0	101.9
BILL-5-11/3	14.9	65.0	1.0	0.0	1.4	14.6	4.7	0.0	101.7
BILL-5-12/1	16.5	63.2	0.9	0.3	2.3	13.8	4.8	0.0	101.7
BILL-5-12/2	15.9	61.7	1.2	0.3	1.5	13.8	4.7	0.0	99.1
BILL-5-12/3	15.9	62.1	1.1	0.0	0.7	14.4	4.6	0.0	98.7
BILL-5-12/4	16.9	61.5	1.1	0.3	1.8	10.7	7.8	0.0	100.1
BILL-5-8/1	15.8	64.1	0.9	0.0	1.7	14.5	4.6	0.0	101.6
BILL-5-8/2	15.3	62.8	0.9	0.0	0.8	14.3	4.8	0.0	98.9
BILL-5-9B/2	14.1	64.2	0.8	0.0	0.0	14.9	4.4	0.0	98.4
BILL-5-9B/3	15.5	63.1	1.0	0.4	0.0	14.2	4.6	0.0	98.9
CAS-A-10/1	28.6	50.9	0.2	0.6	0.1	12.6	5.7	0.0	98.7
CAS-A-10/2	28.6	51.0	0.3	0.1	0.0	13.0	5.4	0.0	98.4
CAS-A-10/3	29.6	51.3	0.2	0.0	0.0	13.0	5.0	0.0	99.1
CAS-A-11/1	30.0	50.1	0.3	0.0	0.3	13.2	5.0	0.0	98.9
CAS-A-11/2	30.0	50.0	0.0	0.2	1.0	13.0	4.9	0.0	99.2
CAS-A-4/1	47.3	34.1	0.3	0.3	0.5	12.0	4.6	0.0	99.1
CAS-A-4/2	47.1	34.2	0.3	0.4	1.1	11.4	4.9	0.0	99.4
CAS-A-5/1	19.8	60.3	0.3	0.0	0.0	11.2	8.2	0.0	99.8
CAS-A-5/2	16.1	63.8	0.5	0.0	0.2	13.9	5.8	0.0	100.3
CAS-A-6/1	16.7	62.1	0.5	0.0	0.3	14.0	5.3	0.0	98.9
CAS-A-6/2	16.0	62.8	0.6	0.0	1.4	13.4	5.5	0.0	99.6
CAS-B-3	28.5	53.3	0.0	0.0	0.0	11.7	7.2	0.0	100.6
CAS-I-1B/1	65.1	18.5	0.4	0.4	0.9	10.1	5.0	0.0	100.4
CAS-I-1B/2	62.0	20.9	0.4	0.3	0.0	9.3	6.2	0.0	99.1
CAS-I-6A/1	53.5	27.9	0.3	0.0	1.9	8.4	6.9	0.0	98.8
CAS-I-6A/2	39.6	43.1	0.3	0.2	0.6	9.9	7.7	0.1	101.5
CAS-I-6B/1	29.5	53.0	0.0	0.0	0.0	10.8	8.1	0.0	101.2
CAS-I-6B/2	30.0	51.4	0.4	0.3	1.7	9.1	8.8	0.0	101.7
CAS-S-8/1	54.8	27.1	1.1	0.0	1.8	11.8	3.5	0.0	100.1
CAS-S-8/2	57.1	25.1	1.1	0.0	1.9	11.1	4.0	0.0	100.4
CAS-S-8/3	46.0	34.2	0.9	0.0	3.5	11.9	3.3	0.0	99.7
CATA-C-4/1	20.0	59.5	0.0	0.0	0.0	9.1	10.1	0.0	98.7
CATA-C-4/2	22.3	56.7	0.0	0.9	0.0	10.8	7.6	0.0	98.3
CATA-C-4/3	63.2	18.8	0.3	0.0	1.1	8.0	6.6	0.1	98.2

Cations based on 24(O)

Ta^{5+}	Nb^{5+}	Ti^{4+}	Sn^{4+}	Fe^{3+}	Fe^{2+}	Mn^{2+}	Ca^{2+}	Total
4.26	3.48	0.18	0.06	0.28	2.38	1.35	0.00	12.00
3.49	4.36	0.09	0.00	0.26	2.56	1.24	0.00	12.00
1.99	5.89	0.05	0.00	0.23	2.20	1.63	0.00	12.00
1.29	6.62	0.05	0.00	0.18	2.15	1.71	0.00	12.00
1.08	6.82	0.04	0.02	0.18	2.36	1.50	0.00	12.00
1.88	6.05	0.07	0.00	0.08	2.75	1.17	0.00	12.00
2.01	5.90	0.06	0.00	0.15	2.67	1.21	0.00	12.00
4.37	3.44	0.00	0.04	0.50	2.79	0.84	0.00	11.98
1.67	6.18	0.12	0.00	0.21	3.04	0.77	0.00	12.00
1.19	6.55	0.25	0.04	0.19	2.93	0.84	0.00	12.00
1.80	5.76	0.49	0.00	0.32	2.86	0.76	0.00	12.00
1.18	6.57	0.20	0.01	0.31	2.89	0.83	0.00	12.00
1.17	6.63	0.24	0.00	0.13	3.02	0.82	0.00	12.00
1.12	6.59	0.28	0.00	0.31	2.84	0.85	0.00	12.00
1.11	6.64	0.31	0.00	0.11	3.01	0.82	0.00	12.00
1.15	6.21	0.68	0.00	0.55	2.62	0.79	0.00	12.00
1.09	6.63	0.24	0.00	0.36	2.61	1.07	0.00	12.00
1.10	6.69	0.18	0.04	0.21	2.87	0.91	0.00	12.00
1.11	6.73	0.16	0.01	0.15	2.89	0.95	0.00	12.00
1.14	6.74	0.16	0.00	0.02	3.01	0.92	0.00	12.00
1.03	6.78	0.15	0.00	0.25	2.87	0.91	0.00	12.00
1.00	6.81	0.14	0.00	0.26	2.74	1.04	0.00	12.00
1.04	6.79	0.16	0.00	0.21	2.90	0.91	0.00	12.00
1.12	6.68	0.18	0.00	0.23	2.83	0.96	0.00	12.00
1.11	6.73	0.16	0.00	0.13	2.89	0.97	0.00	12.00
2.07	5.69	0.19	0.04	0.24	2.45	1.31	0.00	12.00
1.83	6.02	0.16	0.00	0.15	2.92	0.93	0.00	12.00
1.10	6.79	0.14	0.11	0.00	2.97	0.80	0.00	11.91
1.04	6.67	0.24	0.00	0.40	2.63	1.03	0.00	12.00
0.95	6.85	0.18	0.00	0.25	2.84	0.93	0.00	12.00
1.05	6.70	0.16	0.02	0.40	2.71	0.96	0.00	12.00
1.04	6.71	0.22	0.03	0.27	2.77	0.97	0.00	12.00
1.04	6.78	0.19	0.00	0.13	2.90	0.94	0.00	12.00
1.10	6.65	0.19	0.02	0.32	2.14	1.57	0.00	11.99
1.00	6.79	0.15	0.00	0.29	2.84	0.91	0.00	12.00
1.00	6.84	0.17	0.00	0.14	2.88	0.97	0.00	12.00
0.92	6.99	0.15	0.00	0.00	3.01	0.89	0.00	11.97
1.02	6.88	0.18	0.04	0.00	2.86	0.94	0.00	11.92
2.00	5.92	0.04	0.06	0.02	2.71	1.24	0.00	12.00
2.01	5.95	0.05	0.01	0.00	2.80	1.18	0.00	12.00
2.06	5.95	0.04	0.00	0.00	2.80	1.09	0.00	11.94
2.10	5.84	0.06	0.00	0.06	2.85	1.09	0.00	12.00
2.10	5.82	0.00	0.02	0.19	2.80	1.07	0.00	12.00
3.59	4.31	0.06	0.04	0.10	2.80	1.10	0.00	12.00
3.56	4.29	0.07	0.04	0.22	2.66	1.15	0.00	12.00
1.31	6.64	0.06	0.00	0.00	2.29	1.69	0.00	12.00
1.05	6.89	0.08	0.00	0.03	2.78	1.18	0.00	12.00
1.10	6.82	0.09	0.00	0.06	2.84	1.08	0.00	12.00
1.04	6.80	0.10	0.00	0.25	2.69	1.11	0.00	12.00
1.95	6.06	0.00	0.00	0.00	2.46	1.53	0.00	11.99
5.32	2.52	0.10	0.05	0.19	2.55	1.27	0.00	12.00
5.08	2.85	0.08	0.03	0.00	2.34	1.59	0.00	11.98
4.19	3.64	0.05	0.00	0.40	2.02	1.68	0.01	12.00
2.82	5.09	0.05	0.02	0.11	2.17	1.70	0.02	12.00
2.01	6.00	0.00	0.00	0.00	2.25	1.71	0.00	11.98
2.03	5.79	0.08	0.03	0.32	1.90	1.85	0.00	12.00
4.24	3.48	0.23	0.00	0.38	2.81	0.85	0.00	12.00
4.45	3.26	0.23	0.00	0.42	2.66	0.98	0.00	12.00
3.41	4.22	0.18	0.00	0.72	2.71	0.75	0.00	12.00
1.35	6.65	0.00	0.00	0.00	1.88	2.12	0.00	12.00
1.52	6.44	0.00	0.10	0.00	2.27	1.63	0.00	11.95
5.26	2.61	0.07	0.00	0.26	2.05	1.72	0.03	12.00

Sample no.	Ta_2O_5	Nb_2O_5	TiO_2	SnO_2	Fe_2O_3	FeO	MnO	CaO	Total
CATA-I-2	64.0	20.1	0.4	0.2	0.0	8.7	7.0	0.0	100.3
CATA-I-2/2	57.1	26.2	0.0	0.0	0.2	8.7	7.5	0.0	99.7
CATA-I-7/1	61.8	21.9	0.0	0.0	0.0	6.1	8.7	0.0	98.4
CATA-I-7/2	47.3	36.7	0.3	0.0	0.0	8.3	9.1	0.0	101.8
CATA-I-7/3	43.4	38.4	0.0	0.0	0.0	6.6	10.5	0.0	99.0
CATA-I-9	38.9	42.2	0.2	0.0	0.5	6.3	11.1	0.0	99.2
CATA-I-9/1	37.4	42.8	0.2	0.0	0.3	5.2	12.2	0.0	98.1
CATA-I-9/2	40.5	41.5	0.2	0.0	0.6	7.4	10.0	0.0	100.2
CATA-K-1/1	45.7	37.4	0.1	0.2	0.2	4.5	12.8	0.0	100.8
CATA-K-1/2	46.7	36.4	0.1	0.6	0.4	4.0	13.1	0.0	101.3
CATA-Z-1/1	48.3	35.7	0.1	0.5	0.0	7.6	9.3	0.0	101.6
CATA-Z-1/2	53.4	31.0	0.0	1.1	0.0	7.0	8.6	0.0	101.1
CATA-Z-1/3	53.9	27.9	0.0	1.0	0.0	6.6	8.9	0.0	98.2
DR-BOB-5/2	52.3	29.3	0.9	0.7	1.2	15.0	0.9	0.0	100.4
DR-BOB-5/4	54.2	28.0	1.0	0.8	1.2	13.4	2.4	0.0	101.0
EKID-5/1	38.3	43.9	0.3	0.0	0.3	11.8	6.1	0.0	100.6
FI-A-6/1	29.0	51.7	0.0	0.0	0.6	13.8	4.5	0.0	99.6
FI-A-6/2	20.9	60.1	0.2	0.0	0.1	11.6	7.9	0.0	100.8
FI-A-6/3	18.7	62.5	0.3	0.0	0.0	15.5	4.1	0.0	101.1
FI-A-9/1	22.9	57.9	0.5	0.3	0.0	14.8	4.4	0.0	100.9
FI-A-9/2	23.0	58.1	0.3	0.2	0.0	15.0	4.4	0.0	101.0
FI-B-2/1	42.9	39.5	0.2	0.3	0.7	11.9	5.4	0.0	100.9
FI-B-2/2	41.0	41.3	0.4	0.5	0.1	12.3	5.4	0.0	101.0
FI-B-2/3	54.8	26.1	0.5	0.4	1.1	11.0	4.4	0.0	98.3
FLY-1-11/2	60.5	22.4	0.2	0.0	0.0	9.7	6.0	0.0	98.9
FLY-1-11/3	59.6	22.7	0.3	0.1	0.0	9.5	6.2	0.0	98.4
FLY-1-11/5	59.6	22.7	0.3	0.1	0.0	9.5	6.2	0.0	98.4
FLY-1-7/E1	66.1	18.7	0.0	0.0	0.0	7.8	7.8	0.0	100.4
FLY-1-7/E2	74.9	10.3	0.0	0.2	0.6	6.9	7.6	0.0	100.6
FLY-1-7/G1	48.4	34.0	0.0	0.0	0.9	6.4	10.1	0.0	99.9
FLY-1-7/G2	60.3	22.6	0.0	0.2	1.2	5.7	9.6	0.0	99.5
FLY-1-7A	45.9	37.6	0.1	0.1	0.0	7.3	10.1	0.0	101.1
FLY-1-7B	49.0	34.4	0.0	0.5	0.0	4.6	10.5	0.0	99.0
FLY-1-7E	70.5	14.5	0.0	0.1	0.2	7.5	7.7	0.0	100.5
FLY-1-7F	69.3	14.2	0.3	0.4	0.0	6.6	7.9	0.0	98.6
FLY-1-7G	54.3	28.3	0.0	0.1	1.1	6.0	9.9	0.0	99.7
FREDA-14/1	51.4	31.3	0.0	0.0	0.0	10.3	6.3	0.0	99.3
FREDA-14/2	49.2	33.0	0.0	0.3	0.0	9.4	7.3	0.0	99.3
FREDA-3/1	44.4	36.9	0.3	0.5	0.0	11.1	5.6	0.0	98.9
FREDA-3/2	46.0	36.8	0.0	0.7	0.0	11.4	5.8	0.0	100.6
FRGR-PG-1/2	54.5	28.0	0.8	0.5	0.0	12.4	3.0	0.0	99.2
GREG-C-7A/1	23.3	56.2	0.0	0.5	0.1	11.4	7.4	0.0	98.9
GREG-C-7A/2	23.3	56.1	0.5	0.0	0.6	10.8	7.8	0.0	99.1
GREG-C-7A/3	23.2	56.9	0.0	0.0	0.4	11.0	7.9	0.0	99.4
GREG-C-7B/1	23.4	58.6	0.0	0.2	0.0	11.2	8.2	0.0	101.6
GREG-C-7B/2	26.4	55.8	0.0	0.4	0.0	10.4	8.5	0.0	101.5
HEIDI-10-18/1	58.9	23.3	0.8	0.5	1.4	9.5	5.6	0.0	100.1
HEIDI-10-18/2	57.4	24.8	0.7	0.0	0.9	10.4	5.2	0.0	99.3
HEIDI-10-18/3	22.5	58.5	0.3	0.0	0.5	12.9	6.3	0.0	101.0
HEIDI-10-18/4	50.8	31.2	0.8	0.4	0.1	11.3	5.3	0.0	100.0
HEIDI-10-18/5	59.8	22.8	0.6	0.2	0.9	10.0	5.4	0.0	99.8
HEIDI-3-1/1	46.2	36.7	0.9	0.0	0.0	11.5	5.8	0.0	101.1
HEIDI-3-1/2	46.6	35.7	0.9	0.0	0.0	11.0	5.9	0.0	100.2
JAKE-B-2/2	17.7	62.9	0.8	0.0	1.2	7.3	11.8	0.0	101.7
JAKE-B-2/3	14.8	63.8	0.9	0.0	0.9	7.7	11.4	0.0	99.4
JAKE-C-4/1	8.6	70.6	0.0	0.0	0.6	0.0	19.9	0.0	99.8
JAKE-C-4/3	25.8	53.8	0.6	0.0	1.1	9.3	8.8	0.0	99.5
JAKE-C-4/4	25.5	54.2	0.7	0.4	0.3	10.2	8.3	0.0	99.6
JAKE-C-5/2	27.4	52.8	0.4	0.0	0.0	9.2	8.0	0.8	98.5
JAKE-C-5/3	28.3	52.6	0.5	0.0	0.2	9.9	8.7	0.0	100.2
JAKE-G-2/1	18.3	61.1	0.7	0.0	0.0	9.7	9.4	0.0	99.2
JAKE-G-2/2	22.0	59.8	0.4	0.0	0.1	3.2	16.3	0.0	101.8

Cations based on 24(O)

Ta^{5+}	Nb^{5+}	Ti^{4+}	Sn^{4+}	Fe^{3+}	Fe^{2+}	Mn^{2+}	Ca^{2+}	Total
5.21	2.72	0.08	0.03	0.00	2.18	1.77	0.00	11.99
4.53	3.45	0.00	0.00	0.04	2.11	1.85	0.00	12.00
5.09	3.00	0.00	0.00	0.00	1.55	2.23	0.00	11.86
3.48	4.48	0.06	0.00	0.00	1.88	2.09	0.00	12.00
3.24	4.77	0.00	0.00	0.00	1.53	2.45	0.00	11.98
2.83	5.10	0.04	0.00	0.10	1.41	2.52	0.00	12.00
2.74	5.21	0.04	0.00	0.07	1.17	2.77	0.00	12.00
2.93	4.99	0.05	0.00	0.12	1.64	2.26	0.00	12.00
3.38	4.59	0.02	0.02	0.03	1.01	2.95	0.00	12.00
3.45	4.47	0.01	0.06	0.08	0.91	3.01	0.00	12.00
3.58	4.39	0.03	0.05	0.00	1.74	2.15	0.00	11.95
4.08	3.94	0.00	0.12	0.00	1.66	2.05	0.00	11.85
4.29	3.69	0.00	0.11	0.00	1.61	2.20	0.00	11.91
4.00	3.73	0.19	0.08	0.26	3.53	0.21	0.00	12.00
4.15	3.57	0.21	0.09	0.24	3.15	0.58	0.00	12.00
2.73	5.20	0.07	0.00	0.05	2.59	1.35	0.00	11.99
2.01	5.96	0.00	0.00	0.11	2.95	0.98	0.00	12.00
1.38	6.59	0.04	0.00	0.01	2.36	1.61	0.00	12.00
1.22	6.76	0.06	0.00	0.00	3.10	0.83	0.00	11.97
1.52	6.40	0.08	0.03	0.00	3.03	0.91	0.00	11.99
1.53	6.42	0.06	0.02	0.00	3.07	0.90	0.00	12.00
3.13	4.78	0.03	0.03	0.14	2.65	1.23	0.00	12.00
2.96	4.95	0.07	0.06	0.01	2.74	1.21	0.00	12.00
4.36	3.45	0.11	0.05	0.23	2.69	1.10	0.00	12.00
4.93	3.04	0.04	0.00	0.00	2.42	1.54	0.00	11.98
4.88	3.08	0.06	0.01	0.00	2.38	1.59	0.00	11.99
4.88	3.08	0.06	0.01	0.00	2.38	1.59	0.00	11.99
5.44	2.56	0.00	0.00	0.00	1.97	2.00	0.00	11.98
6.46	1.47	0.00	0.03	0.15	1.84	2.05	0.00	12.00
3.66	4.27	0.00	0.00	0.20	1.48	2.39	0.00	12.00
4.86	3.04	0.00	0.02	0.26	1.42	2.41	0.00	12.00
3.38	4.60	0.02	0.01	0.00	1.66	2.31	0.00	11.98
3.75	4.38	0.00	0.05	0.00	1.08	2.49	0.00	11.76
5.95	2.03	0.00	0.01	0.04	1.94	2.02	0.00	12.00
5.94	2.03	0.07	0.04	0.00	1.73	2.10	0.00	11.92
4.24	3.67	0.00	0.01	0.23	1.45	2.40	0.00	12.00
3.98	4.03	0.00	0.00	0.00	2.45	1.52	0.00	11.99
3.77	4.21	0.00	0.03	0.00	2.23	1.75	0.00	11.99
3.34	4.62	0.05	0.06	0.00	2.57	1.32	0.00	11.95
3.42	4.54	0.00	0.07	0.00	2.62	1.33	0.00	11.98
4.27	3.65	0.17	0.06	0.00	3.00	0.72	0.00	11.87
1.59	6.38	0.00	0.05	0.01	2.40	1.58	0.00	12.00
1.58	6.32	0.09	0.00	0.11	2.26	1.64	0.00	12.00
1.57	6.40	0.00	0.00	0.07	2.29	1.66	0.00	12.00
1.54	6.45	0.00	0.02	0.00	2.29	1.69	0.00	11.99
1.77	6.22	0.00	0.04	0.00	2.15	1.77	0.00	11.95
4.66	3.07	0.18	0.06	0.31	2.32	1.39	0.00	12.00
4.56	3.27	0.15	0.00	0.20	2.53	1.28	0.00	12.00
1.49	6.44	0.05	0.00	0.09	2.63	1.30	0.00	12.00
3.88	3.96	0.18	0.05	0.03	2.65	1.25	0.00	12.00
4.79	3.04	0.13	0.03	0.21	2.46	1.34	0.00	12.00
3.40	4.48	0.19	0.00	0.00	2.60	1.32	0.00	11.99
3.47	4.42	0.18	0.00	0.00	2.53	1.38	0.00	11.98
1.13	6.70	0.14	0.00	0.22	1.45	2.36	0.00	12.00
0.96	6.88	0.16	0.00	0.16	1.53	2.31	0.00	12.00
0.54	7.42	0.00	0.00	0.11	0.01	3.92	0.00	12.00
1.76	6.09	0.12	0.00	0.22	1.94	1.88	0.00	12.00
1.74	6.13	0.13	0.04	0.06	2.14	1.76	0.00	12.00
1.90	6.08	0.07	0.00	0.00	1.96	1.72	0.22	11.95
1.93	5.99	0.10	0.00	0.04	2.09	1.85	0.00	12.00
1.21	6.72	0.12	0.00	0.00	1.97	1.94	0.00	11.97
1.44	6.50	0.07	0.00	0.02	0.64	3.32	0.00	12.00

Sample no.	Ta_2O_5	Nb_2O_5	TiO_2	SnO_2	Fe_2O_3	FeO	MnO	CaO	Total
JAKE-G-3/1	22.1	59.3	0.9	0.0	0.3	9.8	9.6	0.0	102.0
JAKE-G-3/3	23.1	57.9	0.6	0.0	1.0	9.2	9.6	0.0	101.4
JAKE-G-4/1	20.4	61.0	0.7	0.0	0.1	6.5	13.1	0.0	101.9
JAKE-G-4/2	20.5	57.7	1.0	0.1	1.8	8.1	9.9	0.0	99.1
JAKE-G-5/1	30.0	51.1	0.0	0.0	0.4	2.4	15.9	0.0	99.8
JAKE-G-5/2	31.5	49.3	0.5	0.0	2.0	5.9	11.4	0.0	100.8
JAKE-G-6/1	34.9	47.1	0.6	0.1	0.3	10.3	7.8	0.0	101.1
JAKE-G-6/2	34.1	46.3	0.9	0.0	0.0	10.0	7.8	0.0	99.0
JAKE-G-6/3	29.4	51.2	0.5	0.0	0.9	7.6	10.4	0.0	100.1
JAKE-H-1/1	18.0	63.1	0.3	0.0	0.0	3.9	15.8	0.0	101.0
JENNE-A-2/2	41.5	39.9	0.3	0.0	0.8	9.9	7.2	0.0	99.5
JENNE-A-2/3	41.6	40.6	0.0	0.1	1.3	9.4	7.7	0.0	100.7
JENNE-A-2/4A	45.0	39.3	0.1	0.0	0.0	9.0	6.4	1.7	101.6
JENNE-A-2/4B	40.0	42.6	0.0	0.0	0.0	9.7	7.2	0.4	99.9
JO-A-18	24.9	57.2	0.6	0.0	0.0	14.3	5.1	0.0	102.2
JOLLY-9/1	34.8	45.4	1.4	0.7	0.0	14.7	2.9	0.0	100.0
JOLLY-9/2	31.4	49.4	1.3	0.4	0.0	15.4	2.9	0.0	100.8
LENS-11/1	25.3	54.3	1.4	0.2	2.3	13.5	4.2	0.0	101.1
LENS-11/2	26.8	52.8	1.2	0.1	3.5	10.2	6.8	0.0	101.3
LIMO-C-1A/1	35.7	44.9	0.3	0.3	0.6	10.0	7.5	0.1	99.3
LIMO-C-1A/2	34.4	46.6	0.4	0.4	0.4	10.6	7.3	0.0	100.1
LIMO-C-1B	35.3	46.1	0.5	0.0	0.8	8.9	8.8	0.0	100.4
LIT-1-10/1	62.6	21.6	0.3	0.5	0.4	9.2	6.5	0.0	101.1
LIT-1-10/2	54.3	28.8	0.5	0.3	0.0	9.3	7.0	0.0	100.3
LIT-1-2/1	52.4	32.0	0.0	0.0	0.8	10.0	6.7	0.0	101.8
LIT-1-2/2	49.5	34.4	0.2	0.6	0.0	9.8	7.1	0.0	101.6
LIT-1-2/3	44.0	38.2	0.0	0.0	0.0	11.1	6.1	0.0	99.5
LIT-1-9/1	56.0	27.5	0.2	0.0	0.0	9.6	6.8	0.0	100.1
LIT-1-9/2	54.8	28.9	0.1	0.0	0.8	9.3	7.0	0.0	100.9
LIT-2-4/1	45.1	36.7	0.4	0.5	1.2	12.2	4.4	0.0	100.5
LIT-2-4/2	44.5	36.5	0.4	0.4	0.4	12.3	4.5	0.0	99.1
LIT-2-4/3	46.5	34.3	0.6	0.7	0.0	12.4	4.2	0.0	98.7
LIT-2-4/4	51.6	30.4	0.6	0.4	0.8	11.6	4.6	0.0	100.0
LU-A-10/1	34.7	47.7	0.1	0.0	0.1	11.1	7.3	0.0	101.0
LU-A-10/2	37.4	44.4	0.2	0.0	0.1	11.1	6.8	0.0	100.2
LU-A-11/1	59.1	25.8	0.4	0.4	0.0	11.5	4.8	0.0	102.0
LU-A-11/2	61.5	23.1	0.3	0.0	0.0	10.6	5.5	0.0	101.0
LU-A-15/1	43.6	39.1	0.0	0.4	0.2	11.1	6.3	0.0	100.8
LU-A-15/2	45.5	37.4	0.0	0.2	0.4	9.0	8.3	0.0	100.7
LU-A-15/3	45.6	37.6	0.0	0.0	0.0	9.0	8.1	0.0	100.5
LU-A-2/1	29.7	51.3	0.0	0.0	0.0	12.1	6.4	0.0	99.5
LU-A-2/2	30.0	50.9	0.0	0.1	0.0	12.0	6.3	0.0	99.3
LU-A-5/1	40.4	42.6	0.4	0.1	0.7	8.8	8.9	0.0	101.9
LU-A-5/2	37.1	46.7	0.0	0.0	0.0	10.7	7.3	0.0	101.9
LU-A-6/1	36.3	46.7	0.0	0.0	0.0	10.4	7.8	0.0	101.2
LU-A-7/1	31.9	50.9	0.0	0.2	0.0	11.7	6.6	0.0	101.4
LU-A-7/2	35.3	47.7	0.0	0.0	0.4	12.9	5.5	0.0	101.8
LU-A-9/4	36.9	44.0	0.0	0.4	0.0	13.9	3.8	0.0	99.1
LU-A-9/5	55.9	24.6	0.0	2.3	0.0	11.7	4.0	0.0	98.4
LU-B-3/2	48.6	34.5	0.3	0.4	0.0	13.6	3.5	0.0	100.9
LU-B-3/4	49.6	33.4	0.0	0.5	0.6	15.4	1.4	0.0	101.0
LU-B-4/2	47.8	35.2	0.2	0.5	0.3	14.6	2.4	0.0	101.1
LU-B-5/4	45.1	38.1	0.0	0.3	1.2	15.7	1.4	0.0	101.8
LU-C-12/1	20.8	58.7	0.2	0.0	0.0	13.4	5.7	0.0	98.8
LU-C-12/2	24.0	57.1	0.0	0.0	0.9	13.0	5.9	0.0	100.8
LU-C-12/3	29.2	52.3	0.0	0.0	0.0	12.6	6.0	0.0	100.2
LU-C-16/1	49.7	33.0	0.3	0.2	1.2	9.7	6.7	0.0	100.8
LU-C-16/3	55.1	28.0	0.2	0.5	0.0	8.5	7.6	0.0	99.8
LU-C-18/1	26.9	54.5	0.0	0.0	0.0	12.0	6.9	0.0	100.3
LU-C-18/2	26.9	54.6	0.0	0.4	0.0	13.6	5.2	0.0	100.7
LU-C-19/1	25.0	56.7	0.3	0.0	0.1	12.8	6.5	0.0	101.4
LU-C-19/2	23.7	58.4	0.2	0.1	0.0	14.0	5.3	0.0	101.6

Cations based on 24(O)

Ta^{5+}	Nb^{5+}	Ti^{4+}	Sn^{4+}	Fe^{3+}	Fe^{2+}	Mn^{2+}	Ca^{2+}	Total
1.44	6.43	0.16	0.00	0.05	1.96	1.95	0.00	12.00
1.52	6.34	0.11	0.00	0.18	1.86	1.98	0.00	12.00
1.33	6.58	0.13	0.00	0.03	1.30	2.64	0.00	12.00
1.36	6.39	0.19	0.01	0.33	1.65	2.06	0.00	12.00
2.08	5.89	0.00	0.00	0.08	0.51	3.43	0.00	12.00
2.17	5.64	0.10	0.00	0.39	1.26	2.45	0.00	12.01
2.44	5.46	0.11	0.01	0.06	2.21	1.71	0.00	12.00
2.42	5.47	0.17	0.00	0.00	2.20	1.72	0.00	11.98
2.02	5.86	0.10	0.00	0.18	1.62	2.23	0.00	12.00
1.17	6.81	0.05	0.00	0.00	0.78	3.19	0.00	11.99
3.05	4.87	0.05	0.00	0.15	2.24	1.64	0.00	12.00
3.01	4.89	0.01	0.01	0.26	2.09	1.73	0.00	12.00
3.26	4.74	0.03	0.00	0.00	2.01	1.44	0.49	11.98
2.90	5.14	0.00	0.00	0.00	2.15	1.62	0.13	11.94
1.65	6.28	0.12	0.00	0.00	2.90	1.05	0.00	11.99
2.46	5.32	0.28	0.07	0.00	3.19	0.63	0.00	11.96
2.16	5.66	0.24	0.04	0.00	3.26	0.60	0.00	11.96
1.68	5.99	0.26	0.02	0.42	2.76	0.84	0.00	11.98
1.78	5.85	0.23	0.01	0.64	2.09	1.38	0.00	11.98
2.55	5.34	0.07	0.04	0.12	2.20	1.66	0.02	12.00
2.43	5.46	0.08	0.04	0.08	2.31	1.60	0.00	12.00
2.48	5.39	0.11	0.00	0.16	1.93	1.93	0.00	12.00
5.01	2.87	0.06	0.06	0.09	2.28	1.62	0.00	12.00
4.21	3.71	0.11	0.04	0.00	2.21	1.69	0.00	11.97
3.94	4.00	0.00	0.00	0.16	2.32	1.57	0.00	12.00
3.69	4.26	0.04	0.06	0.00	2.26	1.65	0.00	11.96
3.30	4.68	0.00	0.01	0.05	2.50	1.46	0.00	12.00
4.39	3.59	0.04	0.00	0.00	2.32	1.66	0.00	12.00
4.22	3.70	0.03	0.00	0.17	2.20	1.67	0.00	12.00
3.33	4.50	0.08	0.05	0.24	2.77	1.02	0.00	12.00
3.34	4.54	0.09	0.04	0.09	2.85	1.05	0.00	12.00
3.54	4.33	0.13	0.08	0.00	2.91	0.99	0.00	11.98
3.96	3.87	0.13	0.04	0.16	2.74	1.10	0.00	12.00
2.43	5.55	0.02	0.00	0.02	2.38	1.59	0.00	12.00
2.68	5.28	0.05	0.00	0.03	2.44	1.52	0.00	12.00
4.60	3.34	0.08	0.04	0.00	2.74	1.17	0.00	11.97
4.90	3.06	0.06	0.00	0.00	2.61	1.37	0.00	12.00
3.19	4.76	0.00	0.04	0.05	2.51	1.44	0.00	12.00
3.36	4.60	0.00	0.02	0.07	2.04	1.91	0.00	12.00
3.38	4.63	0.00	0.00	0.00	2.06	1.88	0.00	11.97
2.07	5.94	0.00	0.00	0.00	2.59	1.38	0.00	11.98
2.09	5.91	0.00	0.01	0.00	2.59	1.38	0.00	11.98
2.86	5.03	0.07	0.01	0.14	1.92	1.96	0.00	12.00
2.59	5.44	0.00	0.00	0.00	2.31	1.60	0.00	11.95
2.56	5.46	0.00	0.00	0.00	2.26	1.70	0.00	11.98
2.20	5.83	0.00	0.02	0.00	2.47	1.42	0.00	11.94
2.46	5.52	0.00	0.00	0.07	2.76	1.20	0.00	12.00
2.68	5.30	0.00	0.04	0.00	3.11	0.86	0.00	11.99
4.51	3.31	0.00	0.27	0.00	2.90	1.01	0.00	12.00
3.64	4.29	0.05	0.04	0.00	3.13	0.82	0.00	11.99
3.74	4.18	0.00	0.06	0.13	3.56	0.33	0.00	12.00
3.56	4.36	0.04	0.05	0.07	3.35	0.57	0.00	12.00
3.28	4.61	0.00	0.03	0.25	3.50	0.32	0.00	12.00
1.40	6.58	0.04	0.00	0.00	2.77	1.20	0.00	11.99
1.60	6.34	0.00	0.00	0.16	2.67	1.22	0.00	12.00
2.01	6.00	0.00	0.00	0.00	2.67	1.30	0.00	11.98
3.73	4.13	0.05	0.02	0.26	2.24	1.56	0.00	12.00
4.32	3.64	0.04	0.06	0.00	2.05	1.85	0.00	11.96
1.84	6.17	0.00	0.00	0.00	2.51	1.46	0.00	11.98
1.83	6.17	0.00	0.04	0.00	2.84	1.09	0.00	11.97
1.67	6.29	0.04	0.00	0.02	2.62	1.35	0.00	12.00
1.57	6.42	0.03	0.01	0.00	2.85	1.09	0.00	11.97

Sample no.	Ta_2O_5	Nb_2O_5	TiO_2	SnO_2	Fe_2O_3	FeO	MnO	CaO	Total
LU-C-19/3	22.2	58.6	0.2	0.4	0.0	14.4	4.9	0.0	100.8
LU-C-21/1	41.9	41.1	0.2	0.0	0.2	11.8	5.9	0.0	101.2
LU-C-21/2	40.6	42.5	0.3	0.4	0.0	11.3	6.7	0.0	101.8
LU-C-21/3	35.3	48.1	0.1	0.1	0.0	12.1	6.0	0.0	101.7
LU-C-3/TAN	51.5	29.3	0.2	0.5	0.8	14.2	1.7	0.0	98.2
LU-C-4/3	55.8	26.9	0.2	0.5	1.0	12.6	3.2	0.0	100.3
LU-C-6/3	58.0	25.1	0.1	0.3	0.5	10.3	5.6	0.0	100.0
LU-D1-4/2	58.5	24.8	0.0	0.4	0.0	9.2	6.8	0.0	99.7
MAC-109/1	52.3	30.9	0.4	0.3	0.0	9.6	7.1	0.0	100.6
MAC-109/2	53.3	29.0	0.7	0.5	0.0	9.3	6.9	0.0	99.6
MAC-109/3	52.8	29.0	0.7	0.4	0.8	9.0	6.9	0.0	99.6
MAC-109/4	53.4	28.9	0.8	0.4	0.2	9.4	6.9	0.0	99.8
MAC-109/5	52.5	29.9	0.4	0.4	0.2	9.4	7.0	0.0	99.8
MAC-111/1	52.9	30.8	0.4	0.2	0.3	9.6	7.1	0.0	101.3
MAC-111/2	52.3	30.5	0.5	0.2	0.0	9.5	6.6	0.0	99.7
MAC-112/1	53.1	29.9	0.5	0.3	0.0	9.1	6.7	0.0	99.7
MAC-112/2	42.1	39.7	0.7	0.0	0.0	10.6	6.2	0.0	99.3
MAC-112/5	42.9	40.9	0.6	0.1	0.0	10.6	6.8	0.0	101.9
MAC-112/6	43.1	40.9	0.5	0.0	0.0	11.0	6.3	0.0	101.7
MAC-112/8	60.9	22.0	1.0	0.5	0.0	8.9	6.8	0.0	100.2
MAC-115/1	54.3	26.8	0.5	0.3	0.4	8.6	7.3	0.0	98.1
MAC-115/2	55.4	26.5	0.5	0.0	0.0	8.8	7.3	0.0	98.4
MEL-1-12/1	28.1	52.3	0.0	0.0	0.0	14.6	3.4	0.0	98.5
MEL-1-12/2	29.3	53.0	0.1	0.0	0.0	15.3	3.3	0.2	101.3
MEL-1-12/4	32.8	48.5	0.2	0.0	0.2	14.6	3.5	0.1	100.0
MEL-5-3/1	43.3	38.7	0.8	0.0	0.0	13.3	3.2	0.0	99.2
MEL-5-3/2	40.9	40.4	0.7	0.0	0.0	14.1	2.9	0.0	98.9
MEL-5-3/3	41.3	40.0	0.7	0.0	0.0	14.2	2.9	0.0	99.1
MEL-6-8	24.9	56.0	0.2	0.0	0.5	13.6	5.3	0.0	100.6
MEL-8-5/1	52.7	28.9	1.4	0.0	1.2	12.4	3.4	0.0	100.0
MEL-8-5/2	23.5	56.5	1.1	0.1	0.1	15.5	3.6	0.0	100.3
MEL-8-5/3	26.0	54.4	1.2	0.0	1.2	14.9	3.4	0.0	101.3
MEL-9-20/1	54.8	27.8	0.4	0.0	0.9	11.3	4.7	0.0	99.9
MEL-9-20/2	58.6	24.5	0.4	0.3	0.0	11.2	4.8	0.0	99.8
MINT-A-2/3	55.4	27.8	0.3	0.3	1.1	8.7	7.2	0.0	101.0
MINT-B-4/2	39.8	42.6	0.2	0.5	0.1	8.6	9.2	0.0	101.0
MINT-B-4/3	39.9	42.7	0.2	0.0	0.0	8.4	8.9	0.0	100.1
MOON-3/1	33.5	48.5	0.2	0.0	0.0	9.1	8.6	0.0	99.8
MOON-3/2	25.2	54.4	0.0	0.3	0.0	10.2	7.9	0.0	98.0
MOOSE-100A/1	24.8	57.4	0.3	0.1	0.0	15.0	4.2	0.0	101.8
MOOSE-100A/2	24.3	57.2	0.5	0.0	0.0	14.8	4.3	0.0	101.0
MOOSE-100B	24.2	58.0	0.4	0.1	0.0	14.7	4.3	0.0	101.8
MOOSE-100B/2	24.5	57.4	0.4	0.2	0.0	14.6	4.3	0.0	101.4
MOOSE-101	24.4	57.7	0.3	0.4	0.0	14.7	4.4	0.0	101.8
MOOSE-102A/1	35.9	45.8	0.4	0.3	1.1	13.2	4.5	0.0	101.2
MOOSE-102A/3	25.5	55.1	0.4	0.3	0.5	15.0	3.8	0.0	100.7
MOOSE-102B/1	52.7	31.0	0.5	0.2	0.2	13.1	3.7	0.0	101.5
MOOSE-102B/2	23.3	56.6	0.4	0.3	0.0	14.3	4.4	0.0	99.4
MOOSE-102B/3	28.9	53.8	0.3	0.0	0.0	14.1	4.4	0.0	101.5
MOOSE-102B/4	31.8	48.3	0.4	0.0	1.8	12.5	4.5	0.3	99.6
MOOSE-104A/1	27.3	53.5	0.4	0.0	0.2	14.4	4.3	0.0	100.1
MOOSE-104A/2	25.4	55.2	0.5	0.4	0.0	14.3	4.3	0.0	100.2
MOOSE-104B/1	24.9	55.8	0.5	0.3	0.0	14.4	4.3	0.0	100.3
MOOSE-104B/2	51.1	31.4	0.3	0.1	0.7	12.9	3.5	0.0	100.1
MOOSE-104B/3	24.8	55.9	0.4	0.0	0.0	14.3	4.5	0.0	99.9
MOOSE-105/1	25.9	55.2	0.3	0.0	0.4	14.5	4.4	0.0	100.8
MOOSE-105/3	25.4	56.1	0.5	0.0	0.2	15.0	4.1	0.0	101.4
MOOSE-112A/1	26.1	55.1	0.5	0.0	1.1	13.3	5.2	0.0	101.4
MOOSE-112A/2	26.4	54.7	0.7	0.4	0.0	14.3	4.2	0.0	100.7
MOOSE-112B	27.1	53.9	0.5	0.3	0.0	14.5	4.3	0.0	100.7
MOOSE-113/1	25.7	55.5	0.5	0.0	0.2	14.7	4.4	0.0	100.9
MOOSE-113/2	25.7	55.7	0.3	0.0	0.0	14.9	4.2	0.0	100.8

Cations based on 24(O)

Ta^{5+}	Nb^{5+}	Ti^{4+}	Sn^{4+}	Fe^{3+}	Fe^{2+}	Mn^{2+}	Ca^{2+}	Total
1.48	6.48	0.04	0.04	0.00	2.94	1.01	0.00	11.98
3.02	4.94	0.04	0.00	0.03	2.63	1.33	0.00	12.00
2.89	5.04	0.06	0.04	0.00	2.47	1.49	0.00	12.00
2.46	5.56	0.02	0.01	0.00	2.60	1.29	0.00	11.94
4.05	3.83	0.04	0.06	0.17	3.43	0.43	0.00	12.00
4.36	3.50	0.04	0.05	0.22	3.04	0.78	0.00	12.00
4.60	3.31	0.03	0.04	0.12	2.51	1.38	0.00	12.00
4.68	3.30	0.00	0.05	0.00	2.26	1.70	0.00	11.99
4.00	3.92	0.08	0.04	0.00	2.27	1.69	0.00	12.00
4.14	3.74	0.15	0.06	0.00	2.22	1.68	0.00	11.98
4.09	3.73	0.14	0.04	0.17	2.14	1.68	0.00	12.00
4.13	3.72	0.16	0.04	0.03	2.23	1.67	0.00	12.00
4.06	3.84	0.08	0.05	0.05	2.24	1.69	0.00	12.00
4.02	3.89	0.09	0.02	0.06	2.25	1.68	0.00	12.00
4.03	3.91	0.11	0.03	0.00	2.26	1.60	0.00	11.95
4.11	3.85	0.11	0.03	0.00	2.18	1.62	0.00	11.91
3.10	4.86	0.14	0.00	0.00	2.40	1.41	0.00	11.91
3.07	4.87	0.13	0.01	0.00	2.35	1.51	0.00	11.94
3.10	4.89	0.10	0.00	0.00	2.43	1.41	0.00	11.92
4.88	2.93	0.22	0.06	0.00	2.20	1.69	0.00	11.99
4.33	3.55	0.11	0.03	0.08	2.10	1.80	0.00	12.00
4.42	3.51	0.10	0.00	0.01	2.15	1.81	0.00	12.00
1.96	6.07	0.00	0.00	0.00	3.14	0.75	0.01	11.94
1.99	6.00	0.02	0.00	0.00	3.21	0.71	0.06	12.00
2.30	5.66	0.04	0.00	0.04	3.16	0.77	0.04	12.00
3.21	4.77	0.16	0.00	0.00	3.02	0.73	0.00	11.88
3.01	4.94	0.15	0.00	0.00	3.18	0.66	0.00	11.93
3.04	4.90	0.13	0.00	0.00	3.22	0.66	0.00	11.95
1.68	6.27	0.03	0.00	0.09	2.82	1.10	0.00	12.00
4.04	3.68	0.29	0.00	0.25	2.91	0.82	0.00	12.00
1.57	6.28	0.20	0.01	0.01	3.18	0.75	0.00	12.00
1.73	6.04	0.22	0.00	0.23	3.06	0.71	0.00	12.00
4.27	3.61	0.09	0.00	0.19	2.70	1.15	0.00	12.00
4.67	3.25	0.08	0.03	0.00	2.75	1.21	0.00	11.99
4.28	3.57	0.06	0.04	0.25	2.08	1.72	0.00	12.00
2.85	5.08	0.04	0.05	0.02	1.90	2.05	0.00	12.00
2.89	5.13	0.04	0.00	0.00	1.87	1.99	0.00	11.93
2.36	5.67	0.03	0.00	0.00	1.97	1.86	0.00	11.89
1.74	6.27	0.01	0.03	0.00	2.17	1.71	0.00	11.93
1.65	6.34	0.04	0.01	0.00	3.06	0.87	0.00	11.97
1.62	6.34	0.09	0.00	0.00	3.03	0.88	0.00	11.96
1.60	6.38	0.08	0.01	0.00	2.99	0.89	0.00	11.95
1.63	6.34	0.08	0.02	0.00	2.99	0.88	0.00	11.94
1.62	6.36	0.04	0.04	0.00	2.99	0.90	0.00	11.95
2.52	5.34	0.08	0.03	0.20	2.83	0.99	0.00	12.00
1.72	6.17	0.08	0.03	0.10	3.10	0.79	0.00	12.00
4.00	3.90	0.10	0.03	0.05	3.06	0.87	0.00	12.00
1.58	6.37	0.07	0.03	0.00	2.99	0.93	0.00	11.97
1.96	6.05	0.06	0.00	0.00	2.94	0.94	0.00	11.94
2.22	5.61	0.07	0.00	0.34	2.68	0.98	0.08	12.00
1.86	6.08	0.07	0.00	0.03	3.03	0.92	0.00	12.00
1.72	6.21	0.10	0.04	0.00	2.98	0.92	0.00	11.97
1.68	6.26	0.09	0.03	0.00	3.00	0.91	0.00	11.97
3.91	3.99	0.07	0.01	0.15	3.04	0.83	0.00	12.00
1.68	6.29	0.08	0.00	0.00	2.98	0.94	0.00	11.98
1.75	6.18	0.07	0.00	0.08	2.99	0.93	0.00	12.00
1.69	6.23	0.09	0.00	0.04	3.08	0.84	0.00	11.98
1.75	6.12	0.10	0.00	0.20	2.74	1.09	0.00	12.00
1.78	6.14	0.12	0.04	0.00	2.98	0.89	0.00	11.95
1.84	6.08	0.09	0.03	0.00	3.03	0.91	0.00	11.99
1.73	6.20	0.09	0.00	0.04	3.03	0.91	0.00	12.00
1.73	6.23	0.07	0.00	0.00	3.09	0.87	0.00	11.99

Sample no.	Ta_2O_5	Nb_2O_5	TiO_2	SnO_2	Fe_2O_3	FeO	MnO	CaO	Total
MOOSE-114A/2	25.1	54.6	0.4	0.0	0.2	14.9	3.8	0.0	99.0
MOOSE-114A/3	22.5	57.4	0.3	0.4	0.0	14.8	4.2	0.0	99.5
MOOSE-114B/1	25.9	53.4	0.4	0.3	1.0	14.7	3.5	0.0	99.1
MOOSE-114B/2	26.5	53.9	0.5	0.0	0.9	13.6	4.8	0.0	100.2
MOOSE-115A	17.2	62.4	0.7	0.0	0.3	15.5	3.9	0.1	100.1
MOOSE-116/1	24.0	56.3	0.3	0.4	1.2	14.0	4.6	0.0	100.7
MOOSE-116/2	25.9	54.9	0.5	0.0	0.0	14.4	4.4	0.0	100.1
MOOSE-117/1	34.4	47.6	0.3	0.4	0.0	13.9	4.4	0.0	101.0
MOOSE-117/2	23.9	57.5	0.4	0.1	0.0	14.7	4.5	0.0	101.2
MOOSE-118/1	53.3	28.0	0.8	0.4	0.3	12.8	3.3	0.0	98.9
MOOSE-118/2	17.5	62.7	0.2	0.0	0.0	15.3	4.4	0.0	100.1
MOOSE-12/A1	21.1	57.8	0.5	0.0	0.0	14.5	4.2	0.0	98.1
MOOSE-12/A2	21.0	58.1	0.4	0.0	0.0	14.7	4.1	0.0	98.3
MOOSE-12/A3	21.4	57.8	0.4	0.0	0.0	14.9	4.0	0.0	98.5
MOOSE-12/A4	20.5	58.8	0.4	0.0	0.0	15.0	4.0	0.0	98.7
MOOSE-12/A5	54.1	27.6	1.0	0.6	0.0	12.3	3.1	0.0	98.8
MOOSE-12/B3	20.7	59.0	0.5	0.0	0.0	14.8	4.0	0.0	99.0
MOOSE-12/B5	54.0	27.8	0.9	0.4	0.0	12.5	3.1	0.0	98.7
MOOSE-120/1	20.5	60.9	0.4	0.0	0.0	15.3	4.1	0.0	101.1
MOOSE-120/2	19.5	61.7	0.5	0.0	0.0	15.2	4.3	0.0	101.2
MOOSE-121/1	19.5	60.4	0.4	0.4	0.0	15.0	4.3	0.0	100.0
MOOSE-121/2	19.4	61.5	0.4	0.0	0.0	15.0	4.4	0.0	100.7
MOOSE-122/1	19.7	60.8	0.4	0.0	0.0	15.0	4.3	0.0	100.2
MOOSE-122/2	25.7	55.3	0.4	0.3	0.8	14.2	4.6	0.0	101.2
MOOSE-16/4	23.0	55.9	0.6	0.0	0.2	15.3	3.4	0.0	98.4
MOOSE-16/5	21.0	59.7	0.5	0.0	0.9	14.3	4.7	0.0	101.3
MOOSE-16/6	50.0	32.6	0.7	0.0	0.1	13.6	3.2	0.0	100.3
MOOSE-7/1	23.0	57.2	0.6	0.0	2.2	13.5	4.6	0.0	101.2
MOOSE-7/4	23.8	56.8	0.7	0.2	0.0	15.6	3.4	0.0	100.6
MOOSE-9/1	27.0	53.0	0.4	0.0	0.3	14.3	4.2	0.0	99.3
MURKY-8/2	24.1	56.0	0.1	0.0	0.0	14.9	4.0	0.0	99.1
MURKY-8/3	24.2	55.9	0.3	0.0	0.0	14.9	4.0	0.0	99.2
MURKY-9/1	36.1	44.8	0.1	0.0	0.8	13.7	3.9	0.0	99.3
MURKY-9/2	34.3	45.7	0.0	0.3	1.0	13.4	4.0	0.0	98.8
MUT-10/1	33.8	44.4	2.0	0.0	2.3	11.0	5.4	0.0	99.0
MUT-10/2	34.7	45.4	1.8	0.1	1.7	12.8	4.3	0.0	100.8
MUT-13/1	45.6	36.9	0.7	0.1	2.3	11.5	4.8	0.0	101.8
MUT-13/2	36.5	42.0	1.8	0.2	0.0	14.1	4.5	0.0	99.2
NITE-A-7/1	67.0	16.6	0.2	0.3	0.7	6.5	8.4	0.0	99.8
NITE-A-7/2	71.6	12.1	0.3	0.4	0.3	5.8	8.9	0.0	99.4
NITE-A-7/3	70.8	12.4	0.4	0.5	0.8	5.4	9.0	0.0	99.2
NITE-A-7/4	68.2	15.1	0.5	0.2	1.9	6.0	8.2	0.0	100.0
NITE-A-8/1	67.4	13.7	0.2	1.7	1.7	4.1	9.6	0.0	98.4
NITE-B-1/1	53.8	29.0	0.2	0.0	0.0	7.4	8.9	0.0	99.4
NITE-B-1/2	45.0	38.8	0.0	0.3	0.0	8.6	8.8	0.0	101.5
NITE-B-4/1	47.8	35.6	0.2	0.4	0.1	10.1	7.1	0.0	101.3
NITE-B-4/2	42.6	39.7	0.2	0.1	0.0	10.2	7.2	0.0	100.1
NITE-B-4/3	41.4	40.9	0.2	0.3	0.4	10.3	7.2	0.0	100.7
ODIN-B-1/1	36.6	45.0	0.3	0.1	0.0	7.3	10.4	0.0	99.7
ODIN-B-8/1A	44.4	37.4	0.0	0.0	0.0	7.6	9.4	0.0	98.9
ODIN-B-8/1B	43.9	37.9	0.0	0.0	1.2	5.4	11.3	0.0	99.7
ODIN-B-8/2A	44.4	36.8	0.2	0.0	1.3	8.4	8.1	0.0	99.2
ODIN-B-8/2B	44.8	35.9	0.0	0.0	1.3	7.9	8.4	0.0	98.3
PAINT-2/1	14.9	63.6	0.4	0.0	0.9	6.7	12.4	0.0	98.8
PAINT-2/2	11.3	67.1	0.4	0.0	0.0	8.2	11.3	0.0	98.2
PEG-1-12	45.1	35.1	0.3	0.1	1.3	12.7	3.4	0.0	98.1
PEG-1-12/1B	45.8	35.3	0.3	0.5	0.0	12.7	3.7	0.0	98.3
PEG-113-1/2	24.0	53.9	0.5	0.0	3.5	10.4	6.4	0.0	98.7
PEG-113-1/3	27.1	51.4	0.5	0.0	2.9	10.8	6.1	0.0	98.8
PEG-118-9/2B	33.0	49.1	0.3	0.0	1.1	7.2	10.8	0.0	101.5
PEG-118-9A/1	36.2	45.4	0.4	0.0	3.1	9.5	6.9	0.2	101.8
PEG-118-9A/2	37.6	44.8	0.3	0.2	1.5	9.9	7.4	0.0	101.8

Cations based on 24(O)

Ta^{5+}	Nb^{5+}	Ti^{4+}	Sn^{4+}	Fe^{3+}	Fe^{2+}	Mn^{2+}	Ca^{2+}	Total
1.72	6.22	0.07	0.00	0.04	3.14	0.81	0.00	12.00
1.51	6.43	0.05	0.04	0.00	3.07	0.87	0.00	11.98
1.78	6.09	0.07	0.04	0.19	3.09	0.74	0.00	12.00
1.80	6.08	0.10	0.00	0.16	2.84	1.01	0.00	12.00
1.13	6.77	0.12	0.00	0.06	3.10	0.79	0.03	12.00
1.60	6.26	0.06	0.04	0.21	2.87	0.95	0.00	12.00
1.76	6.19	0.09	0.00	0.00	3.01	0.92	0.00	11.98
2.40	5.53	0.07	0.04	0.00	3.00	0.95	0.00	11.99
1.59	6.36	0.08	0.01	0.00	3.01	0.93	0.00	11.98
4.18	3.65	0.18	0.05	0.06	3.09	0.79	0.00	12.00
1.15	6.83	0.04	0.00	0.00	3.08	0.90	0.00	12.00
1.43	6.52	0.10	0.00	0.00	3.03	0.88	0.00	11.97
1.42	6.54	0.08	0.00	0.00	3.07	0.86	0.00	11.98
1.45	6.51	0.07	0.00	0.00	3.10	0.85	0.00	11.98
1.38	6.58	0.07	0.00	0.00	3.11	0.83	0.00	11.98
4.25	3.61	0.22	0.07	0.00	2.98	0.76	0.00	11.89
1.39	6.58	0.08	0.00	0.00	3.05	0.84	0.00	11.95
4.25	3.64	0.19	0.04	0.00	3.03	0.76	0.00	11.92
1.34	6.64	0.07	0.00	0.00	3.08	0.84	0.00	11.96
1.27	6.68	0.09	0.00	0.00	3.05	0.87	0.00	11.97
1.29	6.64	0.07	0.04	0.00	3.06	0.88	0.00	11.99
1.27	6.70	0.08	0.00	0.00	3.01	0.89	0.00	11.96
1.30	6.67	0.08	0.00	0.00	3.04	0.89	0.00	11.97
1.72	6.16	0.07	0.03	0.14	2.92	0.95	0.00	12.00
1.57	6.34	0.11	0.00	0.04	3.21	0.73	0.00	12.00
1.37	6.50	0.10	0.00	0.17	2.89	0.97	0.00	12.00
3.79	4.10	0.15	0.00	0.02	3.18	0.76	0.00	12.00
1.51	6.27	0.11	0.00	0.41	2.74	0.94	0.00	12.00
1.59	6.32	0.13	0.02	0.00	3.21	0.71	0.00	11.98
1.86	6.07	0.07	0.00	0.06	3.03	0.91	0.00	12.00
1.64	6.35	0.03	0.00	0.00	3.13	0.85	0.00	11.99
1.65	6.33	0.05	0.00	0.00	3.12	0.85	0.00	11.99
2.59	5.34	0.02	0.00	0.15	3.03	0.86	0.00	12.00
2.46	5.45	0.00	0.03	0.21	2.95	0.90	0.00	12.00
2.38	5.20	0.40	0.00	0.44	2.39	1.17	0.00	11.99
2.41	5.25	0.35	0.01	0.32	2.73	0.93	0.00	11.99
3.30	4.45	0.14	0.01	0.45	2.56	1.08	0.00	11.99
1.91	6.26	0.26	0.01	0.00	2.28	0.72	0.00	11.44
5.58	2.31	0.04	0.04	0.16	1.68	2.18	0.00	12.00
6.16	1.74	0.07	0.05	0.08	1.53	2.37	0.00	12.00
6.08	1.77	0.08	0.06	0.19	1.43	2.39	0.00	12.00
5.68	2.08	0.11	0.03	0.43	1.53	2.14	0.00	12.00
5.75	1.94	0.05	0.21	0.40	1.09	2.56	0.00	12.00
4.21	3.78	0.04	0.00	0.00	1.79	2.18	0.00	11.99
3.29	4.72	0.00	0.03	0.00	1.92	1.99	0.00	11.95
3.55	4.39	0.04	0.04	0.02	2.31	1.65	0.00	12.00
3.13	4.85	0.04	0.01	0.00	2.31	1.65	0.00	11.98
3.00	4.93	0.04	0.03	0.07	2.30	1.62	0.00	12.00
2.62	5.35	0.05	0.01	0.00	1.61	2.32	0.00	11.98
3.33	4.68	0.00	0.00	0.00	1.76	2.21	0.00	11.98
3.25	4.66	0.00	0.00	0.25	1.23	2.60	0.00	12.00
3.32	4.57	0.04	0.00	0.26	1.94	1.88	0.00	12.00
3.39	4.52	0.00	0.00	0.28	1.83	1.98	0.00	12.00
0.97	6.92	0.08	0.00	0.16	1.34	2.52	0.00	12.00
0.73	7.24	0.07	0.00	0.00	1.63	2.28	0.00	11.96
3.42	4.43	0.06	0.01	0.28	2.97	0.82	0.00	12.00
3.49	4.48	0.06	0.05	0.00	2.98	0.88	0.00	11.93
1.63	6.09	0.09	0.00	0.65	2.18	1.36	0.00	12.00
1.87	5.89	0.10	0.00	0.55	2.29	1.31	0.00	12.00
2.28	5.62	0.05	0.00	0.22	1.53	2.31	0.00	12.00
2.51	5.23	0.08	0.00	0.60	2.02	1.49	0.06	12.00
2.64	5.21	0.05	0.02	0.29	2.14	1.63	0.01	12.00

Sample no.	Ta_2O_5	Nb_2O_5	TiO_2	SnO_2	Fe_2O_3	FeO	MnO	CaO	Total
PEG-118-9B/1	24.4	56.3	0.2	0.1	1.9	8.8	9.3	0.1	101.1
PEG-170-16/1	24.1	56.8	0.7	0.0	0.2	16.0	3.1	0.0	101.0
PEG-170-16/2	23.1	57.4	0.7	0.2	0.7	15.3	3.6	0.0	100.9
PEG-170-4/1	51.9	29.4	1.4	0.3	0.0	14.2	2.1	0.0	99.3
PEG-170-4/2	48.8	31.8	1.4	0.0	0.1	14.2	2.2	0.0	98.6
PEG-170-4/3	40.8	39.5	0.8	0.0	0.1	14.9	2.3	0.0	98.4
PEG-170-4/4	41.8	38.8	1.0	0.0	0.0	14.6	2.3	0.0	98.6
PEG-170-8/1	52.4	28.9	1.5	0.3	1.3	13.3	2.4	0.0	100.1
PEG-170-8/2	53.3	28.7	1.5	0.0	0.0	14.1	2.3	0.0	99.9
PEG-170-8/3	54.4	27.9	1.4	0.1	0.1	14.0	2.3	0.0	100.2
PEG-190-7A/1	33.9	47.0	0.3	0.0	1.1	10.2	7.5	0.0	100.0
PEG-190-7A/2	33.6	47.3	0.7	0.0	1.4	9.7	7.8	0.0	100.6
PEG-190-7B/2	43.9	37.7	0.4	0.0	1.4	8.9	7.7	0.0	100.0
PEG-191-12/1	60.8	23.0	0.4	0.0	1.3	9.3	6.1	0.0	100.8
PEG-191-12/2	59.8	23.4	0.4	0.2	0.6	9.4	6.2	0.0	100.1
PEG-191-12/3	61.7	21.5	0.5	0.0	0.9	9.5	5.8	0.0	100.0
PEG-191-4/1	27.8	53.7	0.1	0.0	0.5	9.1	9.5	0.0	100.8
PEG-191-4/2	27.3	54.7	0.3	0.0	0.6	8.8	10.0	0.0	101.7
PEG-191-4A/4	27.6	53.8	0.2	0.0	1.5	9.0	9.2	0.0	101.2
PEG-191-6A/1	49.8	33.2	0.5	0.0	0.0	9.7	6.8	0.2	100.3
PEG-191-6A/2	44.3	36.4	0.5	0.0	0.6	9.4	7.3	0.0	98.5
PEG-191-7A/1	48.0	34.1	1.1	0.0	2.2	9.4	6.5	0.0	101.4
PEG-191-7A/2	37.4	44.2	0.7	0.0	0.6	11.1	6.6	0.0	100.6
PEG-191-7B/1	40.3	40.3	0.5	0.2	1.3	9.8	6.9	0.0	99.3
PEG-191-7B/2	49.6	31.5	0.7	0.0	2.0	8.9	6.7	0.0	99.4
PEG-192-11/1	44.9	34.5	1.3	0.0	2.4	8.4	7.0	0.0	98.6
PEG-192-11/2	49.0	31.3	0.6	0.3	1.2	9.2	6.6	0.0	98.1
PEG-192-11/3	50.1	31.1	0.5	0.1	2.0	8.7	6.9	0.0	99.3
PEG-192-12/1	56.1	25.7	0.5	0.0	0.5	9.3	6.5	0.0	98.7
PEG-192-12/3	54.3	27.9	0.5	0.0	0.5	9.4	6.6	0.0	99.2
PEG-192-13/1	58.2	26.1	0.7	0.0	0.0	9.2	7.1	0.0	101.4
PEG-192-13/2	58.1	26.1	0.7	0.0	0.0	9.2	7.2	0.0	101.3
PEG-192-13/4	55.2	26.9	0.8	0.0	0.0	9.5	6.5	0.0	98.9
PEG-192-7/2	57.0	25.5	0.8	0.0	0.5	8.8	7.0	0.0	99.7
PEG-192-7/3	56.4	27.2	0.7	0.0	1.0	9.2	6.8	0.0	101.3
PEG-192-8/1	63.1	20.8	0.5	0.3	0.5	8.9	6.6	0.0	100.8
PEG-192-8/2	53.6	30.5	0.5	0.6	0.0	9.4	6.5	0.0	101.2
PEG-192-8/3	54.9	28.7	0.6	0.0	0.5	9.1	7.2	0.0	101.0
PEG-196-10/1B	66.2	16.4	0.7	0.3	2.2	5.4	8.6	0.0	99.9
PEG-196-10/2B	36.6	44.8	0.3	0.0	1.9	6.5	10.6	0.0	100.8
PEG-196-3A/1	65.8	18.3	0.6	0.3	0.0	7.0	8.1	0.0	100.2
PEG-196-3A/2	50.6	33.3	0.4	0.0	1.0	6.7	9.9	0.0	102.0
PEG-241-10/1	37.1	44.3	1.0	0.0	0.1	14.8	3.1	0.0	100.5
PEG-241-10/2	35.4	46.5	0.8	0.0	0.5	14.7	3.4	0.0	101.3
PEG-285-4	16.8	64.1	0.4	0.0	1.1	12.5	6.9	0.0	101.8
PEG-285-4/1	52.6	28.9	1.0	0.0	1.6	12.1	3.5	0.0	99.8
PEG-285-4/2	53.3	28.7	1.0	0.3	0.9	10.2	5.8	0.0	100.1
PEG-292-9/1	54.2	26.4	1.1	0.3	1.6	11.7	3.5	0.0	98.7
PEG-292-9/2	55.8	25.5	1.2	0.3	1.0	12.2	3.3	0.0	99.3
PEG-292-9/3	55.8	25.0	1.1	0.4	1.0	12.2	3.2	0.0	98.7
PEG-292-9/4	54.6	25.8	1.6	0.0	0.4	12.6	3.0	0.0	98.0
PEG-300-13/1	59.2	22.9	0.6	0.1	1.3	8.6	6.5	0.0	99.3
PEG-300-13/2	52.6	30.6	0.7	0.0	0.2	9.5	7.1	0.0	100.7
PEG-300-13/3	56.4	27.6	0.4	0.0	1.0	8.9	7.2	0.0	101.6
PEG-300-14/1	29.8	51.9	0.4	0.0	0.0	12.9	5.9	0.0	100.9
PEG-300-3/1	47.8	35.8	0.4	0.1	0.0	11.9	5.2	0.0	101.3
PEG-306-9/2B	57.8	26.2	0.3	0.0	1.9	7.3	8.2	0.0	101.6
PEG-306-9A/1	57.3	25.8	0.4	0.0	3.4	6.9	7.8	0.0	101.7
PEG-306-9A/2	51.2	31.8	0.0	0.1	1.0	8.4	7.9	0.0	100.4
PEG-306-9B	59.0	24.6	0.1	0.0	1.7	7.6	7.8	0.0	100.8
PEG-306-9C	62.3	20.8	0.3	0.0	0.6	8.3	7.1	0.0	99.4
PEG-75-3/1A	37.1	45.1	0.3	0.0	1.3	7.8	9.7	0.0	101.4

Cations based on 24(O)

Ta^{5+}	Nb^{5+}	Ti^{4+}	Sn^{4+}	Fe^{3+}	Fe^{2+}	Mn^{2+}	Ca^{2+}	Total
1.63	6.22	0.04	0.01	0.35	1.80	1.92	0.03	12.00
1.61	6.29	0.13	0.00	0.04	3.28	0.65	0.00	12.00
1.53	6.33	0.13	0.01	0.13	3.13	0.74	0.00	12.00
4.01	3.77	0.29	0.03	0.00	3.38	0.50	0.00	12.00
3.74	4.05	0.31	0.00	0.02	3.35	0.53	0.01	12.00
3.02	4.87	0.16	0.00	0.02	3.40	0.53	0.00	12.00
3.10	4.78	0.21	0.00	0.00	3.34	0.54	0.00	11.96
4.00	3.67	0.32	0.03	0.28	3.12	0.58	0.00	12.00
4.11	3.68	0.32	0.00	0.00	3.34	0.54	0.00	12.00
4.20	3.58	0.31	0.01	0.03	3.33	0.54	0.00	12.00
2.39	5.50	0.06	0.00	0.21	2.20	1.64	0.00	12.00
2.34	5.48	0.13	0.00	0.28	2.08	1.69	0.00	12.00
3.24	4.62	0.07	0.00	0.29	2.01	1.78	0.00	12.00
4.82	3.03	0.09	0.00	0.28	2.27	1.51	0.00	12.00
4.78	3.10	0.10	0.02	0.14	2.32	1.55	0.00	12.00
4.97	2.89	0.11	0.00	0.21	2.36	1.46	0.00	12.00
1.89	6.06	0.02	0.00	0.10	1.90	2.02	0.00	12.00
1.83	6.10	0.06	0.00	0.10	1.81	2.10	0.00	12.00
1.86	6.03	0.03	0.00	0.28	1.86	1.94	0.00	12.00
3.77	4.17	0.11	0.00	0.00	2.26	1.60	0.05	11.98
3.33	4.56	0.10	0.00	0.13	2.17	1.71	0.00	12.00
3.53	4.18	0.22	0.00	0.44	2.12	1.50	0.01	12.00
2.65	5.21	0.14	0.00	0.11	2.43	1.45	0.00	12.00
2.94	4.89	0.11	0.02	0.26	2.21	1.57	0.00	12.00
3.78	3.98	0.14	0.00	0.42	2.08	1.59	0.00	12.00
3.36	4.29	0.28	0.00	0.50	1.93	1.63	0.00	11.99
3.79	4.02	0.13	0.03	0.25	2.18	1.60	0.00	12.00
3.83	3.95	0.10	0.01	0.42	2.05	1.64	0.00	12.00
4.47	3.41	0.12	0.00	0.12	2.27	1.61	0.00	12.00
4.25	3.63	0.11	0.00	0.11	2.26	1.62	0.00	12.00
4.52	3.38	0.16	0.00	0.00	2.20	1.72	0.00	11.98
4.52	3.38	0.15	0.00	0.00	2.20	1.74	0.00	11.99
4.36	3.54	0.16	0.00	0.00	2.32	1.61	0.00	11.99
4.49	3.35	0.18	0.00	0.11	2.14	1.73	0.00	12.00
4.35	3.49	0.14	0.00	0.20	2.18	1.63	0.00	12.00
5.08	2.77	0.11	0.04	0.12	2.20	1.66	0.00	12.00
4.09	3.87	0.10	0.07	0.00	2.21	1.55	0.00	11.89
4.21	3.66	0.13	0.00	0.11	2.15	1.73	0.00	12.00
5.45	2.25	0.16	0.04	0.49	1.38	2.20	0.01	12.00
2.58	5.26	0.06	0.00	0.37	1.41	2.33	0.00	12.00
5.41	2.50	0.15	0.04	0.00	1.76	2.07	0.00	11.94
3.76	4.11	0.09	0.00	0.20	1.54	2.29	0.00	12.00
2.63	5.23	0.19	0.00	0.03	3.23	0.68	0.00	12.00
2.47	5.39	0.16	0.00	0.09	3.15	0.74	0.00	12.00
1.07	6.81	0.08	0.00	0.19	2.46	1.38	0.00	12.00
4.05	3.70	0.21	0.00	0.34	2.86	0.83	0.00	12.00
4.10	3.67	0.22	0.03	0.18	2.41	1.39	0.00	12.00
4.26	3.44	0.25	0.03	0.34	2.81	0.86	0.00	12.00
4.39	3.34	0.26	0.04	0.21	2.94	0.82	0.00	12.00
4.42	3.30	0.25	0.05	0.21	2.97	0.79	0.00	12.00
4.33	3.40	0.35	0.00	0.09	3.07	0.75	0.00	12.00
4.75	3.05	0.13	0.01	0.30	2.12	1.63	0.00	12.00
4.01	3.88	0.14	0.00	0.04	2.23	1.69	0.00	12.00
4.33	3.53	0.09	0.00	0.22	2.10	1.72	0.00	12.00
2.04	5.91	0.07	0.00	0.00	2.71	1.26	0.00	12.00
3.54	4.41	0.09	0.01	0.00	2.72	1.20	0.00	11.98
4.46	3.36	0.05	0.00	0.41	1.73	1.98	0.00	12.00
4.40	3.30	0.09	0.00	0.72	1.62	1.87	0.00	12.00
3.90	4.03	0.00	0.01	0.20	1.98	1.89	0.00	12.00
4.65	3.22	0.03	0.00	0.36	1.84	1.91	0.00	12.00
5.08	2.82	0.07	0.00	0.14	2.08	1.80	0.00	12.00
2.61	5.27	0.05	0.00	0.25	1.69	2.13	0.00	12.00

Sample no.	Ta_2O_5	Nb_2O_5	TiO_2	SnO_2	Fe_2O_3	FeO	MnO	CaO	Total
PEG-75-3/1B	51.3	31.7	0.2	0.0	0.1	8.3	8.5	0.0	100.1
PEG-75-3/2A	35.9	44.3	0.3	0.0	2.0	8.0	8.8	0.0	99.3
PEG-75-3/2B	61.4	20.8	0.0	0.0	1.2	6.8	8.2	0.0	98.5
PEG-75-30/1	16.8	64.3	0.3	0.0	1.0	9.8	9.8	0.0	101.9
PEG-75-30/2	19.1	62.2	0.2	0.0	0.7	8.8	10.6	0.0	101.7
PEG-75-31/1	24.0	58.1	0.2	0.1	0.0	10.4	9.1	0.0	101.9
PEG-75-4/1	25.8	53.7	0.3	0.0	1.7	7.9	9.9	0.0	99.4
PEG-75-4/2	38.3	43.2	0.3	0.0	0.8	4.9	12.5	0.0	99.9
PEG-75-4/3	45.1	37.1	0.3	0.3	1.9	6.5	9.9	0.0	101.1
PEG-75-4/4	52.6	29.2	0.3	0.0	1.5	7.1	8.6	0.0	99.3
PEG-8-1/2	54.5	28.0	0.5	0.0	1.1	9.1	6.7	0.0	100.1
PEG-8-1/3	56.6	26.7	0.7	0.0	0.6	13.1	3.0	0.0	100.7
PEG-8-4/1	54.0	28.8	0.6	0.0	0.2	13.6	2.8	0.0	100.0
PEG-8-4/5	55.8	27.9	0.6	0.0	0.5	13.0	3.3	0.0	101.1
PEG-84-2A/1	62.4	20.1	0.4	0.0	0.5	9.0	5.9	0.3	98.6
PEG-84-2A/2	39.9	41.3	0.5	0.0	3.5	8.3	7.7	0.0	101.2
PEG-84-3A/1	64.8	18.2	1.1	0.0	0.3	11.0	4.3	0.0	99.7
PEG-84-3A/2	55.5	27.0	1.4	0.0	0.7	11.7	4.2	0.0	100.6
PEG-84-3B/1	61.9	21.0	0.8	0.2	0.0	11.3	4.2	0.0	99.4
PEG-84-3B/2	56.7	25.4	1.6	0.0	0.6	11.9	3.8	0.0	100.1
PEG-85-1/1	48.5	34.2	0.3	0.0	1.9	6.3	9.9	0.0	101.0
PEG-85-1/2	35.2	47.4	0.3	0.0	0.0	8.4	9.9	0.1	101.4
PEG-86-2/1	45.3	33.4	2.4	0.0	1.8	8.9	6.6	0.0	98.5
PEG-86-2/2	45.8	33.8	2.0	0.1	1.3	10.5	5.4	0.0	98.9
PEG-93-20/1	60.1	20.6	0.7	0.3	1.9	8.4	6.1	0.0	98.1
PEG-93-20/2	62.1	21.2	0.6	0.0	2.6	8.4	6.2	0.0	101.0
PEG-93-20/5	41.3	40.7	0.6	0.0	1.7	9.4	7.5	0.0	101.2
PEG-93-27/1	45.0	35.0	0.4	0.0	1.8	10.2	5.7	0.0	98.1
PEG-93-31/1	29.4	52.1	0.6	0.1	0.4	12.8	5.9	0.0	101.2
PEG-93-31/2	16.8	63.5	0.5	0.0	1.8	13.7	5.3	0.0	101.6
PEG-93-35/TAN	57.2	25.4	0.8	0.4	2.0	10.3	4.9	0.0	101.0
PEG-93-42/1	38.6	42.1	0.8	0.0	1.6	11.0	5.9	0.0	100.0
PEG-93-42/2	40.0	40.3	0.9	0.3	0.9	11.2	5.7	0.0	99.3
PEG-93-43/1	46.6	35.6	1.0	0.0	0.9	11.1	5.6	0.0	100.8
PEG-93-43/2	45.0	37.5	0.8	0.3	0.6	11.5	5.6	0.0	101.2
PEG-93-43/3	45.0	38.2	0.8	0.0	0.0	12.2	5.3	0.0	101.4
PEG-93-43/4	44.1	38.3	0.8	0.3	0.1	12.1	5.4	0.0	101.1
PEG-93-43/5	45.2	38.1	0.9	0.0	0.0	14.0	3.3	0.0	101.6
PEG-95-12A/1	38.5	42.5	0.6	0.0	1.3	9.8	7.3	0.0	100.0
PEG-95-12A/2	40.6	39.6	0.7	0.1	1.8	10.3	6.1	0.0	99.2
PEG-95-12B/1	59.6	21.8	1.7	0.1	3.4	8.0	6.0	0.0	100.6
PEG-95-12B/2	55.8	26.3	0.9	0.0	3.0	8.4	6.3	0.0	100.7
PEG-95-17A/1	40.9	39.8	0.5	0.0	2.8	9.3	6.6	0.1	99.9
PEG-95-17A/2	39.0	41.9	0.7	0.0	2.2	10.3	6.3	0.0	100.3
PEG-95-17B	41.9	39.1	0.6	0.0	3.4	9.1	6.6	0.0	100.7
PEG-95-17C/1	41.9	37.8	0.8	0.0	2.6	8.4	7.4	0.0	99.0
PEG-95-17C/2	18.8	60.6	0.3	0.0	3.3	8.5	9.3	0.0	100.8
PVILLA-A-7/1	45.4	37.9	0.2	0.4	0.0	11.9	5.2	0.0	101.0
PVILLA-A-7/2	44.8	38.6	0.0	0.3	0.0	11.5	6.0	0.0	101.2
PVILLA-A-7/3	44.2	38.6	0.1	0.0	0.6	11.3	6.0	0.0	100.9
PVILLA-C-4/1	41.1	41.6	0.5	0.5	0.0	12.0	5.8	0.0	101.5
PVILLA-C-4/2	52.6	30.1	0.6	0.4	2.9	9.1	6.3	0.0	101.9
PVILLA-C-4/3	52.9	28.9	1.0	0.5	0.8	10.1	5.8	0.0	100.2
PVILLA-C-7/1	54.5	29.7	0.6	0.0	0.0	11.1	5.6	0.0	101.4
PVILLA-C-7/2	54.5	27.1	0.6	0.3	0.0	10.3	5.7	0.0	98.6
QI-A-3	36.6	43.9	0.0	0.0	0.0	13.2	4.5	0.0	98.2
RIB-A-7-A/2	21.7	59.2	0.1	0.0	0.4	1.8	17.2	0.1	100.5
RIB-A-7-A/3	54.8	29.3	0.3	0.0	0.0	1.9	14.2	0.0	100.6
RIB-A-7-A/5	59.5	24.5	0.6	0.0	0.0	1.5	14.1	0.0	100.2
RIB-A-7-A/6	63.0	19.9	0.8	0.0	0.0	1.7	13.7	0.0	99.1
RIB-15/1	61.0	21.9	0.6	0.1	0.5	3.7	11.7	0.0	99.7
RIB-15/2	55.8	26.1	1.6	1.0	0.5	1.1	14.7	0.0	100.7

Cations based on 24(O)

Ta^{5+}	Nb^{5+}	Ti^{4+}	Sn^{4+}	Fe^{3+}	Fe^{2+}	Mn^{2+}	Ca^{2+}	Total
3.93	4.03	0.05	0.00	0.01	1.96	2.02	0.00	12.00
2.56	5.26	0.06	0.00	0.40	1.76	1.96	0.00	12.00
5.05	2.85	0.00	0.00	0.27	1.71	2.11	0.00	12.00
1.07	6.83	0.06	0.00	0.18	1.92	1.95	0.00	12.00
1.24	6.70	0.04	0.00	0.13	1.76	2.14	0.00	12.00
1.58	6.38	0.04	0.01	0.00	2.11	1.87	0.00	12.00
1.76	6.10	0.05	0.00	0.32	1.66	2.10	0.00	12.00
2.75	5.16	0.06	0.00	0.15	1.07	2.80	0.00	12.00
3.30	4.52	0.06	0.03	0.38	1.45	2.27	0.00	12.00
4.08	3.76	0.07	0.00	0.32	1.68	2.07	0.01	12.00
4.23	3.61	0.11	0.00	0.23	2.18	1.63	0.00	12.00
4.41	3.46	0.14	0.00	0.12	3.13	0.73	0.00	12.00
4.19	3.71	0.13	0.00	0.04	3.25	0.67	0.00	12.00
4.30	3.58	0.13	0.00	0.10	3.08	0.80	0.00	12.00
5.14	2.75	0.10	0.00	0.11	2.28	1.52	0.09	12.00
2.83	4.88	0.09	0.00	0.68	1.81	1.70	0.00	12.00
5.32	2.49	0.24	0.00	0.08	2.77	1.09	0.00	12.00
4.28	3.47	0.30	0.00	0.15	2.78	1.02	0.00	12.00
5.03	2.85	0.17	0.02	0.00	2.83	1.07	0.00	11.98
4.43	3.30	0.34	0.00	0.13	2.87	0.93	0.00	12.00
3.60	4.22	0.07	0.00	0.38	1.43	2.29	0.00	12.00
2.46	5.50	0.07	0.00	0.00	1.80	2.15	0.02	12.00
3.39	4.15	0.49	0.00	0.38	2.05	1.53	0.00	12.00
3.43	4.20	0.40	0.01	0.28	2.42	1.25	0.00	12.00
4.92	2.80	0.16	0.04	0.43	2.10	1.54	0.00	12.00
4.93	2.79	0.14	0.00	0.56	2.05	1.53	0.00	12.00
2.96	4.85	0.12	0.00	0.33	2.07	1.67	0.00	12.00
3.41	4.41	0.08	0.00	0.38	2.37	1.34	0.00	12.00
2.00	5.89	0.11	0.01	0.07	2.67	1.24	0.00	12.00
1.07	6.76	0.10	0.00	0.31	2.69	1.06	0.00	12.00
4.44	3.28	0.18	0.04	0.43	2.45	1.19	0.00	12.00
2.77	5.02	0.16	0.00	0.31	2.42	1.32	0.00	12.00
2.92	4.88	0.18	0.03	0.18	2.52	1.29	0.00	12.00
3.44	4.36	0.21	0.00	0.18	2.52	1.29	0.00	12.00
3.28	4.55	0.16	0.04	0.12	2.59	1.27	0.00	12.00
3.28	4.63	0.16	0.00	0.00	2.73	1.20	0.00	11.99
3.22	4.64	0.17	0.04	0.02	2.70	1.22	0.00	12.01
3.29	4.61	0.18	0.00	0.00	3.14	0.74	0.00	11.97
2.77	5.08	0.11	0.00	0.25	2.17	1.63	0.00	12.00
2.97	4.81	0.13	0.01	0.38	2.32	1.38	0.00	12.00
4.66	2.84	0.38	0.01	0.73	1.92	1.46	0.00	12.00
4.29	3.36	0.20	0.00	0.64	1.99	1.52	0.00	12.00
2.96	4.79	0.09	0.00	0.55	2.08	1.48	0.03	12.00
2.79	4.98	0.13	0.00	0.43	2.26	1.41	0.00	12.00
3.02	4.68	0.12	0.00	0.68	2.02	1.48	0.00	12.00
3.08	4.62	0.17	0.00	0.53	1.90	1.69	0.00	12.00
1.22	6.55	0.05	0.00	0.59	1.70	1.88	0.00	12.00
3.34	4.63	0.04	0.04	0.00	2.69	1.19	0.00	11.95
3.28	4.70	0.00	0.03	0.00	2.59	1.38	0.00	11.98
3.24	4.70	0.03	0.00	0.11	2.53	1.38	0.00	12.00
2.95	4.95	0.10	0.06	0.00	2.63	1.30	0.00	11.99
3.94	3.76	0.12	0.05	0.59	2.09	1.46	0.00	12.00
4.07	3.69	0.22	0.06	0.17	2.39	1.40	0.00	12.00
4.16	3.77	0.12	0.00	0.00	2.60	1.33	0.00	11.98
4.32	3.58	0.14	0.03	0.00	2.51	1.40	0.00	11.98
2.67	5.33	0.00	0.00	0.00	2.96	1.03	0.00	12.00
1.44	6.52	0.02	0.00	0.07	0.37	3.55	0.02	12.00
4.24	3.76	0.06	0.00	0.00	0.45	3.43	0.00	11.94
4.72	3.24	0.13	0.00	0.00	0.36	3.49	0.00	11.93
5.17	2.72	0.17	0.00	0.00	0.43	3.50	0.00	11.99
4.93	2.94	0.13	0.01	0.12	0.92	2.95	0.00	12.00
4.32	3.35	0.34	0.11	0.10	0.25	3.53	0.00	12.00

Sample no.	Ta_2O_5	Nb_2O_5	TiO_2	SnO_2	Fe_2O_3	FeO	MnO	CaO	Total
RIB-17/1	57.3	25.8	0.3	0.0	0.3	5.7	10.3	0.0	99.8
RIB-17/2	56.9	24.6	0.4	0.0	2.6	4.8	9.8	0.0	99.1
RIB-18/2	61.5	22.1	0.5	0.0	0.7	2.9	12.6	0.0	100.3
RIB-18/3	63.1	20.1	0.6	0.6	0.8	2.3	12.9	0.0	100.3
RIB-19/1	13.2	65.4	0.4	0.0	0.4	14.1	5.5	0.0	99.0
RIB-19/2	13.0	64.7	0.6	0.0	0.3	14.7	4.7	0.0	98.1
RIB-9/1	54.3	27.0	0.4	0.0	0.8	6.0	9.7	0.0	98.2
RIB-9/2	48.8	32.5	0.3	0.0	0.9	7.0	9.2	0.0	98.6
SKY-6-1A	34.2	47.4	0.6	0.0	0.8	6.0	11.6	0.2	100.9
SKY-6-1B	27.6	52.6	0.9	0.0	0.2	7.4	11.1	0.0	99.8
SKY-6-2A	37.4	43.9	0.7	0.0	0.0	7.3	10.3	0.0	99.6
SKY-6-2B	33.8	46.1	0.7	0.0	0.1	8.1	9.7	0.0	98.5
TAN-1-1/1	31.9	48.1	1.2	0.3	0.0	14.6	3.3	0.0	99.4
TAN-1-1/2	34.5	45.9	1.5	0.0	0.0	14.3	3.3	0.0	99.5
TAN-3-1/1	55.3	26.3	0.4	0.7	0.0	12.4	3.6	0.0	98.7
TAN-3-1/2	55.7	26.8	0.4	0.4	0.0	12.3	3.6	0.0	99.4
TAN-4-1/3	56.2	25.7	0.7	0.7	0.6	11.3	4.5	0.0	99.6
TAN-4-3/1	56.3	25.9	0.5	0.0	1.2	6.5	9.0	0.0	99.4
THE-AR-A-2/A	22.2	57.5	0.3	0.0	0.0	13.0	5.8	0.0	98.9
THE-AR-A-2/C	40.8	41.8	0.2	0.0	0.0	9.4	7.7	0.0	99.9
THE-C-F-1-1/D	29.3	52.5	0.3	0.0	1.1	9.2	9.1	0.0	101.5
THE-C-F-1-1/E	29.7	52.3	0.1	0.0	1.7	12.6	5.5	0.0	101.9
THE-EN-4/1	34.6	45.7	0.8	0.0	4.3	9.8	6.1	0.0	101.3
THE-EN-4/4	17.2	62.8	0.6	0.0	2.2	12.5	6.2	0.0	101.4
THE-EN-4/5	17.0	62.6	0.8	0.0	2.5	11.8	6.7	0.0	101.4
THE-PN-A-10/A	15.8	62.5	0.5	0.0	0.6	13.1	6.0	0.0	98.4
THE-PN-A-10/C	14.1	64.3	0.5	0.0	0.8	12.4	6.8	0.0	98.9
THE-PN-A-3A/1	64.1	19.5	0.3	0.1	0.8	8.4	6.8	0.0	100.0
THE-PN-A-3A/2	54.9	28.7	0.0	0.0	1.2	8.5	7.5	0.0	100.8
THE-PN-A-3B/2	61.2	21.5	0.3	0.0	1.2	9.4	5.8	0.0	99.5
THE-PN-A-4/A	17.3	61.7	0.8	0.0	0.0	13.4	5.6	0.0	98.9
THE-PN-A-4/C	18.6	60.7	0.4	0.0	0.0	13.8	5.3	0.0	99.0
THE-SN-B-1	13.5	66.4	0.0	0.0	0.0	13.0	6.8	0.0	99.7
THE-T-7/1	25.9	54.8	0.2	0.0	0.0	9.3	8.9	0.0	99.2
THE-T-7/3	29.9	52.0	0.0	0.0	0.0	9.3	8.6	0.0	99.8
THE-T-7/4	28.4	52.3	0.0	0.1	0.0	8.4	9.6	0.1	99.0
THE-W-1/A	48.0	33.9	0.4	0.5	0.0	11.0	4.7	0.0	98.6
THE-W-1/C	47.4	33.5	0.4	0.6	0.0	11.7	4.7	0.0	98.3
THE-W-1/D	49.0	33.8	0.4	0.0	0.0	10.6	5.4	0.0	99.2
THE-W-1/E	50.4	31.6	0.4	0.5	0.0	11.6	4.3	0.0	98.9
THE-W-1/F	49.5	34.5	0.3	0.5	0.0	11.9	4.5	0.0	101.2
THE-W-17A/1	46.0	35.0	0.8	0.3	1.5	12.0	4.1	0.1	99.8
THE-W-17A/2	44.3	37.3	0.7	0.4	0.4	12.9	4.0	0.1	100.2
THE-W-17A/3	56.2	26.2	0.4	0.0	0.8	11.7	4.1	0.0	99.4
TOM-3/1	33.2	48.0	0.2	0.0	0.2	14.0	4.2	0.0	100.0
TOM-3/2	34.9	46.8	0.0	0.0	0.8	13.8	4.1	0.0	100.4
USK-16/1	31.6	49.8	0.4	0.2	0.5	10.0	8.3	0.0	100.8
USK-16/2	34.9	47.6	0.1	0.0	1.6	9.4	8.3	0.0	101.9
USK-18/2	28.4	51.4	0.3	0.2	0.0	10.6	7.8	0.0	98.7
USK-18/3	28.8	52.4	0.3	0.0	0.9	10.1	8.2	0.0	100.7
USK-19/1	37.7	44.5	0.2	0.0	0.0	9.8	8.1	0.0	100.4
USK-19/2	37.3	44.3	0.3	0.4	1.1	9.2	8.2	0.0	100.8
USK-20/1	35.7	46.2	0.2	0.1	0.8	9.3	8.5	0.0	100.9
USK-7A/1	43.3	40.8	0.0	0.0	0.0	9.7	8.2	0.0	101.9
VO-1-10A/1	34.3	43.2	2.9	0.3	0.9	10.4	5.7	0.5	98.2
VO-1-10A/2	26.9	53.7	0.5	0.2	1.3	11.7	6.6	0.0	100.9
VO-4-2A/1	44.2	37.1	1.9	0.1	1.5	12.3	4.2	0.0	101.3
VO-4-2A/2	30.2	48.0	3.0	0.4	2.0	12.1	4.8	0.0	100.5
VO-4-2A/3	44.3	36.5	3.0	0.4	0.9	12.1	4.5	0.0	101.8
VO-5-24/1	52.5	30.4	0.8	0.5	0.3	10.1	6.4	0.0	101.1
VO-5-24/2	40.9	39.2	0.4	0.1	0.3	10.9	6.1	0.0	98.0
VO-5-24A/3	37.0	45.4	0.5	0.4	0.0	10.4	7.0	0.0	100.8

Cations based on 24(O)

Ta^{5+}	Nb^{5+}	Ti^{4+}	Sn^{4+}	Fe^{3+}	Fe^{2+}	Mn^{2+}	Ca^{2+}	Total
4.54	3.39	0.07	0.00	0.07	1.38	2.55	0.00	12.00
4.51	3.24	0.09	0.00	0.56	1.17	2.42	0.00	12.00
4.93	2.95	0.10	0.00	0.15	0.72	3.14	0.00	12.00
5.10	2.70	0.14	0.07	0.18	0.57	3.25	0.00	12.00
0.86	7.06	0.08	0.00	0.07	2.82	1.11	0.00	12.00
0.85	7.05	0.11	0.00	0.06	2.96	0.96	0.00	12.00
4.31	3.57	0.08	0.00	0.19	1.46	2.39	0.00	12.00
3.74	4.15	0.07	0.00	0.19	1.65	2.20	0.00	12.00
2.38	5.49	0.11	0.00	0.15	1.28	2.52	0.05	12.00
1.89	5.98	0.18	0.00	0.04	1.55	2.37	0.00	12.00
2.68	5.24	0.14	0.00	0.00	1.61	2.30	0.00	11.98
2.42	5.48	0.14	0.00	0.02	1.77	2.17	0.00	12.00
2.23	5.60	0.24	0.03	0.00	3.14	0.73	0.00	11.97
2.44	5.39	0.29	0.00	0.00	3.11	0.74	0.00	11.97
4.41	3.49	0.10	0.08	0.00	3.03	0.89	0.00	11.99
4.40	3.52	0.09	0.05	0.00	3.00	0.89	0.00	11.96
4.43	3.37	0.15	0.08	0.13	2.74	1.09	0.00	12.00
4.45	3.39	0.11	0.00	0.27	1.57	2.21	0.00	12.00
1.50	6.47	0.06	0.00	0.00	2.71	1.22	0.00	11.98
2.97	5.06	0.04	0.00	0.00	2.11	1.74	0.00	11.92
1.98	5.92	0.05	0.00	0.20	1.92	1.93	0.00	12.00
2.01	5.88	0.01	0.00	0.31	2.62	1.17	0.00	12.00
2.38	5.23	0.16	0.00	0.82	2.08	1.32	0.00	12.00
1.10	6.70	0.10	0.00	0.39	2.47	1.24	0.00	12.00
1.09	6.67	0.14	0.00	0.44	2.32	1.34	0.00	12.00
1.04	6.86	0.09	0.00	0.11	2.67	1.23	0.00	12.00
0.92	6.98	0.08	0.00	0.14	2.49	1.39	0.00	12.00
5.24	2.65	0.07	0.01	0.18	2.12	1.73	0.00	12.00
4.23	3.68	0.00	0.00	0.26	2.02	1.81	0.00	12.00
4.96	2.90	0.06	0.01	0.27	2.33	1.46	0.00	12.00
1.14	6.77	0.15	0.00	0.00	2.73	1.16	0.00	11.96
1.24	6.72	0.08	0.00	0.00	2.83	1.11	0.00	11.98
0.87	7.14	0.00	0.00	0.00	2.58	1.38	0.00	11.98
1.77	6.25	0.04	0.00	0.00	1.96	1.90	0.00	11.93
2.07	5.99	0.00	0.00	0.00	1.99	1.86	0.00	11.90
1.97	6.04	0.00	0.01	0.00	1.81	2.08	0.03	11.96
3.67	4.31	0.09	0.06	0.00	2.59	1.12	0.00	11.84
3.64	4.28	0.08	0.07	0.00	2.77	1.12	0.00	11.96
3.74	4.29	0.08	0.00	0.00	2.49	1.28	0.00	11.88
3.89	4.06	0.10	0.06	0.00	2.75	1.05	0.00	11.91
3.70	4.29	0.06	0.05	0.00	2.74	1.05	0.00	11.89
3.43	4.33	0.17	0.04	0.31	2.74	0.95	0.04	12.00
3.27	4.57	0.14	0.05	0.08	2.93	0.93	0.02	12.00
4.44	3.44	0.09	0.00	0.17	2.84	1.01	0.00	12.00
2.34	5.62	0.04	0.00	0.04	3.04	0.92	0.00	12.00
2.47	5.48	0.00	0.00	0.15	2.99	0.91	0.00	12.00
2.18	5.72	0.09	0.02	0.09	2.12	1.79	0.00	12.00
2.41	5.47	0.02	0.00	0.30	2.00	1.79	0.00	12.00
1.98	5.97	0.06	0.02	0.01	2.27	1.70	0.00	12.00
1.96	5.94	0.06	0.00	0.17	2.11	1.75	0.00	12.00
2.69	5.29	0.04	0.00	0.00	2.16	1.80	0.00	11.99
2.64	5.21	0.07	0.04	0.22	2.00	1.82	0.00	12.00
2.17	5.70	0.07	0.00	0.26	2.05	1.75	0.00	12.00
3.12	4.88	0.00	0.00	0.00	2.15	1.84	0.00	12.00
2.44	5.10	0.57	0.04	0.17	2.27	1.27	0.14	12.00
1.82	6.03	0.10	0.01	0.24	2.42	1.38	0.00	12.00
3.19	4.45	0.38	0.01	0.29	2.73	0.95	0.00	12.00
2.05	5.42	0.57	0.04	0.38	2.53	1.02	0.00	12.00
3.17	4.34	0.60	0.04	0.18	2.66	1.00	0.00	12.00
3.99	3.83	0.18	0.06	0.07	2.35	1.52	0.00	12.00
3.05	4.86	0.08	0.01	0.05	2.50	1.43	0.00	12.00
2.62	5.34	0.10	0.04	0.00	2.26	1.55	0.00	11.92

Sample no.	Ta_2O_5	Nb_2O_5	TiO_2	SnO_2	Fe_2O_3	FeO	MnO	CaO	Total
VO-5-24B/1	28.1	51.2	0.5	0.4	0.2	7.9	10.3	0.0	98.5
VO-8-3/1	46.8	33.4	0.3	0.0	4.0	2.8	11.9	0.0	99.1
VO-8-3A/2	68.4	15.8	0.2	0.0	0.1	8.6	6.7	0.0	99.7
VO-9-9/1	57.5	25.6	0.5	0.4	0.6	11.5	4.4	0.0	100.6
VO-9-9/2	49.4	32.8	0.3	0.2	0.9	11.9	4.5	0.0	100.0
WACO-A-4/1	44.6	35.2	0.4	1.0	1.1	12.1	4.2	0.0	98.6
WACO-A-4/2	44.0	36.3	0.7	0.6	0.0	12.4	4.2	0.0	98.2
WACO-A-4/3	43.7	36.5	0.4	0.5	0.7	11.9	4.7	0.0	98.4
WACO-A-5/1	45.6	35.3	0.7	0.5	0.0	12.5	4.3	0.0	99.0
WACO-A-5/2	51.2	31.3	0.4	0.0	0.5	11.8	4.6	0.0	99.9
WACO-A-5/3	47.9	32.6	0.6	1.3	1.3	11.7	4.2	0.0	99.7
WACO-A-5/4	61.5	22.5	0.2	0.4	0.2	9.3	6.7	0.0	100.7
WACO-A-9/1	45.2	36.7	0.6	0.0	0.0	5.8	9.9	0.8	99.0
WACO-A-9/2	45.8	37.0	0.8	0.4	0.0	12.7	4.5	0.0	101.2
WACO-A-9/3	45.7	36.4	0.7	0.6	0.0	12.6	4.6	0.0	100.5
WACO-A-9/4	45.3	36.6	0.8	0.6	0.0	12.7	4.3	0.0	100.2
WACO-B-1/2	48.9	31.7	2.2	0.0	0.0	7.6	6.5	1.5	98.5
WACO-B-1/3	51.8	27.6	2.7	1.2	0.0	11.8	3.4	0.5	99.0
WACO-B-1/4	53.4	27.7	2.2	0.8	1.4	10.7	4.8	0.0	100.9
WACO-B-3/1	36.5	42.2	2.1	0.4	0.2	13.3	3.9	0.0	98.7
WACO-B-3/2	36.9	40.9	2.7	0.7	0.0	13.1	3.8	0.0	98.1
WACO-B-3/3	38.4	39.5	2.3	0.7	0.9	12.4	4.0	0.0	98.2
WACO-C-11A/1	28.9	49.8	1.4	0.4	0.9	13.6	4.1	0.0	99.1
WACO-C-11A/2	28.0	51.3	1.1	0.1	1.4	13.6	4.1	0.0	99.6
WACO-C-11B/1	29.7	51.7	1.2	0.1	1.0	14.1	4.2	0.0	102.0
WACO-C-11B/2	26.9	53.8	1.0	0.1	0.9	14.1	4.3	0.0	101.2
WACO-C-6/1	41.6	38.4	2.0	0.4	0.6	12.7	4.0	0.1	99.8
WACO-C-6/2	37.3	42.2	1.5	0.3	0.0	8.9	7.8	0.3	98.4
WACO-C-6A/1	41.6	38.4	2.0	0.4	0.6	12.7	4.0	0.0	99.7
WACO-C-6A/2	37.3	42.2	1.5	0.3	0.0	8.9	7.8	0.0	98.0
WACO-C-6A/3	54.2	26.8	1.2	0.1	0.3	12.1	3.7	0.0	98.5
WACO-C-6A/4	43.4	36.3	1.6	0.6	1.7	12.0	4.0	0.0	99.6
WAS-20/1	44.8	38.7	0.1	0.0	0.1	8.8	8.8	0.0	101.2
WAS-20/2	43.5	39.9	0.2	0.0	0.2	8.7	8.9	0.0	101.5

Cations based on 24(O)

Ta^{5+}	Nb^{5+}	Ti^{4+}	Sn^{4+}	Fe^{3+}	Fe^{2+}	Mn^{2+}	Ca^{2+}	Total
1.96	5.94	0.09	0.04	0.04	1.70	2.23	0.00	12.00
3.52	4.17	0.05	0.00	0.82	0.64	2.80	0.00	12.00
5.76	2.21	0.04	0.00	0.01	2.23	1.75	0.00	12.00
4.51	3.34	0.10	0.05	0.13	2.77	1.09	0.00	12.00
3.75	4.13	0.07	0.02	0.19	2.78	1.06	0.00	12.00
3.37	4.42	0.09	0.11	0.22	2.80	0.98	0.00	12.00
3.32	4.56	0.15	0.06	0.00	2.88	0.99	0.00	11.97
3.29	4.56	0.09	0.05	0.16	2.75	1.10	0.00	12.00
3.44	4.42	0.14	0.06	0.01	2.91	1.02	0.00	12.00
3.92	3.98	0.08	0.00	0.12	2.79	1.10	0.00	12.00
3.62	4.10	0.12	0.14	0.28	2.73	1.00	0.00	12.00
4.93	3.00	0.05	0.04	0.04	2.28	1.66	0.00	12.00
3.38	4.57	0.13	0.00	0.00	1.33	2.31	0.24	11.95
3.37	4.51	0.15	0.04	0.00	2.86	1.03	0.00	11.98
3.38	4.48	0.14	0.07	0.00	2.86	1.06	0.00	11.99
3.35	4.51	0.16	0.06	0.00	2.89	1.00	0.00	11.98
3.71	4.00	0.46	0.00	0.00	1.78	1.54	0.46	11.96
3.99	3.54	0.57	0.14	0.00	2.79	0.82	0.16	12.00
4.05	3.49	0.45	0.09	0.29	2.50	1.13	0.00	12.00
2.63	5.05	0.42	0.04	0.04	2.95	0.87	0.00	12.01
2.68	4.93	0.54	0.07	0.00	2.91	0.85	0.00	11.98
2.80	4.78	0.45	0.08	0.19	2.78	0.92	0.00	12.00
2.01	5.73	0.27	0.04	0.17	2.89	0.89	0.00	12.00
1.92	5.85	0.21	0.01	0.27	2.88	0.87	0.00	12.00
1.99	5.78	0.22	0.01	0.18	2.92	0.88	0.00	12.00
1.81	6.01	0.19	0.01	0.17	2.91	0.91	0.00	12.00
3.02	4.63	0.40	0.04	0.13	2.84	0.90	0.03	12.00
2.71	5.08	0.31	0.03	0.00	1.99	1.77	0.10	11.98
3.02	4.63	0.40	0.04	0.13	2.84	0.90	0.00	11.97
2.71	5.08	0.31	0.03	0.00	1.99	1.77	0.00	11.88
4.27	3.52	0.26	0.01	0.07	2.95	0.91	0.00	12.00
3.19	4.44	0.33	0.06	0.34	2.72	0.92	0.00	12.00
3.28	4.70	0.02	0.00	0.01	1.97	2.01	0.00	12.00
3.15	4.81	0.04	0.00	0.04	1.94	2.01	0.00	12.00

Ixiolite Analyses

Sample no.	Ta_2O_5	Nb_2O_5	TiO_2	SnO_2	Fe_2O_3	FeO	MnO	CaO	Total
BIGHILL-26/3	61.5	10.3	0.0	15.0	0.0	8.2	4.1	0.0	99.0
BIN-20/1	65.6	14.0	0.0	6.3	0.6	8.6	5.5	0.0	100.7
MAC-11/1	63.9	15.2	0.4	4.2	0.3	5.8	8.5	0.0	98.2
MAC-11/5	62.8	6.3	0.5	17.3	1.2	5.1	6.2	0.0	99.4
MAC-112/3	63.7	9.4	0.2	14.0	0.0	5.8	5.8	0.0	98.9
MAC-112/4	64.4	8.3	0.3	15.6	0.0	5.4	6.2	0.0	100.2
MAC-112/7	64.2	8.9	0.2	14.2	0.0	6.0	6.3	0.0	99.8
MAC-9/A	62.8	9.8	0.5	15.0	0.0	5.8	5.3	0.6	99.9
MAC-9/C	65.8	15.9	0.4	3.4	0.0	6.5	7.3	0.2	99.4
MAC-9/D	63.9	11.4	0.3	13.2	0.0	6.1	5.8	0.4	101.2
MINT-A-2/1	67.2	5.3	0.2	15.0	0.3	6.4	5.8	0.0	100.1
MINT-A-2/2	69.9	5.8	0.1	12.8	0.0	7.3	5.1	0.0	100.9
NITE-A-10/1	65.6	6.9	0.0	14.6	0.0	5.8	6.4	0.0	99.3
NITE-A-10/2	66.7	6.5	0.2	14.6	0.0	4.5	7.4	0.0	99.9
NITE-A-10/3	67.0	6.5	0.2	14.4	0.0	5.9	6.5	0.0	100.6
NITE-A-8/2	62.8	6.1	0.2	16.6	1.1	4.8	6.4	0.0	98.0
VO-5-20/5	62.1	5.9	1.3	17.9	0.0	10.9	0.7	0.0	98.8

Cations based on 8(O)

Ta^{5+}	Nb^{5+}	Ti^{4+}	Sn^{4+}	Fe^{3+}	Fe^{2+}	Mn^{2+}	Ca^{2+}	Total
1.77	0.49	0.00	0.63	0.00	0.73	0.36	0.00	3.97
1.83	0.65	0.00	0.26	0.04	0.74	0.47	0.00	3.99
1.81	0.71	0.03	0.17	0.02	0.50	0.75	0.00	4.00
1.81	0.30	0.04	0.73	0.10	0.45	0.56	0.00	4.00
1.84	0.45	0.02	0.59	0.00	0.51	0.52	0.00	3.94
1.85	0.40	0.02	0.66	0.00	0.48	0.55	0.00	3.96
1.85	0.42	0.02	0.60	0.00	0.53	0.56	0.00	3.98
1.78	0.46	0.04	0.63	0.00	0.51	0.47	0.07	3.96
1.84	0.74	0.03	0.14	0.00	0.56	0.63	0.02	3.96
1.79	0.53	0.02	0.54	0.00	0.53	0.50	0.05	3.96
1.96	0.26	0.02	0.64	0.02	0.58	0.52	0.00	4.00
2.03	0.28	0.01	0.54	0.00	0.65	0.46	0.00	3.98
1.92	0.33	0.00	0.63	0.00	0.52	0.58	0.00	3.99
1.94	0.31	0.02	0.62	0.00	0.40	0.68	0.00	3.97
1.94	0.31	0.02	0.61	0.00	0.53	0.59	0.00	4.00
1.85	0.30	0.01	0.72	0.09	0.44	0.59	0.00	4.00
1.80	0.28	0.11	0.76	0.00	0.98	0.06	0.00	4.00

Tapiolite Analyses

Sample no.	Ta_2O_5	Nb_2O_5	TiO_2	SnO_2	Fe_2O_3	FeO	MnO	CaO	Total
BET-112A/A	72.1	7.9	2.2	1.1	2.4	12.3	0.3	0.1	98.4
BET-112B/B	72.1	7.9	2.2	1.1	2.4	12.4	0.3	0.0	98.3
BET-112B/C	71.4	8.5	3.0	1.5	1.3	13.3	0.0	0.0	99.1
BIG-B-25/1	78.7	5.3	0.2	0.2	1.0	13.2	0.5	0.0	99.1
BIG-B-25/3	78.2	5.5	0.3	0.4	1.3	13.0	0.6	0.0	99.2
BIG-B-26	70.8	11.1	1.3	0.3	1.6	12.9	0.9	0.0	98.8
BIG-B-8/2	77.6	5.4	0.0	0.8	0.9	13.1	0.6	0.0	98.4
BIG-B-8/3	77.0	4.7	0.2	1.1	2.2	12.3	0.5	0.0	98.1
BIGHILL-30/1	80.6	2.3	0.2	2.8	0.8	12.2	1.1	0.0	100.0
BIGHILL-30/2	81.1	2.0	0.1	2.8	1.5	11.8	1.2	0.0	100.6
BIGHILL-32/2	78.3	4.9	0.2	1.6	2.2	12.4	0.6	0.0	100.4
BIGHILL-33/1	80.3	2.3	0.2	2.7	1.9	11.2	1.5	0.0	100.2
BIN-19/2	81.2	4.7	0.2	0.7	0.3	13.4	0.9	0.0	101.4
BIN-19/3	80.6	4.4	0.2	0.7	1.1	12.8	1.0	0.0	100.8
BIN-20/2	80.3	4.6	0.2	1.4	0.9	12.9	0.9	0.0	101.2
BIN-20/3	78.4	4.6	0.0	3.9	0.5	12.8	0.9	0.0	101.1
CAS-I-1/1	80.1	3.5	0.5	0.5	2.1	12.0	1.0	0.0	99.6
CAS-I-1/4	81.4	2.3	0.7	0.3	0.3	13.2	0.5	0.0	98.7
CAS-I-2/3	80.4	4.6	0.3	0.3	2.1	10.3	0.5	0.0	98.6
CAS-I-2/4	76.7	6.1	0.7	0.9	0.1	13.4	0.7	0.0	98.7
DR-BOB-3/2	74.3	6.9	2.0	1.1	0.6	13.7	0.0	0.0	98.5
FLY-1-11/1	81.4	1.2	0.0	0.7	3.2	11.4	0.7	0.0	98.6
FLY-1-11/4	79.5	4.0	0.1	0.3	0.6	13.3	0.5	0.0	98.3
FREDA-12/4	74.5	7.7	0.0	1.1	1.2	13.5	0.1	0.0	98.1
LENS-10/1	75.7	7.9	1.5	0.6	1.2	13.5	0.4	0.0	100.8
LENS-10/2	74.9	7.7	1.6	0.6	1.4	13.3	0.3	0.0	99.8
MAC-11/6	79.6	3.7	0.4	1.2	0.1	13.6	0.3	0.0	98.8
MEL-9-11/1	75.1	8.1	0.3	0.5	1.8	12.7	0.9	0.0	99.4
MEL-9-11/2	75.0	8.1	0.3	0.6	1.4	13.3	0.4	0.0	99.3
MEL-9-21/1	75.3	7.5	0.3	0.9	0.3	13.8	0.3	0.0	98.5
MEL-9-21/2	75.7	7.7	0.3	0.7	1.3	13.2	0.6	0.0	99.5
MINT-A-3/1	76.4	7.0	0.7	1.5	0.3	13.7	0.5	0.0	100.0
MINT-A-3/2	77.2	6.6	0.3	0.8	0.5	13.6	0.5	0.0	99.6
MINT-A-6/2	79.5	4.7	0.6	0.6	0.9	13.7	0.1	0.0	100.1
MINT-A-6/4	79.9	3.9	0.3	0.8	0.0	13.0	0.3	0.0	98.3
NITE-A-10/4	81.9	3.5	0.3	0.5	1.8	12.3	1.2	0.0	101.4
NITE-A-3/1	81.9	2.9	0.1	0.5	2.0	11.6	1.5	0.0	100.5
NITE-A-3/2	80.5	3.7	0.1	0.4	1.9	11.9	1.3	0.0	99.9
NITE-A-3/3	80.6	3.7	0.0	0.5	1.4	12.0	1.4	0.0	99.8
NITE-A-6/1	81.6	3.0	0.2	0.8	0.4	12.9	1.0	0.0	99.9
NITE-A-6/2	80.4	4.5	0.2	0.7	0.8	12.8	1.1	0.0	100.5
PEG-196-4/1	82.4	2.3	0.2	0.4	1.5	11.4	1.9	0.0	100.2
PEG-196-4/2	82.7	2.0	0.3	0.0	2.6	11.0	1.8	0.0	100.4
PEG-196-4/3	82.4	1.9	0.3	0.8	2.3	10.4	2.5	0.0	100.4
PEG-196-4/4	82.7	2.0	0.5	0.5	2.2	11.0	2.0	0.0	100.9
PEG-319-1/1	76.5	6.1	1.2	0.0	2.5	12.1	0.9	0.0	99.3
PEG-319-1/2	76.9	6.2	1.1	0.2	2.2	12.3	0.9	0.0	99.7

Cations based on 12(O)

Ta^{5+}	Nb^{5+}	Ti^{4+}	Sn^{4+}	Fe^{3+}	Fe^{2+}	Mn^{2+}	Ca^{2+}	Total
3.12	0.57	0.26	0.07	0.28	1.64	0.04	0.02	6.00
3.12	0.57	0.26	0.07	0.28	1.64	0.04	0.00	5.98
3.04	0.60	0.36	0.10	0.16	1.74	0.00	0.00	6.00
3.54	0.39	0.03	0.01	0.13	1.83	0.07	0.00	6.00
3.50	0.41	0.03	0.03	0.16	1.80	0.08	0.00	6.00
3.04	0.79	0.15	0.02	0.18	1.70	0.12	0.00	6.00
3.52	0.41	0.00	0.06	0.11	1.83	0.08	0.00	6.00
3.49	0.35	0.03	0.08	0.27	1.71	0.08	0.00	6.00
3.65	0.17	0.03	0.18	0.10	1.71	0.15	0.00	5.99
3.66	0.15	0.01	0.18	0.19	1.64	0.16	0.00	6.00
3.46	0.36	0.02	0.11	0.27	1.69	0.07	0.00	5.98
3.61	0.17	0.03	0.18	0.24	1.56	0.21	0.00	5.99
3.60	0.34	0.03	0.04	0.03	1.82	0.12	0.00	5.99
3.58	0.33	0.02	0.04	0.13	1.75	0.12	0.00	5.99
3.55	0.34	0.02	0.09	0.12	1.76	0.12	0.00	5.99
3.47	0.34	0.00	0.25	0.06	1.75	0.12	0.00	6.00
3.59	0.26	0.06	0.03	0.26	1.66	0.13	0.00	6.00
3.73	0.18	0.09	0.02	0.04	1.87	0.07	0.00	6.00
3.69	0.33	0.04	0.02	0.00	1.74	0.07	0.00	5.90
3.44	0.45	0.09	0.06	0.01	1.85	0.09	0.00	6.00
3.27	0.50	0.24	0.07	0.07	1.85	0.00	0.00	6.00
3.74	0.09	0.00	0.05	0.41	1.62	0.10	0.00	6.00
3.64	0.30	0.02	0.02	0.07	1.87	0.07	0.00	6.00
3.33	0.57	0.00	0.07	0.15	1.86	0.01	0.00	6.00
3.24	0.57	0.18	0.04	0.14	1.79	0.04	0.00	6.00
3.24	0.55	0.20	0.04	0.17	1.77	0.03	0.00	5.98
3.63	0.28	0.04	0.08	0.01	1.91	0.04	0.00	6.00
3.29	0.59	0.04	0.03	0.22	1.71	0.12	0.00	6.00
3.29	0.59	0.04	0.04	0.17	1.80	0.06	0.00	6.00
3.37	0.55	0.04	0.06	0.04	1.90	0.04	0.00	6.00
3.33	0.56	0.04	0.05	0.16	1.78	0.09	0.00	6.00
3.36	0.51	0.08	0.10	0.03	1.85	0.07	0.00	6.00
3.43	0.49	0.04	0.06	0.07	1.86	0.06	0.00	6.00
3.54	0.35	0.08	0.04	0.11	1.87	0.01	0.00	6.00
3.68	0.30	0.03	0.06	0.00	1.84	0.04	0.00	5.95
3.63	0.26	0.03	0.04	0.21	1.67	0.16	0.00	6.00
3.68	0.21	0.01	0.03	0.24	1.61	0.22	0.00	6.00
3.62	0.28	0.01	0.03	0.23	1.64	0.19	0.00	6.00
3.64	0.28	0.00	0.04	0.18	1.67	0.20	0.00	6.00
3.70	0.22	0.03	0.05	0.06	1.79	0.14	0.00	6.00
3.58	0.33	0.03	0.05	0.10	1.75	0.15	0.00	6.00
3.73	0.17	0.03	0.02	0.19	1.59	0.26	0.00	6.00
3.71	0.15	0.04	0.00	0.33	1.52	0.25	0.00	6.00
3.71	0.14	0.03	0.05	0.28	1.43	0.35	0.00	6.00
3.69	0.15	0.06	0.04	0.27	1.50	0.28	0.00	6.00
3.36	0.45	0.15	0.00	0.30	1.63	0.12	0.00	6.00
3.36	0.45	0.13	0.01	0.26	1.65	0.12	0.00	6.00

Sample no.	Ta_2O_5	Nb_2O_5	TiO_2	SnO_2	Fe_2O_3	FeO	MnO	CaO	Total
PEG-319-2/1	78.6	5.9	0.8	0.0	1.5	12.6	1.0	0.0	100.6
PEG-8-4/3	78.6	4.8	1.2	0.2	2.3	12.8	0.3	0.0	100.2
PEG-8-4/4	77.3	4.0	1.5	0.0	3.1	11.8	0.4	0.0	98.1
PEG-84-2/2A	76.6	4.8	1.8	0.3	4.6	10.4	1.1	0.1	99.8
PEG-84-2B/1	76.6	4.8	1.8	0.3	4.6	10.4	1.1	0.0	99.7
PEG-84-2B/2	76.5	5.0	1.8	0.3	4.0	11.1	0.9	0.0	99.6
PEG-84-4A/1	72.2	7.0	4.9	0.0	3.0	11.9	0.4	0.0	99.3
PEG-84-4A/2	71.2	7.7	4.7	0.4	3.2	11.8	0.4	0.0	99.3
PEG-84-4B/TAP	71.7	7.1	4.7	0.0	3.3	11.5	0.6	0.0	98.8
PEG-88-2/1	74.8	8.3	0.5	0.3	3.0	12.4	0.6	0.0	99.9
PEG-88-2/2	76.0	8.7	0.5	0.4	0.9	13.8	0.5	0.0	100.8
PEG-88-2/3	74.7	8.8	0.7	0.1	2.0	13.0	0.6	0.0	100.0
PEG-93-35/1	73.6	8.4	0.9	0.7	2.7	12.6	0.4	0.0	99.4
PEG-93-35/2	74.0	8.2	1.2	0.9	2.0	12.7	0.6	0.0	99.7
PEG-93-35/3	75.2	8.4	0.7	0.5	2.0	13.1	0.5	0.0	100.3
PEG-93-37A/3	76.9	7.1	1.2	0.6	1.7	13.2	0.4	0.0	101.2
PEG-93-37A/4	76.8	7.7	1.4	0.2	1.4	13.5	0.4	0.0	101.4
PEG-93-37A/5	76.4	7.2	1.9	0.6	0.8	13.6	0.3	0.0	100.9
PEG-93-37A/6	75.9	7.9	1.3	0.5	0.9	13.7	0.4	0.0	100.6
PEG-93-37A/7	76.0	7.9	1.4	0.3	1.7	13.3	0.4	0.0	101.1
PEG-93-37A/8	75.7	8.2	1.8	0.8	1.3	13.5	0.5	0.0	101.7
PEG-93-37A/9	75.5	7.4	1.7	0.6	1.9	12.8	0.6	0.0	100.6
PVILLA-C-12/1	78.3	5.4	0.3	0.8	0.8	13.0	0.9	0.0	99.5
PVILLA-C-12/2	76.5	6.4	0.2	1.5	1.0	13.0	0.8	0.0	99.4
TAN-2-12/1	75.2	8.2	0.4	1.0	0.0	13.8	0.2	0.0	98.7
TAN-2-12/2	75.1	8.2	0.5	1.1	0.6	13.8	0.4	0.0	99.8
TAN-2-12/3	75.3	8.0	0.8	0.8	1.3	13.3	0.5	0.0	100.1
TAN-2-18/1	77.8	5.3	0.0	2.0	1.0	13.1	0.5	0.0	99.7
TAN-2-18/2	76.9	5.9	0.4	1.8	0.7	13.3	0.5	0.0	99.4
TAN-2-18/3	78.4	5.5	0.0	0.8	1.0	13.3	0.5	0.0	99.5
TAN-2-19/2	79.4	5.5	0.1	0.9	0.7	13.5	0.6	0.0	100.8
TAN-2-19/3	78.9	5.1	0.6	1.1	0.0	13.6	0.0	0.0	99.3
TAN-2-2/1	79.0	4.5	0.1	0.8	1.5	12.7	0.7	0.0	99.2
TAN-2-20/3	77.4	5.9	0.3	1.3	0.7	13.2	0.7	0.0	99.5
TAN-2-20/4	78.9	5.9	0.3	0.9	0.7	13.5	0.6	0.0	100.8
TAN-4-1/1	76.6	6.6	0.0	1.0	0.0	13.5	0.5	0.0	98.2
TAN-4-1/2	74.8	8.0	0.1	1.8	0.1	13.7	0.6	0.0	99.1
TAN-4-1/4	75.5	8.2	0.3	0.7	0.7	13.3	0.9	0.0	99.6
TAN-4-3/5	78.1	5.3	0.0	0.5	0.6	12.9	1.0	0.0	98.3
THE-PN-A-3BTP	78.3	6.5	0.4	1.0	0.0	13.4	0.4	0.0	100.1
USK-15/1	79.5	2.8	1.0	1.2	0.3	12.4	1.1	0.0	98.4
USK-15/2	81.1	2.2	0.4	0.6	1.5	11.9	1.2	0.0	99.0
WACO-B-1/TAP	76.9	5.4	2.0	0.5	0.1	13.5	0.5	0.0	98.8

Cations based on 12(O)

Ta^{5+}	Nb^{5+}	Ti^{4+}	Sn^{4+}	Fe^{3+}	Fe^{2+}	Mn^{2+}	Ca^{2+}	Total
3.44	0.43	0.10	0.00	0.19	1.70	0.14	0.00	6.00
3.45	0.35	0.15	0.01	0.28	1.72	0.04	0.00	6.00
3.45	0.30	0.19	0.00	0.38	1.63	0.06	0.00	6.00
3.31	0.34	0.21	0.02	0.56	1.38	0.15	0.02	6.00
3.31	0.34	0.21	0.02	0.56	1.38	0.15	0.00	5.98
3.32	0.36	0.22	0.02	0.48	1.48	0.12	0.00	6.00
3.02	0.49	0.56	0.00	0.34	1.53	0.05	0.00	6.00
2.97	0.53	0.54	0.03	0.37	1.51	0.05	0.00	6.00
3.02	0.49	0.54	0.00	0.38	1.48	0.08	0.00	6.00
3.23	0.60	0.06	0.02	0.36	1.65	0.08	0.00	6.00
3.28	0.63	0.06	0.02	0.11	1.83	0.07	0.00	6.00
3.22	0.63	0.09	0.01	0.24	1.72	0.08	0.00	6.00
3.19	0.60	0.11	0.05	0.32	1.67	0.06	0.00	6.00
3.20	0.59	0.14	0.06	0.24	1.69	0.08	0.00	6.00
3.24	0.60	0.09	0.03	0.23	1.73	0.07	0.00	6.00
3.30	0.51	0.15	0.04	0.20	1.75	0.06	0.00	6.00
3.28	0.54	0.16	0.01	0.17	1.77	0.06	0.00	6.00
3.28	0.51	0.22	0.04	0.09	1.80	0.05	0.00	6.00
3.27	0.57	0.16	0.03	0.11	1.81	0.05	0.00	6.00
3.25	0.56	0.16	0.02	0.20	1.75	0.06	0.00	6.00
3.20	0.57	0.21	0.05	0.15	1.75	0.06	0.00	6.00
3.24	0.53	0.20	0.04	0.23	1.69	0.08	0.00	6.00
3.51	0.40	0.03	0.05	0.10	1.78	0.12	0.00	6.00
3.40	0.47	0.02	0.10	0.13	1.77	0.10	0.00	6.00
3.34	0.61	0.05	0.07	0.00	1.88	0.03	0.00	5.97
3.29	0.60	0.06	0.07	0.08	1.85	0.05	0.00	6.00
3.27	0.58	0.09	0.05	0.16	1.78	0.06	0.00	6.00
3.48	0.39	0.00	0.13	0.12	1.80	0.07	0.00	6.00
3.42	0.44	0.05	0.12	0.09	1.82	0.07	0.00	6.00
3.51	0.41	0.00	0.05	0.12	1.83	0.07	0.00	6.00
3.51	0.40	0.02	0.06	0.09	1.83	0.08	0.00	6.00
3.55	0.38	0.07	0.07	0.00	1.88	0.00	0.00	5.96
3.56	0.34	0.01	0.05	0.18	1.76	0.09	0.00	6.00
3.45	0.44	0.04	0.09	0.09	1.80	0.09	0.00	6.00
3.48	0.43	0.03	0.06	0.09	1.83	0.08	0.00	6.00
3.47	0.50	0.00	0.07	0.00	1.88	0.07	0.00	5.98
3.32	0.59	0.02	0.12	0.02	1.86	0.08	0.00	6.00
3.31	0.60	0.03	0.05	0.09	1.80	0.12	0.00	6.00
3.55	0.40	0.00	0.03	0.07	1.80	0.14	0.00	6.00
3.47	0.48	0.05	0.06	0.00	1.83	0.05	0.00	5.96
3.63	0.21	0.13	0.08	0.04	1.74	0.16	0.00	6.00
3.71	0.17	0.05	0.04	0.19	1.68	0.16	0.00	6.00
3.41	0.40	0.24	0.03	0.01	1.84	0.07	0.00	6.00

Cassiterite Analyses

Sample no.	Ta_2O_5	Nb_2O_5	TiO_2	SnO_2	Fe_2O_3	FeO	MnO	CaO	Total
BILL-5-12/CAS	0.5	0.0	0.0	100.7	0.4	0.0	0.0	0.0	101.6
CATA-B-1	0.7	0.3	0.0	98.7	0.4	0.0	0.0	0.0	100.0
CATA-T-2/1	1.5	0.5	0.0	96.5	0.0	0.3	0.0	0.0	98.9
CATA-T-2/3	2.6	0.2	0.0	96.9	0.0	0.4	0.0	0.0	100.1
CATA-U-1/1	1.1	0.5	0.0	98.0	0.0	0.3	0.0	0.0	99.8
CATA-U-1/2	0.8	0.5	0.0	98.4	0.3	0.1	0.0	0.0	100.1
CATA-U-1/3	1.0	0.9	0.0	98.2	0.1	0.4	0.0	0.0	100.5
DR-BOB-3/1	2.5	0.0	0.1	96.2	0.4	0.2	0.0	0.0	99.5
DR-BOB-3/4	2.7	0.0	0.0	95.6	0.1	0.4	0.0	0.0	98.8
DR-BOB-5/1	3.2	0.1	0.1	97.7	0.1	0.5	0.0	0.0	101.8
DR-BOB-5/3	1.9	0.0	0.0	98.7	1.5	0.0	0.0	0.0	102.1
FREDA-10/1	3.5	1.6	0.0	94.6	0.2	0.9	0.0	0.0	100.8
FREDA-10/2	2.5	1.2	0.0	94.8	0.2	0.7	0.0	0.0	99.4
FREDA-11/1	1.0	0.8	0.0	97.0	0.6	0.0	0.1	0.0	99.4
FREDA-11/2	0.7	0.3	0.0	99.0	0.4	0.0	0.0	0.0	100.3
FREDA-12/1	6.8	1.8	0.0	88.9	0.0	1.6	0.0	0.0	99.1
FREDA-12/2	7.3	1.3	0.0	88.6	0.1	1.5	0.0	0.0	98.9
FREDA-12/3	7.2	1.4	0.0	88.4	0.3	1.4	0.0	0.0	98.8
FREDA-18/1	1.3	0.0	0.0	99.0	0.0	0.1	0.1	0.0	100.4
FREDA-18/2	0.4	0.0	0.0	99.8	0.0	0.0	0.0	0.0	100.2
FREDA-8	1.3	1.0	0.0	99.0	0.0	0.0	0.0	0.0	101.3
JENNE-A-4/1	1.6	2.3	0.0	95.1	0.3	0.8	0.0	0.0	100.0
JENNE-A-4/2	0.7	0.0	0.0	100.4	0.4	0.0	0.0	0.0	101.5
LU-A-3/1	1.0	0.0	0.0	98.4	0.3	0.0	0.0	0.0	99.7
LU-A-3/2	4.7	0.0	0.0	92.7	1.2	0.2	0.0	0.0	98.9
LU-A-4/2	0.8	0.0	0.0	100.4	0.0	0.0	0.0	0.0	101.2
LU-A-9/1	2.1	0.0	0.0	96.5	0.5	0.1	0.0	0.0	99.3
LU-A-9/3	1.2	0.4	0.0	98.1	0.7	0.0	0.0	0.0	100.5
LU-B-3/1	3.0	0.2	0.0	97.4	0.1	0.5	0.0	0.0	101.2
LU-B-3/3	1.0	0.7	0.0	99.1	0.3	0.2	0.0	0.0	101.4
LU-B-4/1	0.9	0.5	0.0	99.5	0.0	0.3	0.0	0.0	101.2
LU-B-4/3	0.9	0.2	0.0	99.9	0.0	0.0	0.0	0.0	101.1
LU-B-5/1	0.6	0.3	0.0	98.9	0.0	0.1	0.0	0.0	99.9
LU-B-5/2	0.6	0.8	0.0	99.2	0.0	0.0	0.0	0.0	100.6
LU-B-5/3	1.5	0.0	0.0	99.9	0.2	0.1	0.0	0.0	101.8
LU-B-6/1	2.6	1.3	0.0	96.1	0.2	0.7	0.0	0.0	100.9
LU-B-6/2	1.5	0.7	0.0	99.2	0.5	0.2	0.0	0.0	102.0

Cations based on 4(O)

Ta^{5+}	Nb^{5+}	Ti^{4+}	Sn^{4+}	Fe^{3+}	Fe^{2+}	Mn^{2+}	Ca^{2+}	Total
0.00	0.00	0.00	1.98	0.01	0.00	0.00	0.00	1.99
0.01	0.01	0.00	1.97	0.02	0.00	0.00	0.00	2.00
0.02	0.01	0.00	1.95	0.00	0.01	0.00	0.00	2.00
0.04	0.00	0.00	1.94	0.00	0.02	0.00	0.00	2.00
0.01	0.01	0.00	1.96	0.00	0.01	0.00	0.00	2.00
0.01	0.01	0.00	1.96	0.01	0.00	0.00	0.00	2.00
0.01	0.02	0.00	1.95	0.00	0.01	0.00	0.00	2.00
0.03	0.00	0.01	1.93	0.01	0.01	0.00	0.00	2.00
0.04	0.00	0.00	1.94	0.00	0.02	0.00	0.00	2.00
0.02	0.00	0.00	1.92	0.00	0.01	0.00	0.00	1.96
0.02	0.00	0.00	1.93	0.05	0.00	0.00	0.00	2.01
0.05	0.03	0.00	1.87	0.01	0.04	0.00	0.00	2.00
0.03	0.03	0.00	1.90	0.01	0.03	0.00	0.00	2.00
0.01	0.02	0.00	1.94	0.02	0.00	0.00	0.00	2.00
0.01	0.01	0.00	1.97	0.01	0.00	0.00	0.00	2.00
0.09	0.04	0.00	1.80	0.00	0.07	0.00	0.00	2.00
0.10	0.03	0.00	1.80	0.00	0.06	0.00	0.00	2.00
0.10	0.03	0.00	1.80	0.01	0.06	0.00	0.00	2.00
0.02	0.00	0.00	1.97	0.00	0.00	0.00	0.00	2.00
0.01	0.00	0.00	1.99	0.00	0.00	0.00	0.00	2.00
0.02	0.02	0.00	1.95	0.00	0.00	0.00	0.00	1.99
0.01	0.03	0.00	1.88	0.00	0.02	0.00	0.00	1.94
0.00	0.00	0.00	1.98	0.01	0.00	0.00	0.00	1.99
0.01	0.00	0.00	1.97	0.01	0.00	0.00	0.00	2.00
0.07	0.00	0.00	1.88	0.04	0.01	0.00	0.00	2.00
0.01	0.00	0.00	1.99	0.00	0.00	0.00	0.00	1.99
0.01	0.00	0.00	1.95	0.01	0.00	0.00	0.00	1.97
0.02	0.01	0.00	1.95	0.03	0.00	0.00	0.00	2.00
0.04	0.00	0.00	1.93	0.00	0.02	0.00	0.00	2.00
0.01	0.02	0.00	1.95	0.01	0.01	0.00	0.00	2.00
0.01	0.01	0.00	1.96	0.00	0.01	0.00	0.00	2.00
0.01	0.00	0.00	1.98	0.00	0.00	0.00	0.00	2.00
0.01	0.01	0.00	1.98	0.00	0.01	0.00	0.00	2.00
0.01	0.02	0.00	1.97	0.00	0.00	0.00	0.00	1.99
0.02	0.00	0.00	1.97	0.01	0.01	0.00	0.00	2.00
0.03	0.03	0.00	1.90	0.01	0.03	0.00	0.00	2.00
0.02	0.01	0.00	1.94	0.02	0.01	0.00	0.00	2.00

Sample no.	Ta_2O_5	Nb_2O_5	TiO_2	SnO_2	Fe_2O_3	FeO	MnO	CaO	Total
LU-B-8/1	3.5	1.2	0.0	93.9	0.5	0.6	0.0	0.0	99.7
LU-B-8/2	0.0	0.0	0.3	98.4	0.0	0.0	0.0	0.0	98.7
LU-C-10/1	0.5	0.3	0.0	101.0	0.0	0.0	0.0	0.0	101.8
LU-C-10/2	0.4	0.3	0.0	100.2	0.4	0.0	0.0	0.0	101.3
LU-C-11/1	0.4	0.0	0.0	99.7	1.0	0.0	0.0	0.0	101.1
LU-C-11/2	0.3	0.0	0.2	101.0	0.4	0.0	0.0	0.0	102.0
LU-C-16/2	6.1	0.4	0.0	93.5	0.0	1.0	0.0	0.0	100.9
LU-C-3/1	0.7	0.3	0.0	100.5	0.0	0.0	0.0	0.0	101.5
LU-C-3/2	1.4	0.5	0.0	96.9	0.9	0.0	0.0	0.0	99.7
LU-C-4/1	1.0	0.3	0.0	99.5	0.5	0.0	0.0	0.0	101.4
LU-C-4/2	0.5	0.0	0.0	100.1	0.0	0.0	0.0	0.0	100.6
LU-C-5/1	1.0	0.0	0.0	100.6	0.1	0.1	0.0	0.0	101.9
LU-C-5/2	4.0	1.3	0.0	94.8	0.4	0.8	0.0	0.0	101.3
LU-C-6/1	0.6	0.7	0.0	99.2	0.3	0.0	0.1	0.0	101.0
LU-C-6/2	0.4	0.2	0.0	100.1	0.2	0.0	0.0	0.0	101.0
LU-C-7/1	0.6	0.3	0.0	100.3	0.3	0.0	0.1	0.0	101.7
LU-C-7/2	0.9	0.5	0.0	100.4	0.0	0.1	0.0	0.0	101.9
LU-D1-2/1	2.0	0.6	0.0	98.5	0.0	0.4	0.0	0.0	101.4
LU-D1-2/2	0.8	0.5	0.0	99.2	0.6	0.0	0.0	0.0	101.1
LU-D1-4/1	1.6	0.4	0.0	97.7	0.0	0.3	0.0	0.0	100.1
LU-D1-4/3	5.4	0.4	0.0	94.2	0.6	0.5	0.2	0.0	101.3
MAC-9/B	6.2	0.3	0.0	93.6	0.0	0.9	0.0	0.0	101.0
PEG-1-12/1	2.5	1.4	0.3	96.2	0.1	0.7	0.0	0.0	101.4
PEG-1-12/2	2.2	1.2	0.0	96.1	0.6	0.4	0.0	0.0	100.5
PEG-1-12/3	2.5	1.1	0.2	95.8	0.6	0.4	0.0	0.0	100.7
PEG-1-4/1	2.2	1.4	0.2	94.3	0.6	0.5	0.0	0.0	99.1
PEG-1-4/2	3.0	1.5	0.2	94.2	0.0	0.9	0.0	0.0	99.9
PEG-1-4/3	4.2	1.3	0.3	91.9	0.0	1.0	0.0	0.0	98.7
TAN-2-19/1	7.5	0.6	0.0	88.7	0.0	1.3	0.0	0.0	98.0
TAN-2-19/4	11.0	0.3	0.0	88.6	0.5	1.4	0.2	0.0	102.1
TAN-2-20/1	5.4	0.0	0.1	93.2	0.3	0.7	0.0	0.0	99.7
TAN-2-20/2	13.5	0.9	0.0	84.4	0.2	2.1	0.2	0.0	101.4
TAN-4-3/4	5.2	0.0	0.0	93.6	0.4	0.7	0.0	0.0	99.9
VO-5-20/1	0.8	0.0	0.0	100.0	0.3	0.0	0.0	0.0	101.1
VO-5-20/3	5.2	0.3	0.0	92.3	0.2	0.8	0.0	0.0	98.8
WACO-A-3/1	1.0	0.4	0.0	99.0	0.2	0.2	0.0	0.0	100.8
WACO-A-3/2	3.0	1.1	0.0	94.1	3.6	0.0	0.0	0.0	101.7

Cations based on 4(O)

Ta^{5+}	Nb^{5+}	Ti^{4+}	Sn^{4+}	Fe^{3+}	Fe^{2+}	Mn^{2+}	Ca^{2+}	Total
0.05	0.03	0.00	1.88	0.02	0.03	0.00	0.00	2.00
0.00	0.00	0.01	1.99	0.00	0.00	0.00	0.00	2.00
0.00	0.00	0.00	1.98	0.00	0.00	0.00	0.00	1.99
0.00	0.00	0.00	1.97	0.01	0.00	0.00	0.00	1.99
0.01	0.00	0.00	1.96	0.04	0.00	0.00	0.00	2.01
0.00	0.00	0.00	1.97	0.01	0.00	0.00	0.00	1.99
0.08	0.01	0.00	1.86	0.00	0.04	0.00	0.00	2.00
0.00	0.00	0.00	1.98	0.00	0.00	0.00	0.00	1.99
0.02	0.01	0.00	1.94	0.03	0.00	0.00	0.00	2.00
0.01	0.01	0.00	1.96	0.02	0.00	0.00	0.00	2.00
0.00	0.00	0.00	1.99	0.00	0.00	0.00	0.00	2.00
0.01	0.00	0.00	1.98	0.00	0.00	0.00	0.00	1.99
0.05	0.03	0.00	1.87	0.01	0.03	0.00	0.00	2.00
0.01	0.02	0.00	1.96	0.01	0.00	0.00	0.00	2.00
0.00	0.00	0.00	1.98	0.00	0.00	0.00	0.00	1.99
0.00	0.00	0.00	1.97	0.01	0.00	0.00	0.00	1.98
0.01	0.00	0.00	1.97	0.00	0.00	0.00	0.00	1.98
0.01	0.01	0.00	1.94	0.00	0.01	0.00	0.00	1.97
0.00	0.01	0.00	1.95	0.01	0.00	0.00	0.00	1.98
0.01	0.00	0.00	1.95	0.00	0.01	0.00	0.00	1.98
0.04	0.00	0.00	1.87	0.01	0.01	0.00	0.00	1.93
0.04	0.00	0.00	1.87	0.00	0.02	0.00	0.00	1.93
0.02	0.02	0.01	1.89	0.00	0.02	0.00	0.00	1.94
0.01	0.01	0.00	1.90	0.01	0.01	0.00	0.00	1.95
0.02	0.01	0.00	1.89	0.01	0.01	0.00	0.00	1.95
0.03	0.03	0.01	1.89	0.02	0.02	0.00	0.00	2.00
0.04	0.03	0.01	1.88	0.00	0.04	0.00	0.00	2.00
0.06	0.03	0.01	1.86	0.00	0.04	0.00	0.00	2.00
0.10	0.01	0.00	1.82	0.00	0.05	0.00	0.00	2.00
0.15	0.01	0.00	1.76	0.02	0.06	0.01	0.00	2.00
0.07	0.00	0.00	1.88	0.01	0.03	0.00	0.00	2.00
0.18	0.02	0.00	1.69	0.01	0.09	0.01	0.00	2.00
0.04	0.00	0.00	1.88	0.01	0.01	0.00	0.00	1.94
0.01	0.00	0.00	1.98	0.01	0.00	0.00	0.00	2.00
0.07	0.01	0.00	1.88	0.01	0.04	0.00	0.00	2.00
0.01	0.01	0.00	1.96	0.01	0.01	0.00	0.00	2.00
0.04	0.02	0.00	1.82	0.13	0.00	0.00	0.00	2.02

Microlite Analyses

Sample no.	BIG-B-26/4	BIG-B-26/6	CAS-1-1/2	CAS-1-1/3	CAS-1-1/4	CAS-1-2/2	FLY-1-7/C1	FLY-1-7/C2	FREDA-12/5	MINT-A 6/1
Na_2O	0.5	0.0	1.6	1.3	0.3	0.1	0.3	0.0	0.3	2.8
CaO	3.6	3.8	13.1	12.1	10.8	3.8	1.3	3.4	12.4	15.3
MnO	0.0	0.0	0.0	0.0	1.9	0.3	4.0	3.5	0.4	0.4
FeO	2.7	1.4	1.2	1.1	2.2	0.6	4.2	3.6	0.7	0.8
PbO	0.0	0.4	0.2	0.3	0.0	0.4	0.4	0.5	0.1	0.0
UO_2	3.3	4.6	0.7	1.1	0.2	5.1	3.4	2.0	0.9	0.6
TiO_2	0.7	0.8	0.6	0.8	0.3	6.0	0.0	0.0	0.0	0.3
SnO_2	0.0	0.0	0.0	0.0	0.0	0.0	0.0	0.0	0.0	0.0
Nb_2O_5	13.2	6.2	4.4	4.2	24.6	12.6	14.7	18.7	1.0	7.0
Ta_2O_5	69.3	75.8	71.4	72.9	58.9	56.8	68.0	63.4	77.9	68.4
Total	93.3	93.0	93.2	93.8	99.2	85.7	96.3	95.1	93.7	95.6
	Cations based on full B-site occupancy									
Na^{2+}	0.2	0.0	0.6	0.4	0.1	0.0	0.1	0.0	0.1	1.0
Ca^{2+}	0.6	0.7	2.6	2.3	1.7	0.6	0.2	0.6	2.5	3.0
Mn^{2+}	0.0	0.0	0.0	0.0	0.2	0.0	0.5	0.5	0.1	0.1
Fe^{2+}	0.4	0.2	0.2	0.2	0.3	0.1	0.6	0.5	0.1	0.1
Pb^{2+}	0.0	0.0	0.0	0.0	0.0	0.0	0.0	0.0	0.0	0.0
U^{4+}	0.1	0.2	0.0	0.0	0.0	0.2	0.1	0.1	0.0	0.0
Ti^{4+}	0.1	0.1	0.1	0.1	0.0	0.7	0.0	0.0	0.0	0.0
Sn^{4+}	0.0	0.0	0.0	0.0	0.0	0.0	0.0	0.0	0.0	0.0
Nb^{5+}	0.9	0.5	0.4	0.3	1.6	0.9	1.1	1.3	0.1	0.6
Ta^{5+}	3.0	3.4	3.6	3.6	2.3	2.4	2.9	2.7	3.9	3.4
Total	5.2	5.1	7.4	7.0	6.3	5.0	5.6	5.6	6.8	8.2

Sample no.	MINT-A 6/3	PEG-192-12/2	PEG-8-4/2B	PEG-93 35/5	RIB-A-7-A/1	RIB-A-7-A/4	RIB-9/4	RIB-9/5	VO-8-3/1C	VO-8-3/1E
Na_2O	2.2	1.1	2.8	1.0	1.8	1.9	0.3	1.6	1.1	0.0
CaO	17.2	0.9	14.5	9.1	8.4	5.8	2.3	6.4	14.8	9.8
MnO	0.0	4.3	0.0	1.0	0.0	0.0	0.0	0.0	0.0	0.6
FeO	0.0	6.0	1.4	1.7	1.6	4.3	1.8	1.6	0.8	0.4
PbO	0.3	0.0	0.0	0.0	4.4	1.3	1.0	2.7	0.7	1.5
UO_2	1.1	1.5	0.1	1.3	9.6	5.4	7.6	12.6	0.5	0.1
TiO_2	0.5	0.9	4.0	1.5	0.4	0.0	0.6	0.3	1.0	3.3
SnO_2	0.0	0.0	0.0	0.0	0.0	0.0	0.0	0.0	0.0	0.0
Nb_2O_5	7.0	22.3	7.0	25.5	2.6	3.4	9.9	2.9	10.1	17.6
Ta_2O_5	68.0	58.8	68.7	53.4	69.1	74.8	65.4	65.8	66.9	60.0
Total	96.3	95.8	98.5	94.5	97.9	96.9	88.9	93.9	95.9	93.3
	Cations based on full B-site occupancy									
Na^{2+}	0.8	0.3	0.9	0.3	0.7	0.7	0.1	0.6	0.4	0.0
Ca^{2+}	3.3	0.1	2.5	1.4	1.8	1.1	0.4	1.4	2.7	1.6
Mn^{2+}	0.0	0.5	0.0	0.1	0.0	0.0	0.0	0.0	0.0	0.1
Fe^{2+}	0.0	0.8	0.2	0.2	0.3	0.7	0.3	0.3	0.1	0.0
Pb^{2+}	0.0	0.0	0.0	0.0	0.2	0.1	0.0	0.1	0.0	0.1
U^{4+}	0.0	0.0	0.0	0.0	0.4	0.2	0.3	0.6	0.0	0.0
Ti^{4+}	0.1	0.1	0.5	0.2	0.1	0.0	0.1	0.0	0.1	0.4
Sn^{4+}	0.0	0.0	0.0	0.0	0.0	0.0	0.0	0.0	0.0	0.0
Nb^{5+}	0.6	1.5	0.5	1.7	0.2	0.3	0.8	0.3	0.8	1.2
Ta^{5+}	3.4	2.4	3.0	2.1	3.7	3.7	3.1	3.7	3.1	2.4
Total	8.2	5.8	7.6	6.1	7.4	6.7	5.2	7.0	7.2	5.8

Appendix D

STRUCTURE FACTORS FOR YKF-303

OBSERVED AND CALCULATED STRUCTURE FACTORS FOR TAPIOLITE YKF-303

H	K	L	FO	FC	H	K	L	FO	FC	H	K	L	FO	FC	H	K	L	FO	FC	H	K	L	FO	FC
1	1	0	306	287	0	0	2	90	76	1	6	3	73	62	1	1	6	163	177	3	3	8	25	23
0	2	0	219	203	1	1	2	58	60	2	6	3	6	3	0	2	6	137	142	0	4	8	26	25
1	2	0	39	32	0	2	2	50	49	0	0	4	39	37	1	2	6	15	13	1	4	8	4	1
2	2	0	211	224	1	2	2	6	3	1	1	4	40	40	2	2	6	132	146	2	4	8	21	18
1	3	0	163	172	2	2	2	42	49	0	2	4	38	42	1	3	6	110	120	1	5	8	20	17
2	3	0	12	6	1	3	2	39	42	1	2	4	6	2	2	3	6	6	3	0	1	9	102	110
3	3	0	139	148	3	3	2	26	29	2	2	4	27	30	3	3	6	109	104	1	1	9	12	10
0	4	0	151	145	0	4	2	36	36	1	3	4	30	32	0	4	6	99	102	1	2	9	98	102
1	4	0	19	18	2	4	2	22	26	2	3	4	5	5	1	4	6	13	10	2	2	9	4	4
2	4	0	106	120	4	4	2	19	17	3	3	4	17	18	2	4	6	86	87	0	3	9	98	94
3	4	0	9	5	1	5	2	21	22	0	4	4	22	25	3	4	6	6	3	1	3	9	5	3
4	4	0	87	85	3	5	2	17	16	2	4	4	18	19	4	4	6	72	63	2	3	9	78	72
1	5	0	99	103	0	6	2	17	14	4	4	4	15	11	1	5	6	84	75	1	4	9	73	67
3	5	0	68	70	2	6	2	16	14	1	5	4	17	15	3	5	6	58	53	2	4	9	4	3
0	6	0	87	75	0	1	3	256	233	3	5	4	14	12	0	1	7	27	30	0	0	10	9	10
1	6	0	9	5	1	1	3	60	48	0	6	4	13	9	1	1	7	6	6	1	1	10	15	13
2	6	0	63	61	1	2	3	219	217	2	6	4	13	10	1	2	7	20	22	0	2	10	16	16
0	1	1	75	64	2	2	3	16	16	0	1	5	50	52	0	3	7	15	16	2	2	10	10	9
1	2	1	44	48	0	3	3	185	199	1	1	5	8	8	2	3	7	21	19	1	3	10	12	11
2	2	1	7	9	1	3	3	17	12	1	2	5	43	47	1	4	7	15	14	3	3	10	8	6
0	3	1	38	37	2	3	3	118	134	0	3	5	35	42	3	4	7	11	11	0	4	10	10	8
1	3	1	6	5	3	3	3	9	6	2	3	5	28	31	0	5	7	13	13	0	1	11	27	24
2	3	1	28	35	1	4	3	120	127	1	4	5	28	28	2	5	7	10	8	1	2	11	25	24
1	4	1	25	28	2	4	3	9	9	3	4	5	23	22	0	0	8	49	51	0	3	11	23	23
3	4	1	20	22	3	4	3	96	95	0	5	5	21	19	1	1	8	37	39	0	0	12	85	74
0	5	1	22	22	4	4	3	11	9	1	5	5	5	1	0	2	8	30	29	1	1	12	72	65
2	5	1	17	18	0	5	3	90	84	2	5	5	21	20	2	2	8	33	35	0	2	12	61	57
4	5	1	13	10	2	5	3	90	90	1	6	5	18	14	1	3	8	29	27	1	2	12	5	3
1	6	1	16	14	4	5	3	64	57	0	0	6	210	221										